Journal of Geophysical Research

VOLUME 64 AUGUST 1959 NUMBER 8

THE SCIENTIFIC PUBLICATION
OF THE AMERICAN GEOPHYSICAL UNION

Journal of Geophysical Research

An International Scientific Publication

This Journal welcomes original scientific contr
tions on the physics of the earth and its environm
Manuscripts should be transmitted to J. A. Peo
Jr., Geology Department, University of Kan
Lawrence, Kansas. Authors' institutions, if in
United States or Canada, are requested to pay a
lication charge of $15 per page, which, if honored,
titles them to 100 free reprints.
Subscriptions to the *Journal of Geophysical*
search and *Transactions, AGU* are included in m
bership dues.
Non-member subscriptions, *Journal of Geophy*
Research.....$16 per calendar year, $2 per c
Non-member subscriptions, *Transactions, AGU*
.....$4 per calendar year, $1.25 per c
Subscriptions, renewals, and orders for back num
should be addressed to American Geophysical Un
1515 Massachusetts Ave., Northwest, Washingto
D. C. Suggestions to authors are available on requ
Advertising Representative: Howland and H
land, Inc., 114 East 32nd St., New York 16, N. Y

Beginning with the January 1959 issue (Vol. 64, No. 1) the *Journal of Geophysical Research* is publis
monthly by the American Geophysical Union, the U. S. National Committee of the International U
of Geodesy and Geophysics organized under the National Academy of Sciences-National Research Cou
as the U. S. national adhering body. Publication of this journal is supported by the National Science Fo
dation and the Carnegie Institution of Washington. The new monthly combines the type of scien
material formerly published in the bi-monthly *Transactions, American Geophysical Union*, and the quart
Journal of Geophysical Research. The *Transactions, American Geophysical Union* will continue as a quart
publication for Union business and items of interest to members of the Union.

Published monthly by the American Geophysical Union from 1407 Sherwood Avenue, Richmond, Virgi
Second class postage paid at Richmond, Virginia.

YSTEMS
NGINEERING

with standard components

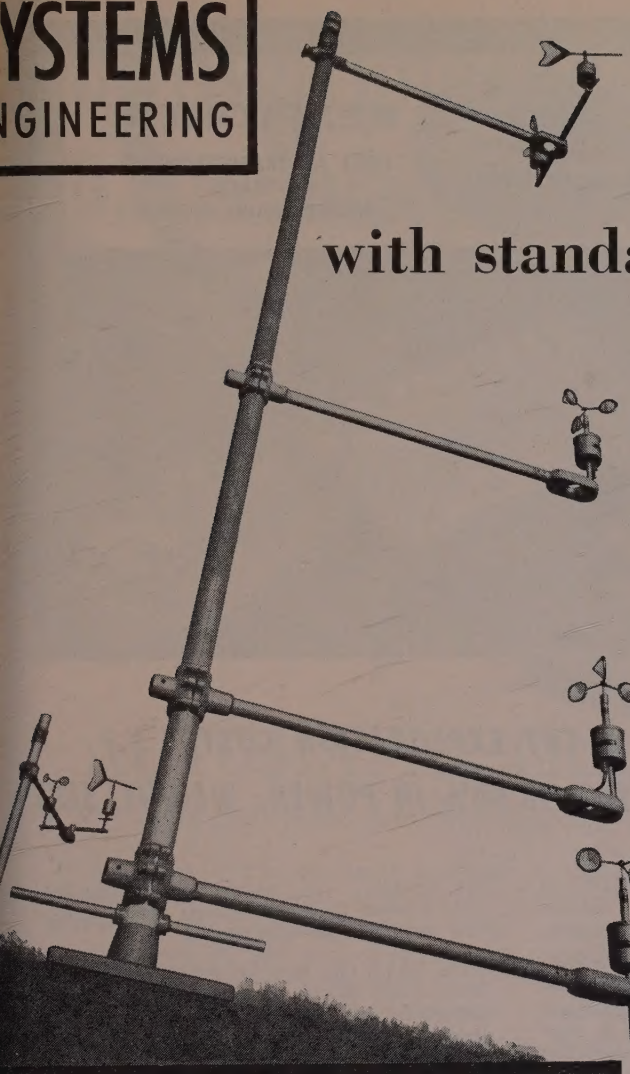

Where a complete meteorological system is required, Beckman & Whitley offers everything you need: 1. Time-tried and proved anemometers, wind-direction units, thermal radiometers, soil heat-flow transducers, etc, of the highest quality and performance, and 2. A knowledgeable and experienced engineering and meteorological group prepared to develop these elements into a complete met system to meet your particular needs.

EXAMPLE: Illustrated here is a complete automatic wind-profile system created for IGY glacier studies. The logarithmic pickup array is composed of standard transmitters mounted on a standard meteorological mast and telemetered to standard translator units driving a special photographic recording unit.

Shown below, this device automatically records the readings from digital counters representing the four wind-speed pickups, together with the indication from a clock face, operating on an interval basis which can be anything from seconds to hours. Wind direction is written on a standard strip-chart recorder.

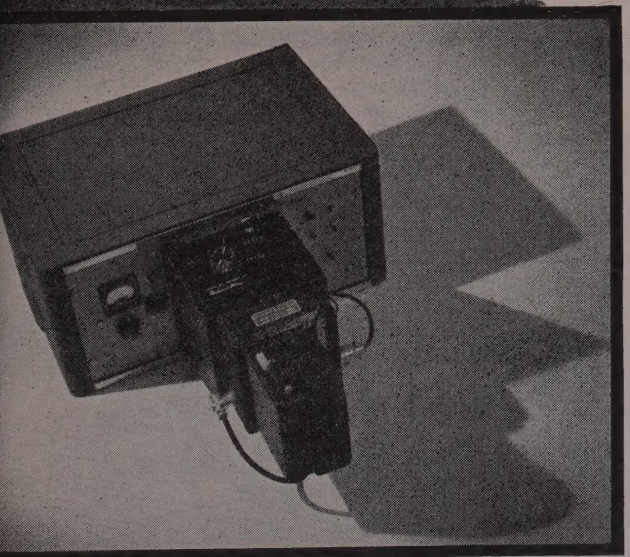

There are many other examples ranging from small portable weather stations to rocket-motor test-tower instrumentation running into dozens of pickup points on numerous towers, and data presentation on punch cards, typewriters, calculator tapes, and the like.

Check with us on your particular problems.

Beckman & Whitley INC.
SAN CARLOS 15, CALIFORNIA

CUT EXPLORATION COSTS . . .

SAVE 50% to 80% IN POWER, WEIGHT, SIZE

Texas Instruments Incorporated has developed a completely new, high-performance seismograph around the functional magic of transistors.

YOU SAVE ON PORTAGE AND TRANSPORTATION . . . For the first time, a 24-channel seismograph, complete with control and test circuitry, is contained in a compact, *one-man* portable case 18″ x 26″ x 8″ weighing only 57 pounds. Other systems require from three to six cases for components performing the same functions. Also, the entire seismograph system, with camera and magnetic recorder (*TECHNO's* new all-transistorized magnetic recorder is a highly compatible system with the EXPLORER) may be mounted in one Jeep or transported in one helicopter trip.

YOU SAVE ON POWER . . . the EXPLORER requires only one 12-volt battery and consumes nine amperes (normally only six amperes after first breaks) . . . no warmup time is required. This is better than a five-to-one power savings over other present seismographs.

YOU SAVE ON MAINTENANCE . . . after initial system checks, 80 per cent of all amplifier difficulties are attributable to vacuum tubes. Transistors used in the EXPLORER, for practical purposes, have infinite life.

Furthermore, the EXPLORER offers a wide practical frequency range, 5 to 200 cps; broad dynamic range; and wide operational latitude in AGC speeds, initial suppression, filtering, inputs, outputs, and test circuitry.

The EXPLORER is literally *jumps* ahead of the exploration industry . . . it pays for itself in REDUCED OPERATING COSTS, INCREASED PRODUCTION, and UNEQUALLED RELIABILITY.

Write for complete EXPLORER information . . . specify Bulletin S-324.

TEXAS INSTRUMENTS
INCORPORATED
INDUSTRIAL INSTRUMENTATION DIVISION
3609 BUFFALO SPEEDWAY • HOUSTON, TEXAS • CABLE: HOULAB

Other TI/IID Products

- Complete Seismic Instrumentation
- TI Worden Gravity Meters
- DATA-GAGE Measurement and Control Systems
- "recti/riter" Recorders and Accessories
- Automatic Test Equipment

(TI handles export sales and service for TECHNO transistorized recorder)

MINIATURIZED RAYDIST DM SYSTEM

SAVES OIL COMPANY THOUSANDS OF DOLLARS

HYDROGRAPHIC AND GEOPHYSICAL SURVEY ALONG 75 MILES OF COASTLINE COMPLETED WITHIN 40 WORKING DAYS

The Pacific Petroleum Company, an affiliate of Richfield Oil, selected the new, miniaturized Raydist Type DM system for use in a geological survey off the coast of Peru.

According to the Chief Geophysicist for the survey, the selection of Raydist over other position determining systems resulted in an over-all savings of thousands of dollars.

Since time was limited, the equipment was shipped by air from Hampton, Virginia, to Peru, South America. Raydist, weighing only one-tenth of competitive systems, saved $4,000 in shipping costs alone. Within twenty-four hours after clearing customs, Raydist was on the job.

The new, miniaturized Raydist system saved many days of installation time since the small, light, battery-operated shore stations can be set up within thirty minutes.

Raydist, maintained by only two operators, saved additional transportation costs and also reduced the logistics problem especially important in this remote area.

Raydist provided a continuous permanent record of the vessel's position with relation to two selected shore sites which enabled the survey boat to return to any point at a later date with extreme accuracy.

Raydist left Hampton, Virginia, on December 10 and returned home February 2 after having completed a hydrographic survey along a 75 mile coastline in Peru, South America.

An observer from another oil company, after seeing Raydist in operation, said, "I was favorably impressed by the portability and compactness of the system. I was also favorably impressed by the apparent accuracy and repeatability of the system. The whole set-up appeared efficient, and I feel sure it would be of value in our operation."

In case after case, Raydist has proved itself a superior tool for all hydrographic operations. We welcome your inquiries.

HASTINGS-RAYDIST, INCORPORATED

TEL: PARK 3-6531 HAMPTON, VIRGINIA

GEOPHYSICAL MONOGRAPH SERIES

AMERICAN GEOPHYSICAL UNION

1515 Massachusetts Avenue, N.W. Washington 5, D. C., U.S.A.

Antarctica in the International Geophysical Year—Geophysical Monograph No. 1 (Publication No. 462, National Academy of Sciences—National Research Council); Library of Congress Catalogue Card No. 56-60071; 133 pp. and large folded map of the Antarctic, 1956, 7" x 10", $6.00. Contains 16 papers by various American authorities on the Antarctic under the headings: General, Geographic and Meteorological, Geological and Structural, Upper Atmospheric Physics, and Flora and Fauna. Map (41" x 41") compiled by the American Geographical Society. Introduction by L. M. Gould, President of Carleton College and internationally recognized authority on the Antarctic.

Geophysics and the IGY—Geophysical Monograph No. 2 (Publication No. 590, National Academy of Sciences—National Research Council); Library of Congress Catalogue Card No. 58-60035; 210 pp., 1958, 7" x 10", $8.00. Contains 30 papers by leading American authorities under the headings: Upper Atmospheric Physics, The Lower Atmosphere and the Earth, and The Polar Regions. Preface by Joseph Kaplan, Chairman of the U. S. National Committee for the IGY.

Atmospheric Chemistry of Chlorine and Sulfur Compounds—Geophysical Monograph No. 3 (Publication No. 652, National Academy of Sciences—National Research Council); Library of Congress Catalogue Card No. 59-60039; 129 pp., 1959, 7" x 10", $5.50. Based on a symposium held jointly with the Robert A. Taft Sanitary Engineering Center of the U. S. Public Health Service in Cincinnati in November, 1957. Contains 23 papers (some as summaries) with discussion. Preface by James P. Lodge, Jr., of the Taft Sanitary Engineering Center and Chairman of AGU's Committee on Chemistry of the Atmosphere.

Contemporary Geodesy—Geophysical Monograph No. 4 (Publication No. 708, National Academy of Sciences—National Research Council); Library of Congress Catalogue Card No. 59-60065; about 120 pp., 7" x 10", to be published in late summer, 1959, $5.50. Based on a Conference held at Cambridge, Massachusetts, in December 1958 jointly by the AGU with the Smithsonian Astrophysical Observatory and the Harvard College Observatory. Contains 14 papers by leading authorities, with verbatim discussions on topics ranging from classical geodesy to trilateration by underwater sound to space navigation in the solar system under the general headings: Geodetic Fundamentals, Problems of Modern Geodesy, and Geodesy and Space.

Prices plus postage, unless payment accompanies order. Quantity discounts: 5–19 copies, 10%; 20–49 copies, 15%; 50 or more copies, 20%.

It is anticipated that Geophysical Monograph 5 will be issued during 1959. Watch "Special Announcements" in the *Transactions* for word of this.

Purchase Order

To AMERICAN GEOPHYSICAL UNION

1515 Massachusetts Avenue, N.W., Washington 5, D. C., U.S.A.

Please enter our order for the following:

_____ copies of Geophysical Monograph No. 1, *Antarctica in the International Geophysical Year,* at $6.00* $_____

_____ copies of Geophysical Monograph No. 2, *Geophysics and the IGY,* at $8.00* $_____

_____ copies of Geophysical Monograph No. 3, *Atmospheric Chemistry of Chlorine and Sulfur Compounds,* at $5.50* $_____

_____ copies of Geophysical Monograph No. 4, Contemporary Geodesy, at $5.50* _____

☐ Payment of $_____ is enclosed.

☐ Please send invoice, adding postage charges.

☐ Enter our standing order for _____ copies of subsequent Geophysical Monographs at the special prepublication rates, e.g., prepublication rate for Monograph No. 4 for non-members was $4.00, payment in advance, or $4.75 (plus postage) on invoice.

* List price is net for quantities up to four; see above for discounts on quantity purchases. Special discounts to members.

Typed name _____ Signature _____

Address _____

_____

Journal of
GEOPHYSICAL RESEARCH

VOLUME 64 AUGUST, 1959 No. 8

SYMPOSIUM ON SCIENTIFIC EFFECTS OF ARTIFICIALLY INTRODUCED RADIATIONS AT HIGH ALTITUDES

Introductory Remarks*

RICHARD W. PORTER

General Electric Company
New York, New York

The existence of corpuscular radiation of high intensity in the vicinity of the earth was discovered by accident in the course of the first successful experiment of the United States IGY satellite program. The scientific equipment on our first satellite, 1958α—or, as it was popularly called, Explorer I—had been designed to measure the intensity of primary cosmic rays entering the upper layers of the earth's atmosphere. Although this equipment was capable of detecting and counting the number of ionizing events well in excess of any expected cosmic-ray intensity, the telemetered recordings showed that the satellite was passing in and out of regions where the number of counts rose abruptly to a level where it saturated not only the counting circuits but even the Geiger-Müller tube itself. Fortunately, by means of laboratory tests on similar instruments, it was possible to identify, at least approximately, the levels at which this saturation occurred and thereby to establish a lower limit for the magnitude of the radiation that was being encountered.

The data from this first US-IGY satellite, launched on 31 January 1958 by the Army Ballistic Missile Agency and the Jet Propulsion Laboratory of the California Institute of Technology, and also from the next IGY Explorer, 1958γ, launched on 26 March 1958, again by ABMA and JPL, led to the following preliminary conclusions, which were presented by Dr. Van Allen at an historic joint meeting of members of the National Academy of Sciences and the American Physical Society here in Washington a year ago:

1. Below approximately 700 km, at latitudes between 33° north and south, the satellites were encountering only radiation that was essentially in accord with expectations on the basis of previous cosmic-ray measurements in rockets and balloons and at the earth's surface.

2. At higher altitudes, generally around 1000 km or above, depending somewhat on longitude and latitude, the intensity of the radiation began to increase very rapidly with altitude in a manner that could not be explained on the basis of cosmic-ray phenomena.

3. At the highest altitudes, on the assumption that the radiation consisted entirely of penetrating charged particles, that is of electrons having an energy of at least 3 Mev or of protons having at least 30 Mev, the omnidirectional intensity was found to exceed 1700 counts

* Opening statement by the Chairman on the occasion of the Symposium, April 29, 1959, held at the National Academy of Sciences, Washington, D. C. These remarks and the other papers presented are being published simultaneously in the August 1959 issue of the *Proceedings of the National Academy of Sciences.*

per square centimeter per second. If, on the other hand, the energy were assumed to consist exclusively of electrons in the range between approximately 50 kev and 3 Mev, where the electrons themselves could not penetrate the absorber but could produce Bremsstrahlung energetic enough to penetrate without much attenuation, the omnidirectional intensity must have been in excess of 10^8 per square centimeter per second.

4. Because of the rapid change in observed intensity between 700 and 1000 km, where the air density is insignificantly small, it was evident that the primary radiation must be restrained from reaching lower altitudes by the earth's magnetic field and therefore must consist of charged particles having energies substantially less than those normally associated with cosmic rays.

On the basis of these conclusions, it was suggested that the observed radiation might originally have come from the sun in the form of ionized gas clouds, portions of which subsequently entered the earth's magnetic field by means of local magnetic disturbances created by the clouds themselves. Having once entered the earth's field, the particles might remain trapped in a manner suggested previously by Störmer and others. It was, therefore, quite natural to relate this radiation to the "soft auroral radiation" that had been observed in the arctic and antarctic regions, both before and during the IGY. Both Van Allen and Bennett had suggested that observations be made of auroral corpuscular radiation using satellites having highly inclined orbits. It had not been anticipated, however, that this radiation would be found at such low altitudes so near the equator. Nevertheless, on the basis of this previous experience there was a tendency to favor the alternative of Bremsstrahlung from low-energy electrons as the predominant source of the radiation.

The National Academy of Sciences' IGY Committee, and particularly its Satellite Panel, were anxious to conduct further experiments as soon as possible with instrumentation more suitably designed to observe this newly discovered belt of natural radiation. Work was started immediately to prepare instrumentation, and the Department of Defense was asked t provide at least two more Jupiter C vehicles.

One of the two additional satellites, Explore IV, was launched by ABMA and JPL on 2 July and became 1958ε; the other failed to g into orbit.

While Explorer IV was still in the planning stage, the Advanced Research Projects Agency of the Department of Defense carried forward plans for the Argus experiment which we are here to talk about this morning. Inasmuch as the objective of the Argus experiment was to observe the behavior of electrons trapped in the earth's magnetic field, instrumentation was provided for Explorer IV which was suitable for study of both the natural radiation belt and any Argus effects. Pertinent scientific results relating to the natural radiation effects observed by this satellite were presented at the American Physical Society meeting in Chicago earlier this year and were published in the March issue of the *Journal of Geophysical Research*.

Despite some newspaper stories to the contrary, there was no commitment under the IGY to exchange information with other nations on the Argus experiment. Argus was not an IGY program; it was a Department of Defense effort. Some confusion on this point has arisen entirely from the circumstance that a single satellite gathered data on two subjects—one, natural-radiation phenomena; the other, artificial phenomena from Argus. However, the Department of Defense and the Atomic Energy Commission have now released the information you are about to hear this morning so that it can be made a part of the synoptic geophysical record of this interesting period in science.

Presentation of these results necessarily waited upon reduction and analysis of the scientific data and upon declassification of the Argus experiment.

The first Argus burst produced a yield of between 1 and 2 kilotons at approximately 02 hr 30 min UT on August 27 at a nominal altitude of 480 km in the neighborhood of longitude 12° west, latitude 38° south. A fascinating sequence of observations followed, which will be described in some detail by the speakers on this morning's program. For the first time in history, geophysical phenomena on a world-wide scale were being measured and related to

quantitatively known cause—namely, the injection into the earth's magnetic field of a known quantity of electrons of known energies at a known position and at a known time.

The diverse radiation instruments in Explorer IV recorded and reported to ground stations the absolute intensity and position of this man-made shell of high-energy electrons as the satellite continued to lace back and forth through the trapped radiation, hour after hour and day after day. The rate of decay of electron density as a function of altitude provided new information on the density of the remote upper atmosphere, since atmospheric scattering was the dominant mechanism for loss of particles. Moreover, the continuing observation of the thickness of the shell served to answer the vital question about the rate of diffusion of trapped particles transverse to the shell. All these matters, which are of essential importance to a thorough understanding of the electrodynamics of the natural radiation, thus became subject to direct study by means of the electrons released from Argus I.

At approximately 03 hr 20 min UT on August 30, a second detonation of the same size was produced, also at nominal altitude of 480 km in the neighborhood of longitude 8° west, latitude 50° south. A similar succession of phenomena followed.

The third and final detonation, of the same size, was at about 22 hr 10 min UT on September 6 at the same nominal altitude in the neighborhood of longitude 10° west, latitude 50° south. Again a series of remarkable geophysical phenomena was produced. And, for the third time, Explorer IV faithfully observed the power of artificially produced trapped radiation.

Throughout the testing period a series of firings of high-altitude sounding rockets was carried out successfully, yielding valuable results in the lower fringes of the trapping region.

Explorer IV continued to observe the artificially injected electrons from the Argus tests, making some 250 transits of the shell, until its batteries were exhausted in the latter part of September. By that time the intensity had become barely observable above the background of natural radiation at the altitudes covered by the orbit of this satellite. It also appears likely that the deep space probe Pioneer III detected a small residuum of the Argus effect at very high altitudes on December 6, 1958, but the effect appears to have become unobservable before the flight of Pioneer IV on March 3, 1959.

An immense body of directly related observations has now been under study and interpretation by a large number of persons for about 7 months, and, as you will shortly hear, useful scientific results are being derived. It is also possible that other important contributions will arise as the many diverse geophysical observations being conducted by other countries participating in the International Geophysical Year are accumulated and analyzed.

The Argus Experiment*

N. C. CHRISTOFILOS

Lawrence Radiation Laboratory, University of California
Livermore, California

Abstract—A geophysical experiment on global scale was conducted last fall. Three small A-bombs were detonated beyond the atmosphere at a location in the south Atlantic. The purpose of the experiment was to study the trapping of the relativistic electrons (produced by the β-decay fission fragments) in the geomagnetic field. The released electrons are trapped by this field oscillating along the magnetic lines between two mirror points. In addition to this motion the electrons drift eastward, creating a thin electron shell around the earth. The lifetime and location of the thus-created global electron shell were measured by satellite- and rocket-borne instruments. Auroral luminescence was observed at the conjugate points. The electron shell exhibited remarkable stability during its lifetime. *No* motion of the shell or change in its thickness was detected.

This experiment was proposed by the writer a few weeks after the launching of the first Sputnik. After intensive investigations by several scientists it was decided by the end of April 1958 to go ahead with the experiment. All the necessary preparations were accomplished in the amazingly short time of 4 months.

The usefulness of such electron shells for interpreting geophysical phenomena and possible future experiments are discussed.

With the advent of the satellite era the thoughts of scientists have extended to outer space, since means have become available for measurements and experimentation in the region of the upper atmosphere. Two classes of experiments are possible with satellite-carried instruments: (1) measurements of natural phenomena; (2) creation of artificial effects under controlled conditions. The second is more interesting, as the initial conditions are known and therefore physical quantities can be measured under completely different conditions from those which the natural phenomena allow.

Just after the first Sputnik was launched I was attracted by problems of outer space. The second class of experiments appeared very intriguing, and I started thinking about possible experiments. The first one that occurred to me stemmed from my main field of endeavor in the past five years, namely, the Astron thermonuclear device. In this device it is the aim to establish a cylindrical layer of relativistic electrons between two mirror coils. The electron layer, in turn, will establish a magnetic bottle for plasma confinement, while the relativistic electrons will subsequently heat the plasma by Coulomb collisions up to fusion temperature. It then occurred to me to extrapolate the idea of the electron layer to global dimensions, inasmuch as the earth's magnetic field provides a natural mirror effect. The trapping phenomenon was known theoretically for many years from the work of Störmer, Alfven, and others, namely, that charged particles released at one point will spiral about a magnetic line, being reflected at two points along this line, which came to be known as mirror points. In addition to this motion the electrons drift eastward, since the earth's field decreases with distance from the earth. Consequently, it was obvious that, if sufficient electrons were released at one point, they would spread all around the earth, creating a rather thin layer, but of global dimensions. Thus the first conclusion was that the electrons could be released from one point

* Work was performed under the auspices of the U. S. Atomic Energy Commission, Contract W-7405-eng-48, Rept. UCRL-5548.

Presented at the Symposium on Scientific Effects of Artificially Introduced Radiations at High Altitudes held at the National Academy of Sciences, April 29, 1959. This paper is being published simultaneously in the August 1959 issue of *Proceedings of the National Academy of Sciences.*

source, provided that the source was large enough.

The question then arose whether or not these electrons would survive long enough to complete several circuits around the earth. The time for one circuit around the earth is approximately inversely proportional to the electron energy. The lifetime has been calculated. The conclusions from the calculations were that most of the losses are due to Coulomb scattering with air atoms. Since the density of the atmosphere decreases exponentially with altitude it turned out that most of the losses occur near the mirror points. The result of the scattering is that the mirror points move down toward denser atmosphere. The electrons are practically lost after the mirror points have moved downward by about one scale height. The lifetime is proportional to the air density at the mirror points and approximately to the square of the electron energy, and is proportional to the length of the magnetic line. The conclusion was that electrons of 1 to 2 Mev energy injected at an altitude of a few hundred miles would survive several hours or more, depending on the air density at the mirror points. In more detail the results of these calculations were as follows (see also the Appendix).

The energy loss ($\dot{E}$) of the electrons by Coulomb scattering is equal to the energy loss ($\dot{E}_0$) corresponding to the air density at the mirror points divided by the length (ψ) of the magnetic line from the mirror point to the equatorial plane, measured in units of earth radii, times the square root of the ratio of the earth's radius (r_0) to the scale height (h):

$$\dot{E} = \dot{E}_0/(\psi\sqrt{r_0/h}) \qquad (1)$$

or

$$\dot{\gamma} = 3.10^{-8}N_0Z/(\psi\sqrt{r_0/h}) \quad \text{rest mass units/day} \qquad (2)$$

From the energy loss we can compute the square of the scattering angle and thus the downward velocity of the mirror points.

$$\frac{\dot{r}}{r_0} = \frac{Z(Z+1)}{\gamma^2}\frac{10^{-8}N_0}{\psi}\sqrt{\frac{h}{r_0}} \quad \text{days}^{-1} \qquad (3)$$

where Z is the atomic number, N_0 the numerical density, r_0 the earth radius, and γ the electron energy in rest mass units.

Electrons in the few Mev range are lost scattering without appreciable energy loss this case the lifetime is

$$T = 1.7 \times 10^6(\psi\gamma^2/N_0)\sqrt{h/r_0} \quad \text{days}$$

For the following parameters

$$(r_0/h)^{1/2} = 8 \qquad N_0 = 10$$

$$\psi = 1.5 \text{ (latitude } 45°) \qquad \gamma = 3$$

$$T = 2.86 \quad \text{days}$$

These results pointed toward a conveni source of a large quantity of electrons, nam to an A-bomb. This source is so plentiful t even 1 megaton of fission would create an el tron layer so dense as to constitute a radia hazard in outer space. To illustrate this I the following example: 1 megaton of fis yields 10^{26} fissions, approximately. If we assu that 4 electrons per fission are above 1 M energy and that half will be trapped in earth's field we derive the number of trap electrons, namely, 2×10^{26}. Then let us assu that these will be spread in a volume in ou space equal to the earth's volume, or 10^{27} c The resulting electron density is 0.2 electro cm^3. The flux against any surface exposed the electrons is

$$N_e = n_e c/4 \qquad (4)$$

or

$$N_e = 1.5 \times 10^9 \quad \text{electrons/cm}^2\,\text{sec}$$

A small part of the energy of the electrons converted to bremsstrahlung. The efficiency this conversion is proportional to the atom number of the target material.

The radiation level inside a space vehicle is

$$R = 8Z\gamma(\gamma - 1)n_e \quad \text{roentgens/hr} \qquad (6)$$

where Z and γ are as defined previously. A suming an atomic number $Z = 10$ and $\gamma =$ we observe that the radiation level is more tha 100 r/hr, which is a good fraction of the leth dose. Consequently, it is obvious that any e plosion of such magnitude can create a radiatio hazard in outer space, and any space exper ments involving A-bomb explosions must b carefully designed to avoid creation of hazardou radiation.

Fortunately a much smaller yield, namely in the kiloton range, is sufficient to yield detectable quantities without creating any radiation hazard at all.

It is obvious that the scientific aspect of such experiments is extremely important. Consequently, as soon as I suggested this experiment, about the end of October 1957, the matter was discussed with interest within the Radiation Laboratory for several weeks. In January 1958, I had completed preliminary calculations and a paper was prepared. The matter was further discussed with scientists from other laboratories. Finally, a group of scientists was appointed to evaluate the proposal, and it was recommended to proceed with a test employing a small-yield A-bomb in the kiloton range. Further, an altitude was selected so that the effect would not last more than a few days. In the meantime the belt of natural radiation was discovered by Dr. James Van Allen.

This discovery was partial proof that the trapping effect actually exists as postulated, so that about the end of April 1958 it was decided to proceed with the Argus test (the code name given to the experiment). The most pertinent question then was the location of the tests. Since the magnetic axis of the earth is tilted and the center of the dipole is displaced toward the Pacific Ocean, it is obvious that the trace of the mirror points will have their closest distance from the surface of the earth over the south Atlantic Ocean. Hence a location in the south Atlantic was finally selected for the test.

The over-all responsibility for the preparation and conduct of the experiment was vested in the Advanced Research Projects Agency (ARPA), then just established. Only 4 months from the time it was decided to proceed with the tests, the first bomb was exploded. This is a remarkable achievement in organization, and if we were to single out one man as most responsible for the accomplishment it would be Dr. Herbert York, who was then Chief Scientist of the ARPA. During this short time a task force including the rocket launching ship, *Norton Sound,* was organized, and special instrumentation on satellites was prepared by Dr. Van Allen. Many other activities were coordinated with the help of dozens of scientists.

In addition to the trapping effect the creation of an artificial aurora was predicted. The non-trapped electrons would be guided along the magnetic lines of force (which pass through the burst point) toward the upper atmosphere, producing strong ionization along these magnetic lines. Hence in both points where these lines re-enter the atmosphere auroral luminescence was expected.

The persons responsible for organizing the observations of auroral phenomena and magnetic disturbances as well as some of the minitrack stations were Dr. Philip Newman (AFCRC) and Dr. Allen Peterson (SRI). Besides the satellite observations, some rocket launchings were scheduled for observations at the very beginning of the formation of the Argus shell. This responsibility was assumed by a group of scientists in the AFSWC.

The experiment was successful in all respects except that Explorer V was not placed in orbit. However, the one satellite available, Explorer IV, yielded most of the important information, although valuable information resulted from other observations.

The bursts occurred on August 27 and 30 in the early morning hours and on September 6 shortly before midnight, Greenwich time. The locations were respectively 38°S, 12°W; 50°S, 8°W; and 50°S, 10°W, approximately.

A very interesting sequence of observations was obtained. The initial flash of the burst was followed by an auroral luminescence extending upward and downward along the magnetic line where the burst occurred. Simultaneously, at the point where the same magnetic line returns to the earth's atmosphere (the so-called conjugate point) in the north Atlantic, another auroral luminescence appeared in the night sky near the Azores Islands.

The instruments of Explorer IV recorded and reported to ground stations, around the earth, the electron density in the shell, as well as the position and thickness of the shell. The satellite continued to penetrate the shell several times a day at various altitudes, so that the density as a function of altitude and time was measured. The apogee of the electrons was about an earth's radius out in space, or approximately 4000 miles. Thus, for the first time, the earth's magnetic field was being plotted experimentally. The conjugate points were a few hundred miles

away from where the theoretical calculations indicated. This is rather a small error, considering that ring currents at high altitudes are not yet well known and that all the measurements of the earth's field had thus far been taken at the earth's surface.

When the location in the south Atlantic was selected, the data on the belt of natural radiation were rather meager, but it turned out that the Argus shell was located at a region where the intensity of the radiation passes through a minimum. If the location had been south or north of the one selected, the Argus shell effects would have disappeared in the background much earlier. For the first time there had been conducted in outer space on a global scale an experiment in which all the measured quantities were related to a known cause, namely, to the trapping in the earth's field of a known number of electrons of a known energy, injected at a known location at a known time.

The satellite measurements are described in detail by Dr. James Van Allen [1959]. The general conclusion on electron lifetime is that the electrons died a natural death, namely, by scattering with the air molecules near the mirror points. No effect was observed which appeared to hasten or increase the loss of the electrons.

Other important observations were that, within the limit of observational error, the electron shell did not move at all across the magnetic lines, nor did the electrons diffuse across these lines. The theory that there are two adiabatic invariants, namely, the magnetic moment and the action or the integral of the momentum along the magnetic lines, is thus verified. The first adiabatic invariant has been known for a long time. The second was postulated in 1953 by Marshall Rosenbluth. According to a theory by T. Northrup and E. Teller (*Univ. Calif. Radiation Lab. Rept.* 5615, to be published), the particles follow a closed magnetic surface even if the field is not axially symmetric. A rigorous proof that these quantities are invariants in all orders has been provided by Dr. Martin Kruskal (Princeton University), for the first about two years ago, for the other recently. Also it was believed that invariance in time exists, and therefore any change of the magnetic field in time, in a period that is long in comparison with the period of one oscillation between mirror points, will not permanently affect the position of the shell.

Since the changes in the earth's field occur in a matter of hours, very rarely in minutes, whereas the oscillation period is less than a second, no effect in the position of the shell should be expected. These postulations have been verified. In connection with the position stability of the shell another conclusion can be drawn concerning hydromagnetic instabilities. According to hydromagnetic theory the relevant quantity in generating unstable motions is the ratio of the energy density of the particles to the energy density of the magnetic field. For the Argus shell this ratio was negligible, hence the trapped electrons could not create any instability. However, an ionized plasma either permanently existing there or temporarily trapped as a result of the sun's activity would create such motions characterized by unstable magnetic line interchange. In such a case the Argus shell would have followed the motion of the magnetic lines and be deformed and change location. The fact that no such motion has been observed is a good indication that such instabilities are not occurring in the earth's field, at least at the latitudes of the Argus shell or lower (toward the equator). This is a useful observation, and some possible conclusions will be discussed later.

The first Argus experiment provided very important information, though only a fraction of what is possible with experiments of this nature. A variety of experiments is possible, as well as a variety of methods of injecting electrons into the geomagnetic field. We can classify the means of injection into three categories: (*a*) injection through atomic explosions as in the Argus experiment; (*b*) injection from a satellite carrying a payload of radioactive β-decay material; (*c*) injection from a satellite-borne electron accelerator. Comparing the three categories, we observe that the first is the easiest, but the last affords much better-controlled experiments since monoenergetic electrons can be injected in any desirable direction. Experiments of the first category are already being conducted, however; a satellite-borne accelerator might require 2 years to be developed and launched. Consequently, a sequence of experiments can be planned over a number of years

so that the satellite-borne accelerator experiments will be scheduled 2 to 3 years hence. In such a sequence of experiments several important results of geophysical interest may be obtained:

1. Complete mapping of the earth's magnetic field and defining the extent of the region of closed lines of the earth's field. According to current theories this region ends at a distance from the earth, at the equatorial plane, where the magnetic pressure equals the gas pressure. Since this distance is many earth radii, the residual gas there is the solar corona, consisting of hydrogen atoms in an ionized state. The equivalent gas pressure is half the mass density times the square of the orbital velocity of the earth. Owing to this effect, according to these theories, the earth's magnetic field is swept away beyond this distance. A magnetic line passing through the equatorial plane at a distance of 10 radii returns to the earth at 70° north or south latitude. This is the latitude of the auroral zones. Hence, it is quite possible that lines originating in the polar regions beyond this latitude do not return to the earth but vanish in outer space, intermixing with the sun's field or the interplanetary field. It is of extreme interest to determine the earth's field in this fringe region. Quite probably the region is very turbulent and the region of the closed magnetic lines is variable during magnetic storms or other disturbances created by the interaction of plasma streams originating in the sun and the earth's magnetic field. By conducting well designed Argus experiments it will be possible not only to monitor these changes but also to measure approximately the density of the solar corona near the earth. Further, it will be possible to clarify and advance the theory of auroral phenomena.

2. To shed light on the origin and lifetime of the belts of natural radiation. The first indications are that the region of the outer belt is very turbulent. Hence we cannot exclude the possibility that particles that originated in the sun are responsible for the outer belt.

A continuous monitoring of the density of artificially injected electrons in that region might shed light not only on the origin of the outer radiation belt but on the origin and behavior of the auroral phenomena as well.

The lifetime of the radiation belts cannot be directly determined since the density is more or less constant under steady-state conditions, but by injecting labeled electrons and measuring their lifetime we can determine the lifetime of the particles in the belt. Consequently, the required source strength will be derived. Thus it will be easier to explain the origin of the natural radiation belts. As a matter of fact, one observation from the Argus experiment already appears to be very useful and to offer tentative conclusions on the origin of the inner belt. The Argus shell was located beyond the maximum of the inner belt. As was mentioned above, this shell exhibited remarkable stability and did not move at all during the few weeks when observations were possible—an indication that no convection currents existed. Consequently, plasma cannot be transferred from the outside to the inner belt. This conclusion, however, must be considered only tentative at present, since, during the Argus experiment, no extremely violent solar disturbances occurred. Then, according to this tentative conclusion, the inner-belt particles are born within this region. The only explanation therefore is that the particles in the inner belt are neutron decay products, the neutrons originating from cosmic-ray interactions with the upper atmosphere. It seems that this radiation consists of protons and electrons, both products of neutron decay. During the initial discussion on Argus, I suggested the possibility of neutron decay and I postulated that electrons must already be trapped up there. I did not proceed with the quantitative calculations, however; they were done later by Dr. Kellog.

In suggesting this effect I had thermal neutrons in mind. Professor Singer, however, thought that high-energy neutrons could be responsible, yielding upon decay high-energy protons. These theories of neutron decay origin seem to be verified by the stability of the Argus shell. Final conclusions will be possible only after further experiments, particularly an Argus experiment during a period of intense solar activity.

The above result was not expected when the Argus experiment was first proposed since the natural radiation belt had not yet been discovered. Continuation of the Argus experiments in any of the three categories may yield unex-

pected new information, as has happened many times in physical experiments, particularly when a new class of experiments has been conducted in a relatively new field.

In conclusion I should like to say that a new tool is now available for exploring the part of outer space encompassed by the geomagnetic field and for clarifying the phenomena of interaction of the earth's magnetic field with various charged particles of natural or artificial origin.

Appendix. Calculation of the Lifetime of the Electrons

The electron loss is due mainly to Coulomb scattering near the mirror points. A given increase ($\Delta\theta^2$) of the square of the scattering angle will cause an increase of the square of the parallel velocity by $\Delta W_\parallel{}^2$, namely

$$\Delta W_\parallel{}^2 = c^2\,\Delta\theta^2 \qquad (1)$$

From the invariance of the magnetic movement we have the relation

$$W_\parallel{}^2 = c^2[1 - (B/B_m)] \qquad (2)$$

where

$$B/B_m = (r_0/r)^3 \qquad (3)$$

r_0, B_m are the radius and field at the mirror point, respectively. Equation 3 is valid at high latitudes where the lines are almost normal to the earth's surface.

Equations 2 and 3 yield

$$W_\parallel = \dot{R} = c[1 - (r_0/r)^3]^{1/2} \qquad (4)$$

From the above equations we derive

$$\Delta R = (r_0/3)\,\Delta\theta^2 \qquad (5)$$

where ΔR is the downward shift of the mirror points caused by an increase of the square of the scattering angle by $\Delta\theta^2$.

By differentiating equation 5 we obtain

$$\dot{R} = (r_0/3)\,\dot{\theta}^2 \qquad (6)$$

The value of θ^2 is given by the known equation

$$\dot{\theta}^2 = -[(Z + 1)\dot{\gamma}]/\gamma^2 \qquad (7)$$

where $\dot{\gamma}$ is the energy loss by scattering measured in rest mass units (γ is the electron energy in rest mass units). The energy loss by scattering is given by the known Bethe formula. In the present case, after substituting the numeri values we obtain

$$\dot{\gamma} = -3 \times 10^{-8} NZ \qquad \text{rmu/day} \qquad (8$$

The value of the air density is a function position, which in turn is a function of tim We shall express the air density as a function time and integrate along a trajectory from t point of reflection to the equational plane.

By integrating equation 4 we obtain

$$\frac{ct}{r_0} = \int \frac{d(r/r_0)}{[1 - (r_0/r)^3]^{1/2}} \qquad (9$$

Since most of the losses occur at a distan $(r - r_0)$ from the mirror points much less th r_0, we can substitute, $x = r - r_0$, in equati 9, which upon integration yields

$$x = \frac{3}{4}\frac{c^2}{r_0}\,t^2 \qquad (10$$

The air density varies with the distance from the mirror points as $N_0 e^{-x/h}$, where N_0 the air density and h the scale height at t mirror points, respectively. From the abo equations we obtain

$$\dot{\gamma} = -3 \times 10^{-8} N_0 Z \exp\left(-\frac{3c^2}{4r_0 h}\,t^2\right) \qquad (11$$

Integration of this equation from zero to infinit will yield the energy loss along one trajector from the reflection point to the equator. The considering the oscillation time we derive th average energy loss, namely

$$\langle\dot{\gamma}\rangle = \frac{3 \times 10^{-8} N_0 Z}{\psi}\sqrt{\frac{h}{r_0}} \qquad \text{rmu/day} \qquad (12$$

where $(r_0\psi)$ is the length of the magnetic lin from the mirror point to the equator. The rat of change of the scattering angle ($\dot{\theta}^2$) is a func tion of $\dot{\gamma}$, just evaluated, and of γ^2. The value o γ is reduced from Coulomb scattering an Schwinger radiation loss. However, the contri bution from Schwinger radiation is small fo N_0 more than 10^5 atoms per cm^3. Equations 6, 7 and 12 yield

$$\dot{x} = \dot{R} = -\frac{10^{-8} Z(Z + 1) N_0}{\psi\gamma^2}\, r_0 \sqrt{\frac{h}{r_0}} \qquad (13$$

As the mirror points move downward the ai density increases. Consequently, at a distance

(downward) from the initial mirror point the ownward velocity is

$$\dot{r} = -\frac{10^{-8}Z(Z+1)}{\psi\gamma^2} N_0 e^{-x/h} r_0 \sqrt{\frac{h}{r_0}} \qquad (14)$$

In the case of electrons having energies of a ew Mev, the loss of the electrons is due more o scattering than to energy loss; i.e., the mirror oints move downward one scale height without appreciable energy loss. Then equation 14 yields upon integration

$$T = 1.7 \times 10^6(\psi\gamma^2/N_0)\sqrt{h/r_0} \text{ days} \qquad (15)$$

REFERENCE

VAN ALLEN, J. A., C. E. MCILWAIN, AND G. H. LUDWIG, Satellite observations of electrons artificially injected into the geometric field, *J. Geophys. Research*, **64**, 877–891, 1959.

(Manuscript received June 18, 1959.)

Satellite Observations of Electrons Artificially Injected into the Geomagnetic Field*

JAMES A. VAN ALLEN, CARL E. MCILWAIN, AND GEORGE H. LUDWIG

Department of Physics
State University of Iowa
Iowa City, Iowa

Abstract—Our four radiation detectors in satellite 1958ϵ (Explorer IV) easily and promptly observed the geomagnetically trapped electrons resulting from the three high-altitude nuclear detonations Argus I, II, and III in August–September 1958. An account of over 160 satellite passes through the three Argus "shells" of artificially injected electrons is given herein, and a preliminary appraisal of the geophysical significance of these experiments is offered.

INTRODUCTION

After our discovery with Explorer I (satellite 1958α) and with Explorer III (satellite 1958γ) that there were very great intensities of charged particles trapped in the geomagnetic field [*Van Allen et al.*, 1958], we undertook to make arrangements for a further satellite flight of equipment of greater discrimination and much greater dynamic range for the purpose of detailed study of the properties and the spatial distribution of the radiation. The progress of such arrangements was greatly aided by Richard W. Porter, chairman of the Technical Panel for the Earth Satellite Program of the U. S. National Committee for the International Geophysical Year, and by Herbert York, then chief scientist of the Advanced Research Projects Agency of the Department of Defense.

In October 1957 Nicholas C. Christofilos of the Lawrence Radiation Laboratories of the University of California at Livermore had suggested in an unpublished memorandum that many observable geophysical effects could be produced by an atomic detonation at high altitude above the earth in the tenuous upper atmosphere. Of the various effects contemplated, one of the most interesting promised to be the temporary trapping of high-energy electrons at high altitudes in the geomagnetic field. Such electrons result from the radioactive decay of fission fragments and, less importantly, of neutrons.

A subsequently organized study group carried out more detailed estimates of the various effects to be expected, concluding that the proposed experiments (later named "Argus" experiments) were indeed feasible. The group, led by W. K. H. Panofsky, also concluded that satellite observations would be of great value.

Meanwhile, the discovery of the existence of the natural trapped radiation served as an overall validation of the Argus proposal by showing that a high intensity of charged particles can indeed be trapped in the geomagnetic field. And to the IGY workers at the State University of Iowa and elsewhere it was clear that the artificial, impulsive injection of known particles along a known line of force at a known time would be a powerful technique for elucidating many of the uncertain aspects of the dynamics of geomagnetic trapping.

After a series of conferences, the Advanced Research Projects Agency agreed to provide, among other things, two Jupiter C satellite vehicles for the joint IGY-Argus undertaking.

The Department of Physics of the State University of Iowa (SUI) had charge of the design,

* Presented at the Symposium on Scientific Effects of Artificially Introduced Radiations at High Altitudes held at the National Academy of Sciences, April 29, 1959. This paper is being published simultaneously in the August 1959 issue of the *Proceedings of the National Academy of Sciences.*

TABLE 1—*Summary of detector characteristics (Explorer IV)*
(See *Van Allen et al.*, 1959, for more complete description)

Channel	Detector	Shielding	Sensitive to	Geometric Factor
1	Geiger-Müller counter (Anton 302) Cylinder approximately 7 mm × 9 mm Scaler: 64	1.2 g/cm² Fe + 1.6 g/cm² Pb (minimum)	Electrons of $E >$ 5 Mev Protons of $E >$ 40 Mev X-rays of $E >$ 80 kev with low efficiency	Omnidirectional geometric factor 0.14 cm² for minimum stopping powe 0.82 cm² for penetrability greater tha 7 g/cm²
2	Plastic scintillator 0.76 cm diameter, 0.18 cm thick Pulse detector Scaler: 16	0.14 g/cm² Al over window	Electrons of $E >$ 580 kev Protons of $E >$ 10 Mev Axis of detector ⊥ to payload axis X-rays of $E >$ 300 kev with low efficiency	0.040 cm² steradian for minimum stoppi power; 4.2 cm² steradian for pene trability greater tha 5 g/cm²
3	Same as channel 1 except less shielding Scaler: 2048	1.2 g/cm² Fe (minimum)	Electrons of $E >$ 3 Mev Protons of $E >$ 30 Mev X-rays of $E >$ 20 kev with low efficiency	Omnidirectional geometric factor 0.14 cm² for minimum st ping power; 0.70 cm² for greater than 5 g/cm² stopping power
4	Cesium iodide crystal 0.76 cm diameter, 0.20 cm thick Total energy—d-c electrometer	1.0 mg/cm² Ni and Al over window	Electrons of $E >$ 20 kev Protons of $E >$ 400 kev X-rays Axis of detector ⊥ to payload axis	0.0235 cm² steradian for minimum stoppi power 4.4 cm² steradian for penetrability greater than 5 g/cm²
5	Same as 2 except scaler: 2048			

development, construction, and calibration of the detectors, associated electronics, etc. The apparatus was designed for two objectives: (1) to study the natural radiation in further detail; (2) to detect and study quantitatively the artificially injected electrons from the Argus experiments. Final environmental tests and overall specifications of the flight payloads were in the hands of the Army Ballistic Missile Agency (ABMA), as were the supply of payload shells, thermal design of the shells, and, of course, many other essential aspects of the flight operations. Telemetry transmitters and other electronic components were provided by the Jet Propulsion Laboratory (JPL), by Project Va guard, and by the Army Signal Engineeri and Development Laboratory.

Four flight payloads were built, fully ca brated, and subjected to the full gamut of e vironmental tests. One payload was flown Explorer IV, which entered a 51° inclinati orbit successfully at 1506 UT on July 26, 19 thus earning the astronomical designation sat lite 1958ε. The apparatus performed in all r spects fully up to expectations, though the lif time of its batteries was somewhat shorter th had been expected.

A second payload was flown on Explorer

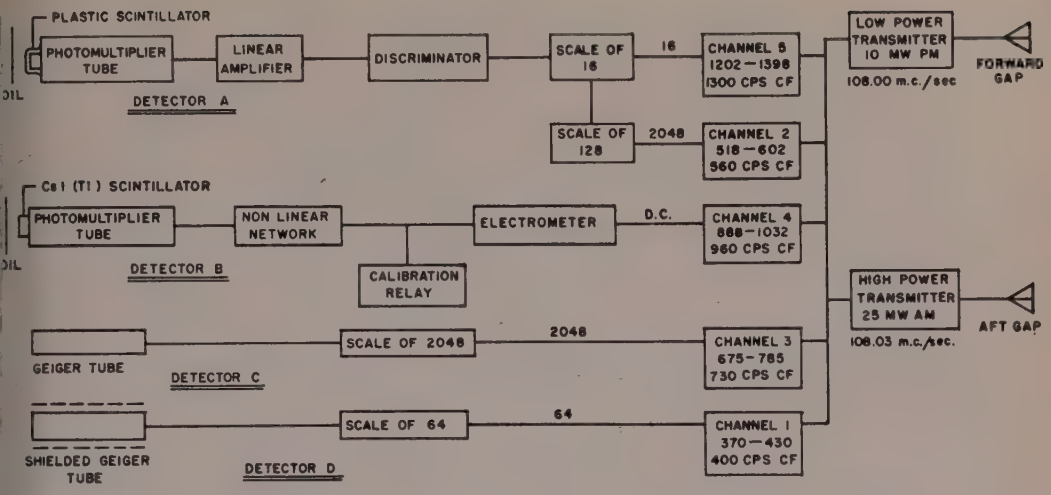

FIG. 1—Block diagram of detectors and associated circuitry of Explorer IV.

aunched on August 24, 1958. This rocket failed o go into orbit, but the on-board apparatus unctioned properly during its brief flight.

A full description of the observing equipment f Explorer IV and a preliminary account of he observations of the natural radiation have been published [*Van Allen et al.*, 1959]. For the convenience of the present reader, Table 1 summarizes the principal characteristics of the apparatus. Figures 1 and 2 show the circuit schematic and physical arrangement respectively. See *Van Allen et al.* [1959] for further experimental details as well as for discussion of interpretative aspects.

THE ARGUS DETONATIONS

A series of three multistage rockets, fired from the *U. S. S. Norton Sound* in the south Atlantic Ocean, delivered small fission bombs to high altitude, where they were detonated. A variety of considerations led to the choice of site for detonations:

(*a*) An isolated firing area was desired for reasons of safety.

(*b*) An intermediate latitude was desired in order that the expected lifetime of the trapped particles be at least a few days in order to permit comprehensive observations. At low latitudes the trapped particles spend a greater fraction of their paths in denser air, and at high latitudes the corresponding magnetic line of force goes farther from the earth in the equatorial plane and a shorter lifetime of the trapped particles is to be expected on account of perturbations in the outer reaches of the geomagnetic field.

(*c*) It was necessary that the chosen magnetic shell be such that it could be intercepted by a low-altitude satellite in an orbit inclined at not more than 51° to the equatorial plane (the highest inclination that was practical with United States facilities at that time). An intermediate latitude was preferable to a low latitude, also, because the satellite orbit would then intercept the shell of trapped particles at a less oblique angle.

(*d*) From the observations of Explorers I and III, it was known that the intensity of the natural radiation diminished rapidly, at a given altitude, with distance from the magnetic equator (either north or south). Hence the "background" radiation would be less at intermediate latitudes.

(*e*) The scalar magnitude of the geomagnetic field is less in the south Atlantic than at any other point on the earth in intermediate latitudes. Hence, for a given altitude of injection, the trapped lifetime of charged particles would be the greatest for this firing site [cf. *Van Allen et al.*, 1959].

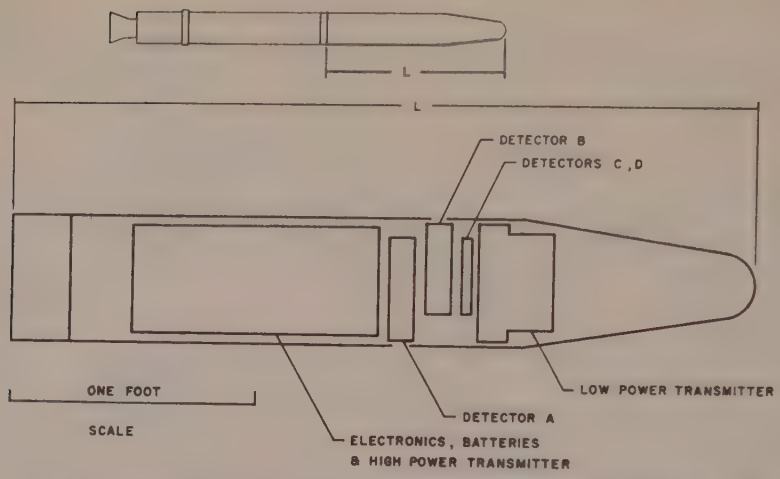

FIG. 2—Outline sketch of arrangement of principal components of payload of Explorer IV (satellite 1958ϵ); small diagram in upper part of figure shows appearance of orbiting body, of which payload was a permanent part.

(*f*) It was desirable that an island or other convenient observing site be located near the point conjugate to the firing point (the Azores Islands, in this case).

In Table 2 are summarized the pertinent data on the three Argus bursts.

TABLE 2—*Data on bursts*

	Argus I	Argus II	Argus III
Nominal yield	1 to 2 kilotons	1 to 2 kilotons	1 to 2 kilotons
Approximate time of burst	27 August 1958 0230 UT	30 August 1958 0320 UT	6 September 1958 2210 UT
Approximate geographic coordinates	38°S, 12°W	50°S, 8°W	50°S, 10°W

Nominal altitude of all bursts = 480 km.

NATURE AND SCOPE OF SATELLITE OBSERVATIONS

During the month preceding Argus I (26 July to 26 August) an extensive body of observations served to establish the detailed spatial dependence of the natural trapped radiation and many of its properties in terms of the characteristics of the four detectors which we had devised for the twofold program of observation.

Typical geometric relationships between the orbit of Explorer IV (satellite 1958ϵ) and chosen magnetic shell are illustrated schem ically in Figures 3 and 4. It is seen that i favorable case the satellite orbit intersects Argus shell four times during each revolu around the earth, at points *A*, *B*, *C*, and These intersections are, of course, at vari altitudes, latitudes, and longitudes. In prac the number of observed intersections from wh significant data were obtained was much than four per orbit, for a variety of reaso (*a*) Many of the intersections were at such altitudes that the intensity of Argus electr was immeasurably small with the equipm used. (*b*) In many cases, fewer than four int sections occurred, owing to the distortion a tilt of the chosen magnetic shell. (*c*) Many tersections occurred beyond radiotelemet range of any one of the receiving stations. Some of the intersections occurred at poi where the artificially injected radiation w unobservably small in comparison with t natural radiation. After enough time, of cour this situation prevailed at all points within t reach of Explorer IV.

Table 3 gives a brief summary of the numbe of observed intersections which yielded signi cant data. It should be noted that the batteri supplying the lower-powered of the two tran mitters and telemetry channels 2 and 5 we exhausted on about September 3. The highe

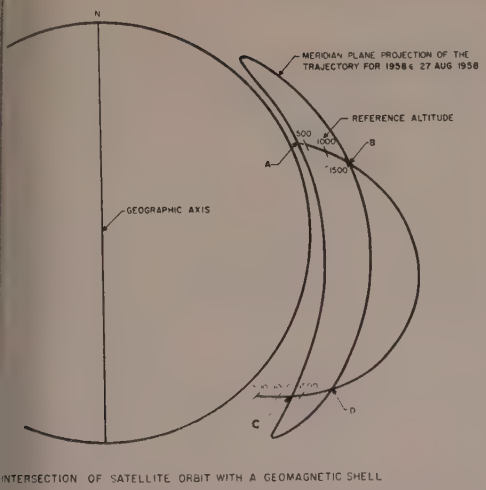

FIG. 3—Illustrative diagram showing sample geometric relationship between the orbit of satellite 1958ε and a chosen magnetic shell at a given longitude.

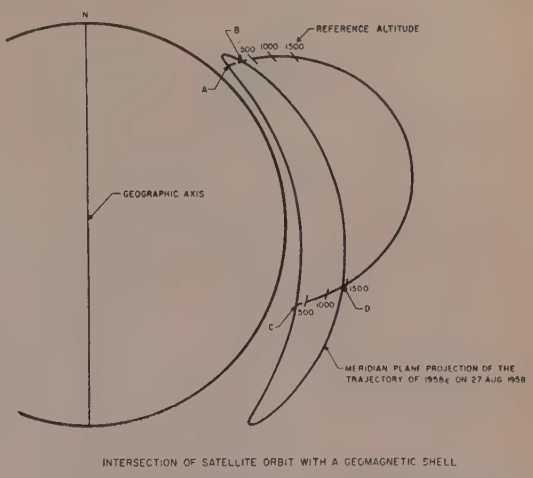

FIG. 4—Same as Figure 3, except at a different longitude.

powered transmitter and channels 1, 3, and 4 continued to operate properly until about September 21. At this time the Argus III particles were still being detected above the background on occasional favorable intersections.

It appears probable that a residuum of the Argus electrons was also detected near the geomagnetic equator with Pioneer III on December 6, 1958. But no observable intensity was present there on March 3, 1959 (Pioneer IV).

DETAILED OBSERVATIONS

The "Argus effect" was easily and promptly observed by Explorer IV after each of the three detonations.

Figure 5 shows a record of measurements of the natural radiation taken on the day *before* Argus I. Figure 6 shows a record taken on a satellite pass through a similar geographic region about 3½ hr after Argus I. The same data are plotted with a linear scale of ordinates in Figure 7. The great peak which was intersected at 0608 UT on August 27 had no precedent in 4 weeks of previous observations of the natural radiation. Moreover, it was encountered on the first observed intersection with the planned magnetic shell following the Argus I detonation. Further reasons for the validity of identifying such observed peaks with the "Argus effect" are as follows:

(*a*) The observed energy spectrum and the nature of the radiation were found to be in essential agreement with those expected for the decay electrons from fission fragments.

(*b*) A peak with similar characteristics was found at every observed intersection of the orbit of the satellite with the appropriate magnetic shell, irrespective of latitude or longitude.

(*c*) The geometric thickness of the shell was similar to that of pretest estimates.

(*d*) The observed intensity of trapped electrons was in order-of-magnitude agreement with pretest estimates.

TABLE 3—*Summary of observed intersections giving significant data*

Burst	Number in northern hemisphere	Number in southern hemisphere	Period of observations (1958)
Argus I	28	9	27 August to 6 September
Argus II	27	12	30 August to 6 September
Argus III	61	27	6 September to 21 September
Totals	116	48	

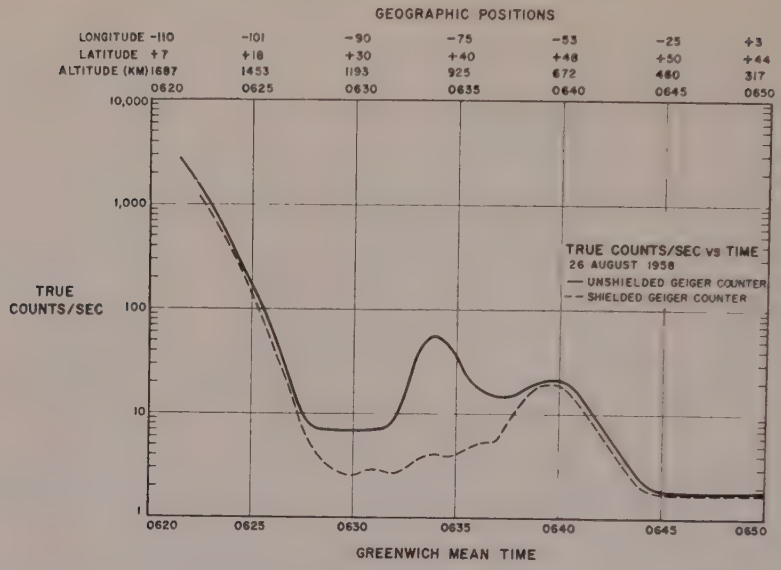

FIG. 5—A plot of observations of the natural radiation on the day before Argus I.

(*e*) The temporal decay of trapped intensity resembled pretest estimates.

The above remarks apply to the sequences of observations after each of the three shots Argus I, II, and III. During the entire active period of Explorer IV (July 26 to Septem 21, 1958) no such peaks were observed ex those having the proper temporal and spa relationship to the artificial ones expected. observing period included a number of imp

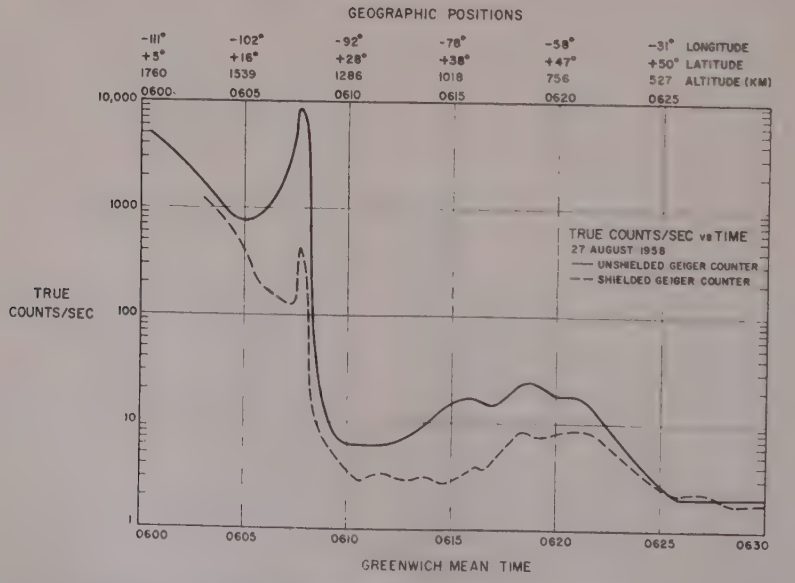

FIG. 6—A plot of radiation observations showing the Argus I peak at 0608 UT on August 27, 1958, about 3½ hr after the burst. The geographic region is similar to that of Figure 5.

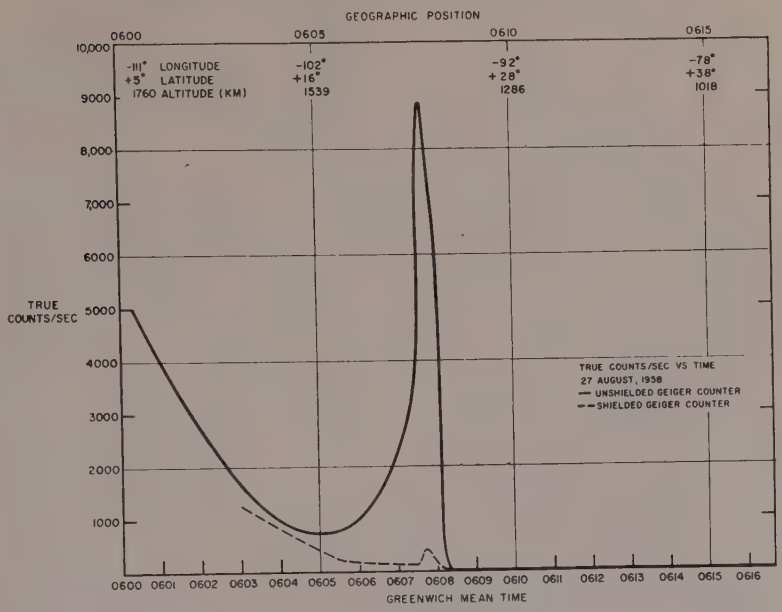

FIG. 7—Same data as on Figure 6, plotted with a linear scale of ordinates.

tant geophysical perturbations in the radiation around the earth. But these perturbations were of a quite different nature.

Figure 8 is a record on August 31, 1958, which shows the decaying peak due to Argus I (at 0446 UT) and the fresh peak due to Argus II (at 0449 UT); Figure 9 is a sample record on September 9, 1958, which shows the peak due to Argus III. Figure 10 is a photograph of a raw telemetry record of the passage of Ex-

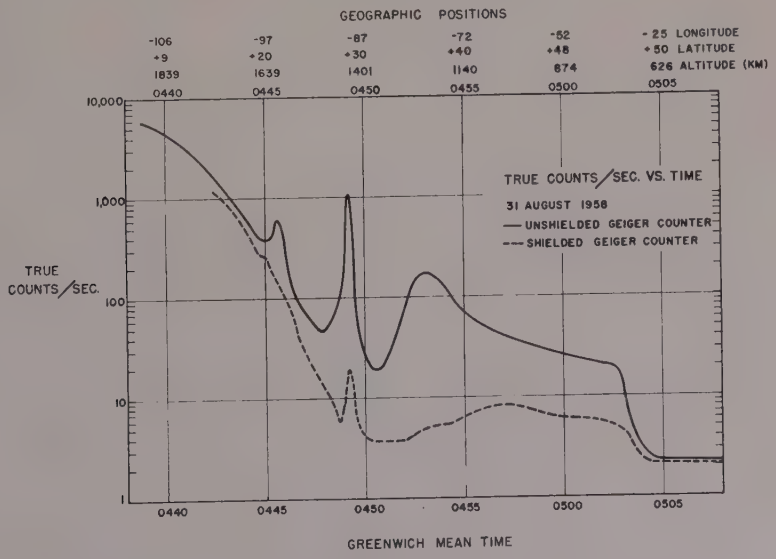

FIG. 8—A plot of radiation observations on August 31, 1958, showing the decaying Argus I peak (at 0446 UT) and the fresh Argus II peak (at 0449 UT).

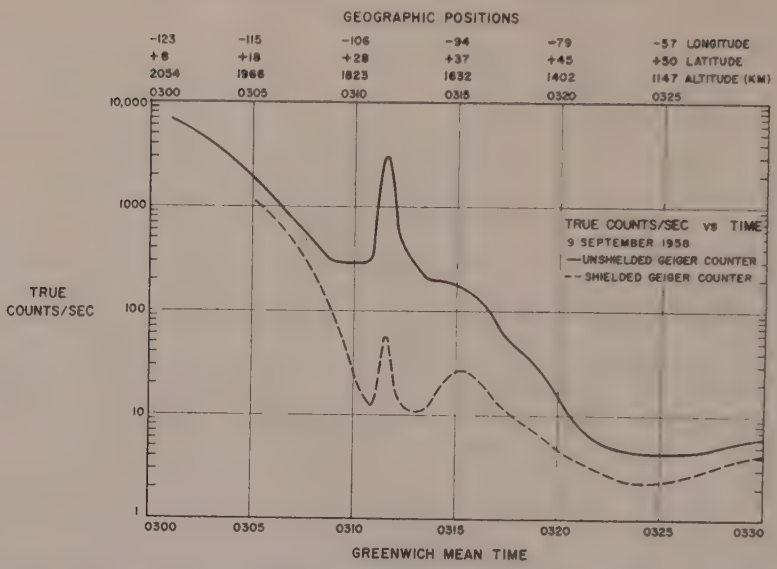

FIG. 9—A plot of radiation observations on September 9, 1958, showing the Argus III peak at about 0312 UT.

plorer IV through the Argus II shell, and Figure 11 gives plots of the reduced corrected data from all four detectors. These two figures exemplify the data-reduction procedure.

Figure 12 (expanded time scale) gives an example of the variation of counting rate of [illegible] pulse scintillation detector as the satellite ro[illegible] and tumbled in its passage through the Argu[illegible] shell. As previously described [*Van Allen et al.*, 1959], this type of "random" angular motion[illegible]

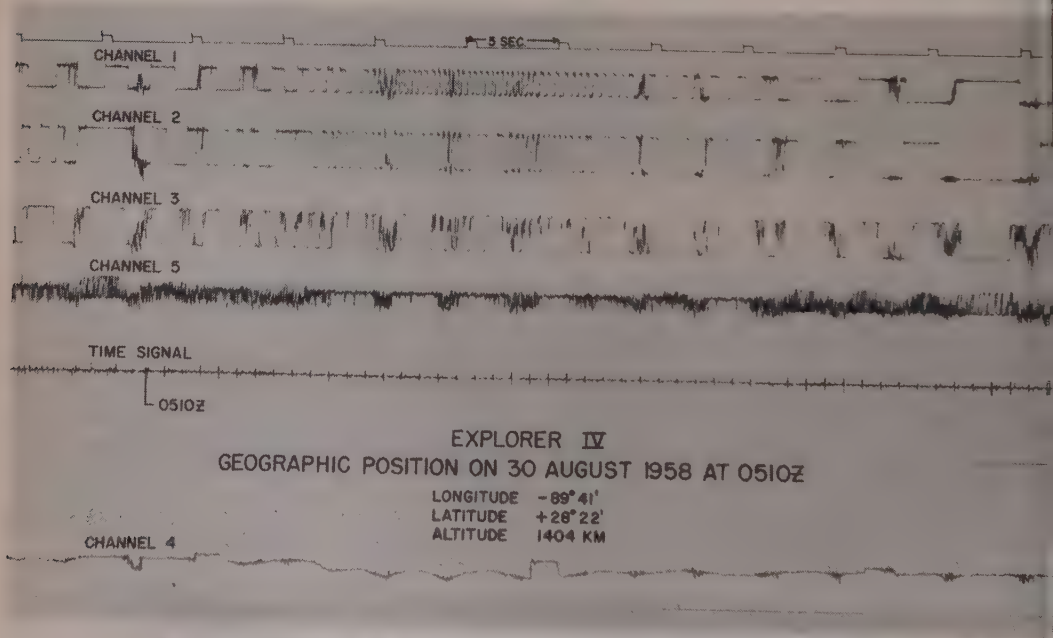

FIG. 10—Photograph of raw telemetry record (Offner pen-and-ink recorder) of a pass through the Argus II shell on August 30, 1958.

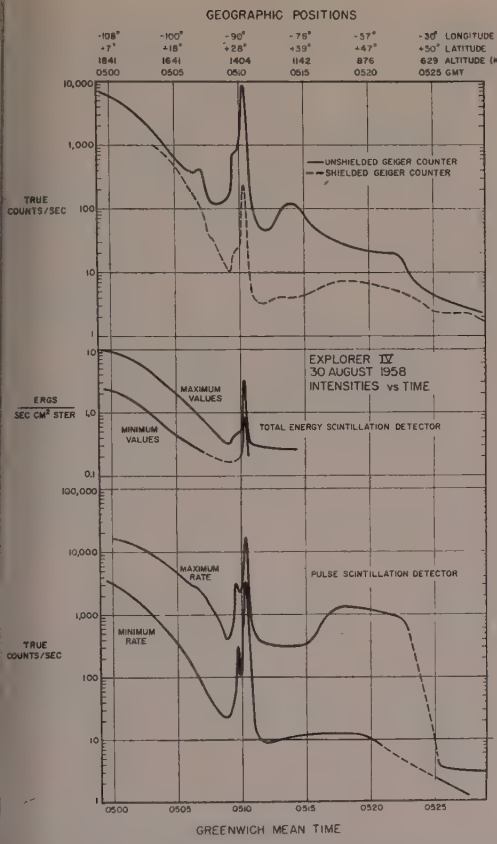

FIG. 11—Plots of reduced corrected data from all four detectors as derived from the record of Figure 10 and from the preflight calibrations of detectors.

highly advantageous for the measurement of angular distributions. The angular distributions of the Argus electrons (as observed near their mirror altitudes) were found to be disk-like, as is suggested by magnetic-trapping theory and as has been extensively observed on the natural radiation.

In each set of observations (cf. Figs. 10 and 11), the output of each detector was converted either to true counting rate (channels 1, 2, 3, and 5) or to absolute directional energy flux (channel 4) using preflight calibration data; and from the corrected plots the following quantities were estimated: (*a*) net intensity above background of observed Argus electrons, obtained by subtraction of the interpolated background values; (*b*) time width of the Argus peak at half-maximum intensity; (*c*) time width

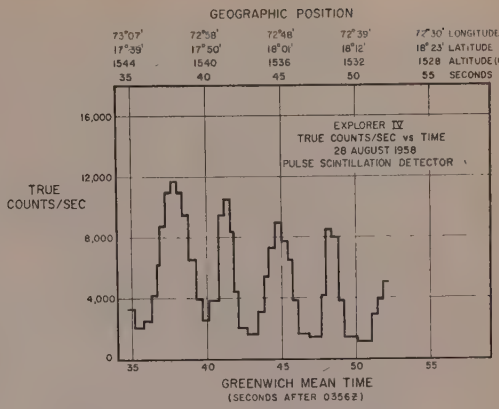

FIG. 12—A plot on an expanded time scale of the detailed counting rate of the pulse scintillation counter as a function of time during passage through the Argus I shell. This plot illustrates the disk-like angular distribution of the radiation. The tumble period was 7 sec.

of the Argus peak at 0.1 maximum intensity; (*d*) local maximum and minimum values of intensity near the center of the peak; (*e*) time at which the center of the peak occurred. Then, from the ephemeris of the satellite [*Van Allen et al.*, 1959], the following were tabulated: (*f*) geographic location (latitude, longitude, and altitude) of the center of the observed peak; (*g*) geometric thickness of the "shell" of electrons at half-maximum intensity, measured perpendicular to the shell.

Organization and Analysis of Observations

The work sketched in the present section was considerably advanced by a 10-day study session arranged and conducted by the Department of Defense during February 1959 at the Lawrence Radiation Laboratories in Livermore, California. The group specifically concerned with satellite observations consisted of the following persons: George Bing (Chairman), Donald Chandler, Rolf Dyce, William Karzas, John Killeen, Charles Lundquist, Hans Mark, Carl McIlwain, Paul Nakada, Theodore Northrup, Ralph Pennington, Russell Shelton, James Van Allen, and Ernest Vestine.

As was mentioned earlier, the various observations occurred at a great variety of positions in space; and, of course, the irregular nature of the geomagnetic field produces essential complications. The foundations for organizing the

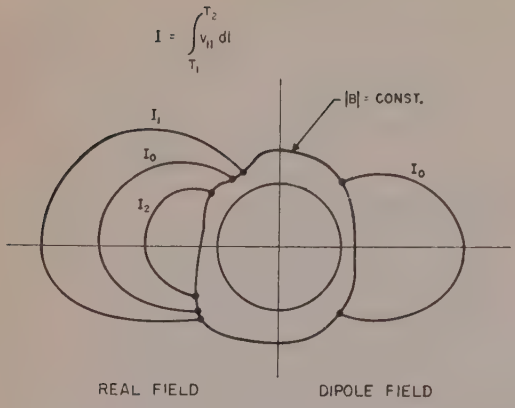

FIG. 13—A diagram to illustrate the principles of conservation of μ and I in geomagnetic trapping. (See text.)

data are indicated in Figure 13. By the basic Poincaré-Störmer-Alfven theory of the trapping of charged particles in the geomagnetic field the magnetic moment of a spiraling particle is an adiabatic invariant of the motion. That is,

$$\mu = \tfrac{1}{2} m v_{\perp}^{2}/B = \text{constant}$$

Since the speed v (having components $v_{\parallel}$ and $v_{\perp}$ at any moment parallel and perpendicular respectively to the magnetic vector **B**) is also a constant of the motion in a static magnetic field, the turning points (or mirror points) of the oscillatory helical path of a given particle always occur at the same scalar value, B. Indeed, the locus of the turning points of all particles of given magnetic moment is a surface of $B =$ constant. (Cf. Figure 13.)

Also, as first conjectured by *Rosenbluth* and *Longmire* [1957] and later discussed in detail by others, the line integral along a line of force between turning points for a given particle

$$I = \int_{\tau_1}^{\tau_2} v_{\parallel}\, dl = v \int_{\tau_1}^{\tau_2} \sqrt{1 - B/B_{\tau}}\, dl$$

is an adiabatic invariant (under an important class of physical conditions) of its motion, where B_{τ} is the scalar value of B at the turning points τ_1 and τ_2.

This principle makes possible the identification of a unique sequence of magnetic lines of force that constitute a single-valued, three-dimensional surface on which the guiding center of the particle will forever lie—to the extent that the conditions for the conservation of μ and I are met—as it moves about in the irregular geomagnetic field. The argument is illustrated in Figure 13. Let the surface $B =$ constant shown there represent the locus of turning points for a particle having a given magnetic moment μ. Let the particle's motion at a chosen period of time be along the line of force shown in the right-hand side of the figure with the integral I having the value I_0. The question then is: Along which of the infinite number of segments of lines of force having values of $I = I_1$, I_2, etc. (sketched in the left-hand side of Fig. 13), and having turning points on the specified surface of constant B, will the guiding center of the particle's trajectory be moving at some later time? The Rosenbluth principle assures us that it will be the segment characterized by I_0, or more precisely by I_0/v.

To the extent that the above discussion is applicable to electrons having energies up to several million electron volts and trapped in the real geomagnetic field it may be expected that an Argus shell of trapped electrons will maintain its integrity and will be fixed with respect to the earth.

Moreover, elementary consideration of perturbations by localized magnetic irregularities and by atmospheric scattering and energy loss indicates that the tendency for diffusion of guiding centers transverse to the shell will be greatly exceeded by the tendency for diffusion of turning points along the shell, and that the latter tendency will result in progressive leakage of particles downward into the denser atmosphere and eventual loss.

Hence, the temporal decay of the total number of trapped particles resulting from an impulsive injection may be expected to proceed by way of loss of particles out of the ends of the shell; it may be further expected that the geometric thickness and position of the shell with respect to the earth will be substantially constant.

In the first instance, the observations following each detonation are functions of four apparently independent parameters: latitude, longitude, altitude, and elapsed time from the time of the detonation.

The considerations of the preceding paragraphs (which have been most clearly advocated

by T. Northrup and implemented by E. H. Vestine) suggest that important progress can be made in systematizing the observations for the purpose of interpretation if the three positional parameters, latitude, longitude, and altitude, be supplanted by a single one—the scalar value B at the position of the observation. Apart from perturbations whose effects are important during one longitudinal precession period (of the order of a fraction of an hour in the present case), a surface of constant B may be expected, at a given time, to be a surface of constant particle intensity irrespective of the distorted shape of this surface in the real geomagnetic field.

Hence, it may be hoped that observable features of the trapped Argus radiation will be functions of only two parameters, B and elapsed time.

The geomagnetic field has a slow secular rate of change, and B is not accurately known as a function of geographic coordinates during August–September 1958. In the present work Vestine and associates have derived pertinent B values from the recent British 48-coefficient potential function (era of 1955). Small errors also arise from the imperfect knowledge of the orbit of the satellite (± 10 km) and from the observational uncertainty in locating the center of the shell of electrons.

Preliminary Summary of Significance of Observations

Thickness of Argus shells—The observed mean thickness of the Argus shells at half-intensity, measured perpendicular to the boundaries of the shells, was about 90 km for events I and II and 150 km for event III. The thickness of the shells did *not* have a systematic dependence on elapsed time, but the scatter of the measured values of thickness is of the order of 30 per cent, and no lesser broadening (or thinning) of the shell during the observing period could be discerned. It is presumed that the basic shell thickness was determined by the very complex injection situation at and immediately after the detonation. This surmise is supported by crude consideration of the dynamics of the detonation in the earth's magnetic field.

It does seem to be of importance that the leakage of particles from the shell (by energy loss and "longitudinal" diffusion) proceeded at a sufficiently rapid rate that the transverse diffusion was, in general, unobservably small. (See, however, a later section remarking on the influence of the geomagnetic storm of September 3 ff.) And it may be noted that the magnetic shell in question reaches outward to a radial distance of about 2 earth radii from the center of the earth.

These results, of course, provide a quantitative validation of the principle of conservation of I in the geomagnetic field.

Position of the shell in space—Each observation of the center of each Argus shell (I, II, and III) was projected down to the surface of the solid earth by means of a simplified model of the geomagnetic field, the eccentric dipole model. A comprehensive plot of the results of this process is shown in Figure 14, together with conjugate points calculated with the full 48-coefficient potential function. The three resulting loci of points, interlaced in time, are notably smooth and regular, suggesting the positional stability of the several shells during the observing period. This question can be more critically examined by a study of Figure 15, a large-scale plot of projected observations on Argus III. In view of the interlacing of observations at various sequences of times, we conclude that the shell could not have drifted monotonically in latitude by more than about 0.03° of latitude per day (about 2 km of distance per day at 1500 km) without resulting in an unreasonable "ripple" in the implied geomagnetic field contour.

These results are confirmatory both qualitatively and quantitatively of the principles sketched in preceding sections.

Angular distribution—As typified by Figure 12 (see also *Van Allen et al.*, 1959), the angular distribution of the trapped electrons was always observed to be disk-like, with an angular thickness of the order of $\pm 20°$ or less. In terms of the basic dynamics of the trapping of charged particles this fact shows that, at the relatively low altitudes of observation, most particles being measured have their turning points not more than a few hundred kilometers below the observing point—a reasonable result.

Trapped lifetimes—The product of the maximum observed intensity C at the center of the

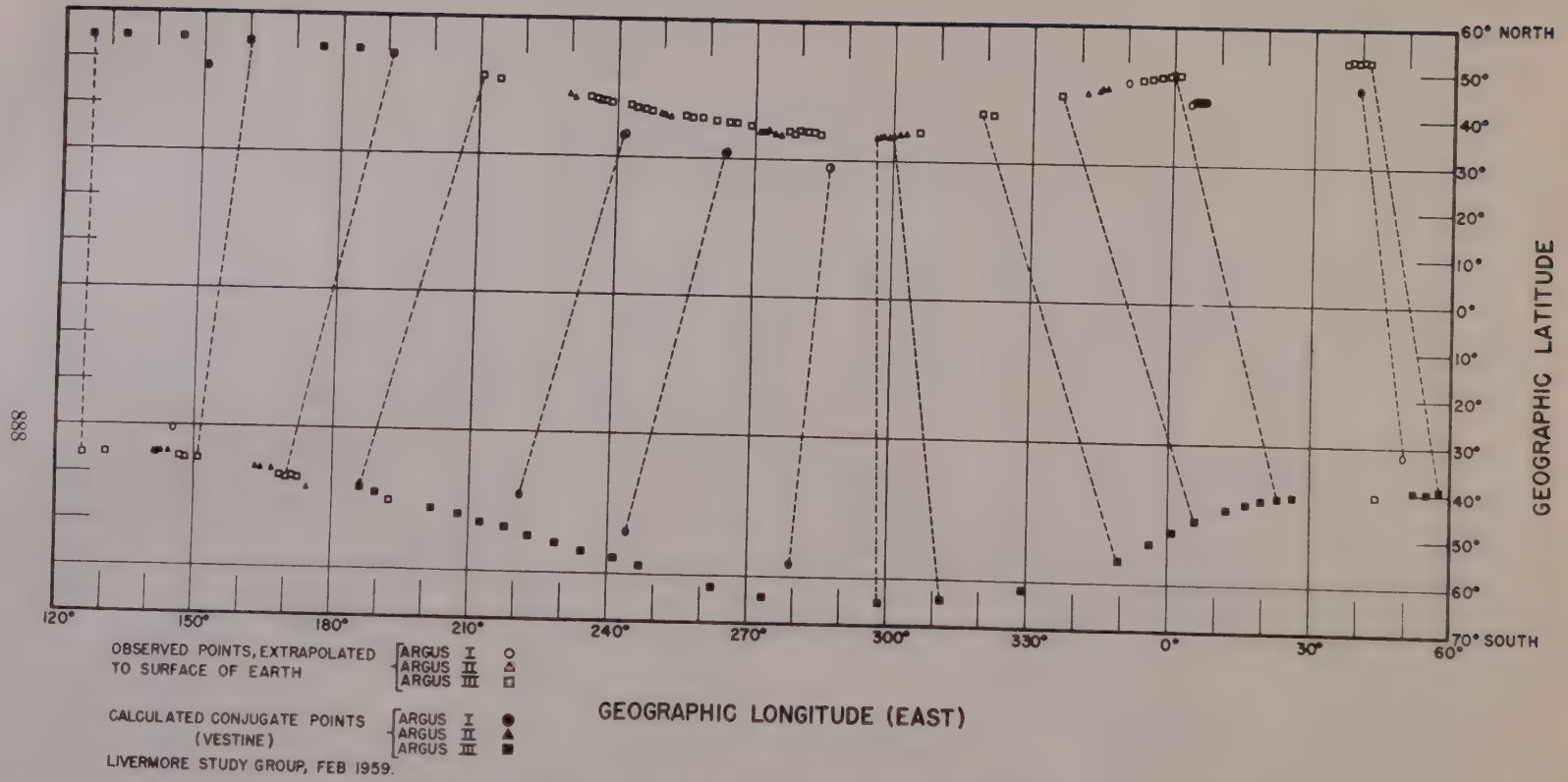

FIG. 14—Plot of (extrapolated) observed intersections of Argus "shells" I, II, and III with surface of the earth, and computed conjugate points (after Vestine and Pennington) (Livermore study group).

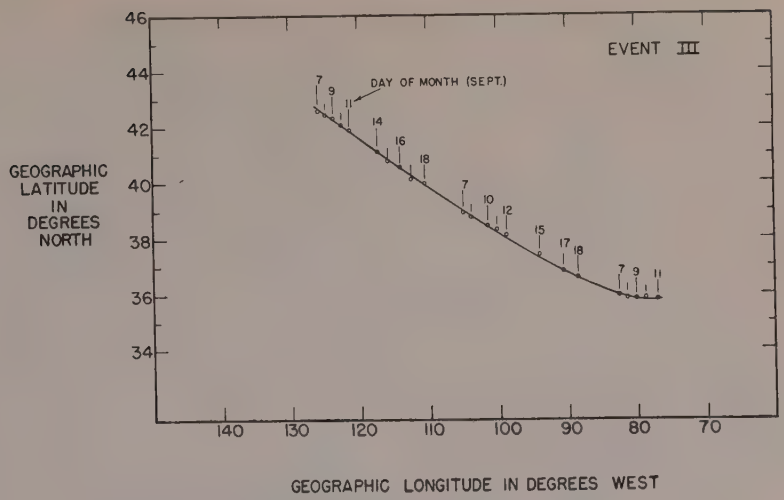

FIG. 15—An expanded plot of a portion of Figure 14.

shell by the thickness W of the shell at half-intensity has been taken as a measure of the total intensity of trapped particles (within the detection range of the detector in question). Several preliminary plots of this quantity, CW, versus elapsed time, t, for two different ranges of B are given in Figures 16, 17, and 18. The plots are of data from channel 3 (the unshielded Geiger tube). Closer examination of several selected cases suggests that the scatter of data will be reduced by taking proper account of the average aspect of the satellite equipment as it passed through the shells. It is seen that CW varies approximately as the negative first power of the elapsed time. This law of time decay of trapped intensity, namely

$$CWt = \text{constant}$$

is in general accord with a theory of the loss mechanism due to Ernest C. Ray of this laboratory (to be published). The above curves based on our channel 3 data (the most extensive and

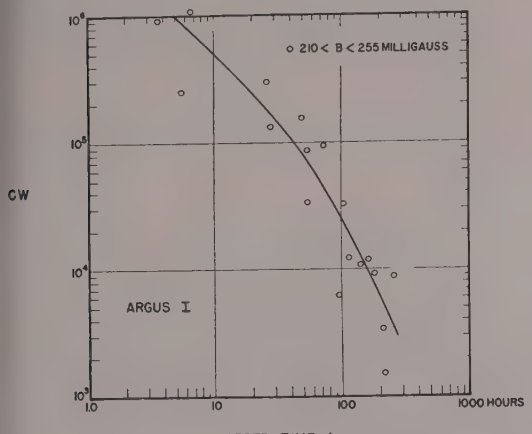

FIG. 16—The product of maximum true counting rate, C, of channel 3 at center of Argus I shell by the geometric width (thickness) at half-maximum, W, versus elapsed time, t (Livermore study group).

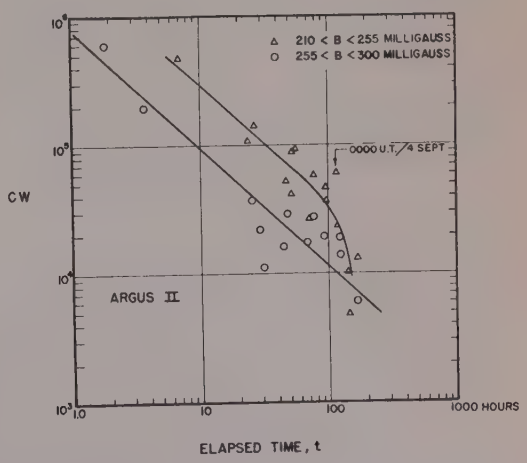

FIG. 17—The product of maximum true counting rate, C, of channel 3 at center of Argus II shell by the geometric width (thickness) at half-maximum, W, versus elapsed time, t (Livermore study group).

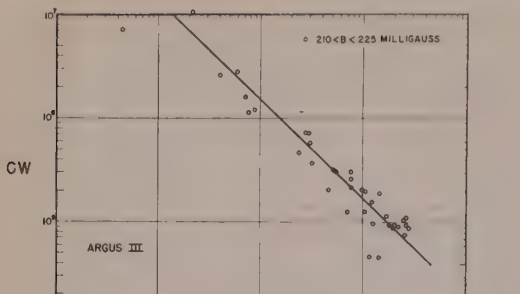

FIG. 18—The product of maximum true counting rate, C, of channel 3 at center of Argus III shell by the geometric width (thickness) at half-maximum, W, versus elapsed time, t (Livermore study group).

simplest body of data) pertain to an effective electron energy of about 3.5 Mev. By comparison with the theory, Ray finds that the effective atmospheric density at 1000 km required to reduce the intensity as rapidly as observed is at least 10 times as great as would be supposed from the plausible extrapolation of the Jastrow "satellite-drag" atmosphere.

It is of interest to note that the Argus shells occurred (Fig. 19) within the "slot" between the two natural radiation zones [*Van Allen* and *Frank*, 1959; *Vernov et al.*, 1959]. It may be that the atmospheric density is anomalously high there.

An alternative line of speculation would suppose that the rapid decay was, at least in part, the result of "magnetic diffusion" due to small-scale and perhaps time-dependent irregularities of the geomagnetic field. A more conclusive discussion of this point is in process, making use of the results from all four detectors (different effective particle energies).

The gross decay rate is presumably a composite of atmospheric and magnetic effects.

The present experimental results on artificially injected electrons are of far-reaching importance in understanding the dynamics of the natural radiation.

The discontinuously rapid drop of intensity of Argus I and Argus II on about September 4 suggests that the great magnetic storm of that date may have caused a much higher rate of loss of stored particles. Also, the thickness of the Argus II shell appears to have increased s nificantly during the same period.

These observations may provide an impr tant clue to the understanding of the struct and the intensity of the natural radiation be

Injection efficiency—By means of our E plorer IV observations, it is possible to estima the total number of trapped Argus electro having turning points below the highest altitu of observation. This estimate, made as of ze elapsed time, serves to place a lower limit the fraction of electrons effectively injected in the geomagnetic field, since the nominal yi and the nominal spectrum of electrons a known.

Distribution of turning points—Figure 20 a plot of CWt versus B for Argus I, II, and I The distribution of turning points along a l of force is implicit in these curves. It is seen t there is a monotonic increase in the density turning points with decreasing B (increasi altitude). It is therefore evident that injecti of the longer-lived electrons occurred, in lar part, at altitudes much greater than that of t atomic detonations.

The general geomagnetic field—The geometr form of the Argus shells is known to a precisi of the order of ±10 km with respect to t earth. Hence, these experiments provide a si nificant new method for the harmonic analys of the general geomagnetic field. This analys is not yet completed, but it is already cle that at least the dipole and quadrupole term will be determined with useful accuracy.

Acknowledgments—The Argus work at the Sta University of Iowa has been supported, in larg

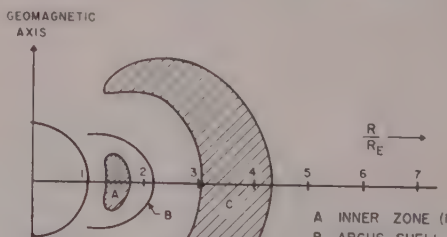

FIG. 19—The general relationship of the Argu shells to the structure of the natural radiation zones. See *Van Allen* and *Frank* [1959] and *Ver nov et al.* [1959].

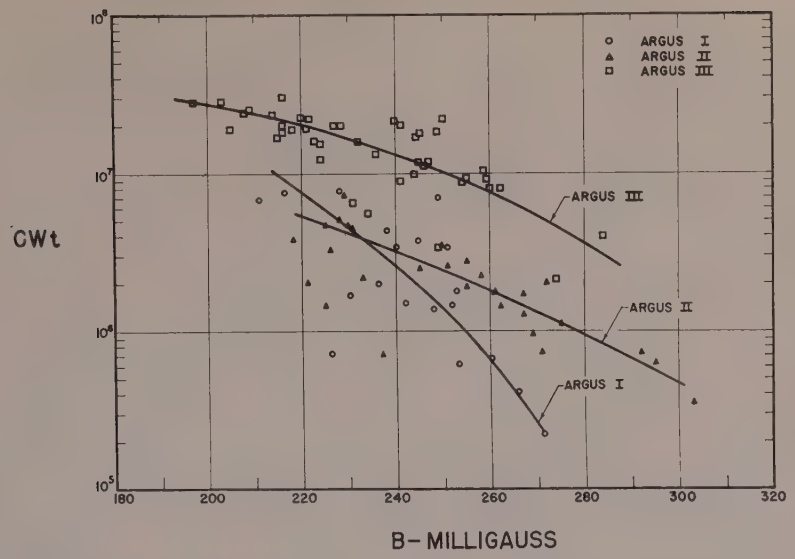

FIG. 20—The triple product of C by W by t for channel 3 versus scalar magnetic field intensity B for Argus I, Argus II, and Argus III (Livermore study group.)

part, by Contract DA-11-022-ORD-2788 with the Chicago Ordnance District of the Department of the Army, which support is gratefully acknowledged.

REFERENCES

ROSENBLUTH, M. N., AND C. L. LONGMIRE, Stability of plasmas confined by magnetic fields, *Ann. Phys.*, 1, 120–140, 1957. (Apparently the first paper on the matter in the open literature.)

VAN ALLEN, J. A., AND L. A. FRANK, Radiation around the earth to a radial distance of 107,400 km, *Nature*, 183, 430–434, 1959.

VAN ALLEN, J. A., G. H. LUDWIG, E. C. RAY, AND C. E. MCILWAIN, Observation of high intensity radiation by Satellites 1958 Alpha and Gamma, *Jet Propulsion*, 28, 588–592, 1958.

VAN ALLEN, J. A., C. E. MCILWAIN, AND G. H. LUDWIG, Radiation observations with Satellite 1958ε, *J. Geophys. Research*, 64, 271–286, 1959.

VERNOV, S. N., A. YE. CHUDAKOV, P. V. VAKULOV, AND YU. I. LOGACHEV, Study of terrestrial corpuscular radiation and cosmic rays during flight of the cosmic rocket, *Doklady Akad. Nauk S. S. S. R.*, 125, 304–307, 1959.

Project Jason Measurement of Trapped Electrons from a Nuclear Device by Sounding Rockets*

LEW ALLEN, JR., JAMES L. BEAVERS, II, WILLIAM A. WHITAKER, JASPER A. WELCH, JR., AND RODDY B. WALTON

Physics Division, Research Directorate
Air Force Special Weapons Center
Air Research and Development Command
Kirtland Air Force Base, New Mexico

Abstract—Solid-propellant rockets were sent to altitudes of 800 km from three stations in the eastern United States to observe electrons injected into the geomagnetic field from a small high-altitude nuclear detonation. The electron flux was measured by an assembly of Geiger counters. Shortly after a nuclear detonation above the south Atlantic, a narrow region of high counting rate was observed. The geometry of the observations is related to the geomagnetic field. The region consisted of an intense band about 20 km wide (half-width at half maximum counting rate) and less intense wings extending at least 700 km north and perhaps 700 km south of the band. Neither position nor width of the band changed during the observations, which consisted of periodic soundings until 100 hr after the nuclear detonation. The intensity of both the wings and the band decayed during the measurements as $1/t$, which is consistent with the hypothesis that small-angle scattering is the dominant loss mechanism. The angular distribution of the radiation was measured, and the electron flux was observed to be confined very nearly to a plane perpendicular to the field lines. Spectral measurements show far fewer electrons above 4 Mev than were expected from the fission beta spectrum. Betas trapped from the decay of neutrons emitted from large-yield high-altitude weapon tests in the Pacific were also noted.

Equipment—Project Jason is the name for the Air Force Special Weapons Center's participation in the Argus experiment. It consisted of the firing of 19 high-altitude sounding rockets to measure the electrons created by the Argus detonations. The carrier vehicle was a five-stage solid-propellant rocket consisting of an Honest John for the first stage, Nike boosters for the second and third stages, a Recruit for the fourth stage, and a T-55 for the fifth stage. These were capable of delivering a 50-lb payload to an altitude of 800 km when launched at an elevation of 80°. They were launched from three sites: Cape Canaveral, Florida (Air Force Missile Test Center); Wallops Island, Virginia (NASA Pilotless Aircraft Test Station); and Ramey Air Force Base, Puerto Rico. Table 1 gives some particulars of each launching. The flights are referred to by Patrick Air Force Base test number and are listed in chronological, rather than numerical, order. The table shows the launch site; date of launch; launch time after the appropriate burst; and the apogee and splash coordinates of the flight. Also shown are the rocket spin and tumble periods.

The instrumentation used in this project was basically a radiation-sensing system composed of eight Geiger-Müller tubes and a system for providing a data link to ground receiving. Inasmuch as new phenomena were being investigated, it was necessary to provide a radiation-detecting system with various thresholds and dynamic ranges that would best serve the angular distribution of the electron flux. The selected values for thresholds and dynamic ranges proved quite adequate. In the design of the instrumentation system, effort was made to provide a minimum number of components and maximum reliability. The package was designed and constructed under contract by Lockheed MSD;

* Presented at the Symposium on Scientific Effects of Artificially Introduced Radiations at High Altitudes held at the National Academy of Sciences, April 29, 1959. This paper is being published simultaneously in the August 1959 issue of the *Proceedings of the National Academy of Sciences.*

TABLE 1—*Test data*

Launch coordinates for the Jason flights were: Wallops (75°29′W, 37°50′N); Patrick (80°32′W, 28°27′ Ramey (67°7′W, 18°32′N).

Event/ flight	Launch site	Date	After burst (launch time), hr:min	Per- formance	Apogee, km	Splash latitude	Splash longitude	Spin period, sec	Tum peri sec
Pacific I	Johnston I.	1 Aug.	...		...	...	...	...	..
Pacific II	Johnston I.	12 Aug.	...		...	...	...	...	..
1822	Patrick	15 Aug.	65:46	O.K.	693	27.91°N	76°49′W	2.0	2.
1841	Ramey	20 Aug.	182:57	Failure	...	...	...	...	..
1859	Wallops	25 Aug.	319:43	Failure	...	...	...	...	..
Event 1		27 Aug.	...		...	...	...	...	..
1909	Patrick	27 Aug.	1:03	O.K.	937	30.62	74.01	15.1	120.
1914	Ramey	27 Aug.	1:54	Failure	...	...	...	...	..
1917	Ramey	27 Aug.	4:12	O.K.	817	25.40	68.49	2.33	2.
1913	Wallops	27 Aug.	4:59	Failure	...	...	...	...	..
Event 2		30 Aug.	...		...	...	...	...	..
2019	Wallops	30 Aug.	0:28	O.K.	817	29.90	74.88	5.0	3
2022	Patrick	30 Aug.	1:11	O.K.	878	28.19	70.21	1.07	38.
2021	Wallops	30 Aug.	1:58	O.K.	830	31.51	80.30	6.5	30
2023	Ramey	30 Aug.	2:32	O.K.	825	25.51	70.86	3.8	8
2025	Patrick	30 Aug.	3:16	O.K.	699	27.32	70.52	3.2	1.
2024	Wallops	30 Aug.	4:01	O.K.	815	27.56	72.56	1.97	17.
2027	Wallops	30 Aug.	18:42	O.K.	745	30.08	71.08	1.50	1
2026	Ramey	30 Aug.	19:43	Failure	...	...	....	...	...
2020	Patrick	31 Aug.	20:47	O.K.	800	25.96	67.47	5.4	13.
2041	Ramey	2 Sept.	87:42	Failure	...	...	...	...	..
2042	Wallops	2 Sept.	88:43	O.K.	789	29.61	70.19	4.3	9.
2043	Patrick	2 Sept.	90:55	O.K.	789	27.96	67.27	20.7	138.

Figure 1 shows a breakdown of the complete instrumentation package. The transducer head, some aspects of which are shown schematically in Figure 2, consisted of eight Geiger-Müller tubes arranged around the circumference of the forward portion of the instrumentation package. The tubes were protected during the lower atmospheric portion of the flight by a nose cap, which was jettisoned at an altitude of about 400,000 ft. After jettison of nose cap, all the detector circuitry became exposed to the radiation environment. The possibility of arcing necessitated "potting" of all electrical connections in the instrumentation section. Table 2 gives specific information on each tube used in the transducer head.

The output pulses of the Geiger-Müller tubes were sequentially sampled and transmitted directly to ground. As no analog data were involved, calibration of the FM deviation was not necessary. The telemetry system was AM/FM at 217.5 Mc. Power output was a minim of 6 watts. The radiating antenna was form by the outer shell of the instrument packa and the fifth-stage rocket, each composing h of a resonant antenna system. The telemet receiving equipment of the Air Force Miss Test Center range was used, particularly t TLM-18 60-ft parabolic dishes. The minimu received signal of all flights at apogee was 1 microvolts input to the receiver from the TL 18.

Counters—The relationship between cou ing rates and incident flux is given by

$$R = \int_{\Omega,E} G(E,\Omega)\, F\,(E,\Omega)\, dE\, d\Omega$$

where

R = counts per seconds.

G = absolute geometrical factor for ele tron of energy E incident within so

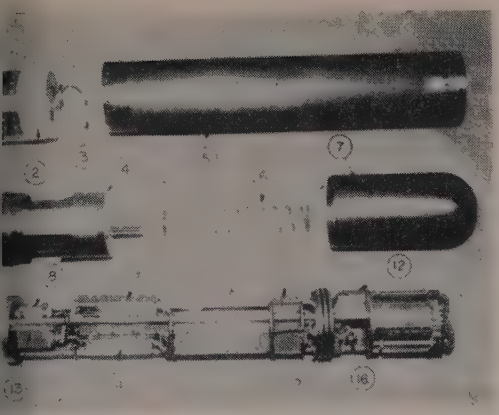

FIG. 1—Instrumentation components.

1. Package-to-rocket mating fixture.
2. Antenna insulator.
3. Antenna feed coaxial line.
4. Housing of nose-cap-ejector mechanism.
5. Outer skin of instrument package.
6. Nose-cap ejection spring.
7. Nose cap.
8. Acceleration-actuated switch.
9. Commutator and modulation-amplifier tray.
10. Plate supply battery box.
11. Filament supply battery box.
12. Timer and telemetry actuation switches.
13. RF power amplifier.
14. FM transmitter.
15. "O" ring seal.
16. Nose-cap-ejection timer.

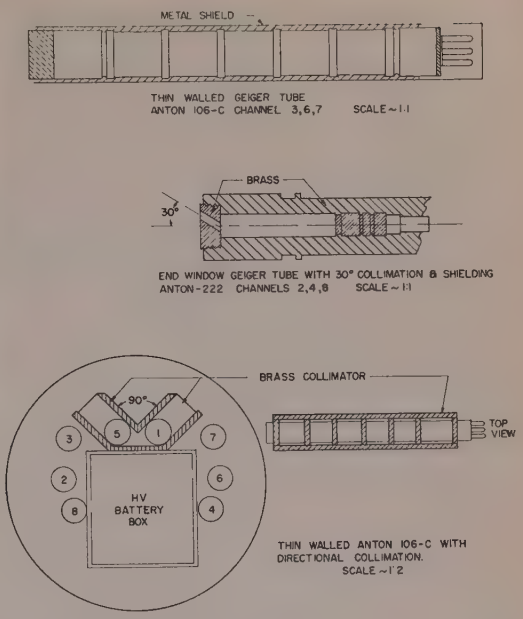

FIG. 2—Schematic representations of the Geiger tubes and their orientation in the instrument head.

angle Ω with respect to the counter (cm^2 ster).

F = flux in electron/cm^2 ster Mev at energy E within Ω.

As will be shown, the electron flux is essentially confined to a plane perpendicular to the geomagnetic field; therefore, we may consider two simplifying cases: *A*, where the long axis of counters 1, 3, 5, 6, and 7 is perpendicular to the plane; and *B*, where the axis is parallel. For these cases the integration over the incident directions can be performed and the result expressed as

$$R = \int_E G_0(E) F_0(E)\, dE$$

TABLE 2—*Detector details*

Channel	Window	Directional	Area, cm^2	Material	Window thickness, mg/cm^2	Approximate maximum flux	Minimum energy, kev
1	Side	Yes	13	Steel	30	1.3×10^4	190
2	End	Yes	0.08	Aluminum	28	5×10^6	170
3	Side	No	13	Aluminum	400	3.3×10^3	1000
4	End	Yes	0.08	Brass	400	5×10^6	900
5	Side	Yes	13	Steel	30	1.3×10^4	190
6	Side	No	18	Brass	2000	1.7×10^3	4000
7	Side	No	13	Aluminum	150	2.4×10^3	460
8	End	Yes	0.08	Aluminum	150	5×10^6	470

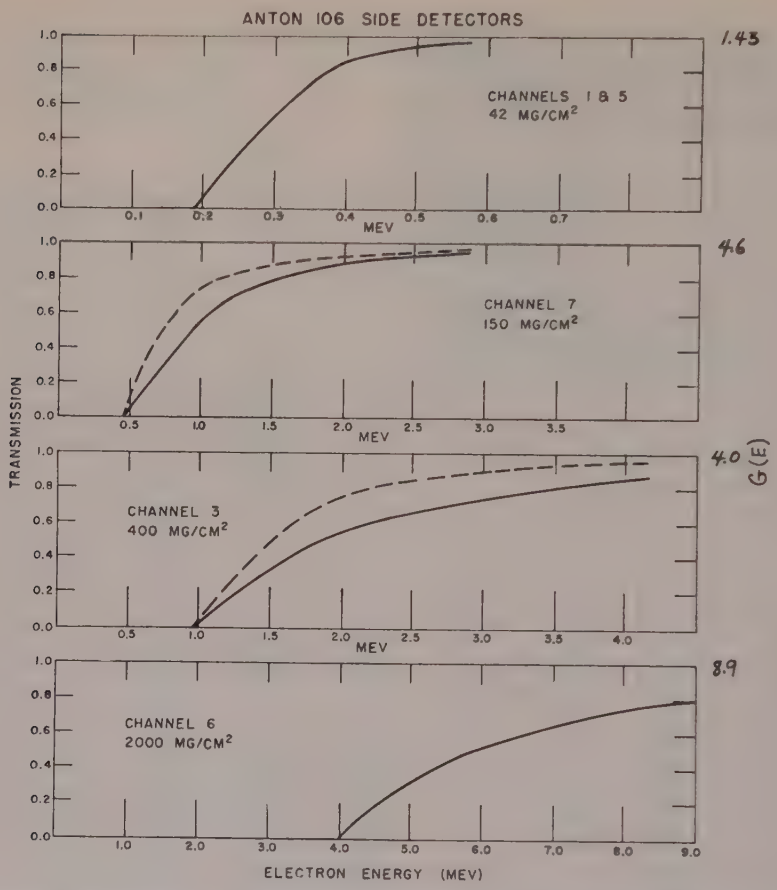

FIG. 3—Calculated transmissions as a function of electron energy for high-sensitivity detectors. T dashed curves refer to orientation A and the solid curves to orientation B.

We note now that $F_0(E)$ = planar electron flux (electrons per cm² sec); i.e., a planar monoenergetic flux of F_0 would produce a counting rate of F_0 in an isotropic detector having a transmission of unity and a cross-sectional area of 1 cm². An isotropic flux F_0 would also count F_0 in the same detector; hence, G_0 is numerically the same as the absolute omnidirectional geometrical factor for these cases. Representative angular resolution curves are shown in Figure 5.

$G_0(E)$ is plotted in Figures 3 and 4. The dashed curves in Figure 3 represent the results for orientation A when they differ from results calculated for orientation B. In these cases the results for orientation B are indicated by solid curves. Because of the narrow collimations used for the small end windows 2, 4, and 8, and the side detectors 1 and 5, the transmissions these detectors were the same for both orien tions considered. The calculation for detecto

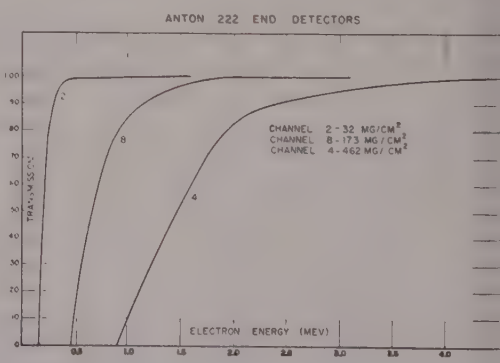

FIG. 4—Calculated transmissions of low sensitivi and detectors as a function of electron energy

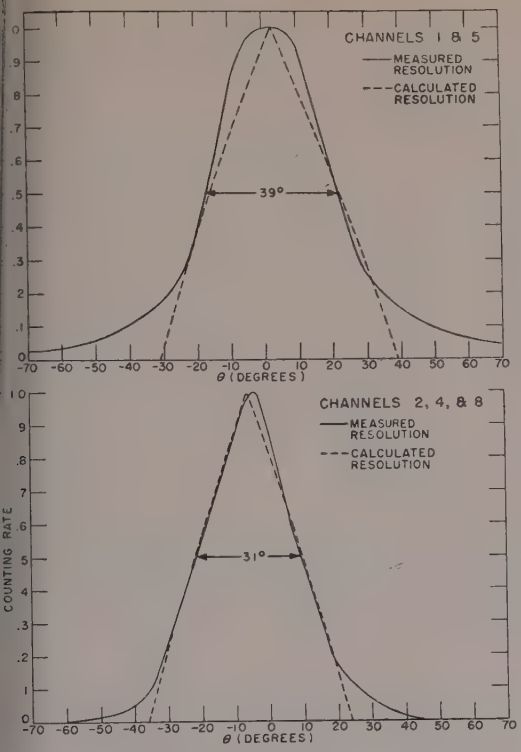

FIG. 5—A comparison of experimental and calculated angular resolutions.

was treated somewhat uniquely because the thickness of the brass shield, 2 g/cm^2, was so great that the root mean square scattering angle of a 4-Mev electron transversing the shield would exceed $\pi/2$. In this case, an electron penetrating the shield would not remember its direction of entry into the shield; hence, the transmission was a function only of energy and shield thickness.

Dead-time corrections were made to all data, assuming a value of 10^{-4} sec, the value recommended by the tube manufacturer. Experiments were performed which verified this value for a representative number of tubes used in this project.

Data requirements and data reduction—The exact data required in this project were counting rates as a function of time for each Geiger-Müller tube, and the rocket trajectory. Continuous recording of each channel was not accomplished. A commutator sampled each channel 5 times per second for a period of 1/75 sec.

Because of the low-frequency response of the tape recorder, synchronization and reference pulses suffered severe differentiation, which, however, had no effect on the quality of the counter pulses recorded. To provide synchronization and reference pulses for data-reduction purposes, the composite signal was used to modulate a 22-kc subcarrier oscillator at the ground stations. The discrimination of this subcarrier returned the desired information. The data were played back at low speed onto an oscillograph with a 3-kc response, and individual pulses were counted on the resulting record.

The total missile flight time for the 13 firings of interest was about 200 min. It was found sufficient to analyze only about one-half of the total flight time, and this playback required 21 miles of oscillograph paper. Data processed in this manner were carefully edited to minimize reading errors, which were always less than 10 per cent.

Each flight trajectory was determined by using the azimuth and elevation time histories from the TLM-18 antennas located at Cape Canaveral and the Island of Antigua. These antennas are 60-ft parabolic dishes used to track the data link telemetry. Ballistic trajectories were calculated, which minimized the squares of the errors between these trajectories and the azimuths and elevations observed. A summary plot of all the trajectories is shown in Figure 6. In order to correlate the results from all rockets with their trajectory variations, launch point, and launch time, any longitude variations have been suppressed by projecting all trajectories onto a plane containing the 75°W meridian.

It was also desirable to construct a model of the earth's magnetic field in the plane of the projection. Since the observed field differs greatly from the dipole approximation in this region, the observed dip angle at the earth's surface is used. For the magnetic lines of force, arcs of circles were drawn which had the observed dip at the surface and a curvature derived from the dipole field. These lines were labeled by the geographic latitude at which they intersect the surface, and thus form a magnetic field line coordinate.

In Figure 6 the projected trajectories are shown together with the constructed magnetic lines. It should be noted that the geometry of this plot is distorted. First, the curvature of the

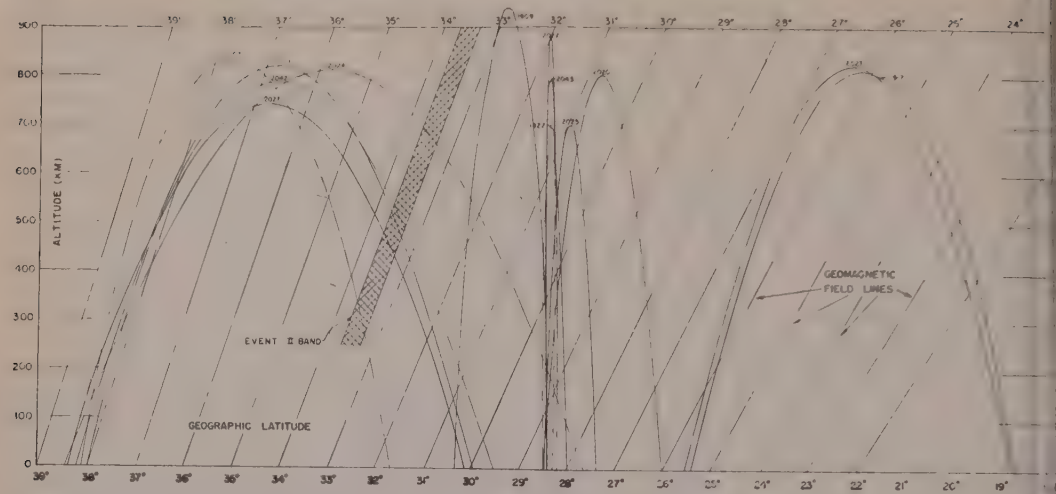

FIG. 6—Jason rocket trajectories presented as altitude versus geographic latitude. Trajectories ha been projected on the plane containing the 75° meridian. The position and width of the event 2 ban together with the magnetic field lines, are shown. The apparent launch points of the trajectories are ra coincident, since a ballistic path was fitted to the unpowered portion of the flight. Slight angular diffe ences at the end of the powered portion cause significant differences in apparent origins.

earth is suppressed; second, the abscissa is in degrees of latitude, which are about 105 km, whereas the ordinate is given in hundreds of kilometers. This distortion causes the magnetic field lines to appear straight. It will become clear that it was more natural and meaningful to use the magnetic line coordinate than the geographic latitude.

Should the dipole approximation be accurate, the geomagnetic latitude at the surface would be given by the latitude of the line of force plus 11°. Any comparison of this experiment with others at far distant places, however, should be made on the basis of exact geographic position and height and a more accurate model of the earth's magnetic field.

Results, general—As Table 1 indicates, there was a total of 13 successful rocket flights out of 19 attempts. One of them (1822) was launched before any of the south Atlantic shots and was therefore used as a background measurement. Actually, it was less than 3 days after a high-altitude shot in the Pacific, and there are indications that this flight counted trapped betas from the decay of neutrons. Nevertheless, this flight served as a background measurement for the detectors having a threshold above the end point of the neutron beta decay spectrum. Of the other 12 flights, 2 were used on the first of the south Atlantic events, and 10 on the second The third south Atlantic event was not mon tored in this project. This report presents r sults from the second event for the most part unless otherwise specified, all remarks refer t this event.

Event 2 was monitored by a total of 10 suc cessful rocket flights that covered the tim period from H plus 28 minutes to H plus 9 hours. A well defined band of electrons wa found immediately after the shot along a magn netic line of force which intersects the earth a a geographic latitude of 33.5°N, 75°W. Thi band persisted throughout the observation period and remained in a fixed position within the accuracy of the measurement. Increased counting rates (10 to 100 times background) were observed several hundred kilometers north and south of the band. In this report we assume that the observed counts are caused by electrons, although they could conceivably be caused by any charged particle with the same range in the absorbers.

Results are given for such parameters as the position of the trapped electron band, the energy spectrum, and the rate of decay of the trapped particles. A discussion is presented of how the orientation of the instrument package was determined unambiguously for several

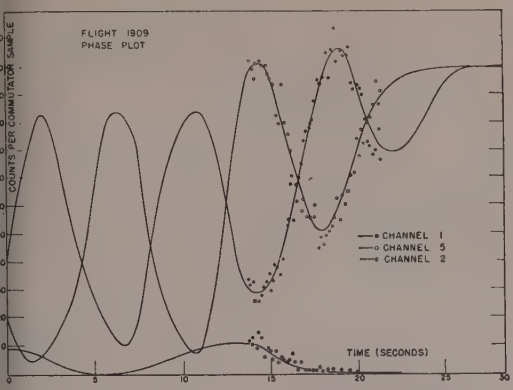

FIG. 7—A phase plot for flight 1909. Both smoothed data and several typical points are shown.

flights, and how it was determined from this that the election flux is perpendicular to the magnetic field. Generally, channel 3 is the most useful one for following the events qualitatively, since its threshold was above the neutron decay beta spectrum and the observed low-energy background. Furthermore, the threshold was still low enough to count a large fraction of the fission-product electrons.

Angular distribution of trapped electrons—The directionality of the radiation field was obtained from plots like that in Figure 7. In this figure, counts per commutator sample have been plotted against time (uncorrected for the dead time of the counters) for channels 1, 2, and 5 of flight 1909. Zero time is an arbitrarily chosen reference point. These detectors all have a threshold of about 180 kev; 1 and 5 are collimated at right angles to the missile axis and to each other, and 12 views of the field at 30° to the missile axis. The counting data were extracted from flight 1909 because the spin and tumble periods and the orientation of the total angular momentum with respect to the magnetic field for this flight were optimum for showing the planar nature of the electron flux.

It can be seen that counts on channels 1 and 5 oscillate out of phase for the first 20 sec and then coalesce. This behavior indicates that these counters at first pass in and out of the electron field as the rocket spins and then count at equal rates later in the tumble period when they are both completely in the field for several spin cycles. Thus, in the time period shown in Figure 7, the missile tumbles from a position where it is parallel to the plane of the radiation field (or perpendicular to the magnetic field) to one in which the axis is perpendicular to the plane of radiation. Because detectors 1 and 5 were almost completely saturated for counts greater than 100 per commutator sample, the peaks for these detectors are greatly depressed.

The angular distribution of the electrons was obtained by means of the known angular resolution of the collimated detectors. Flight 2019 was used in this study. It was launched from Wallops Island 28 minutes after event 2, and it passed through the electron band at H plus 41 minutes. It turned out to be a particularly favorable flight for this measurement because of the orientation of the rocket in space and its spin period. The analysis was done for two portions of the flight, in the wings and in the band.

Figure 8 shows the counting rate observed with channels 1 and 5 at an altitude of 465 km and along the 38° magnetic line. At this position, the package is 5° (of magnetic line) north of the electron band. Dead-time corrections have been applied to the data. The uncertainties shown in the figure are statistical; errors from dead-time corrections are negligible. The counting rates of the other directional counters were too low to be statistically meaningful. As indicated in Figure 8, the spin rate of the package was determined by measuring the time between consecutive maxima in the counting rate of detectors 1 or 5. By means of the known spin

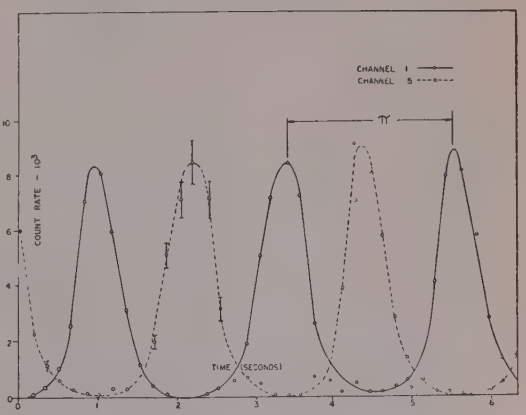

FIG. 8—Counting rates on channels 1 and 5 for flight 2019. One-half of a revolution of the instrument package is indicated by π. The spin period is 2π.

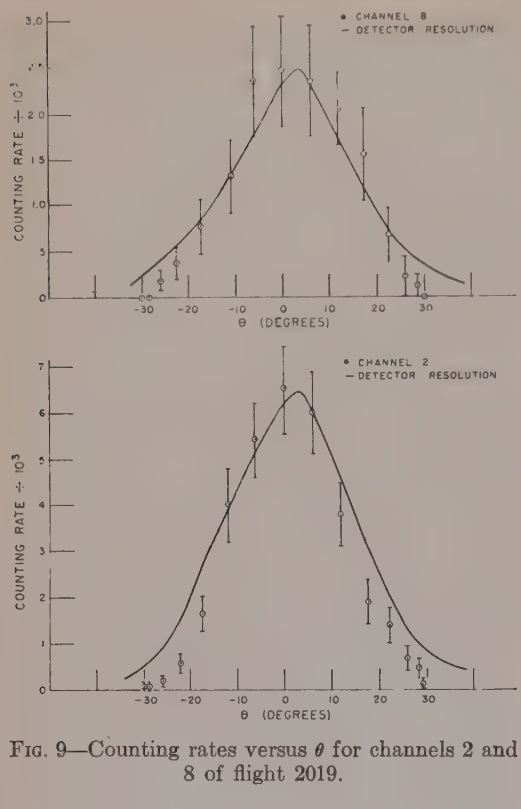

FIG. 9—Counting rates versus θ for channels 2 and 8 of flight 2019.

rate it was possible to replot the data as counting rate versus angle. This manipulation showed that the measured angular distribution was indistinguishable from the known angular resolution of the detectors, and therefore the electron flux was very nearly confined to a plane. The maximum half-width at the half-height of this angular distribution, consistent with the uncertainties of the measurement, gave an upper limit of 15° for the half-angle of electron distribution about a plane in space. It is shown in the next section that this plane was actually perpendicular to the magnetic field.

The angular distribution near the center of the trapped band was measured with channels 2 and 8, since 1 and 5 were saturated and 4 had an insufficient counting rate. The altitude of this measurement was 500 km when the package was in the electron band. In Figure 9, counting rates are presented as a function of θ, the angle about the plane of radiation. The smooth curves represent the experimental angular resolutions of the detectors. From these data an upper limit of 15° is derived for the half-an of the electron distribution. The sharpness the angular distribution is further illustrated the fact that the counting rate goes to zero these counters when they are at an angle of 3 to the plane of the radiation. Thus, for t detector geometries used in this experiment, t electron distribution is indistinguishable from delta function centered on a plane in spa Since the packages were always spinning a tumbling, it was virtually impossible for t side detectors not to become aligned in the po tion of maximum counting rate at some part the cycle. Since the angular resolution of t counters was larger than the observed angul distribution of the flux, only the peak counti rate during a complete spin-tumble cycle w necessary to define the field completely. Ph plots of counting rates (e.g., Fig. 7) for t directional detectors were made for each flig to ensure that detectors were oriented in a po tion to observe the maximum flux.

Orientation of instrument package—Becau of the rather strong anisotropy of the radiati pattern of the telemetry transmitter, it w possible to determine the orientation of the in strument-package axis in space. For purpos of analyzing its rotation the package could b considered a long cylinder. It had two larg principal moments of inertia and one sma moment (1/90 of the large moments). Suc configuration has a tendency to transform an angular motion into a flat spin or tumble there is a means of energy loss. Since the rocke burned out deep in the atmosphere (120,000 ft) aerodynamic forces provided this means. A examination of signal-strength records shows transformation from last-stage burnout to stable mode of tumble established at abou 300,000 ft. The flatness of the tumble can b determined from the ratios of moments of inerti and rates of spin and tumble. Since, with th large receiving antennas, it was always possibl to receive signals far above the noise, a recor of signal strength as a function of time may b related to points on the cylindrically symmetri pattern of the telemetry transmitter.

A careful examination of the records per mitted the detemination of the angle betwee the longitudinal axis of the package and th line of sight between the package and the re

ceiving station. From this information, it was concluded that the axis of the package lay on a cone about a line of sight having that angle as half-angle. Data from other stations provided similar cones. In this manner, the axis of the rocket was found as the intersection of the various cones. Up to five of the six available down-range stations could be used at any one time, and the orientation determinations made at the stations showed good agreement. The stations were located from Patrick to Antigua and covered a look angle from the rocket of almost 150°. As only three stations were necessary to obtain the absolute orientation, the confirmation provided by other stations encourages confidence in the results. This determination was done in selected cases to an accuracy of 3° with respect to a set of axes fixed in space.

To verify that the flux was perpendicular to the lines of force, it was necessary to determine the relation of the axis of the rocket to the field line at the time when counters 1 and 5 were equal and at a relative maximum. Determinations of the direction of the axis of the rocket on favorable flights (3 sec $<$ spin period $<$ tumble period) showed that the plane of the flux and the direction of the line of magnetic field were perpendicular within 3°.

Method of presentation of data—It should now be possible to present the data in the form of peak counting rates versus either altitude or magnetic line. However, it was not possible to choose peak counting rates directly for all portions of a flight because either the counters were too near saturation or the counting rates were so low that a peak counting rate was not statistically reliable. If a high-sensitivity detector was saturated, the counting rate of the low-sensitivity detector having the same energy threshold was used. The latter counting rate was normalized in the region where the high-sensitivity detector was not yet saturated. Where counting rates of the high-sensitivity detectors were too low, the average counting rates of those detectors were plotted and normalized to the peak counting rates where the latter became statistically significant. Corrections for counting losses caused by dead time were applied to all data before normalizations were made.

Two questions may arise about these procedures. The first is the validity of using a low-sensitivity detector as a back-up for the high-sensitivity detector when the transmissions of the pair were slightly different. This difference produced a negligible error for the energy spectrum observed. The second question concerns the use of average counting rates to extend the peak counting-rate curves. For this procedure to be correct, the ratio of average to peak counting rates had to be constant throughout the flight. These ratios were taken from the data at several points along the trajectory of every flight and were found to be constant to within the accuracy of the measurement. This result is to be expected, since the modes of spin and tumble were constant throughout each flight and the direction of the plane of the trapped particles was almost constant over the geographical extent of a rocket flight.

Except for the discussion of absolute flux, the data in this report have been presented as peak counting rates normalized to the high-sensitivity detectors: 1 (180 kev threshold), 3 (1 Mev), 6 (4 Mev), and 7 (500 kev). By the procedures just described, peak counting rates were extended for rates about 2×10^4 counts/sec using the low-sensitivity detectors and for rates below about 6×10^2 counts/sec using the average counting rates of the high-sensitivity detectors.

Plots of peak counting rates against magnetic line for channels 1, 3, and 7 for all flights are shown in Figures 10 through 12. The direction of flight is indicated by arrows. Altitudes of several points for each flight are shown in hundreds of kilometers. In these, as in several succeeding figures, the statistical errors in a few selected points are shown by error bars. The Wallops flights are on the left of the figure, the Patrick flights in the middle, and the Ramey flights on the right. On the flights following event 2, a rather sharp peak is seen to exist at the 33.5° magnetic line; this region is referred to in this report as the band. An expanded view of the band is shown in Figure 13, where, again, statistical errors are shown. The band width is shown for counters 2, 4, and 8; excellent agreement is seen to exist between them. The high count rates observed both to the north and south of the band are known as wings.

Event 1—Because of the location of the band

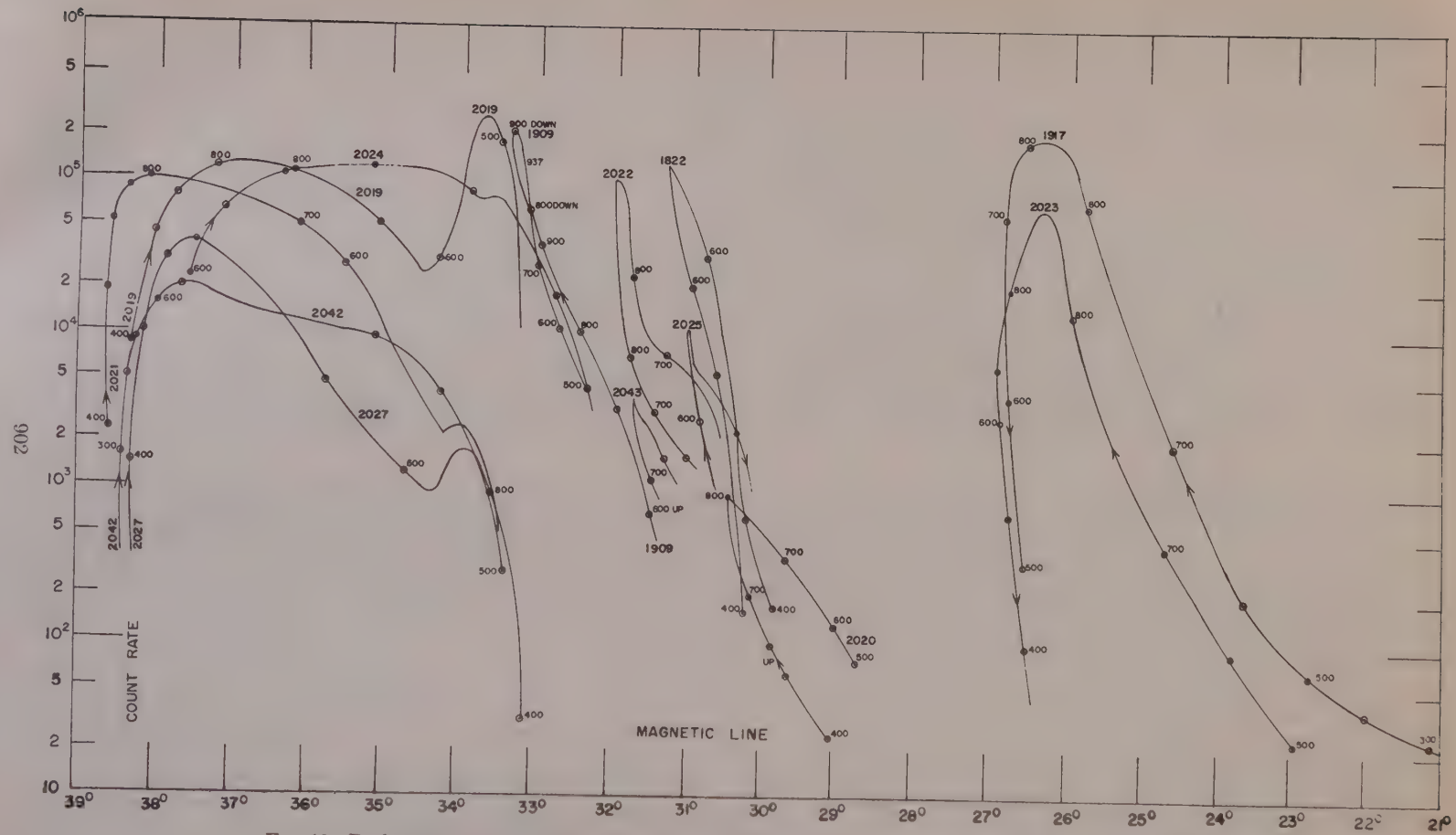

FIG. 10—Peak count rate versus magnetic line for channel 1 on all successful flights. Hundred-kilometer points are indicated.

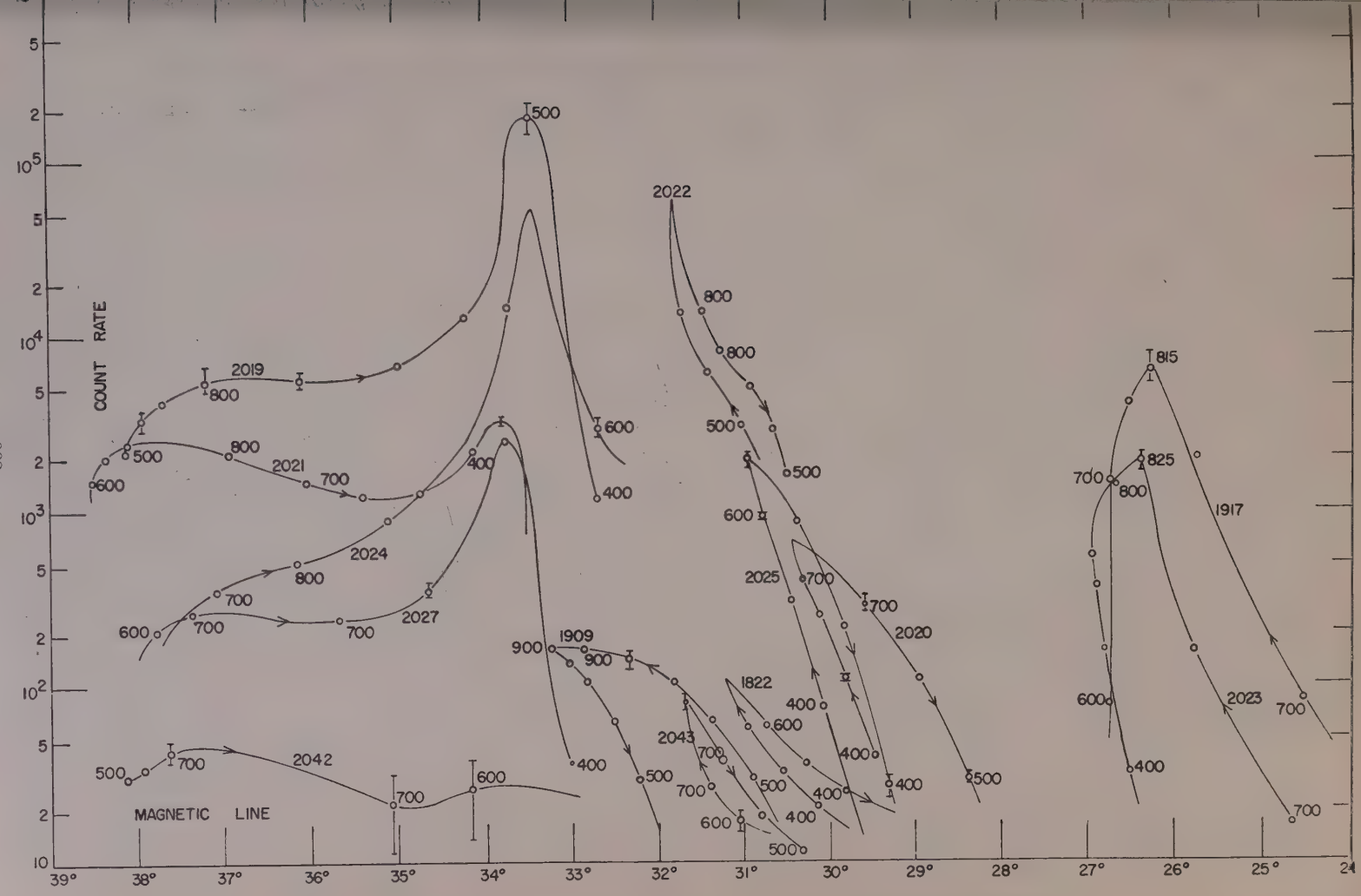

FIG. 11—Peak count rate versus magnetic line for channel 3 on all successful flights.

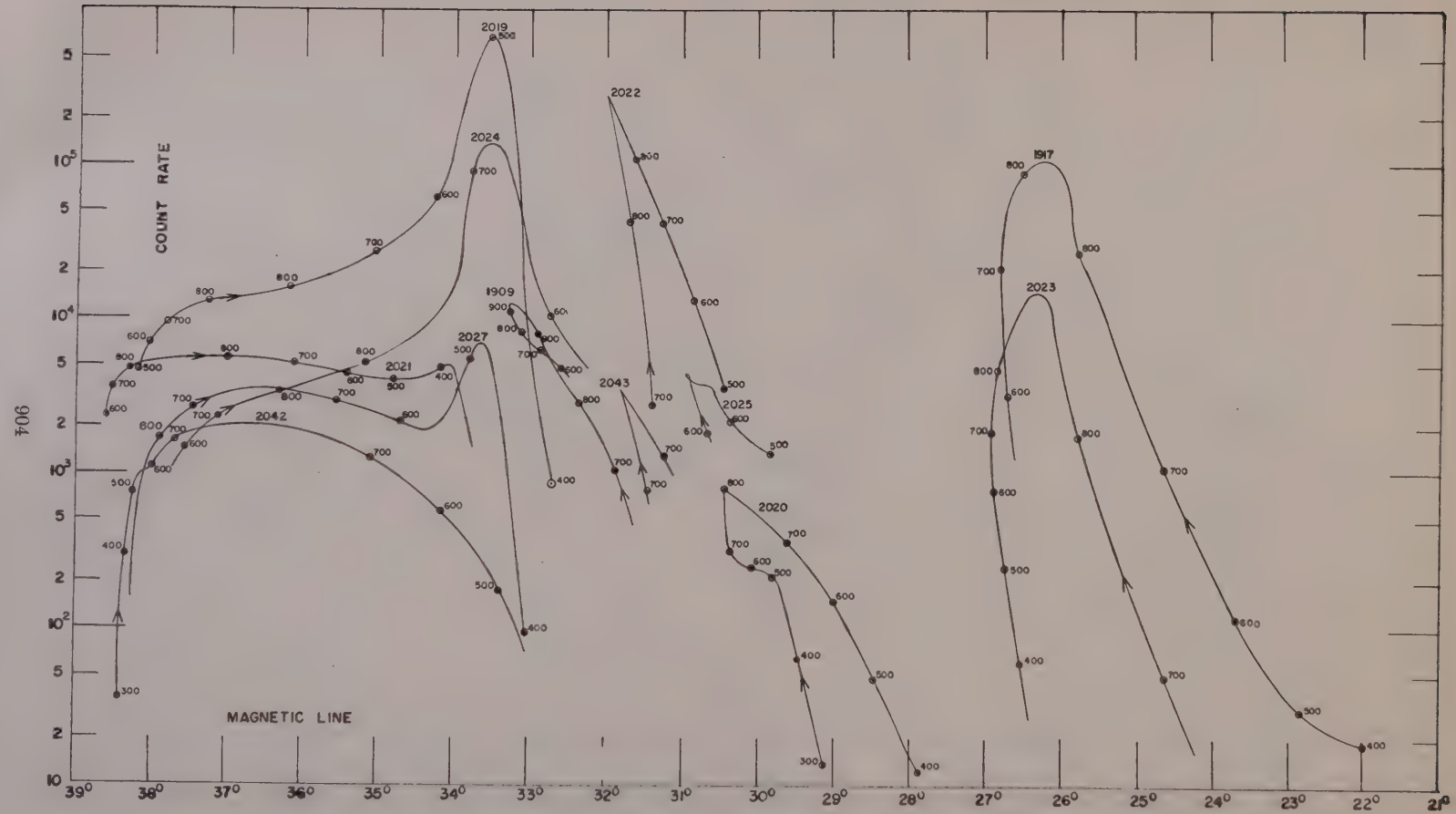

FIG. 12—Peak count rate versus magnetic line for channel 7 on all successful flights.

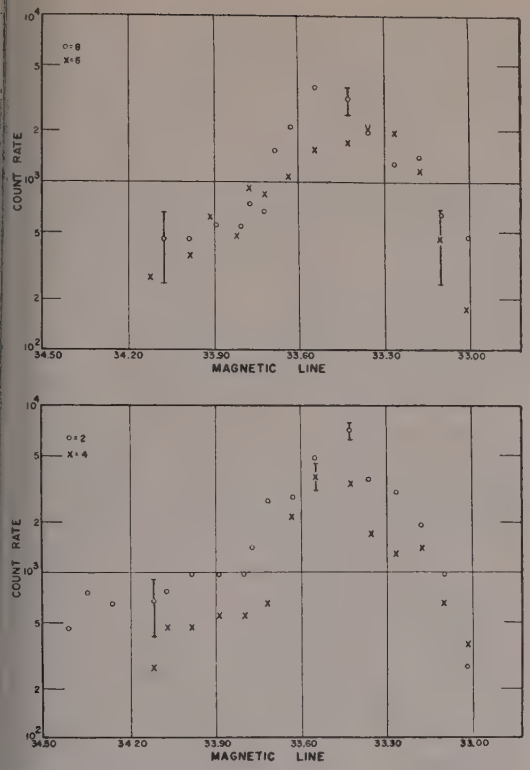

FIG. 13—Expanded view of the band as seen on channels 2, 4, 6, and 8 of flight 2019.

in event 1, only three sounding rockets were launched, of which only two were successful. Even these results are complicated considerably by the fact that 1909, the Patrick flight, went considerably more northerly than any other Patrick flight. Therefore, it is only possible to make comments on the effects on both sides of the band. Referring to Figures 10 through 12, the Ramey flight (1917) shows a low counting rate until about 600 km on the ascending part of the flight, when the counting rate begins to rise rapidly. It continues to increase until apogee, after which it recedes only slowly. It may be observed that at the same altitude on the ascending and descending portions of the trajectory the counting rate is considerably higher at the higher magnetic line. Channel 3 is the most indicative of the presence of any effect added by event 1, as the background for this high-energy channel (as illustrated by flight 1822) was much lower than it was in either channels 1 or 7. On channel 7, the counting rates at similar altitudes are higher on the Ramey flight than on the Patrick flight. This effect is even more pronounced on channel 3. Detailed analysis of effects indicates that the data are consistent with the presence of a band located at the 28° magnetic line ±1°.

Event 2—The band from event 2 was more favorably located. The first flight from Wallops after event 2 was launched at H plus 28 min. This shows the band clearly and locates it along the 33.5° magnetic line. As a result of this observation an effort was made to fire north from Patrick, but because of air traffic problems it proved to be impossible. Therefore, only the firings from Wallops went directly through the band. Nevertheless much valuable information on structure was obtained from the Patrick firings. Because of missile and telemetry failures, there was only one successful firing from Ramey after event 2.

From Figures 10 through 12 it can be seen that the structure of the effect was, in general, a broad plateau upon which was set a narrow band or peak. The location of this band was constant in time. Small apparent changes in location are interpreted as a result of errors in the magnetic field model and the method of projecting the trajectories onto the 75° meridian. Since the magnetic field is not pure dipole at the earth's center, the predominately eastward electron drift had both small vertical components and north-south components. The simplification of the projection of the trajectory to a purely east-west direction shows up as slight shifts in the plotted position of the band in these figures. The true deviation of the position of the band was less than 1/10° in period from 40 min to 4 days after the event. It should be noted that there was a large area north of the band extending to at least the 38° magnetic line which exhibited counting rates considerably above background though more than an order of magnitude down from the peak and decay properties similar to the band. This region will be known as the northern wing. It is further noted that in this region the counting rate was relatively independent of magnetic line or altitude. A partial explanation of this behavior is that, as the package neared the band, the counting rates would tend to increase; but the package was also descending, and the counting rates

would normally decrease. The two effects tended to cancel each other, keeping the counting rates fairly constant.

The Patrick flights show a very large effect due to the deviations of our model from the true magnetic field. This is a result of the great longitudinal spread from the eastward-fired Patrick flights, and it causes some disparity between the ascending and descending portions of the trajectories. This disparity, however, does not seriously affect the interpretations of the experiment. The Patrick flights show a large southern wing which extends to at least the 29° magnetic line and possibly even farther south. In shape and decay the southern wing is similar to the northern wing. The best measurement of the location of the band was flight 2019, the trajectory of which was almost exactly along the 75° meridian. The data that have been

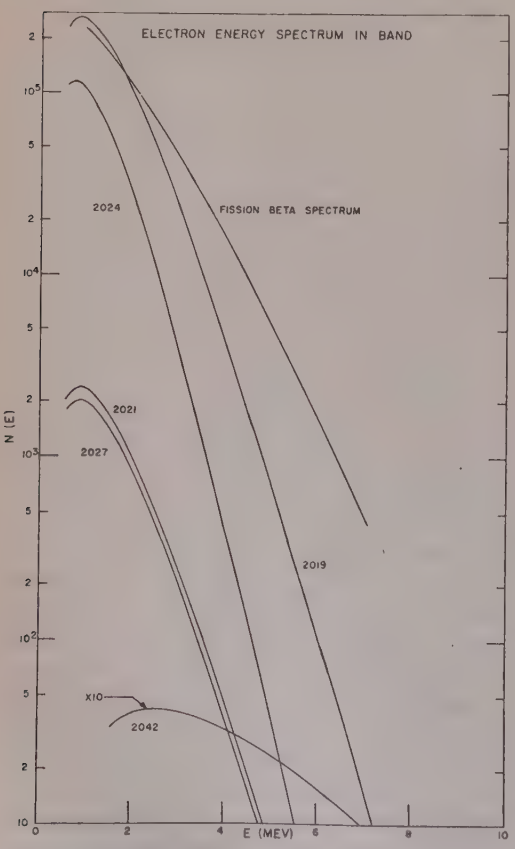

FIG. 14—Electron energy distribution (electrons per cm² sec Mev) in the bands. The fission beta spectrum is also shown for comparison.

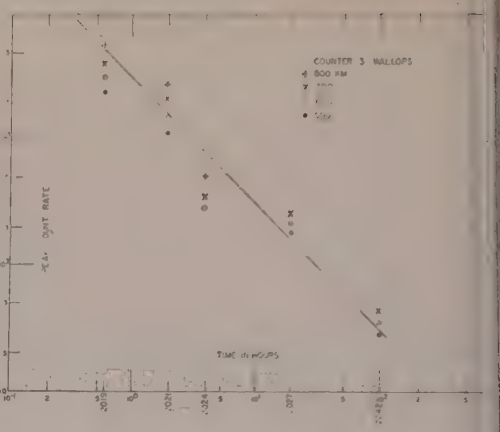

FIG. 15—Isoaltitude plot of peak count rate channel 3 versus time after event 2. The data taken at 100-km intervals on the ascending portion of the Wallops flights.

presented were selected from curves smoothed through the raw data.

Spectrum—It had been predicted that the trapped particles would give a fission spectrum enhanced in the high energies at late times because of the increased scattering and loss at low energies. The prediction was not fulfilled. Figure 14 shows the spectrum measured in the band for flight 2019 compared with the fission product spectrum. Other flights after the south Atlantic events give the same spectrum within the limits of the data. It is noted that there is a severe discrepancy at high energies.

Lifetime of the Argus effect—In order to correlate the results from several rocket firings, it was necessary to display the data by holding one parameter fixed from flight to flight. The parameter chosen was altitude. A plot of the peak counting rate versus time after event 2 is shown in Figure 15 from the Wallops Island flights. Data are given for counter 3 (1 Mev). They were selected at a series of constant altitudes in the northern wing of the trapped electron shell. From this plot, it can be seen that the effective decay is roughly $1/t$. Other plots from Patrick firings and on other channels, give basically the same results. On channels 1 and 7 the Wallops flights decay less rapidly since they are also observing a neutron decay beta background from a far earlier time. (See following sections.)

Pacific events—The high-altitude shots in the

Pacific were of large yields and therefore might be expected to have contributed to the electron backgrounds observed in this project, except that they were at much lower magnetic altitude. Even if it were impossible for these shots to inject fission products into the earth's magnetic field, the large number of neutrons produced would decay, producing betas which might have been trapped. Calculations of the trapped-particle density expected from these neutron betas indicate that three missile flights may have detected effects attributable to the Pacific shots. These were flight 1822, which took place 2¾ days after the last Pacific shot; 1909, which was designed to investigate event 1 but was far to the north of the band; and 2043, which occurred long after events 1 and 2. These three flights had very similar characteristics on counter 3, which was not expected to be affected by the neutron decay betas, and its threshold was above the end point of the beta spectrum. Counters 1 and 7, however, should be expected to detect such betas. Flight 1822 was notable for the extremely high counting rates in counter 1. These counting rates are in fact an order of magnitude higher than those at similar altitudes immediately after event 2. Flight 2043 came much later and had considerably lower counting rates on this counter. Channel 7, which failed on flight 1822, was backed up by channel 8, which provided some information. Because of the location of the threshold of these counters with respect to the neutron decay spectrum, it was possible to compare the ratios of the counting rates of these channels with that expected for a neutron beta spectrum. It was found that the ratios of the 180-kev channels to the 460-kev channels on flight 1822 were those expected for a neutron spectrum within a factor of 1.5.

This is the first experimental verification of the expected effect of the trapping of neutron decay betas from an atmospheric neutron source.

Pacific lifetimes—It is difficult to obtain reasonable lifetimes for the neutron decay betas from the Pacific shots, because there was only one flight immediately after a Pacific shot but before the south Atlantic events. There were many flights, of course, but they were affected by intervening injections. In Figure 16, a plot is shown of peak counting rate on channel 1 for

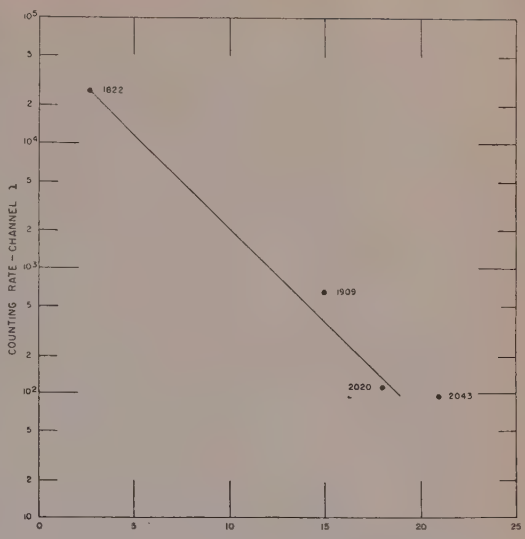

FIG. 16—Count rate for selected flights as a function of time in days after last Pacific event. All points were taken at 600 km on the ascending portion of the Patrick flights.

the Patrick flight versus time after the last Pacific event. It is seen that, at long times, the decay of the effect is not consistent with the $1/t$ law which would seem to be valid for short times after event 2. There may be two explanations: that the particles sometime after 1822, but before 1909, were catastrophically removed by some geophysical event, or that at long times an exponential decay may dominate. Such decay might result from the scattering of electrons out of the shell by hydromagnetic waves.

Conclusions—The results of the experiment agree qualitatively with those measured by the satellite Explorer IV. If it is assumed that all losses take place by small-angle scattering in the region about Capetown where the mirror points dip low into the atmosphere as a result of the magnetic anomaly, this experiment agrees quantitatively with the satellite. Certain unique results are obtained from the rocket data: the angular distribution is measured carefully and shown to be distributed about the plane perpendicular to the magnetic lines of force; the location of the band at one point is shown to be quite constant; spectral measurements indicate a deficiency of high-energy particles; and the neutron decay betas from the large-yield Pacific shots are detected.

Theory of Geomagnetically Trapped Electrons from an Artificial Source*

JASPER A. WELCH, JR., AND WILLIAM A. WHITAKER

Physics Division, Research Directorate
Air Force Special Weapons Center
Air Research and Development Command
Kirtland Air Force Base, New Mexico

Abstract—A theoretical formulation has been made for the history of an artificial shell of geomagnetically trapped electrons resulting from low-yielding nuclear detonations in the exosphere. The formulation assumes a source distribution and gives the spatial distribution of trapped electrons along the magnetic field lines, the drift rate around the world, and the configuration of the resulting shell. Interactions of the shell with the atmosphere lead to an electron density decaying inversely with time from injection for times longer than a characteristic lifetime that is a function of altitude and electron energy. The electron flux is found to be very nearly confined to a plane perpendicular to the field direction after several characteristic lifetimes. Scattering by geomagnetic fluctuations is probably not an important loss mechanism for the artificial shell, but it may be important for the hard component of the natural trapped belt. The effect of the geomagnetic anomaly over the south Atlantic has been described qualitatively. Jason rocket data and Explorer IV satellite data have been compared with the theoretical results.

INTRODUCTION

This paper reports some of the theoretical predictions and interpretations for the Argus experiment. This experiment consisted of three small-yield nuclear detonations approximately 300 miles above the south Atlantic Ocean in the late summer of 1958. Beta decay of the fission products from the explosions injected relativistic electrons into trapped orbits in the geomagnetic field. It is the history of these electrons with which we are concerned here. Experimental measurements of this history were made by the satellite Explorer IV and the Jason sounding rockets. Details of these and other measurements performed during the Argus experiment are found in accompanying papers by Van Allen et al.; Allen et al.; Newman et al.; and Peterson et al. A general description of the entire experiment is given in the accompanying paper by Christofilos.

I. GENERAL CONCEPTS

We shall take as our point of departure a source function which is the number of particles per cubic centimeter injected into the geomagnetic field. We shall take the injection to be isotropic. Our first step is to show how the particles rearrange themselves in the field according to the geometry of the trapped orbits. Most of the features are obtained by considering a dipole field and many by even omitting the angular dependence of the dipole. Departures from a static dipole are treated in later sections as perturbations.

We shall make use of the mirror equation of *Alfven* [1950], $B = B_m \sin^2 \alpha$, where the pitch angle α is the angle between the velocity vector of the particle and the magnetic field vector, B is the field strength, and B_m is the field strength where the particle is mirrored (i.e. where α becomes $\pi/2$). This is equivalent to the conservation of the magnetic moment of the particle orbit. That is,

* Presented at the Symposium on Scientific Effects of Artificially Introduced Radiations at High Altitudes held at the National Academy of Sciences, April 29, 1959. This paper is being published simultaneously in the August 1959 issue of the *Proceedings of the National Academy of Sciences*.

$$\mu = (\text{Area} \perp \text{to } \vec{B})(\text{Current} \perp \text{to } \vec{B})$$

$$= \pi R_c^2 e\omega_c \sim V_\perp^2/B \tag{1}$$

where R_c and ω_c are the cyclotron radius and frequency, and $V_\perp$ is the component of the velocity perpendicular to B. Alfven has shown that μ is an adiabatic invariant, i.e., not strictly a constant of the motion, so long as space and time variations of the field are large with respect to the cyclotron radius and period. Section VI will discuss the consequences of the breakdown of these conditions. Since the static magnetic field does no work on the particle, the total velocity is conserved and we obtain

$$V_\parallel^2 = (V^2 - V_\perp^2) = (1 - B/B_m)\, V^2$$

as the equation of motion of the guiding center along the line of force.

In addition to the particle density $p(r)$ (i.e., the number of particles per cubic centimeter) we shall have use for what we call the mirror-point density $w(r)$. This is the number of particles whose guiding centers mirror in a particular cubic centimeter. This concept is useful, as the lifetime of a particle depends almost exclusively on the location of its mirror point. Or, to put it another way, all particles with the same mirror point have the same lifetime (aside from dependence on energy and type of particle), whereas all particles found at the same altitude, for example, do not have the same lifetime. These three densities—injection, $n(r)$; particle, $p(r)$; and mirror-point, $w(r)$—are related in the following ways.

The number of particles injected into a volume of length dl' along the field line at r' having cross-sectional area dA' and having pitch angles between α and $\alpha + d\alpha$ is $dv' = dA'\, dl' n(r') \sin\alpha\, d\alpha$ where α runs from 0 to $\pi/2$ since a particle emitted in the direction $(\pi - \alpha)$ will appear at the injection point with angle α after one reflection, and vice versa.

These particles will be mirrored in a volume of length

$$dl = \left|\frac{dl}{d\alpha}\right| d\alpha$$

and of cross section

$$dA = \frac{B(r')}{B(r)}\, dA'$$

at the point r. But the number of mirror points per unit volume is the mirror-point density. Thus

$$dw(r) = \frac{dv'}{dA\, dl} = \frac{B}{B'}\, n' \sin\alpha \left|\frac{d\alpha}{dl}\right| dl' \tag{2}$$

where $B = B(r)$, $B' = B(r')$, etc.

But, since

$$\sin\alpha \left|\frac{d\alpha}{dl}\right| = \frac{d}{dl}\cos\alpha = \frac{d}{dl}\sqrt{1 - \frac{B'}{B}} = \frac{B'}{2B^2\sqrt{1 - B'/B}}\frac{dB}{dl} \tag{3}$$

$$dw = \frac{n'}{2B\sqrt{1 - B'/B}}\frac{dB}{dl}\, dl' \tag{4}$$

and the total mirror-point density is obtained by integrating along the field line of which dl' is the arc line element.

$$w(r) = \frac{1}{2B(r)}\frac{dB(r)}{dl}\int_B^{B^*} \frac{n(r')}{\sqrt{1 - B'/B}}\, dl' \tag{5}$$

The limits refer to the values of $B(r')$; B and B^* are numerically equal to each other and to $B(r)$, and the integral is taken along the field line from the point r in the direction of decreasing field strength and continues past the equator and on until $B(r')$ attains the value $B(r)$ again. This point is called the conjugate point to r; hence, the notation on the limit B^*.

Since we shall find that the mirror-point density is most directly affected by losses, let us compute the particle density from mirror-point density, although we could go directly from injection density. The time taken by a particle in going from one mirror point to the conjugate mirror point (let us call this the bounce period) is given by the integral

$$T(v, B_m, I) = \int_{B_m}^{B_m^*} \frac{dl}{v_\parallel} = \frac{1}{v}\int_{B_m}^{B_m^*} \frac{dl}{\sqrt{1 - B/B_m}} \tag{6}$$

where B_m is the field at the mirror points, and

the dependence of T on the particular line of force is denoted by I. The symbol I refers to the integral invariant of the motion

$$I = \int_{B_m}^{B_{m^*}} v_\parallel \, dl$$

and is more fully developed in Section III. For a dipole the equation of a field line is $r = r_0 \sin^2 \theta$, where θ is the colatitude, r is the distance from the dipole (i.e., we use the spherical polar coordinates r, θ, ϕ), and r_0 is the value of r at the equator. We shall call r_0 the field-line constant.

The bounce period for a dipole field is very nearly proportional to the field-line constant r_0, and independent of the angle through which the particle travels. The numerical value for relativistic electrons for an r_0 of 2 radii is about 0.2 sec.

Let $dv = w' \, dA' \, dl'$ be the number of particles with mirror points in the volume of length dl' and cross section dA' at r'. These particles will spend the fraction of their bounce period $dl/(v_\parallel T')$ in the volume element of length dl and cross section $dA = dA'(B'/B)$ at the point r. Thus we have

$$dp = \frac{dv}{dl} \frac{(dl/v_\parallel T')}{dA} = \frac{w'B}{v_\parallel T' B'} \, dl' \tag{7}$$

$$p(r) = \frac{B(r)}{v} \int_B^{B_{max}} \frac{w' \, dl'}{B' T' \sqrt{1 - B/B'}} \tag{8}$$

where the integral is taken along the field line in the direction of increasing B from the point r and continuing until w' goes to zero for good (say at the earth's surface). As we noted before, although T' is strictly a variable, it is slowly varying for any particular field line and hence can usually be taken out of the integral.

We should like to point out that the radical in the denominator of the integrand for both p and w goes to zero at the limit of integration. While not making the integral blow-up, the radical does tend to cause most of the contribution to the mirror-point density w to come from injection points near by and, likewise, most of the contribution to the particle density p to come from mirror points near by.

Several other useful integrals—angular distribution of the particle flux, flux parallel to B, etc.—will be developed by similar methods in Section V.

For our source function, we shall take electrons injected with constant injection density into a tube of force. We shall consider a dipole field and let the tube lie along the line of force that intersects the earth at 45° magnetic latitude. The tube will have a circular cross section. The cross section will be inversely proportional to the total field strength. The mirror-point density is then calculated according to equation 5,

$$w(r) = \frac{n_0}{2B} \frac{dB}{dl} \int_B^{B^*} \frac{dl'}{\sqrt{1 - B'/B}}$$

n_0 is electron density which is plotted in Figure 1.

We will later need the arc length from the equator along the field line $r = r_0 \cos^2 \lambda$, where λ is now the latitude. This is given for a dipole field by

$$s(\lambda) = \frac{r_0}{2\sqrt{3}} \{(3 \sin^2 \lambda)^{1/2}(1 + 3 \sin^2 \lambda)^{1/2} + \ln [(3 \sin^2 \lambda)^{1/2} - (1 + 3 \sin^2 \lambda)^{1/2}]\}$$

which can be approximated for $\lambda \leq \pi/4$ by

$$S(\lambda) = r_0(\lambda + \lambda^2/10)$$

II. The Drift in Longitude

This tube filled with electrons does not, however, remain stationary. There are several phenomena which give rise to drifts. First, there is the gradient of the magnetic field. As given in *Spitzer* [1957], this drift velocity is in the direction $\nabla \vec{B} \times \vec{B}$ for electrons (i.e., east) and has the value

$$V_{DG} = V_\perp \frac{\mathcal{R}_c \nabla_\perp B}{2B} = \frac{V_\perp \mathcal{R}_c}{2} \frac{1}{\mathcal{R}} = V_\perp^2 \frac{1}{2\mathcal{R}\omega_c}$$

where

V_{DG} = drift velocity due to gradient of magnetic field.

$V_\perp$ = particle velocity perpendicular to $\vec{B}$.

$\nabla_\perp B$ = gradient of the scalar B in plane perpendicular to $\vec{B}$.

We have replaced $B/\nabla_\perp B$ by $\mathcal{R}$, the radius of curvature of the field line, which is valid if curl $\vec{B} \equiv 0$.

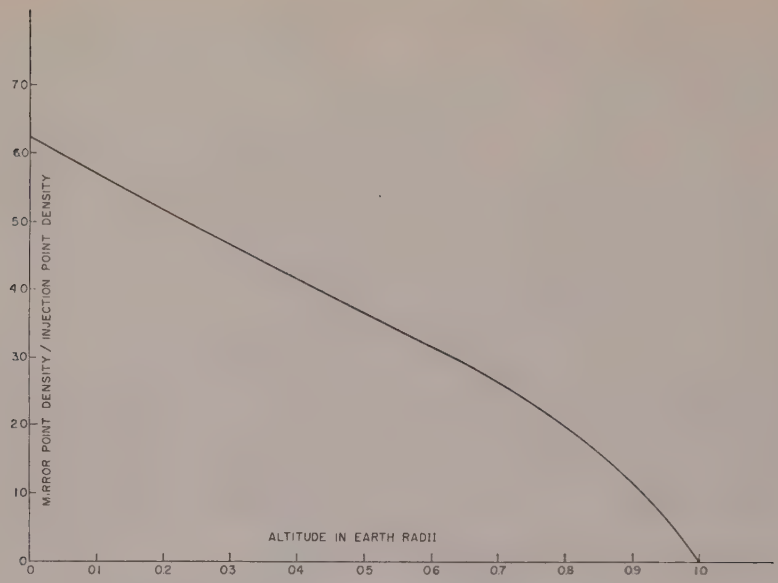

FIG. 1—Initial mirror-point density versus altitude.

Second, there is a drift if the particle is moving with a velocity $V_\parallel$ along a line of force which is curved. From Spitzer this gives rise to a drift velocity

$$V_{DC} = V_\parallel^2 \frac{1}{(\Re\omega_c)}$$

where $V_\parallel$ = particle velocity parallel to field line. This drift is in the same direction as the gradient drift.

Third, there is the drift from the earth's gravitational field, $V_{DE} = g/\omega_c$. This is very small, as

$$\frac{V_{DE}}{V_{DC}} = \frac{g/\omega_c}{V_\parallel^2/\Re\omega_c} = \frac{g\Re}{V_\parallel^2}$$

$$\approx \frac{10^3 \times 10^9}{(3 \times 10^{10})^2} \approx 10^{-9}$$

Fourth, the direction of the drifts from the gradient and curvature are west for positively charged particles. Thus, the electrons and positive ions would tend to pull apart until the resulting charge separation built up enough electric field strength to overcome the drift forces. This electric field will be in the east-west or ϕ direction and will itself cause a drift radially outward. If unchecked, this drift would tend to disperse the electrons. However, the earth is supposed to be immersed in a hydrogen plasm originating from the solar corona. This plasm has an estimated 10^3 protons and thermal ele trons per cubic centimeter. If the estimate i correct, the electric field will never build up, a this comparatively dense plasma will shif around to neutralize the charge separation. Th uncertainties about this point and the presenc and effect of electric fields in general seem to b satisfactorily dispelled by the observed stabilit of the Argus electron shell.

The curvature for a dipole field is given by

$$\frac{1}{R} = \frac{3}{r_0 \sin\theta}\left[\frac{1 + \cos^2\theta}{(1 + 3\cos^2\theta)^{3/2}}\right]$$

and the cyclotron frequency by

$$\frac{1}{\omega_c} = \left(\frac{\gamma m_0 c}{eB_0 r_e^3}\right)\left(\frac{r_0^3 \sin^6\theta}{[1 + 3\cos^2\theta]^{1/2}}\right)$$

and the velocity term by

$$V_\parallel^2 + \tfrac{1}{2}V_\perp^2 = V^2 - \tfrac{1}{2}V_\perp^2$$

$$= \beta^2 c^2\left[1 - \frac{B}{2B_m}\right]$$

But we really want the drift velocity in radians per second,

$$\dot{\phi} = V_D/r \sin\theta = V_D/r_0 \sin^3\theta$$

ombining we obtain

$$\dot{\phi} = \left(\frac{r_0\beta^2\gamma}{r_e}\right)\left(\frac{3m_0c^2}{eB_0r_e}\right)\left(\frac{c}{r_e}\right) \cdot\left\{\left[\frac{1+\cos^2\theta}{(1+3\cos^2\theta)^2}\right]\left[1-\frac{B}{2B_m}\right]\left[\sin^2\theta\right]\right\}$$

The numerical constant is easily evaluated as

$$\left(\frac{3m_0c^2}{eB_0r_e}\right)\left(\frac{c}{r_e}\right) = \left(\frac{1.53\ \text{Mev}}{6.02\times10^4\ \text{Mev}}\right) \cdot\left(\frac{3\times10^{10}\ \text{cm/sec}}{6.38\times10^8\ \text{cm}}\right) = 1.20\times10^{-3}\ \text{sec}^{-1}$$

We must remember that B/B_m is also a function of θ and θ_m, the colatitude of the mirror point. For our case the line intersects the earth at $\theta = 45°$, $r_0 = 2r_e$, and we can easily evaluate $\dot{\phi}$ for the case of particles mirroring on the equator: we always have $\theta_m = \pi/2$ and $B = B_m$. Then

$$\dot{\phi} = 1.20\times10^{-3}(2\beta^2\gamma)\{[1]\ [\tfrac{1}{2}]\ [1]\}$$
$$= 1.20\times10^{-3}\beta^2\gamma\ \ \text{sec}^{-1}$$

The drift period is then

$$T_D(\theta_m) = T_D(\pi/2) = 2\pi/\dot{\phi}$$
$$= 5.23\times10^3/\beta^2\gamma\ \ \text{sec}$$
$$= 87/\beta^2\gamma\ \ \text{min}$$
$$\approx 30/E\ \text{Mev}\ \ \text{min}$$

For other values of θ_m we need to average $\dot{\phi}$ weighted by $v/v_\parallel$, the relative time spent at each angle θ. This weighted average value turns out to vary by less than 8 per cent over the range $\pi/6 \leq \theta_m \leq \pi/2$. Using an average value over θ_m we have constructed Table 1.

TABLE 1—*Time to drift around the world versus energy*

E, Mev	T average, min/rev
0.5	57
1.0	33
2.0	18
3.0	12.5
4.0	9.7
6.0	6.6
8.0	5.2

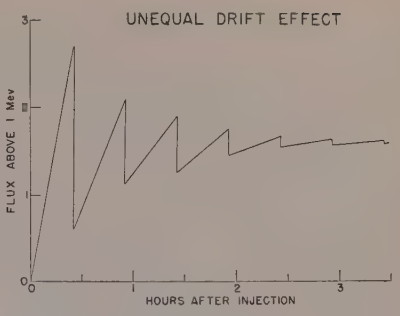

FIG. 2—Total electron flux above 1 Mev versus time after an injection.

The energy dependence of the drift has the effect of a gigantic time-of-flight spectrometer. If we station ourselves at the eastern coast of the United States (which is almost one revolution from the initial tube for the eastward-drifting electrons) and observe at such a time that the 1-Mev electrons just get to our station, we will also see 2-Mev electrons that have gone around twice and 3-Mev electrons that have gone around three times, and so forth.

When we add up all the contributions we will get a total flux above 1 Mev that varies in time as shown in Figure 2. This figure is for a fission-product beta spectrum which drops off rapidly above 1 Mev. The large discontinuities occur just as the large 1-Mev contribution passes by the station. For any detector, some time variation of the flux will be associated with the energy-dependent drift and it will take about six drift periods before the spectrum is completely smeared out. Thus, at early times some care needs to be taken in the proper interpretation of the flux levels.

III. The Shape of the Electron Shell

For a pure dipole field, or any other field where B has no components in the ϕ (i.e., azimuthal) direction, the drift will be entirely in the ϕ direction. However, the geomagnetic field does have ϕ components even when referred to an eccentric dipole. These components were of some concern to us in locating the launch sites and trajectories of our rockets. We needed an estimate of what we call the conjugate trace—the intersection of the electron shell with the earth's surface. We shall define magnetic latitude as latitude with respect to the

position and direction of the best-fit (eccentric) dipole.

If the field is pure dipole field, the conjugate point trace will follow a constant magnetic latitude with respect to the dipole. Since the eccentric dipole is located a small fraction of the earth's radius from the earth's center, we can lay off constant latitude approximately as small circles from the point of emergence of the eccentric dipole axis from the earth's surface.

If we examine a plot of the field at the earth's surface, we see that there are moderate deviations from the dipole approximation. We shall now give two estimates of the effect of these perturbations on the trace of the conjugate point.

As we go away from the earth's surface, the surface perturbations can be expected to wash out and the field to approach that of a dipole. Calculation of the eastward drift for a dipole field shows that most of the drift occurs at the maximum altitude. Further, for a dipole field, the drift has no radial components. Carrying these tendencies to the limit, we can form a model in which the electrons always orbit about lines that cross the equatorial plane at a fixed distance from the dipole location. We need now to find where these lines intersect the earth. If the field were pure dipole, these lines would have a constant dip angle at the earth's surface and would intersect the earth along a parallel of magnetic latitude. That is, the conjugate trace, the magnetic parallel, and the iso-dip line would be coincident.

For a dipole field, the dip angle D (the angle between the line of force and the earth's surface) is related to the latitude, λ, by $\tan D = 2 \tan \lambda$. Thus, the dip angle associated with 45° latitude is 63°. Consider now a particular longitude in the northern hemisphere where high-order multiples have caused the 63° iso-dip trace to lie south of 45° magnetic latitude (see Fig. 3). From the figure we see that the line of force intersecting the earth at 45° latitude for a pure dipole field now intersects at a lower latitude, but not so low as the 63° iso-dip trace. This new intersection is precisely the position of the conjugate trace at this longitude.

The first estimate is to place the conjugate trace halfway between a parallel of magnetic latitude and the perturbed iso-dip trace charac-

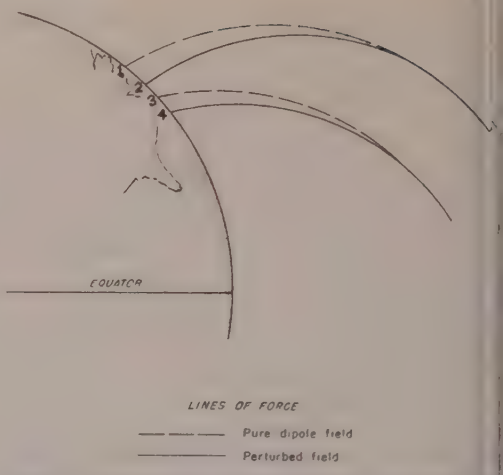

FIG. 3—Illustration of the earth's magnetic fi along the east coast of the United States. Poin is 44° magnetic latitude and unperturbed positi of 60° iso-dip line. Point 2 is perturbed position 1, i.e. the conjugate trace. Point 3 is the unp turbed position of line that is now at point Point 4 is 60° iso-dip line, perturbed positi Note that the conjugate trace lies between 4 magnetic latitude and the 60° iso-dip line. For dipole field all three would be coincident.

teristic of this latitude for a dipole field (e.g 63° iso-dip trace for 45° latitude). There a generally a large number of latitudes and co responding iso-dip traces that lie equally fa north and south of a given initial conjuga point. The pair with smallest separation w probably give the best results. The conjuga trace as seen by the Explorer IV agreed wc with this approximation.

A second approximation is to assume that a the drift takes place at or near the earth's su face. Then the direction of the drift is alway perpendicular to both the magnetic field an that part of the gradient of the magnetic fiel perpendicular to the field itself (roughly mag netic east). Thus, we can take the publishe values for the magnetic field and find this direc tion for all points on the earth. Starting fro the initial conjugate point we can then win our way around the earth, guided by the direc tion of the drift as described above. This ap proximation gives results close to those fro the iso-dip approximation.

A more elegant method is to make use of th two adiabatic invariants of the particle motio —the magnetic moment and the integral in

ariant. The constancy of magnetic moment nplies that a given particle will always mirror t a constant value of the field strength. Thus, s far as loss times are long compared with drift imes, we should find the same number of elec- rons in the shell at various longitudes if we eep on a surface of constant field strength. he integral invariant,

$$I = \int_{B_m}^{B_{m'}} V_\parallel \, dl$$

s conserved since the bounce period (<1 sec) s small compared with the azimuthal drift pe- iod (~1000 sec). Thus, to construct the shell t each longitude, one moves north and south long a surface of constant field strength until he integral invariant comes out correctly. For zimuthally distorted fields, particles with dif- erent mirror-point field strengths that share a ommon field line at one longitude may not hare a common field line at other longitudes. That is, the shell need not have a constant hickness as a function of longitude, even on a surface of constant field strength. Wherever the shell is wider, however, the electron density will be lower, and wherever it is narrower the electron density will be higher. This effect is noted in the satellite data.

IV. Atmospheric Losses and the Characteristic Lifetime

Small-angle scattering—It has been shown by *Christofilos* [1958] that small-angle scattering of electrons by the air is a more important loss mechanism than energy loss by either radiation or ionization. We shall see in this section that the role of scattering is to move the mirror point of the electrons to lower and lower altitudes. As they encounter denser air, the electrons eventually lose all their energy by ionization.

On the basis of small-angle scattering, the mean lifetime of an electron as a function of its initial mirror-point altitude will now be calculated. We will call this the characteristic lifetime. Many of the approximations will be based on the case of those lines of force that intersect the earth's surface near 45° latitude. Here the dip angle is large, $\approx 70°$, and motion parallel to the lines of force (near the mirror point) may be approximated to motion along an earth radius. At this latitude the angular factor in the field strength, $(1 + 3 \cos^2 \theta)^{1/2}$, has increased to only 1.5 from its value of unity at the equator. Because of the slow change and the large dip angle we will refer all field strengths to their value at the mirror point and keep only the $1/r^3$ dependence in field strength. To account for the effect of the eccentric dipole we shall construct a model atmosphere in which the air density has been averaged over longitude. These densities will be referred to the altitude of closest approach to the earth's surface. For 45° magnetic latitude and 100-km scale height the averaged density is down by a factor of 3.6 from the density at closest approach.

With this approximation to the field the mirror equation becomes $r_m{}^3 = r^3 \sin^2 \alpha$, where the subscript m denotes a value at the mirror point. Now, physically, scattering of the electron by the atmosphere represents a change in α at constant r, hence a change in r_m. Let ϵ be an elemental scattering angle. Expanding $\sin^2 (\alpha + \epsilon)$ in a Taylor series about α.

$$\sin^2 (\alpha + \epsilon) = \sin^2 \alpha + \sin (2\alpha)\epsilon + \cos (2\alpha)\epsilon^2 + \cdots$$

But we are interested in the average behavior of the particles, and ϵ is distributed in a symmetric, random distribution about $\epsilon = 0$. Thus, let us average over this distribution. Then we have

$$\langle \sin^2 (\alpha + \epsilon) \rangle = \sin^2 \alpha + \cos (2\alpha) \langle \epsilon^2 \rangle$$

neglecting higher terms. Let the symbol D denote a differential averaged over the distribution in ϵ. Then we have

$$D (\sin^2 \alpha) = \cos (2\alpha) \langle \epsilon^2 \rangle$$

But from *Fermi* [1950] we obtain

$$\langle \epsilon^2 \rangle = [7 \times 10^{-3} \, D(s)]/E^2$$

where $D(s)$ is the elemental path length in STP air, and E is the electron energy in Mev.

For relativistic electrons,

$$\langle \epsilon^2 \rangle = \frac{7 \times 10^{-3} Nc \, D(t)}{E^2 N_{STP}} = KN \, D(t)$$

where N is the atomic particle density where

the scattering occurs (we will be interested in altitudes of several hundred miles, hence the choice of atomic particle density), c is the velocity of the electrons set equal to light velocity. Remembering that D refers to an event happening at constant r,

$$D(r_m^3) = 3r_m^2\ D(r_m) = r^3\ D(\sin^2\alpha)$$

or

$$D(r_m) = \frac{r^3}{3r_m^2}\cos(2\alpha)KN\ D(t)$$

We can then define a velocity of the mirror point of the mean scattered particle

$$V' \equiv \frac{D(r_m)}{D(t)} = \frac{r^3}{3r_m^2}\cos(2\alpha)\ KN$$

Let us now calculate what is of more interest, the average of V' over the path of the particle. If the scattering per trip is small we can simply take the average over the unperturbed path

$$V = \frac{\int_0^T V'\,dt}{\int_0^T dt}$$

where the integrals are taken over the path from the mirror point to the equator.

$$Y \equiv \int_0^T V'\,dt$$

$$= \int_{r_m}^{r_0}\left(\frac{r^3}{3r_m^2}\right)\cos(2\alpha)\ KN(r)\,dt$$

Now $N(r) = N_m \exp(-x/a)$, where $x = (r - r_m)$ and a is the e-folding distance for the atmospheric density. We can express all variables inside the integral in terms of x, expanded about r_m.

$$\cos(2\alpha) = -1 + 6(x/r_m) + \cdots$$

$$r^3/3r_m^2 = (r_m/3)(1 + (x/r_m) + \cdots)$$

$$dV_\parallel/dt \equiv u(r, r_m) = u(x, r_m)$$

$$= (3c^2/2r_m)(1 - 4(x/r_m)\cdots)$$

where u is the acceleration along the line of force.

At the altitudes of most interest, a few hundred miles, $a \leqq r_m$ and the exponential fa is dominant. Specializing to the case w $(r_0 - r_m)$ is also much larger than a, we express everything in terms of x and make limits of integration zero to infinity.

Then Y becomes

$$Y = -\frac{r_m KN_m}{3(2u_m)^{1/2}}\int_0^\infty \frac{\exp(-x/a)}{\sqrt{x}}\,ds$$

$$= -\frac{r_m KN_m}{3(2u_m)^{1/2}}\sqrt{a\pi} \qquad u_m =$$

Expressing

$$T = f(2r_m/u_m)^{1/2} = f\sqrt{4/3}\,(r_m/c)$$

we find that $f = 2.0$ almost independent of Thus

$$V = \frac{Y}{T} = -\frac{\sqrt{\pi}\ KN_m}{6f}(ar_m)^{1/2}$$

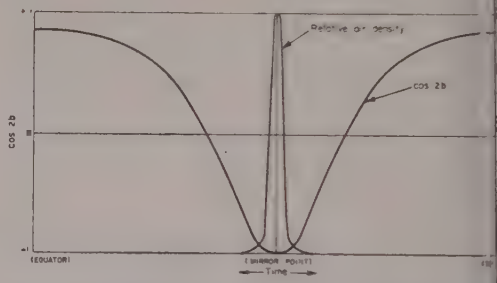

FIG. 4—Relative air density encountered by particle mirrored at 45° magnetic latitude ver time. Also cos 2α, where α is the angle betw the velocity vector and the magnetic field.

Figure 4 shows how the air density throu out a bounce period is appreciable only wh cos 2α is close to −1. That is, since all scatt occur when α is nearly π/2, all scatters lead a lowering of the mirror point. The statisti nature of the scattering relates then only to amount of lowering.

It can be seen that the average velocity proportional to the density at the mirror po and is downward into the exponentially incre ing atmosphere. Under these circumstances, a again neglecting the slow variation of a and compared with N, we find the characteris lifetime for complete loss to be the e-foldi distance, a, divided by the initial downward locity. To show this, let $V(x)$ be the veloc

TABLE 2—*Characteristic lifetime for 1-Mev electrons versus altitude*

Altitude h, km	Air density N, atoms/cc	Scale height a, km	Centered dipole, days	Characteristic lifetime for 1-Mev electron Eccentric dipole where h is minimum altitude, days
0	5.4×10^{19}	10	1.4×10^{-14}*	1.8×10^{-13}*
100	1×10^{14}	20	1.1×10^{-8}*	1.0×10^{-7}*
200	2.5×10^{10}	50	7.0×10^{-5}	4.0×10^{-4}
300	3.5×10^{9}	100	7.1×10^{-4}	2.6×10^{-3}
400	1.2×10^{9}	100	2.0×10^{-3}	7.3×10^{-3}
500	4.5×10^{8}	100	5.5×10^{-3}	2.0×10^{-2}
600	1.8×10^{8}	100	1.4×10^{-2}	5.1×10^{-2}
700	6.5×10^{7}	100	3.7×10^{-2}	0.14
800	3×10^{7}	100	8.2×10^{-2}	0.30
900	1×10^{7}	100	0.24	0.88
1000	4.4×10^{6}	100	0.50	1.8
1100	1.7×10^{6}	100	1.3	4.7
1200	8×10^{5}	100	2.8	10.2

* Less than time for one orbit ($\sim 10^{-6}$ day); hence particles with these mirror-point altitudes die on heir first encounter with the atmosphere.

ositively downward as a function of $x = r_i - r_m$), where r_i is the initial mirror point. Then

$$V(x) = V(0) \exp (x/a)$$

eglecting the variation of V with $(ar_m)^{1/2}$. Then the characteristic lifetime is

$$\tau(r) = \int_0^\infty \frac{dx}{V(x)} = \frac{1}{V(0)} \int_0^\infty \exp\left(-\frac{x}{a}\right) dx = \frac{a}{V(0)}$$

ubstituting for K and setting $18/\sqrt{\pi} = 10$,

$$\tau(r) = \frac{10^7 E^2 f}{N} \left(\frac{a}{r}\right)^{1/2} \doteq \frac{2 \times 10^6 E^2}{N} \quad \text{days}$$

This result is valid for $(r_0 - r_1) \gg a$ and $r_0 - r_i) \approx r_i$. This equation has been evaluted in Table 2 for *Harris* and *Jastrow* [1958] tmosphere (curve A).

Time variation of the mirror-point density—Ve have calculated, in the previous section, the ean time for a particle's mirror point to drift own to the earth. This process was controlled y small-angle scattering. We shall now investiate the cumulative effect on the mirror-point ensity at a given altitude from the mirror points that are lost to lower altitudes and those that are gained from higher altitudes. We shall define w as the integral of the mirror-point density w over the cross-sectional area of the shell perpendicular to the field line.

We have seen that the mean velocity of a mirror point downward is proportional to the air density, $N(h)$, at the mirror altitude, h. That is, $dh/dt = -K_1 N(h)$, where K_1 is a constant. Let us approximate the function $N(h)$ by an exponential, $N(h) = N_0 e^{-h/a}$, where N_0 and a are constants chosen to fit the density in the region of interest. Now define a new variable, z, such that

$$dz = dhe^{+h/a} \qquad z = \int_0^h dhe^{h/a} = a[e^{h/a} - 1]$$

$$h = a \ln\left(\frac{z + a}{a}\right) \qquad \frac{dh}{dz} = \frac{a}{z + a}$$

Then we obtain $dz/dt = -K_1 N_0 = -V_0$, where V_0 is a constant. That is, in "z-space" the mean velocity downward is constant. Let us now make the approximation that all mirror points drift with the mean drift velocity. This assumption will have the effect of maintaining peaks and valleys in the mirror-point density. Physically, they should wash out because of the sta-

tistical nature of the scattering process. However, we have seen in Section I that peaks and valleys are not expected for the initial condition of our particular problem. Paul Nakada at Livermore has checked this in some detail and has applied more rigorous scattering theories. He obtains essentially the same results.

Proceeding, then, our assumption implies that $\tilde{w}(z, t) = w(z - V_0 t, 0)$, where $\tilde{w}(z, t)$ is the mirror-point density in "z-space" at time t, and is related to the density in "h-space" by $\tilde{w}(z, t)\, dz = 2(h, t)\, dh$. We can now find the time variation of

$$\tilde{w}(h, t) = \tilde{w}(z, t) \frac{dz}{dh_z} = \tilde{w}(z + V_0 t, 0) \frac{dz}{dh_z}$$

as

$$\tilde{w}(h, t) = \tilde{w}(h', 0) \left(\frac{dh}{dz}\right)_{z - V_0 t} \left(\frac{dz}{dh}\right)_z$$

where

$$h' = h(z + V_0 t)$$

$$\tilde{w}(h, t) = \tilde{w}(h', 0) \left(\frac{a}{z + V_0 t + a}\right)$$

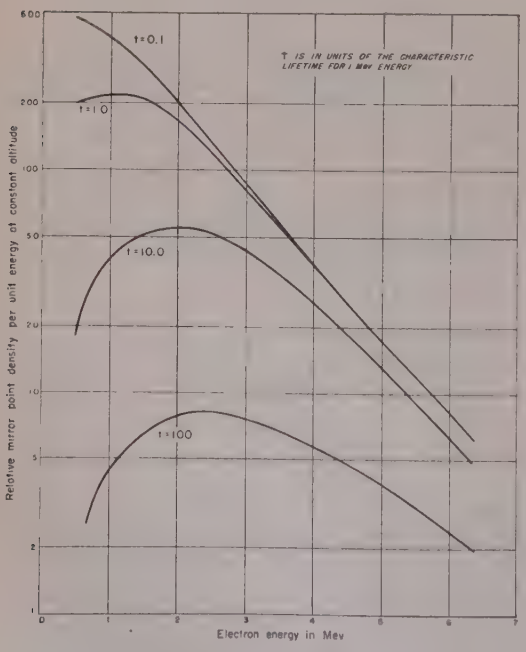

FIG. 5—Change in the electron spectrum with time caused by the dependence of the characteristic lifetime on electron energy.

$$\cdot \left(\frac{z + a}{a}\right) = w(h', 0) \left(\frac{1}{1 + (+V_0/a +}\right.$$

But

$$-\frac{V_0}{a + z} = \frac{V_0}{a + ae^{h/a} - a} = \frac{V_0 e^{-h/a}}{a} \equiv$$

Therefore we have the result

$$\tilde{w}(h, t) = \tilde{w}(h', 0) \left[\frac{1}{1 + t/(h)}\right]$$

where

$$h' = h + a \ln \left(1 + \frac{t}{\tau(h)}\right).$$

Time variation of the electron spectr
For the initial beta-spectrum we make u
the neutrino research which has developed
theoretical and experimental methods to
the total beta-spectrum for reactors. *M*
hause and *Oleska* [1957] give a spectrum
is very nearly $P(E) = P_0 \exp(-E/1.3)$
0.5 Mev $< E <$ 6 Mev. We found $\tau \approx E^2$

$$\tilde{w}(h, t) = \tilde{w}(h', 0) \left[\frac{1}{1 + t/\tau}\right].$$

Using these, and setting $w(h', 0) = 1$, we
compute the spectrum as a function of t
This has been done in Figure 5, where times
measured in units of the characteristic life
at 1 Mev.

We can integrate these spectra to get the
crease in the total mirror-point density. Th
plotted in Figure 6, where the time units

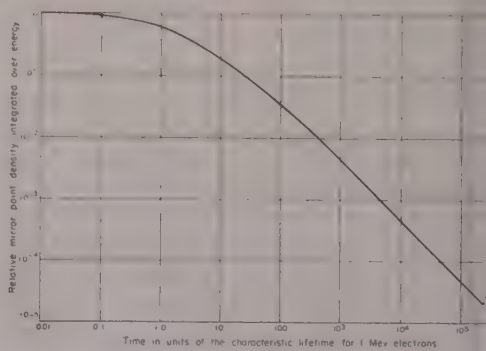

FIG. 6—Change in the mirror-point density i
grated over energy with time at constant altitu

in the characteristic time for 1 Mev. At long es, this goes as

$$h, t) \to w(h', 0)\,\frac{5.2\tau\,(E = 1)}{t}$$

$$\text{i.e., for} \quad t \gg \tau\,(E = 1)$$

ich shows that the mean energy of the long- ed electrons is

$$\sqrt{5.2} = 2.3 \text{ Mev}$$

This "$1/t$ law" has been verified fairly well the rocket and satellite results. One difficulty, wever, is that no evidence of turning over at rly times, i.e., $t < \tau(h)$, was observed. An planation may be tied into the effect of the uth Atlantic anomaly as discussed in Section I.

For times greater than the characteristic time, (itself a function of altitude and energy), the irror-point density is inversely proportional average air density by continuity arguments. his fact will simplify some of the integrals in e next section.

V. Electron Flux and Angular Distributions

The isotropic flux is, of course, the product particle density and mean velocity. This roduct can be obtained from the mirror-point ensity by the formula developed in Section I.

$$\rho v = B \int_B^{B_{\max}} \frac{w'\,dl'}{B'T'\sqrt{1 - B/B'}}$$

gain expanding in terms of $x = r - r_m$, setting $' = T$, a constant, and setting $w = w_0 e^{-x/a}$, we et

$$\rho v = \sqrt{\pi a r/3}\; w_0/T$$

his shows the almost direct relationship of flux n mirror-point density.

The angular distribution of the flux is obtained y starting with the differential flux.

$$v\,d\rho = \frac{vw'B}{v_\parallel T'B'}\,dl' = \frac{vw'B}{v_\parallel\, T'B'}\,\frac{dl'}{d\alpha}\,d\alpha$$

he flux per steradian at angle α is then

$$\frac{j}{\Omega} = \frac{v\,d\rho}{2\pi \sin\alpha\, d\alpha} = \frac{vw'B}{v_\parallel T'B'}\,\frac{dl'}{d\alpha}\,\frac{1}{2\pi \sin\alpha}$$

$$= \frac{vw'B}{\pi T'B'v_\parallel\sqrt{1 - B/B'}}\,\frac{(B')^2\sqrt{1 - B/B'}}{B\,dB'/dl'}$$

$$= \frac{vw'B'}{T'v_\parallel}\,\frac{dl'}{dB'}$$

Although it is not evident from this formula, if w' is exponential with a 100-km relaxation distance, the angular distribution will be symmetric about $\alpha = \pi/2$ and have a half-width at half-height of around 11°. That is, the flux will be very nearly confined to a plane perpendicular to the magnetic field vector. Even if w' is fairly constant, the $v_\parallel$ in the denominator tends to emphasize the flux near $\alpha = \pi/2$.

Another interesting integral is the flux parallel to the magnetic field. This is

$$j_\parallel = \rho v_\parallel$$

$$= \frac{B}{v}\int \frac{v\sqrt{1 - B/B'}}{B'T'}\,\frac{w'\,dl'}{\sqrt{1 - B/B'}}$$

$$= \frac{B}{T}\int \frac{w'\,dl'}{B'} \approx \frac{1}{T}\int w'\,dl'$$

if w' is a rapidly decreasing function of B'. That is, $j_\parallel TA$, where A is the cross-sectional area of the entire shell, is just $A\int w'\,dl'$, the total number of mirror points below the point of observation. Now $j_\parallel$ is not an easy quantity to measure, but it is related to $j_\perp$ through the width of the angular distribution.

VI. Magnetic Scattering

Let us investigate how much space and time variations in the geomagnetic field might affect the conservation of the magnetic moment. That is, we seek breakdown of the conditions.

$$B\Big/\frac{\partial B}{\partial r} \equiv R_I \ll R_c \quad \text{and} \quad \frac{\partial B}{\partial t}\Big/B \equiv \omega_I \ll \omega_c$$

Taking 2-Mev electrons and measuring distances in earth radii, we find on the equator

$$\omega_c = \frac{eB}{\gamma m_0 c} = \frac{1.5 \times 10^6}{r^3} \quad \text{sec}^{-1}$$

and

$$R_c = \frac{\gamma m_0 c}{eB}\,v_\perp = \frac{\gamma m_0 c v}{e\sqrt{BB_m}}$$

$$= 2.7 \times 10^3 [r_m{}^3 r^3]^{1/2} \quad \text{cm}$$

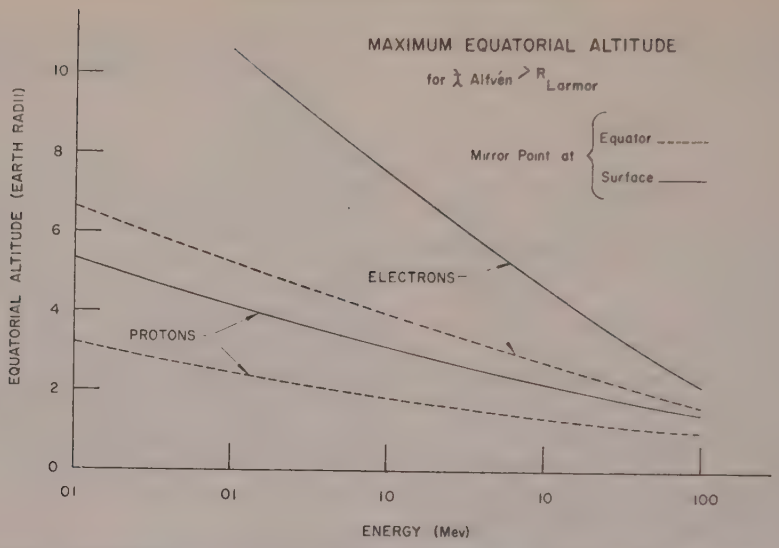

FIG. 7—Maximum equatorial altitude versus energy for stability of electrons and protons against magnetic scattering.

where r_m is the position of the mirror point.

Now, we really have no measurements in the upper atmosphere of small-scale fluctuations in the field. However, it is postulated that the solar wind acting on the earth will set up Helmholz instabilities in the outer reaches of the earth's field and that these fluctuations in the field will be propagated as Alfven waves throughout the field. If so, we can, perhaps, take the frequency spectrum of the surface fluctuations as typical of the frequency spectrum of these Alfven waves. To estimate the upper limit of the wavelength of these Alfven waves, we use the fastest speed by taking as the ionization density 10^3 protons per cubic centimeter which has been postulated for the solar corona. This wavelength will decrease as the inverse cube of the distance from the center of the dipole while the cyclotron radius of a particle mirrored at the equator will increase as the cube of this distance. As we go up, therefore, there is an altitude above which the cyclotron radius will exceed the Alfven wavelength. Above this altitude we would not expect the magnetic moment to be conserved. These altitudes are shown as dotted lines in Figure 7 versus energy for both protons and electrons.

Above these critical altitudes the particle will experience what we may call magnetic scattering off these Alfven fluctuations and will find the magnetic moment either increase[s] decreased. Now, if it is decreased, the par[t] goes to a lower mirror point and the cyclo[tron] radius is reduced, and so the magnetic sca[t]ing is reduced. On the other hand, if the m[a]netic moment increases to a higher mi[r]point, the scattering is larger.

The statistical average of all this will be[e] force the mirror points to lower and lower a[l]tudes, and eventually the atmospheric lo[ss] will take over. The solid lines we have plot[ted] show the altitudes at the equator for the mir[ror] point at the surface which is the maxim[um] allowable. For the Argus experiment—electr[ons] of several Mev with an equatorial altitude[s] about one earth radii—there is no trouble w[ith] magnetic scattering. On the other hand fai[nt] energetic protons would not be expected on t[his] basis to remain in the outer Van Allen belt.

You will notice that the critical altitude[s] very insensitive to energy. This insensitivity [to] energy is equivalent to an insensitivity of t[he] assumed frequency spectrum which we ha[ve] taken. If this idea of Alfven waves in the upp[er] atmosphere has anything to it, we have an e[f]fective way of removing protons from the ou[ter] Van Allen belts. This idea can then also be co[n]nected with the changes in the nature of t[he] Van Allen belts associated with magnetic storm[s] which are generally accompanied by large sol[ar]

inds and large fluctuations in the outer fringes f the field.

II. Effect of Static Magnetic Anomalies

We mentioned in Section III that the three-imensional drift of the mirror point can be ollowed by staying on a surface of constant ield strength and adjusting the north-south osition so as to keep the integral invariant onstant. Any particle will have two closed aths, one in the northern hemisphere and one n the southern, traced out by its mirror points. or magnetic latitudes near 45° (that is, for the rgus shell) the northern path is fairly well be-aved with north-south excursions of 500 km or o and vertical excursions somewhat less. The outhern path is very distorted, however, owing o the large area in the South Atlantic where he total field strength is much less than that iven by the eccentric dipole (see Fig. 8). This nomaly causes the path to swing south of outh America to maintain the integral in-variant and to dip very low just west of Cape-town to find the surface of constant field strength. This last point is of greatest interest, since, as was shown in Section IV, it is the aver-age air density around the drift path that de-termines atmospheric loss rates. Because the air density is exponential, a small downward change in altitude over a fraction of the drift period may contribute overwhelmingly to the average density.

For the Argus data, the situation is more ex-treme. An electron mirroring over the eastern United States at altitudes below 800 km will find its southern drift path plunging into the ocean west of Capetown. That is, all the elec-trons seen by Jason rockets never lived to drift around the earth again. In passing through the anomaly, some particles at higher altitudes will be scattered down, however, to repopulate the low altitudes. The only change is from a picture of slow, steady loss to an impulsive loss once each drift period.

The time of transit through the anomaly is about 5 min for a 1-Mev electron. But the characteristic lifetime is just 5 min at 400 km. Now 400 km over the anomaly corresponds to a field strength of about 0.28 gauss. This field strength, then, is the dividing line between par-ticles that survive passage through the anomaly

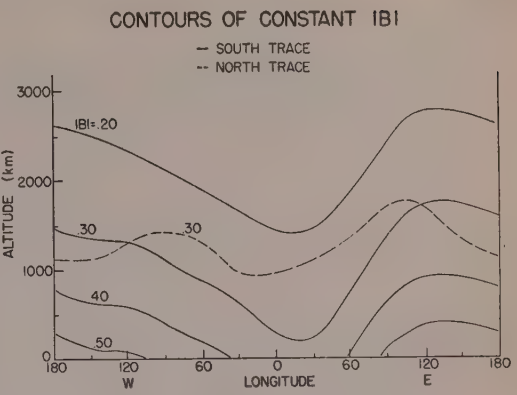

Fig. 8—The altitude of surfaces of constant scalar magnetic field strength versus longitude at the intersection of these surfaces with the Argus electron shell.

and those that do not. Inspection of the mirror-point density versus field strength curves com-piled from rocket and satellite data reveals a sharp change in slope at $B = 0.28$.

A further effect of the anomaly is to increase appreciably the average air density for particles high enough to survive several drift periods. This increased density shortens the character-istic lifetime over the data in Table 2, and may explain why the flux was not constant at early times. That is, we may never have made a measurement at any times shorter than a char-acteristic lifetime.

Having looked at the great effect of the anomaly, we believe now that future calcula-tions should start with the anomaly as the cen-terpiece instead of introducing it as a perturba-tion as we have done in this paper.

Acknowledgments—The role of the ambient plasma in checking the charge separation drift was pointed out by Dr. Conrad Longmire. The magnetic invariant formulation for the configura-tion of the electron shell was suggested by Dr. Theodore Northrup. Dr. Paul Nakada has con-firmed by more rigorous methods the results of the simple scattering theory used here.

References

Alfven, H., *Cosmical electrodynamics*, Oxford University Press, 1950.

Christofilos, N. C., Trapping and lifetime of charged particles in the geomagnetic field, *Univ. Calif. Radiation Lab. Rept.*, UCRL 5407 (un-published), 1958.

Fermi, E., *Nuclear physics,* Chicago University Press, 1950.

Harris, I., and R. Jastrow, Upper atmosphere densities from Minitrack observations on Sputnik I, *Science, 127,* 471–472, 1958.

Muehlhause, C. O., and S. Oleska, Antineu flux from a reactor, *Phys. Rev.,* 105, 1332– 1957.

Spitzer, L., *Physics of fully ionized gases,* I science Publishers, New York, 1957.

Optical, Electromagnetic, and Satellite Observations of High-Altitude Nuclear Detonations, Part I*

PHILIP NEWMAN

Propagation Sciences Laboratory
Electronics Research Directorate
Air Force Cambridge Research Center
L. G. Hanscom Field, Bedford, Mass.

Abstract—After each of the high-altitude detonations in the Argus experiment, visual auroras were observed in the detonation area. After the third event an aurora was observed in the conjugate area. After the second and third events, signals attributed to hydromagnetic waves were detected in the conjugate region; these signals had a periodicity of about 1 cycle per second. The maximum change in the magnetic field was about 1 gamma. If propagated along the magnetic line of force the velocity was about 2000 km/sec. Sporadic *E* was observed after the third event in the conjugate area. Comparative records of the 5577 A and 3914 A lines were obtained in the detonation area.

INTRODUCTION

In the planning of the Argus program it was realized that there might be effects that could be observed on the ground. The Air Force Cambridge Research Center (AFCRC) in cooperation with the Stanford Research Institute received the assignment for a setting up of surface instrumentation to make optical and electromagnetic observations. Originally, the chief emphasis was to be placed on the area magnetically conjugate to the detonation area. In the conjugate area some of the trapped electrons after each transit along the magnetic line would enter the atmosphere and possibly cause auroral and associated phenomena. As the electron shell spread around the earth, the conjugate area would move along the geomagnetic latitude. Later the program was enlarged to include the detonation area and a station in Spain to monitor Explorer IV. It should be stressed that the shortage of time made more than a minimal program impossible. It was planned to detonate the nuclear bombs so that the conjugate area would be in the vicinity of the Azores. An obvious problem was the possible occurrence of natural geomagnetic disturbances. There was an appreciable disturbance on the day of event I and for several days between events II and III.

POSSIBLE EFFECTS

Auroral phenomena—In addition to the luminosity of the aurora which can be observed visually or by cameras, in particular the all-sky camera [*Little et al.*, 1956] developed by auroral investigators, natural auroras have characteristic spectral lines, the most prominent being the atomic oxygen lines, the red one at 6300 A, the green line at 5577, and the violet nitrogen lines at 4278 and 3914. In addition, there are hydrogen lines, which are attributed to protons. Since an Argus aurora, if any, would be caused primarily by electrons [*Fowler and Waddington*, 1958], the oxygen and nitrogen lines would be of principal interest. It was decided to employ the lines 3914, 5577, and 6300 and a spectrograph, but we were not successful in obtaining the latter two items. The spectrophotometers used were built in AFCRC shops. With increasing height, 3914 increases relative to 5577 [*Harang*, 1951a]; another important difference between the lines is that in the ever-present night airglow at non-auroral latitudes the 3914 line is generally very weak or absent whereas the 5577 line is always present and moreover shows a strong preference for the 100-km level [*Koomen et al.*, 1957].

* Presented at the Symposium on Scientific Effects of Artificially Introduced Radiations at High Altitudes held at the National Academy of Sciences, April 29, 1959. This paper is being published simultaneously in the August 1959 issue of the *Proceedings of the National Academy of Sciences.*

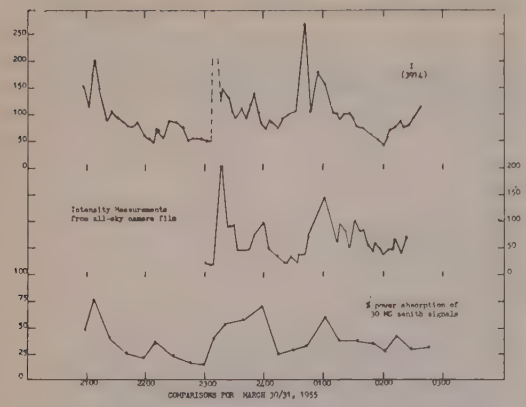

FIG. 1—Comparison of auroral intensity with zenith absorption.

During natural aurora the absorption of radio waves in the HF band by the *D* layer of the ionosphere is increased. This effect can be observed by the diminution in the strength of reception on the ground of cosmic radio noise. Figure 1 shows how these effects are correlated; it was taken from a report of the University of Alaska on investigations sponsored by AFCRC [*Little et al.*, 1956].

A second important property of most auroras is their ability to reflect *radio waves* [*Bullough and Kaiser*, 1954, 1955; *Kaiser*, 1955; *Peterson et al.*, 1955]. This effect is most pronounced in the 10 to 100 Mc/s range, but by employing high power and large antennas, reflections have been obtained up to 800 Mc. Figure 2 shows a reflection from an aurora near the city of Quebec, Canada, observed on the scope of an 18-Mc radar operated by AFCRC at Plum Island, north of Boston. The lower return is ground backscatter via *F*-layer reflection. Beyond the aurora is ground backscatter via reflection from the aurora or from sporadic *E* accompanying the aurora. The distance to the aurora is about 250 miles. The optimum position for the radar beam is in the direction of geomagnetic north and intersecting the magnetic lines at right angles at ionospheric heights. The frequency selected for the Argus tests was 27 Mc.

Other effects that frequently accompany auroras are disturbances in the earth's magnetic field, changes in ionospheric electron densities, formation of sporadic *E*, and variations in earth current. Figure 3, from Harang's *The Aurorae*, illustrates the change of ionospheric struct during an aurora. Figure 4 shows reflect from a sporadic *E* layer, and also multiple flections, as obtained on an ionosonde [*Wri et al.*, 1957].

Magnetic and electromagnetic effects—T explosion would cause a shock wave in the m dium which should propagate as a hydrom netic wave or Alfven wave, the preferred mo being along the magnetic line of force [*Spita* 1956; *Grad*, 1959]. This effect should then detectable on the ground by very low fi quency (VLF) equipment or by magnetomet A change in the magnetic field not only co be caused by the hydromagnetic wave but a could be induced by an electric current in t atmosphere. Several equipments were availa in the Azores region to monitor possible effe A VLF (300 cps to 30 kcs) receiver was up with a whip antenna which would meas the electrical field of an electromagnetic eff of the whistler type [*Gallet*, 1959; *Helliw and Morgan*, 1959; *Hines*, 1957; *Morgan*, 195 This was supplemented by ELF equipment (

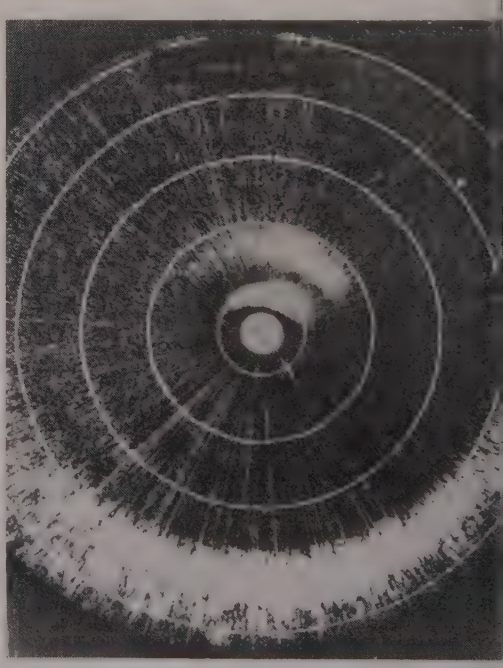

FIG. 2—Eighteen-megacycle-per-second radar r turn obtained at Plum Island, Mass. Concentr circles indicate 500-mile range. Innermost retu is auroral reflection. Ground backscatter reflect via F_2 layer appears at bottom of illustration.

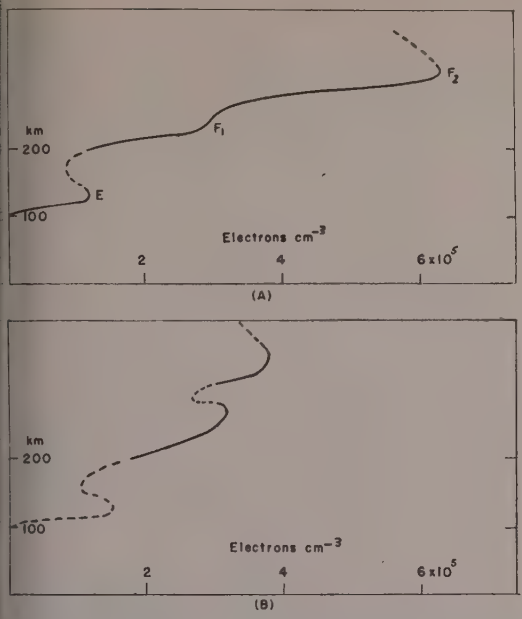

FIG. 3.—Changes in the constitution of the ionosphere from a quiet day (*A*) to a disturbed day (*B*).

to 30 cycles) attached to three mutually orthogonal loops which would measure the rate of change of the magnetic field (Fig. 5). In addition there was a heliflux magnetometer and a variable-μ magnetometer to measure the static magnetic field.

SITING OF EQUIPMENT

The VLF, ELF, and magnetic equipment just

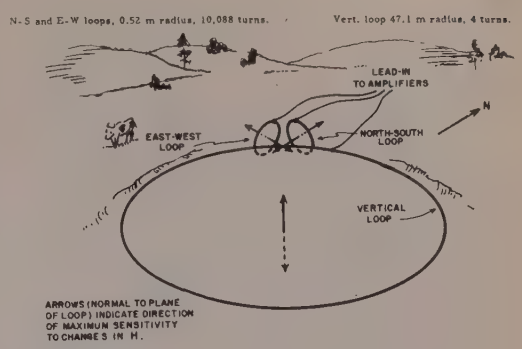

FIG. 5—Positions of the detector loops used for the ELF detector.

alluded to were located on the Azores. At the same location there were riometers [*Little and Leinbach,* 1959], which are essentially receivers designed to measure the absorption of the cosmic radio noise; they were at 30, 60 and 120 Mc. There were also an all-sky camera and photometers. Two C-97 aircraft were based on the Azores, each carrying an ionosonde and one carrying also an all-sky camera and photometers. The photometers had inference filters 80 A wide at 3914 and 5577 and employed an RCA 6810-A 14-stage photomultiplier. The 27-Mc radar for observing radar reflections was on the *USS Albemarle.* The plan called for the *Albemarle* to be sited about 400 miles south of the expected conjugate point; it also carried an all-sky camera, a set of photometers, and a set of riometers. This equipment, like the equip-

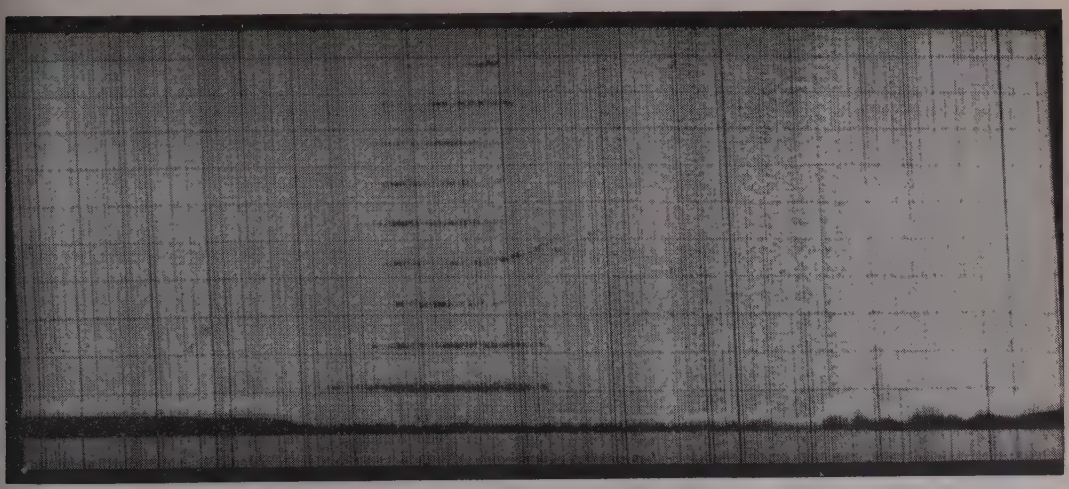

FIG. 4—Ionosonde records of sporadic *E* and multiple reflections.

ment in the aircraft, served as insurance if the conjugate area for any reason did not occur where planned.

At the site in Spain there was a Microlock receiver to monitor Explorer IV. In addition, an all-sky camera, photometers, VLF receivers, and riometers were placed there should the auroral effect spread eastward. Regular magnetic stations as well as IGY airglow and auroral stations were also available to observe effects.

In the detonation area, there were magnetic detectors, all-sky cameras, and other equipment including VLF receivers, a 30-Mc riometer, a 27-Mc radar, and photometers at 3914 A and 5577 A.

Brief Summary

Visual aurora were sighted for all events in the launch area; in the conjugate area, possibly for the first and unmistakably for the third.

Radar reflections were obtained for all events except in the conjugate area for event II.

Changes in magnetic field were observed in the launch and conjugate area; in the conjugate area, for events II and III; in the launch area, for event III.

Very low frequency. Field-strength recordings of GBZ on 19.6 kc made in the Azores and Spain showed decreases of 6 to 12 db after events II and III. Recordings at Stanford, California, on 18.6 and 17.1 kc showed slight increase.

Sporadic *E* was noted in the conjugate area.

The Explorer IV transmissions were successfully monitored at the Spanish site. The data were incorporated with other satellite data upon which Dr. Van Allen has reported.

Part I of this paper will discuss briefly the aurora and ELF results; in Part II, which follows, the radar, riometer, and satellite results will be covered.

The Visual Aurora in the Conjugate Area

After shot 1 an observer in one of the aircraft reported that he sighted an orange glow, in a direction which made sense, 23 min after the burst. No sighting was reported after the second, although the reported position of one of the aircraft was not too far from the computed conjugate point.

After shot 3 a brilliant auroral display wa witnessed by Captain Minter and the cre of the *USS Albemarle* and by civilian scientis aboard. The direction was given as 282°T whereas geomagnetic north was about 340 The estimated spread in azimuth varied fro 3° to 8° to 45°, but the last estimate may b the result of reflection from clouds which co ered seven-tenths of the sky. The elevation wa estimated to be from 15° to 30°.

One observer estimated the distance to b about 300 to 600 miles, and the duration given as about 0.5 hr. The aurora observed a the Apia observatory [*Cullington*, 1958] in th south Pacific after the August 1 Johnston Islan detonation was reported to have lasted 14 mi

The description of one of the observers, M Orange of AFCRC, follows:

> The effect began as a blue-green "spear" star ing close to the horizon, climbing in back of cloud, and reappearing above the cloud. The e fect first appeared about a half a minute aft detonation. This is within a few seconds as I ha previously set my watch by WWV. A short tim after the onset of the effect, about a half a mi ute, a red crown developed at the head of th bluish spear. The red was distinct but not as bright as the green. For the next minute the re spread out while the blue-green lost intensity The red aurora deepened in color, began to fade and after 4 minutes was no longer visible. Th blue-green spread out and became an indistinc luminous glow covering about 45 degrees of hori zon up to about 30 degrees high. This glow slowl faded and was gone about 32 minutes after aurora began.
>
> The brightest part of the initial display wa extremely intense as the edges of the cloud whic obscured the center of the display were outline clearly, as if the moon were behind the cloud.
>
> My position was on the fantail of the *Albe marle* with a clear view of the northern sky. My eyes were adjusted to the darkness and I was ex pecting the event.

The other observers placed the duration a varying periods, 5 min to 0.5 hr. One observe thought that the aurora spread from a cente and did not observe an upshooting pulse, bu this he could easily have missed. The observa tions were complicated by cloud cover whic was placed at about seven-tenths. In fact, th observations were made possible only by a opportune break in the clouds just before the event.

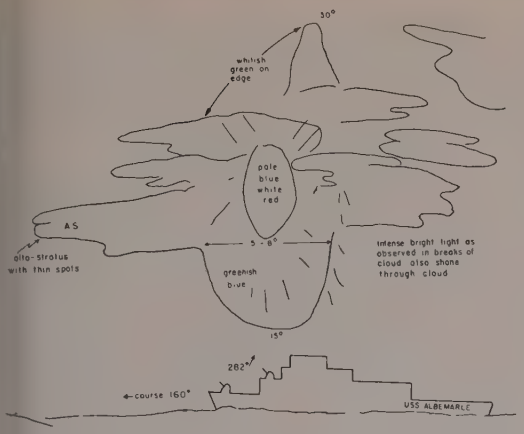

FIG. 6—Sketch of view from *USS Albemarle*.

One of the sketches is presented here (Fig. 6). The top crown of red noted by Mr. Orange would appear to come under Vegard's classification of Type A [*Vegard*, 1957] attributed in natural aurora to proton excitation. It was generally assumed that the effects in the conjugate area, if any, would be produced by electrons from the detonation [*Koomen et al.*, 1957] rather than by heavy ions. In this connection it is worth noting that a recent article by the Russian *Galperin* [1959] gives a high degree of correlation between the occurrence of radar returns and the presence of protons as evidenced by the hydrogen lines in the spectrum of the aurora. Perhaps the movement of heavy ions into the conjugate area should receive more serious consideration.*

It is notable that the duration of the red crown is given as about 4 min. During two of them the radar return was expanding in range, as will be seen later. Table 1 shows possible heights of the aurora and corresponding ranges for given elevation angles. It will be observed that the estimated distances correspond to auroral heights of about 150 to 350 miles. The initial radar range of 500 miles gives a height in this bracket, if we assume that the radar return comes from the region in which the visual aurora is taking place. The greater radar ranges would imply returns from even greater altitudes unless the returns were from nonluminous parts of the sky.

A height of 100 km for the aurora at a range of 800 km requires an elevation angle of 2°48′, apparently below the visual aurora. In this case, the ground conjugate point is deviated by about 170 km to the northeast of the conjugate point for event III computed at the RAND Corporation by Vestine and Karzas. The range of 800 km and elevation angle of 15° yields a minimum height of about 200 km for the aurora and a deviation of the ground conjugate point of about 280 km to the northwest.

Figure 2 shows the possibility of extension of range by ground scatter; this does not appear a satisfactory explanation in view of the smooth extension of radar range reported in Part II, Figure 5, of this paper, but may be applicable to later stages of the radar return.

If we accept the value of 8° for the width of the visual aurora, and employ the radar range

TABLE 1—*Range versus height for various elevation angles*

Elevation angle	Height, miles	Range, miles
10°	60	290
	100	440
	130	545
	160	640
	200	760
15°	60	215
	100	325
	130	440
	160	525
	200	615
	375	1015
20°	60	170
	100	270
	130	340
	160	415
	200	505
	300	720
30°	60	115
	100	195
	130	250
	160	310
	200	375
	300	500
	400	715

* However, A. Omholt in a paper presented at the May 1959 AGARD Symposium, "Ionization above F_{max}," attributes both high and low auroras to fast primary electrons.

of 500 miles, we find a width of about 75 miles for the visual aurora.

Visual Observations in the Launch Area

(*a*) All three events were accompanied by colorful aurora which elongated in a direction making an angle of 10° with the magnetic *N-S* direction. A sketch of the aurora produced by shot 3 is shown in Figure 7.

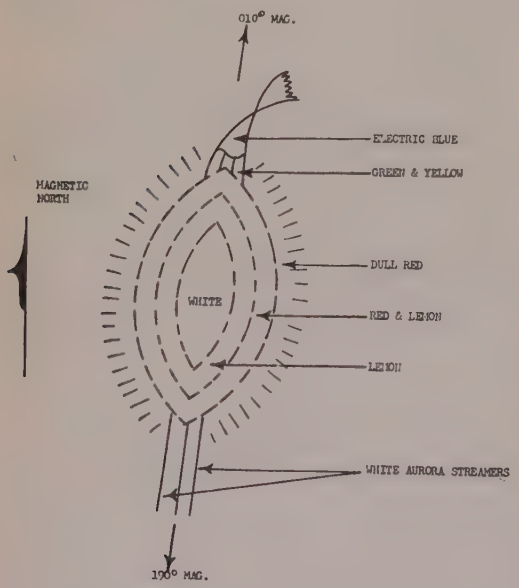

Fig. 7—Sketch of short 3 phenomena by pilot of aircraft in launch area.

(*b*) Records obtained for each of the events on the 5577 and 3914 photometers served as a check on detonation time. We may assume that the effect is mainly caused by the excitation of atmospheric oxygen and nitrogen, since the prompt flash is over in microseconds. The high ratio of 5577 to 3914 (Fig. 8), about 10 to 1, for event III is much higher than is usually found in natural auroras [*Harang*, 1951b]. The result suggests strong excitation of the 100-km level by fission products.

Magnetic Field Effects

ELF in conjugate area—The ELF receiver operating in the frequency range 0.3 to 30 cps obtained results on events II and III but not on event I. Two points should be made about event I: it took place during a geomagnetic disturbance which was accompanied by unusually severe radio blackout; the magnetic line on which the detonation took place and along which an effect presumably would have been propagated passed through the lower of the recently discovered radiation belts.

For event II, two of the coils *N-S* and vertical were operational. Unmistakable signals were obtained distinguishable from the background by their greater amplitude and lower-frequency components. The frequency components of the signal, equated to harmonic equivalent, varied from 1/2 to 2 cps. The equipment is about 2 times more sensitive at 10 than at 1 cps, so that 10 cps tends to dominate the noise background (Fig. 9). The *N-S* signal appeared at about plus 13 sec. Large changes were in evi-

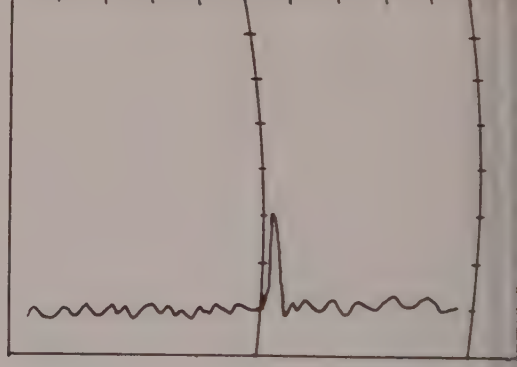

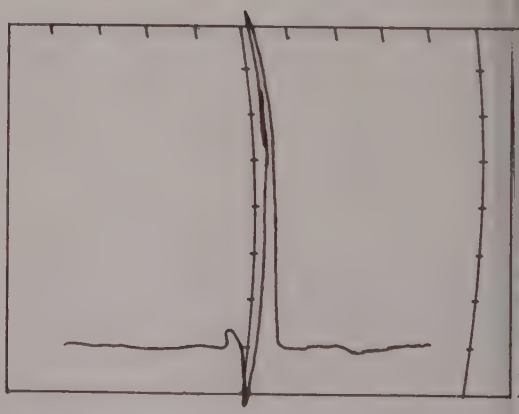

Fig. 8—Photometer measurements at detonation point. Above, 3914 A line, deflection 0.1 volt per division. Below, 5577 A, 0.2 volt per division. Chart speed, 1 large division per second.

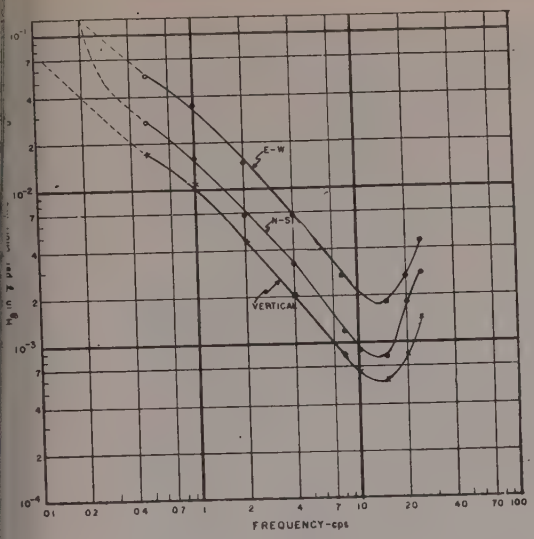

FIG. 9—Calibration of magnetic detector coils. ($1\gamma = 10^{-5}$ gauss.)

dence for about 13 sec., with the highest rate of change off scale occurring at about plus 16 sec. The *V* component attained its maximum rate of change about 0.5 sec earlier. Assuming a 1 cps frequency, the *N-S* magnetic component had a maximum change of about 1/2 γ; the *V* component had a much smaller change.

For event III (Fig. 10), all equipments operated and the signal went off scale. There may be a signal between plus 4 and plus 6 sec, but the first large rate of change occurs at about plus 12 sec on the *E-W*. The strong signals were not harmonic. Estimates of the amplitudes, assuming a 1 cps pulse, give the amplitude of the magnetic change as 3/4, 3/2, and 1/2 γ for *N-S*, *E-W*, and *V* components.

A sinusoidal waveform signal of 1 cps can be observed at plus 31, at plus 42, and possibly at plus 14 sec, all lasting for about 4 to 6 sec. It was strongest at plus 42, with amplitude of 1/4, 1/2, and 1/25 γ for the *N-S*, *E-W*, and *V* components.

The *ground speed* of propagation of the strong disturbance from the detonation point would be about 700 km/sec. If we assume that the disturbance followed the magnetic line through the detonation, the average speed would be about 2000 km sec. If we accept a signal at 4 to 6 sec for event III we find a speed almost 3 times as great. Recent estimates by *Dessler* [1958a, b] give propagation speeds for an Alfven wave in the upper atmosphere of 300 to 1000 km/sec. Unpublished theoretical work of J. H. Piddington, privately communicated by G. R. A. Ellis (CSIRO, Australia), indicates the possibility of much higher velocities than those given by Dessler [*Gerard*, 1959].

It is of interest that a magnetic station operated by the Signal Corps employing a 52 square mile horizontal loop appears to have picked up signals after event III of about 1/400 γ with a periodicity of about 1 cps (Fig. 11). The signals appeared at plus 4 and at plus 20 sec. Using the plus 4, we find a ground speed of about 3000 km/sec, and for an upper atmosphere path this figure would have to be approximately doubled.

The ELF receiver was built at AFCRC for this project. The horizontal loop was 141 meters in diameter and had four turns of wire. The other two, 1 meter in diameter, had 10,000 turns.

A magnetic detector in the launch area recorded an initial 1-sec-pulse signal of about 1 cps for event III, with a strength of over 10 γ followed by longer-period pulses (Fig. 12). The total duration with irregular fluctuation was about 1.5 min.

The Ionosondes

The ionosondes carried in the two C-97's at the Azores were generally not in good position to observe ionospheric effects except possibly for event II, as mentioned earlier. One effect may be worth noting, however, although its direct relation to the event is open to question. For event III, one aircraft, because of weather, flew east, the other remaining on the ground at Lajes. When the ionosonde in the grounded plane was turned on, about 18 min after the event it observed sporadic *E*. The airborne sounder was about 120 miles east of Lajes and not observing any sporadic *E*. On returning, the airborne sounder found sporadic *E* about 330 miles east of Lajes about 1 hr and 50 min after the event (see Fig. 4). The sporadic *E* at Lajes had disappeared. Sporadic *E* continued to be observed by the airborne sounder for about 50 min as the aircraft approached Lajes.

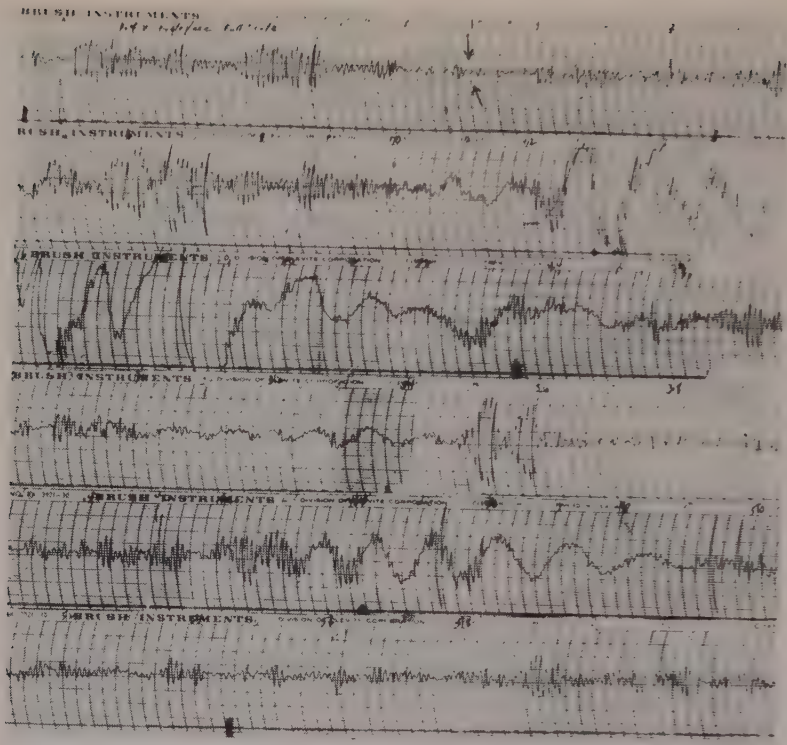

FIG. 10—ELF magnetic signals received in Azores Sept. 6, 1958. Chart speed, 5 divisions per second. Arrow indicates detonation. *E-W* coil.

CONCLUSIONS

The high-altitude nuclear detonations showed that it is possible to generate auroras of limited extent and hydromagnetic waves; a new tool is available for making controlled auroral and upper-atmosphere studies.

Acknowledgment—The Air Force Cambridge Research Center effort involved the participation of many people. Mr. R. Harvey had general charge of equipment, and Mr. N. Oliver and Mr. T. Markham installed the all-sky cameras. Lt. R. Koehler constructed and calibrated the ELF equipment and participated in its operation. Mr. E. J. Chernosky was in charge of the magnetic program. The advice of E. Maple in the analysis of the ELF records was very helpful. Messrs. Orange, Eng, Straka, and McCabe operated equipment on the naval vessels. Messrs. Miner, Cameron, Shapiro, and Romano operated the ionosondes in the C-97. The formidable logistics was under the able management of Major C. Wood, Captain R. Yates, Captain E. Angell, and Mr. J. Murphy.

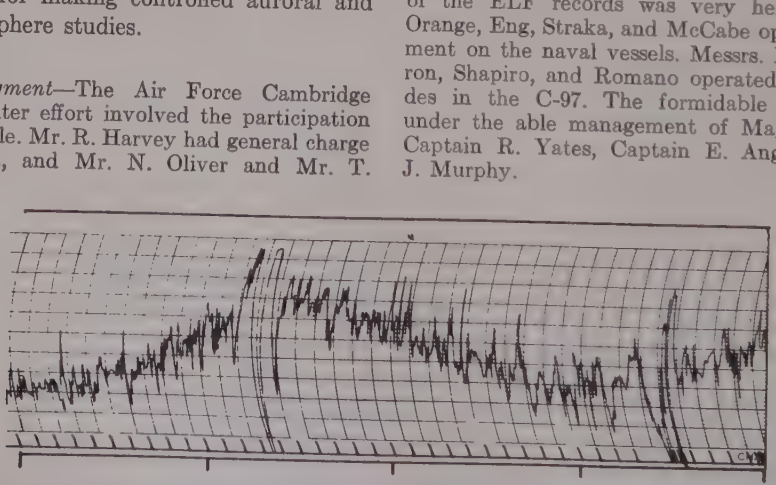

FIG. 11—One cycle per second magnetic bursts, Grand Canyon, Sept. 6, 1958, full scale: ± 2.5 mv. (after A. K. Harris and H. Berthold).

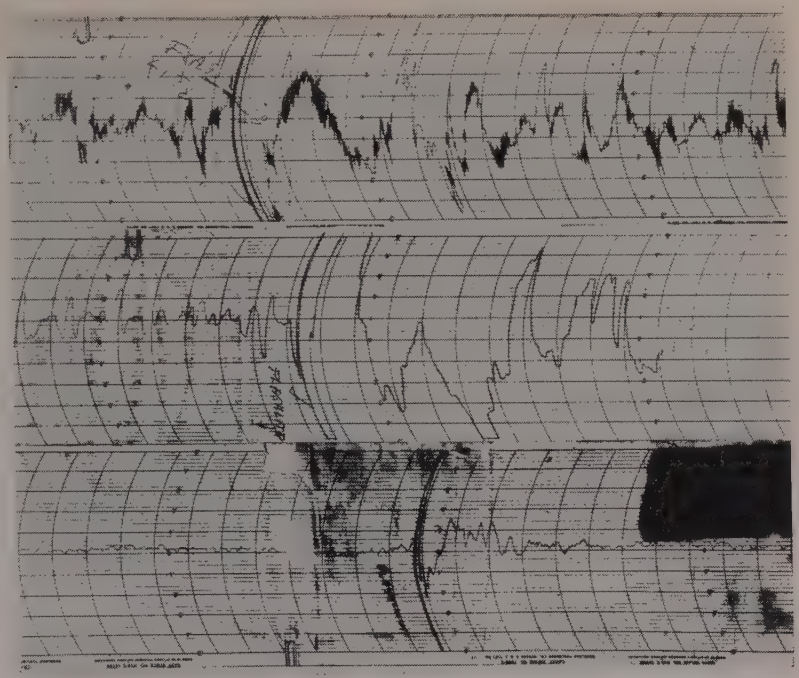

FIG. 12—Magnetic record at launch point, Sept. 6, 1958. Chart speed: top two rows, 8 divisions per minute; bottom row, 4 divisions per minute.

REFERENCES

BULLOUGH, K., AND T. R. KAISER, Radio reflections from aurorae, *J. Atmospheric and Terrest. Phys.*, 5, 189–200, 1954.

BULLOUGH, K., AND T. R. KAISER, Radio reflections from aurorae—II, *J. Atmospheric and Terrest. Phys.*, 6, 198–214, 1955.

CULLINGTON, A. L., A man-made or artificial aurora, *Nature*, 182, 1365–1366, 1958.

DESSLER, A. J., The propagation velocity of world-wide sudden commencements of magnetic storms, *J. Geophys. Research*, 63, 405–408, 1958a.

DESSLER, A. J., Large amplitude hydromagnetic waves above the ionosphere, *J. Geophys. Research*, 63, 507–511, 1958b.

FOWLER, P. H., AND C. J. WADDINGTON, An artificial aurora, *Nature*, 182, 1728, 1958.

GALLET, R. M., The very low-frequency emissions generated in the earth's exosphere, *Proc. IRE*, 47, 211–231, 1959.

GALPERIN, G. L., Hydrogen emissions and two types of auroral spectra, *Planetary and Space Sci.*, 1, 60, 1959.

GERARD, V. B., The propagation of world-wide sudden commencements of magnetic storms, *J. Geophys. Research*, 64, 593–596, 1959.

GRAD, H., Propagation of magnetohydrodynamic waves, *N. Y. Univ. Report TID 4500*, Jan. 15, 1959.

HARANG, L., *The Aurorae*, John Wiley and Sons, New York, 1951: (*a*) p. 152; (*b*) p. 77.

HELLIWELL, R. A., AND M. G. MORGAN, Atmospheric whistlers, *Proc. IRE*, 47, 200–208, 1959.

HINES, C. O., Heavy-ion effects in audio-frequency radio propagation, *J. Atmospheric and Terrest. Phys.*, 11, 36–42, 1957.

KAISER, T. R., in *The Airglow and the Aurorae* (a symposium held at Belfast in Sept. 1955), ed. by E. B. Armstrong and A. Dalgarno, Pergamon Press, New York, 156–173, 1955.

KOOMEN, M. J., et al., in *Threshold of Space*, ed. by M. Zelikoff, Pergamon Press, New York, p. 222, 1957.

LITTLE, C. G., et al., Radio propagation in the Arctic, *Univ. of Alaska, Final report on contract AF(604)-1089*, 15 April 1956.

LITTLE, C. G., AND H. LEINBACH, The riometer—a device for the continuous measurement of ionospheric absorption, *Proc. IRE*, 47, 315–320, 1959.

MORGAN, M., Whistlers and dawn chorus, *IGY Ann.*, 3, Part 4, 315–321, 1957.

PETERSON, A. M., O. G. VILLARD, JR., R. L. LEADABRAND, AND P. B. GALLAGHER, Regularly-observable aspect-sensitive radio reflections from ionization aligned with the earth's magnetic field and located within the ionospheric layers at middle latitudes, *J. Geophys. Research*, 60, 497–512, 1955.

SPITZER, L., *Physics of Fully Ionized Gases*, Interscience Publishers, Inc., New York, 1956.

VEGARD, L., in *Threshold of Space*, ed. by M.

Zelikoff, Pergamon Press, New York, 22–31, 1957.

Wright, J. W., R. W. Knecht, and K. Davies, Ionospheric vertical soundings, *IGY Ann.*, Part 1, 1957.

(Manuscript received June 15, 1959.)

Optical, Electromagnetic, and Satellite Observations of High-Altitude Nuclear Detonations, Part II*

ALLEN M. PETERSON

Stanford University
Stanford Research Institute
Stanford, California

Abstract—The radio effects of the Argus detonations were measured using (1) 30-Mc radars designed to obtain echoes from the aurora or from the earth's surface mirrored in an enhanced ionospheric layer, (2) VLF receivers for monitoring distant transmitters or atmospheric noise sources in search of changes in signal strength, (3) riometers for recording cosmic noise absorption or VHF shot-created noise at 30, 60, and 120 Mc.

Results included (1) auroral echoes in the vicinity of the launch point after all three shots and near the conjugate points after the first and third shot, (2) sudden depressions of 6 to 12 db of the signal from England (19.6 kc) at Madrid and the Azores, (3) no ionospheric absorption at the conjugate location.

RADAR OBSERVATIONS OF AURORAL IONIZATION

It was anticipated that a by-product of the explosion of a nuclear device at very high altitudes might be the generation of an artificial aurora. Not only would a fraction of the high-energy β-decay electrons enter orbits which would result in penetration of the ionosphere, but highly ionized heavy-particle debris from the explosion might also enter the ionosphere and participate in the generation of an aurora. Since ionized particles are constrained to follow the earth's magnetic field, it was believed that auroral displays might be observable both in the southern hemisphere near the explosion and in the northern hemisphere near the magnetic conjugate point. See Figure 1.

It has been discovered that the mechanism which creates the visual display of the natural aurora also creates ionization [*Nichols*, 1959; *Schwinger*, 1949] in the upper atmosphere which is capable of reflecting and absorbing radio waves. As a result, within the last two decades radio and radar methods have become very valuable in research on the aurora. A radar does not see exactly the same thing as the eye or the camera, but it has the great advantage that it can detect auroral ionization through clouds or in daylight. Radio and radar echoes have, in the case of the natural aurora, been observed at radio frequencies between a few megacycles and a few hundred megacycles. The number of auroral radar echoes observed and their strength are markedly dependent on the orientation of the earth's magnetic field lines with respect to the observing location. Reflection of radio waves from the aurora behaves as if scattering takes place in a region filled with long thin columns of ionization aligned along the earth's magnetic field. Radar echoes are obtained most readily when it is possible to

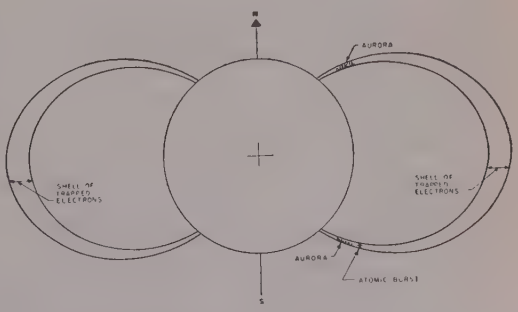

FIG. 1—Generation of auroras at atomic explosion and at magnetic conjugate region.

* Presented at the Symposium on Scientific Effects of Artificially Introduced Radiations at High Altitudes held at the National Academy of Sciences, April 29, 1959. This paper is being published simultaneously in the August 1959 issue of the *Proceedings of the National Academy of Sciences.*

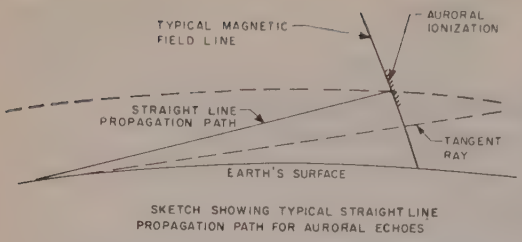

FIG. 2—Reflection at perpendicular incidence from elongated ionization irregularities aligned with the earth's magnetic field.

make a perpendicular reflection at an earth's magnetic field line in a region in which auroral ionization is being produced. The requirement for perpendicular incidence is not an absolute one and is a function of frequency. A sketch showing the geometry involved is presented in Figure 2.

The net effect of the aspect-sensitive reflection geometry is to limit the region of the sky from which radar echoes are observed. As a result of the geometrical considerations, radar echoes are difficult to interpret. Not only is the occurrence of the aurora required in the region which the radar is surveying, but also the geometrical conditions must be appropriate.

Figure 3 illustrates the regions in which perpendicular reflection at an earth's magnetic field line can take place for a radar location near 45° magnetic latitude. It can be seen in Figure 3(*a*) that, looking in the geomagnetic north direction, perpendicularity can be achieved at heights to about 300 km. In (*b*) is shown a polar plot of the contours of perpendicular reflection for different heights above the earth. Reflection geometry is favorable only for regions to the north of the radar for a location in the northern hemisphere, such as was assumed in constructing Figure 3; for radar locations in the southern hemisphere, the favorable reflection regions would lie to the south of the radar.

It is known from the natural aurora that the height region of most intense ionization occurs near 100 km and that radar echoes are most often observed from such heights. However, just as visual displays are observed at heights of several hundred kilometers [*Störmer*, 1955], radar echoes are sometimes observed up to 300 or 400 km.

TABLE 1

Frequency	27 Mc
Peak power	7.5 kw
Pulse length	Adjustable, 150–10(μsec
Pulse repetition frequency	Adjustable, 15–30 p
Antenna	3-element Yagi arr horizontally pola ized, mounted fon tation in azimuth
Receiver bandwidth	1–6 kc

In the interest of obtaining maximum det tion sensitivity for auroras with relatively s ple equipment, experimental radars operat at a frequency near 27 Mc were designed constructed for use in the Argus experime

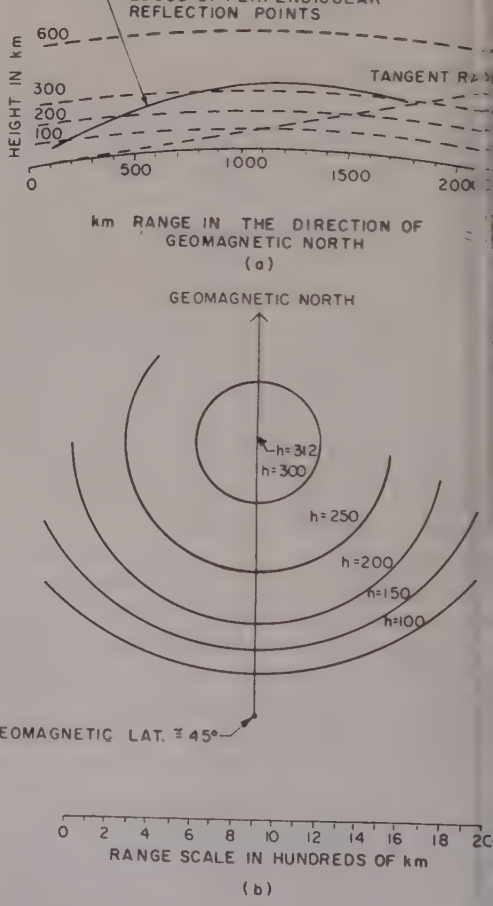

FIG. 3—Regions at which perpendicular reflection at an earth's magnetic field line can take place

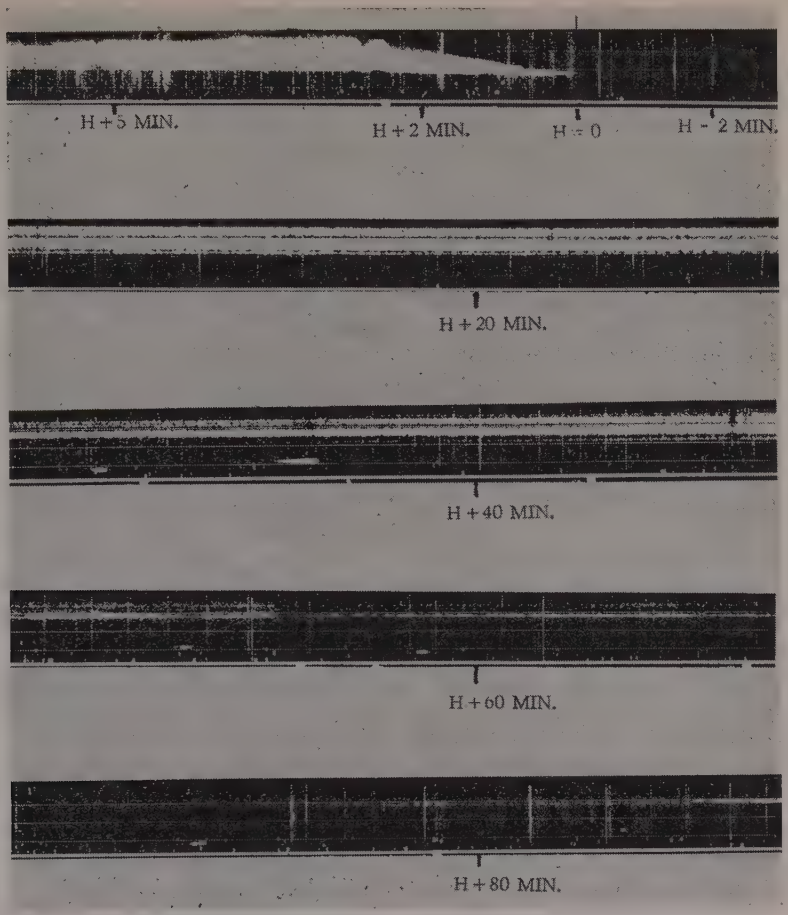

FIG. 4—Auroral echoes following explosion 3. Radar in region near magnetic conjugate point.

Equipment with similar characteristics has been installed in many parts of the world as a part of the United States IGY program in ionospheric physics [*Peterson et al.*, 1959]. These radars (backscatter sounders), operating at frequencies near 30 Mc, have proved very satisfactory in studies of echoes from field-aligned irregularities in the aurora. The characteristics of the 27-Mc radars used in the Argus experiments are shown in Table 1. In the Argus experiments, two of these special radars were used, one on a ship near the explosion, and one on a ship near the conjugate magnetic field point.

Auroral radar echoes were obtained on all three explosions by the radar near the launch end, and on events I and III by the radar near the conjugate points. Negative results on the conjugate end radar for event II were probably caused by unfavorable location of the ship. Range-versus-time photographs of the echoes observed at the conjugate-region radar are shown in Figure 4. The echoes appeared within seconds after the explosion at the launch radar, and somewhat later, although less than a minute, at the conjugate-region radar. The echoes were observed in one case for 1 hr and 15 min at the conjugate-region radar, and in one case for 5 hr at the launch-region radar.

In Figure 4 it can be seen that the echoes moved outward in range. Although initially there is a single well defined echo, at some stages in the echo development more than one trace is visible, and the echo at times becomes

very spread in range. It appears probable that part of the time a sporadic ionization patch existed, which was capable of reflecting the 27-Mc radio waves down to earth at a distant point and which produced "ground scatter" echoes. However, it is believed that most of the observed echoes were directly back-scattered from field-aligned irregularities. A combination of visual auroral observations and the radar records of Figure 4 permitted the conjugate magnetic point to be located. This measured conjugate point agreed with theoretical expectations to within less than 100 km.

VLF Radio Observations

Observations of the variations in propagation characteristics of radio waves in the VLF range (300 to 30,000 kc) have for many years been known to be a sensitive indication of conditions in the lower ionosphere (below 100-km height). In addition to VLF communications transmitters, operated in many parts of the world, the "atmospherics," signals propagated from lightning strokes, provide a source of signals that can be recorded in the VLF range. The VLF signals can be enhanced by increased ionization at the height of reflection in the ionosphere and reduced by absorption caused by increased ionization at lower levels of the ionosphere through which the signals must pass.

For the Argus experiments, VLF equipment was designed, constructed, and installed at operating locations by personnel of the Stanford University Radio Propagation Laboratory u der the direction of Professor R. A. Helliw It consisted of a broad-band receiver, loop a tenna, magnetic tape recorder, and associat calibration equipment, and was similar to t IGY whistler recorders [*Helliwell and Morg* 1959].

During the Argus experiments, VLF reco ings were made in the launch region, at a nu ber of locations in the conjugate region, and Stanford University. These recorded data ha been studied in a search for possible effects the ionosphere which might result from t trapped shell of electrons extending around t world [*Christofilos,* 1958] or for possible lo effects in the launch or conjugate area. T broadband VLF recordings (300 to 30,000 p include the narrow-band signal from a nu ber of VLF radio stations which was stud by observing the tape recordings through tunable narrow-band filter. Signals of particu interest in the conjugate area were those fr station GBZ in England on a frequency 19.6 kc (Fig. 5). Recordings of this stati taken in the Azores and in Spain showed abr decreases in signal strength, after Argus eve II and III, which amounted to 6–12 db. (Eve I data have not yet been analyzed.) The signa remained reduced in strength for nearly 0.5 h Decreases in signal strength in Spain co menced a few seconds later than in the Azore which are closer to the conjugate area. A Stanford in California, the signals from NPG Seattle (18.6 kc) and NDT in Japan (17.1 k

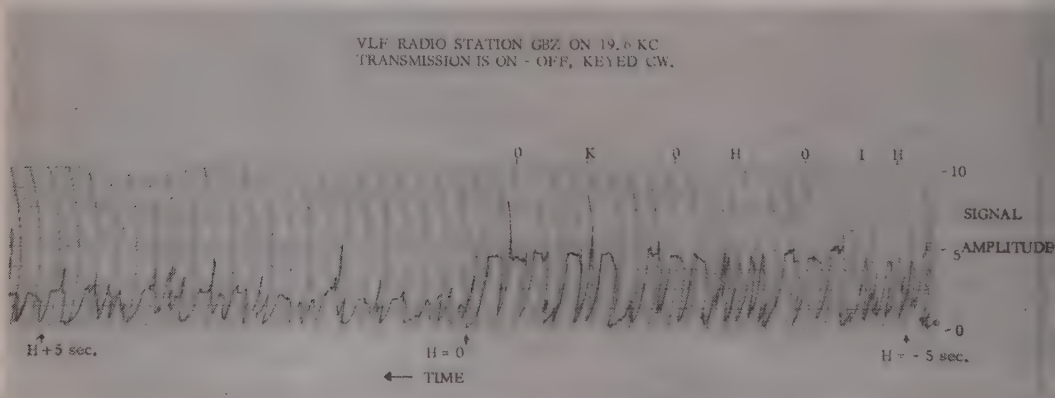

Fig. 5—Recording taken in the Azores of VLF station GBZ in England.

re analyzed for events II and III, and both owed slight increases in strength for some nutes after the explosions. A possible explana- n for these observations is that the elec- ons scattered from the Argus shell (and near e conjugate area the ionized debris) actually anged the ionization in the lower ionosphere, parently penetrating to lower heights and oducing absorption in regions relatively near e conjugate area. In the Pacific, far removed om the original injection region in the Atlan- , an enhancement of signal strength was ob- rved, perhaps indicating increases in ioniza- n density near the reflection points.

In addition to these observations, the level signal strengths from distant atmospherics being analyzed to seek further substantiation these results. It had been suggested that histlers or other VLF noise emissions [*Dyce id Nakada,* 1959; *Gallet,* 1959; *Helliwell and Morgan,* 1959] might accompany the nuclear xplosions and might be observable in the unch or conjugate areas. A search of the VLF cordings has been made for signals of this ype, but none have been found.

Riometer Measurements

The riometer [*Little and Leinbach,* 1959] is a ensitive, self-balancing, noise-measuring piece f equipment that has been designed for rou- ne determination of ionospheric absorption y monitoring the power level of cosmic noise hat has propagated through the ionosphere. pplication of this technique during the IGY as resulted in quantitative measurements of nospheric absorption in the high-frequency and during auroral disturbances and sudden nospheric disturbances (SID's).

In the riometer a local noise source is con- nuously made equal to the noise power from he antenna. The receiver is used merely as a etector of inequalities between the noise out- ut of a temperature-limited vacuum noise iode and the noise from the antenna; it gen- rates a d-c output voltage proportional to his noise difference. The d-c voltage is used o change the filament temperature and hence he output noise power of the noise diode in uch a direction as to reduce the inequality of ntenna and noise diode powers to zero. The oise power from the noise diode is directly proportional to the direct current flowing through it, and, therefore, the antenna noise power can be measured on a linear scale by recording the noise diode current on a pen recorder.

The IGY riometers operate on a single frequency near 30 Mc and have been used with great success in a synoptic network during the IGY. As a part of the Argus measurements, three riometers stations were operated in a network near the conjugate region. These installations made use of three receivers operating on frequencies near 30, 60, and 120 Mc. The antennas were vertically directed three-element Yagi arrays of about 60° half-power beamwidth. A single-frequency (30-Mc) riometer was operated near the launch end during the Argus experiments.

All these units operated satisfactorily during the Argus experiments, although the results were negative in that no significant absorption increases were recorded following the three events.

The riometer measurements demonstrated that, although there was sufficient perturbation of the ionosphere by the Argus experiments to produce reduced signal strength or absorption of VLF signals, the perturbations were either not large enough or not widespread enough to be detectable on equipment sensitive to absorption in the high-frequency range.

Another purpose of the riometer network during the Argus experiments was to provide a sensitive indication of noise generation by trapped electrons. High-energy relativistic-velocity electrons spiraling in magnetic fields have been postulated as a possible mechanism for the generation of cosmic noise in nebulae. In addition, a number of years ago *Schwinger* [1949] calculated the radiation to be expected from high-energy electrons circulating in strong magnetic fields in the synchrotron particle accelerator. The generation of synchrotron radiation was confirmed by *Tomboulian and Hartman* [1956] at optical frequencies both as to spectra and as to angular distribution in the ultraviolet frequency range, using the Cornell synchrotron. On the basis of the paper by Schwinger and the high-energy particle counting rates measured by Van Allen in the natural radiation belt, calculations have been made by

Dyce and Nakada [1959] of the possibility of detecting radiofrequency radiation from the Van Allen belts. Their calculations show that, assuming the Van Allen belts to be of trapped electrons, in the vicinity of 30 Mc the ratio of synchrotron radiation to cosmic radiation from the coldest part of the sky is about 0.4 per cent. The noise ratio is expected to drop off rather rapidly with increased observation frequencies. Thus the synchrotron radiation is not likely to have been observed on existing equipment, but might reasonably be extracted by careful radiometric methods. Dyce and Nakada suggest that, although synchrotron noise from the Van Allen belts and cosmic noise are difficult to resolve because they are both wide-band noise and both are present at all times, they are unalike in the following ways: (1) they have a different power spectrum; (2) synchrotron radiation is mainly radiated normal to the magnetic field lines, whereas cosmic noise arrives from wide angles in the sky; (3) synchrotron radiation is linearly polarized when viewed normal to the magnetic field, whereas cosmic noise has been experimentally shown to be unpolarized. Antenna directivity and resolution by polarization determination both appear to offer promise for a means to observe synchrotron radiation from the Van Allen belts experimentally.

As a result of the satellite particle-counting studies in the Argus experiments and comparison of electron density in the trapped electron shells with counting rates in the Van Allen belts, it is now believed that the level of synchrotron noise from the Argus experiments should have been below the detectable level with even very refined equipment such as outlined above. The riometer experiments provide confirmation that the noise level was in fact below the level of conventional cosmic noise radiometers even in the 30-Mc frequency range. No detectable increases in noise levels were observed at any time on the riometers operated in the conjugate area during the Argus experiments.

Conclusion

The Argus nuclear detonations affected ra propagation to a minor extent. Auroral ech were obtained near the launch point and conjugate point by radar equipment operat at 30 Mc. Marked absorption of VLF propa tion was observed over a path between Engla and Spain. Slight signal enhancements w noted over Pacific paths. Absorption of cosm noise was not detectable at 30, 60, or 120 nor was any shot-associated radio noise served.

References

Christofilos, N. C., Trapping and lifetime charged particles in the geomagnetic field, *U Calif. Radiation Lab. Rept.*, UCRL 5407, N 28, 1958.

Dyce, R. B., and M. P. Nakada, On the possibil of detecting synchrotron radiation from hig energy electrons in the Van Allen belts, *St ford Research Inst. Mem.*, March 24, 1959.

Gallet, Roger M., The very-low-frequency er sions generated in the earth's exosphere, *P IRE*, **47** (no. 2), 211–232, February 1959.

Helliwell, R. A., and M. G. Morgan, Atm pheric whistlers, *Proc. IRE*, **47** (no. 2), 200–2 February 1959.

Little, C. G., and H. Leinbach, The riometer a device for the continuous measurement ionospheric absorption, *Proc. IRE*, **47** (no. 315–319, February 1959.

Nichols, Benjamin, Auroral ionization and ma netic disturbances, *Proc. IRE*, **47** (no. 2), 24 255, February 1959.

Peterson, A. M., R. D. Egan, and D. S. Pra The IGY three-frequency backscatter sounde *Proc. IRE*, **47** (no. 2), 300–315, February 1959

Schwinger, J., On the classical radiation of a celerated electrons, *Phys. Rev.*, **75** (no. 1 1949.

Störmer, C., *The Polar Aurora*, Clarendon Pre Oxford, 1955.

Tomboulian, D. H., and P. L. Hartman, Spectr and angular distribution of ultraviolet radi tion from the 300 Mev Cornell synchrotro *Phys. Rev.*, **102** (no. 6), 1423–1447, June 1956.

(Manuscript received June 15, 1959.)

Turbulence at Meteor Heights

C. O. HINES

Radio Physics Laboratory
Defence Research Telecommunications Establishment
Defence Research Board, Ottawa, Canada

Abstract—A preliminary outline of a new approach to the study of motions at meteor heights is given, the fundamental assumption being that these motions are perturbation velocities associated with propagating atmospheric waves. Several observed features of the large-scale motions are thereby explained, and a basis is laid for the study of associated smaller-scale "turbulent" motions. It is found that smaller-scale motions having appreciable amplitude need not be anticipated a priori, contrary to an earlier conclusion derived from conventional turbulence theory.

trong winds and large-scale wind shearing at eor heights have been revealed by the optical observation of long-enduring meteor trails *hipple*, 1954]. There has been considerable ate about whether these motions represent large-scale end of an extensive spectrum of bulent eddies [*Booker*, 1956, 1958] or ether they exist independently of—and to the lusion of—any appreciable smaller-scale wind ucture [*Manning* and *Eshleman*, 1957].

have suggested elsewhere [*Hines*, 1959] that large-scale motions could be interpreted in ms of atmospheric waves, and that, when y are so interpreted, many of their observed perties can be explained. A single assumption is required: that the optically observed nds are perturbation motions associated with illatory waves propagating through the atsphere. Immediate inferences may be drawn m the observations: the vertical scale of ase variation is of the order of 1 km, and the iods of oscillation greatly exceed a few mins. The effects of gravity are critical at such g periods, and they introduce the following sotropies as may be deduced from the ory for a non-viscous isothermal atmosphere: The winds are primarily horizontal, being ined to the horizontal at angles $\lesssim 15°$. (2) e variation of the wind occurs primarily in direction perpendicular to it, and lying in same vertical plane; such variations appear nearly vertical wind shearing. (3) The amude of the wind increases exponentially with height, the height scale being twice the scale height of the atmosphere. These deductions are in full accord with the optical observations, and the wave hypothesis appears to be substantiated.

The wave analysis may now be applied to the question of the existence of smaller-scale structures. Wave interaction occurs through the operation of non-linear processes, and provides a means of generating short-wavelength highly dissipative modes of oscillation in the actual viscous atmosphere. The process might proceed in a manner analogous to that envisaged in turbulence theory [*Booker*, 1956], and indeed it may even provide a useful approach in the extension of that theory to the study of compressible fluids under the influence of gravity. In the latter case, the following conclusions about atmospheric turbulence may be inferred from the wave analysis.

Two sequences of turbulent eddies are to be expected, rather than a single one, because of gravitational effects. One sequence is associated with long-period oscillations, and is highly anisotropic; it appears to correspond to the large-scale structures revealed by meteors. It is damped out at structure sizes not much smaller than those observed optically, and therefore should not be expected to give rise to smaller eddies. On the contrary, the smallest of the optically observed eddies at 80- to 90-km heights should be damped out at 100- to 110-km heights, and such is observed to be the case.

The second turbulence sequence is associated

with short-period oscillations, and is essentially isotropic; the criterion for extinction of the sequence is the Reynolds criterion as in ordinary turbulence. This sequence might be generated by the large-scale wind shearing of the other sequence, but the rate of energy input to it is not readily calculable. Since the optically observed winds are highly anisotropic, it is unlikely that the energy input to the large-scale end of the isotropic sequence is nearly as large as has been assumed in previous work [*Booker*, 1956]. The importance of isotropic small-scale eddies [*Booker*, 1956, 1958; *Booker* and *Cohen*, 1956] may therefore have been greatly overestimated. It is difficult to agree a priori with the suggestion [*Booker*, 1958] that a model of the winds which excludes small eddies is in any way incompatible with the principles of fluid dynamics. On the contrary, such a model—which has been claimed to be appropriate observationally [*Manning* and *Eshleman*, 1957]—now seems quite appropriate theoretically.

The foregoing remarks have obvious bearing on the scattering and reflection of radio waves in the *D*- and *E*-regions of the ionosphere, some points of contact with large-scale traveling disturbances in the *F*-region, and possible associations with tidal oscillations. These relations are now receiving preliminary study. The complete analysis will be presented in due course.

Discussions with many colleagues have of value in the development of these stu and I wish particularly to acknowledge t held with Dr. P. C. Clemmow of the Caven Laboratory during a period of association at Radiation Laboratory of the University Michigan.

References

Booker, H. G., Turbulence in the ionosphere applications to meteor trails, radio star scin tion, auroral radar echoes, and other phenom *J. Geophys. Research*, **61**, 673–705, 1956.

Booker, H. G., Concerning ionospheric turbul at the meteoric level, *J. Geophys. Researc* 97–107, 1958.

Booker, H. G., and R. Cohen, A theory of enduring meteor echoes based on atmosp turbulence with experimental confirmatio *Geophys. Research*, **61**, 707–733, 1956.

Hines, C. O., Motions in the ionosphere, *Inst. Radio Engrs.*, **47**, 176–186, 1959.

Manning, L. A., and V. R. Eshleman, Di sion of the Booker and Cohen paper 'A th of long-enduring meteor echoes based on at pheric turbulence with experimental conf tion,' *J. Geophys. Research*, **62**, 367–371, 195

Whipple, F. L., Evidence for winds in the atmosphere, *Proc. Natl. Acad. Sci. U. S.*, **40**, 972, 1954.

(Manuscript received May 11, 1959.)

Evidence Concerning Instabilities of the Distant Geomagnetic Field: Pioneer I

C. P. SONETT, D. L. JUDGE, AND J. M. KELSO

Space Technology Laboratories, Inc.
Los Angeles 45, California

Abstract—The search-coil magnetometer carried on Pioneer I has yielded evidence of complex geomagnetic behavior at great distances from the earth. This paper is intended to report only some preliminary observations; in particular, what appears to be directional instability in the field. A comprehensive statistical analysis, to be reported later, is still in progress.

Preliminary results of the flight of Pioneer I* ve indicated that certain instabilities appar- ly occur in the geomagnetic field at great tances from the earth. A comprehensive sta- tical analysis of the data is in progress. Since e results of this analysis are pending, it was nsidered desirable to present qualitatively me of the characteristics of the data at the esent time.

The magnetometer which was used to obtain e data consisted of a search coil wound about nickel-iron alloy core. The emf generated by e search coil was applied to an amplifier hich had a center frequency of 2 cps and a ssband 2 cps wide. The dynamic range of the nplifier was approximately 3000. The 2-cps in rate of the vehicle was utilized to generate e emf, the coil being fixed in the vehicle's ame of reference.

As a consequence of the low frequency, the rrow passband, and the large amount of auto- atic gain control, the transient response for e amplitude excursions highly modified the ta. On the other hand, the phase transient sponse time was considerably shorter than the ne associated with a number of phase shifts hich have appeared in preliminary examina- on of the data. The geometry for the apparatus indicated in Figure 1 where XYZ is an iner- tial frame centered in the vehicle and $X'Y'Z$ is a rotating frame fixed in the vehicle.

Since the rocket was spin stabilized, the orientation of the spin axis was fixed inertially. The distance from the center of the earth for the particular discontinuity which is shown in Figures 2 and 3 is 84,000 km. The geocentric latitude was 5° and the orientation of the spin axis was approximately 85° to the dipole field di-

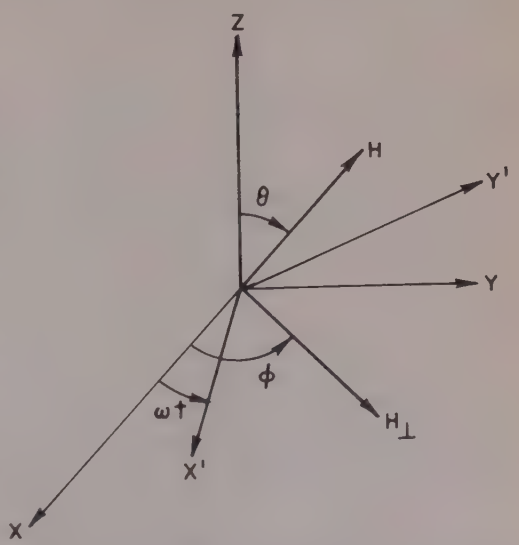

FIG. 1—The magnetometer frame X'Y'Z referred to an inertial set XYZ. The spin axis of the vehicle is colinear with Z and the search coil is mounted in the plane X'Z.

* This program was carried out under the direc- on of the National Aeronautics and Space Ad- inistration.

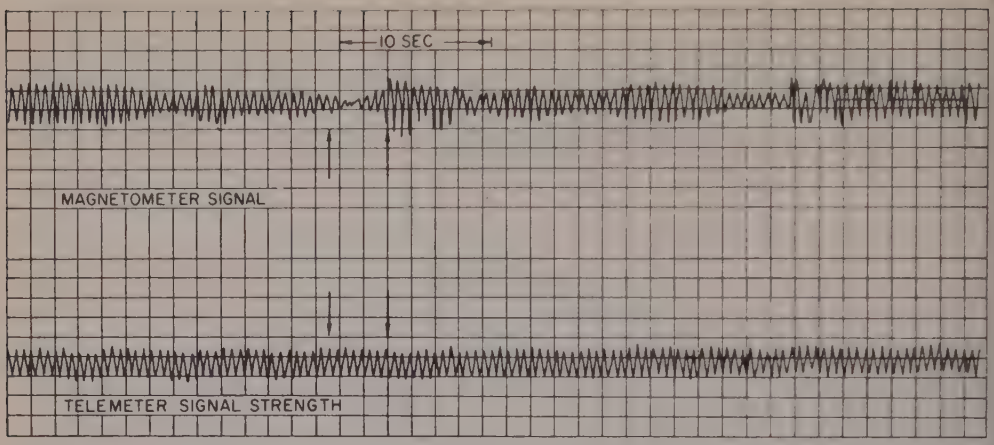

FIG. 2—A typical magnetometer recording showing a signal zero associated with large phase cl (between arrows), signal oscillations, and rapid changes in signal level. The magnetometer trace a characteristic spin rate. The telemeter rf signal strength is shown below, so as to serve as a reference for the magnetometer. The scale for the magnetic field is indicated at the right-hand the units being oersted (emu). This record represents the signal at approximately 86,300 km fro earth's surface.

rection; thus, within the error assignment for the experiment, the magnetometer, at this distance, measured the total field. The velocity of the vehicle at this time was 2.2 km/ sec.

The received data shown in Figures 2 and 3 consists of the spin-rate sinusoid corresponding to $\mathbf{H}_\perp$. Comparison of the phase of $\mathbf{H}_\perp$ with the rf signal-strength spin modulation can be made. Referring to Figure 1, we note that amplitude excursions of $\mathbf{H}_\perp$ would be explained by ch in $|H|$, the polar angle θ, or a combinati the two. In Figure 2, the arrows isolate a with which is associated a phase change (tion of ϕ) of about π radians. Because o amplitude zero, this appears to be a com tion of a rotation of $\mathbf{H}$ through the spin coupled with a change in $|H|$. The asymm form of the signal to the right of the zero w

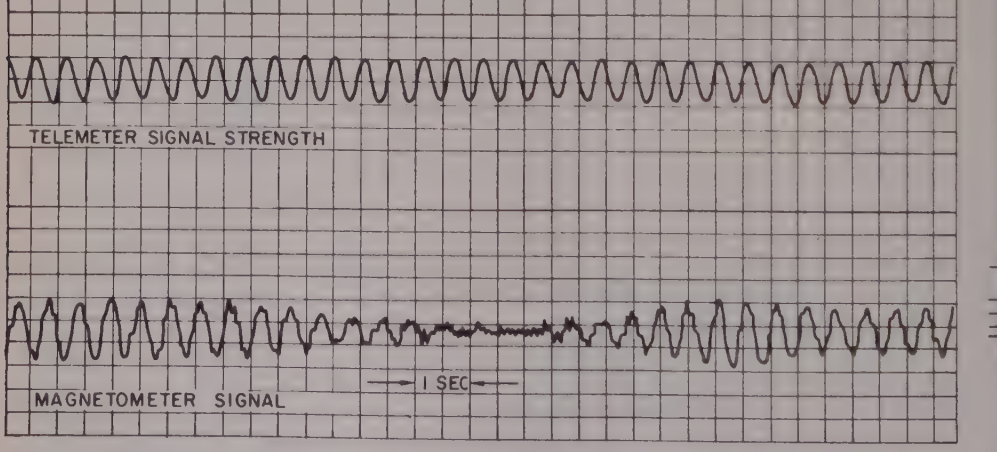

FIG 3—A time-expanded section of Figure 2 (the region about the indexing arrows) showing cle the phase change of about π radians associated with the zero. The scale at the right of the diagra the same as for Figure 2.

ly fast ($\tau < \frac{1}{2}$ sec) changes in either or n $|H|$ and θ. Preliminary examination of the a has not disclosed large phase changes oc- ring in this time.

igure 3 is a more expanded version of the a between the arrows. This figure distinctly icates the phase changes discussed in the pre- is paragraph. The amplitude excursions are entuated by the amplifier gain character- cs; and thus the time fluctuations, if real, not as extreme as shown. The removal of plifier effects from the data is planned as a t of the computer program.

The generation of hydromagnetic waves at the magnetic field termination due to a magnetic tability associated with a coronal wind has n proposed by both *Biermann* [1957] and *yle* [1956]. Slow variations in amplitude are n in Figure 2. The periods were typical for region of 13 to 15 earth radii. The day of ng (October 11, 1958) was extremely quiet gnetically. A proton magnetometer at Palo to disclosed surface fluctuations of about 10^{-6} uss rms (A. J. Dessler, private communica- n). Extrapolation of these values to about 13 rth radii would yield wave amplitudes con- tent with those obtained [*Dessler*, 1958]. It s been suggested that 10 earth radii represent suitable geomagnetic-field coronal-wind in- rface for a quiet day, though the region of stability sampled by Pioneer I is much broader an that suggested by J. A. Simpson (private mmunication). A further flight will be neces- ry to determine the boundaries of the ob- rved phenomena, if, in fact, an outer bound- ary exists. The possibility that some or all of the fluctuations represent a deep and random infusion of interplanetary gas into the geomagnetic field is being explored. A detailed statistical analysis of the available data is being prepared at the present time.

Some of the amplitude discontinuities in the data appear to occur in times limited by amplifier response. These would be attributable to compressional waves. Sudden phase changes associated with the above amplitude discontinuities may enable longitudinal and transverse wave motion to be sorted out, since Alfvén waves would be expected to show an abrupt phase discontinuity.

The following conclusions can now be drawn:

1. Rotations of the magnetic intensity vector, through both large and small angles, appear for the distant field. At least some of those associated with large angular excursions have characteristic times of the order of 10 seconds.

2. Almost periodic oscillations in amplitude occur (sometimes accompanied by rotational changes) having lifetimes of 2 to 5 cycles and periods of the order of 10 seconds.

References

L. Biermann, *Observatory*, **77**, 109, 1957.

F. Hoyle, Suggestion concerning the nature of the cosmic-ray cutoff at sunspot minimum, *Phys. Rev.*, **104**, 269–270, 1956.

A. J. Dessler, Large amplitude hydromagnetic waves above the ionosphere, *J. Geophys. Research*, **63**, 507–511, 1958.

(Manuscript received April 2, 1959.)

The Faraday Fading of Radio Waves from an Artificial Satellite

F. H. HIBBERD

University of New England
Armidale, N.S.W., Australia

Abstract—Faraday fading of signals from an artificial satellite is analyzed in terms of the difference between the Doppler shifts of the ordinary and extraordinary components in the ionosphere. A procedure is outlined for determining the vertical distribution of electron density in the upper ionosphere. Explanations are given for the apparently excessive values of electron content yielded by measurements of Faraday fading and for the observation that the rate of Faraday fading is not exactly inversely proportional to the square of the wave frequency.

Introduction—Faraday fading is observed in dio signals received from an artifical satellite ecause of the presence of the ionosphere and ie earth's magnetic field. As the satellite moves, ie amount of ionized medium between satelte and observer changes, and the direction of ropagation relative to the direction of the agnetic field also changes. As a result, the polarzation ellipse of the wave received on the ground ontinually rotates, and this gives rise to the 'araday fading.

Within the ionosphere the wave emitted from he satellite is split into ordinary and extraordinary components, with electric vectors otating in opposite senses. These travel with lightly different phase velocities and by slightly ifferent paths to the ground. If the emitter vere stationary, both components would have he same frequency and their phase difference at he receiver would be constant. At the receiver hey would combine to produce a polarization llipse whose major axis would be stationary, lthough inclined at some angle to the major xis at the emitter.

When the emitter is moving, however, both omponents suffer Doppler shifts, and these are lightly different for the two components. The eceived wave then consists of two elliptically olarized waves, rotating in opposite senses, with slightly different frequencies. The resultant polarization may be represented by a single llipse whose major axis rotates continuously with a frequency equal to half the difference between the frequencies of the two components. This rotation frequency will be called the Faraday frequency F. The observed frequency of the fading of the signal that is induced in a receiving aerial is simply related to the Faraday frequency in a manner which depends on the polar pattern and the aspect of the aerial.

The frequency of the Faraday fading—It has been shown by *Hibberd* [1958] that the frequency f, observed on the ground, of a radio signal emitted from a satellite traveling in the ionosphere is given by

$$f = f_0 + \frac{f_0 V \mu_e}{c} (\cos \alpha \sin \psi_e - \cos \beta \cos \psi_e) \quad (1)$$

where f_0 is the emitter frequency, μ_e is the refractive index of the ionosphere adjacent to the emitter, c is the velocity of light in free space, and V is the velocity of the satellite relative to the observer. The angles α and β (defined by *Hibberd* [1958]) specify the direction of motion of the satellite at any instant, and ψ_e is the angle between the observed ray as it leaves the satellite and the inward radial direction from the satellite to the center of the earth.

In deriving equation (1) we neglected the effect of the earth's magnetic field. When this is included it is necessary to distinguish between the direction of the ray and the wave normal. In the presence of the magnetic field, equation (1) is applicable to both the ordinary and extraordinary magneto-ionic components, provided that ψ_e is interpreted as the angle between the

wave normal at the satellite and the radial direction. We use the superscripts ′ and ″ to indicate quantities associated with the ordinary and extraordinary components, respectively, and we write

$$f' = f_0 + \frac{f_0 V \mu_s'}{c} (\cos \alpha \sin \psi_s' - \cos \beta \cos \psi_s') \quad (2)$$

$$f'' = f_0 + \frac{f_0 V \mu_s''}{c} (\cos \alpha \sin \psi_s'' - \cos \beta \cos \psi_s'') \quad (3)$$

The frequency F of the Faraday rotation is then equal to one half the difference between (2) and (3). That is,

$$F = \tfrac{1}{2}(f' - f'') = \frac{f_0 V}{2c} [\cos \alpha(\mu_s' \sin \psi_s' - \mu_s'' \sin \psi_s'') - \cos \beta(\mu_s' \cos \psi_s' - \mu_s'' \cos \psi_s'')] \quad (4)$$

The angles ψ_s' and ψ_s'' depend on the wave frequency, the distribution $N(h)$ of the electron density as a function of height throughout the region traversed by the wave, the magnetic field in this region, and the relative positions of satellite and receiver. The refractive indices μ_s' and μ_s'' depend only on the values at the satellite of the electron density, the magnetic field, and the respective angles ψ_s' and ψ_s''.

Suggested procedure for determining the $N(h)$ curve above h_m—We now outline a procedure for obtaining $N(h)$ in the upper ionosphere by the application of equation (4) to observations of Faraday fading. In addition to the record of Faraday fading one needs to have the $N(h)$ curve up to the height h_m of the ionization maximum, as deduced from conventional $h'(f)$ ionograms. The satellite orbit elements are also required; those obtained from good radio observations are sufficiently accurate for this purpose.

Values of V, α, and β can be calculated from the orbit data at a number of selected instants during the period for which the fading record is available. A model monotonic $N(h)$ curve can be assumed above h_m and combined with the known $N(h)$ curve below h_m to yield a com $N(h)$ curve for the whole ionosphere up t greatest height attained by the satellite d the period considered. For each of the sel positions of the satellite the angles ψ_s' an can be determined by ray tracing (with th of an automatic computer) through the com ionosphere, if the earth's magnetic field is t to be a dipole field (or modified dipole fi The refractive indices μ_s' and μ_s'' at the sat are then computed. The appropriate valu of the various quantities can then be substit into equation (4) to obtain a value for Faraday frequency F at each of the sele instants. These computed values of F sh then be compared with the observed val The whole procedure must be repeated various assumed monotonic $N(h)$ curves a h_m until that model is found which gives cl agreement with observation.

Discussion of approximate calculations an effects of refraction—Several workers [S *Mullard Radio Astronomy Observatory*, 1 *Burgess*, 1958], using a simplified approxi analysis, have made estimates of the integ electron content $\int_0^h N dh$ up to the height of satellite, from observations of Faraday fad They obtained values for the electron con which were so large that they could not reconciled with the known electron content to h_m.

We shall now use the result (4) of the pres analysis to show how the neglect of refract can lead to an incorrect estimate of the integra electron content in the ionosphere. In order do this we consider three idealized cases, ill trated in Figures 1(a), (b), and (c), respectiv

The refractive indices for the two magne ionic components within the ionosphere different, and when both refractive indices less than unity we may put

* The effects of the receiving aerial must be tak into account in determining the Faraday frequen F from the fading record. Because of these effe and the occurrence of other fading phenome including the effect of rotation of the satelli probably the simplest procedure is to count fr the record the number of Faraday rotations $\int$ over a suitable interval. This can then be compar with the value of $\int F dt$ which is determined grap cally from a set of values of F computed for t model ionosphere at a number of instants duri the selected interval.

$$\mu_s' > \mu_s'' \qquad (5)$$

ithout loss of generality in the conclusions.

Case (a): The ionosphere has a uniform ectron density that extends indefinitely upards from a lower boundary. Refraction is eglected, and both the ordinary and extraordinary rays follow a straight-line path from tellite to receiver. However, the phase velocities the two components are different. These are actly the same assumptions as those under hich the approximate calculations mentioned ove were made.

or this case

$$\sin \psi_s' = \sin \psi_s'' \qquad (6a)$$

Case (b): The ionosphere has a uniform electron ensity that extends indefinitely upwards from lower boundary. Refraction is included. This orresponds approximately to the situation in hich a satellite is traveling in the actual ionophere at a height *less* than h_m. With the relation 5) it may be seen from Figure 1(b) that $\psi_s' < \psi_s''$, and therefore

$$\sin \psi_s' < \sin \psi_s'' \qquad (6b)$$

Case (c): The ionosphere consists of a parallel lab of uniform ionization, and the satellite is raveling above the slab. Refraction is included. his corresponds approximately to the situation n which a satellite is traveling in the actual onosphere at a height *greater* than h_m. It is een from Figure 1(c) that the ordinary and extraordinary rays intersect within the slab so that, with relation (5), we must have $\psi_s' > \psi_s''$ and

$$\sin \psi_s' > \sin \psi_s'' \qquad (6c)$$

In equation (4), which gives the Faraday frequency, the effect of the ionosphere is accounted for by the terms within the square brackets. Because, in general, $|\cos \alpha| \gg |\cos \beta|$ for an orbit with small eccentricity, we shall consider only the magnitude of the dominant. quantity

$$|\mu_s' \sin \psi_s' - \mu_s'' \sin \psi_s''| \qquad (7)$$

For a given electron density, height of the lower boundary, and position of the satellite we compare the relative values of the quantity (7), and therefore of F, which corresponds to each of the cases (a), (b), and (c). On combining the relation (5) with (6a), (6b), and (6c) in turn, we see that the smallest value of F is obtained in case (c), a greater value in case (a), and a still greater value in case (b). Conversely, and in particular, it is clear that for a satellite traveling above h_m one would deduce, from a given value of F, a greater value of electron density and electron content if one made the approximations implicit in case (a) than if one took account of refraction and of the existence of N_m, as is done roughly in case (c). The inconsistency between the early estimates and the known upper limit to the electron content may thus be accounted for. This effect is quite distinct from the contri-

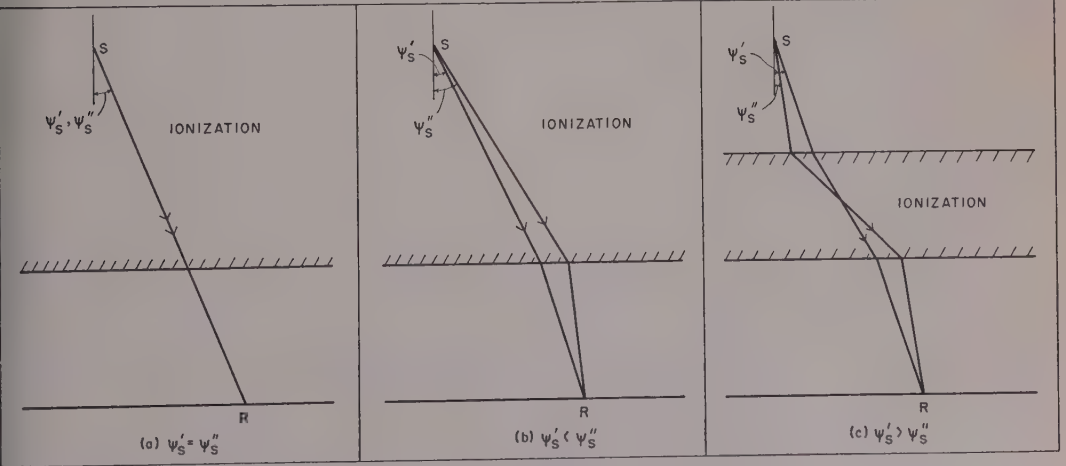

FIG. 1

bution to the fading due to radial motion in a non-circular orbit [*Daniels* and *Bauer*, 1958]. The latter effect is here included separately in the $\cos \beta$ term in equation (4).

A further apparently puzzling observation may also be explained in terms of equation (4). According ot the conventional treatment of the Faraday effect, for straight-line propagation through a uniform medium the rotation should be inversely proportional to the square of the wave frequency f, when f is considerably greater than the gyro frequency. Thus one might expect the Faraday frequency of the 20-Mc/s signal from the Sputniks to be exactly equal to four times that of the 40-Mc/s signal. However, it has been commonly observed that this relationship is not strictly satisfied. The reason is that, although the difference between the refractive indices, $\mu_s' - \mu_s''$, is to a close approximation proportional to f^{-3} (so that $f(\mu_s' - \mu_s'')$ is proportional to f^{-2}), the quantities $\sin \psi_s'$ and $\sin \psi_s''$ are not simply related to the wave frequency. Therefore, when refraction is included, the Faraday frequency F, by (4), cannot be exactly inversely proportional to the square of the wave frequency, quite apart from the effect of the $\cos \beta$ term which is associated with the non-circular orbit.

Further Remarks—It has been shown how the $N(h)$ distribution above N_m can be deduced from observations of the Faraday fading, provided $N(h)$ is known below N_m and the magnetic field is known or assumed. The same information can be obtained from simultaneous Dop observations on two frequencies (for exam 20 and 40 Mc/s from the Russian sate [*Thomas* and *Hibberd*, 1959]). These two met should provide a useful check on each o but because the Faraday rotation can be n accurately and more easily measured it probably turn out to be more generally usefu

Further, it has been shown by *Hibberd* [1 that the angle of arrival of a signal from a sate is directly related to the Doppler shift. I thus interesting to notice that measurem of Faraday rotation, Doppler shift, and a of arrival in the vertical plane all yield the sa ionospheric information, at least to a first or

References

Burgess, B., Discussion on radio observation the Russian satellite, *Proc. Inst. Elec. Engrs London* 105, 112–113, 1958.

Daniels, F. B., and S. J. Bauer, Faraday fadin earth satellite signals, *Nature*, 182, 599, 195

Hibbard, F. H., The effect of the ionosphere the Doppler shift of radio signals from an a ficial satellite, *J. Atmospheric and Terrest. P* 12, 338–340, 1958.

Staff of the Mullard Radio Astronomy Ob vatory, Radio observations of the Russian e satellite, *Nature*, 180, 879–883, 1957.

Thomas, J. A., and F. H. Hibberd, Satellite D pler measurements and the ionosphere, *J. mospheric and Terrest. Phys.*, 13, 376–379, 19

(Manuscript received March 23, 1959; revise April 30, 1959.)

Auroras, Magnetic Bays, and Protons *

R. C. BLESS, C. W. GARTLEIN, D. S. KIMBALL, AND G. SPRAGUE

Cornell University
Ithaca, New York

Abstract—Various statistical and detailed studies of the relation between auroras and bays are presented. It appears that bays and auroras are manifestations of the same phenomenon. Numerical estimates are presented which indicate that the bay can be caused by atmospheric winds operating on ionized particles produced by incoming 50-kev solar protons. It is not necessary to postulate any dynamo action.

Introduction—Magnetic bays have been studd almost as long as the earth's magnetic field as been measured, and the known relation beween magnetic storms and auroras is almost as ld [*Hiorter*, 1747].

The present paper is the result of work underaken to establish a quantitative cause-and-ffect connection between the two phenomena. t appears reasonable to assume that the bay s an integral part of the aurora, being due to n atmospheric drift of ions produced by solar rotons. Part of the visible aurora is due to the ecombination energy of these same ions. A bay s, therefore, a definite indication of the presence f an aurora, and it can be used to complete isual records.

There are three general topics to be discussed. The first is a brief discussion of the current system which is responsible for the magnetic bays; the second is a summary of old and new studies of the bay-auroral relationship; and the third is a short, semi-quantitative study of the magnitudes involved.

Magnetic bays—In the magnetic records an extreme fluctuation which may maintain maximum displacement for an hour or two before returning to normal value is referred to as a magnetic bay. For a complete description of bays and their current systems reference should be made to a standard text, such as *Chapman* and *Bartels* [1940] or *Vestine* and others [1947].

Since the earth's magnetic field has been measured and records have been kept over a long period of time, good data on the behavior of bays are available. From these data the magnetic field due to an average bay can be represented, free from the other variations of the earth's main field. From this average bay field and other experimental data, it is possible to determine the current that caused the bay. The assumptions and limitations of the results are discussed in the references.

The basic conclusion is that the current which is responsible for the bays is heavily concentrated in the auroral region at the auroral heights. In addition, the relative behavior of bays and the normal diurnal variation of the earth's field indicate that the bay can be generated by increasing the number of charges in the ionospheric regions. These charges, moved by the atmospheric circulation system, cause the bay [*Mitra*, 1940; *Vestine*, 1954]. Therefore, if an aurora contains enough charges, and if their behavior is like that of the other charges in the ionosphere, the aurora can cause the bay.

Bay-aurora relationship—Celsius, in the infancy of magnetic and auroral studies, noticed that the earth's magnetic field was strongly affected during an aurora. There have been many investigations since that time, covering various aspects of auroral behavior. Most of these works show that the geographic positions of the aurora indicate that it is due to the motion of charged particles in the earth's field, but little study has been made of the effect of these particles on the field itself.

This latter point has been approached by studies of the relation between the aurora and the disturbed field. One measure of the disturb-

* This analysis was supported in part by the U. S. Signal Corps.

ance is the three-hour K index, published by magnetic observatories throughout the world. A typical [*Gartlein*, 1944] relation between the K index from Cheltenham, Maryland, and L, the geomagnetic latitude of the southern edge of the aurora, is

$$L = 65 - 1.4K \pm 3$$

This specific relationship, determined from a statistical study of 4036 North American observations covering the period from 1938 to 1946, is sufficiently accurate to predict the K index to within one unit from the position of the aurora.

The major cause of the fluctuation is that the K index is not sufficiently fine, especially in time. For this reason auroral and magnetic records have been examined more closely. Comparison of photoelectric records of the auroras and magnetograms shows a more detailed relationship than the K indices permit [*Gartlein*, 1944]. Figure 1 shows a sample comparison.

Magnetograms taken at Cheltenham, Maryland, during the years 1946 to 1950 were compared with the photoelectric records taken at Ithaca, New York. The times of occurrence of short increases (at least 50 gammas) in the horizonatal intensity were noted from the magnetic records, and the simultaneous photoelectric traces were investigated. Many of these latter were of no value for comparison because of the effects of moonlight, inclement weather, or operative equipment. Only twenty-five nig were found with records free of complicatio These were divided into two groups, one of greatly disturbed days, and the other of moderately disturbed days.

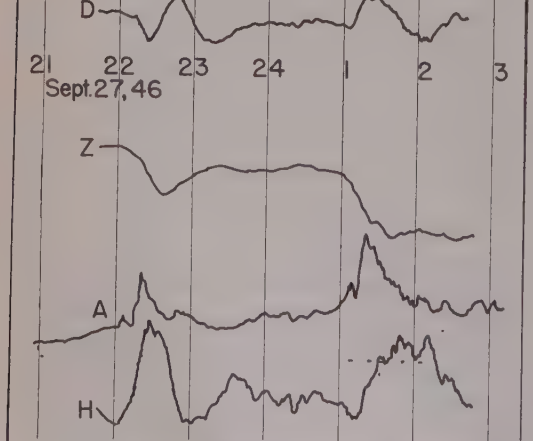

FIG. 1—Magnetic elements D, Z, and H and photoelectric aurora records on same time scale

During the 12 moderately disturbed days, relationship was found between the bays in and the most prominent features of the phot electric record of the auroral night. (Both re ords can be read to within three minutes.) Th changes in H were found to occur shortly aft the change in auroral light intensity. The ave age lag was about 15 minutes, but occasiona it was smaller or even unobservable. Howev the bay never preceded the aurora. Correspon ence of auroral light peaks was found with bay but not with SC's.

In the 13 remaining cases, correlations of th same type were found between the Z compone of the earth's field and the record of auror light. (In general, H was so disturbed on th nights that correlation with anything could ha been found.) The Z component record is l sensitive to bays than is the H component re ord, and it is less ambiguous on very disturb nights. On moderately disturbed nights there practically no noticeable variation in Z. Th behavior is connected with the relative position of the aurora and the magnetic observatory.

In order to test this association of bays wit auroras, the Cheltenham magnetograms for 19 were examined, and the times were noted c bays in H which, from the above analysis, wer expected to be associated with auroras. Daytim bays were rejected, and the records of visua aurora observations made every night at Ithac were checked to see if a display had occurred a these times. The results are tabulated below

Bays	101	Aurora	68
		Cloudy	28
		Doubtful	5
	101		101

There can be little doubt that bays and auro ras are closely related. Of the auroras counte above, approximately six were weak glows: th rest were strong diffuse surfaces, veils risin high in the sky, or, more often, displays whic developed into arcs and rays.

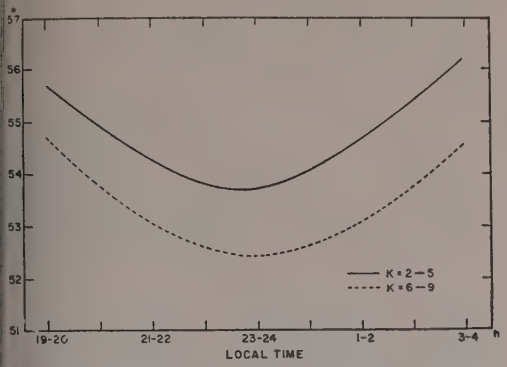

FIG. 2—Corona position as a function of local time; average for 28 well-observed auroras

There were, in addition, 70 nights during hich small auroras appeared but were not icked up by the list of bays; ten of these were aint northern arcs or rays in the north, and the thers were weak glows seen very low in the orthern sky. Perhaps these weak northern auroas would have been recorded on magnetograms rom a more northerly observatory.

Part of a more detailed study of visual records f well-observed auroras is represented in Figure . This shows the average southern extent of 28 uroras as a function of local time. The two urves are for two different ranges of K values nd indicate (1) the K dependence with southern xtent discussed above and (2) a maximum outhern extent near local midnight, which is a haracteristic of the bay current system.

Pre-IGY auroral records are incomplete, but n spite of this the statistical relation between he aurora and K, the detailed relation in a few ases between photoelectric and magnetic records, the good correspondence between visual ecords and the bay occurrence, and the agreenent between the bay current system and the uroral position indicate that the aurora and he magnetic bay are inseparable. This means hat magnetic records can be used to extend and orroborate visual records of auroral occurrence.

Estimated magnitudes—The preceding secions indicate that the bay is caused by a curent which coincides with the visible part of the urora in space and lags a few minutes in time. (In a later paper a more detailed study of this ime lag, based mostly on time spectrum data, vill be presented.) In a previous paper [*Gartlein* and *Sprague*, 1957], evidence was presented which indicated that solar protons could be the initiator and energy supply for the aurora. It is therefore pertinent to decide whether the same protons could cause the bay. The rough hypothesis is that the protons produce positive ions which drift in the atmospheric circulation system and cause the bay. It is necessary to decide whether enough positive charges are produced and why the electrons do not drift along with them and cancel the magnetic effects.

The wind system responsible for diurnal magnetic effects and bays is frequently derived by application of the *Balfour Stewart* 'dynamo' theory [1882]. This raises certain difficulties regarding the electrical properties of the ionosphere [*Chapman*, 1929] and the phases of the tidal components [*Kertz*, 1957]. A fundamental assumption of the theory is that ions and electrons in the ionosphere will acquire the velocity of the surrounding neutral atmosphere. If this is correct and the other difficulties are surmounted, the electrons in the ionosphere will acquire velocities of the same magnitude as the surrounding air, and the heavy ions will not.

It seems equally possible that a different mechanism is operating, which leads to the same result as far as the purpose of this paper is concerned. Calculations indicate that at auroral altitudes (around 100 km) only the protons will move with the surrounding wind. The necessary equations are worked out by *Chapman* and *Cowling* [1952] in another connection, but a simplified explanation of the result can be given here.

The complicating factor is the magnetic field. Charged particles in a magnetic field tend to travel in circles, and if they are to move with the wind this tendency must be removed by collisions with the air molecules. The possibility of moving charged particles with a neutral air mass depends upon the relative times for collision of a charged particle with an air molecule and the time for a complete revolution in the magnetic field. If a charged particle is turned around in a circle between collisions with air molecules, it is not moving in the wind direction. In other words, it has a large transverse (to the field) resistance. The fact that the driving force is due to collisions between molecules and charged particles, rather than to electrical attraction,

makes the case different from that for the calculation of conductivities.

If solar protons produce a large number of electrons and nitrogen molecular ions, the magnitudes of the important quantities can be rapidly determined.

The time for one revolution in the magnetic field is proportional to the mass of the particle involved. From measurements of E-layer reflections

$$T_e = 7 \times 10^{-7} \text{ sec at 90 km [Mitra, 1940]}$$

$$T_{N_2} = 28 \times 1800 \times 7 \times 10^{-7} = 4 \times 10^{-2} \text{ sec}$$

The collision time for electrons, at the same levels, is found to be 5×10^{-6} sec from the Luxembourg effect, and 10^{-4} from E-layer absorption data [*Mitra*, 1940]—both greater than T_e.

From these figures it appears that the electrons will tend to spiral in one location rather than assume the neutral stream velocity. Since the pressure and the collision frequency are proportional, the electrons would acquire the stream velocity if the pressure were higher. To gain the required factor of ten, it would be necessary for the electrons to drop 15 km in the atmosphere —to about 75 km above the ground.

The collision time for nitrogen molecular ions must be calculated from their sizes and thermal velocities. The expression is approximately

$$T = (760/P) \times 3 \times 10^{-9} \text{ sec at } 300°K$$

where P is the pressure in mm of Hg. This is less than the gyroperiod given above if P is greater than 6×10^{-5} mm Hg.

This pressure occurs at a height of about 115 km [*Rocket Panel*, 1952]. The critical heights are roughly 75 and 115 km. Above 115 km neither electrons nor ions would acquire the wind velocity; below 75 km both would. In the intervening range only the positive ions would acquire the wind velocity; the electrons would remain relatively stationary. It is in this region that the bay current flows, that auroras are seen, and that solar protons stop.

It is not the purpose of this paper to decide between the dynamo theory and that outlined above. Both lead to the result that charges of one sign acquire a velocity whose magnitud that of the wind (about 50 m/s) [*Lovell*, 19

The total atmospheric current produced the solar protons [*Gartlein* and *Sprague*, 19 can be estimated. The proton current wh caused the visible aurora was estimated to 10^4 amp of 50-kev particles. At 28 elect volts per ion-pair, each proton would prod 50000/28 ions, giving a total ion population

$$Q = \frac{5 \times 10^8}{28 \times 1.6 \times 10^{-19}} D \text{ ions}$$

$$Q = 1.6 \times 10^7 D \text{ couloumbs}$$

D is the duration of the proton current or ion lifetime, whichever is shorter. This cha flows in a rough circle 30° from the pole an driven by a wind of the order of 50 m/s. T amount of charge passing a plane perpendic to the flow in one second is thus

$$i = \frac{D(8 \times 10^2)}{(12\pi \sin 30°} \text{ amperes}$$

From studies of the duration of hydrogen a nitrogen ions in auroral spectra it seems pro able that D is about one hour, or

$$i = 10^5 \text{ amp}$$

Since the limiting bay was chosen to be abo 50 gammas in magnitude at Cheltenham, whi is roughly 1000 km south of the auroras se from Ithaca, the necessary current can also l calculated in this way, if one assumes that it a straight-line current 1000 km away.

$$B = 50 \times 10^{-5} \times 10^{-4} \text{ webers/meter}^2$$

Also,

$$B = \mu_0 i/2r = 6 \times 10^{-13}(i)$$

Equating these two expressions gives

$$i = 8 \times 10^4 \text{ amp}$$

This agrees reasonably well with the othe estimate. Only one significant figure is held i the numerical work, and only orders of mag nitude are held in the final answers.

In a recent paper, *Nichols* [1957] has show that the electron component of the ionized ga is in rapid motion, velocities of as high as 50

s being observed. This is ten times the ve-
ity of the atmospheric wind, and it would
respond to a larger bay than the average one
d above. Therefore, mechanism for produc-
a velocity of 500 m/s could not be either the
nd or the dynamo effect.

Conclusions—(1) Observational evidence in-
ates that the aurora and the magnetic bay
caused by the same agent and occur in the
ne place, the aurora slightly antedating the
y.

(2) Order-of-magnitude calculations do not
ntradict the hypothesis that the bay is pro-
ced by the wind movement of positive ions
nerated by incoming solar protons.

(3) The bay-auroral relationship is close
ough so that magnetic records can be used to
l in incomplete visual records.

References

HAPMAN, S., On the theory of the solar diurnal variation of the earth's magnetism, *Proc. Roy. Soc. A.*, **122**, 369–386, 1929.

HAPMAN, S., AND J. BARTELS, *Geomagnetism*, Oxford University Press, 1940.

HAPMAN, S., AND F. COWLING, *The mathematical theory of non-uniform gases*, Cambridge University Press, 1952.

GARTLEIN, C. W., Relation of three-hour-range index K to aurora seen at Ithaca, New York, *Trans. Am. Geophys. Union*, 533–547, 1944.

GARTLEIN, C. W., AND G. SPRAGUE, Hydrogen in auroras, *J. Geophys. Research*, **62**, 521–526, 1957.

HIORTER, P. O., Von der Magnetnadel verschiedenen Bewegung, *Svenski Vet. Acad. Hand.*, 27–28, 1747.

KERTZ, W., Atmospheric tides, *Handbuch der Physik*, **48**, 928–956, 1957.

LOVELL, A. C. B., Physics of meteors, *Handbuch der Physik*, **48**, 427–432, 1957.

MITRA, S. K., *The upper atmosphere*, Asiatic Society, Calcutta, 1940.

NICHOLS, B., Drift motions of auroral ionization, *J. Atmospheric and Terrest. Phys.*, **11**, 292–293, 1957.

ROCKET PANEL REPORT, Pressures, densities, and temperatures in the upper atmosphere, *Phys. Rev.*, **88**, 1027–1032, 1952.

STEWART, BALFOUR, Terrestrial magnetism, *Encyclopedia Brittannica*, 9th Ed. 36, 1882.

VESTINE, E. H., I. LANGE, L. LAPORTE, AND W. E. SCOTT, The geomagnetic field, its description and analysis, *Carnegie Inst. Wash., Publ. 580*, 1947.

VESTINE, E. H., Winds in the upper atmosphere reduced from the dynamo theory of geomagnetic disturbance, *J. Geophys. Research*, **59**, 93–128, 1954.

(Manuscript received May 14, 1958; revised March 24, 1959.)

Some Properties of the Luminous Aurora as Measured by a Photoelectric Photometer *

W. B. MURCRAY

Geophysical Institute, College, Alaska

Abstract—Intensity of the auroral radiation from the entire sky as a function of time was monitored photoelectrically at College, Alaska. Measurements extended over two years. Very good correlation was found between the 3914A band of N_2^+ and the 5577A line of OI. An intensity-time curve of a typical auroral display is shown. A diurnal variation curve is obtained which is very consistent, giving the same form for weak, moderate, and strong aurorae, and showing no evidence of seasonal variation. A rapid fluctuation in the intensity of radiation is reported.

Introduction—It is desirable, for many reasons, to know the manner in which the light from the sky as a whole varies as a function of time during an auroral display, since this may be interpreted as showing the intensity-time curve for the excitation of the luminous portion of the disturbance. An approximate means of accomplishing this is to monitor the brightness of a diffusing surface, mounted horizontally so as to be exposed to radiation from the entire sky. It is evident that this method will discriminate heavily in favor of light sources in the vicinity of the zenith, so that what is investigated will be events which occur principally in the vicinity of the observing station.

Observations were commenced in the spring of 1955 at the Geophysical Institute, College, Alaska. The diffusing surface was sometimes unglazed porcelain and sometimes snow surface. It was found that these surfaces were roughly equivalent, and, in consequence, no effort was made to keep the surface clean of snow. College has an arctic climate, so most of the observations were made on a snow surface.

The brightness of the diffusing surface was monitored by a photoelectric photometer, which has been described fully elsewhere [*St. Amand*, 1953]. It consists essentially of a telescope which puts an out-of-focus image on the photo-cathode of a 1P21 photo-multiplier tube. Output of the tube goes to a dc amplifier and thence to an Esterline-Angus recorder. Chart speed was 6 in/hr.

The radiation of interest was that of auroral origin; accordingly, filters were used to isolate wavelengths which are prominent in the auroral spectrum. The filters were a combination of Baird interference filters with the appropriate Corning glass filters. Half intensity width of the combination was about 150A. Two wavelengths were used, the green auroral line at 5577A which is due to atomic oxygen, and the 3914A band of the first negative system of N_2^+. These are the two strongest radiations of the visible aurora and are well suited to this type of observation. The green oxygen line is also present in the airglow; the 3914 band is not. The 3914 band, however, is subject to strong twilight enhancement, and the 5577 line is not.

Correlation of the two wavelengths—Records taken simultaneously in both wavelengths show that the intensities of the two radiations are very closely related. ("Intensity" as used here will always refer to an effective intensity for the whole sky, rather than to the actual intensity of any specific area.) Indeed, the relation is so close that a constant ratio of the two intensities in any specific area of the sky, as was observed by *Rees* [1959], appears to be the most reasonable explanation. Rees has suggested that the 5577A radiation may be due to excitation of the oxygen atoms by the electrons produced during the ionization of nitrogen molecules. Since the 3914A radiation is a result of excitation during the

* This work was supported by Electronics Research Directorate of Air Force Cambridge Research Center.

nitrogen ionization process, it would be expected from this hypothesis that the intensity ratio for the two wavelengths would be a constant. Rees' observations indicated that this was the case in the display he analyzed. In the present observations the raw data does not show a constant intensity ratio, but the variation is not wide. It could result from the fact that the zenith angle from which most of the light comes is constantly changing, so that the relative extinction of the two wavelengths is not constant. It is not possible to correct for this.

Close examination of the records shows that there are occasional small variations in the 3914A intensity which are not present in the intensity of 5577A. This has been observed by *Ashburn* [1955] for a limited area of sky. The present observations show that such variations also occur for the sky as a whole. Instances in which 5577A intensity shows variations not matched by 3914A are extremely rare if not entirely absent. There is also a slight time crepancy; sharp increases in 5577A intens seem to follow similar increases in 3914A some seconds. This is not easy to see from records, but it is very evident if one watches instruments while the record is being tak Measurement of the delay has not been succe ful because the chart speeds were low and cause the time constants of the recorders a amplifiers distort the records sufficiently to ma it very difficult to determine precisely when increase starts, but the delay is of the order a few seconds. It is not easy to see how such delay could be a result only of the mean life sociated with the emission of the 5577A line, cause the delay is much too long. A hypoth which might explain such a time lag follows

If the 5577A emission is excited by the el trons produced in the formation of the exci N_2^+ ions which are responsible for the fi negative group emissions (included the 391

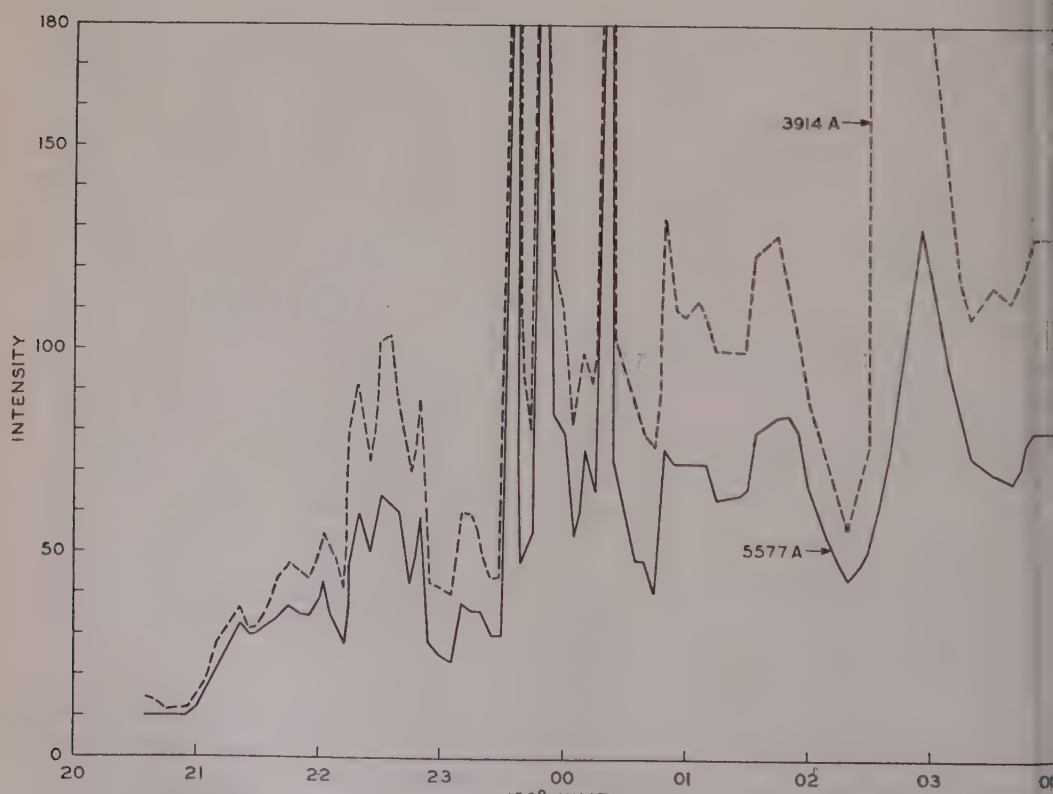

FIG. 1—Typical night's record; intensity versus time; intensity units arbitrary

nds), the intensity of the 3914A emission will proportional to the rate of production of e electrons, and the rate of excitation of the ygen atoms will be governed by the density free electrons in the required energy range. might be expected, therefore, that in the case very rapid increases in the 3914A intensity, ere might be a noticeable lag while the elec- n density built up to the point where the in- ase in 5577A intensity became appreciable. ring periods of rapidly changing intensities, uilibrium conditions would not be reached, d this could cause minor discrepancies in the I_{5577}/I_{3914} ratio. The above considerations will ply provided that oxygen atoms are present such large numbers that saturation effects ay be ignored.

Figure 1 shows a typical intensity-time curve r a moderately active auroral display. It can seen that the agreement in intensity varia- ns for the two wavelengths is extremely good. all available records, there is no instance of ajor discrepancy between the two curves. It ould be borne in mind, however, that the easurement is influenced by aurora anywhere the sky; thus it is some type of mean value r all auroral forms above the horizon, though eighted heavily in favor of the neighborhood the zenith. In this connection it is interesting note that during a portion of the display corded in Figure 1, visual observation showed lsating surfaces in the zenith. The pulsations d not appear on the record because, although e pulsating forms covered a considerable area the sky, they consisted of numerous cloud- ke forms, each one of rather small area. Since e pulsations of these surfaces were in random hase, the effect on the photometers was small.

General Features of Auroral Displays—The cord shown is typical of the intensity-time rve for nearly all auroral displays in form, ough the magnitude differs considerably from e display to another. This particular record as obtained on the night of March 17–18, 955, from an active, though not extremely right, aurora. It shows a rather low intensity rly in the evening, which increased until local idnight; then the activity remained at a high vel until daylight. Large bursts of activity in hich the intensities rose at a rate near the mit of response of the recorder to a peak and fell very rapidly afterward are of considerable interest because they indicate the rapidity of variation of the excitation. The photometer generally goes off scale during such events, so that the maximum level is not known. The intensity, however, has been observed to increase by a factor of eight from a moderate level in less than 20 seconds. These 'bursts' are a characteristic feature of auroral displays and must therefore be accounted for in any theory of the mechanism of the luminous aurora.

That the record above is indeed typical may be seen by reference to Figure 2. This is a plot of the average intensity versus time for the 3914A radiation. It was obtained by scaling records for the mean intensity over the appropriate intervals, which in this case was one hour.

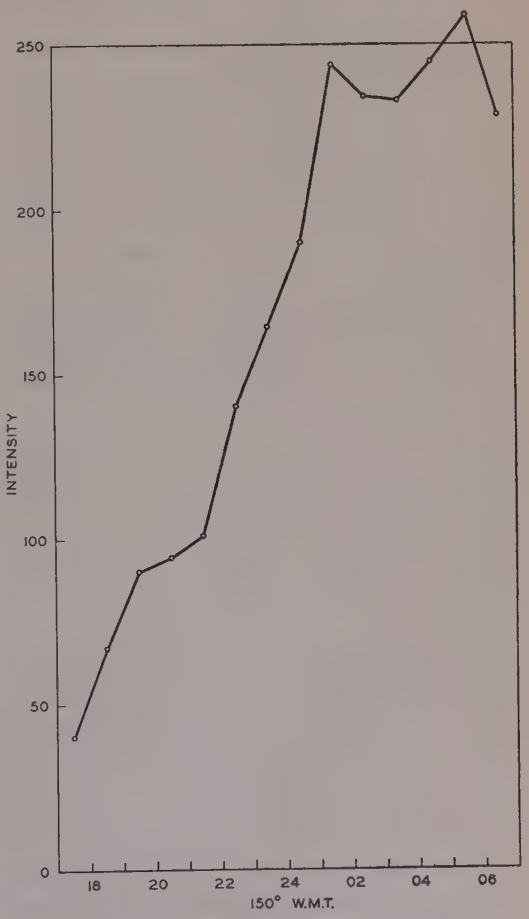

FIG. 2—Diurnal variation of 3914A intensity; intensity units arbitrary

It can be seen that this is essentially the area under the intensity-time curve for the hour, and it should therefore be an indication of the brightness and area of the luminous aurora in the sky during that time. The curve of Figure 2 represents the diurnal variations of this quantity. It was obtained by averaging the hourly values obtained during about nine months of observation, including October, November, and December of 1955, and January, February, March, October, November, and December of 1956. Records for 180 nights were used. Corrections were applied for moonlight but not for cloud cover, as it was found that clouds had little effect on the observations. This was deduced from the fact that the average for cloudy days was about the same as that for clear days. The clouds do not absorb the radiation but merely act as a diffusing screen, which reduces the intensity of the source and increases its area so that the total light received is not much changed.

It can be seen from Figure 2 that the average intensity of the luminous aurora increases steadily from the time of the earliest evening observations to sometime between local midnight and magnetic midnight. From this time on, the level does not change much until daylight ends the observations. In spite of the difference in the type of observation, and the different position in the solar cycle, this agrees very well with the diurnal variation found from visual observations by *Elvey's* group [1955, 1956] for the years 1951–53 and 1953–55. It does not agree with the curve given by *Fuller* [1935] from visual observations in 1933–34, nor does it agree with earlier statements from many sources that auroral activity falls off after midnight, with or without a second maximum before morning [*Harang*, 1951]. The reason for the difference is not known. In some cases, such a discrepancy may be geographic (a latitude effect) or it may be a result of the solar cycle. Sometimes it seems likely that the observations may be at fault. None of these explanations appears to apply in the case of the two sets of visual observations at College; nevertheless, the discrepancy exists and it seems that there may be an actual change in the character of the diurnal variation, at least for College, between 1934 and 1951. Whether the change would apply only at College or is world-wide is not known.

The diurnal variation curve which was tained by the photometers seems remarka constant; data for a very few days was su ient to reproduce it in its essentials. Mont average curves show much the same shape do the total averages, and there is no evide of systematic variation from month to mo or from equinox to solstice, though the pe covered is too short for firm conclusions in respect. There seems to be no essential dif ence between the curves obtained from la disturbances, medium disturbances, and sm disturbances. Except in the actual intens values, the form of the curve remained same.

What may be called an "auroral storm" m last from one to several nights; the longer du tions are complicated by the difficulty of ciding whether two or more storms are overl ping. In storms lasting more than one nig the same general development will be observ on successive nights. A record for any of th nights resembles in its broad features the reco of Figure 1, and there is no particular way decide whether or not all events belong to t same storm.

Rapid Fluctuation in Intensity—An interes ing feature of the photometric records is a ra fluctuation in the light from the whole sky. typical example of this is shown in Figure 3. T amplitude of the variations may be 20 per ce of the total intensity, and the time betwe maxima may be anywhere up to a half minu or so. It should be emphasized that this do not refer to an ordinary pulsating aurora, whic as mentioned before, generally has a negligibl effect on the total intensity, but to some proce which must involve simultaneous action over large portion of the sky.

The phenomenon is somewhat unusual, bu not rare. During the nine months mentione above, the records show 44 instances of suc fluctuations, with individual durations rangin from a few minutes to several hours. The pe centage of auroral records showing this fluctua tion, however, is quite small. The phenomeno seems to be characteristic of some particula 'auroral storms,' since it frequently occurs o two or three successive nights but does not re appear for a considerable time. It is definitel a morning phenomenon; only one instance i

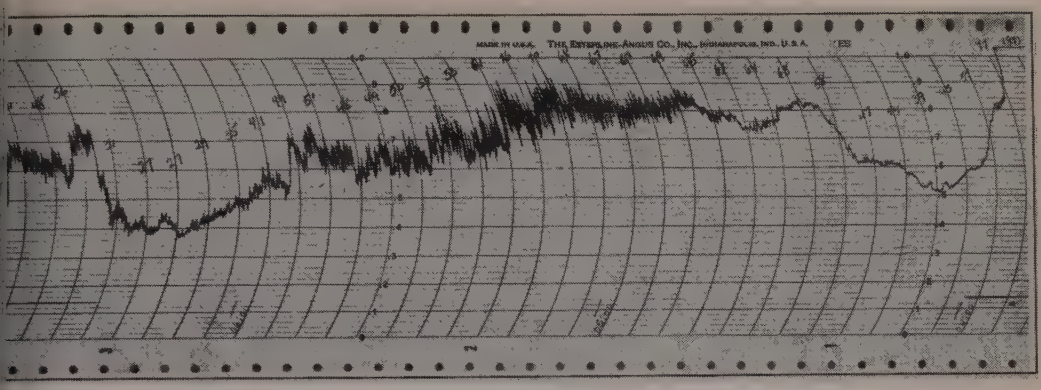

FIG. 3—Record showing rapid fluctuations in 3914A intensity

ıich it occurred before midnight was recorded, d this one started only a few minutes before dnight.

The records obtained during the rapid fluc- ation resemble those obtained from rapid fluc- ation of the earth currents [*Hessler* and *Wes- tt*, 1959], and the two phenomena sometimes ›pear to be related. However, the relation can- ›t be very close, as either phenomenon can ːcur without the other. The earth-current ıctuations are much more common and also ːe frequently observed before midnight. Study the magnetograms does not show association ith any definite magnetic feature, except that ıey always occur during a disturbance.

The fluctuations generally occur at two or ıree A.M.; consequently there are not many isual observations available for determining hat sort of auroral activity produces them. In ne instance, at least, such a record was ob- ained during a flaming aurora. At another time, isual observation showed multiple pulsating rcs at the time of the fluctuating record. Vis- al observation is necessary to establish the ause of any particular fluctuating record, be- ause all-sky camera records will not show this. ll-sky camera observations are related to the hotometric readings about as would be ex- ected; the maxima in intensity occur when the ll-sky camera shows large areas of bright au- rora. The photometers, however, are influenced considerably by large diffuse auroral forms which do not show up well on the all-sky pictures.

REFERENCES

ASHBURN, E. V., Photometry of the aurora, *J. Geophys. Research*, 60, 205–212, 1955.

ELVEY, C. T., H. LEINBACH, J. HESSLER, AND J. NOXON, Preliminary studies of the distribution of auroras in Alaska, *Trans. Am. Geophys. Union*, 36, 390–394, 1955.

ELVEY, C. T., Visual observations of the aurora in Alaska, Appendix, pp. 1–13, *Quart. Progr. Rept. 5., Signal Corps Contract DA-36-039-SC-56739*, Geophys. Inst., College, Alaska, 1956.

FULLER, V. R., A report on the aurora borealis for the years 1932–34, *Terrest. Magnetism and Atmospheric Elec.*, 40, 269–275, 1935.

HARANG, L., The aurorae, John Wiley & Sons, New York, 1951.

HESSLER, V. P., AND E. M. WESCOTT, Rapid fluctuations in earth currents at College, Alaska, *Geophys. Inst. Rept.*, College, Alaska, 1959, (in press).

REES, M. H., Absolute photometry of the aurora, *J. Atmospheric and Terrest. Phys.*, 1959 (in press).

ST. AMAND, PIERRE, *A possible relation between the night airglow and the ionosphere*, Doctoral thesis, Calif. Inst. Technol., Pasadena, 1953.

(Manuscript received March 5, 1959; presented at the Fortieth Annual Meeting, Washington, D. C., May 5, 1959.)

Analysis of Photoelectrons from Solar Extreme Ultraviolet

H. E. HINTEREGGER AND K. R. DAMON

Air Force Cambridge Research Center
Bedford, Massachusetts

AND

L. A. HALL

Comstock and Wescott, Inc.
Cambridge, Massachusetts

Abstract—The first rocket experiment for analysis of photoelectrons from a metal surface exposed to solar extreme ultraviolet around 115 miles altitude is evaluated. The soundness of the experimental techniques is confirmed, and the first data on photoelectron energy distribution are presented. Details on the simplified 'photoelectric method' of radiation analysis are discussed, and the preliminary results of applying this method to the first flight data are given.

Introduction—The scientific significance of studying photoelectrons ejected from a solid under solar irradiation at high altitudes may be divided into two areas. The first is concerned with the role of photoelectric emission in the over-all mechanism of charge transfer between a solid body and its environment of the upper atmosphere or interplanetary space. The other area is related to the fact that the energy distribution of the emerging photoelectrons is sensitive to the spectral composition of the incident radiation, and a crude but reliable intensity analysis [*Hinteregger*, 1958, pp. 146–156] of solar extreme ultraviolet (EUV) can be obtained with relatively simple satellite experiments.

The choice among the various possible experimental methods of photoelectron energy analysis was determined largely by practical considerations. The EUV radiation flux received by the solid sample had to be large enough to make possible the accurate measurement of small partial photoelectron currents with rocket-borne instrumentation. In the EUV this condition can be fulfilled only by providing a sufficiently large area of direct exposure. Optical means of collimating radiation of wavelengths shorter than about 1100A not only are inadequate but also would seriously falsify the spectral composition of the incident solar EUV. For the same reason, no material 'window' could be used to protect the photoelectron analyzer from the high density of ions and electrons in the ionospheric environment.

The photoelectron analyzer is of the retarding potential type (Fig. 1). A large plane cathode serves as the radiation receiver, and a grid in a parallel plane in front of it creates the variable retarding field. Since this retarding field depends only on the differential voltage $V_s - V_c$, it is possible to bias the cathode negatively with respect to the system ground (the rocket body and the shield) to guard against the collection of environmental electrons. The protection of the analyzer space against environmental positive ions is achieved by an auxiliary grid at a positive potential with respect to the rocket. The specific values of auxiliary grid and cathode bias voltage determine the highest kinetic energy of the environmental positive and negative charge carriers beyond which the protection is no longer effective. These limits refer to the kinetic energy with which an electron or ion actually reaches the vehicle surface. This energy differs from the corresponding value in an undisturbed environment to a degree which depends on the charge on the vehicle and the effects of the motion of the vehicle. For the

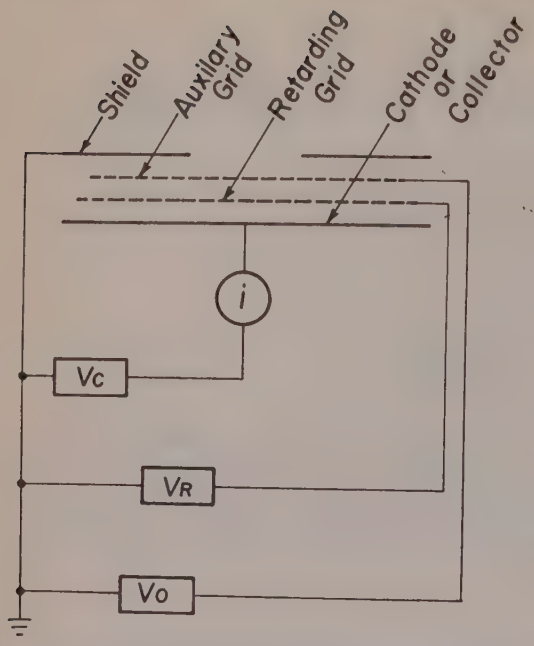

FIG. 1—Schematic diagram of retarding potential analyzer. The following voltages (with respect to vehicle skin) were used: $V_0 = +22$ v (constant); $V_c = -5.4$ v (constant); V_R sweeping between -1.0 v and -26.5 v (that is, between $+4.4$ v accelerating and -21.1 v retarding potential with respect to cathode).

rocket flight discussed here, the effects of the rocket motion can be disregarded.

Judgment of the charge voltage of the vehicle with respect to space potential is still rather controversial, mainly because of insufficient data on the energy distribution of the ionospheric electrons. (Their distribution may be far from that of 'thermal' equilibrium with the ions and the neutral gas.) There is, however, reasonable agreement in assuming negative polarity of the vehicle charge and in expecting a magnitude of potential difference of no more than a few electron volts for the altitude range in which the experiment was conducted. The results from the rocket experiment reported here are compatible with these assumptions but do not contribuite any further information on this interesting question. In future rocket and satellite experiments the same detector structure will be used to provide for analysis of environmental ions, environmental electrons, and EUV photoelectrons. It is hoped that these experiments will help to correlate the phenomena photoelectric emission and charge collection natural or artificial bodies moving through t upper ionosphere or interplanetary space.

Because of the parallel plane geometry of t retarding potential analyzer, the derivative the current-voltage diagram does not represe the distribution of the total energy of the ph toelectrons, but rather represents the distrib tion of energy related to the component of m mentum normal to the cathode surface ('norm energy distribution'). Undoubtedly the adoptic of a method which gives the total energy di tribution would have been much more desirab for drawing conclusions about the spectral co position of incident solar EUV. The difficulti inherent in such experiments on rocket an satellites, although not insurmountable, ha dictated the choice of a parallel plane geometr for the first experiment. For the purpose of ob taining information on the role of electron em sion due to solar EUV in the over-all charge ex change mechanism, the disadvantage of th adopted geometry is less serious because i many instances the distribution with respect t the energy of motion perpendicular to the sur face is as interesting as the total energy distri bution. Also, the normal energy distribution s obtained can be used to infer the total energ distribution by correlating it with data col lected in the laboratory.

Preflight study of instrument—The retarding potential analyzer used in the flight experiment was operated with the voltages indicated under Figure 1. The detector was of rectangular shape and had a large cathode of tungsten (18 cm × 8 cm); the parallel plane grid to which the retarding sweep voltage was applied also consisted of tungsten. The provisions against unwanted collection of environmental charged particles from the ionosphere have already been discussed. The unfiltered solar radiation was admitted through an opening of 74.4 cm² in the cover plate (shield). Since the combined optical transmission of the two grids was 90 per cent and the cathode plane was kept perpendicular to the incident rays by a biaxial pointing control, the effective radiation receiving area for our experiment was 67 cm².

Before flight, the entire detector was exposed to nearly monochromatic EUV radiation of an

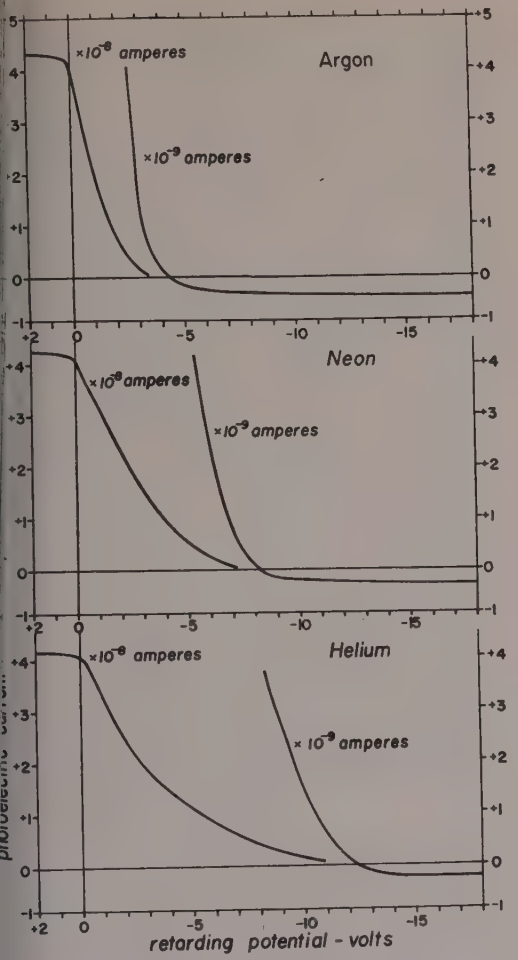

FIG. 2—Laboratory current-voltage diagrams of light instrument; obtained for photon energies of about 11.5, 16.8, and 21.2 ev corresponding to resonance radiation from argon, neon, and helium, respectively.

ntense photon flux in order that current-voltage diagrams could be obtained accurately. These diagrams formed the basis for constructing current-voltage diagrams for various hypothetical compositions of EUV spectra for comparison with flight data. The method of the corresponding 'photoelectric analysis' and its application to the first flight results will be discussed in a later paragraph. Figure 2 shows the current-voltage diagrams corresponding to nearly monochromatic radiation with photon energies of about 11.5, 16.8, and 21.2 ev produced respectively by argon, neon, and helium discharges. Previous studies with a vacuum monochromator had established the discharge conditions under which almost all of the EUV radiation is due to the respective resonance transitions. This allowed the use of undispersed (high intensity) radiation as a nearly monochromatic source. A magnetic trap prevented charged particles in the discharge from reaching the retarding potential detector and was sufficiently far removed from the latter so that its magnetic field presented no problems.

The curves of Figure 2 are uncorrected and show good saturation characteristics and low 'reverse currents' (less than 1 per cent of the saturation current in all cases). It will be noticed that the ratio of reverse current to saturation current decreases with increasing photon energy. This is quite understandable. The reverse current consists largely of photoelectrons from those parts of the retarding grid which face the cathode, whereas photoelectrons ejected from the opposite side (that is, by the direct incident radiation) are preferably drawn to the positive auxiliary grid (V_0 in Fig. 1). As the cathode reflectivity in this wavelength range is known to drop with decreasing wavelengths, the decrease in reverse current in the observed order must be expected. In principle, one could easily correct for considerably larger reverse currents, as they are essentially constant. (Over the retarding voltage range of interest here, the current of electrons from the grid to the cathode is saturated.)

However, in the radiation from the sun the relative number of EUV quanta is only a minute fraction of the intense photon flux of longer wavelengths. The reverse currents due to the latter could be considerably larger than the forward current due to EUV. As a consequence, one would be either off scale or limited to a rather insensitive negative scale on which the variation of the significant forward current with retarding voltage could no longer be recognized. It is known from previous laboratory experiments that commercially pure tungsten in its natural state of slight surface oxidation exhibits a particularly rapid decrease of photoelectric yield toward the longer wavelengths. The retarding grid was therefore made of tungsten in order to keep at a tolerable level the reverse

current expected for the actual rocket experiment.

The decision to use a tungsten cathode was related to this same property of the material, for a reason, however, which was not solely related to reverse currents. Whereas large reverse currents make it impractical to obtain information from the part of the current-voltage diagram around higher retarding potentials, any significant cathode sensitivity to longer wavelengths would have a similar effect in the range of low retarding voltages. If there is an excessive amount of low-energy electrons due to longer wavelength radiation, it is not practical to identify the low-energy electron contribution corresponding to EUV.

In order to study these effects on experimental detector structures under representative laboratory conditions before flight, an intense high-pressure xenon light source with a quartz collimator (mounted as a vacuum seal) was added to the vacuum system. The detector could then be exposed either simultaneously or successively to EUV and to undispersed intense radiation of wavelengths longer than 2000A. It should be noted that Figure 3 illustrates this procedure only schematically.

The relative reverse currents which were obtained for illumination with this xenon lamp

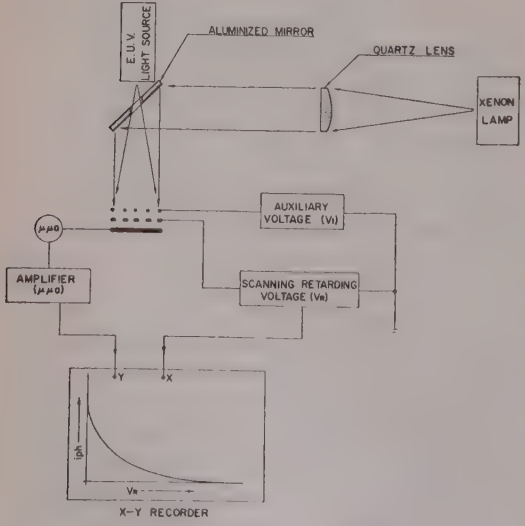

FIG. 3—Schematic diagram showing combination of extreme ultraviolet and near ultraviolet illumination for laboratory tests.

were actually found to be smaller than for argon discharge. This apparent deviation fr the previously indicted 'rule' is, of course, qu desirable from a practical viewpoint, and ac ally it is not surprising. The rule of decreas reverse current for decreasing wavelengths ho only for monochromatic EUV radiation and identical spectral distribution of photolect quantum efficiency of cathode and retardi grid. The first condition is obviously not f filled here since the xenon spectrum is contin ous from about 2000A up, and the observed fect can be explained as the interplay of t wavelength dependence of the cathode refle tivity and the rapid decrease of photoelect yield of the retarding grid towards the lon wavelengths. With respect to the second con tion, it should be emphasized that good agr ment of the spectral yields of cathode and g can be expected only in the EUV and not i longer wavelengths. In the latter region pho electric emission shows the well-known extre sensitivity to differences in sample treatme and slight contaminations. The 'normal' ene distribution obtained with the actual flight strument for illumination by this xenon lamp shown in Figure 4, where it is compared wi the distributions for monochromatic EUV radi tion. The character of these curves shows clear that even in the case of a dominating contrib tion of longer wavelengths to the 'saturatio current' the remaining current rapidly becom quantitatively determined by electrons due t EUV radiation as one progresses toward in creasing retarding potentials.

First results on energy distribution—An Aero bee-Hi rocket launched at 0845 MST on Aug ust 15, 1958 from Holloman Air Force Bas New Mexico, was the first well-behaved vehicl to carry an experiment designed for the analysi of EUV photoelectrons. The vehicle reached a altitude of 125 miles, and a readable telemetr record of the experiment was obtained. Over th interesting period of the flight, 15 diagrams o photoelectron current versus retarding voltag could be reconstructed. The sweep from + volts to −21 volts (grid voltage with respec to the cathode) took about 12 seconds, as it ha on the ground. The dc amplifier was provide with automatic range-switching over seve scales of forward current (electrons leaving the

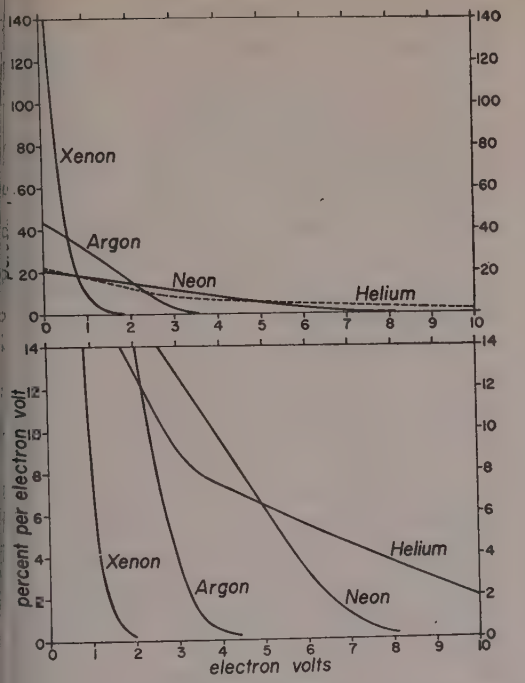

FIG. 4—Relative energy distributions; showing 'normal energy distribution' of photoelectrons for flight instrument exposed to nearly monochromatic EUV radiation (argon, neon, helium, and undispersed nearer ultraviolet from a xenon high-pressure lamp, respectively).

irradiated cathode) and two scales of reverse current (electrons being collected by the cathode). All scales were linear, and successive sensitivities were arranged to overlap in the ratio of 1:5. Of the nine scales, eight had actually been used during exposure in flight and neither the saturation current nor the maximum reverse current was off scale.

Figure 5 shows a plot which was derived from a preliminary evaluation of the flight telemetry record. The currents are given on an absolute scale and correspond to our effective area of 67 cm² for receiving the unfiltered solar radiation in normal incidence at an altitude near the peak of the rocket trajectory. Unfortunately, the flight data showed that there was a small positive parasitic current. It disappeared gradually during ascent towards zenith and did not reappear noticeably during the descent over the period covered by the data of Figure 5. The possibility of a corresponding zero shift of the dc amplifier was eliminated, and it has been

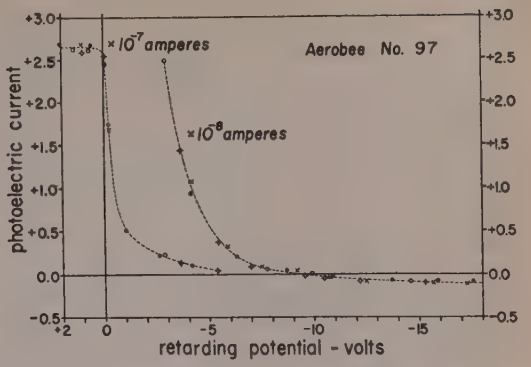

FIG. 5—Current-voltage diagram of flight experiment. The dashed line is considered characteristic for an altitude of approximately 115 miles (0847 MST, August 15, 1958, Holloman Air Force Base, New Mexico). The absolute values refer to an area of 67 cm² exposed at normal incidence. To correct for 'reverse current' the curve should be shifted along the ordinate axis by approximately 1.4×10^{-9} amp.

concluded that the effect was actually due to inadvertent pickup of environmental positive ions, not by the detector cathode itself, but by components used for the capacitive compensation of the displacement current which was induced by the retarding potential sweep. The effect can be remedied by a relatively simple redesign for future experiments; for the flight discussed here, however, it is the dominating limitation in the accuracy of interpreting details. As a discrimination of altitudes for the points of Figure 5 did not seem to be warranted, the dashed line represents an average current-voltage diagram which may be considered characteristic for an altitude of approximately 115 miles. This figure shows the current-voltage diagram without correction for the small reverse current. This correction is relatively insignificant for small retarding voltages. To obtain an accurate correction for the higher retarding potentials, however, the determination of the reverse current should be based on measurements over a larger range of retarding voltages. Because of the limitation in the actual experiment, the reverse current correction for the curve of Figure 5 is estimated as 1.4×10^{-9} ampere (−10 per cent, +50 per cent).

The derivative of the dashed line in Figure 5 gives a reasonably quantitative normal energy distribution of the photoelectrons from tungsten

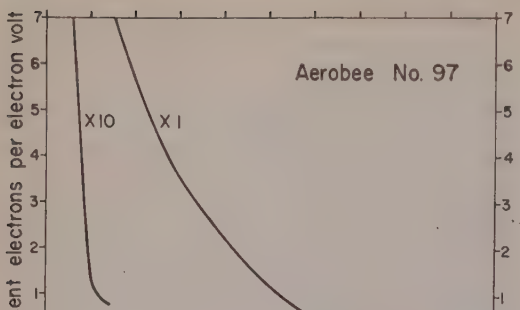

FIG. 6—Relative energy distribution of photoelectrons emitted from tungsten sample exposed to unfiltered solar radiation at about 115 miles (derived from experimental result shown in Fig. 5).

under direct solar radiation at this altitude (Fig. 6). The energy distribution shown in Figure 6 is representative only for the specific cathode material used in the flight experiment; however, the energy distributions for other materials exposed to the same radiation are expected to be fairly similar, except for the region near zero energy.

Estimate of spectral composition—The problem of obtaining information about the spectral intensity distribution of the incident light from an analysis of the current-voltage diagrams is complicated by two facts. First, monochromatic radiation does not cause monoenergetic photoelectric emission. Second, the retarding potential experiment in parallel plane geometry does not permit analysis of the total energy of the emitted electrons. Only the so-called normal energy may be analyzed, and its distribution always starts with a maximum value at zero energy. This would be the case even if the emitted electrons were monoenergetic. Because of the complications and limitations of an elaborate theoretical approach, a strictly empirical method was adopted for the actual analysis. This method consists of matching the current-voltage diagram (CVD) of flights to the monochromatic CVD's of the laboratory, their scale factors adjusted so as to provide a good fit. The scale factors are adjusted in the following way. At the high retarding-voltage end, the curve of the flight CVD is matched to a properly reduced laboratory CVD of the shortest wavelength considered important in the actual spectrum. T first 'partial CVD' is now extended to saturati and subtracted from the flight CVD. The sulting CVD is then matched to a suitably duced laboratory CVD for the next represen tive wavelength, and so on. This procedure rigorously applicable only if the spectrum concentrated in lines at given wavelengths. B even in more general cases the method still giv a valuable analysis of approximate intensit The resolution of this analysis naturally is lim ited because one cannot take too many parti CVD's of different wavelengths for the form tion of improved composite CVD's witho reaching a point of diminishing returns. Ther fore, this method is not in competition with t superior means offered by spectral photomet with diffraction gratings, but it is a desira substitute in cases where the installation of real monochromator may be prohibitive.

The procedure of matching the flight CVD laboratory CVD's is illustrated in Figure 7. T EUV range in this case is represented by on three partial CVD's, which correspond to wav lengths 584A, 740A, and 1060A, respectivel Besides these three extreme ultraviolet CVD's fourth CVD is used to approximate the contr butions of ordinary ultraviolet. Since the spec tral intensity distribution of the high-pressur xenon lamp is similar to solar radiation of abou 2000A, CVD's which had been obtained wit this lamp may be considered sufficiently repre sentative. A more accurate simulation was no considered necessary because this radiation doe not contribute photoelectrons of sufficiently hig energy to interfere with that part of the cur

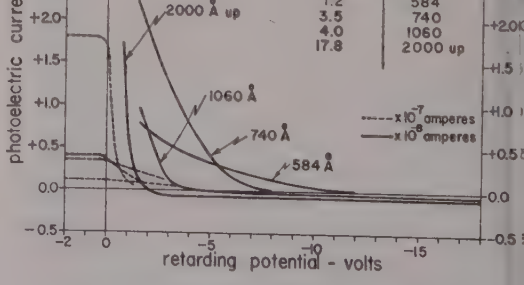

FIG. 7—Superposition of 'partial current-voltage diagrams' as explained in text.

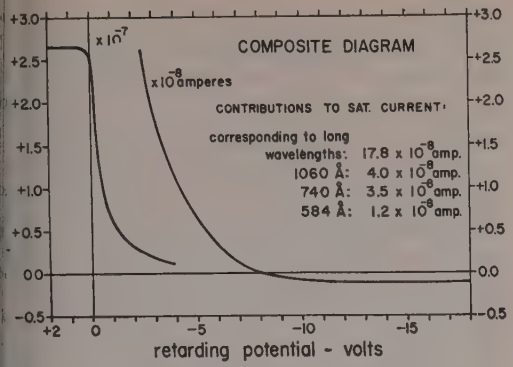

FIG. 8—Composite diagram resulting from superposition of partial current-voltage diagrams of Fig. 7.

ent-voltage diagrams which is most interesting or the EUV (compare Figure 4). The superposition of the partial CVD's of Figure 7 is hown separately in Figure 8. This CVD would e obtained by the actual detector under simulaneous irradiation by the three chosen EUV avelengths and the nearer ultraviolet continuum in a specific mixture of absolute intenities. To obtain the partial intensities in terms f photons/sec cm², the partial saturation curents (Fig. 7) must be divided by the effective rea (67 cm²) of the detector and by the corresponding photoelectric yield (number of electrons emitted per incident photon). Below 900A this yield, fortunately, is nearly constant. Above 900A the photoelectric yield decreases rather rapidly from about 12 per cent to about 1 per cent at 1300A. Within the limited accuracy of the CVD from the rocket flight (Fig. 5), it did not seem worth while to attempt an improved analysis by using many monochromatic partial CVD's. However, hydrogen Lyman alpha (at 1216A) is known as a line of outstanding intensity in the part of the solar spectrum above 1000A, and the inclusion of one additional partial CVD for this particular wavelength is most reasonable. In the revised analysis, which is based on five partial CVD's for 584A, 740A, 1060A, 1216A, and the xenon lamp, the contributions assigned to 584A and 760A remain unchanged, of course, but the distribution among 1060A, 1216A, and the long wavelengths is noticeably altered. The corresponding partial saturation currents and their conversions to intensity estimates are listed in Table 1.

Since the wavelengths shown in the top row of Table 1 represent only our convenient but arbitrary choice of monochromatic CVD's for the analysis, the figures of estimated solar radiation flux (last two rows) must not be mistaken for monochromatic intensities at these specific wavelengths. The figures actually represent integrated intensities for four spectral subsections. Although one cannot assign accurate wavelength limits to the individual subsections, a reasonable division, with probably no more than about 100A uncertainty, can be made. The corresponding bands under their nominal wavelengths of Table 1 are as follows: from soft x-ray wavelengths to 650A (under 584A); from 650A to 900A (under 740A); from 900A to 1100A (under 1060A); and from 1100A to 1350A (under 1216A). Therefore, the intensity estimate under 584A in Table 1, for instance, includes not only the He I (584A) and He II (303A) lines, which were discovered spectrographically in a recent

TABLE 1—*Spectral composition of solar extreme ultraviolet at 115 miles altitude*
(The flux data reflect integrated intensities over adjoining subsections around the wavelengths listed in the first column.)

Wavelength of partial CVD (A)	Partial saturation current (10^{-8} amp)	Partial current density (10^{-10} amp/cm²)	Yield in electrons per photon	Corresponding photon flux (10^{10} cm^{-2} sec^{-1})	Estimated energy flux (erg cm^{-2} sec^{-1})
584	1.2	1.8	0.13	0.86	0.3
740	3.5	5.2	0.14	2.3	0.6
1060	1.8	2.7	0.064	2.6	0.5
1216	8.0	12	0.022	34.0	5.5
2000 up	12.2	18	10^{-4}	...	...

rocket experiment by W. A. Rense (private communication, 1958), but also any other emission lines or continuum in this range. The intensity estimate of the band around 740A also deserves some comment (Table 1). The estimated intensity of solar radiation under this column could, of course, be distributed over the range of about 600A to 950A in any number of different arrangements. It could consist of many weak lines, one or more strong ones, an actual continuum, or a mixture of continuum and lines. The present experimental record provides no basis for determining the spectral distribution.

Discussion—There are practical difficulties in the determination of absolute intensities in the EUV spectrum of solar radiation. Both the nature of these difficulties and their degree of seriousness strongly depend on the specific wavelength section of this spectral range and on the experimental method. Photographic records of the solar EUV spectrum have been obtained by various workers [*Rense,* 1953; *Jursa,* 1955; *Johnson* and others, 1958] using rocket-borne grating spectrographs, but the determination of absolute intensities with this technique becomes increasingly difficult towards the shorter wavelengths. For instance, Rense's spectrographic discovery of obviously strong lines at 303A (He II) and 584A (He I) in the solar spectrum allows only an order-of-magnitude estimate of the intensity. Even the latter is possible only for such strong single lines, and the situation is considerably worse for the determination of integrated absolute intensities of certain subsections of the EUV range (for example, wavelength bands one or several hundred angstrom units wide). At least at present, photographic spectrophotometry does not offer significant information on absolute integral intensities of wavelength bands below about 1000A. There the implementation with nonspectrographic techniques, such as photon counters or ionization chambers sensitive only to specific wavelength bands, is extremely valuable. This has been demonstrated by the well-known work of Friedman and his co-workers during the past ten years at the U. S. Naval Research Laboratory [*Byram* and others, 1953, 1956; *Chubb* and others, 1957]. The region of applicability of their techniques, however, has a gap extending from 1050A (transmission limit of lithium fluorid down to the much shorter wavelengths of t x-ray range, for which significantly 'transpa ent' window materials are again available. Fo tunately, the photoelectric method is best suit to this wavelength range, below about 1000A, b cause the photoelectric yield [*Hinteregger* a *Watanabe,* 1953; *Wainfan* and others, 195 *Walker* and others, 1955] is very high and al shows conveniently little wavelength depen ence.

As far as we know, Table 1 presents the on data on absolute integral radiation flux co tained in sections of the solar EUV emissio spectrum between about 1000A and x-rays. A these data are based on a single rocket fligh the figures should be used with some reserv tion; however, the actual flux values are b lieved to deviate no more than +200 per ce or −70 per cent from those listed in Table Naturally, the most significant improvement our knowledge of the absolute intensity dist bution of solar EUV would be expected [*Hi teregger* and *Watanabe,* 1953] from a combin tion of diffraction-grating spectrometry wi proper photoelectric detection techniques. Th most serious disadvantage of photographi rocket spectrometry in the EUV—the proble of abundant stray light of longer wavelengths can thereby be virtually eliminated. The gra ing-incidence rocket monochromators for th EUV range from 250A to 1300A, developed fo this purpose, have already been completed an are presently being subjected to the last pre flight tests and calibrations in the laboratory Their successful performance, however, will no eliminate the need for continuing experiment of the type described in this paper, at least fo the purpose of clarifying the role of photoelec tric emission in the balance of charge transfe between bodies in the upper atmosphere an interplanetary space. Whereas the contributio of those photoelectrons which are specifically due to solar EUV is relatively insignificant u to moderately high satellite altitudes, it become increasingly important for larger distances from the earth. From our present results (Fig. 5) we must expect that electron emission due to EUV would actually be the dominant factor in estab lishing the equilibrium charge of a body in in terplanetary space, provided the density o

vironmental ions and electrons is not much gher than is generally believed.

References

YRAM, E. T., T. A. CHUBB, H. FRIEDMAN, AND N. GAILAR, Lyman-alpha radiation in the solar spectrum, *Phys. Rev.*, **91**, 1278, 1953.

YRAM, E. T., T. A. CHUBB, H. FRIEDMAN, AND J. E. KUPPERIAN, JR., Observations of the intensity of solar Lyman-alpha emission, *Astrophys. J.*, **124**, 480–482, 1956.

CHUBB, T. A., H. FRIEDMAN, R. W. KREPLIN, AND J. E. KUPPERIAN, JR., Lyman-alpha and x-ray emissions during a small solar flare, *J. Geophys. Research*, **62**, 389–398, 1957.

HINTEREGGER, H. E., *Vistas in astronautics*, Pergamon Press, New York, 330 pp., 1958.

HINTEREGGER, H. E., AND K. WATANABE, Photoelectric cells for the vacuum ultraviolet, *J. Opt. Soc. Am.*, **43**, 604–608, 1953.

JOHNSON, F. S., H. H. MALITSON, J. D. PURCELL, AND R. TOUSEY, Emission lines in the extreme ultraviolet spectrum of the sun, *Astrophys. J.*, **127**, 80–95, 1958.

JURSA, A., Results of recent attempts to record the solar spectrum in the region of 900 to 3000 A, *J. Opt. Soc. Am.*, **45**, 1085–1086, 1955.

RENSE, W. A., Intensity of Lyman-alpha line in the solar spectrum, *Phys. Rev.*, **91**, 229–302, 1953.

WAINFAN, N., W. C. WALKER, AND G. L. WEISSLER, Preliminary results on photoelectric yields of Pt and Ta and on photoionization in O_2 and N_2 in the vacuum ultraviolet, *J. Appl. Phys.*, **24**, 1318–1321, 1953.

WALKER, W. C., N. WAINFAN, AND G. L. WEISSLER, Photoelectric yields in the vacuum ultraviolet, *J. Appl. Phys.*, **26**, 1366–1372, 1955.

(Manuscript received February 18, 1959.)

A Theory of Spread F Based on a Scattering-Screen Model*

J. RENAU

Cornell University
Ithaca, New York

Abstract—To shed some light on the phenomenon of spread F, a thin scattering screen is postulated above the E region. The virtual height which is associated with a pulse radiated from the sounder, forward scattered by the screen and then reflected back to the sounder via the F region, is calculated.

For frequencies appreciably larger than the penetration frequency, the minimum virtual height versus the operating frequency, on a linear scale, is a straight line, the slope of which depends on the height of the screen. As the height of the screen increases, the slope decreases. When the scattering screen is assumed at the level of reflection, the slope of the line coincides with the tangent from the origin to the regular vertical-incidence trace.

Experimental ionograms are presented that fit with the suggested mechanism.

Introduction—Over the past twenty years experimental observations with ionospheric sounding equipment have established the existence of the spread F phenomenon [*Kasuya* and others, 1955; *Reber*, 1954, 1956; *Singleton*, 1957; *McNicol* and *Webster*, 1956], but the mechanism responsible for this effect is still not understood.

Assuming that spread F is due to a scattering mechanism [*Dieminger*, 1951; *Eckersley*, 1937; *Briggs* and *Phillips*, 1950; *Briggs*, 1958], we postulate a thin scattering screen at a level above the E region. The existence of the screen permits echoes to return to the sounder from off-vertical ray paths. Calculations of virtual heights associated with such rays have been made with a view to estimating the type of ionogram that would result from such a model. It was hoped that by varying the height of the scattering screen some idea would be obtained of the height principally responsible for spread-F occurrences.

Calculation of virtual height—Figure 1 illustrates a scattering screen at a height h_s above the surface of the earth. This screen has been drawn below the F region, the bottom of which is supposed to be at a height h_0; TR denotes a transmitter and receiver at an ionospheric sounder, a ray from which in the direction of point P on the screen can be scattered back to the sounder via the F region, as shown. Let θ' be the angle of incidence of the ray before scattering and θ the angle of incidence after scattering. To write an expression for the virtual height, which is defined as half the time taken for a signal to travel from the ionospheric sounder to the point P and back to the ionospheric recorder via the F region, multiplied by the velocity of light, it is convenient to make use of the function $h'(\theta, f/f_p)$. This is the equivalent height of the F region for a fixed angle of incidence θ and an operating frequency f when the vertical penetration frequency is f_p. For a parabolic F region this function is

$$h'(\theta, f/f_p) = h_0 + (Hf \cos \theta/f_p) \ln \frac{1 + f \cos \theta/f_p}{1 - f \cos \theta/f_p}, \quad (1)$$

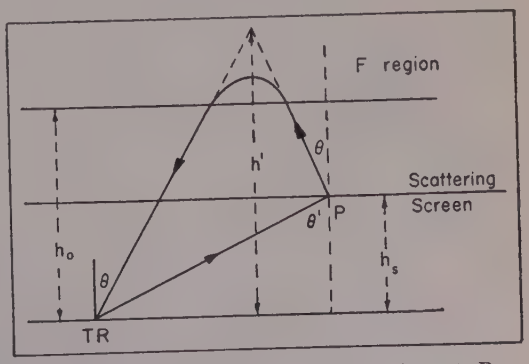

FIG. 1—Ray path illustrating scattering at P

* This research was supported by the U. S. Signal Corps under Contract No. DA-36-039-sc-74903.

where $2H$ is the semithickness of the layer. In terms of this function the virtual height ct is given by

$$ct = h' \sec \theta + \tfrac{1}{2}h_s (\sec \theta' - \sec \theta) \qquad (2)$$

where t is half the time of travel of the path and c is the velocity of light in free space.

A relation between the angles θ and θ' is obtained by equating two expressions for the distance of the scattering point P from the vertical through the sounder. In this way we obtain

$$h_s \tan \theta' = (2h' - h_s) \tan \theta. \qquad (3)$$

To obtain the dependence of the virtual height ct on the angle of arrival θ, we eliminate θ' between (2) and (3) and thereby obtain

$$ct = h' \sec \theta + \tfrac{1}{2}h_s \cdot \left[\left\{1 + \frac{(2h' - h_s)^2 \tan^2 \theta}{h_s^2}\right\}^{\frac{1}{2}} - \sec \theta\right], \qquad (4)$$

where h' is given by equation (1) and is independent of the angle θ'.

In Figure 2, the virtual height ct is plotted as a function of the arrival or the departure angle θ for a series of constant values of f/f_p. This diagram has been drawn for a situation in which the level of maximum electron density in the F region is at 400 km, the bottom of the F region is at 270 km, and the screen height is at 180 km. It can be seen that the curves associated with a low value of f/f_p exhibit a single extreme value; namely, a minimum which occurs at zero angle of incidence. As the operating frequency approaches the penetration frequency, the curves exhibit two extreme values, a minimum for a nonzero angle of incidence and a maximum for a zero angle of incidence. The two types of curves are separated by a curve corresponding to a frequency f^* which is less than the penetration frequency f_p; for the frequency f^* the extreme values of virtual height coincide. For frequencies less than f^* the minimum virtual height occurs for rays leaving the

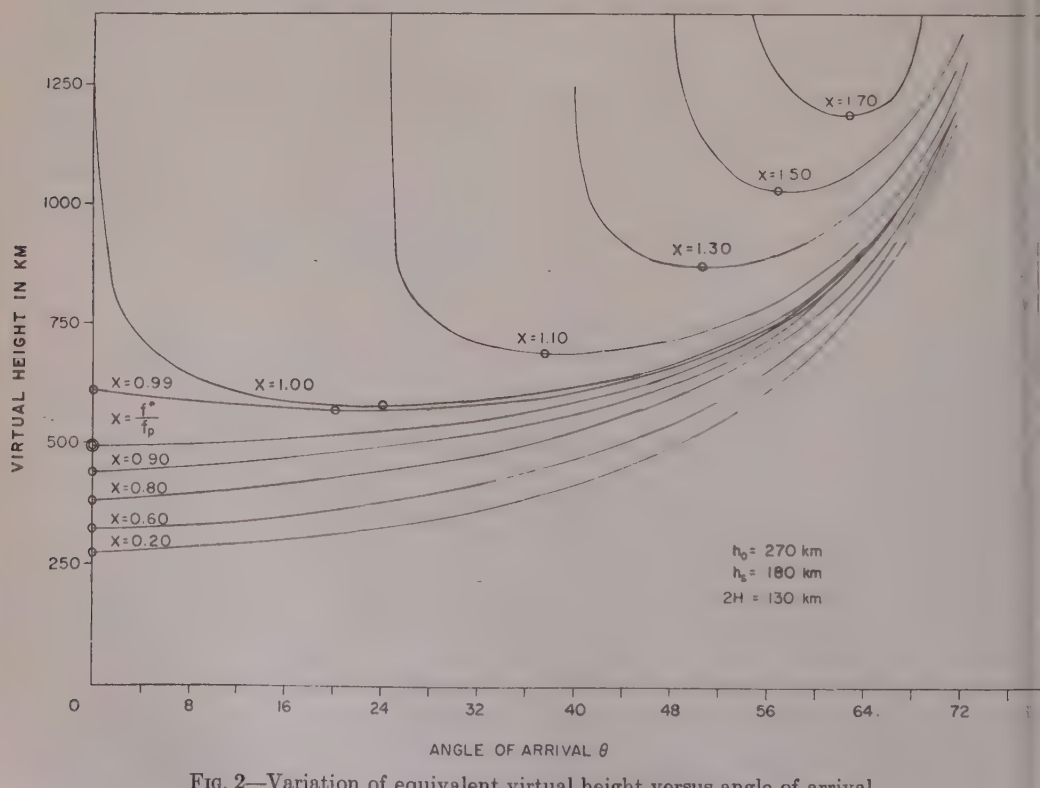

FIG. 2—Variation of equivalent virtual height versus angle of arrival

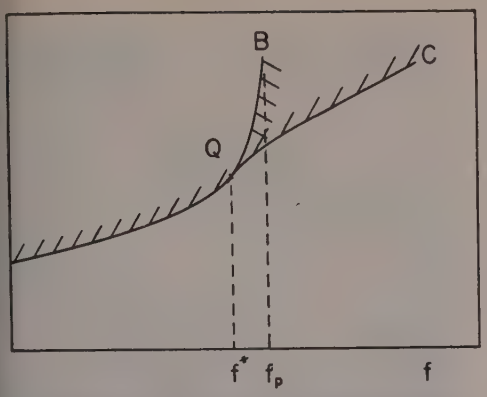

IG. 3—Sketch of theoretical spread-F ionogram

ounder in the vertical direction. For frequencies reater than f^* the minimum virtual height ccurs for a value of θ that increases with the perating frequency f. For frequencies between * and f_p the virtual height exhibits, in addition o the minimum value, a maximum value as nentioned above. If these extreme values of he virtual heights are plotted as a function of perating frequency, we obtain a curve with two ranches AQB and AQC as shown in Figure 3.

The branch AQB is identical with the regular curve of vertical equivalent height versus frequency. The branch QB in Figure 3 corresponds to the maximum virtual height occurring for $\theta = 0$ and for frequencies between f^* and f_p. The branches AQ, QC, and QB shown in Figure 3 correspond to values of virtual heights that are stationary with respect to the angle θ in Figure 2. Each point on the branches corresponds, therefore, to a situation in which radiation from the sounder over a range of angles arrives back at the sounder with practically the same delay time, thus bringing about time focusing. For the branch AQ and the branch QC, the indicated virtual height is a minimum value, and departures from this value can occur upward on the ionogram as indicated by the shading in Figure 3. For the branch QB, the indicated virtual height is a maximum, and spread can occur from this curve downward. The type of ionogram that should be observed, therefore, should consist of a trace AQC, with a sharp underedge and upward spreading from this edge. In addition, however, there should be a trace QB which is sharp on the left and spread

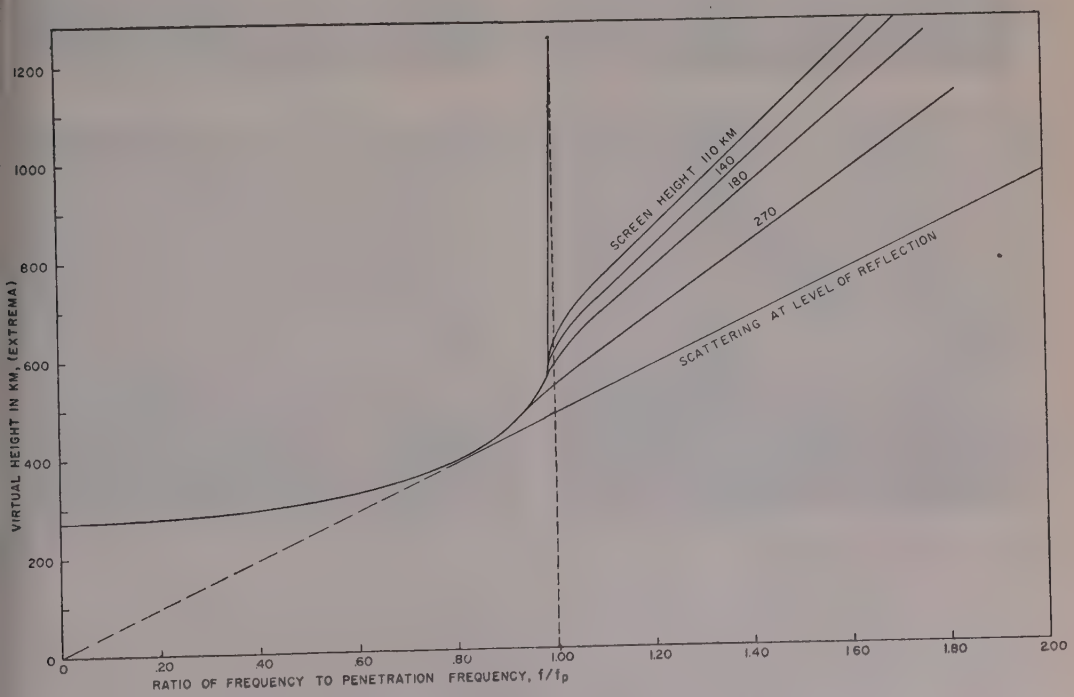

FIG. 4—Theoretical spread-F ionogram

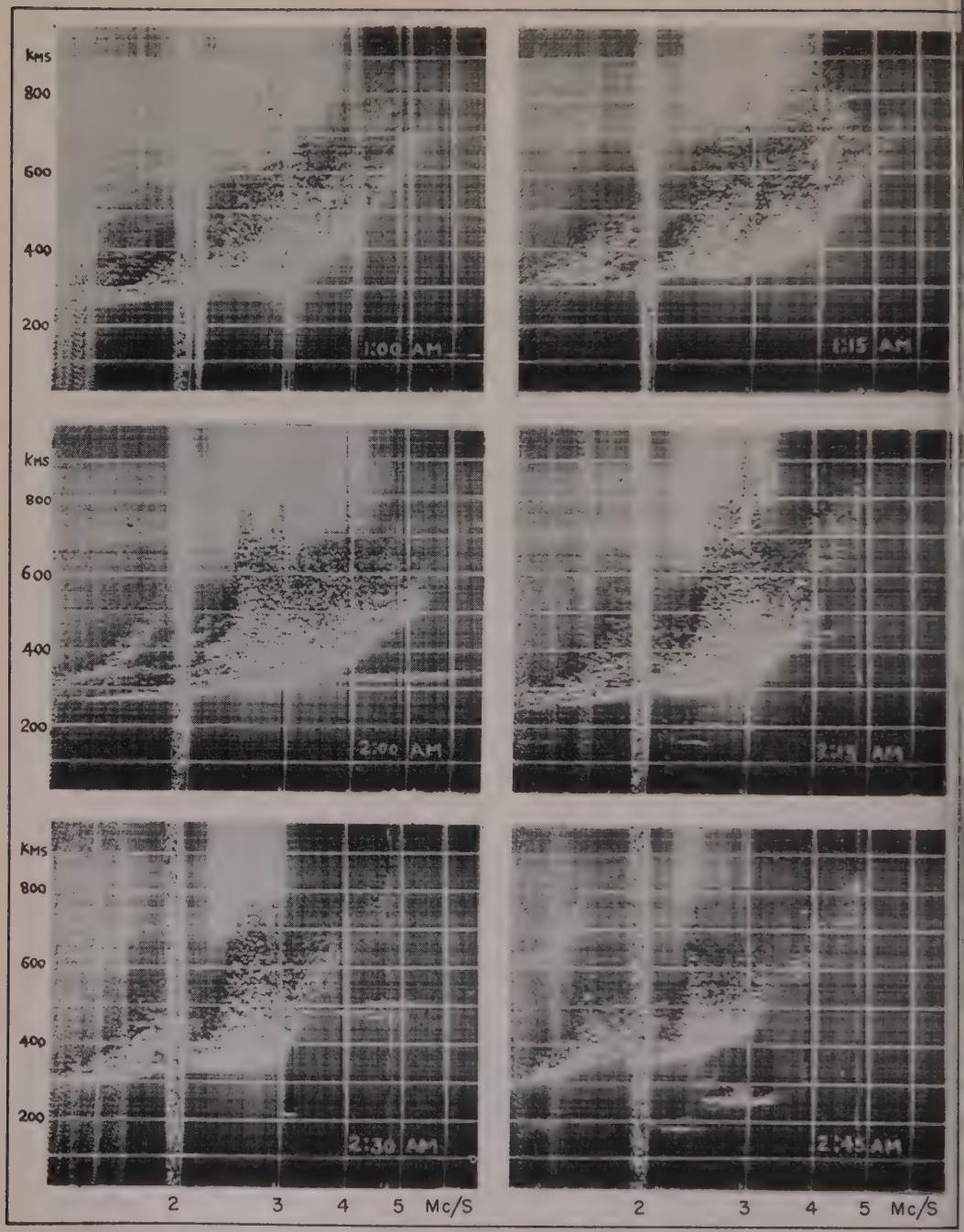

FIG. 5—Records from Godhavn Ionospheric Station, March 9, 1955

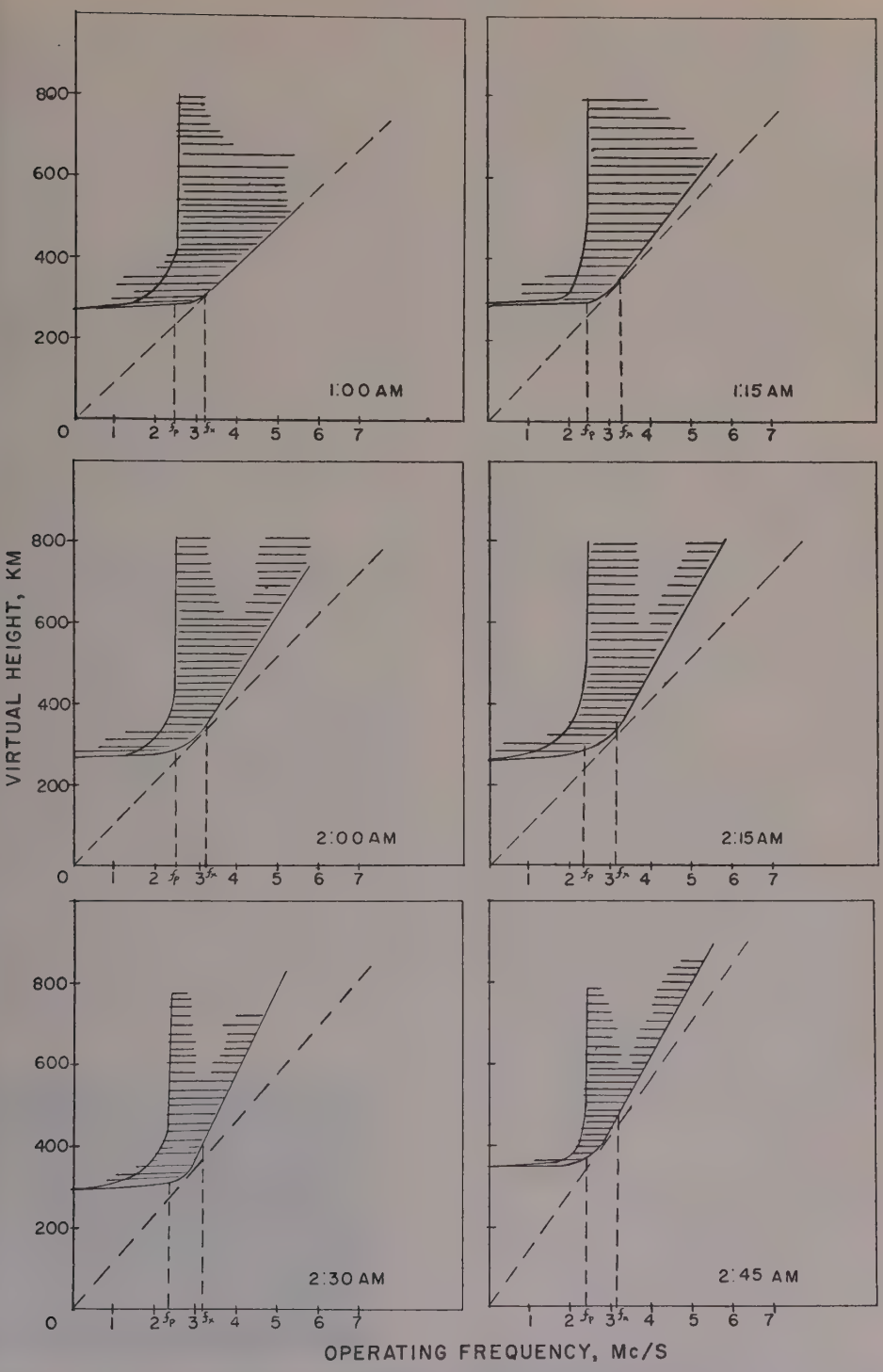

Fig. 6—Records from Godhavn Ionospheric Station, March 9, 1955, replotted on linear-frequency scale

to the right. In a qualitative way the type of ionogram indicated by Figure 3 is a type frequently observed during disturbed ionospheric conditions. The existence of the branch *QB* which is sharp on the left and spread to the right is quite well known and is frequently used for assessing the ordinary penetration frequency of spread-F ionograms. We note also that, on a linear frequency scale and for operating frequencies larger than f_p, the theoretical branch *QC* is a straight line whose slope is greater than the slope of the tangent from the origin of the coordinate system to the regular trace.

Calculations were repeated for a series of values of the height of the scattering screen with the results plotted in Figure 4. It will be observed that, for frequencies larger than the frequency of penetration, the slope of the branch *QC* substantially decreases as the height of the scattering screen increases. Finally, calculations were made for the situation in which the scattering screen is at the level of reflection; in this case the forward scattering screen model reduces to backscattering from the level of reflection, where it is assumed that irregularities exist. The minimum virtual height involved in this case is one-half the virtual height involved in backscattering from the ground via the ionosphere, as previously studied by *Peterson* [1951]. For the case of backscattering from the level of reflection and for a linear-frequency ionogram rather than the usual logarithmic one, the branch *QC* is a tangent from the origin of the coordinate system to the regular trace, as indicated in Figure 4. Thus the slope of the branch *QC* decreases, as the height of the scattering screen increases, until it coincides with the tangent to the normal trace. Figure 4, therefore, is a theoretical prediction of the type of spread one may obtain for each height of the scattering screen.

To incorporate the approximate effect of the earth's magnetic field in the model, the regular trace, corresponding to the extraordinary wave, may be used to replace that which exists when the earth's magnetic field is neglected.

Comparison with observations—The ionograms illustrated in Figure 5 were selected from the records available at the National Bureau of Standards, Boulder, Colorado; they are from the Godhavn Ionospheric Station and were recorded on March 9, 1955. These have been r plotted on a linear-frequency scale in Figure According to present practice the inner fr quency edge of a spread ionogram is the pen tration frequency. Therefore the penetrati frequency of the ordinary wave is scaled about 2.4 Mc/s. If the gyrofrequency of t electrons at Godhavn (dip 81°) is taken as 1. Mc/s at an altitude of 300 km, the penetrati frequency f_x of the extraordinary trace is calc lated to be about 3.2 Mc/s. The observed sprea is indicated by the horizontally shaded are The tangent from the origin to the regular tra which corresponds to the extraordinary wav has been drawn as a guide. The shaded area in the neighborhood of this tangent line, an for frequencies f larger than the penetrati frequency of the extraordinary trace, the co tour of the shaded area is roughly a straigh line. The spread ionograms, therefore, agree re sonably well with the theoretical predictions the scattering-screen model. The screen heig responsible for the spread seems to vary wit time and an estimate places it appreciably abov the E region. Indeed, a screen at the level reflection in the F region is a possible case, a shown by the first ionogram of Figures 5 and

Figure 7 represents another example of arct spread-F ionogram published by *Reber* [1956] This ionogram has been replotted on a linear frequency scale in Figure 8. Once more it i seen, according to the present practice of scal ing the penetration frequency, that the ordinary penetration frequency is 2.65 Mc/s and th penetration frequency of the extraordinary trace is calculated to be about 3.5 Mc/s. The ob-

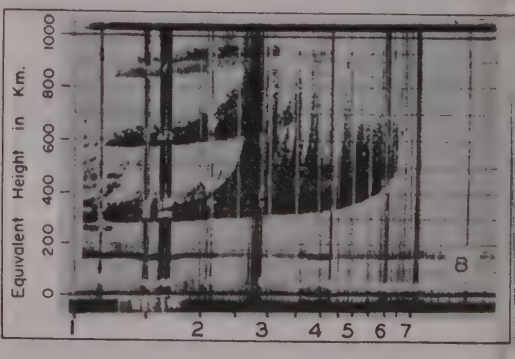

FIG. 7—Arctic spread-F ionogram published by *Reber* [1956]

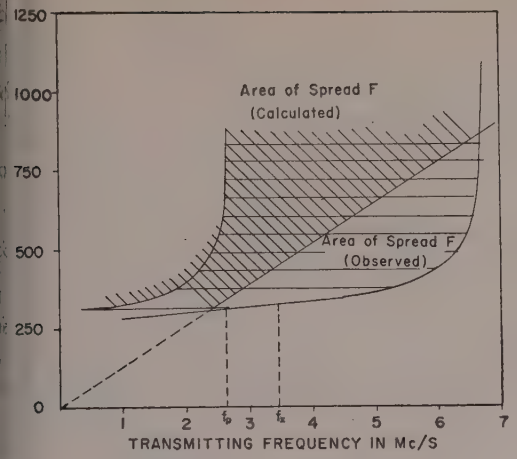

FIG. 8—Arctic spread-F ionogram of Figure 7, replotted on linear-frequency scale

erved spread is indicated by the horizontally haded area. The extreme spread that would be xpected on the basis of the calculations of the receding sections, including the approximaion for the effect of the earth's magnetic field, s indicated by the diagonal shading. It is clear hat, whatever the height of the screen, the shape of the theoretical ionogram indicated in Figure 8 does not correspond well with the observed spread F of Figure 7. In general, when the inner and the outer frequency edges of a spread ionogram are so separated that the frequency difference of the two edges is much larger than the gyrofrequency (in the artic ionograms) or half the gyrofrequency (in the middle latitude ionograms), and both of the edges resemble normal ionogram traces in shape, then the results of the scattering-screen model fail to explain the observations. The ionogram of Figure 7 is of this type.

In conclusion, the scattering-screen theory in its present form cannot explain all observed types of spread F, but it does provide an explanation for the many ionograms of the form of Figure 5. Moreover, the results of this theory can be applied to a larger class of spread ionograms if features of observed spread F are re-interpreted and the current procedure of determining the penetration frequency is revised. This assertion will be discussed in a future paper which will contain a detailed study of the formation of the observed spread F and its structure.

Acknowledgment—The author wishes to thank H. G. Booker for his helpful criticism and suggestions. Thanks are also due to the officials of the IGY Ionospheric Data Center, CRPL, Boulder, Colorado.

References

Briggs, B. H., and G. J. Phillips, A study of the horizontal irregularities of the ionosphere, *Proc. Phys. Soc. London, B,* **63**, 907–923, 1950.

Briggs, B. H., A study of the ionospheric irregularities which cause spread-F echoes and scintillation of radio stars, *J. Atmospheric and Terrest. Phys.,* **12**, 34–45, 1958.

Dieminger, W., The scattering of radio waves, *Proc. Phys. Soc. London, B,* **64**, 142–158, 1951.

Eckersley, T. L. Irregular ionic clouds in the E layer of the ionosphere, *Nature,* **140**, 846–847, 1937.

Kasuya, I., S. Katano, and S. Taguchi, On the occurrences of spread echoes in the F region over Japan, *J. Radio Research Lab., Japan,* **2**, 239, 1955.

McNicol, R. W. E., and H. C. Webster, A study of 'spread F' ionospheric echoes at night at Brisbane, *Australian J. Phys.,* **9**, 272–285, 1956.

Peterson, A. M., The mechanism of F layer propagated backscatter echoes, *J. Geophys. Research,* **56**, 221–237, 1951.

Reber, G., Spread F over Hawaii, *J. Geophys. Research,* **59**, 257–265; Spread F over Washington, *ibid.,* 445–448, 1954.

Reber, G., World-wide spread F, *J. Geophys. Research,* **61**, 157–164, 1956.

Singleton, D. G., A study of spread-F ionospheric echoes at night at Brisbane, *Australian J. Phys.,* **10**, 60–76, 1957.

(Manuscript received March 30, 1959.)

The Possible Occurrence of Negative Nitrogen Ions in the Atmosphere

F. D. STACEY

Geophysics Department
Australian National University
Canberra, A.C.T., Australia

Abstract—Liquid conduction counter experiments give evidence of N_2^- ions, so that their possible occurrence in the atmosphere cannot be discounted. It is shown that a strong pressure dependence of electron-ion recombination coefficient, as found in laboratory experiments on nitrogen gas, would result from the formation of metastable negative ions. At very low pressures negative ion formation could result in an attachment law $-dn_e/dt = \beta n_e$ for decay of electron density n_e.

Negative ions of molecular or atomic nitrogen have been sought unsuccessfully for a number of years, so it is generally assumed that they do not exist and that nitrogen has no electron affinity [*Massey*, 1950; *Branscomb*, 1957]. However, significant positive evidence arising from liquid conduction counter experiments appears to have been ignored, and the purpose of this note is to assess the evidence and to consider its possible implications. The principal conclusions are that if negative ions are formed a strong pressure dependence of electron-ion recombination coefficient is to be expected and that at very low densities (corresponding to the F2 layer) the rate of disappearance of free electrons could follow an attachment law.

Experimental Evidence—Davidson and *Larsh* [1950] measured the pulses of electrical conduction occurring in an ionization chamber in which the ionized media were dilute solutions of nitrogen and oxygen in liquid argon. They found that both of the added gases destroyed the conduction pulses by removing free electrons from the liquid. Although the effect was about 20 times greater for oxygen than for nitrogen, their conclusion that N_2^- ions were formed and therefore that N_2 has an electron affinity appears to be inescapable. (It also explains why pure liquid nitrogen does not give electron conduction.) More recent work [*Williams*, 1957; *Williams* and *Stacey*, 1957] showed unmistakably that Davidson and Larsh's pulses were due to electron and not ion motions, and independent qualitative confirmation of their results has been obtained (Stacey, unpublished data).

The conditions prevailing in the liquid state may be particularly conducive to the formation of N_2^-, but it appears unlikely that its formation is completely impossible in the gaseous state; lack of direct observation is only presumptive evidence. Such negative evidence was also used to discount He^- until it was discovered by *Hiby* [1939]. Useful support for Davidson and Larsh's conclusion that N_2^- ions occurred in their experiments is given by the evidence for He^- in the liquid helium conduction counter [*Williams*, 1957; also discussed briefly by *Stacey*, 1959].

Estimate of Cross Section for Capture of Electrons by N_2—The cross section can be estimated from the results of Davidson and Larsh, although N_2^- apparently has a short life which cannot be taken into account properly so that the value obtained depends to a certain extent on the choice of experimental readings. Taking the ratio of maximum observed pulse size in the solution to that observed in pure argon, at an electrode separation $d = 0.36$ mm, to be 0.5 at a mole fraction 1.1×10^{-2} of nitrogen, we have

$$0.5 = (1 - e^{-x})/x,$$

where

$$x = NQ\,d,$$

N being the number density of nitrogen molecules (2.3×10^{20} cm^{-3}) and Q the required

cross section. Then

$$Q \sim 2 \times 10^{-19} \text{cm}^2$$

This estimate is not necessarily appropriate to electrons at 90°K, as it was obtained from measurements made with an applied electric field.

Pressure Dependence of Electron-Ion Recombination

Coefficient in N_2—Bialecke and *Dougal* [1958] measured this coefficient by a microwave transmission method and observed a strong pressure dependence, which is to be expected if metastable negative ions are present but is otherwise difficult to explain. Apart from the direct recombination processes discussed by Bialecke and Dougal, recombination may occur via negative ion formation as indicated by equations (1).

$$N_2 + e \rightleftharpoons N_2^- \qquad (1a)$$

$$N_2^- + N_2^+ \rightarrow 2N_2 \qquad (1b)$$

Equation (1a) is represented as reversible, since it is assumed that N_2^- is metastable. However, it acts as a reservoir of electrons which are not observed in microwave-transmission experiments. The detailed mechanism of (1b) is not of interest here.

The observed recombination coefficient α_0, for the rate of disappearance of electrons of density n_e is defined by the equation

$$-dn_e/dt = \alpha_0 n_e^2 \qquad (2)$$

since it is supposed that the positive ion density n_+ is equal to n_e. α_0 is the quantity measured by Bialecke and Dougal. It may be related to the coefficients α_e for direct recombination of electrons with positive ions and α_i for recombination of negative ions with positive ions. If the negative ion density is represented by n_i, the total rate of disappearance of electrons and negative ions is given by

$$-d(n_e + n_i)/dt = \alpha_e n_e n_+ + \alpha_i n_i n_+ \qquad (3)$$

For gases of moderate density we may make the simplifying but reasonable assumption that the density of neutral molecules is always so much greater than that of any of the ions that the equilibrium represented by equation (1a) is established in a time short by comparison w that required for the other processes. Then

$$n_i/n_e = \tau_i/\tau_e$$

where τ_i is the mean lifetime of N_2^- with resp to separation into a neutral molecule plus electron, and τ_e is the mean lifetime of an el tron between successive captures to form N Combining (3) and (4) and noting that n_+ $n_e + n_i$ for over-all neutrality of the gas, obtain

$$-dn_e/dt = n_e^2(\alpha_e + \alpha_i\tau_i/\tau_e)$$

so that from (2) and (5)

$$\alpha_0 = \alpha_e + \alpha_i\tau_i/\tau_e$$

For electrons of velocity v in nitrogen molecular density n

$$\tau_e = 1/nQv$$

where Q is the capture cross section, which w estimated above but is almost certainly a fu tion of v. We may write n in terms of pressure

$$n = Ap$$

where

$$A = n_0T_0/p_0T$$

and T is absolute temperature, values at stan ard temperature and pressure being denoted the subscript zero. Inserting (7) and (8) into (we obtain an approximation to the variation recombination coefficient with pressure.

$$\alpha_0 = [\alpha_e] + [A\alpha_i\tau_iQv]p$$

Of the quantities in square brackets in equa tion (9) only τ_i can be a significant function of (It is possible that more frequent collisions wit neutral molecules may reduce the lifetime ions), but by considering only low gas densiti this effect can be neglected and we find α_0 to l a linear function of p at constant temperatur When the results of Bialecke and Dougal a replotted on a linear scale, a stronger (quadrati variation with p is indicated. This could be e plained by the formation of N_4^- by attachmen of neutral molecules to N_2^-. It is important t note that in this way we can avoid the conclusio that the recombination coefficient has a funda mental dependence upon pressure. α_e and α_i a independent of pressure.

Rocket Experiments—The possibility of direct servation of all the ion types in the upper nosphere is intriguing, and the experiments *Johnson* and *Heppner* [1956] are of interest this connection. At altitudes between 93 km d 131 km negative ions were observed with asses 46, 32, 29, 22, and 16, of which 46 was edominant. Masses 14 and 28 were not re-rded, but masses 22 and 29 were not satis-ctorily identified. Errors of one mass unit have en discounted so that two possibilities not eviously considered may be suggested. Mass could be N_2^- with nitrogen isotopes of masses and 15; mass 22 could be an isotope of neon. owever, the absence of masses 28 and 20, hich are more abundant isotopes of the same ses, is then difficult to explain. (The formation Ne^- would not be surprising since He^- is own and A^- has been suggested [*Stacey*, 1959]).

Very Low Pressures—We may consider also e rate of disappearance of free electrons in itrogen gas at a pressure corresponding to the 2 layer. At very low pressures the equilibrium presented by (1a) would not be reached until ecombination was nearly complete, and this quation would become

$$N_2 + e \rightleftharpoons N_2^- \qquad (10)$$

Under conditions in which photo-detachment ay occur, for example, the F2 layer in day-ight—τ_i is reduced so that the importance of he return arrow in (10) increases slightly.) urther, if $\alpha_i \gg \alpha_e$, (10) becomes the rate-ontrolling process for electron disappearance. t gives an attachment law

$$-dn_e/dt = \beta n_e \qquad (11)$$

where

$$\beta = nQv$$

s in (7). *Ratcliffe* and others [1956] and *Martyn* 1956] have shown that an equation of the form 11) represents electron disappearance in the F2 ayer. Using high-altitude-density figures given n the conference review by *Boyd* [1959] we find an exponential atmosphere with density 2.7×10^{-14} gm cm^{-3} at 300 km and a scale height of 30 km. (Figures given by *Schilling* and *Sterne* [1959] are not in disagreement with this.) For an atmosphere of N_2 we find that $n = 5.8 \times 10^8$ cm^{-1}. Thermal electrons at 1000°K have $v = 1.7 \times 10^7$ cm sec^{-1}, so that under these conditions $\beta = 20 \times 10^{-4}$ sec^{-1} if we make the crude assumption that the above estimate of Q is applicable to this electron energy.

It cannot be suggested that N_2^- is a major constituent of the F2 layer, but these estimates show that even as a minor constituent it could have a significant influence. It must be allowed that the variety of negative ions in the upper atmosphere is much wider than has usually been considered and that their combined effect could be the observed attachment law in which $\beta \sim 10^{-4}$ sec^{-1} at 300 km.

References

Bialecke, E. P., and A. A. Dougal, Pressure and temperature variation of the electron ion recombination coefficient in nitrogen, *J. Geophys. Research*, **63**, 539–546, 1958.

Boyd, R. L. F., Space research, *Nature*, **183**, 361–364, 1959.

Branscomb, L. M., Negative ions, *Advances in Electronics and Electron Phys.*, **9**, 43–94, 1957.

Davidson, N., and A. E. Larsh, Conductivity pulses induced in insulating liquids by ionizing radiations, *Phys. Rev.*, **77**, 706–711, 1950.

Hiby, J. W., Massenspektrographische Untersuchungen an Wasserstoff-und Heliumkanalstrahlen (H_3^+, H_2^-, HeH^+, HeD^+, He^-), *Ann. Physik*, **34**, 473–487, 1939.

Johnson, C. Y., and J. P. Heppner, Positive and negative ion composition of the E-region from rocket-borne mass spectrometer measurements (Abstr.), *Trans. Am. Geophys. Union*, **37**, 350–351, 1956.

Martyn, D. F., Processes controlling ionization distribution in the F2 region of the ionosphere, *Australian J. Phys.*, **9**, 161–165, 1956.

Massey, H. S. W., Negative ions, 2nd Ed., Cambridge University Press, 136 pp., 1950.

Ratcliffe, J. A., E. R. Schmerling, G. S. G. K. Setty, and J. O. Thomas, The rates of production and loss of electrons in the F region of the ionosphere. *Phil. Trans. Roy. Soc. London, Ser. A*, **248**, 621–642, 1956.

Schilling, G. F., and T. E. Sterne, Densities and temperatures of the upper atmosphere inferred from satellite observations, *J. Geophys. Research*, **64**, 1–4, 1959.

Stacey, F. D., Electron mobility in liquid argon, *Australian J. Phys.*, **12**, 105–108, 1959.

Williams, R. L., Ionic mobilities in argon and helium liquids, *Can. J. Phys.*, **35**, 134–146, 1957.

Williams, R. L., and F. D. Stacey, Ionization currents in argon and helium liquids, *Can. J. Phys.*, **35**, 928–940, 1957.

(Manuscript received February 6, 1959; revised May 13, 1959.)

Diurnal and Semidiurnal Variations of Wind, Pressure, and Temperature in the Troposphere at Washington, D. C.

MILES F. HARRIS

U. S. Weather Bureau, Washington, D. C.

Abstract—The diurnal and semidiurnal variations of wind, pressure, and temperature in the troposphere are obtained for a summer season by combining two series of 6-hourly observations made at different times at Washington, D. C. Order-of-magnitude estimates of terms in the equation of motion at the 5-km level suggest that a linearized form of the equation of motion describes the diurnal motions closely. On the assumptions that the pressure wave moves westward at an even rate without change of amplitude and that friction is absent, the local pressure variation is computed from the wind observations. At levels above 4 km in the case of the diurnal wave and above 1 km in the case of the semidiurnal wave, the phase computed from the wind agrees reasonably well with the observed phase of the pressure variation, although the calculated amplitude is too large. Discrepancies between the pressure changes determined from the winds and the observed pressure variation can be traced to the basic assumption of a simple progressive wave, to obvious wind errors that are revealed by an absence of vertical continuity, and probably to the vertical exchange of momentum in the layer near the earth's surface.

Introduction—In spite of the great increase in the number of upper air observations during the past 20 years, relatively little new information has been gained about the diurnal variations of wind, pressure, and temperature in the free atmosphere. Early studies of the diurnal variations [*Ballard*, 1933; *Hergesell*, 1922] were necessarily confined to the lowest 2 or 3 km of the atmosphere, and in recent years the frequency of radiosonde and rawinsonde observations during the day has not been sufficient to determine the diurnal variations accurately. In a few instances [*Riehl*, 1947; *Gentry*, 1958; *Angell*, 1958] it has been possible to obtain the semidiurnal component of the variation as well as the first harmonic, but these computations have generally been based on short series of observations made for special purposes.

Johnson [1955], by combining two series of 6-hourly observations made at differently scheduled times, computed the diurnal wind variation in the lower stratosphere over the British Isles. He concluded that the variations were real and not the result of systematic errors of measurement in either the temperature or the wind observations. Although there is an apparent diurnal variation of pressure in the stratosphere, believed to be largely the result of solar radiation on the radiosonde instrument itself [*Johnson*, 1955; *Teweles* and *Finger*, 1958], the vertical wind shear in the stratosphere over Britain was found to be too small to account for the observed wind changes on the basis of false pressure-height values.

As a result of a recent change in the scheduled times of upper air observations it is possible to compute the diurnal variation of wind, pressure, and temperature in the free air at those points where soundings are made four times daily and at levels where no large systematic errors associated with the time of day are present in the observations. Prior to June 1, 1957, upper air observations were scheduled by international agreement at 0300, 0900, 1500, and 2100 UT; since that date the schedule has been 0000, 0600, 1200, and 1800 UT. These two series can be combined to form a single series of eight observations equally spaced throughout the day—more than the number required for determining the semidiurnal component of the variation.

Combination of the two series is legitimate if the mean of the four observations in each case provides an unbiased estimate of the daily mean. If the variation could be exactly represented by the sum of the first two terms of a

Fourier series, any four equally spaced observations would determine the daily mean exactly. At many stations the first two harmonics are sufficient to reproduce the daily course of surface temperature and pressure quite closely. Thus it is not surprising to find that at Washington, D. C., the normal daily surface temperature (during the summer months), based on 24 observations, can be determined with an error of at most 0.2°C by any four observations spaced 6 hours apart. The normal daily surface pressure is similarly specified with an error of less than 0.1 mb. These errors are small compared with the deviations, which are of the order of 5°C and 1 mb. It is reasonable to assume that the upper air temperature, pressure, and wind can also be closely represented by two terms with periods of 24 hours and 12 hours, and therefore that the two series can be combined throughout the troposphere without introducing appreciable errors resulting from inadequate estimates of the true daily mean. This assumption is consistent with *Johnson's* [1955] evidence that it is unnecessary to use harmonics of higher order than the second to account for the tidal winds in the stratosphere over Brita

A preliminary study was made of the da variation of the upper air winds and heights isobaric surfaces, at elevations between t ground and 10 km, for the months of June, Ju and August, 1956–1957, at Washington, D. (The word *daily* is used here interchangeab with *diurnal* to denote the variation of an e ment during the course of the day; and t *daily variation* is assumed to be composed e tirely of *diurnal* and *semidiurnal* components variation, i.e, of harmonics with periods of hours and 12 hours, respectively.) The wind o servations were obtained from the *Daily Bulle* [*U. S. Weather Bureau,* 1956–1957a] and t height observations from monthly summaries constant pressure data [*U. S. Weather Bure* 1956–1957b]. Although a much longer series observations is desirable, the data are probab sufficiently representative of long-term avera to reveal features of general interest. Consis ency in the pattern of variations from mon to month suggests that these features are re provided there are no systematic errors due insolation or other causes. It is especially di

TABLE 1—*Amplitude and phase of the diurnal and semidiurnal variations of wind during the summer months, 1956–1957, at Washington, D. C.*

Level (km)	u' (West wind component)				v' (South wind component)			
	Diurnal		Semidiurnal		Diurnal		Semidiurnal	
	Amplitude (cm sec^{-1})	Phase (degrees)	Amplitude (cm sec^{-1})	Phase (degrees)	Amplitude (cm sec^{-1})	Phase (degrees)	Amplitude (cm sec^{-1})	Phase (degrees
0.09(Sfc)	35	278	36	53	58	128	3	223
0.5	61	49	29	41	161	135	55	132
1.0	62	71	16	356	111	152	22	119
1.5	33	62	32	291	58	156	28	51
2.0	17	344	34	292	35	84	29	27
2.5	31	322	44	290	88	53	36	54
3.0	70	317	43	305	111	44	44	78
4.0	104	306	38	302	102	17	48	71
5.0	104	293	42	287	107	12	20	67
6.0	106	278	35	309	102	341	24	65
7.0	98	249	34	300	118	331	24	84
8.0	88	214	10	23	96	308	49	75
9.0	75	197	24	238	99	294	27	351
10.0	56	165	6	291	120	284	44	94
100 mb*	25	130	26	331	27	257	33	44

* Johnson's data. See text.

lt to conceive of such errors giving rise to the rnal wind variation observed, since the radio- nde temperature error in the troposphere is lieved to be small.

While the primary purpose of this paper is to esent the harmonic analysis of the data, some ditional computations based on the analysis e discussed. These computations have a bear- g on the reliability of the observations and ould also be useful in planning more elaborate udies of the diurnal changes.

Diurnal and semidiurnal variation of wind—he components of the wind, u and v, directed ward the east and the north, respectively, ere computed for each observation time for ch month at the levels indicated in Table 1. he daily mean values of u and v for each onth were then assumed to be the means of e four observations, and the deviations from e daily means, u' and v', were obtained. In ese computations, and in those involving eight values also, only days having observa- ons at all four scheduled times were used. The umber of observations ranges from 92 at the rface to 85 at 10 km. The deviations for June 956 and June 1957 were then combined into single sequence of eight observations spaced hree hours apart, and the first and second harmonic components were computed at each level [*Conrad* and *Pollak*, 1950]. The same procedure was followed for July and August and for the summer season as a whole. The amplitudes and phase angles of the diurnal and semidiurnal variations of u' and v' for the summer season are presented in Table 1 according to the convention:

$$u_1' = U_1 \sin(\psi + \alpha_1)$$

$$u_2' = U_2 \sin(2\psi + \alpha_2)$$

where ψ represents the hour angle, α is the phase, U is the amplitude, and the subscripts 1 and 2 indicate the first and second harmonics with periods of 24 hours and 12 hours, respectively.

The negative of the phase angle in the case of the diurnal variation, and the negative of one-half the phase angle in the case of the semidiurnal wave, is the hour angle at which the curve crosses the *x-axis* upward. An hour angle of zero corresponds to midnight, EST. *Johnson's* values [1955] for the wind variation (annual averages) at the 100- to 150-mb level over the British Isles are included in Table 1 for comparison.

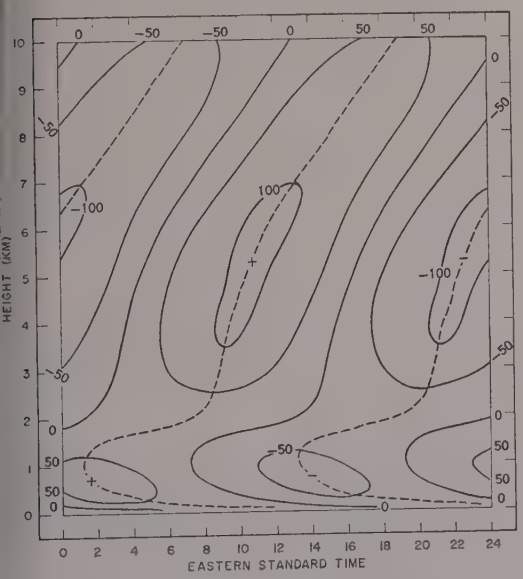

FIG. 1—Diurnal variation of west wind component, cm sec^{-1}, during the summer months, 1956–57, at Washington, D. C.

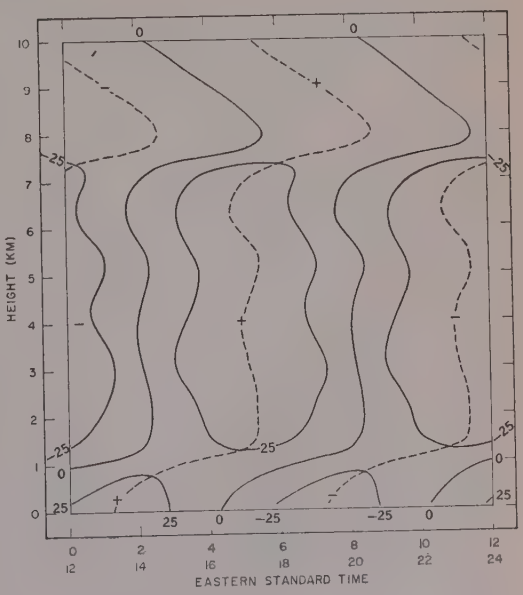

FIG. 2—Semidiurnal variation of west wind component, cm sec^{-1}, during the summer months, 1956–1957, at Washington, D. C.

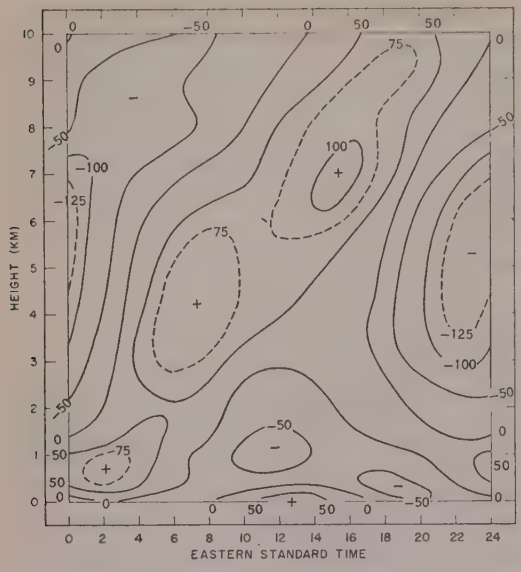

FIG. 3—Daily variation of west wind component, cm sec^{-1}, during the summer months, 1956–1957, at Washington, D. C.

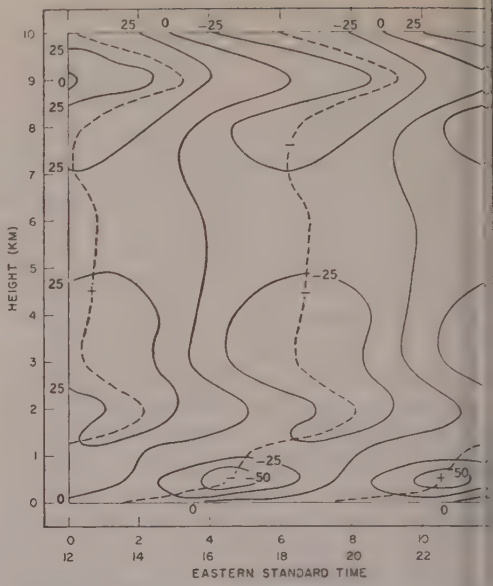

FIG. 5—Semidiurnal variation of south w component, cm sec^{-1}, during the summer mon 1956–1957, at Washington, D. C.

An analysis of the observed deviations of u and v according to elevation and time of day showed that the individual monthly patterns of u' and v' were quite similar. This similarity suggests that the seasonal pattern of deviations obtained by combining the data for the th months represents a real and not merely a tuitous variation. The u' and v' component the wind are characteristically about 90° out phase, a feature more closely approximated

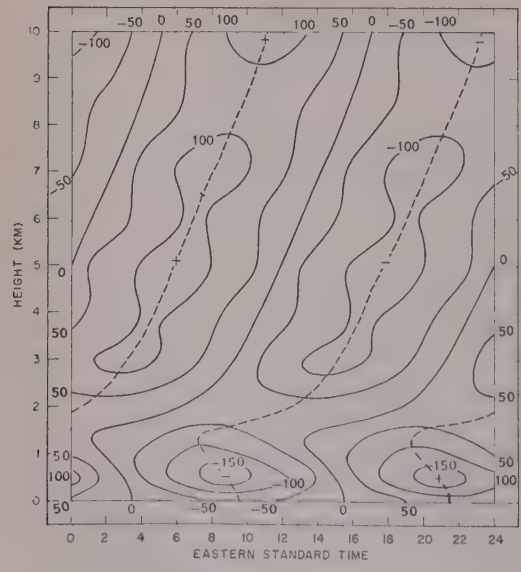

FIG. 4—Diurnal variation of south wind component, cm sec^{-1}, during the summer months, 1956–1957, at Washington, D. C.

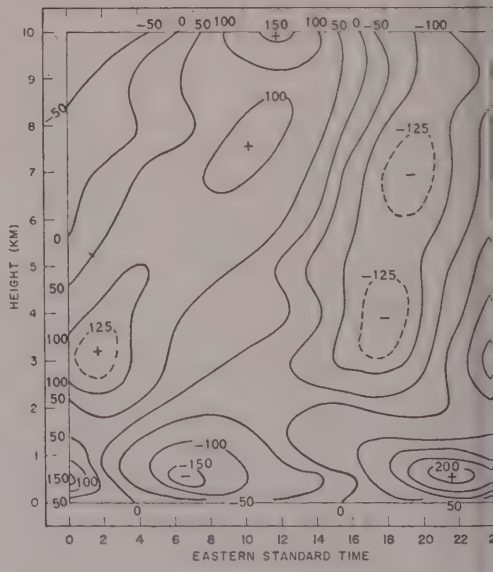

FIG. 6—Daily variation of south wind com nent, cm sec^{-1}, during the summer months, 19 1957, at Washington, D. C.

TABLE 2—*Percentage variance of observed diurnal wind at Washington, D. C., explained by the first two harmonics; data are for the summer months, 1956–1957.*

Level (km)	Sfc	1	2	3	4	5	6	7	8	9	10
West component	.962	.947	.940	.856	.980	.939	.984	.925	.686	.974	.454
South component	.990	.920	.387	.843	.918	.994	.869	.806	.876	.885	.750

e case of the diurnal than the semidiurnal ave.

In Figures 1 to 6, the diurnal, the semidiurnal, d the daily or composite variations of u' and for the summer season are shown as functions elevation. The broken curves are dividing es between regions of rise and fall. Figures 3 d 6 are representations of the raw data ob- ined by adding the harmonic components. The egree of smoothing of the original data is indi- ted by the squares of the correlation coeffi- ents between the observed and fitted values of and v' shown in Table 2. These values sug- st that, in general, a large percentage of the ariation of u' and v' has been accounted for y the harmonic analysis, but that more ob- rvations, and perhaps some refinement in the ethod of determining the deviations, are re- uired to represent accurately the details of the hanges at individual levels.

The sharp changes in phase and amplitude of $'$ and v' below 3 km, evident in Table 1 as well s in the figures, are probably associated with rtical exchanges of momentum [*Haurwitz*, 941], known to be of importance in the varia- ion of wind speed in the lower atmosphere. t higher elevations, the amplitude and phase f the semidiurnal components exhibit irregu- arities which appear to be due to random errors n the determination of u' and v'. The low cor- elation at 2 km (Table 2) is probably the re- ult of the rapid phase shift of the south compo- ent of the diurnal wind between 1 and 3 km; he observed data for v' at this level show rregular variations of small amplitude.

The diurnal and semidiurnal wind variations re presented in addition to the daily variation ecause it is generally believed that these two omponents of the atmospheric tide have differ- ent physical origins [*Chapman*, 1951; *Godske* and others, 1957]; if this is true, the diurnal and semidiurnal components of the wind also have different origins and should be analyzed separately from the combined oscillation. But even if both components of the tide are induced by thermal changes alone, as suggested in an earlier article [*Harris*, 1955], it is convenient for analytical purposes to represent the wind variation by means of its harmonic components.

Diurnal and semidiurnal variations of pressure—The height values at 12 isobaric surfaces for the period June-August, 1956–1957, were analyzed in the same way as were the wind components. The height deviations were con-

TABLE 3—*Amplitude and phase of the diurnal and semidiurnal variations of pressure during the summer months, 1956–1957, at Washington, D. C.*

Level (km)	Diurnal		Semidiurnal	
	Amplitude (mb)	Phase (degrees)	Amplitude (mb)	Phase (degrees)
0.09 (Sfc)	0.77	343	0.54	136
0.5	0.59	300	0.43	120
1.0	0.48	274	0.59	111
1.5	0.42	250	0.55	108
2.0	0.40	244	0.52	106
2.5	0.40	240	0.50	104
3.0	0.40	238	0.48	102
4.0	0.44	234	0.48	101
5.0	0.45	232	0.48	78
6.0	0.46	230	0.47	96
7.0	0.45	228	0.46	98
8.0	0.45	226	0.44	102
9.0	0.44	223	0.43	102
10.0	0.44	221	0.42	102

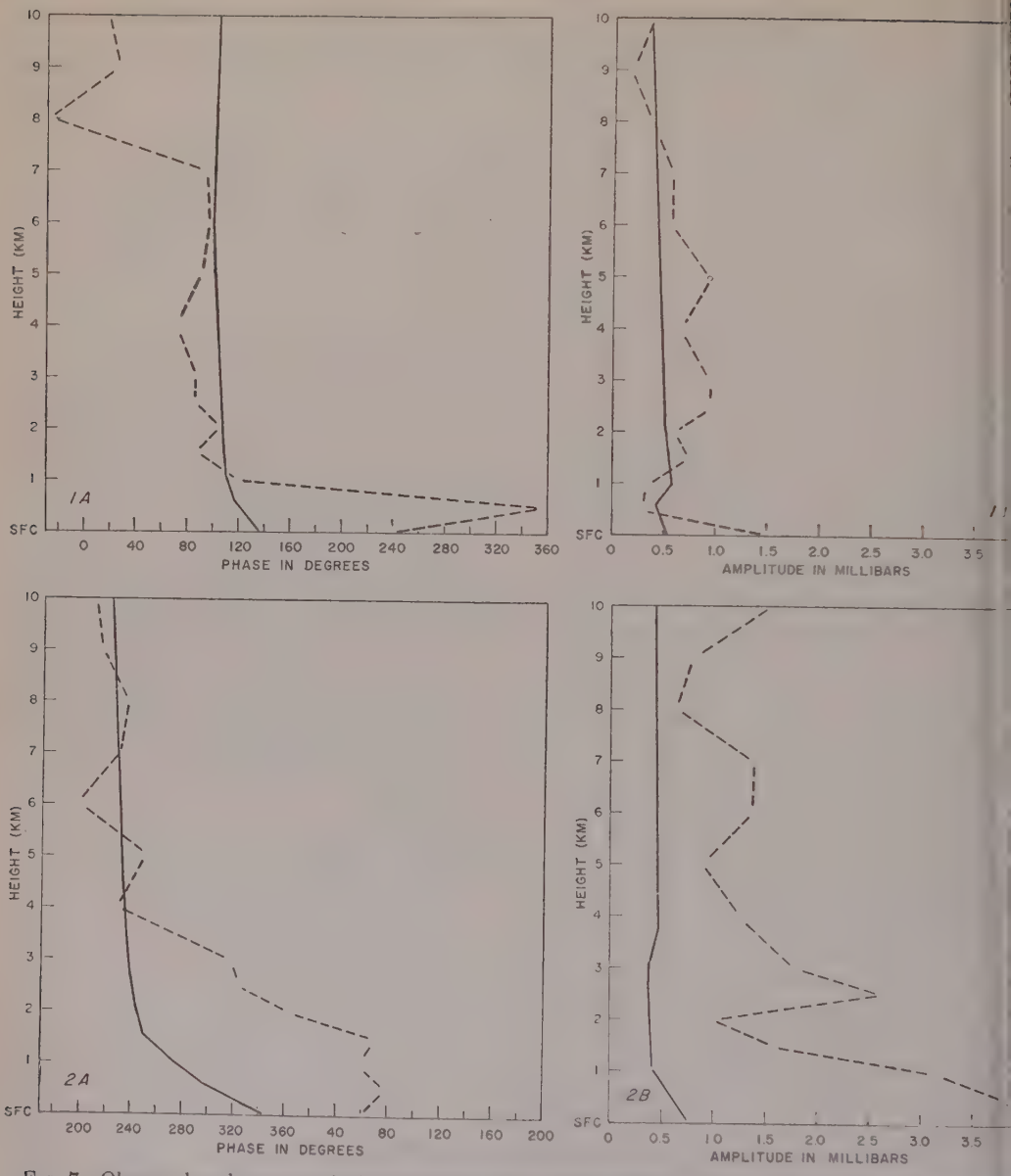

FIG. 7—Observed and computed phase and amplitude of the diurnal (bottom figures) and semidiurn (top figures) pressure variation during the summer months, 1956–1957, at Washington, D. C., observ variation, solid lines; computed variation, dashed lines.

verted to pressure deviations at standard heights by means of the normal summer pressure-height-density relationship at Washington [*Ratner*, 1957]. Pressure changes at the surface were read from graphs of normal station pressures in *Technical Paper No. 1* [*U. S. Weather Bureau*, 1943]. The phase and amplitude of the diurnal and semidiurnal variations of pressure are sho in Table 3 and also in Figure 7.

The hourly deviations of pressure as a fu tion of height, for the diurnal, semidiurnal, a combined waves, are shown in Figures 8 to The vertical structure of the diurnal pressu wave is in one important respect unlike t

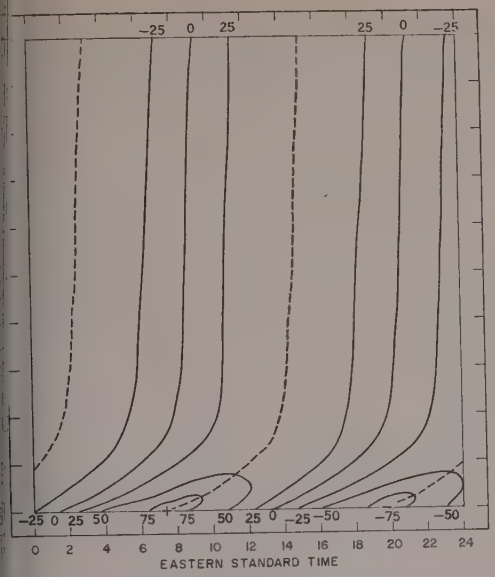

FIG. 8—Diurnal variation of pressure (units 10^{-2}) during the summer months, 1956–1957, at shington, D. C.

resentation [*Godske* and others, 1957] ob- ned from Wagner's Alpine summit data *Vagner*, 1932–1938]. Thus the diurnal pres- re wave in the free atmosphere at Washing-

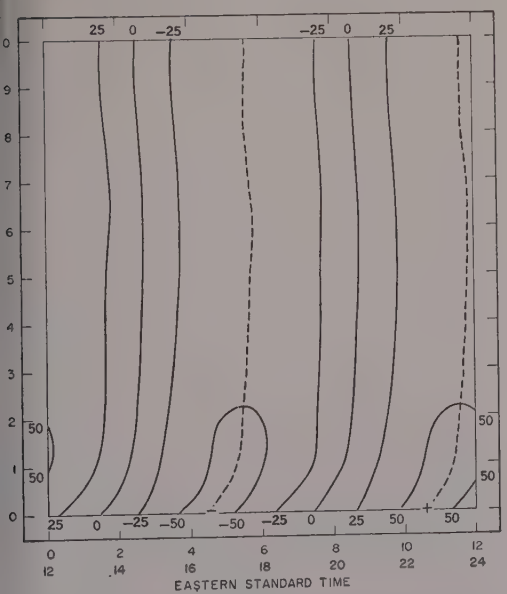

FIG. 9—Semidiurnal variations of pressure (units 10^{-2} mb) during the summer months, 1956–1957, t Washington, D. C.

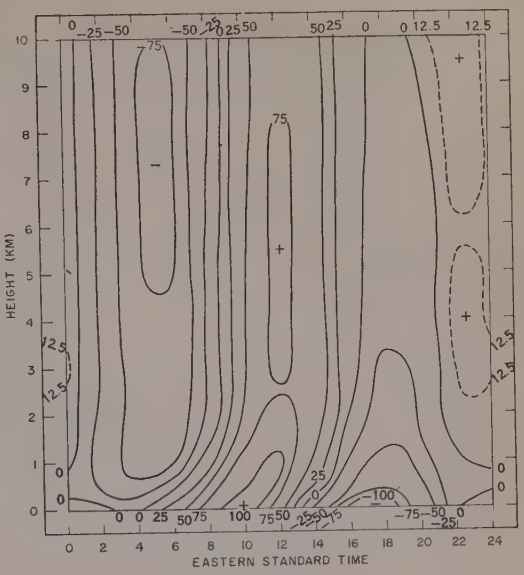

FIG. 10—Daily variation of pressure (units 10^{-2} mb) during the summer months, 1956–1957, at Washington, D. C.

ton during the summer months does not reverse phase near the 1-km level, as suggested by the mountain observations; instead, a phase lag of one-quarter wavelength is attained near this elevation, and from that point upward, at least to a height of 10 km, the phase variation is quite small. The phase of the semidiurnal pres-

TABLE 4—*Amplitude and phase of the diurnal and semidiurnal variations of temperature during the summer months, 1956–1957, at Washington, D. C.*

Leval (km)	Diurnal		Semidiurnal	
	Amplitude (°C)	Phase (degrees)	Amplitude (°C)	Phase (degrees)
0.09 (Sfc)	4.23	221	0.55	129
0.5	1.87	160	0.65	57
1.5	0.62	160	0.15	345
2.5	0.18	198	0.11	43
3.5	0.25	214	0.15	90
4.5	0.21	212	0.19	73
5.5	0.25	215	0.21	78
6.5	0.16	201	0.19	122
7.5	0.27	218	0.25	142
8.5	0.25	190	0.19	102
9.5	0.25	199	0.18	102

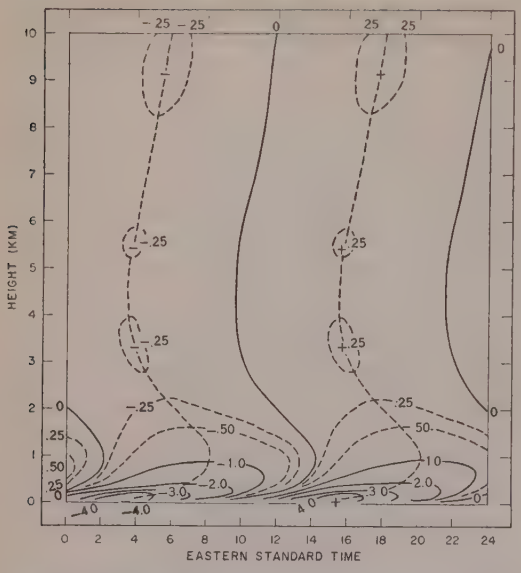

FIG. 11—Diurnal variation of temperature (°C) during the summer months, 1956–1957, at Washington, D. C.

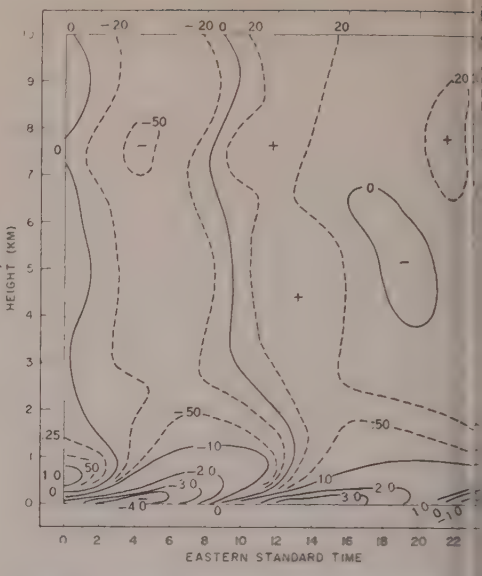

FIG. 13—Daily variation of temperature during the summer months, 1956–1957, at W ington, D. C.

sure wave shows only a slight change with elevation, the time of maximum aloft occurring an hour to an hour and a half later than at the surface. This result is in substantial agreement with those of a recent study by *Haur* [1958], who obtained the semidiurnal varia of pressure in the stratosphere by combi the data from pairs of stations each having observations daily.

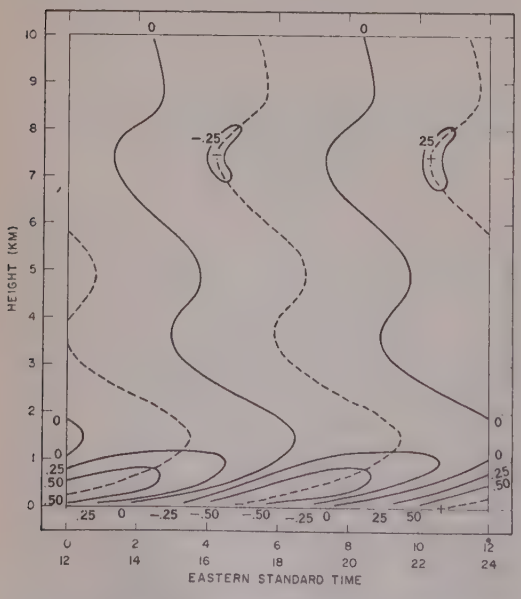

FIG. 12—Semidiurnal variation of temperature (°C) during the summer months, 1956–1957, at Washington, D. C.

Diurnal and semidiurnal variations of te perature—The hourly deviations of mean tual temperature were obtained from the pr sure variation by means of the hydrostatic eq tion, except at the surface where normal val [*U. S. Weather Bureau*, 1949] were used. T phase and amplitude of the diurnal and se diurnal temperature waves are shown in Ta 4, and the temperature variations as functi of height in Figures 11 to 13. The ratio of amplitude of the diurnal to the semidiur temperature oscillation, which at the surface 7.69, approaches unity at a height of 2.5 k The semidiurnal temperature wave of Figure is similar to that obtained from mountain servations below 1.5 km, but it differs at high elevations in that the time of maximum a minimum (Fig. 12) occurs earlier with incre ing height above this level. Seasonal and la tudinal variations may account for some of t differences between the Washington data and t Alpine observations.

Figure 13 brings out the pronounced se

LE 5—*Order of magnitude of quantities and terms in the first equation of motion for diurnal flow at 5 km, estimated from data for the summer months at Washington, D. C. For explanation of terms see text. Terms without parenthesis represent observed data.*

	Velocity components (cm sec^{-1})					
aponent	$\bar{u}$	u'	$\bar{v}$	v'	$(\overline{w})$	(w')
t monic	7.0×10^2	0.6×10^2	2.0×10^2	0.7×10^2	0	6.5×10^{-3}
ond monic	7.0×10^2	0.3×10^2	2.0×10^2	0.3×10^2	0	5.0×10^{-3}

	Velocity gradients (cm sec^{-1})					
nponent	$\left(\frac{\partial \bar{u}}{\partial x}\right)$	$\left(\frac{\partial u'}{\partial x}\right)$	$\left(\frac{\partial \bar{u}}{\partial y}\right)$	$\left(\frac{\partial u'}{\partial y}\right)$	$\frac{\partial \bar{u}}{\partial z}$	$\frac{\partial u'}{\partial z}$
st monic	5.0×10^{-6}	1.3×10^{-7}	5.0×10^{-6}	1.3×10^{-7}	1.6×10^{-3}	3.0×10^{-4}
ond monic	5.0×10^{-6}	1.0×10^{-7}	5.0×10^{-6}	0.5×10^{-7}	1.6×10^{-3}	3.0×10^{-5}

	Terms in the equation of motion (10^{-5}-cm sec^{-2})						
mponent	$\frac{\partial u'}{\partial t}$	$\left(\bar{u}\frac{\partial u'}{\partial x}\right)$	$\left(\bar{v}\frac{\partial u'}{\partial y}\right)$	$\left(\overline{w}\frac{\partial u'}{\partial z}\right)$	$\left(u'\frac{\partial \bar{u}}{\partial x}\right)$	$\left(v'\frac{\partial \bar{u}}{\partial y}\right)$	$\left(\frac{1}{\bar{\rho}}\frac{\partial p'}{\partial x}\right)$
rst rmonic	500	9	3	0	30	35	100
cond rmonic	400	7	1	0	15	15	200

	Term						
omponent	$\left(w'\frac{\partial \bar{u}}{\partial z}\right)$	$\left(u'\frac{\partial u'}{\partial x}\right)$	$\left(v'\frac{\partial u'}{\partial y}\right)$	$\left(w'\frac{\partial u'}{\partial z}\right)$	$(2\omega \cos \phi \cdot w')$	$2\omega \sin \phi \cdot v'$	F_x'
irst rmonic	1	1	1	<1	1	600	—
econd rmonic	1	<1	<1	<1	1	300	—

iurnal character of the temperature variation bove 2.5 km. The graph suggests that upward ux of heat from the earth's surface may contribute to a secondary temperature maximum t 3 km and above, in the late hours of the eveing, whereas the primary maximum near noon t these elevations may be the result of direct bsorption of solar radiation [*Godske* and thers, 1957].

Order of magnitude of terms in the equation of motion—The data summarized in Tables 1 and 3 can be used to compute estimates of the order of magnitude of terms in the equations of motion which describe the diurnal variations. Such estimates, computed from the data for the 5-km level, are presented in Table 5.

Since the diurnal motions can be treated as small perturbations superimposed on an undis-

turbed state of the atmosphere, the equations may be linearized by the perturbation method [*Haurwitz*, 1941] to describe the variations. Because the variation of density is small (of the order of 2×10^{-7} gm cm^{-3} at 5 km), the first equation of motion can be written

$$\frac{\partial u'}{\partial t} + \bar{u}\frac{\partial u'}{\partial x} + \bar{v}\frac{\partial u'}{\partial y} + \bar{w}\frac{\partial u'}{\partial z} + u'\frac{\partial \bar{u}}{\partial x} + v'\frac{\partial \bar{u}}{\partial y} + w'\frac{\partial \bar{u}}{\partial z} + u'\frac{\partial u'}{\partial x} + v'\frac{\partial u'}{\partial y} + w'\frac{\partial u'}{\partial z} + 2\omega \cos\phi \cdot w' - 2\omega \sin\phi \cdot v' + \frac{1}{\bar{\rho}}\frac{\partial p'}{\partial x} - F_x' = 0 \qquad (1)$$

with those terms omitted which satisfy the undisturbed motion. Non-linear terms representing the products of perturbation quantities have been retained. In equation (1) the barred quantities represent the mean or undisturbed quantities, and the primes indicate departures from the mean; that is, the deviations associated with the diurnal or semidiurnal waves. The velocity components u, v, and w are directed along the x-, and y-, and z-axes, respectively, the latter being positive toward the east, the north, and the zenith; p is the pressure, ρ the density, t is time, ω is the angular speed of rotation of the earth, and ϕ is the latitude. F_x' is the component of frictional or eddy forces directed along the x-axis.

The magnitude of some of the terms in equation (1) can be obtained from data presented in Tables 1 and 3, and from the graphs; the size of other terms has to be estimated. In Table 5, whereas the quantities enclosed in parentheses are estimated, the magnitudes of the remaining quantities were determined from observations. All of the computations were based on data at the 5-km level.

The horizontal gradients of the perturbations are not known from observation, but estimates of the east-west gradients may be obtained if it is assumed that the pressure wave with its associated wind variation moves westward without change of amplitude or phase. In this case,

$$\frac{\partial}{\partial t} = c\frac{\partial}{\partial x} = \omega\frac{\partial}{\partial \theta} \qquad (2)$$

where c is the speed of propogation of the v and θ is the longitude. Since the time varia of u', v', and p' are known, the magnitud $\partial u'/\partial x$ and $\partial p'/\partial x$ can be computed from The quantity $\partial u'/\partial y$ was estimated by assun that u' is zero at the pole and varies lin with latitude, the phase being assumed cons with latitude. The y-component of the F zontal shear of the undisturbed motion $\partial \bar{u}/\partial y$ approximated by the shear between Norf Virginia, and Washington, D. C., for the sum months, 1956–1957, and $\partial \bar{u}/\partial x$ was assume have the same order of magnitude as $\partial \bar{u}/\partial y$. vertical motion of the undisturbed atmosp is assumed to be zero.

The magnitude of the vertical velocity sociated with the diurnal motions w' was mated by assuming that the individual varia of density is small compared with the velo divergence and that individual terms in horizontal divergence tend to cancel, as is case in large-scale atmospheric motions. The

$$\frac{\partial w'}{\partial z} \sim \frac{1}{10}\frac{\partial u'}{\partial x}$$

the factor 1/10 being inserted because of the sumed negative correlation between $\partial u'$ and $\partial v'/\partial y$. If the vertical velocity at the grou is zero,

$$w_h' \sim \frac{1}{10}\int_0^h \frac{\partial u'}{\partial x}\,dz \sim \frac{h}{10}\overline{\frac{\partial u'}{\partial x}}$$

where h is some level above the ground (5-km level, specifically), and $\overline{\partial u'/\partial x}$ represe the mean divergence in the layer between ground and the level h. The mean diverge in this layer was assumed to be no greater th the divergence at 5 km. From Figures 1 an it can be seen that the individual terms in t horizontal divergence are negatively correlat and do indeed tend to cancel, provided v' creases toward the pole.

The largest terms in Table 5 are the Cori acceleration, the 'local acceleration,' and t pressure gradient force, in that order. T magnitude of F_x' may be equally large at l elevations, for there is good reason to belie that the eddy exchange of momentum accou in large part for the diurnal variation of wi speed near the ground [*Haurwitz*, 1941].

The terms $v'(\partial \bar{u}/\partial y)$ and $u'(\partial \bar{u}/\partial x)$ appear

relatively large, but they are equivalent errors of only about 5 per cent in the determination of the Coriolis acceleration. Similary, the $\bar{u}(\partial u'/\partial x)$ is equivalent to an error of per cent in the determination of $\partial u'/\partial t$. Thus equations of motion in the linearized form

$$\frac{\partial u'}{\partial t} - fv' + \frac{1}{\bar{\rho}r\cos\phi}\frac{\partial p'}{\partial \theta} - F_\theta' = 0 \qquad (5)$$

$$\frac{\partial v'}{\partial t} + fu' + \frac{1}{\bar{\rho}r}\frac{\partial p'}{\partial \phi} - F_\phi' = 0 \qquad (6)$$

pear to describe the horizontal components of e diurnal motions satisfactorily at the 5-km vel, provided the pressure wave progresses stward without change.

No order-of-magnitude estimates were obined at a level close to the ground because re the basic assumption of a simple progressive ave is not, in general, appropriate.

Computation of pressure variation from the inds—It follows from equations (5) and (6) at one should be able to compute the pressure *adients* from the observed wind variation oove the layer of vertical momentum exchange. the pressure wave can be approximated by a rogressive wave which does not change amplide or phase as it moves westward, equation (5) ith the aid of (2) can be written

$$\frac{\partial u'}{\partial t} - fv' + \frac{1}{\omega\bar{\rho}r\cos\phi}\frac{\partial p'}{\partial t} = 0$$

or

$$\omega\frac{\partial u'}{\partial \theta} - fv' + \frac{1}{\bar{\rho}r\cos\phi}\frac{\partial p'}{\partial \theta} = 0 \qquad (7)$$

neglecting friction. Since u', v', and p' are sine functions of θ,

$$p' = \omega\bar{\rho}r\cos\phi\left[2\sin\phi\int v'\,d\theta - u'\right] \qquad (8)$$

by integration with respect to θ.

Equation (8) was used to compute the amplitude and phase of the diurnal and semidiurnal pressure waves, at each level, by adding vectorially the harmonic components of u' and $2\sin\phi\int v'd\theta$. The results are plotted in Figure 7 to facilitate comparison with the observed amplitude and phase of p'. This graph shows that the phase agreement between computed and observed changes is good above 4 km (in the case of the diurnal wave) and between 1 and 7 km (for the semidiurnal wave). However, the computed amplitude of the diurnal pressure variation is much too large, even above 4 km, and the computed amplitude of the semidiurnal change is also somewhat too great.

Although it is tempting to assume that the level where phase agreement is first reached coincides with the upper limit of significant vertical momentum exchange, this inference probably is not justified. A vector difference between the observed and computed harmonic components of p' at the various levels indicates one or both of two possibilities: (1) equation (7) is not applicable at this level; (2) errors in the determination of the true wind and pressure variations are too large to permit an accurate comparison.

Above 7 km, the error in the computed value of the semidiurnal pressure variation is probably the result, to a large extent, of erroneous values of u_2' and v_2'; as noted previously, the amplitude and phase of the semidiurnal components of the wind exhibit irregularities at these levels that are suggestive of large random errors.

Equation (7) is not appropriate at levels near the earth's surface because neither the basic assumption of a simple progressive wave nor the supposition of frictionless motion is valid here. Wherever the amplitude or the phase of the pressure wave varies with longitude, expression (2) does not hold. Instead of the substitution $\omega(\partial p'/\partial\theta) = \partial p'/\partial t$ in equation (5), we should then use an expression taking account of changes in the form of the wave as it moves westward. For the 24-hr wave, for example,

$$\omega\frac{\partial p_1'}{\partial\theta} = \frac{\partial p_1'}{\partial t} + \omega^2 P_1\frac{\partial\tau_1}{\partial\theta}\cos\omega(t+\tau_1) + \omega\frac{\partial P_1}{\partial\theta}\sin\omega(t+\tau_1) \qquad (9)$$

where P_1 is the amplitude, t is time measured from local midnight, and τ_1 is the phase of the pressure variation represented at the point of observation by

$$p_1' = P_1\sin\omega(t+\tau_1) \qquad (10)$$

Substituting from (9) into (5) and integrating the resulting equation with respect to time, we find

$$\left(1 + \omega \frac{\partial \tau_1}{\partial \theta}\right) p_1' + \omega \frac{\partial P_1}{\partial \theta} \int p_1' \, dt = \omega \bar{\rho} r \cos \phi \left[f \int v_1' \, dt - u_1' \right] \tag{11}$$

An analogous equation holds for the semidiurnal wave.

In equation (11), p_1' is the local pressure deviation described by (10). The quantity on the right-hand side of (11), which is the vector quantity compared with p_1' in Figure 7, is therefore greater than the local pressure deviation when the phase of the pressure wave increases eastward; that is, when $\partial \tau_1 / \partial \theta$ is positive. Further, the computed vector is nearly in phase with p_1', provided $\partial P_1 / \partial \theta$ is not unduly large. Under these conditions, therefore, the error of the diurnal pressure variation computed from the wind observations on the assumption of a simple progressive wave is associated largely with an amplitude error rather than with a phase error; and this is, in fact, what is observed with the present data. At Washington the phase of the surface diurnal wave does increase eastward [*Wexler*, 1951], at least in June. Since the surface pressure change is reflected at every level above the surface in the ratio p/p_0, it seems probable that a large portion of the error in the computed diurnal pressure variation is due to a change in amplitude and phase of the wave as it moves across the eastern seaboard. Because of hydrostatic considerations, the error should decrease with elevation, unless variations in the westward-moving temperature wave also introduce an appreciable effect on the pressure changes aloft.

Expression (2) is more nearly applicable to the semidiurnal wave than to the diurnal wave, for the semidiurnal wave shows less variation with longitude. It must be at least partly for this reason that the vector errors of the computed semidiurnal pressure change (at 7 km and below) are smaller than those of the computed diurnal change. A possible contributing factor to the better agreement in the case of the semidiurnal changes is the relative size of the semidiurnal and diurnal frictional terms. Because the vertical transport of momentum depends upon the stability, and because the temperature lapse rate must be predominantly diurnal in character near the earth's surface, one would expect frictional coupling between the earth and the atmosphere to be much greater for the diur than for the semidiurnal motions. Such an planation conceivably could account for fact that the semidiurnal pressure wave appe to be less influenced by surface irregulariti than the diurnal wave.

Conclusions and suggestions for further search—This study suggests that the diur pressure and wind variations obtained fr upper air observations during the summ months, 1956–1957, at Washington, D. C., substantially consistent to a height of 10 k for the phase of the pressure variation obtai from wind data (that is, from data proba independent, for all practical purposes, of temperature and pressure measurements) agr reasonably well with the observed phase. seems unlikely that large time-dependent err could be present in the pressure or height com tations in this layer without seriously affect the phase of the diurnal and semidiurnal wav A discrepancy between the computed a observed amplitudes of the pressure change c be explained as the result of an assumptio not true in this particular case—that the wa progresses westward without change of for Wherever this assumption is satisfied it sho be possible to compute the actual diurnal pr sure change in the upper air from wind data a single station, provided a sufficient number observations is available. Perhaps a more re istic approach, making it unnecessary to assu a simple progressive wave, would be to make u of data from neighboring stations at the sam latitude.

The diurnal pressure variation determine from a long record of winds in the stratosphe could serve as a check on the reliability radiosonde temperature measurements at hig elevations. At heights of 24 km, for exampl systematic errors in the thermistors of som instruments result in spurious diurnal heig variations so large as to make isobaric analys difficult; it is desirable either to avoid thes errors in the routine observations or to provi adequate corrections for the various instrumen now in use [*Teweles* and *Finger*, 1958]. In eithe case it would be useful to have independen evidence of the diurnal pressure variation ob tained from wind observations.

Insofar as the results of the study may contrib ute to an understanding of the diurnal an

nidiurnal tides, the most interesting points pear to be (1) confirmation of the relative crease in magnitude of the semidiurnal vari- ion of temperature with elevation [*Godske* and hers, 1957; *Harris*, 1955] and (2) the evidence esented in Table 5 that the equation of motion a simple linearized form should suffice to plain the horizontal motions of the atmospheric des. The study does not show the magnitude frictional or eddy forces in the equations for ie diurnal motion; however, it is proposed iat the semidiurnal variation of the vertical xchange of momentum may be much smaller nan the diurnal variation, and that the compara- ve regularity of the semidiurnal wave, and to ome extent the relative magnitudes of these wo primary components of the atmospheric ide, may be partially explained on this basis. This idea could be tested by utilizing observa- ions from neighboring stations at the same atitude or possibly by analyzing the upper air lata for a single station where the assumption of a progressive wave should be more closely realized than it is at Washington.

It should be emphasized that the results of this preliminary study, being based on a comparatively short record of observations at one locality for a single season, need to be verified by additional data. The results appear to be sufficiently consistent to suggest that information of both practical and theoretical value can be obtained by extending the harmonic analyses of wind, pressure, and temperature to higher levels and to other localities and seasons.

Acknowledgment—The author expresses his appreciation to those members of the Office of Meteorological Research, U. S. Weather Bureau, who contributed through discussion and criticism, or through computations on the data, to the completion of this paper.

References

Angell, J. K., Some evidence for tidal oscillations obtained from 300 mb transosonde data, *J. Am. Meteorol. Soc.*, **15**, 566–567, 1958.

Ballard, J. C., The diurnal variation of free-air temperature and of the temperature lapse rate, *Monthly Weather Rev.*, **61**, 61–79, 1933.

Chapman, S., Atmospheric tides and oscillations, *Compendium Meteorol.* (T. F. Malone, ed.), Am. Meteorol. Soc., Boston 510–530, 1951.

Conrad, V., and L. W. Pollak, *Methods in climatology*, 2nd Ed., Harvard Univ. Press, 459 pp, 1950.

Gentry, R. C., Diurnal variation of wind, temperature, and pressure at upper levels in the tropics, (unpublished manuscript), 1958.

Godske, C. L., T. Bergeron, J. Bjerknes, and R. C. Bundgaard, *Dynamic meteorology and weather forecasting*, Am. Meteorol. Soc., Boston, and Carnegie Inst. Wash., Washington, 579–590, 1957.

Harris, M. F., Pressure change theory and the daily barometric wave. *J. Am. Meteorol. Soc.*, **12**, 394–404, 1955.

Haurwitz, Bernhard, *Dynamic meteorology*, McGraw-Hill Book Co., New York, 1941.

Haurwitz, Bernhard, The semidiurnal pressure oscillation in the stratosphere, *Sci. Rept. 7*, Dept. Meteorol. and Oceanog., Coll. of Engineering, N. Y. Univ., 15 pp, 1958.

Hergesell, H., der Tägliche Gang der Temperatur in der Freien Atmosphäre über Lindenberg, *Arb. Preuss. Aeron. Obs. Lindenberg*, **14**, 1–43, 1922.

Johnson, D. H., Tidal oscillations of the lower stratosphere, *Quart. J. Roy. Meteorol. Soc.*, **81**, 1–8, 1955.

Ratner, B., Upper-air climatology of the United States, pt. I, Averages for Isobaric Surfaces, *Tech. Pap. 32*, U. S. Weather Bur., 1957.

Riehl, H., Diurnal variation of pressure and temperature aloft in the eastern Caribbean. *Bull. Am. Meteorol. Soc.*, **28**, 311–318, 1947.

Teweles, S., and F. G. Finger, Reduction of diurnal variation in the reported temperatures and heights of stratospheric constant pressure surfaces, (unpublished manuscript), 1958.

U. S. Weather Bureau, 10-year normals of pressure tendencies and hourly station pressures for the United States, *Tech. Pap. 1*, 1943

U. S. Weather Bureau, *The climatic handbook for Washington, D. C., Tech. Pap. 8*, 1949.

U. S. Weather Bureau, Northern Hemisphere data tabulations, Daily Series, Synoptic Weather Maps, Pt. II, *Daily Bulletin*, June-Aug., 1956–1957a.

U. S. Weather Bureau, Summary of constant pressure data, *WBAN 33*, June-Aug., 1956–1957b.

Wagner, A., Der Tägliche Lufdruck—und Temperaturgang in der freien Atmosphäre und in Gebirgastälern, *Gerlands Beitr. Geophys.*, **37**, 315–344, 1932.

Wagner, A., Theorie und Beobachtung der Periodischen Gebirgswinde, *Gerlands Beitr. Geophys.*, **52**, 408–449, 1938.

Wexler, H., Unpublished data available from Office of Meteorological Research, U. S. Weather Bureau, Washington, D.C., 1951.

(Manuscript received April 22, 1959.)

Horizontal Convergence as a Factor for Fog and Stratus at Calcutta (Dum Dum)

M. GANGOPADHYAYA AND C. A. GEORGE

Regional Meteorological Centre
Calcutta, India

Abstract—Fog or stratus at Calcutta (Dum Dum) was found to be associated with horizontal convergence and rarely, if at all, with divergence of air flow within the surface inversion. It is considered that turbulent eddies likely to be caused by convergence and divergence will respectively tend to augment or retard cooling of the surface air layers. It is also shown that low level convergence will usually increase moisture advection, while divergence will lead to desiccation of surface air layers, thereby aiding or inhibiting, as the case may be, formation of fog or stratus over the station. A few specific situations, favorable as well as adverse to fog formation at Calcutta (Dum Dum) have been discussed in the light of the observed horizontal divergence of air flow at the 1000-ft. level.

Introduction—Successful prediction of the incidence of most cases of fog at an individual station is an extremely difficult problem owing to the fact that the very delicate balance between the various favorable factors essential for its occurrance is not easily tractable. Winter fogs at Dum Dum may broadly be classified into four distinct types: radiation, frontal, low stratus settling on ground, and advection-cum-radiation [*Chakravorty*, 1948; *Roy*, 1951; *S. C. Basu*, 1952; *A. Basu*, 1954]. Of these, the first two are more or less interrelated and are generally easier to forecast than the rest, since they occur in the wake of or before sufficient precipitation, usually caused by western disturbances [*Roy*, 1951], and at times after the passage across the station of the fronts associated with such moving pressure systems. The third class of fog, though rare, is essentially a case of formation of low stratus cloud in a moist inversion [*George*, 1948], with the stratus so formed building downwards and settling on the ground as the cooling of the lower air layer progresses under weakening surface wind conditions. The advection-cum-radiation type of fog, which is far more frequent than the other classes of fog at Dum Dum, is very often extremely difficult to forecast because of some unknown factor. Thermal stability indicated by the surface inversion is a normal feature at Dum Dum as elsewhere during the winter months; only the height and the lapse rate in the inversion layer undergo slight fluctuations from day to day. Fog has failed to form even under apparently ideal meteorological conditions, such as a combination of stable atmosphere, high moisture content, small dew point depression, calm or light surface winds, and clear nights. It was, therefore, thought to be worth-while to investigate whether the dynamic characteristics of the low-level wind circulation within the thermal inversion have sufficient influence on fog formation to be considered as an additional contributory factor for incidence of fog. The results of this study, together with illustrations of two specific situations of 'fog' and 'no-fog' at Calcutta Airport (Dum Dum), are discussed in this paper.

Velocity divergence and its relation to fog and stratus—Figure 1 shows the diurnal variation of horizontal divergence of winds at the 1000-ft level over and near Dum Dum for the period January 22 to March 22, 1953. The period March 1 to 14 has been left out, being insignificant, as there was only one incidence (March 6) of fog at the station during this period.

The velocity divergence is computed by the objective method of *Bellamy* [1949] over a triangular area formed by three pilot balloon stations, Asansol, Cuttack, and Chittagong. For lack of a closer triangular grid of upper wind observations, it has not been possible to

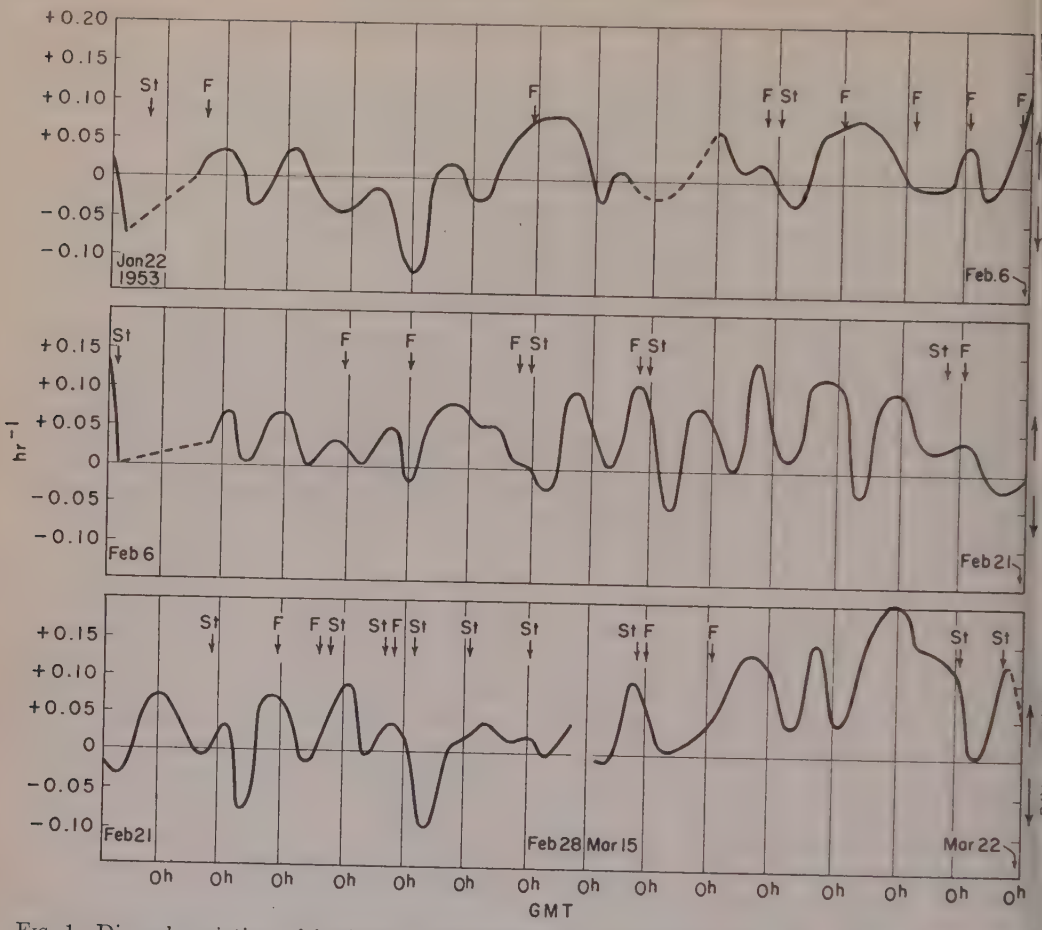

FIG. 1—Diurnal variation of horizontal divergence of winds at 1000-ft. level over Calcutta and neighborhood as computed from wind observations at 0200, 0900, and 2000 GMT at Asansol, Cuttack, and Chittagong. [F = fog; St = stratus.]

compute the divergence over a smaller area around Dum Dum. However, this may be desirable for a study of fog or stratus owing to their localized nature on most occasions. It is assumed that the computed value will represent the divergence at and near Calcuttta, which is approximately at the orthocenter of the triangular area. Winds at 1000 ft msl were chosen for estimating the divergence, as they were the winds at the lowest reported level. This altitude was also comparable to the lowest height of the surface inversion on most of the days. Moreover, the winds at this level were chosen because, in synoptic practice, a noticeable change in the moisture content and circulation in the surface air layers at least up to 1000 ft is reckoned as very significant for formation of appreciably thick fog or stratus. If the divergence of the winds at the surface is ignored, the average vertical velocity within the layer up to the 1000-ft level will be half the value of the divergence at the 1000-ft level, expressed in units of 500 ft hr^{-1}. The direction of the vertical velocity at all levels from surface up to 1000 ft is assumed to be similar to that at the 1000-ft level, as the vertical variation of wind at the three stations is likely to be in the same sense, especially when the surface inversion extends to 1000 ft or more.

The Forecasting Office, Dum Dum, recorded special reports in the current weather register for the occurrence of fog or stratus during the period under consideration. These points are indicated by arrows in Figure 1 (*F* for fog and *St*

TABLE 1

Date	At 1500 GMT			At night			Fog (*F*) or Stratus (*St*)	Conv. (*C*) or Div. (*D*) at 1000-ft level
	Height of inversion (ft)	Lapse rate in inversion (°F)	Dew point depression at surface (°F)	Surface wind: Direction	Surface wind: Speed (knots)	Sky condition		
53								
n. 22	1350	1.8	2.7	WNW	6	Cloudy	*St*	No data
23	750	4.5	4.5	SW	Light	Trace	*F*	*C*
24	1200	2.7	1.8		Calm	Clear		*D*
25	No inversion		15.3	NW	5	Clear		*D*
26	900	9.9	6.3	NE	Light	Clear		*D*
27	1650	8.1	7.2		Calm	Clear		*D*
28	1350	9.9	3.6		Calm	Clear	*F*	*C*
29	No inversion		6.8	NW	3	Partly cloudy		*D*
30	900	11.7	6.8		Calm	Trace		No data
31	900	—	12.6	NNW	12	Cloudy		No data
eb. 1	No inversion		5.0	NW	2	Cloudy	*F*, *St*	*C*
2	1650	4.5	5.4		Calm	Partly cloudy	*F*	*C*
3	1410	14.4	5.4		Calm	Clear	*F*	None
4	990	10.8	6.3		Calm	Clear	*F*	*C*
5	No inversion		7.2	SE	Light	Clear	*F*, *St*	*C*
6	No inversion		5.9	NW	3	Cloudy		No data
7	1050	3.0	10.8		Calm	Partly cloudy		*C*
8	1050	11.7	3.6	NNE	3	Trace	*F*	*C*
9	600	13.1	9.4		Calm	Clear	*F*	*C*
10	900	10.8	5.9		Calm	Clear		*C*
11	1350	9.9	9.0		Calm	Clear		*C*
12	900	13.5	9.0		Calm	Clear	*F*, *St*	None
13	990	16.2	6.3		Calm	Clear		*C*
14	750	14.9	10.0	W	3	Clear	*F*, *St*	*C*
15	990	15.3	7.2		Calm	Trace		*C*
16	600	21.6	7.2	WSW	4	Partly cloudy		*C*
17	1350	19.8	7.2	WSW	4	Trace		*C*
18	600	6.8	15.3	SW	6	Trace		*C*
19	1680	11.7	12.6	SSW	3	Trace	*St*, *F*	*C*
20	1050	4.5	16.2		Calm	Trace		*D*
21	1650	4.5	9.0		Calm	Trace		*C*
22	2190	3.2	13.5	S	2	Partly cloudy	*St*	None
23	1740	4.5	6.3		Calm	Partly cloudy	*F*	*C*
24	690	8.1	5.4		Calm	Clear	*F*, *St*	*C*
25	1140	4.1	17.4	S	Light	Partly cloudy	*St*, *F*	*C*
26	No inversion		7.2	S	3	Partly cloudy	*St*	*C*
27	No inversion		7.2	S	3	Partly cloudy	*St*	*C*
28	No inversion		5.4	S	4	Partly cloudy		—
Iar. 15	No sounding		3.3	SW	Light	Partly cloudy	*St*, *F*	*C*
16	1950	4.5	5.4	S	Light	Clear	*F*	*C*
17	No inversion		7.2	S	Light	Clear		*C*
18	No inversion		9.0	S	4	Clear		*C*
19	3300	5.4	7.2	S	10	Clear		*C*
20	No inversion		4.4	S	9	Trace		*C*
21	No inversion		5.4	SSE	4	Trace	*St*	*C*
22	No inversion		7.2	SSE	7	Partly cloudy		—

for stratus). Times of occurrence of mist or haze have not been taken into account in this study.

Table 1 gives the height of the surface inversion layer, the lapse rate within it, the dew point depression at the surface at 1500 GMT, the surface wind and sky condition at night over Dum Dum on days for which divergence at the 1000-ft level has been depicted in Figure 1. This table shows that although such well-known favorable factors as surface inversion, low dew point depression, light winds, and clear skies existed on many occasions, fog or stratus occurred on only a few days. It will be seen from Figure 1, however, that fog or stratus which occurred was associated with horizontal convergence and rarely, if at all, with horizontal divergence of the winds at the 1000-ft level over and near the station. This fact would, no doubt, suggest that weak horizontal convergence within a shallow layer of air close to the ground might contribute to the strengthening of factors like augmentation of influx of moisture and cooling due to ascent within the layers close to the ground which favor condensation. Horizontal divergence will have an opposite effect. The probable reasons for these aspects of convergence and divergence are suggested in the succeeding sections.

Convergence and cooling within an inversion—The role of vertical mixing by turbulance in the formation of fog or stratus within the surface inversion, and the correlation of turbulence with wind velocities have been generally recognized. Slight turbulence causing vertical mixing of a shallow layer of air close to the ground leads to fog; whereas moderate turbulence associated with stronger winds leads to vertical mixing within a thicker layer and results in stratus formation [*O'Connor,* 1945 p. 727]. The influence of vertical velocities arising out of the horizontal divergence and the opposing hydrostatic drag on the air particles on the formation of turbulent eddies in an inversion is quite apparent, and the resulting thermal changes within the surface inversion are qualitatively assessed below.

If the circulation is non-divergent, vertical velocities are practically absent within the inversion, and the cooling of the surface air layers is controlled by radiation alone. Such a situation is depicted schematically in Figure 2a, in which the broken line *B* represents the modi-

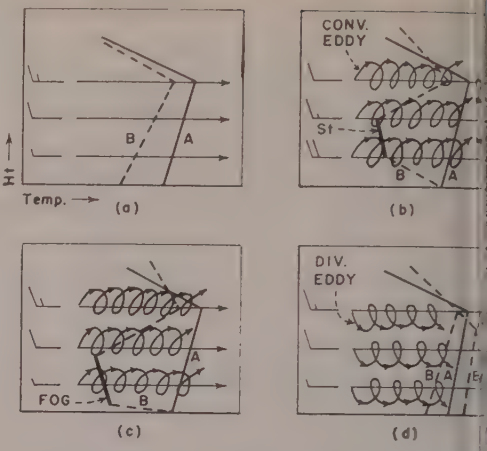

FIG. 2—Horizonal divergence and 'dynam cooling or heating within an inversion. Diag (a) depicts cooling by radiation alone in a divergent wind field; (b) and (c) cooling by ra tion as well as by ascent by horizontal con gence causing stratus and fog respectively; and radiation cooling retarded by descent by horiz tal divergence. [A-inversion at 1500 GMT; B B'-inversion modified by nocturnal radiation horizontal divergence.]

fication by nocturnal radiation of the earlier version (at 1500 GMT) represented by the co tinuous line *A*. The effect of mechanical edd caused by ground friction can be ignored as ing insignificant on account of very light calm surface winds on occasions of fog. Wh the vertical velocity due to horizontal div gence overbalances the stable tendency of t air particles, vertical eddies are likely to fo in an inversion. The upward velocities associat with convergent air flow will continually pu up the coldest moist air in contact with t ground and cool it further at the adiabat lapse rate. As a result, the air layers above t ground *are cooled more than they would be radiation alone,* and under favorable conditio of humidity condensation may occur. The d scending limb of the eddies, on the other han may transport potentially warmer super-incu bent air to the lower levels and may result the formation of approximately a dry adiabati or, in rare cases, super-adiabatic lapse ra within a thin layer close to the ground. Th process produces the well-known conditio which are favorable for stratus formation [*Pe tersson,* 1940 p. 95] (Fig. 2b). The mechanis

ormation of fog is apparently similar to that stratus formation, except that in the case of the adiabatic lapse rate may not extend re than a few feet above the ground, if at all; ereas in the case of stratus it may well extend a few hundred feet above ground level (Fig. . This difference is apparently due to higher ues of convergence and the associated greater tical mixing in the case of stratus formation n in the case of fog. Thus, under certain iting conditions of lapse rate, horizontal con-gence and the resulting turbulent eddies tend supplement the radiational cooling of the air ers and to aid formation of fog or stratus thin an inversion. By a process opposite to at which had been described in the case of nvergent air flow, eddies produced by diver-nt air flow generally tend to retard the effect radiational cooling due to warming by descent thin the inversion as shown in *B′* in Figure . The formation of a fog or stratus is thereby hibited in an otherwise favorable situation.

Convergence and advection of moisture—Hor-ontal divergence over India has been studied *Koteswaram* and *Parthasarathy* [1954]. The rve in Figure 1 generally corroborates their bservation, which was mainly based on the orning [0200 GMT] and the afternoon [0900 MT] winds, with respect to the low-level di-ergence over Northeast India. It is interesting note, however, that although the airflow at 000 ft above sea level over the area under con-deration is mostly divergent during daytime, becomes generally convergent during the night ours in January and February. In March, how-ver, the circulation is generally convergent at ll times, with a minimum value in the after-oon and a maximum at night.

The reason for the above diurnal variation of orizontal divergence at 1000 ft and its role in ncreasing or decreasing moisture at and near Calcutta can be assessed only in relation to the vind circulation with which the convergence nd divergence are usually associated. In Jan-ary and February the semipermanent pressure ystems affecting the wind circulation over the rea are the Indian anticyclone to the west and he Indo-China anticyclone to the east of Cal-utta; in addition, a transient shallow 'high' lso develops over the northern regions of the Bay of Bengal at night on many occasions. Con-

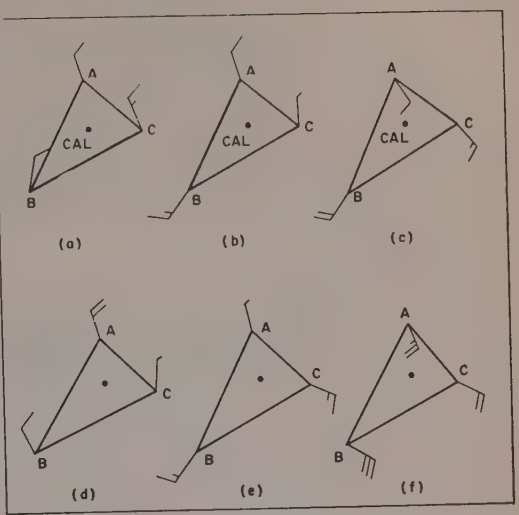

FIG. 3—Horizontal divergence of winds at 1000-ft level over the area between Asansol (A), Cuttack (B), and Chittagong (C), having Calcutta (CAL) at its orthocenter, under various synoptic situations. Diagram (a) depicts divergence during day; (b) convergence with 'high' over northern Bay of Bengal; (c) convergence in March; (d) convergence of dry air; (e) convergence with strong Indo-China 'high'; and (f) divergence of moist air

sidering the winds at the three stations, Asansol, Cuttack, and Chittagong, which form the triangle *ABC* having Calcutta at its orthocenter, the air flow associated with the Indian anticyclone is usually divergent (Fig. 3a.) During late evening or night, the moist on-shore winds from the 'high' over northern Bay of Bengal converge with the prevailing current over the region (Fig. 3b). This explains the observed diurnal variation of horizontal divergence at and near the station during these months. In March, however, the heat low gets established over the northern part of Indian Peninsula and the associated circulation at the 1000-ft level produces convergence of moist air over southern Bengal at all times (Fig. 3c). The convergence increases at night owing to the steepening of the isobaric gradient and the consequent accentuation of the coastal winds.

When the Indian and the Indo-China anticyclones are strong, and when the fractional divergent flow at Chittagong is reduced under the influence of the opposing pressure gradients of these 'highs,' a situation of dry air convergence

HOUR GMT	12	16	18	21	23	00*
CLOUD COVER	⊕	○	○	◔	◑	○
SURFACE WIND	CALM	S/2K	CALM	CALM	CALM	CALM
D. B. (°F)	78.2	68.0	66.2	62.6	62.3	61.1
D. P. (°F)	62.0	65.0	63.0	61.0	–	55.0

(a)

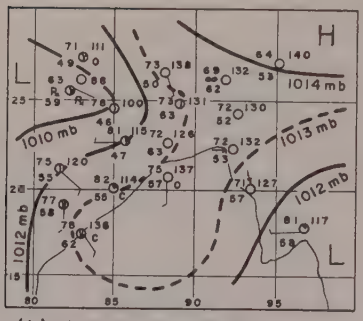

(b) 12 GMT, Feb. 5, 1953

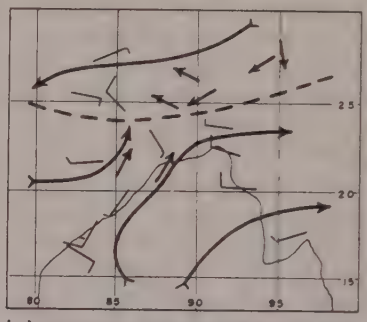

(c) 09 GMT, Feb. 5, 1953, 0.3 Km

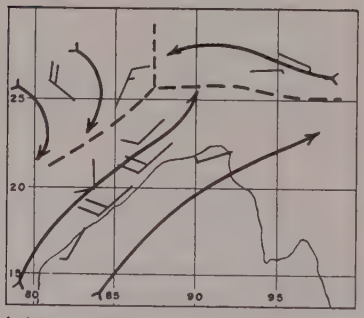

(d) 20 GMT, Feb. 5, 1953, 0.3 Km.

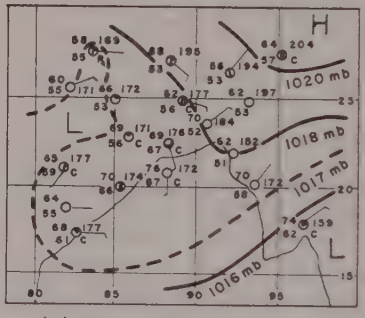

(e) 03 GMT, Feb. 6, 1953

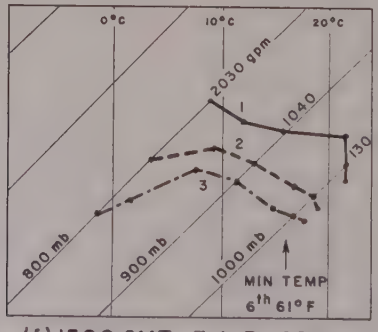

(f) 1500 GMT, Feb. 5, 1953,
ASCENCION

FIG. 4—Synoptic and meteorological conditions leading to fog over Calcutta (Dum Dum). Diagra
(a) depicts nocturnal cloud cover, surface wind, D.B., and D.P. conditions at Dum Dum; (b) and (e
sea level charts at 1200 GMT and 0300 GMT respectively; (c) and (d) wind charts at 1000-ft level a
0900 and 2000 GMT respectively; and (f) 1500 GMT radiosonde data up to 880-mb level plotted c
T-ϕ gram: (1) D.B. curve (2) W.B. curce (3) D.P. curve. Minimum temperature recorded next morn
ing is indicated. Asterisk indicates hour nearest to the time of commencement of fog at the static

HOUR GMT	12	16	18	21	23	00
CLOUD COVER	O	O	O	O	O	O
SURFACE WIND	NNW 2KT	CALM	CALM	CALM	CALM	CALM
D.B. (°F)	66.2	61.3	57.0	53.8	52.9	51.2
D.P. (°F)	45.0	52.0	51.0	51.0	52.9	49.0

(a)

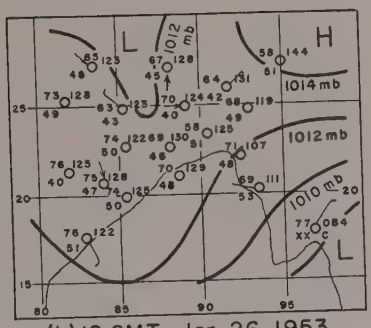

(b) 12 GMT, Jan. 26, 1953

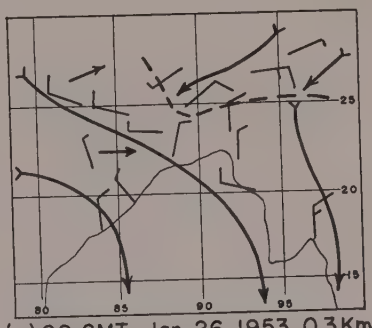

(c) 09 GMT, Jan. 26, 1953, 0.3 Km

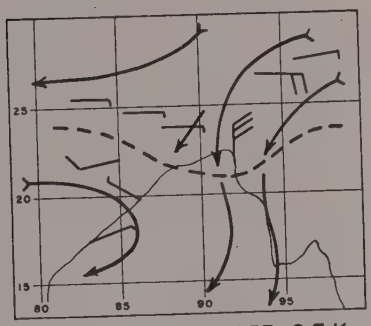

(d) 20 GMT, Jan. 26, 1953, 0.3 Km

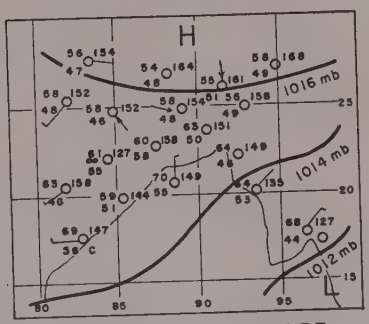

(e) 03 GMT, Jan. 27, 1953

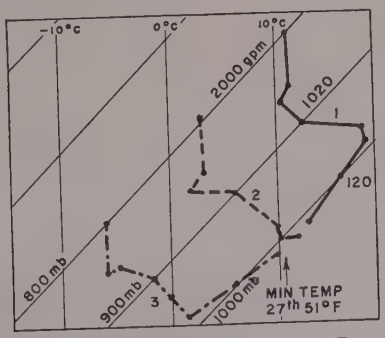

(f) 1500 GMT, Jan. 26, 1953
ASCENCION

FIG. 5—Synoptic and meteorological conditions depicted on the lines of Figure 4 for a 'no—fog' situation.

may arise (Fig. 3d). Because of the high degree of dryness within the converging continental air, this situation, like divergence, is normally not conducive to fog or stratus except when the air in the surface layers around the station is already near saturation. If the Indo-China high predominates, the winds over the western limb of this circulation will arrive over the Calcutta area from the sea, and the resulting circulation will cause convergence (Fig. 3e) as well as advect moisture. This is a favorable situation for fog or stratus at Calcutta, depending on the relative strength of the winds blowing into the area concerned. This situation gradually develops into the type of convergent flow in March which has been considered above. A case of low-level divergence of moist air over the region may occasionally arise (Fig. 3f) when a low pressure system lies over Chotanagpur and eastern Madhya Pradesh, situated to the west of the area under consideration. Besides the thermal changes caused by the divergence, such a situation generally leads to cloudiness which prevents formation of fog or stratus.

It will be clearly seen from the foregoing that convergence, except when it is caused by continental air flow as represented in Figure 3d, will generally be associated with inflow of moist air. This increases the moisture content of the air in the surface layers and favors formation of fog or stratus; whereas divergence, except in situations such as are represented in Figure 3f, generally desiccates the air and inhibits formation of fog or stratus over Calcutta during the winter months. The copious condensation of water vapor which follows eventually in the case of convergent air flow will lead to greater opacity of the atmosphere in proportion to the magnitude of convergence; this is characteristic of fog or stratus. In addition to the change in moisture content, 'dynamic' change of temperature associated with eddies produced by convergence or divergence within the surface inversion also makes it an important factor for the formation or non-formation of fog or stratus.

Discussion of two specific situations—The role played by low-level horizontal divergence in producing fog or stratus can be easily judged from a study of Figure 1 along with Table 1. Two typical situations, one of fog and another of no-fog, are illustrated in Figures 4 and 5 respectively. Only wind, pressure, D.B., D. present and past weather, and total cloud cov have been plotted on these charts according the usual station model. At Calcutta, observa tions of Alipore are plotted on these char Significant points concerning these situations, the light of the horizontal divergence shown Figure 1, are briefly described below.

(a) *Fog-situation on February 6, 1953*—Fi ure 4 represents a situation of sea air advecti over the area around Calcutta in associati with a 'high' over the Bay of Bengal. The a vection is noticeable even on the evening char of February 5 (Figs. 4b and 4c) a little earli than usual owing to the presence of shallow lo over eastern Uttar Pradesh on this day. As t low moved northeastwards, the inflow of moi air over the station was accentuated by 20 GMT (Fig. 4d). The isothermal layer notic on the ascent curve in Figure 4f would, n doubt, have become an inversion later in t night. The horizontal convergence at 1000 ft o this night is noteworthy (Fig. 1). This is a ideal case of fog caused by high dew point a cooling by convergence and radiation.

(b) *'No-fog' situation on January 26-27, 195* —The synoptic situation on the evening of Ja uary 26, 1953 is depicted in Figure 5. Judgin from the prevailing sky conditions at night, th surface inversion, and the observed variation o the dew point depression, this case may appea to be even more favorable for the occurrence o fog at Dum Dum than that of February 3–4 Yet there was no fog on this night or the follow ing early morning. This is a typical case o horizontal divergence inhibiting the incidenc of fog; whereas on Feburary 3–4, fog was caused by horizontal convergence within the surface in version (Fig. 1).

Conclusion—The present study has shown that, except in the case of convergence of dry continental air, a high correlation exists between fog or stratus and horizontal convergence of air flow in the surface layers bounded by the thermal inversion, whereas horizontal divergence generally inhibits incidence of fog or stratus at Calcutta (Dum Dum). A plausible reason has been adduced for the physical process responsible for this observed relationship: turbulent eddies likely to be produced by convergent or divergent air flow within an inversion layer

and respectively to augment or retard the effect of radiational cooling of the surface air layers; furthermore, by virtue of the seasonal circulation and geographical features of the region under study, convergence of air flow over the area will, as a rule, be associated with inflow of moister air, whereas divergence desiccates the air over the station. Hence, a knowledge of the actual trend of horizontal divergence within the surface layer of inversion will be a helpful guide, in addition to the other well-known factors, for more successful forecasting of the occurrence of fog or stratus at a given station than is available at present.

For qualitative assessment of the nature of air flow, one has to forecast the type of low-level wind circulation likely to prevail over a comparatively small area surrounding the station at night and towards the probable time of formation of fog or stratus. It is necessary to take due account of the wind circulation and the isobaric field and prognosticate them with the help of the isallobaric gradient observed earlier. It will be seen from Figure 1 that the divergence usually observed at 0900 GMT changes to convergence at an intermediate hour between 0900 and 2000 GMT in the months of January and February. Since the 2000 GMT pilot balloon observations are too late for use in fog forecasting, upper wind observations restricted to about 2000 ft at about 1500 GMT from three stations around Calcutta may provide a useful tool for predicting fog or stratus at the station. This can be done by the computation of horizontal divergence within the surface inversion at that hour.

References

Basu, A., Frequency of fog at Alipore, Dum Dum and Barrakpore, *Indian J. Meteorol. Geophys.*, 5, 349–355, 1954.

Basu, S. C., Fog forecasting over Calcutta and neighbourhood, *Indian J. Meteorol. Geophys.*, 3, 281–289, 1952.

Bellamy, J. C., Objective calculation of divergence, vertical velocity and vorticity, *Bull. Am. Meteorol. Soc.*, 30, 45–49, 1949.

Chakravorty, K. C., Fog at Calcutta, *Sci. Notes*, vol. 10, no. 124, India Meteorol. Dept., 1948.

George, P. A., Low stratus clouds over Bangalore, *Sci. Notes*, vol. 10, no. 123, India Meteorol. Dept., 1948.

Koteswaram, P., and S. Parthasarathy, The mean jet-stream over India in the premonsoon and postmonsoon season and vertical motions associated with the sub-tropical jet stream, *Indian J. Meteorol. Geophys.*, 5, 138–156, 1954.

O'Connor, J. F., *Handbook of meteorology*, McGraw-Hill Book Co., New York, 1056 pp., 1945.

Petterssen, S., *Weather analysis and forecasting*, McGraw-Hill Book Co., New York, 490 pp., 1940.

Roy, A. K., Rainmaking and its possibility in India, *Indian J. Meteorol. Geophys.*, 2, 241–249, 1951.

(Manuscript received July 21, 1958; revised February 17, 1959.)

A Note on the Growth of the Spectrum of Wind-Generated Gravity Waves as Determined by Non-Linear Considerations

WILLARD J. PIERSON, JR.

Department of Meteorology and Oceanography
College of Engineering
New York University
New York, N. Y.

Abstract—Non-linear wave properties lead to the conclusion, according to Phillips, that "where non-linear effects are important" the spectrum of wind-generated gravity waves must have the form $S(\mu) = \alpha g^2 \omega^{-5}$. To second order, it has been shown by Tick that non-linear effects are important in producing sharp crests above a frequency corresponding to twice the frequency of the dominant peak in the wave spectrum and that the second-order contribution is due to contributions from the linear part obtained from both sum and difference frequencies. In the representation due to Tick it is possible to represent the wave spectrum as a first-order part, $S^1(\mu, v)$, and a second-order correction, $S^2(\mu, v)$.

If these results are accepted, and if several additional assumptions are made, it is shown that the first-order family of wave spectra, $S^1(\mu; v)$, for fully developed seas, cannot form a nested family of curves. The results suggest that the various theoretical forms for the first-order spectrum of a fully developed sea are each correct over a limited range of wind speeds. However, since they are nested curves, they cannot be correct over the whole range of sea states.

If the breaking of waves is the dominant consideration in limiting their height, it has been shown by *Phillips* [1958] that the spectrum of the waves must have the form given by

$$S^{(\infty)}(\mu) = \alpha g^2 \mu^{-5} \tag{1}$$

over *"that range of frequencies where non-linear effects are important."* The value of α according to Phillips is 7.4×10^{-3}. In his analysis, the waves are treated as a random process. This random process certainly cannot be a Gaussian random process since non-linear effects are so strongly present. The probability structure of the model is therefore unknown. Also, the interpretation of the spectrum itself is difficult from a physical point of view.

A random model of waves that is highly dependent on linear assumptions has been studied actively for a number of years and is the basis of considerable work in the field [*Longuet-Higgins*, 1957; *Pierson*, 1955; *Roll*, 1957; *St. Denis* and *Pierson*, 1953]. This short-crested Gaussian sea surface has been shown to represent numerous properties of the actual sea surface, although the application of the probabilistic results obtained for such a model may have been pushed beyond the limits of applicability to actual waves.

A non-linear random model of gravity waves that satisfies the equations of motion to second order for long-crested gravity waves has been obtained by *Tick* [1958]. Let $\eta^{(1)}(x, t)$ and $\phi^{(1)}(x, z, t)$ be stationary Gaussian processes such that the linearized equations of motion with $p = 0$ at $z = 0$ are satisfied for deep water. Let the spectrum of $\eta^{(1)}(x, t)$ be given by $S^{(1)}(\mu)$ when studied at a fixed x as a function of time.

Then

$$\eta(x, t) = \eta^{(1)}(x, t) + \eta^{(2)}(x, t) \tag{2}$$

and

$$\phi(x, z, t) = \phi^{(1)}(x, z, t) + \phi^{(2)}(x, z, t) \tag{3}$$

can be found such that $\eta(x, t)$ and $\phi(x, z, t)$ satisfy the equations of motion to second order.

The spectrum of $\eta^{(2)}(x, t)$ as observed at a fixed point is given by

$$S^{(2)}(\mu) = \frac{1}{g^2} \cdot \int_{-\infty}^{\infty} K(\lambda; \mu) S^{(1)}(\mu - \lambda) S^{(1)}(\lambda)\, d\lambda \tag{4}$$

where

$$K(\lambda;\mu) = \begin{cases} \lambda^2(\mu^2 - 2\mu\lambda + 2\lambda^2), \\ \quad 0 < \lambda < \mu, \mu > 0 \\ (\mu - 2\lambda)^2\mu\lambda \\ \quad \lambda < 0, \lambda > \mu, \mu > 0 \end{cases} \tag{5}$$

The spectrum that would be estimated from a wave record would be given by

$$S^{\infty}(\mu) = S^{(1)}(\mu) + S^{(2)}(\mu) + \quad + \cdots \tag{6}$$

where the higher order non-linear contributions are unknown. It is a problem of interest to determine how closely

$$S(\mu) = S^{(1)}(\mu) + S^{(2)}(\mu) \tag{7}$$

approaches what is actually determined by assuming that some part of a spectrum computed from observations represents $S^{(1)}(\mu)$ and computing $S^{(2)}(\mu)$ to see if the sum nearly equals the original spectrum. In many ways the linear model has proved adequate, so that second-order corrections may be more than adequate to explain many additional features of waves.

If $S^{(1)}(\mu)$ (for a Gaussian process) is a spectrum that is zero for $0 < \mu < \mu_1$ and that rises very steeply to a sharp peak for μ slightly greater than μ_1 and then falls off smoothly toward zero for large μ, it is found that $S^{(2)}(\mu)$ is very low, but detectable, over the range $0 < \mu < 2\mu_1$ and that, for μ slightly greater than $2\mu_1$, $S^{(2)}(\mu)$ rises to a peak and then falls off to zero gradually. The sum, $S^{(1)}(\mu) + S^{(2)}(\mu)$, could then have small values at frequencies between zero and the peak (due to the non-linear effect of the difference between two frequencies in the linear spectrum) and a secondary peak at about twice the frequency of the dominant peak in the spectrum (due to the non-linear effect of the sum of two frequencies in the linear spectrum). These two features appear in the spectrum given in the original work of *Chase* and others [1957], but in this case computations show that $S^{(2)}(\mu)$ is far too small to account for the observed spectral irregularities as is shown in *Chase* and others [1959]. *Burling* [1955] also pointed out such a feature but could not definitely establish its existence.

According to Tick (current work at New York University), more needs to be done in the study of this non-linear model. It has to be extended to the short-crested case, and the probability structure of the random process has to be discovered. Preliminary calculations indicate that the second-order correction can be appreciable when compared with the first-order contribution at the same frequency. The total area under the spectrum is not much changed, however.

Under the assumptions that equation (1) is correct, that equations (4), (5), and (7) will still apply in a short-crested seaway, and that equation (7) represents a major part of equation (6), it is possible to obtain some general results on how the spectrum of the waves will grow when the growth of the spectrum is controlled by non-linear effects. The last of the above three assumptions is perhaps the weakest. A sharp wave crest is found in the spatial representation when wave numbers near k, $2k$, $3k$, $\cdots$ combine to produce a sharp crest, and thus a second-order theory should not be expected to produce sharp crests. Probably, since the dominant contribution of non-linearity propagates by means of convolutions such as (4) to higher frequencies, the analysis due to *Phillips*]1958] can be extended to include this new result.

A number of authors have presented theoretical forms for the family of wave spectra that would exist for fully developed seas as a function of the wind speed at anemometer level that generated the waves [*Darbyshire*, 1955; *Neumann*, 1954; *Roll* and *Fischer*, 1956]. These theoretical spectra were derived under linear assumptions and, from the above discussion, cannot be proved to be incorrect simply on the basis of observations that tend to show that equation (1) holds at the high-frequency end of a computed wave spectrum.

These theoretical families of spectra all have one feature in common. They are nested in such a way that

$$S^{(1)}(\mu; v_2) \geq S^{(1)}(\mu; v_1) \tag{8}$$

if

$$v_2 > v_1$$

for all values of μ for which they are defined. If equation (1) is to apply when $S^{(\infty)}(\mu)$ is identified with $S(\mu) = S^{(1)}(\mu) + S^{(2)}(\mu)$ over

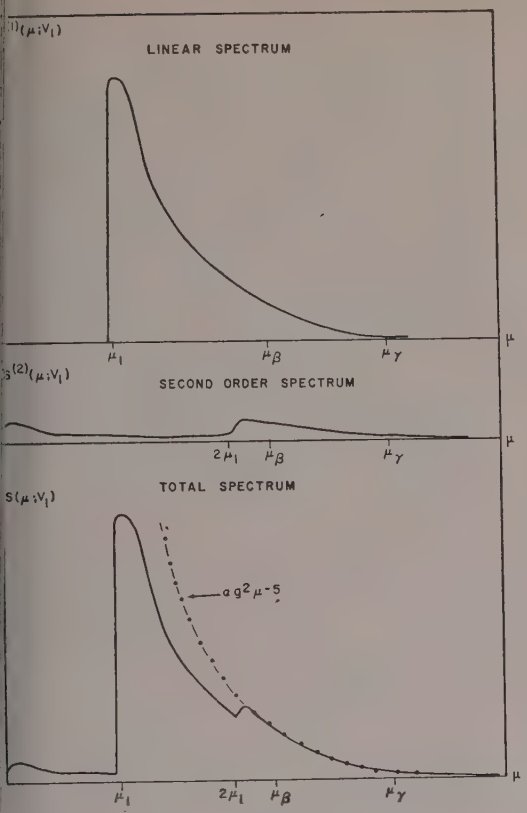

FIG. 1—Sketch to illustrate how $S^{(1)}(\mu; v_1)$ and $S^{(2)}(\mu; v_1)$ combine to produce $S(\mu; v_1)$ equal to $\alpha g^2\mu^{-5}$ over the range $\mu_\beta < \mu < \mu_\gamma$

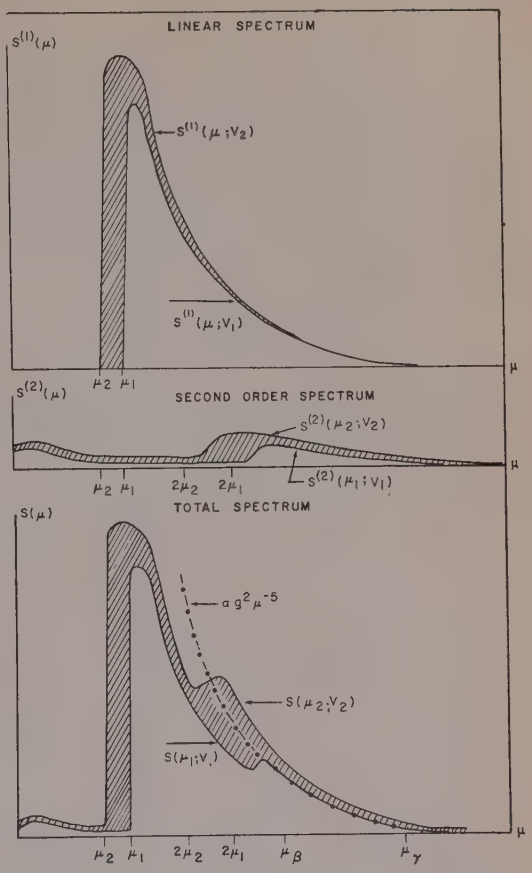

FIG. 2—Sketch to illustrate how another member of a family of nested spectra cannot form a total spectrum equal to $\alpha g^2\mu^{-5}$ over the range $\mu_\beta < \mu < \mu_\gamma$; shaded areas indicate the effect of an increase in wind speed from v_1 to v_2

that range of frequencies where non-linear effects are important, this one feature is enough to prove that these families of spectra cannot adequately describe fully developed seas.

Suppose, for example, that, for a particular $v = v_1$, $S^{(1)}(\mu; v_1)$, as defined in any of the above references [or in *Neumann* and *Pierson*, 1957], after proper modification to conform with the notation and definitions of Phillips and Tick that are used here, has the property that when $S^{(2)}(\mu; v_1)$ is computed and added to $S^{(1)}(\mu; v_1)$ to obtain $S(\mu; v_1)$, it is found that $S(\mu; v_1) = \alpha g^2\mu^{-5}$ for $2\mu_1 < \mu_\beta < \mu < \mu_\gamma$. Here $2\mu_1$ is at twice the dominant peak in the linear spectrum, μ_β is slightly greater than $2\mu_1$ to allow the non-linear contribution to settle down, and μ_γ is the upper range of applicability where surface tension and the effects of, say, eddy viscosity due to the turbulence created by the breaking waves becomes important. The range of $\mu_\beta < \mu < \mu_\gamma$ is the range where non-linear effects are important in the sense that the second-order correction to the Gaussian model makes the crests sharper and the troughs shallower by means of contributions at these frequencies. This condition is shown schematically in Figure 1.

Consider now another member of the family of nested curves for the wind speed v_2 where $v_2 > v_1$ (Figure 2). In the theoretical families of spectra referred to above, the most important effect of increasing wind speed is a sharp increase at values of μ less than μ_1, although an increase also exists for all μ.

If equation (4) is applied to $S^{(1)}(\mu; v_2)$ when written in the form

$$S^{(1)}(\mu; v_2) = S^{(1)}(\mu; v_1) + S^{(1)*}(\mu; v_2, v_1), \quad (9)$$

it is seen that the new contribution to the linear spectrum is strongest for frequencies just above μ_2 where $\mu_2 < \mu_1$. This contribution, however, interacts with all other parts of the linear spectrum and increases $S^{(2)}(\mu; v_2)$ for all values of μ over the range $\mu_\beta < \mu < \mu_\gamma$. The spectrum $S(\mu; v_2) = S^{(1)}(\mu; v_2) + S^{(2)}(\mu; v_2)$ therefore has the property that

$$S(\mu; v_2) > \alpha g^2 \mu^{-5} \quad (10)$$

over the range $\mu_\beta < \mu < \mu_\gamma$. This violates the assumption that equation (1) is the controlling condition for the growth of the wave spectrum. Therefore, if this assumption holds, it must follow that a correct version of the family of spectra, $S^{(1)}(\mu; v)$, for fully developed seas as a function of wind velocity cannot form a nested family of curves.

Two new theoretical forms for $S^{(1)}(\mu, v)$ have been given by *Darbyshire* [1959] and by *Bretschneider* [1959], as described by *Phillips* [1958]. The new results of Darbyshire that supersede the results referred to above still have the property defined by equation (8) at high frequencies for large wind speeds. The results of Bretschneider agree with equation (1) for high frequencies, so, if valid, they must be interpreted in terms of non-linear considerations. They do not, however, show the secondary peak in the spectrum that seems to be evident in some computed spectra.

Possible form for the spectrum of a wind-generated sea—It is evident, therefore, if the assumptions given above are correct, that most (and perhaps all) of the currently proposed families of theoretical spectra are not correct. In order to maintain equation (1) at the high frequencies as the waves grow in height, the linear spectrum must decrease at intermediate and high frequencies at the same time that it increases sharply at the lower frequencies. The results of *Burling* [1955], *Roll* and *Fischer* [1956], *Neumann* [1954], *Chase* and others [1959], and *Darbyshire* [1955] thus all tend to become consistent, since the low waves observed by Burling can certainly have a spectrum with a linear part that behaves more or less like $C_1/\omega^{5.5}$ (say), the linear spectrum of the waves of intermediate height observed by Chase, Cote, and others could look more or less like a member from the family of curves obtained by Neumann, and behave like C_2/ω^6 and the generally higher waves that were studied by Darbyshire could mostly (although they certainly all cannot) have spectra that behave like C_3/ω^7 (if we ignore, for the moment, the difficulty that C_3 depends on the wind speed). Asymptotic spectral behavior like C_4/ω^8 advocated by *Roll* and *Fischer* [1956] is, in a sense, an upper limit for the behavior of the linear part of the spectrum. Each theory would be almost correct over a certain range of wind speeds, but each would lead to errors if used for other ranges of wind speeds. There are other questions, such as the significant height of the highest waves generated by a given wind, that remain unanswered, however.

Darbyshire [1955] has given non-nested spectra that describe the growth of waves as a function of fetch. The analysis given above supports these results in a general way, although the actual formulas derived by Darbyshire need further confirmation.

Some specific quantitative results need to be obtained with the above qualitative analysis used as a basis. Such work is in progress.

References

Bretschneider, C. L., Revisions in wave forecasting, *Tech. Memo. Beach Erosion Board*, Washington, D. C., 1959 (in press).

Burling, R. W., Wind generated waves on water, Ph.D. Dissertation, Imperial College, University of London, 1955.

Chase, J., L. J. Cote, W. Marks, E. Mehr, W. J. Pierson, F. C. Rönne, G. Stephenson, R. C. Vetter, and R. G. Walden, The directional spectrum of a wind generated sea as determined from data obtained by the Stereo Wave Observation Project, New York University, College of Engineering, Research Division, Technical report prepared for the Office of Naval Research, 1957.

Chase, J., L. J. Cote, J. O. Davis, W. Marks, E. Mehr, R. J. McGough, W. J. Pierson, F. C. Rönne, J. F. Ropek, G. Stephenson, R. C. Vetter, and R. G. Walden, The directional spectrum of a wind generated sea as determined from data obtained by the Stereo Wave Observation Project, 1959. (To be published in *Marine Research*.)

Darbyshire, J., An investigation of storm waves in the North Atlantic Ocean, *Proc. Roy. Soc., A* 230, 560–569, 1955.

RBYSHIRE, J., A further investigation of wind generated waves, *Deut. Hydrograph. Z.*, **12**, Heft 1, 1959.

NGUET-HIGGINS, M. S., The statistical analysis of a random moving surface, *Phil. Trans. Roy. Soc., Ser. A*, **249**, 321–387, 1957.

EUMANN, G., Zur Charakteristik des Seeganges, *Arch. Meteorol. Geophys. U. Bioklimatol., Ser. A* **7**, 352–377, 1954.

EUMANN, G., AND W. J. PIERSON, JR., A detailed comparison of theoretical wave spectra and wave forecasting methods, *Deut. Hydrograph. Z.*, **10**, Heft 3, 73–93, Heft 4, 139–146, 1957.

HILLIPS, O. M., The equilibrium range in the spectrum of wind generated waves, *J. Fluid Mech.*, **4**, 426–434, 1958.

IERSON, W. J., JR., Wind generated gravity waves, *Advances in geophysics*, **2**, 93–175, 1955.

OLL, H. U., Oberflächenwellen des Meeres, *Handbuch der Physik*, **48**, Berlin, Göttingen, Heidelberg, 1957.

ROLL, H., AND G. FISCHER, Eine kritische Bemerkung zum Neumann-Spektrum des Seeganges, *Deut. Hydrograph. Z.*, **9**, Heft 9, 1956.

ST. DENIS, M., AND W. J. PIERSON, JR., On the motions of ships in confused seas, *Soc. Naval Architects Marine Engrs. Trans.*, **61**, 280–357, 1953.

TICK, L. J., A non-linear random model of gravity waves I, *N. Y. Univ., Coll. Eng., Research Div. Sci. Pap. 11*, technical report prepared for the Office of Naval Research and the David Taylor Model Basin, 1958. (To be published in the *J. Math. and Mech.*, Univ. Indiana.)

(Manuscript received April 27, 1959; presented at the Fortieth Annual Meeting, Washington, D. C., May 5, 1959.)

Wind-Induced Changes in the Water Column Along the East Coast of the United States*

JOSEPH CHASE

Woods Hole Oceanographic Institution
Woods Hole, Massachusetts

Abstract—Two types of changes in the water column at certain lightships are linked to the wind pattern. In one type there is a replacement of the whole water column, whereas in the other there is a fluctuation in the thickness of the upper layer.

Introduction—A program** of bathythermographic and water sampling observations at seven lightships along the east coast of the United States was begun late in 1955. The data thus collected provide an interesting daily record of hydrographic events [*Bumpus,* 1957; *Day,* 1959]. Of particular interest are parts of the records from Frying Pan Shoals, Chesapeake, Winter Quarter, Five Fathom, Barnegat, and Ambrose lightships.

Frying Pan Shoals lightship is located about 45 miles southwest of Cape Hatteras. The others are spread along the coast from the mouth of Chesapeake Bay to the offing of New York (Fig. 1).

FRYING PAN SHOALS, FALL 1956

Temperature—From October 1, 1956 to the end of the year, the water column at Frying Pan Shoals lightship was essentially homogeneous, the temperature difference between top and bottom (70 ft) being generally less than 0.5°F and the bottom salinity being generally within 0.10‰ of the corresponding surface salinity. (Bottom salinity samples are taken once a week and surface samples are taken daily.) The bathythermograph profile and salinity graphs of Figure 2 illustrate the general vertical homogeneity.

The surface temperature, which is thus a very good indicator for the whole column, provides a convenient means of studying the temporal changes during this season. A graph of the daily (0945 EST) surface temperatures, together with a dashed straight 'trend' line connecting its ends, is seen in Figure 3A.

At first the temperature line was close to the trend line, later (November 9 through Dec. 7) it was consistently below it, and still later (December 8 through 25) it was consistently above it. Reasons for this behavior were sought in daily 1230z weather maps. It soon appeared that temperature fluctuations were associated with air-mass movements. In general, warming occurred ahead of cold fronts (when southwesterly winds are prevalent) and cooling occurred after passages of cold fronts (when northerly winds prevail). The times of cold frontal passages are marked in the figure by arrows. (Note that the graph contains only one temperature per day and therefore does not show exactly when each temperature change began.)

The cold period from November 9 through December 7 was marked by many cold frontal passages, whereas during the subsequent warm period only three cold fronts passed the lightship. During this latter period on three occasions lasting two, six, and four days, respectively, the lightship was less than 300 miles south of a system of waves on a cold front.

The foregoing suggests the transfer of heat to the atmosphere as a mechanism for the lowering of water temperature in the wake of cold fronts, and indeed, rough calculations of heat loss yield figures of the right order of magnitude. How-

* Contribution No. 1032 from Woods Hole Oceanographic Institution.

** This program was instituted by the Woods Hole Oceanographic Institution under a contract with the U. S. Fish and Wildlife Service. The observations at the lightships were made by the U. S. Coast Guard.

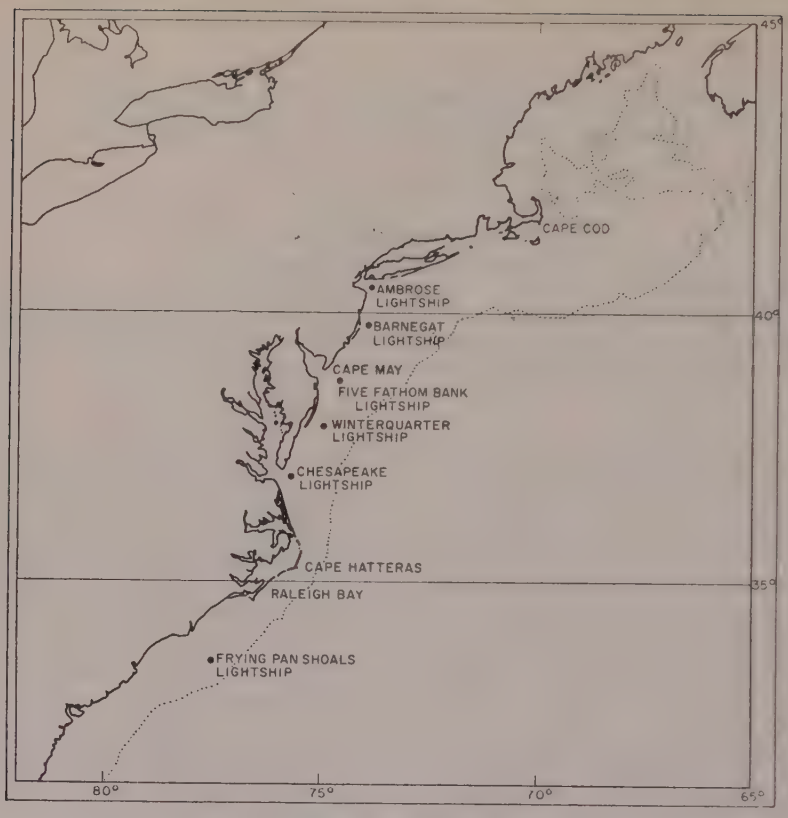

FIG. 1—East coast of the United States

ever, corresponding drops in the curve of salinity make such an explanation inadequate.

Salinity—The salinity at Frying Pan Shoals lightship is normally about 36‰ but during the period from October 6 through December 2, 1956 it ranged between 32.66‰ and 35.11‰ and averaged about 34‰ (Fig. 3B).

Water fresher than 34‰ is often found close to shore in this area. *Bumpus* [1955, p. 603] found that the amount of this 'fresh' water reflected the trends in runoff. He also found that the outflow from Pamlico Sound could account for considerable amounts of water fresher than 34‰ in Raleigh Bay. However, the amount of water available from these sources is hardly sufficient to account for the 34‰ found in the 70-ft column at the lightship.

A further and sufficient source is water from the Virginia coast which occasionally breaches the hydrographic barrier at Cape Hatteras and extends into Raleigh Bay. *Bumpus* and *Pierce* [1955, p. 96] reported such a breaching, whi occurred in January 1954 after a three-da northeast storm.

During October and the first half of Nove ber 1956, well over half of the winds record at 0945 EST at the lightship were from t north-northeast, northeast, and east-northea This is about twice the normal frequency. T chart of mean surface pressure for October 19 (Fig. 4) indicates that northeasterlies prevail as far north as New England; that is, about degrees of latitude farther than normal.

Average surface-pressure charts of two p riods of persistent northeasterly winds at t lightship are seen in figures 5A and 5B. One these is for October 23 to 29, the days leadi up to the regime of lower salinity, and the oth is for November 2 to 7, early in the regim Characteristic of all three charts is the indic tion of (1) northeasterly flow along the Car lina coast and (2) a long sweep of northeaster

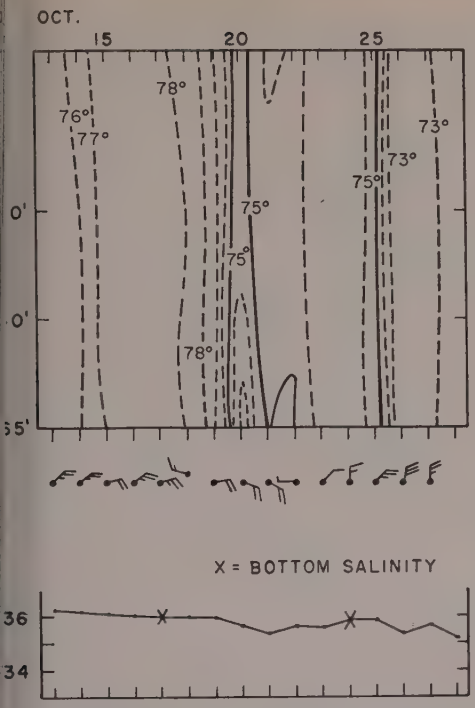

g. 2—Typical bathythermograph profile and ity record at Frying Pan Shoals lightship, fall

easterly winds toward the coast between e Hatteras and Cape Cod.

hese same characteristics are found in the ts of the storm of January 22 to 24, 1954 . 6), after which *Bumpus* and *Pierce* [1955] d water from the Virginia coast in Raleigh . And it was after such a pattern of isobars appeared on four successive days that two t bottles released off Cape May by *Miller* 52] were found on the shores of Raleigh . *Bumpus* [1955, p. 604] stated, "These are only bottles on record to have rounded the e in that direction or, for that matter, to e been recorded as moving southerly in this on."

hree of Bumpus' figures show the distribu- of salinity off Cape Hatteras. During the *atross III* cruises in May 1949, the 34‰ aline was found at about the latitude of e Hatteras, although during the surveys of uary and February 1950 it was found far- north. The northeast pattern described ve was prevalent (though the winds were light) just prior to the May 1949 cruises but was not prevalent just before the cruises of January and February 1950.

Thus there is a consistent record of association of the northeast pattern with the movement of water southward to or past Hatteras.

A connection between characteristic (1), local northeast winds, and invasions of water from the Virginia coast into Raleigh Bay is not surprising, but the importance of characteristic (2), a long broad northeasterly or easterly flow of wind toward the coast north of Hatteras, is less obvious. However, *Miller* [1957, p. 30] showed that there was a maximum of setup* at Atlantic City under just such conditions. Presumably the effect is felt elsewhere along the coast and as far as Cape Hatteras. Possibly a pressure head thus developed contributes to the southward flow of water off the Cape. As a partial check on this concept, the surface-temperature records from Ambrose, Barnegat, Five Fathom, Winter Quarter, and Chesapeake lightships were examined. All showed a definite though slight lessening of cooling rate during late October and early November when the northeast pattern was prevalent. No greater effect would be expected, since the gradient of surface temperature between these lightships and the continental slope is very small at that time of year [*Bigelow*, 1933, Fig. 54].

The occasions when the northeast pattern was present for two or more successive days are indicated by the bars of Figure 3C. The incidence of the pattern was greater in this case than in any of the other cases studied, and it is not surprising that this corresponds to the greatest known excursion of Virginia coastal water. Four northeasterly regimes occurred in October and early November, and a fifth occurred on November 19 and 20.

The salinity at the lightship first dropped sharply after the third regime, fell still lower after the fourth, and fell again after the fifth. Superimposed on this record are the smaller drops associated with cold fronts. A possible explanation of the foregoing is that:

A. As a result of (1) northeast winds along the Carolina coast and (2) a long broad northeasterly or easterly wind flow toward the coast

* Or wind tide.

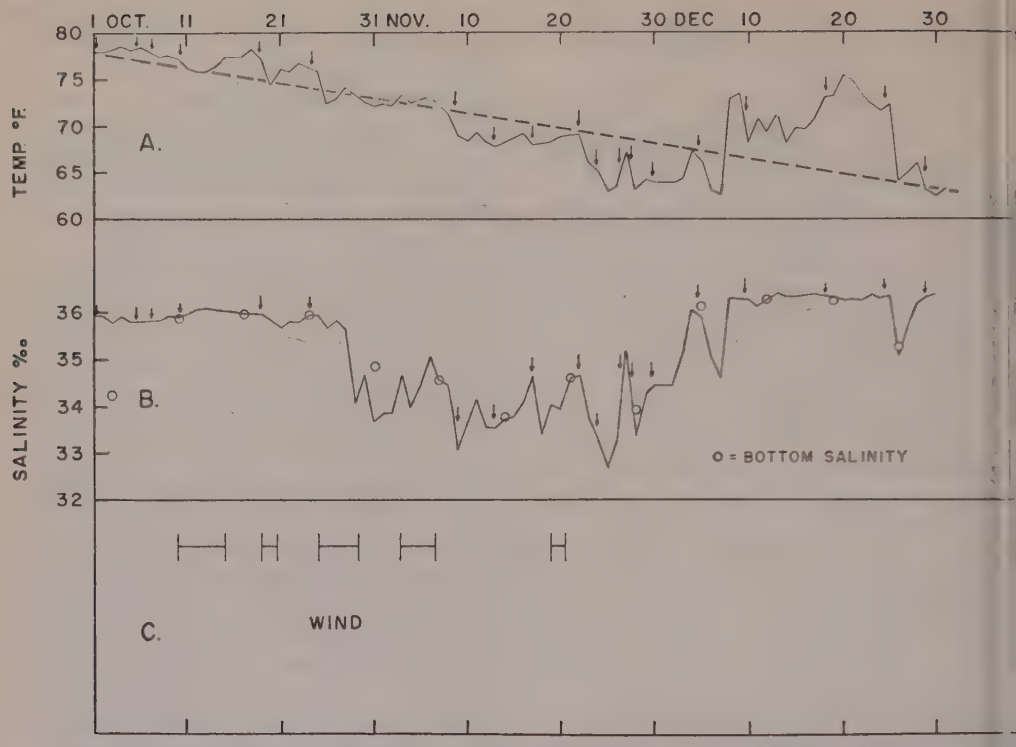

FIG. 3—(A) Daily surface temperature, Frying Pan Shoals lightship, fall 1956; (B) Daily salinity ing Pan Shoals lightship, fall 1956; (C) Graph of occurrence of typical northeast pattern, Fryin Shoals lightship, fall 1956

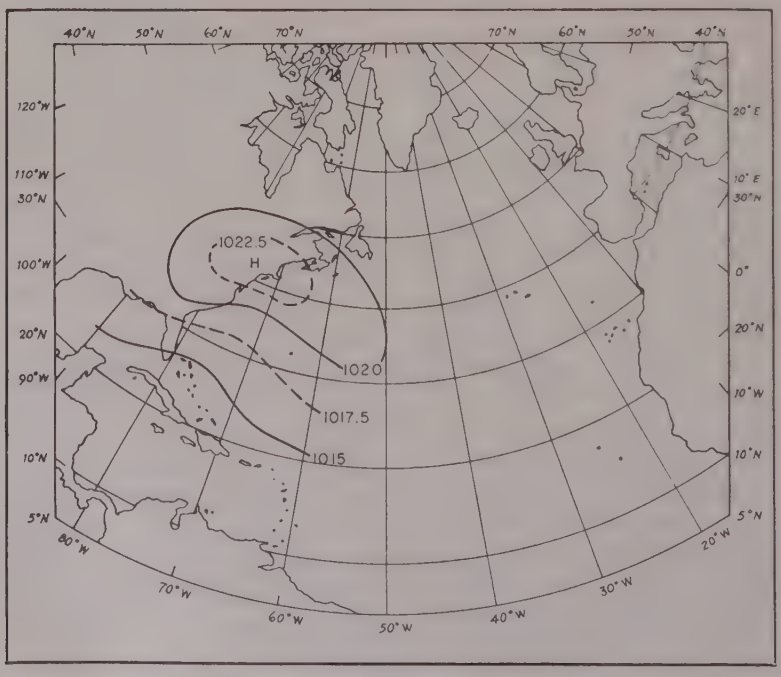

FIG. 4—Mean surface pressure, October 1956

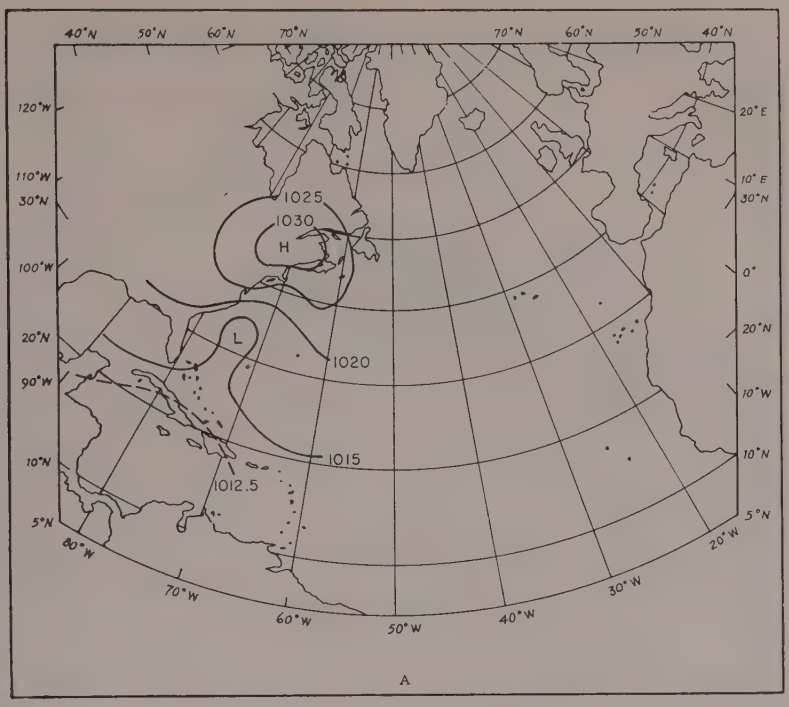

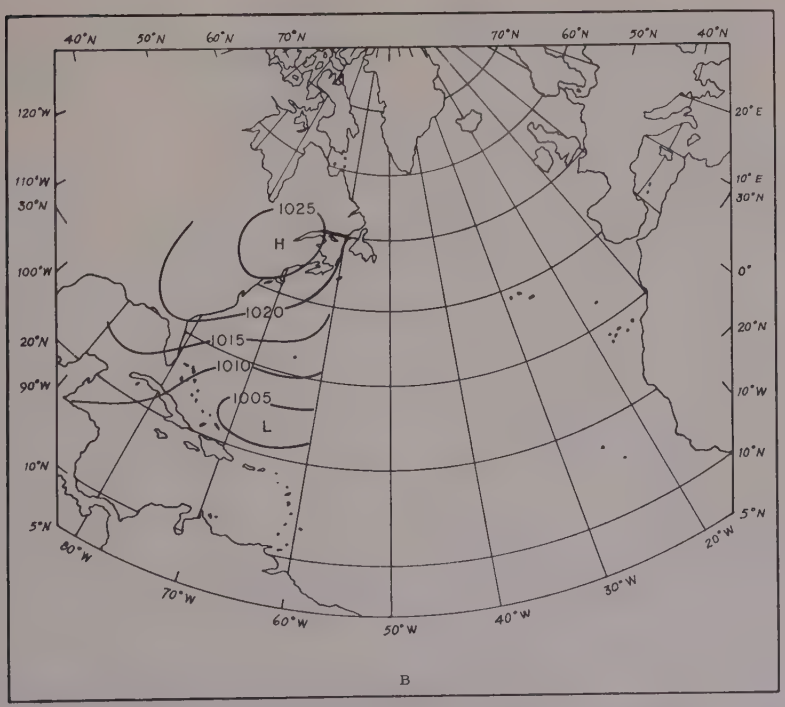

5—Average surface pressure during two periods of persistent northeasterly winds at Frying Pan Shoals lightship; (A) October 23–29, 1956; (B) November 2–7, 1956

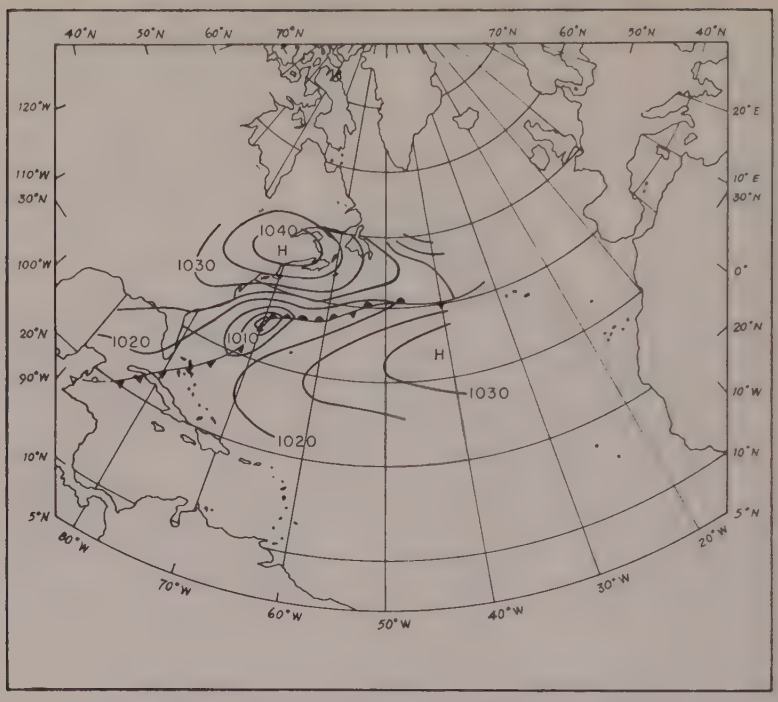

FIG. 6—Surface pressure, January 23, 1954

between Cape Hatteras and Cape Cod, Virginia coastal water can be swept southward around Cape Hatteras. This is an extension of a theory proposed by *Bumpus* and *Pierce* [1955, p. 95].

B. When, in the fall, this pattern of northeast wind occurs with sufficient frequency and wind strength, large volumes of water from the Virginia coast can be carried as far south as Frying Pan Shoals. This results in a lowering of both temperature and salinity in the whole water column.

C. In the fall, under the action of post-cold-frontal winds, relatively cold water is blown seaward as far as Frying Pan Shoals lightship. When a large column of Virginia coastal water is in the immediate vicinity, the temperature drop tends to be large, and an appreciable drop in salinity is also observed.

From November 25 to December 8 there was an over-all upward trend in salinity toward the normal value of 36‰. This suggests a gradual mixing of the previously advected Virginia coastal water with the more saline Carolina coastal or Florida Current waters which are normally found in the area.

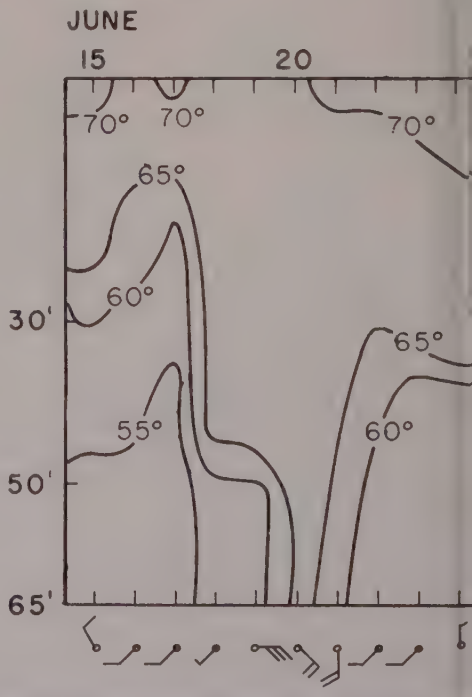

FIG. 7—Temperature profile, Chesapeake light
June 15–25, 1956

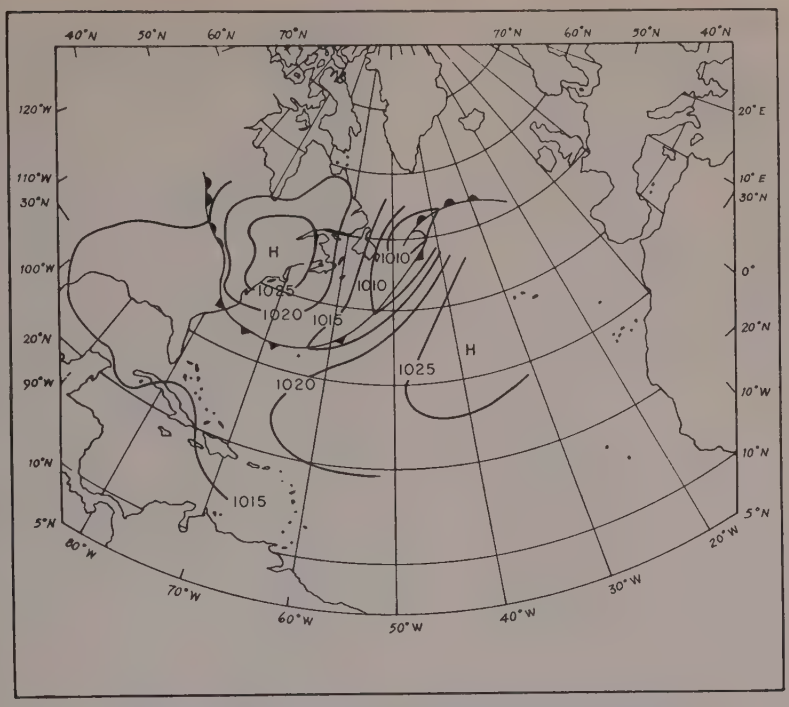

FIG. 8—Surface weather map, 0730 EST, June 19, 1956

The drop in salinity to about 35‰ on December 26, after the passage of a sharp cold front, suggests that the mixture had migrated northward from Frying Pan Shoals but was then pushed southward by the post-frontal winds.

CHESAPEAKE TO AMBROSE, JUNE TO SEPTEMBER

The summer data from Chesapeake, Winter Quarter, Five Fathom, Barnegat, and Ambrose lightships reveal many instances when the thermocline rose or fell as the warm surface layer became thinner or thicker. Particularly dramatic were three occasions in 1956 when at Chesapeake warm water flooded the entire column, driving out the cold water normally found at the bottom. These occasions were June 17 to 20, August 5 to 7, and August 21 to 24. Each was accompanied by an easterly wind at the lightship and, farther offshore, a large area of northeasterly or easterly winds. *Bumpus* [1957] noted the basic relationship in his discussion of ten-day means of temperature.

The situation is analogous to that at Sambro (Nova Scotia) Light Vessel as described by *Longard* and *Banks* [1952]. Whereas at Sambro a force 6 wind was needed to fill the 300-ft water column with warm water, force 4 was enough at Chesapeake (65 ft).

Figures 7, 9, and 11 are temperature profiles showing the thickening of the warm surface layer and the increase of temperature in the deeper water. The weather charts of Figures 8, 10, and 12 give the type of pressure distribution associated with the periods of warming. Each indicates that a large off-shore area was subject to northeasterly or easterly winds.

It is interesting that at a depth of 30 ft, on June 17 and 18, there was an increase of nearly 14°F (Fig. 7), even though the local wind was southwesterly; whereas on August 2 and 3 (Fig. 9), when the local winds were easterly, the temperature was virtually unchanged. These two cases indicate the importance of the winds at sea. In the former case a large area of easterlies was advancing southward from New England but had not yet reached the lightship. In the latter, although there were some easterlies off shore, they were weak, of short duration, and of small extent.

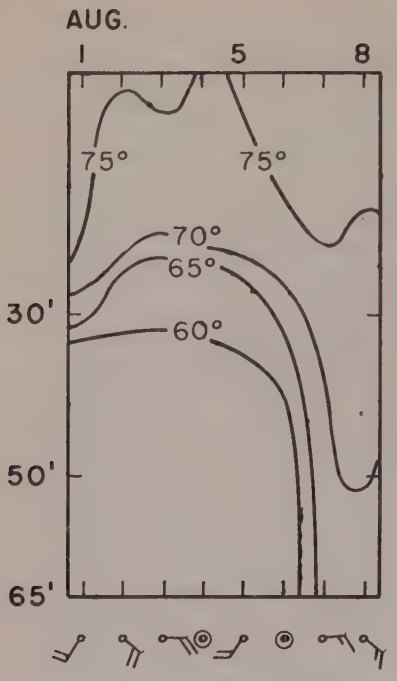

FIG. 9—Temperature profile, Chesapeake lightship, August 1–8, 1956

At Winter Quarter, Five Fathom, Barnegat and Ambrose lightships, similar though not always parallel reactions to wind occur. During June 17 to 20, 1956, Chesapeake showed the largest reaction and Winter Quarter the second largest. Evidently, the more northerly ships were somewhat in the lee of Cape Cod and Long Island. From September 16 to 20, 1958, on the other hand, the bottom temperature at *Ambrose* rose 12°F while the other stations showed little response. At this time *Ambrose* was in a field of easterly winds on the north side of a front, while the other lightships were south of the front where the southwesterly winds evidently prevented an accumulation of surface water.

It is not always easy to find an explanation for such selectivity. Possibly some of the floods may have a period of considerably less than 24 hours and thus can be missed by daily observations. The column at Winter Quarter responded markedly (11° at 50 ft) to the easterlies of August 2, 1956, while no response was evident at the other ships.

Immediately after the flooding of June 17–20, 1956 (Fig. 7), cold water flowed back

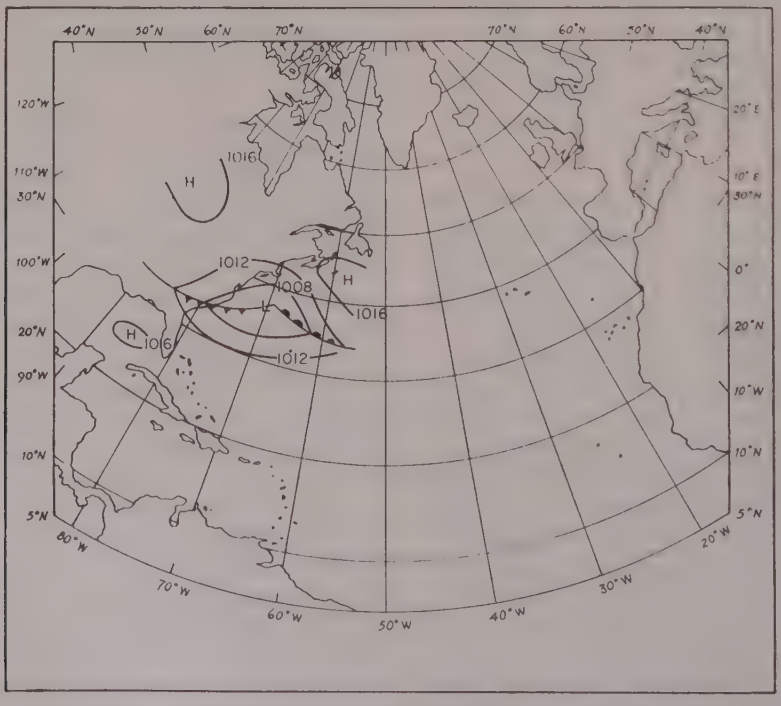

FIG. 10—Surface weather map, 0130 EST, August 7, 1956

lower 25 ft of the column at Chesapeake. is return was probably helped by the south- y winds of June 21 to 23, but, since the winds re rather light, it appears that this was, in main, a return to hydrostatic equilibrium. e cold water became much thicker in early y after a period of stronger southwesterly nds. *Taylor* and *Steward* [1959] have re- rted similar upwelling along the east coast of rida.

It would be interesting to know the thickness the warm and the cold layers, the thermocline der equilibrium conditions, and to what ex- t these thicknesses may change during the son. The averages probably will not reveal is, for the average wind, which is southwest- y, would tend to push surface water seaward d thus disturb the balance. Equilibrium con- ions can probably be determined most easily rough the examination of data taken in peri- s of extended calm. This is a study for some ture time when sufficient data have become ailable.

In the summers of 1957 and 1958 there were

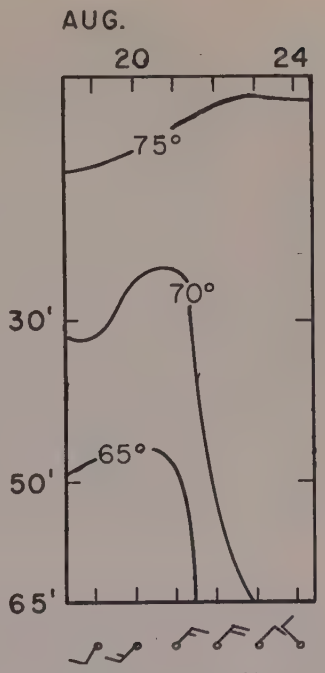

FIG. 11—Temperature profile, Chesapeake lightship, August 19–24, 1956

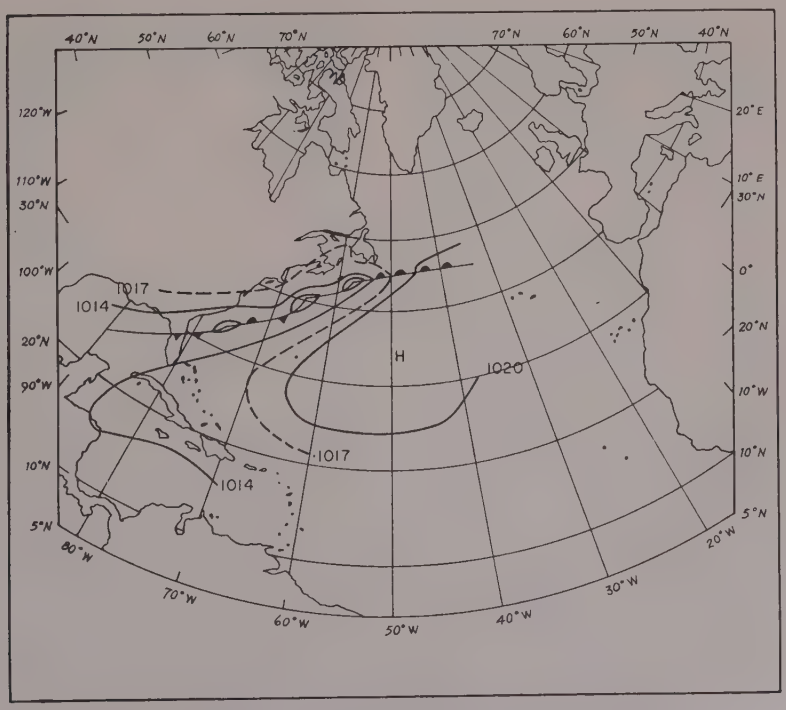

FIG. 12—Surface weather map, 0730 EST, August 22, 1956

many responses to wind like those of 1956, but none so abrupt. A gradual warming at all five stations occurred during the first three weeks of August 1957, a period when northeasterly winds far outnumbered the southwesterlies. In 1958, hurricane Daisy caused warming at all five stations as it moved northward along the coast. This hurricane caused warming in the lower part of the column at Frying Pan Shoals lightship also, although much of the time this column fails to respond to wind in the manner of the columns from Chesapeake to Ambrose.

No use has been made of the Chesapeake salinity data to indicate water movement because (1) the distribution of salinity off the mouth of Chesapeake Bay is too complicated [*Miller* 1952, Fig. 4] and (2) the data are insufficient for determining the exact times of maxima and minima.

The relationship between northeasterly or easterly wind fields and the flooding of surface waters along the Middle Atlantic coast is essentially the same as that conjectured in the section on fall conditions at Frying Pan Shoals lightship.

Acknowledgements—The writer wishes to express his appreciation to Dean Bumpus for his interest and guidance and to Raymond Wexler and G. Godfrey Day for their helpful suggestions.

This study was sponsored by the Office of Naval Research under contract Nonr 2196(00) NR 083-004.

References

Bigelow, H. B., Studies of the waters on the tinental shelf from Cape Cod to Chesap Bay, I—The cycle of temperature, *Pap. Oceanog. and Meteorol.*, 2(4), 1–135, 1933.

Bumpus, D. F., The circulation over the conti tal shelf south of Cape Hatteras, *Trans. Geophys. Union*, 36, 601–611, 1955.

Bumpus, D. F., Oceanographic observations, East Coast of the United States, *U. S. Wildlife Serv. Spec. Sci. Rept., Fisheries 233*, 132 pp., 1957.

Bumpus, D. F., and E. L. Pierce, The hydro and distribution of chaetognaths over the c nental shelf off North Carolina, *Deep-Sea search, Suppl.*, 3, 92–109, 1955.

Day, C. G., Oceanographic observations, 1957, Coast of the United States, *U. S. Fish. Wil Serv. Spec. Sci. Rept., Fisheries Ser., 282*, 123 1959.

Longard, J. R., and R. E. Banks, Wind-ind vertical movement of the water on an coast, *Trans. Am. Geophys. Union*, 33, 377– 1952.

Miller, A. R., A pattern of surface coastal c lation inferred from surface salinity-tempera data and drift bottle recoveries, *Woods H Oceanogr. Inst. Tech. Rept. 52–28*, unpubl. 14 pp., 1952.

Miller, A. R., The effect of steady winds o level at Atlantic City, *Meteorol. Monograph* 24–31, 1957.

Taylor, C. B., and M. B. Stewart, Jr., Sum upwelling along the east coast of Florid *Geophys. Research*, 64, 33–40, 1959.

(Manuscript received April 13, 1959.)

The Climatic Factor in the Radiocarbon Content of Woods

W. W. WHITAKER, S. VALASTRO, JR., AND MILTON WILLIAMS

Production Research Division, Humble Oil & Refining Company
Houston, Texas

Abstract—Past research has shown significant variations in radiocarbon contents of woods from different environments and in the degrees to which these radiocarbon contents reflect dilution of atmospheric carbon dioxide by carbon dioxide from fossil fuels. The present work attempts to relate these variations to climatic factors. Comparison of radiocarbon contents of individual tree rings with thicknesses of the rings and, in some cases, with meteorological records suggests that the radiocarbon contents of rings produced in years of heavy rainfall may be relatively low and that the contents of rings added in times of drought may be comparatively high. The year-to-year fluctuations in radiocarbon content observed in individual trees probably cannot be ascribed to rainfall alone, but likely also depend upon other factors. The apparent dependence of radiocarbon content on climate seems to be a result of a varying contribution to the tree of carbon from the pedosphere.

Introduction—An important quantity in the termination of the age of carbon-containing aterials by the radiocarbon method is the contration of radiocarbon which the material ntained initially—the so-called contemporary say. Any error in the choice of the value of e contemporary assay results in an error in e radiocarbon age. The absolute value of the ror in age is independent of the age of the mple and depends only on the error in choice the contemporary assay. The error in age is proximately 80 years for an error in conmporary assay of 1 per cent and is proporonately more for larger errors in contemporary say.

It is desirable that the error in age that is troduced by improper choice of the contemrary assay be kept less than the uncertainty age that results from statistical uncertainty the determination of the radiocarbon content a sample. The latter uncertainty is dependent on the age of the sample and also upon the rticular method and counting time used in the diocarbon determination. Generally, for methds of radiocarbon assay and counting times rrently in use, the statistical uncertainty in e is less than 1 per cent for samples up to ore than a thousand years old; it becomes rge only in the case of very old samples. It is us desirable that the error in contemporary say be no more than about 0.75 per cent for the use in the determination of age of samples no older than about 5,000 years. For the dating of samples in the age range of 5,000 to 10,000 years, the permissible error should probably be no greater than about 1 per cent, and even for samples as old as 15,000 years it is desirable that the contemporary assay be known to within approximately 2 per cent.

It is accordingly obvious that the contemporary assay must be known with assurance if radiocarbon ages are to be as accurate as present methodology permits. In order to develop information on the contemporary assay, work was initiated in this laboratory several years ago on those factors which influence the contemporary assay of various carbon-containing materials. Part of this work has been described previously [*Brannon* and others, 1957]. Although the previous publication was concerned primarily with the degree to which natural radiocarbon has been diluted by 'dead' carbon from the combustion of fossil fuels, several questions were raised which pertain to the radiocarbon contents of woods, which form an important class of materials amenable to radiocarbon dating,

In the previous work it was shown that four different woods varied not only in their contemporary assays but also in the extents to which they exhibited dilution by carbon from fossil fuels. The results are summarized in Table 1.

TABLE 1—*Contemporary assays and extents of dilution shown by various woods [from Brannon and others, 1957]*

Wood	Contemporary assay, extrapolated to present, from data on tree rings antedating the Industrial Revolution (cpm)	Dilution from fossil fuels (pct)
Douglas fir (*Pseudotsuga taxifolia*)	21.00 ± 0.17	3.6 ± 1.1
Gum (*Liquidamber styraciflua*)	20.23 ± 0.17	3.3 ± 1.1
Oak (*Quercus stellata* [?])	20.52 ± 0.17	2.8 ± 1.1
Swamp cypress (*Taxodium distichum*)	19.81 ± 0.17	1.7 ± 1.2

The Douglas fir of Table 1 grew in the region of the Rocky Mountains, the oak and the gum were from an area in southeast Texas approximately 75 miles north of Houston, and the swamp cypress was from Tangipahoa Parish, Louisiana. All of the radiocarbon assays were made by proportional counting of the samples as carbon dioxide gas, and in all assays the same counter was used. The counter was filled to a gas pressure of five atmospheres absolute [*Brannon* and others, 1955]. The comparative assay for the National Bureau of Standards' oxalic acid radiocarbon standard is 21.59 ± 0.12 cpm.

In a discussion of these results it was pointed out that both the differences in contemporary assays of the woods and the differences in the indicated degrees of dilution by fossil carbon could probably be attributed to differences in ecologies of the trees. More specifically, it was suggested that some older carbon from ground water or from the pedosphere was incorporated into the woody materials of the trees and that the amounts of older carbon utilized were dependent upon the moisture and organic contents of the soils in which the trees grew. Such a view is consistent with the data of *Deevey* and others [1954], who found that vegetation growing in hard-water lakes contains an abnormally low radiocarbon concentration, presumably because of the utilization by the plants of old carbon in the form of inorganic carbon compounds dissolved in the lake water. It was also pointed out that *Wickman* [1952] had postulated mechanisms by which older carbon could be introduced into plants either by uptake of carbon dioxide dissolved in ground waters or by utilization in photosynthesis of carbon dioxide released f the pedosphere.

In seeking an explanation of the differe in radiocarbon contents of the various wo attention was given in the present work fir the mechanism by which older carbon migh introduced into plants and then to the fac which might determine the degree of upt of older carbon. Among these factors the m obvious was that of climate, particularly of r fall.

Mechanism of uptake of older carbon trees—That variations in radiocarbon conte of the different woods are the result of vary amounts of uptake of older carbon, rather t the reflection of isotopic fractionation due differences in physiological behavior of the tr is demonstrated by results of measurement the stable carbon isotopic compositions of woods. These determinations, made by A. Daughtry and Douglas Perry of Humble Oi Refining Company, showed that the C^{12}- ratios of all of the woods of Table 1 were pr tically the same within a range of no more t about two parts per mil. Should isotopic fr tionation have been the cause of the variat of the radiocarbon contents, it might be pected that differences of as much as 30 pa per mil would have been found in the C^{12}- ratios.

Lack of variation of the C^{12}-C^{13} ratios of woods also indicated an absence of the mec nism proposed by *Wickman* [1952], which volves cycling of carbon through the air. In t mechanism, atmospheric carbon is first fracti ated in the process of photosynthesis to g

ghter' vegetable material. As part of the veg- able material finds its way into the pedosphere nd decays in time to yield carbon dioxide, part this carbon dioxide rises through the air to e utilized in photosynthesis and again under- oes fractionation to yield still lighter vegetable aterial. *Craig* [1954] has raised objections to is cycle on the ground that it is not supported y the existence of sufficiently large differences observed C^{12}-C^{13} ratios.

Even though the uniformity of C^{12}-C^{13} ratios or the four woods was evidence against the ransfer of older carbon from the pedosphere to ne trees via an aerial route, data presented by *undegårdh* [1954] suggest that large quanti- ies of carbon dioxide may be liberated from the edosphere and utilized by trees. He reported hat on a still day in a dense forest the carbon ioxide content of the air was several times the ormal amount close to the ground and that it iminished upward to less than the normal con- ent at leaf level.

In view of Lundegårdh's observations, it eemed desirable to plan and execute a definitive xperiment in an attempt to determine whether here is significant aerial transfer of old carbon rom the pedosphere to the leaves of growing rees. To this end, C. W. Arnold of Humble Oil & Refining Company designed and built equip- ment for the sampling of carbon dioxide in air. The equipment, which is portable and which ab- stracts carbon dioxide quantitatively, consists of a countercurrent extraction tower filled with ceramic 'saddle' packing, an electrically powered blower for blowing air vertically upward through the tower, and an electric pump for circulating the absorbent (2.0 molar sodium hydroxide so- lution, initially free of carbonate ion) from a sump at the bottom of the tower to a distributor spray at the top of the column, from which the absorbent percolates downward through the packed tower. Tests made on this equipment showed that more than 99 per cent of the car- bon dioxide in air is absorbed at the design rate of air intake, 5.0 liters per second. The high re- covery of carbon dioxide virtually precludes there being any detectable fractionation of car- bon isotopes in the sampling procedure.

By use of this equipment, samples of atmos- pheric carbon dioxide were obtained by Doug- las Perry and P. A. Kolodzie of Humble Oil & Refining Company at various heights above the water surface in a dense and extensive cy- press swamp in Iberville Parish, Louisiana. An exceptionally hot day in July 1957 was chosen for the sampling. The samples were secured at midday, at a time when there was no detectable breeze. Small samples of air were taken at the same time for later determination of carbon di- oxide content. Table 2 presents radiocarbon as- says of the atmospheric carbon dioxide samples and the results of the determinations of carbon dioxide contents of the air samples. For com- parison with the radiocarbon assays, an assay is shown of carbon dioxide in an air sample (obtained with the same extraction equipment) which had been secured about a month earlier on a beach of Galveston Island, Texas, which faced the Gulf of Mexico. Hurricane Audrey (1957) was moving coastward at the time, and strong onshore winds were blowing at the sam- pling location. The radiocarbon determinations of Table 2 and all succeeding ones presented in this report were made by use of the same coun- ter and of the same sample size utilized in ob- taining the assays of Table 1.

TABLE 2—*Carbon dioxide contents and radiocarbon assays, air from cypress swamp*

Height above Water surface at which air sample taken (meters)	Carbon dioxide content (pct by volume)	Radiocarbon assay (cpm)
0.2	0.0314	22.31 ± 0.17
0.9	0.0305	22.15 ± 0.17
2.1	0.0306	22.09 ± 0.17
Air sample from Galveston beach	—	22.12 ± 0.17

From the carbon dioxide contents of the air samples from the swamp it is apparent that there was no significant vertical gradient of car- bon dioxide concentration, even though the time and conditions of sampling were so chosen that they presumably offered maximum opportunity for the existence of a gradient. Likewise, the radiocarbon assays of the carbon dioxide sam- ples from the cypress swamp exhibited no vari- ation which was outside statistics. Within statis-

tics, too, the carbon dioxide samples from swamp air had the same radiocarbon content as the atmospheric carbon dioxide sample from Galveston beach.

These data demonstrate the absence of any significant amount of aerial transport of old carbon in the particular case investigated. Since this case was chosen because it would likely afford a definitive example, it was concluded that, if old carbon is indeed incorporated in woody plants, the mechanism is not that of cycling of carbon dioxide from the pedosphere to the leaves of trees by an aerial route.

The only other route by which older carbon might be introduced into a plant is through the plant's root system. The likelihood of uptake of carbon by roots involves complex problems of plant physiology, and whether appreciable amounts of carbon can be taken up through the roots appears to have been disputed among plant physiologists. Current thoughts on the matter have been summarized by *Stolwijk* and *Thimann* [1957], who performed laboratory experiments in which carbon dioxide was introduced into young pea and barley plants through the root systems. The uptake by the roots, according to these authors, was small. Whether uptake by roots of trees occurs in amounts sufficient to account for observed variation in radiocarbon contents is, from the standpoint of plant physiology, apparently still unresolved. Under the circumstances, however, the authors favor uptake of older carbon by the root system as the most likely explanation of differences in radiocarbon contents of trees from different environments.

Possible influence of climate on radiocarbon content of woods—If it is assumed that some older carbon from the pedosphere or from ground water is assimiliated by trees, then the degree of the resultant reduction in radiocarbon assay of the wood is dependent both upon the relative amount of older carbon utilized and upon the age of the older carbon. It might be expected that the amount of older carbon utilized would be related, at least qualitatively, to the amount of carbon dioxide or bicarbonate ion present in the soil in which the roots grow. This, in turn, should be dependent upon the amount of organic material resident in the soil and upon the extent of microbial activity. The age (more specifically, the average age) of the older c bon, if fractionation in the conversion of ganic material to carbon dioxide by microorg isms is neglected, should be dependent upon time of residence of the organic material in pedosphere. This again involves the extent microbial activity.

The foregoing ignores carbon which might derived from solution of ancient limestone. though such carbon may have been import in diluting the radiocarbon content of pla growing in the hard-water lakes with wh *Deevey* and others [1954] were concern lack of variation in the C^{12}-C^{13} ratio of woods which are listed in Table 1 implies t little or no carbon derived from limestone w taken up in these particular woods. Furth with the possible exception of the Douglas the trees grew in areas in which limestones virtually absent. Accordingly, the assumptio made in the present work that limestone-d rived carbon is not ordinarily an important f tor in determining the radiocarbon assay woods.

Following the argument that both amount of organic material and the extent microbial activity in soil are relevant to upta of older carbon, one may postulate the enviro ment in which a tree grows as being a prima factor in governing the amount and age of old carbon utilized. For example, a tree growing a cypress swamp or in muskeg might be e pected to partake of relatively large amounts older carbon. A tree growing in an arid regi or in a thin tropical soil in which the rate turnover of organic material is high might log cally be expected to yield a contemporary ass which is only slightly affected by dilution wi older carbon. In this connection, the conte porary assay, extrapolated to the present fro old rings, of a recently-felled chicle (*Sapo achras*) which grew in Palenque, Chiapas, Me ico, was found to be 20.68 ± 0.17 cpm. Co parison of this with the contemporary assays Table 1 shows the chicle assay to be in t higher part of the range of values. Parenthet cally, although the chicle tree grew in limesto bedrock, the relatively high radiocarbon conte and the C^{12}-C^{13} ratio, which was essentially t same as for those of the woods of Table 1 a quite different from those of limestones, is ev

e against the incorporation of an appreci- amount of carbon derived from the weath- g of the limestone.

lthough the effects on contemporary assay extreme environmental conditions, such as se which prevail in cypress swamps or in erts, might be predicted with some confi- ce, the woods of interest in many radiocar- dating problems are from temperate zone s which are not restricted to such character- habitats. Such trees often undergo changes climatic conditions during their lifetimes, , in effect, are thus exposed to a succession environmental conditions. Alternate periods drought and of heavy rainfall may result in tuations of soil moisture and in variations of robial activity. Consequently, it might be ected that woods of different ages from a gle tree should show variations in radiocar- n content as a result of climatic fluctuation.

Variations in radiocarbon content of tree rings l possible relationship to climate—In order investigate woods from individual trees for variations in radiocarbon content that might ult from climatic fluctuations, a series of as- vs was made on rings from a gum (*Liquid- ber styraciflua*) from Liberty County, Texas, ated approximately at 30°25′N, 94°55′W. is tree, somewhat more than 50 years old at e time of its felling in October 1957, grew on sandy slope in an area relatively remote from tensive industrial activity. The site was atypi- l in that it was reasonably well drained, hereas the gum usually grows in a more moist cation. The locality is very close to that from hich came the oak and the gum of Table 1.

Samples for radiocarbon analysis were taken om a cross section of trunk several feet above e ground. Each sample represented a single ear's growth of the tree. Thicknesses of the an- ual growth rings were also measured. Figure 1 ows the thicknesses of all rings and radio- rbon assays, extrapolated to the present, of a mber of the individual rings.

A striking feature of the radiocarbon data is e marked increase in the radiocarbon content ithin the last several years. This is attributable radiocarbon contributions from nuclear ex- losions.

Particularly noticeable in the pre-1950 radio- rbon results is the wide range of variation of

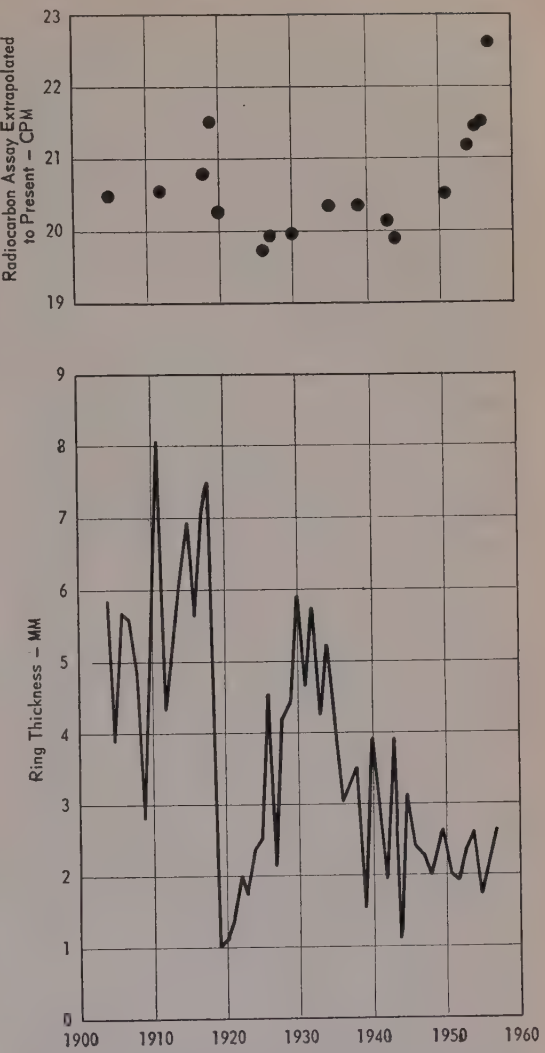

FIG. 1—Thickness and radiocarbon assays of rings; gum tree, Liberty County, Texas

the assays. The extreme values were as low as 19.73 ± 0.17 cpm and as high as 21.50 ± 0.17 cpm. As far as is known, these variations are real and are not due to experimental error or to fractionation in sample preparation.

The highest pre-1950 radiocarbon assay shown in Figure 1 is that of the 1919 ring, which was exceedingly narrow. Weather Bureau records both for Houston and for College Station, Texas (both of which are within about 75 miles of the locality in which the tree grew) show that an exceptionally high rainfall was recorded

for the entire year of 1919. Most of the rainfall occurred in late summer and fall, however; the growing season—the early part of the year —was drier than normal. The lowest radiocarbon assay is that of the 1926 ring, which, compared with adjacent rings, is relatively wide. Weather records show that rainfall during the growing season of that year was heavy.

Although the radiocarbon assays for these two years, 1919 and 1926, appear to corroborate the view that the radiocarbon content is higher in time of drought and lower in years of heavy rainfall, other examples from Figure 1 may be cited which are not in accord. For example, the radiocarbon assay of the 1920 ring is relatively low, yet both the thickness of the ring and weather records show that the rainfall during the growing season was sparse. Again, the radiocarbon content of the 1944 ring is low, although the ring thickness indicates a dry year and the weather records show normal rainfall. It is unfortunate that the results for the prolonged period of drought extending from about 1950 to 1957 are obscured by additions of radiocarbon from nuclear explosions.

Some additional information may be gained from the trend of the radiocarbon assays of Figure 1. If a smooth curve, monotonically decreasing with increasing time, is drawn through the pre-1950 points, the extrapolated asymptotic value for average pre-1900 wood is in the neighborhood of 20.6 cpm, which is somewhat higher than the contemporary assay of the gum of Table 1. Since the latter tree grew in a normal moist habitat, while that of Figure 1 grew in a well-drained location, the difference in their extrapolated assays substantiates the idea that a more moist environment results in a reduced contemporary assay.

Although the data of Figure 1 certainly do not provide a clear correlation of ring thickness and radiocarbon content, they suggest the existence of a climatic factor which influences radiocarbon content. In general, then, there is some reason to believe that higher radiocarbon contents may be associated with thin rings and lower contents with thicker rings.

In order to investigate further those variations in radiocarbon content which might be related to climatic fluctuations, a number of radiocarbon determinations were made on a section of Douglas fir (*Pseudotsuga taxifolia*
section, made available by Terah L. Smi
the University of Arizona, was from an o
which grew in the Santa Catalina Mou
Pima County, Arizona, and which was fe
1951. The Douglas fir normally grows in
sitive' site in the sense that moisture in t
and subsoil is derived almost entirely fr
cent rainfall or snowfall. Because of t
might be expected that the Douglas fir wo
particularly responsive in exhibiting climat
induced variations in radiocarbon content
though the organic content of the soil i

Figure 2 shows the thicknesses of the
vidual rings of the Douglas fir specimen a
radiocarbon assays, extrapolated to the pr
of a number of rings. The thicker rings
sufficient in quantity to allow radiocarbon
of only a single year's growth, but the
size of some of the thinner ring samples
it necessary to combine the growth of t
more years to obtain enough sample for

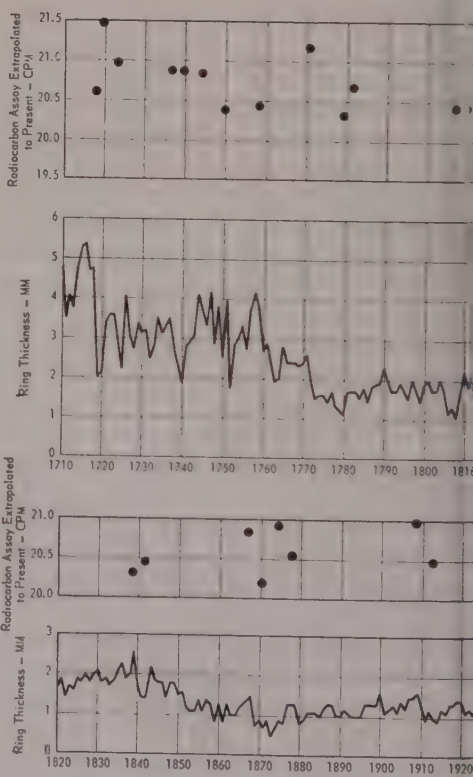

FIG. 2—Thickness and radiocarbon assays of ri
Douglas fir tree, Pima County, Arizona

ne range of variation of the radiocarbon as-
, as in the case of the gum tree, was rela-
y great. The lowest assay was 19.88 ± 0.17
and the highest 21.47 ± 0.17 cpm. There
me indication of a secular periodicity in
radiocarbon content (with the period being
erhaps 200 years in duration) of the general
re of that visualized by *de Vries* [1958].
ike the periodic variation described by de
s, which indicates a maximum of small am-
de early in the 19th century, that which
ht be deduced from Figure 2 would have a
imum around the years 1820 to 1830.

comparison of the radiocarbon assays with
ring thicknesses (Fig. 2) shows again that
ome cases high assays were associated with
rings and low assays with thicker rings,
reas in other cases the reverse was true.
teworthy is the highest value of the assay,
the years 1719 and 1720, which was obtained
rings which were relatively narrow for two
cessive years. A rough statistical appraisal
wed that the radiocarbon content, when com-
ed with ring thickness corrected for the gen-
l trend of decreasing thickness with increas-
age of the tree, tended to be higher for the
nner rings and lower for the thicker rings,
t the correlation was very poor at best. It
st be borne in mind that the objective of the
nparison was to assess the influence of pos-
le climatic factors on the radiocarbon assay
d that the tacit assumption of a relationship
tween ring thickness and rainfall is itself sub-
t to question.

As in the case of the gum tree data, the data
r the Douglas fir again suggest, but do not
monstrate, that there is a reduction in the
diocarbon content of wood added in times of
avy rainfall.

Conclusions—From this work it is apparent
at there may be significant year-to-year varia-
ns in the radiocarbon content of woods from
dividual trees, as well as appreciable differ-
ces in the contemporary assays of trees from
fferent environments. The magnitudes of these
riations are sufficiently large to be of concern
radiocarbon dating.

From the evidence at hand it is likely that
ese variations are a reflection of varying con-
tributions to the trees of older carbon from the pedosphere. The nature of the environment in which a tree grows is certainly a factor in governing the amount and age of older carbon incorporated into the tree, and the evidence suggests that climate, directly or indirectly, is also a factor. The amount and age of older carbon which is in the soil and available to a tree are probably determined by the amount of organic material present, its time of residence in the pedosphere, and the extent of microbial activity. Climate influences these.

In spite of the fact that this work has revealed complexities in the contemporary assays of woods which, if ignored, might limit the reliability of the radiocarbon ages of recent vegetable materials, the recognition of these and allowance for their effects should permit greater reliability in radiocarbon dates of the future.

References

Brannon, H. R., M. S. Taggart, and M. Williams, Proportional counting of carbon dioxide for radiocarbon dating, *Rev. Sci. Instr.*, **26**, 269–273, 1955.

Brannon, H. R., A. C. Daughtry, D. Perry, W. W. Whitaker, and M. Williams, Radiocarbon evidence on the dilution of atmospheric and oceanic carbon by carbon from fossil fuels, *Trans. Am. Geophys. Union*, **38**, 643–650, 1957.

Craig, H., Carbon 13 in plants and the relationship between carbon 13 and carbon 14 variations in nature, *J. Geol.*, **62**, 115–149, 1954.

Deevey, E. S., M. S. Gross, G. E. Hutchinson, and H. L. Kraybill, The natural C-14 content of materials from hard-water lakes, *Proc. Natl. Acad. Sci., U. S.*, **40**, 285–288, 1954.

de Vries, Hl., Variation in concentration of radiocarbon with time and location on earth, *Koninkl. Ned. Akad. Wetenschap Proc., Ser. B*, **61**, 94–102, 1958.

Lundegårdh, H., *Klima und Boden*, Veb Gustav Fisher Verlag, Jena, 1954.

Stolwijk, J. A. J., and K. V. Thimann, On the uptake of carbon dioxide and bicarbonate by roots, and its influence on growth, *Plant Physiol.*, **32**, 513–520, 1957.

Wickman, F. E., Variations of the relative abundance of the carbon isotopes in plants, *Geochim. et Cosmochim. Acta*, **2**, 243–254, 1952.

(Manuscript received April 9, 1959; presented at the Fortieth Annual Meeting, Washington, D. C., May 5, 1959.)

JOURNAL OF GEOPHYSICAL RESEARCH VOLUME 64, NO. 8 AUGUST, 1959

Ground-Water Studies in New Mexico Using Tritium as a Tracer, II

HARO VON BUTTLAR*

Research and Development Division, New Mexico Institute of Mining and Technology
Socorro, New Mexico

Abstract—The monitoring of the tritium concentration of rain-water and ground-water samples in New Mexico has been continued. A third peak in the rain water was found in the summer of 1957. By comparison of the tritium content of a ground-water sample with that of the rain water, hydrologic quantities such as the age and velocity of flow of the ground water could be determined. The tritium method shows considerable promise as a hydrologic tool.

INTRODUCTION

A method of studying ground-water problems by means of natural tritium as a tracer has been described in an earlier paper [*von Buttlar* and *Wendt,* 1958]. Essentially, the method consists of measuring the tritium concentration of water samples collected from streams and wells and relating the results to the tritium concentration found in rain water.

Rain water previous to 1954 had a tritium concentration of about 10 *T* units, the tritium being due to cosmic-ray action [*Kaufman* and *Libby,* 1954; *von Buttlar* and *Libby,* 1955]. As found in the world-wide distribution studies by *Begemann* and *Libby* [1957], *Begemann* and *Turkevich* [1958], and *Brown* and *Grummitt* [1956], and in the New Mexico data reported by von Buttlar and Wendt, marked peaks occurred in the tritium concentration of meteoric water after the hydrogen-bomb explosions in the years 1954 and 1956. A third peak, in 1957, resulting from the British test series, is indicated by the present study.

Part of the surface water of high tritium content will enter the ground and contribute to the recharge of the ground-water reservoirs. It mixes with the ground water already present and takes part in its underground motion. The tritium concentration of a ground-water sample, therefore, is related to its underground age. If no tritium is found, the sample must have been out of contact with meteoric water for at least 30 years; if the tritium concentration is higher than the prebomb level, the sample contains at least a sizable admixture of recent surface recharge. If the tritium concentration of a well is monitored in time, inferences can be drawn as to the rate of motion of the ground water, its age, and the ratio of recharge to total water in an aquifer.

In the previous article the method of such study was described in detail, and some results were presented. In the present paper further data on the tritium concentration of natural waters are given, and the implications thereof are discussed. Three groups of data will be distinguished: (1) rain and river waters, (2) ground waters from an area south of Carrizozo, New Mexico, and (3) miscellaneous other ground waters from New Mexico. An evaluation of the method will conclude the paper.

RAIN AND RIVER WATERS

As mentioned above, peaks occurred in the tritium concentration of waters of meteoric origin in the years 1954 and 1956, and peak heights as high as 100 times the level produced by cosmic-ray action on the atmosphere were recorded. A third peak, during the summer of 1957, was discovered in the rains at Socorro, New Mexico (Table 1). A considerable scatter of the tritium concentration is noticed following the main peak, a phenomenon which was found also by Begemann and Turkevich after the 1956 maximum. Our scanty data do not allow a clear explanation of this effect, since the rains which occur at Socorro usually comprise a complicated mixture of water derived from the Pacific Ocean, the Gulf of Mexico, and re-evaporated rain

* Present address: Institut für Kernphysik, Technische Hochschule, Darmstadt, Germany.

TABLE 1—*Tritium concentration of rain at Socorro, New Mexico*

(All results given have an estimated analytical error of 10 per cent.)

Date	*T* units (tritium/protium × 10^{-18})
1956	
Oct. 17	63.5
1957	
Jan. 4	42.0
Feb. 17	57.5
Mar. 20	73.9
Apr. 29	133
June 6	260
June 7	252
July 4	95
July 13	162
July 25	81
July 26	63.5
Aug. 2	166.2
Aug. 3	135
Aug. 8	89.7
Aug. 14	53.3
Aug. 18	73.2
Aug. 21	53.1
Oct. 11	170
Oct. 12	178.5
Oct. 16	107.5
Oct. 21	62
1958	
Jan. 4	172.5
Mar. 4	179
Mar. 6	331
Mar. 13	500
Mar. 24	338

TABLE 2—*Tritium concentration of New Mexico river water*

(All results given have an estimated analytical error of 10 per cent.)

River	Date	*T* units (tritium/protium × 10^{-18})
	1957	
Rio Grande, near Socorro	Feb. 1	47.5
Pecos River, near Carlsbad	Feb. 23	33.8
Rio Grande, near Socorro	May 10	82.0
Rio Grande, near Socorro	June 27	116
Rio Grande, near Socorro	July 31	56.8
Rio Grande, near Socorro	Sept. 4	67.5
Rio Grande, near Socorro	Nov. 7	73
	1958	
Rio Grande, near Socorro	Jan. 16	71
Rio Grande, near Socorro	Mar. 5	65.5

water which had fallen earlier. It is believed that the latter source is mainly responsible for the high tritium concentration of the rains during the winter of 1957–1958.

Compared with the rain water, the New Mexico river samples (mainly from the Rio Grande; see Table 2) exhibit a slower rise and a smaller magnitude of the 1957 tritium peak. This is to be expected since the river water is composed of (1) rain water which fell a few weeks before the sampling date and (2) ground water which may have been underground for a long time and thus would have a smaller tritium concentration. Furthermore, surface reservoir accumulation may delay and broaden the tritium peak for samples taken in the river below the reservoir. For Mississippi River water, a similar trend of the tritium concentration was found by Begemann and Turkevich after the H-bomb explosion in 1956.

Three tritium-concentration peaks have been detected within the past few years in the surface waters of the Northern Hemisphere, one each occurring during the summer months of the years 1954, 1956, and 1957. A fourth test series appears to have originated another peak in March 1958 (Table 1).

GROUND WATER FROM AN AREA SOUTH OF CARRIZOZO, NEW MEXICO

The study of the tritium concentration of ground waters in the Carrizozo area described in the previous paper was continued. The results are plotted in Figure 1. It is evident that during 1957 no peak as large as those of 1956 occurred in the tritium concentrations of the waters from wells 1, 2, and 7. Since it is unlikely that well contamination by surface runoff could show such differences from one year to the next, this finding suggests that the peak found in

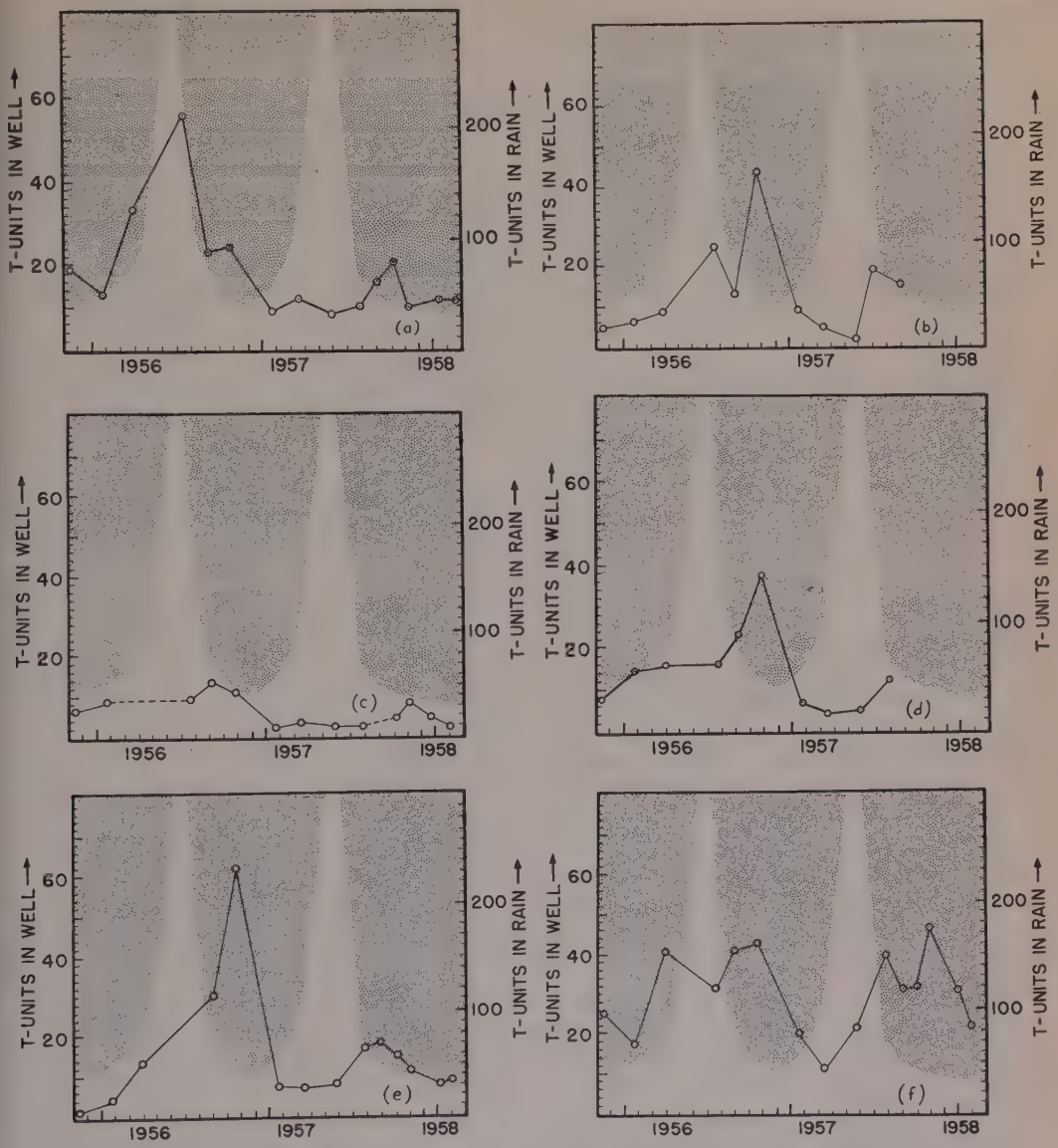

FIG. 1—Comparison of the tritium concentration found in the Carrizozo wells with the tritium concentration of rain water. Shaded area outlines rain peaks (units on right); solid line joins points measured for well water (units on left); (a) well 1; (b) well 2; (c) well 4; (d) well 6; (e) well 7; (f) well 8

1956 might not be the result of the 1956 rain peak. If so, the ground water that feeds these wells must have an age of about two years with respect to its influx as rain water, and the tritium peak must have been due to the 1954 rain water. Confirmation will be obtained if the wells again exhibit a larger peak in 1958. This would reflect the presence of the 1956 rain water that entered the aquifer at the main recharge area located in the mountains.

The small rises in the tritium concentration of wells 1, 2, and 7 during the fall of 1957 can be attributed to vertical percolation of rain water into the ground-water zone. From the data one may conclude that this water appears in the discharge of the wells about three months

TABLE 3—*Tritium concentration of water from a mountain creek near well 1, south of Carrizozo, New Mexico*

(All results given have an estimated analytical error of 10 per cent.)

Date	*T* units (tritium/protium $\times 10^{-18}$)
1957	
Jan. 24	28.6
Mar. 4	31.4
May 28	44.0
July 30	42.6
Nov. 4	50.5
1958	
Jan. 11	47.8
Feb. 23	46.5

TABLE 4—*Tritium concentration of Socorro, New Mexico, municipal water supply*

Date	Source	*T* units (tritium/protium $\times 10^{-18}$)
1957		
May 16	Hot spring	1.8 ± 0.4
May 16	Well	1.8 ± 0.9
July 26	Hot spring	3.2 ± 0.3
July 26	Well	4.0 ± 0.4
Sept. 4	Hot spring	3.1 ± 0.3
Nov. 7	Hot spring	(10.0 ± 1.0)
1958		
Jan. 16	Hot spring	1.8 ± 0.5
Mar. 5	Hot spring	2.7 ± 0.4

after it falls as rain. Since the thickness of the unsaturated top strata is about 100 ft, the approximate rate of vertical percolation is calculated to be 1 ft/day. Whereas the tritium content of the rain water during the summer of 1957 is about 200 *T* units, the well water reaches peaks of about 10 *T* units above the previous level. Thus, during 1957 the surface percolation contributed about 5 per cent to the water produced by the wells.

Well 8, as in 1956, shows an altogether different behavior. This well appears to receive a much larger contribution of recent surface waters than wells 1, 2, and 7, as was suggested previously.

Well 4, the Carrizozo municipal water well, has not yet shown an appreciable peak of tritium concentration. The somewhat elevated tritium contents during the autumns of 1956 and 1957, which are proportional to those in wells 1, 2, and 7, suggest that the well is mainly pumping water from the Cretaceous formation underlying the alluvial bed. The water contribution from the upper strata cannot amount to more than 20 per cent of the total water produced, as is seen when the peak heights of wells 4 and 1 (or 7) are compared.

In summary, it may be said that the second interpretation offered in the earlier paper to explain the tritium-concentration trends in the Carrizozo wells can be ruled out. The data presented in Figure 1 of this article support the first previous interpretation. But there remains latitude for further attempts to interpret the data.

In addition to the wells, a mountain creek situated about one-half mile northeast of well 1 was monitored for its tritium concentration during the same period. The data obtained (Table 3) show that the creek carries water derived from both rain and ground water; its tritium concentration is of intermediate magnitude.

MISCELLANEOUS GROUND-WATER SAMPLES FROM NEW MEXICO

Socorro municipal water supply—The hot spring and the well that contribute to the municipal water supply of Socorro were described in the previous paper. The monitoring of the tritium concentration of these waters was continued and the results are listed in Table 4. The well was not used during the winter months because the discharge of the spring was sufficient to cover the city's water demand. The tritium data indicate that the 1954 recharge to the ground water which feeds the spring had not reached the spring site by March 1958. The velocity of the ground-water flow in the area west of Socorro Mountain (Snake Ranch Flats) is thus smaller than 10 miles in four years, or 35 ft/day. The high concentration found for the November 7, 1957 sample may be explained by local recharge subsequent to the 1957 rain peak; or, possibly, an analytical error caused the high value. This water is being reanalyzed.

Ground-water samples from an area west of

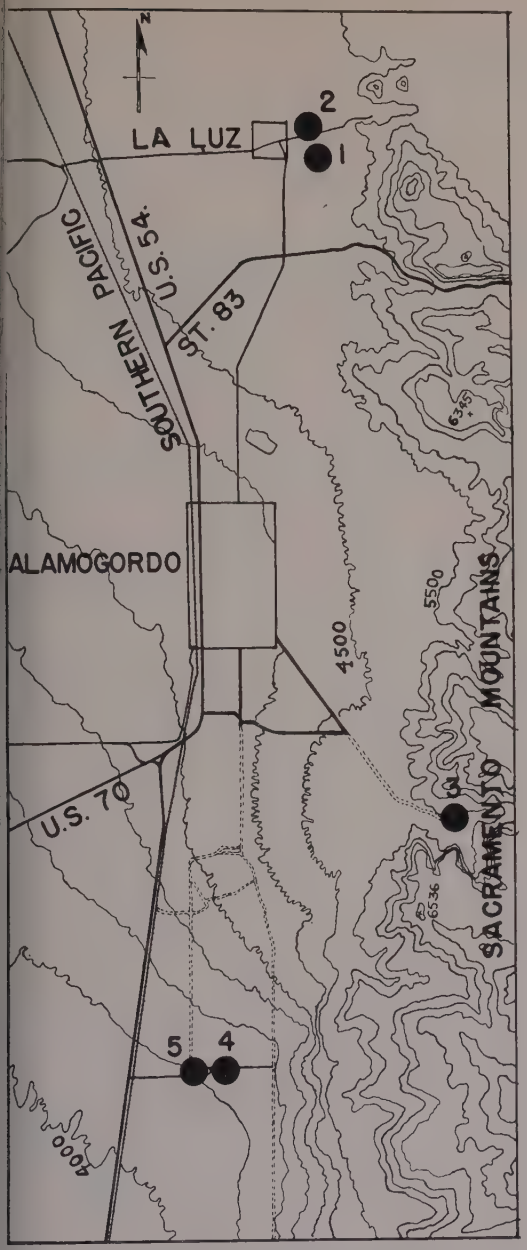

FIG. 2—Map of the area near Alamogordo, New Mexico, showing the collection stations

Alamogordo, New Mexico—In connection with the recent increase in the demand for water at Alamogordo and the Holloman Air Force Base, a Government project was initiated to effect more efficient utilization of the surface- and ground-water resources in that area. A large surface-water reservoir has been constructed near the village of La Luz, which is located about 5 miles north of Alamogordo. This reservoir collects water derived from the easterly slope of the Sacramento Mountains, mainly from La Luz Creek. Another reservoir of good-quality ground water was developed south of Alamogordo. The probable recharge area of the ground-water reservoir is also the easterly slope of the Sacramento Mountains, although *Vacquier* and others [1957] were led by their induced-polarization measurements to believe "that the water issues from an underground spring."

Five sampling stations were selected for the tritium investigation (Fig. 2):

Station 1. Surface-water reservoir, 0.4 mile east of La Luz.

Station 2. Well 500 ft deep, 0.3 mile east of La Luz. The water is used as part of the municipal supply of La Luz.

Station 3. Surface water from a water tank for cattle in the Alamo Canyon, 0.6 mile east of the mouth of the canyon. Even though this water does not contribute recharge to the ground-water reservoir south of Alamogordo, its tritium concentration is probably similar to that of the recharge.

Station 4. Well water from the main pumping station of the ground-water development area south of Alamogordo.

Station 5. Tapwater from the guard's house, 0.3 mile from the main pumping station (station 4). This water is said to come from the wells of the pumping station; however, the tritium concentration indicates that it is not the same as the water from station 4.

The tritium-concentration data from the samples collected at these stations are listed in Table 5. It is seen that both the deep well at La Luz (station 2) and the main pumping station in the ground-water development area (station 4) show low tritium concentrations, whereas the surface waters (stations 1 and 3) exhibit a trend similar to that of the previously mentioned mountain creek near Carrizozo; possibly the runoff near Alamogordo contained a somewhat higher admixture of ground water during the spring of 1957 than the Carrizozo mountain creek.

It is seen definitely that the good-quality ground water produced at the Government de-

TABLE 5—*Tritium concentration of miscellaneous ground-water samples from an area near Alamogordo, New Mexico*

(The tritium results have an estimated error of 10 per cent.)

Station	Location Sec	T	R	*T* units (tritium/protium $\times 10^{-18}$) Nov. 29, 1956	May 1, 1957	Nov. 14, 1957
1	25	15 S	10 E	14.4	11.6	60.6
2	25	15 S	10 E	5.8	1.0	6.5
3	34	16 S	11 E	13.1	18.7	52.0
4	19	17 S	10 E	3.2	4.6	11.6
5	19	17 S	10 E	20.1	23.8	23.2

velopment area has not received much recharge from recent rains or runoff from the Sacramento Mountains; otherwise its tritium concentration would have been higher. However, the data are too scanty at this stage to draw definite conclusions as to the origin of this water. In particular, the behavior of the samples from station 5 cannot be explained as yet.

Ground-water samples from west and south of Deming, New Mexico—The Mimbres River, which starts as a perennial stream in the mountains to the north of Deming, becomes intermittent toward the south and actually has been dry near the city of Deming during the last decade. It is believed that the river water recharges underground aquifers several miles north of Deming. The water then travels underground toward the city and contributes to

TABLE 6—*Tritium concentration of miscellaneous ground-water samples from an area near Deming, New Mexico*

Station	Location Sec	T	R	*T* units (tritium/protium $\times 10^{-18}$) Aug. 16, 1957
1	30	23 S	9 W	5.8 ± 0.6
2	31	23 S	9 W	8.6 ± 0.9
3	6	24 S	9 W	7.2 ± 0.7
4	7	24 S	9 W	9.0 ± 0.9
5	18	24 S	9 W	9.3 ± 0.9
6	19	24 S	9 W	4.0 ± 0.6
7	6	25 S	9 W	6.6 ± 0.7

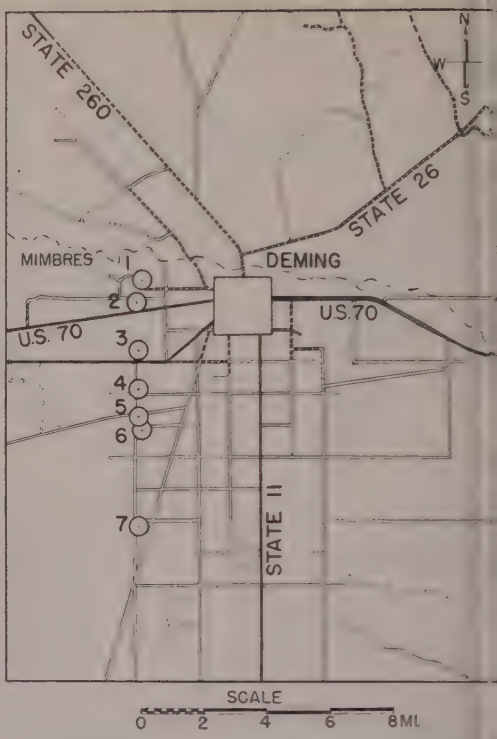

FIG. 3—Map of the area near Deming, New Mexico, showing the collection stations

the irrigation water which is pumped from the ground in large quantities throughout the Mimbres Valley. The depth to water has increased from about 80 ft to about 100 ft in the entire area during the last 15 years.

For the tritium study, seven wells were selected along a line about 8 miles long, running north-south from a point about 3 miles west of Deming (Fig. 3). As can be seen from the tritium data (Table 6), no definite trend exists in the tritium concentrations of the well waters. Not much tritium from nuclear bombs could have reached the sampling sites by March 1957. It is hoped that further monitoring of the wells may supply some information on the influence of the heavy irrigation in this area on the tritium pattern.

Deep-well samples from the artesian water basin near Artesia, New Mexico—Three samples were collected from deep wells approximately 2½ miles east of Artesia, New Mexico. The tritium concentration of these samples was generally low (Table 7) and was very low

TABLE 7—*Tritium concentration of other ground-water samples*

Description	Depth (ft)	Location Sec	T	R	Date	*T* units
					1957	
Deep well near Artesia, New Mexico	1,050	14	17 S	26 E	June 3	1.5 ± 0.2
Deep well near Artesia, New Mexico	240	14	17 S	26 E	June 3	1.7 ± 0.2
Deep well near Artesia, New Mexico	90	14	17 S	26 E	June 3	5.1 ± 0.5
Ice caverns near Grants, New Mexico	200	23	9 N	12 W	June 6	6.0 ± 0.6
Silver City, present municipal supply	243	11	18 S	15 W	April 1	3.5 ± 0.3
Silver City, well near site of new municipal supply	377	25	18 S	15 W	April 1	4.0 ± 0.4
Faywood Hot Spring	—	20	20 S	11 W	May 1	3.2 ± 0.3

the deeper wells. This indicates that the water has been underground for at least 30 years and is unmixed with recent rain water.

Ice caverns near Grants, New Mexico—A sample of ice from the cave known as the Big Room, approximately 200 ft below the surface, was melted and analyzed for its tritium content. The concentration was relatively high. Yet a rerun yielded the same result within the error of the measurement; namely, 6 *T* units (Table 7). This indicates either that the ice, or at least part of it, is younger than 30 years, or perhaps that moisture condensed from the atmosphere caused the relatively high tritium concentration of the sample.

Ground-water samples from Silver City, New Mexico—Three ground-water samples from the Silver City area were analyzed for tritium concentration. One sample was taken from one of the present municipal water-supply sources of Silver City (Frank's Ranch well field), a well drilled into bolson deposits of late Tertiary age which produces about 300 gpm of water. It has a tritium concentration of only 3.5 *T* units. This indicates that water of recent origin has not yet reached the well. During the past 12 years, the water level has declined by about 35 ft.

The city is presently developing another well to the east of the Continental Divide, with the hope of developing a supply independent of the Frank's Ranch well field. The tritium concentration of a well near the new location, however, fails to show any evidence of recent recharge (Table 2d).

The third sample is from the Faywood Hot Spring, about 22 miles southeast of Silver City. The temperature of the spring water is 128°F; the discharge is about 40 gpm. The water rises from a single orifice, and a tufa cone 300 ft in diameter and 30 ft high has been built up on bolson fill at the spring site. The cone is reported to be radioactive. The origin of the water is not definitely known. From the chemical analyses available, it apparently is meteoric water which rises in part from the Tertiary volcanic rocks that underlie bolson deposits of Quaternary age and in part from the bolson deposits. The water is believed to rise along a concealed fault scarp that has a northwest trend. This fault also may be responsible for the existence of warm springs about 2 miles to the northwest and for the occurrence of warm to hot waters encountered in the wells of the area.

The tritium concentration of only 3.2 *T* units indicates that the water, if meteoric, cannot be of very recent origin; its apparent age is certainly greater than 10 years.

EVALUATION OF THE TRITIUM METHOD

It has been demonstrated that the tritium method provides a useful new tool for hydrology. From the data available to date, the following conclusions can be drawn regarding the applicability of the method to the study of ground waters:

(1) Natural and bomb tritium is present in near-surface layers of ground water for areas underlain by alluvium.

(2) The tritium content of ground water is related to the amount of recent recharge into the reservoir.

(3) Age determinations of ground-water sam-

ples with respect to their origin as surface waters are possible within the following ranges: (a) age greater than 30 years, (b) age of at least part of the water less than 30 years, (c) age of at least part of the water less than 3 to 4 years, and (d) age of most or all of the water less than 3 to 4 years.

(4) If the tritium concentration of the waters produced by a number of (shallow) wells of the same area is monitored as a function of time, the rate of motion of the ground water and the rate of vertical percolation of rainwater into the ground can be determined.

(5) By proper identification of the tritium-concentration peaks occurring in the ground water and comparison with peaks exhibited by the rainwater some time previously, the exact age of the ground water can be found.

References

Begemann, F., and W. F. Libby, Continental water balance, ground-water inventory and storage times, surface ocean mixing rates and world-wide water circulation patterns from cosmic-ray and bomb tritium, *Geochim. et Cosmochim. Acta*, **12**, 277–296, 1957.

Begemann, F., and A. Turkevich, *Tritium assays of natural waters measured in 1956–1957*, AFOSR TR 58–41, Contract Number AF 18(600)-564, December 31, 1957.

Brown, R. M., and W. E. Grummitt, The determination of tritium in natural waters, *Can. J. Chem.*, **34**, 220–226, 1956.

Kaufman, S., and W. F. Libby, The natural distribution of tritium, *Phys. Rev.*, **93**, 1337–1344, 1954.

Vacquier, V., C. R. Holmes, P. R. Kintzinger and M. Lavergne, Prospecting for ground water by induced electrical polarization, *Geophysics*, **22**, 660–687, 1957.

von Buttlar, H., and W. F. Libby, Natural distribution of cosmic-ray produced tritium, *J. Inorg. & Nucl. Chem.*, **1**, 75–91, 1955.

von Buttlar, H., and I. Wendt, Ground-water studies in New Mexico using tritium as a tracer, *Trans. Am. Geophys. Union*, **39**, 660–668, 1958.

(Manuscript received July 21, 1958; revised April 13, 1959.)

Nitrogen Probe for Soil-Moisture Sampling

H. D. BURKE AND A. W. KRUMBACH, JR.

*Vicksburg Research Center**
Vicksburg, Mississippi

Abstract—Moisture determinations were made on soil cores frozen to hollow probes into which liquid nitrogen had been poured. Values compared closely with those from samples extracted by more conventional methods.

In this paper a method of using liquid nitrogen to obtain soil-moisture samples is described. It is applicable where very high moisture content makes conventional techniques difficult or impossible. It is also useful because the full range of moisture may be gauged with a single type of sampler.

The results reported here were secured by thrusting hollow probes into the soil and pouring liquid nitrogen into the probes. A two-minute period was found to be adequate for freezing the sample. The probes were then withdrawn and the adhering soil was removed in lengths corresponding to the soil layers for which a sample was desired.

Although other gases might have been used, nitrogen was chosen because it boils at −320.4°F and freezes the soil quickly. Only neon, hydrogen, and helium have lower boiling points than nitrogen has. Of these, neon and helium are more expensive and hydrogen is highly explosive. Dry ice is readily available but it sublimates at only −109.3°F. Nitrogen is available commercially and is nontoxic, odorless, and nonexplosive.

There are but few reports concerning the use of freezing agents for soil sampling. *Krynine* [1947] mentioned a report made in 1939 by Kollbrunner and Langer of an experiment wherein an unidentified cold mixture at a temperature of between −112° and −130°F was introduced into 2.5-inch pipes surrounding a casing to obtain samples of quicksand. *Hvorslev* [1940] described a freezing technique used by Falquist for obtaining undisturbed cohesionless soil samples by circulation of grain alcohol at −30°C through a chamber surrounding the lower end of the soil sampler. *Shapiro* [1958] has described a method of freezing soft sediment cores *in situ* with a sampling tube surrounded by a jacket filled with dry ice.

Study procedure—After preliminary trials had shown that the method could be used over a wide range of soil moisture, it was tested on silt and sandy loam soils. The characteristics of the soils are shown in Table 1.

TABLE 1—*Soil Characteristics*

	Texture			Liquid limit	Plastic limit
	Sand	Silt	Clay		
	Per cent				
Silt	10	83	7	20.6	Non-plastic
Sandy loam	36	51	13	24.8	24.3

Three probes were tried (Fig. 1). The largest was of 1.5-inch aluminum tubing, 2.5 feet long, and the smallest was of 0.75-inch stainless steel tubing. Both tubular probes had pointed tips. A third probe was flat —0.5 inch thick, 2.5 inches wide, and 18 inches long. Its bottom was beveled to a cutting edge at the front face, which was of stainless steel. The back was made of two thin sheets of steel with asbestos sandwiched between to prevent freezing on that side.

Tests of each probe began with a silt soil that

* Maintained at Vicksburg, Mississippi, by the Southern Forest Experiment Station, Forest Service, U. S. Department of Agriculture, in cooperation with the Waterways Experiment Station, Corps of Engineers, U. S. Army.

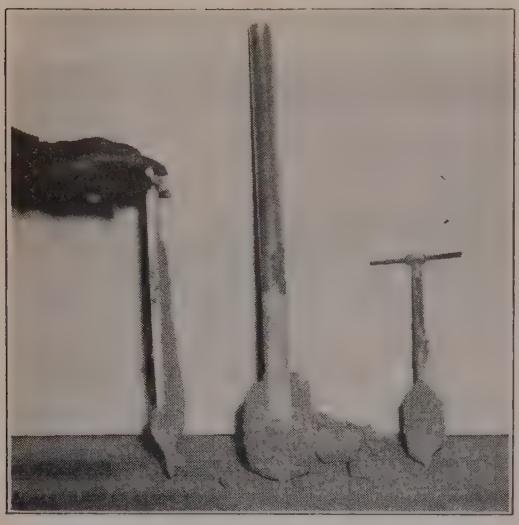

FIG. 1—Left to right are the flat probe, the large tubular probe, and the small tubular probe. The soil is silt loam at 4 per cent moisture by weight.

contained between 2 and 3 per cent moisture by weight and a sandy loam that contained about 14 per cent. The soils were screened to remove foreign objects and stones, and they were then placed in a container on a specially constructed platform and vibrated with a power hammer for one minute to settle the soil and distribute the moisture evenly. The hollow probes were thrust into the soil and the liquid nitrogen was poured into the probes. After a 2-minute period, which generally was sufficient to allow cores of a sufficient size to be frozen, the probes were withdrawn. The soil samples were removed from the surface of the probes in 3-inch lengths. At the same time samples were taken with one of the mechanical samplers at depths corresponding to those removed from the nitrogen probe.

After the soil had been sampled, a small amount of water was added. The soil was then thoroughly mixed, vibrated, and again sampled. This process was continued until the moisture reached or exceeded 100 per cent by weight.

The mechanical samplers were (1) an open-sided tube, (2) a *Hvorslev* [1940] sampler, and (3) a bulb from a relatively large syringe. The open-sided tube was used until the soil became too soft. The Hvorslev sampler was used until the soil became almost liquid (about 40 per cent moisture), and the rubber bulb was used to take samples with greater moisture conten

Results—T-tests revealed that the sampl taken with the probes did not deviate signi cantly from those secured mechanically. T small probe had the smallest mean differen for each soil. The largest mean difference w obtained with the large probe on sandy s (Table 2). The close association between t results obtained by the small nitrogen pro and the mechanical sampler is illustrated Figure 2.

To investigate the possibility that water w moving into the frozen sample from the su rounding soil, a nitrogen-filled probe was ke in the soil for periods of 2, 10, and 20 minute This was done several times at moisture co tents of 30 per cent and saturation. Averages several runs at each of the three time-interva revealed negligible differences ranging fro —0.38 per cent to + 0.15 per cent—within a between time-intervals. Figure 3 illustrates san ples taken over periods of 2, 10, and 20 mi utes.

The samples that adhered to the tubul probes always had a teardrop shape which b came more pronounced as the moisture conte of the soil increased. The nitrogen evaporate so rapidly that it was almost impossible t keep a full 12 inches in the large probe or

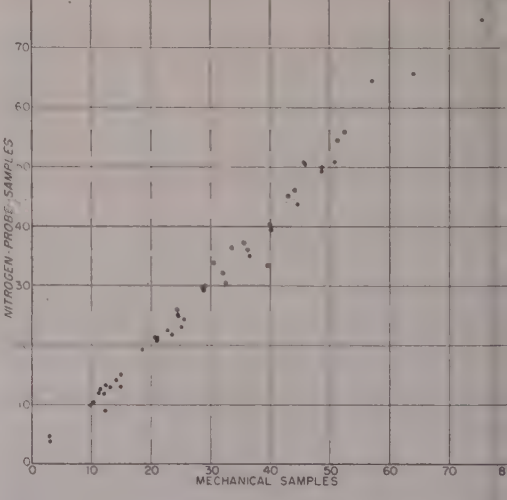

FIG. 2—Moisture contents, in percentage b weight, as determined from samples taken wit mechanical samplers and with the small nitroge probe.

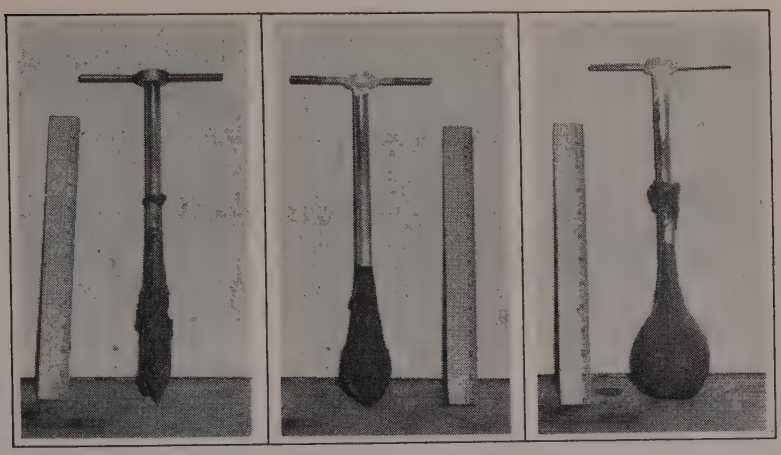

FIG. 3—Left to right are cores obtained in 2, 10, and 20 minutes with the small nitrogen probe in silt with 108.5 per cent moisture by weight.

inches in the other two. Freezing action was therefore least and core thickness smallest near the top of the sample. The cores taken with the flat probe showed a similar thickening near the bottom. With all three probes, the upper 3 inches of the sample sometimes contained less than 10 grams of soil—an amount too small to be analyzed.

As the moisture content of the soil increased, the hardness of the samples increased and the size of the samples decreased. This may be explained by the fact that water has higher latent and specific heat but lower heat conductance than soil has.

Discussion—This study was exploratory. The immediate aim was to devise a means for sampling soils that contain free water. It appears, however, that the liquid-nitrogen technique may be useful in other phases of soils and hydrological research. For example, nuclear or electrical soil-moisture measuring devices must be calibrated over a full range of moisture. No single mechanical sampler known to the authors can be used to estimate moisture over the full range.

Ascribing moisture contents to natural soil horizons is at best difficult and often impossible. Where the soil structure to be measured is shallow, nitrogen sampling allows a profile to be extracted and the moisture content to be isolated by horizons. A single trial in a stream bottom, when a sample 17 inches long was extracted with the large probe, revealed that soil layers—in this case thin sediment deposits—were very sharply delineated. The probe might also be used for measuring suspended sediment in still water or in a slow-moving stream.

Volume-weight determinations with present equipment are often suspect because of loss of water from the sample while it is being lifted, compaction, plastering, and other effects. A frozen sample from a probe can be placed in a plastic bag or tight can (to keep it free of condensed moisture) and sent to the laboratory in dry ice.

The simple equipment reported here is adequate for the required measurement of moisture in the surface foot. To obtain samples at greater depths or of greater uniformity of shape, probes to fit the need must be developed. If the deep boring techniques that are used with coolants having lower freezing capability were

TABLE 2—*Mean differences in soil-moisture content between samples taken with the nitrogen samplers and with the mechanical samplers*

Probe	Mean differences ± standard error of mean difference[a]	
	Silt	Sandy loam
Large	1.36 ± 0.21	2.59 ± 0.63
Small	1.14 ± 0.22	1.12 ± 0.30
Flat	1.68 ± 0.19	1.89 ± 0.25

[a] In percentage of moisture by weight.

adapted to liquid nitrogen, as good or better results should be obtained. The usefulness of liquid nitrogen as a means of freezing soil samples quickly was demonstrated by the relatively simple tests made in this study.

References

Hvorslev, J. M., The present status of the art of obtaining undisturbed samples of soil, *Prelim. Rept., Comm. on Sampling and Testing,* Soil Mech. and Foundations Div., Am. Soc. Civ. Engrs., Cambridge, Mass., 88 pp., 1940.

Krynine, D. P., *Soil mechanics,* McGraw-Hill Book Co., 511 pp., 1947.

Shapiro, J., The core-freezer—a new sampler for lake sediments, *Ecology,* 39, 758, 1958.

(Manuscript received March 23, 1959; presented at the Fortieth Annual Meeting, Washington, D. C., May 4, 1959.)

Nonsteady Flow to Flowing Wells in Leaky Aquifers

MAHDI S. HANTUSH*

New Mexico Institute of Mining and Technology
Socorro, New Mexico

Abstract—Potential distribution is found for a flowing well discharging by natural flow from a uniform aquifer into, and/or out of, which there is leakage in proportion to the drawdown. The leaky aquifer is of uniform compressibility and of uniform transmissibility. Three cases are considered: (1) that of a well draining an infinite leaky aquifer; (2) that of a well at the center of a circular aquifer with zero drawdown on its outer boundary; (3) that of a well situated at the center of a closed circular aquifer (that is, the flow across the outer boundary is zero). The variation of the discharge with time is formulated in the three cases. The drawdown distribution and the discharge variation for the corresponding systems of nonleaky aquifers are obtained. It is shown how the formation constants (the coefficient of transmissibility, the coefficient of storage, and the coefficient of leakage) are obtained from variations in the rate of discharge of wells flowing at constant drawdown.

Introduction—The drawdown distribution around a well assumedly pumping at a constant rate from an effectively infinite and perfectly elastic leaky aquifer of uniform thickness has been obtained by *Hantush* and *Jacob* [1955]. This solution has been applied to the determination of the formation constants and to the prediction of drawdowns at distances and times beyond those immediately observed. The purpose of this paper is to obtain the solution for the related problem of a well of constant drawdown that is discharging by natural flow from a leaky aquifer of similar characteristics. It is shown that under these conditions the discharge declines with time, attaining finally a constant value which is entirely sustained by leakage, or by leakage and another source of recharge, depending on the boundary conditions of the case treated. *Jacob* and *Lohman* [1952] have obtained the solution of the problem in an infinite nonleaky aquifer.

Figure 1 is a diagrammatic representation of a leaky aquifer penetrated by a flowing well.

THEORY

Statement of the problem—The problem is to determine the drawdown distribution around a flowing well that is draining a leaky aquifer. The usual assumptions are made with regard to the uniformity of thickness, of permeability, of compressibility, and of leakage. Initially the drawdown is zero throughout the aquifer. As the well is opened, its water level drops instantaneously to some lower elevation, and it maintains a constant drawdown thereafter.

Translated mathematically, solutions are sought for the following boundary-value problems.

Case 1: *Infinite leaky aquifer*—In this case, the boundary conditions are

$$\partial^2 s/\partial r^2 + (1/r)\partial s/\partial r - s/B^2 = (1/\nu)\partial s/\partial t \qquad (1)$$

$$s(r, 0) = 0 \qquad (2)$$

$$s(r_w, t) = s_w \qquad (3)$$

$$s(\infty, t) = 0 \qquad (4)$$

where $s(r, t)$ is the drawdown at any time from the start and at any point in the region of the flow r distant from the axis of the well; $\nu = T/S$; S is the storage coefficient; $T = Kb$ is the transmissibility coefficient; K, K' and b, b' (Fig. 1) are respectively the hydraulic conductivities and the thicknesses of the artesian aquifer and its semiconfining bed; $K'/b' = T/B^2$ is the leakance

* On leave from the College of Engineering, University of Baghdad, Baghdad, Iraq.

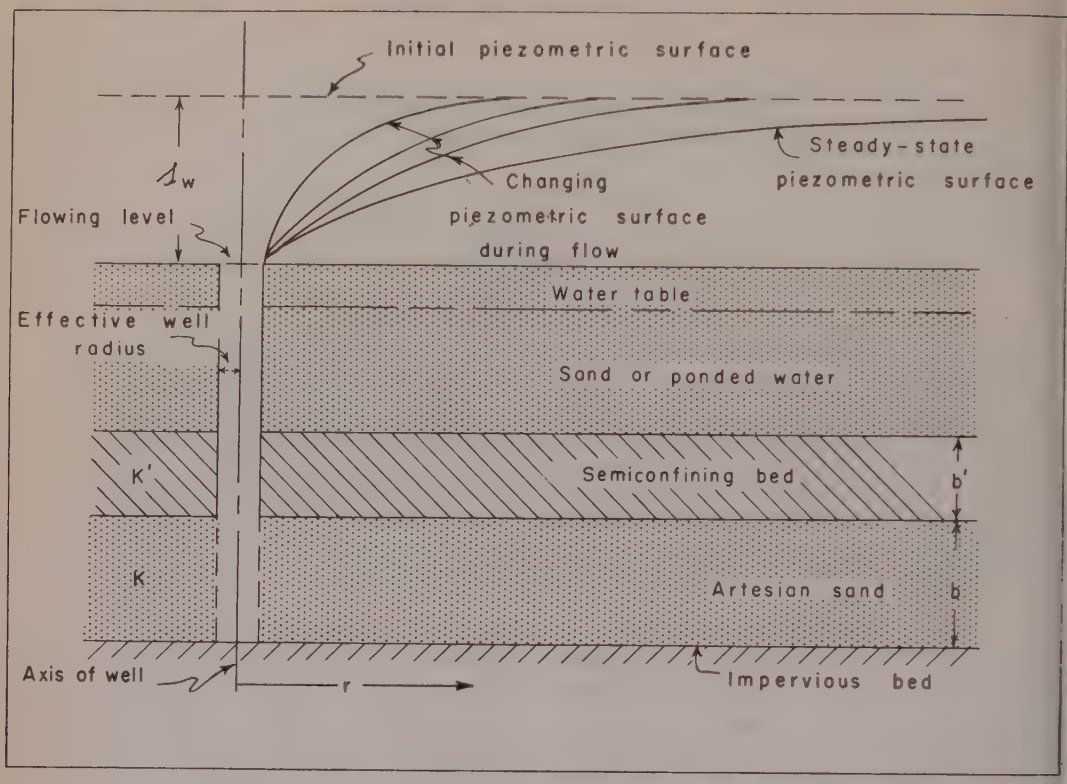

FIG. 1—Diagrammatic representation of a flowing well in a leaky aquifer

or the coefficient of leakage (see *Hantush* and *Jacob*, [1955], and *Hantush*, [1956] for the definition of these terms); s_w is the drawdown at the face of the well; and r_w is the effective radius of the well.

If one uses the Laplace transformation in solving the differential equation and applies boundary condition (2), the transformed boundary-value problem will be

$$\partial^2\bar{s}/\partial r^2 + (1/r)\partial\bar{s}/\partial r - (1/B^2 + p/\nu)\bar{s} = 0 \qquad (5)$$

$$\bar{s}(r_w, p) = s_w/p \qquad (6)$$

$$\bar{s}(\infty, p) = 0 \qquad (7)$$

where $\bar{s}(r, p)$ is the Laplace transform of the function $s(r, t)$.

A solution that satisfies (5), (6), and (7) can be shown as

$$\bar{s} = \frac{s_w K_0(r\sqrt{p/\nu + 1/B^2})}{pK_0(r_w\sqrt{p/\nu + 1/B^2})} \qquad (8)$$

where K_0 is the zero-order modified Bessel function of the second kind.

As the Laplace transform of the function $s \exp(\nu t/B^2)$ is $\bar{s}(r, p - \nu/B^2)$, it follows that

$$L\{s \exp(\nu t/B^2)\} = s_w K_0(r\sqrt{p/\nu})/(p - \nu/B^2)K_0(r_w\sqrt{p/\nu}) \qquad (9)$$

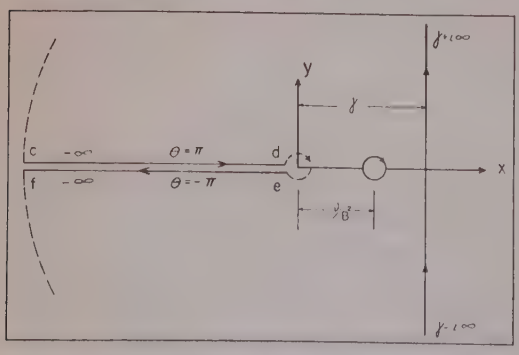

FIG. 2—The contour along which the integral of equation (10) is performed

where the notation $L\{F\}$ means the Laplace transform of the function F.

Using the Inversion Theorem, one obtains

$$s \exp(\nu t/B^2) = (s_w/2\pi i) \cdot \int_{\gamma-i\infty}^{\gamma+i\infty} \frac{\exp(zt)\, K_0(r\sqrt{z/\nu})}{(z - \nu/B^2) K_0(r_w\sqrt{z/\nu})}\, dz \qquad (10)$$

The integrand of (10) has a simple pole at $z = \nu/B^2$ and a branch point at $z = 0$. To evaluate the line integral in (10), one uses the contour shown in Figure 2. Inasmuch as $K_0(r\sqrt{z/\nu})$ has no zeros in this contour [*Watson*, 1944, sec. 15.7], the line integral in (10) may be replaced by the sum of the integrals over *cd*, *ef*, and the small circle around $z = \nu/B^2$.

The integral around the small circle reduces in the limit to $2\pi i \exp(\nu t/B^2) K_0(r/B)/K_0(r_w/B)$ as its radius tends to zero.

On *cd*, let $z = \nu\gamma^2 \exp(i\pi)$ and obtain for the integral I_{cd} the following.

$$I_{cd} = 2 \cdot \int_0^\infty \frac{\exp(-\nu t\gamma^2) K_0[r\gamma \exp(i\pi/2)]}{(\gamma^2 + 1/B^2) K_0[r_w\gamma \exp(i\pi/2)]}\, \gamma\, d\gamma \qquad (11)$$

As $K_0[x \exp(i\pi/2)] = -(1/2)i\pi[J_0(x) - iY_0(x)]$, (11) becomes

$$I_{cd} = 2 \cdot \int_0^\infty \frac{\exp(-\nu t\gamma^2)[J_0(\gamma r) - iY_0(\gamma r)]}{[\gamma^2 + 1/B^2][J_0(\gamma r_w) - iY_0(\gamma r_w)]}\, \gamma\, d\gamma \qquad (12)$$

where J_0 and Y_0 are the zero-order Bessel functions of the first and second kind, respectively.

The integral over *ef* gives minus the conjugate of (12).

Nonsteady-drawdown distribution. Combining the results of the above integration and making the substitution $\gamma r_w = \mu$, one obtains, after simplification, the drawdown distribution in the following form

$$s/s_w = K_0(r/B)/K_0(r_w/B) + (2/\pi) \exp(-\alpha r_w^2/B^2) \int_0^\infty \frac{\exp(-\alpha\mu^2)}{\mu^2 + (r_w/B)^2} \cdot \frac{J_0(\mu r/r_w) Y_0(\mu) - Y_0(\mu r/r_w) J_0(\mu)}{J_0^2(\mu) + Y_0^2(\mu)}\, \mu\, d\mu \qquad (13)$$

where $\alpha = Tt/Sr_w^2$.

The infinite integral in the above expression cannot be integrated directly; however, it can be evaluated by numerical integration.

Steady-drawdown distribution. As time becomes great, α goes to infinity and the steady-state distribution is realized. Thus, as α becomes infinite, (13) reduces to

$$s_s = s_w K_0(r/B)/K_0(r_w/B) \qquad (14a)$$

$$= (Q_s/2\pi T) K_0(r/B) \qquad (14b)$$

and

$$s_s \approx s_w \log_{10}(0.89r/B)/\log_{10}(0.89r_w/B) \qquad (15)$$

$$\approx (-2.3Q_s/2\pi T) \log_{10}(0.89r/B)$$

for

$$r/B < 0.05 \qquad (16)$$

where s_s is the steady-state drawdown or the maximum drawdown that can be attained under the prescribed conditions.

Discharge. The discharge at the face of the well is given by

$$Q = -2\pi T r_w\, \partial s(r_w, t)/\partial r \qquad (17)$$

If $\partial s(r_w, t)/\partial r$ is obtained from equation (13), and if it is recalled that $J_0(x)Y_0'(x) - Y_0(x)J_0'(x) = 2/\pi x$, then (17) reduces into

$$Q = 2\pi T s_w G(\alpha, r_w/B) \qquad (18)$$

where

$$G(\alpha, r_w/B) = (r_w/B) K_1(r_w/B)/K_0(r_w/B) + (4/\pi^2) \exp[-\alpha(r_w/B)^2] \cdot \int_0^\infty \frac{\mu \exp(-\alpha\mu^2)}{J_0^2(\mu) + Y_0^2(\mu)} \cdot \frac{d\mu}{\mu^2 + (r_w/B)^2}$$

and where K_1 is the first-order modified Bessel function of the second kind. The infinite integral in (17) cannot be integrated directly and therefore is evaluated numerically for the practical range of the parameters involved. Table 1 and Figure 3 give values of $G(\alpha, r_w/B)$ in terms of the practical range of α and r_w/B.

The steady-state discharge, or, in other words, the minimum yield of the well under the assumed conditions, is obtained when α or t becomes very large. Thus, if α goes to infinity, (17) reduces to

TABLE 1—*Values of the function* $G(\alpha, r_w/B)$

r_w/B / α	0	1×10^{-5}	2×10^{-5}	4×10^{-5}	6×10^{-5}	8×10^{-5}	10^{-4}	2×10^{-4}	4×10^{-4}	6×10^{-4}	8×10^{-4}	10^{-3}	2×10^{-3}	4×10^{-3}	6×10^{-3}	8×10^{-3}	10^{-2}
1×10^{2}	0.346																
2	0.311																0.344
3	0.294												0.311	0.311	0.311	0.312	0.312
4	0.283												0.294	0.294	0.294	0.295	0.295
5	0.274												0.283	0.283	0.283	0.284	0.285
													0.274	0.274	0.275	0.275	0.276
6	0.268																
7	0.263												0.268	0.268	0.268	0.269	0.271
8	0.258												0.263	0.263	0.263	0.264	0.265
9	0.254												0.258	0.258	0.259	0.260	0.261
													0.254	0.255	0.255	0.257	0.258
1×10^{3}	0.251																
2	0.232												0.251	0.252	0.252	0.254	0.255
3	0.222												0.232	0.233	0.234	0.234	0.239
4	0.215												0.222	0.223	0.225	0.227	0.231
5	0.210												0.215	0.216	0.219	0.222	0.226
													0.210	0.212	0.215	0.218	0.222
6	0.206																
7	0.203												0.206	0.208	0.211	0.215	0.220
8	0.201												0.203	0.205	0.209	0.213	0.219
9	0.198												0.201	0.203	0.207	0.212	0.218
													0.198	0.201	0.205	0.210	0.217
1×10^{4}	0.196																
2	0.185											0.196	0.197	0.200	0.204	0.209	0.216
3	0.178											0.185	0.185	0.190	0.197	0.205	0.213
4	0.173											0.178	0.179	0.184	0.194	0.203	0.212
5	0.170											0.173	0.176	0.183	0.193	0.202	
												0.170	0.173	0.181	0.192		
6	0.168																
7	0.166											0.168	0.171	0.180	0.192		
8	0.164										0.166	0.167	0.170	0.179	0.191		
9	0.163										0.164	0.165	0.169	0.179			
											0.163	0.164	0.168	0.179			
1×10^{5}	0.161																
2	0.152								0.161	0.162	0.162	0.162	0.167	0.178			
3	0.148							0.152	0.153	0.153	0.154	0.155	0.163	0.177			
4	0.145							0.148	0.148	0.149	0.150	0.152	0.162				
5	0.143							0.145	0.145	0.146	0.147	0.150	0.162				
								0.143	0.143	0.144	0.145	0.148	0.161				
6	0.141																
7	0.140							0.141	0.142	0.143	0.144	0.147	0.160				
8	0.138							0.140	0.140	0.141	0.143	0.146	0.160				
9	0.137							0.138	0.139	0.141	0.143	0.145	0.160				
								0.137	0.138	0.140	0.142	0.144	0.160				
1×10^{6}	0.136																
2	0.130						0.136	0.137	0.138	0.139	0.141	0.144	0.159				
3	0.127						0.130	0.131	0.133	0.135	0.139	0.143	0.159				
4	0.124						0.127	0.127	0.130	0.134	0.138	0.142	0.158				
5	0.123						0.124	0.125	0.129	0.134							
							0.123	0.124	0.128	0.133							
6	0.121																
7	0.120						0.121	0.123	0.128								
8	0.119						0.120	0.122	0.127								
9	0.118						0.119	0.121	0.127								
							0.118	0.121	0.127								
1×10^{7}	0.118																
2	0.114						0.118	0.120	0.127								
3	0.111					0.111	0.114	0.116	0.126								
4	0.109				0.109	0.110	0.112										
5	0.108				0.108	0.109	0.111										
							0.110										
6	0.107																
7	0.106			0.107	0.108	0.109	0.110										
8	0.105			0.106	0.107	0.108	0.109										
9	0.104		0.104	0.105	0.106	0.107	0.108										
1×10^{8}	0.104		0.104	0.104	0.105	0.106	0.108										
2	0.100	0.100	0.101	0.102	0.103	0.105	0.107										
3	0.0982	0.0982	0.0986	0.100	0.103												
4	0.0968	0.0968	0.0974	0.0994	0.102												
5	0.0958	0.0958	0.0966	0.0989													
6	0.0950	0.0951	0.0959	0.0986													
7	0.0943	0.0944	0.0954	0.0984													
8	0.0937	0.0939	0.0949	0.0982													
9	0.0932	0.0934	0.0946	0.0981													
1×10^{9}	0.0927	0.0930	0.0943	0.0980													
2	0.0899	0.0906	0.0927	0.0977													
3	0.0883	0.0893	0.0920	0.0976													
4	0.0872	0.0885	0.0917														
5	0.0864	0.0880	0.0916														
6	0.0857	0.0876	0.0915														
7	0.0851	0.0873	0.0915														
8	0.0846	0.0870	0.0915														
9	0.0842	0.0869	0.0914														
1×10^{10}	0.0838	0.0867	0.0914														
2	0.0814	0.0862															
3	0.0861	0.0860															
4	0.0792																
5	0.0785																
6	0.0779																
7	0.0774																
8	0.0770																
9	0.0767																
10	0.0764	0.0860	0.0914	0.0976	0.102	0.105	0.107	0.116	0.126	0.133	0.138	0.142	0.158	0.177	0.191	0.202	0.212

$$= 2\pi T s_w (r_w/B) K_1(r_w/B)/K_0(r_w/B) \quad (19)$$

practice, $r_w/B < 0.01$; thus, if one recalls for small values of x, $xK_1(x) = 1$, the limit 8) for small values of r_w/B is

$$= 2\pi T s_w / K_0(r_w/B) \quad (20)$$

$$= (Q_s/2\pi T) K_0(r_w/B) \quad (21)$$

$$= -(2.3Q_s/2\pi T) \log_{10} (0.89 r_w/B) \quad (22)$$

h, as expected, gives the steady-state drawn at the face of a steady well draining an ite leaky aquifer [*Hantush* 1956].

symptotic solutions.

) Small values of time. For small values of r small relative values of t), the approximate tion is obtained as follows.

the asymptotic expansions of the Bessel tions in (9) are used—that is, $K_0(z) \approx \sqrt{\pi/2z} \exp(-z)$ for $z > 5$ (or $(r^2p/\nu) > 25$), $r^2/\nu t) > 25$—equation (9) becomes

$$s \exp(\nu t/B^2)\} \approx s_w \sqrt{r_w/r}$$

$$\exp[-(r - r_w)\sqrt{p/\nu}]/(p - \nu/B^2) \quad (23)$$

If tables of Laplace transforms [*Carslaw* and *Jaeger*, 1947] are used, the inverse transform of (23) is

$$s \approx (s_w \sqrt{r_w/r}/2) \cdot \{ \exp[(r_w/B)(1 - r/r_w)] \cdot \operatorname{erfc}[-(r_w/B)\sqrt{\alpha} - (1 - r/r_w)/2\sqrt{\alpha}] \cdot + \exp[-(r_w/B)(1 - r/r_w)] \cdot \operatorname{erfc}[(r_w/B)\sqrt{\alpha} - (1 - r/r_w)/2\sqrt{\alpha}]\} \quad (24)$$

where, as before, $\alpha = \nu T/r_w^2$, and erfc = the complementary error function.

Equation (24) can be used for values of $(r/r_w)^2/\alpha > 25$, with results accurate in the third decimal.

In a similar procedure, the discharge for the same range of time can be approximated by

$$Q = 2\pi T s_w \cdot [1/2 + (1/\sqrt{\pi\alpha}) \exp[-(r_w/B)^2\alpha]] \quad (25)$$

(b) Large values of time. For large values of α or large relative values of t, it can be shown that the drawdown can be approximated, for $\alpha(r_w/B)^2 > 5$, by

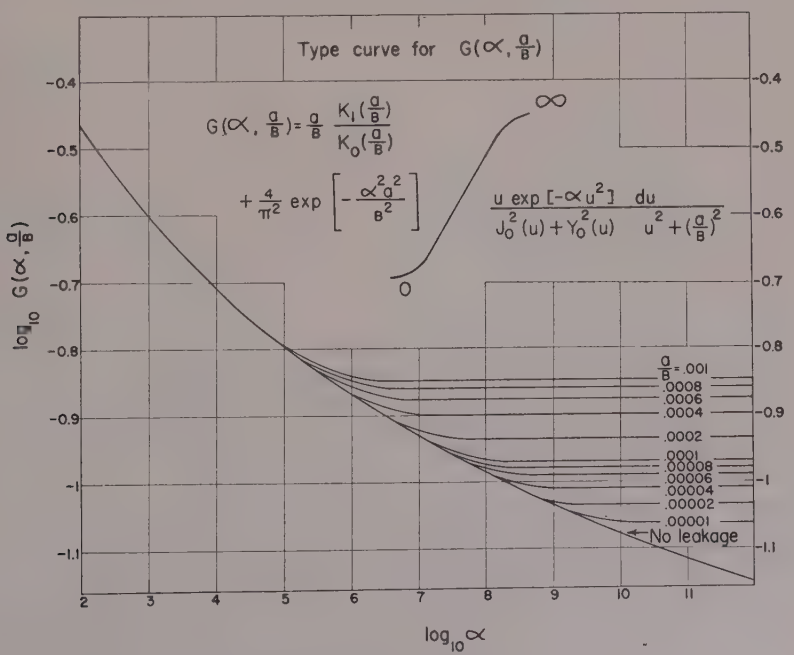

FIG. 3—Type curve of the function $G(\alpha, r_w/B)$

TABLE 2—*The roots* β_n, *of* $J_0(\beta_n)Y_0(k\beta_n) - Y_0(\beta_n)J_0(k\beta_n) = 0$
$k = r_e/r_w$

k	$(k-1)\beta_1$	$(k-1)\beta_2$	$(k-1)\beta_3$	$(k-1)\beta_4$	$(k-1)\beta_5$	$(k-1)\beta_6$	$(k-1)\beta_n$
1.0	3.142	6.283	9.425	12.566	15.708	18.850	$n\pi$
1.2	3.140	6.282	9.424	12.566	15.708	18.849	$18.849 + (n -$
1.5	3.135	6.280	9.423	12.565	15.707	18.848	$18.848 + (n -$
2.0	3.123	6.273	9.418	12.561	15.704	18.846	$18.846 + (n -$
2.5	3.110	6.266	9.413	12.558	15.701	18.843	$18.843 + (n -$
3.0	3.097	6.258	9.408	12.553	15.697	18.839	$18.839 + (n -$
3.5	5.085	6.250	9.402	12.549	15.694	18.836	$18.836 + (n -$
4.0	3.073	6.243	9.396	12.545	15.690	18.832	$18.832 + (n -$
5.0	3.053	6.228	9.39				$9.39 + (n -$
10	2.983	6.172	9.34				$9.34 + (n -$
20	2.911	6.104					$6.104 + (n -$
30	2.87	6.06					$6.06 + (n -$
40	2.85	6.03					$6.03 + (n -$
50	2.83	6.02					$6.02 + (n -$
	2.405	5.520	8.654	11.792	14.931	18.071	$18.071 + (n -$

$$s \approx [s_w/2K_0(r_w/B)] \cdot \int_u^\infty \frac{1}{y} \exp[-y - (r^2/B^2)/4y]\, dy$$

$$\approx [s_w/2K_0(r_w/B)]W(u, r/B) \qquad (26)$$

where $u = r^2S/4Tt$, and $W(u, r/B)$ is the well function for leaky aquifers, which has been obtained and tabulated by *Hantush* [1956].

Similarly, the discharge can be approximated, in the same range of time, by

$$Q \approx 4\pi T s_w / W(1/4\alpha, r_w/B) \qquad (27)$$

Equation (27) is the same as that giving the drawdown [*Hantush*, 1956] in a well of radius r_w discharging at a steady rate Q for a period of time t. In other words, the ratios of discharge to drawdown in two isolated wells (one with constant discharge, the other with constant drawdown) approach equality at sufficiently large relative values of time. It is assumed, of course, that the two wells tap the same aquifer and are so spaced that interference is not appreciable, or that they tap two aquifers of the same hydraulic properties.

Case 2: Circular leaky aquifer with zero drawdown on outer boundary—In this case the boundary conditions are those given by (1) to (3), and

$$s(r_e, t) = 0 \qquad (4a)$$

where r_e is the radius of an outer circle on w the drawdown remains zero.

Nonsteady-drawdown distribution. By the of the Laplace transformation, or by combi elementary solutions of (1) and expanding Fourier-Bessel series in the interval $(0, r_e)$, can, after mathematical manipulation, put solution in the following form

$$s/s_w = R_0(r/B)/R_0(r_w/B) + \pi \sum_{n=1}^{\infty} (A_n/C_n)\, U_0(\beta_n r/r_w) \qquad (2$$

where

$$A_n = \beta_n^2 J_0(\beta_n) J_0(\beta_n r_e/r_w) \cdot \exp[-(\beta_n^2 + (r_w/B)^2)\alpha]$$

$$C_n = [\beta_n^2 + (r_w/B)^2] \cdot [J_0^2(\beta_n) - J_0^2(\beta_n r_e/r_w)]$$

$$R_0(x/B) = K_0(x/B) - K_0(r_e/B) I_0(x/B)/I_0(r_e/B) \approx K_0(x/B)$$

(for cases of practical interest)

$$U_0(\beta_n r/r_w) = J_0(\beta_n r/r_w)\, Y_0(\beta_n r_e/r_w) - J_0(\beta_n r_e/r_w)\, Y_0(\beta_n r/r_w)$$

s the zero-order modified Bessel function first kind, and the β_n's are such that

$$= J_0(\beta_n)Y_0(\beta_n r_e/r_w) - J_0(\beta_n r_e/r_w)Y_0(\beta_n) = 0$$

ues of $(-1 + r_e/r_w)\beta_n$ for various values $/r_w)$ are tabulated in the literature (see and *Emde* [1945] or *Carslaw* and *Jaeger*]). These roots are given in Table 2.

ady-drawdown distribution. As time be- s great, α goes to infinity, and the steady is realized. Thus, for $\alpha = \infty$, the infinite in (28) drops out, and the solution reduces

$$s = s_w R_0(r/B)/R_0(r_w/B) \qquad (29)$$

n is another form of that obtained by b [1946].

scharge. The discharge is obtained by ying (17) to (28), which, after mathematical ction, becomes

$$\pi T s_w = (r_w/B)R_1(r_w/B)/R_0(r_w/B) + 2\sum_{n=1}^{\infty}(1/C_n)\beta_n^2 J_0^2(\beta_n r_e/r_w) \cdot \exp[-(\beta_n^2 + (r_w/B)^2)\alpha] \qquad (30)$$

re

$$_w/B) = K_1(r_w/B) + K_0(r_e/B)I_1(r_w/B)/I_0(r_e/B) \approx K_1(r_w/B)$$

cases of practical interest)

$$= [\beta_n^2 + (r_w/B)^2] \cdot [J_0^2(\beta_n) - J_0^2(\beta_n r_e/r_w)]$$

I_1 and K_1 are the first-order modified Bessel ctions of the first and second kind, respec- ely.

Case 3: Closed circular aquifer—In this case boundary conditions are those given by to (3), and

$$\partial s(r_e, t)/\partial r = 0 \qquad (4b)$$

Nonsteady-drawdown distribution. In a man- similar to that followed in the preceding e, the solution finally can be put as

$$s/s_w = R_2(r/B)/R_2(r_w/B) + \pi\sum_{n=1}^{\infty}(\epsilon_n^2/E_n)J_1^2(\epsilon_n r_e/r_w) \cdot \exp[-(\epsilon_n^2 + (r_w/B)^2\alpha] \cdot V_0(\epsilon_n r/r_w) \qquad (31)$$

where

$$R_2(x/B) = K_0(x/B) + K_1(r_e/B)I_0(x/B)/I_1(r_e/B) \approx K_0(x/B)$$

(for cases of practical interest)

$$E_n = [\epsilon_n^2 + (r_w/B)^2][J_0^2(\epsilon_n) - J_1^2(\epsilon_n r_e/r_w)]$$

$$V_0(\epsilon_n r/r_w) = J_0(\epsilon_n r/r_w)Y_0(\epsilon_n) - Y_0(\epsilon_n r/r_w)J_0(\epsilon_n)$$

and the ϵ_n's are such that $V_0'(\epsilon_n r_e/r_w) = 0$, or

$$J_0(\epsilon_n)Y_1(\epsilon_n r_e/r_w) - J_1(\epsilon_n r_e/r_w)Y_0(\epsilon_n) = 0$$

A few roots of the above equation are given in Table 3.

Steady distribution. As α goes to infinity, (32) reduces to the steady-state solution, which is

$$s = s_w R_2(r/B)/R_2(r_w/B) \qquad (32)$$

Discharge. In a manner similar to that followed in Case 2, the discharge may be put finally as

$$Q/2\pi T s_w = (r_w/B)R_3(r_w/B)/R_2(r_w/B) + 2\sum_{n=1}^{\infty}(\epsilon_n^2/E_n)J_1^2(\epsilon_n r_e/r_w) \cdot \exp[-(\epsilon_n^2 + (r_w/B)^2)\alpha] \qquad (33)$$

where

$$R_3(r_w/B) = K_1(r_w/B) - K_1(r_e/B)I_1(r_w/B)/I_1(r_e/B) \approx K_1(r_w/B)$$

for practical cases.

Functions used. The different functions appearing in the equations obtained in the above treatment are tabulated and may be found in the literature [*Janke* and *Emde*, 1945; *Watson*, 1944; *Gray, Mathews*, and *MacRobert*, 1931; *McLachlan*, 1946; and *National Bureau of Standards*, 1952]. However, manual computations in (28), (30), (31), and (33) become labo-

TABLE 3 *Values of β corresponding to the roots $\epsilon_n = (n - 0.5)/(k - 1)\beta\pi$ of $J_0(\epsilon_n)Y_1(R\epsilon_n) - Y_0(\epsilon_n)J_1(R\epsilon_n) = 0$*

k	$n = 1$	2	3	4	5	6	∞
1000	0.36	0.87	0.93	0.95	0.97	0.97	1.00
900	0.37	0.88	0.93	0.96	0.97	0.97	1.00
800	0.37	0.88	0.93	0.96	0.97	0.97	1.00
700	0.37	0.88	0.93	0.96	0.97	0.97	1.00
600	0.38	0.88	0.94	0.96	0.97	0.97	1.00
500	0.38	0.88	0.94	0.96	0.97	0.98	1.00
400	0.39	0.88	0.94	0.96	0.97	0.98	1.00
300	0.40	0.88	0.94	0.96	0.97	0.98	1.00
200	0.42	0.89	0.94	0.96	0.97	0.98	1.00
100	0.45	0.90	0.95	0.97	0.98	0.98	1.00
90	0.46	0.90	0.95	0.97	0.98	0.98	1.00
80	0.46	0.90	0.95	0.97	0.98	0.98	1.00
70	0.47	0.91	0.95	0.97	0.98	0.99	1.00
60	0.48	0.91	0.96	0.97	0.98	0.99	1.00
50	0.50	0.91	0.96	0.98	0.98	0.99	1.00
40	0.51	0.92	0.96	0.98	0.98	0.99	1.00
30	0.54	0.92	0.97	0.98	0.99	0.99	1.00
20	0.57	0.93	0.97	0.98	0.99	0.99	1.00
10	0.63	0.94	0.98	0.99	0.99	0.99	1.00
9	0.64	0.95	0.98	0.99	0.99	1.00	1.00
8	0.66	0.96	0.98	0.99	0.99	1.00	1.00
7.00	0.677	0.960	0.9822	0.9911	0.9947	0.9966	1.00
6.25	0.696	0.962	0.9840	0.9920	0.9952	0.9969	1.00
6.00	0.702	0.963	0.9846	0.9923	0.9954	0.9970	1.00
5.00	0.728	0.967	0.9870	0.9935	0.9961	0.9974	1.00
4.00	0.755	0.971	0.9894	0.9947	0.9968	0.9978	1.00
3.00	0.796	0.977	0.9919	0.9959	0.9975	0.9983	1.00
2.00	0.864	0.986	0.9949	0.9974	0.9984	0.9990	1.00
1.00	1.000	1.000	1.0000	1.0000	1.0000	1.0000	1.00
0.90	1.021	1.003	1.0009	1.0004	1.0003	1.0002	1.00
0.80	1.045	1.005	1.0020	1.0010	1.0006	1.0004	1.00
0.70	1.073	1.009	1.0032	1.0016	1.0010	1.0007	1.00
0.60	1.105	1.013	1.0048	1.0025	1.0015	1.0010	1.00
0.50	1.142	1.019	1.0070	1.0036	1.0022	1.0015	1.00
0.40	1.187	1.027	1.0101	1.0052	1.0032	1.0021	1.00
0.30	1.242	1.039	1.0150	1.0080	1.0047	1.0032	1.00
0.20	1.311	1.058	1.0247	1.0126	1.0077	1.0052	1.00
0.10	1.402	1.093	1.0658	1.0314	1.0173	1.0110	1.00
0.00	1.531	1.171	1.1018	1.0724	1.0562	1.0459	1.00

rious in the range where r_e/r_w is large. In order to make these formulae useful in practical applications, sufficient tabulation for all practical purposes would not be difficult if mechanical computation were employed. This would make (28), (30), (31), and (33) as simple to use as any other drawdown formula.

The following asymptotic expressions may be helpful in computations.

$$J_0(z) \approx 1 \qquad \text{for } z < 0.10$$

$$\approx \sqrt{2/\pi z}\cos(z - \pi/4) \qquad \text{for } z > 16$$

$$J_1(z) \approx (1/2)z \qquad \text{for } z < 0$$

$$\approx \sqrt{2/\pi z}\sin(z - \pi/4) \qquad \text{for } z > 1$$

$$Y_0(z) \approx (2/\pi)(0.5772 + \ln(z/2)) \qquad \text{for } z < 0$$

$$\approx \sqrt{2/\pi z}\sin(z - \pi/4) \qquad \text{for } z > 1$$

$$Y_1(z) \approx -2/\pi z \qquad \text{for } z < 0$$

$$\approx -\sqrt{2/\pi z}\cos(z - \pi/4) \qquad \text{for } z > 1$$

$$I_0(z) \approx 1 \qquad \text{for } z < 0$$

$$\approx (e^z/\sqrt{2\pi z})(1 + 1/8z) \qquad \text{for } z > 1$$

$(z) \approx (1/2)z$ for $z < 0.10$

$\approx (e^z/\sqrt{2\pi z})(1 - 3/8z)$ for $z > 10$

$(z) \approx -(0.5772 + \ln (z/2))$ for $z < 0.01$

$\approx \sqrt{\pi/2z}\, e^{-z}(1 - 1/8z)$ for $z > 10$

$(z) \approx 1/z$ for $z < 0.01$

$\approx \sqrt{\pi/2z}\, e^{-z}(1 + 3/8z)$ for $z > 10$

Nonleaky Aquifers

When $B = \infty$, the coefficient of leakage $/b'$ (equal to T/B^2) is zero. In other words, kage does not take place. Thus, if in the utions presented above, B is taken as ∞, the ulting expressions, which are readily obtained, l be the corresponding solutions in a non- ky system.

Graphical Determination of the Formation Constants

Graphical methods based on (14), (15), (16), d (18) can be outlined for determining field lues of the formation constants; namely, the efficients of storage, of transmissibility, and leakage. These are:

Steady distribution of drawdown

Type-curve method. Based on the solution presented by (14a), Theis' graphical method ay be used to obtain field values of r_w, T, B, d hence of K'/b'. In this case, however, the pe curve' is a plot of the function $K_0(r/B)$ ainst r/B on logarithmic paper, and the servational data (data on the steady distri- tion of drawdown in the vicinity of a flowing ell—that is, a well with constant drawdown— a flowing center) are plotted on logarithmic per of the same scale, with r as abscissa and as ordinate.

Application. The procedure for computing , B, T, and then the leakage coefficient (K'/b') as follows. (1) Place the observational curve er the type curve and obtain the best fitting sition. (2) From this position, select any point natching point) and note its coordinates on ie observational curve and the type curve; amely, (s_s, r) and $(K_0(r/B), r/B)$, respectively. 3) Knowing r and r/B, compute B. (4) Knowing , $K_0(r/B)$, s_w, and B, compute r_w from equation 4a); namely, $K_0(r_w/B) = (s_w/s_s)K_0(r/B)$. (5) Knowing s_s, $K_0(r/B)$, B, and Q_s, compute T from equation (14b); namely, $T = (Q_s/2\pi s_s)$ $K_0(r/B)$. (6) Knowing B and T, compute K'/b' from the relation $K'/b' = T/B^2$.

Asymptotic-curve method. Equations (15) and (16) represent the approximate drawdown distribution in the range $r/B < 0.05$. Thus, a plot of s_s against r on a semilogarithmic paper, with r on the logarithmic scale, will exhibit a straight-line relationship in the range where r/B is small. In the range where r/B is large, the points fall on a curve that approaches the zero-drawdown axis asymptotically. The slope of the straight portion of the curve, or $\Delta s_s/\Delta \log_{10} r$, is equal to $s_w/\log_{10}(0.89r_w/B)$. The intercept (r_0) of this line on the zero-drawdown axis is given by $B = 0.89r_0$.

Application. If observational data are plotted on a semilogarithmic paper and most of the points fall on a straight line (several points are necessary to establish this condition), the procedure for computing r_w, B, T, and then K'/b' is as follows: (1) Construct the best-fit straight line through the points which appear to fall on a straight line, and measure its slope $\Delta s_s/\Delta \log_{10} r$. (2) Compute (r_w/B) from the relation $\Delta s_s/\Delta \log_{10} r = s_w/\log_{10}(0.89r_w/B)$. (3) Compute T from the relation $\Delta s_s/\Delta \log_{10} r = -2.3Q_s/2\pi T$. (4) Select any point on the straight line and note its coordinates s_s and r. Knowing the slope of the line and these values, compute B from either (15) or (16); or determine (r_0), the intercept on the zero-drawdown axis, and then compute B from the relation $B = 0.89r_0$. (5) Knowing r_w/B and B, compute r_w. (6) Knowing T and B, compute K'/b' from the relation $K'/b' = T/B^2$.

Discharge-time variation

Type-curve method. Based on the solution represented by (18), field values of S, T, B, and hence K'/b' can be found by a process similar to that described under the type-curve method, provided the effective radius of the well r_w is known. (Values of r_w are generally obtained by careful inspection of the drilling and casing records and, where possible, by questioning the drillers as to the exact size of bit used, the amount of bit wobble suspected, the possibility and probable amount of caving, and other similar factors. If there is any doubt

about the reported value of r_w, the well calipers should be used.) In this case, the type curve is a plot of the function $\log_{10} G(\alpha)$ against $\log_{10} (\alpha)$, and the observational data are a plot of $\log_{10} Q$ against $\log_{10} t$ with the same scale as that of the type curve. The type curve may conveniently be prepared from Table 1 as shown in Figure 3. A convenient scale is not less than 50 centimeters to the cycle.

Application. The procedure for computing B, T, S, and then K'/b' is as follows (1) Place the observational curve over the type curve and obtain the best fitting position. (2) From this position, and from the position of the observational curve between the two theoretical curves of r_w/B, obtain the value of r_w/B by interpolation. Also, select any point on the drawing sheet (matching point) and note its coordinates; namely, $\log_{10} Q$, $\log_{10} t$, and $\log_{10} G(\alpha)$, $\log_{10} (\alpha)$, from which the corresponding values of Q, t, $G(\alpha)$ and α are obtained. (3) Knowing r_w/B and r_w, compute B. (4) Knowing s_w, s, and $G(\alpha)$, at the matching point, compute T from the relation $T = 2\pi s_w G(\alpha)/s$. (5) Knowing r_w, T, t, and α, at the matching point, compute S from the relation $S = Tt/\alpha r_w^2$. (6) Knowing T and B, compute the leakage coefficient K'/b' from the relation $K'/b' = T/B^2$.

Acknowledgment—The author is indebted to C. R. Cassity, of the New Mexico Institute of Mining and Technology, for preparing Tables 2 and 3.

References

Carslaw, H. S., and J. C. Jaeger, *Conduction of heat in solids*, Oxford Univ. Press, London, 19

Gray, A., G. B. Mathews, and T. M. MacRobe *Bessel functions*, Macmillan and Co., Ltd., Lo don, 1931.

Hantush, M. S., Analysis of data from pump tests in leaky aquifers, *Trans. Am. Geoph Union*, 37, 702–714, 1956.

Hantush, M. S., and C. E. Jacob, Non-ste radial flow in an infinite leaky aquifer, *Tr Am. Geophys. Union*, 36, 95–100, 1955.

Jacob, C. E., Radial flow in a leaky artesian a fer, *Trans. Am. Geophys. Union*, 27, 198–2 1946.

Jacob, C. E., and S. W. Lohman, Nonsteady to a well of constant drawdown in an exten aquifer, *Trans. Am. Geophys. Union*, 33, 5 569, 1952.

Janke, E., and F. Emde, *Table of functions*, D Publications, New York, 1945.

McLachlan, N. W., *Bessel functions for en neers*, Oxford Univ. Press, London, 1946.

National Bureau of Standards, *Tables of Be functions*, App. Math. Series, no. 25, U. S. G Printing Office, Washington, 1952.

Watson, G. N., *Theory of Bessel functions*, Macmillan Co., New York, 1944.

(Manuscript received April 16, 1959; presented the Regional Meeting, Stanford University, C fornia, February 6, 1956.)

A Note on the Muskingum Flood-Routing Method

J. E. NASH

Hydraulics Research Station
Department of Scientific and Industrial Research
Wallingford, Berks., England

Abstract—An exact method of solution of the flood-routing equation, when the storage is a linear function of weighted inflow and outflow, is developed. This operation is shown to be equivalent to routing a multiple of the inflow through reservoir storage and subtracting the excess inflow. Modified coefficients for the Muskingum equation are developed which do not depend on the routing interval being small relative to K.

Introduction—The Muskingum method, which a finite difference method of solution of the d routing equation, under the assumption t storage is a linear function of a weighted an of inflow and outflow, $S = K[xI + (1 - x)]$, is widely used, both in its original form *cCarthy*, 1938] and as the basis of a number graphical or semi-graphical methods. In the of these methods, however, it is sometimes rlooked that an essential requirement, to ure accuracy in such finite difference calcu- ions, is that the finite interval T must be small ative to the other time elements involved. is fact was emphasized by *Clark* [1945] in cussing the Muskingum flood-routing method. vertheless, it still happens that values of T sibly equal to K are recommended for use actual calculation.

Whereas it is possible that in practice the ccuracies so introduced are generally not nificant relative to the inaccuracies intro- ced by the basic storage assumption, and the ual inaccuracies of the data, it may happen, rticularly in theoretical work, that a high lative accuracy is required. The failure of the uskingum method when T/K is not small is monstrated by the widely accepted belief that uting through linear storage with $x = 0.5$ erates as a pure delay. This conclusion is sed on the fact that the substitution of $T = K$ d $x = 0.5$ in the Muskingum equation yields $= I_0$, the other coefficients being zero. That is conclusion is erroneous is demonstrated in is note. An exact method of solution under e storage assumption is developed, and modified equations for the Muskingum coefficients are derived. These equations are true even when T is not small relative to K.

Notation—

$I(t)$ = inflow, ft³/sec
$Q(t)$ = outflow, ft³/sec
x = a numerical parameter
$S(t)$ = storage, ft³ hrs/sec
K = a time parameter, hours
k = $K(1 - x)$
D = the differential operator d/dt
C_1 C_2 C_3 the Muskingum coefficients
c = $\exp - T/K(1 - x)$
q = the outflow from routing I through $S = K(1 - x)q$
T = the routing interval, hours
m = slope of inflow curve

The exact solution—The fundamental equations are

$$I = Q + \frac{ds}{dt} \tag{1}$$

$$S = K(xI + (1 - x)Q) \tag{2}$$

from which

$$I - xK\frac{dI}{dt} = Q + (1 - x)K\frac{dQ}{dt}$$

$$Q(t) = \frac{1 - xKD}{1 + (1 - x)KD} I(t) \tag{3}$$

When x = zero we have the corresponding reservoir case

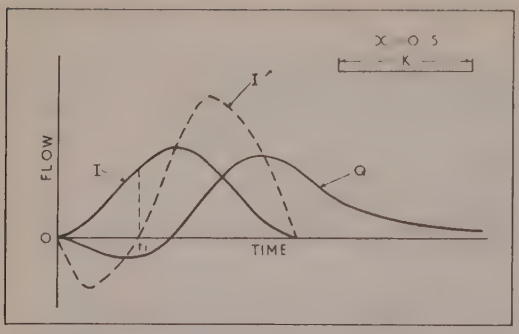

FIG. 1—Routing through storage with $x = 0.5$

$$Q(t) = \frac{1}{1 + KD} I(t) \qquad (4)$$

which has the solution

$$Q = \frac{1}{K} e^{-t/K} \int e^{t/K} I \, dt \qquad (5)$$

Now (3) may be looked upon as the result of operating on $I(t)$ successively with $1 - xKD$ and $1/[1 + (1 - x)KD]$. The operation $1 - xKD$ merely involves differentiation of the inflow and $1/[1 + (1 - x)KD]$ represents reservoir routing with $S = (1 - x)KQ$. Therefore (3) is equivalent to subtracting xK times the first derivative of I from I and routing the remainder through reservoir storage with $S = (1 - x)KQ$. These operations generally can be carried out graphically, and mathematically as well, when I is a simple function of time. We can learn more from (3). Let us define

$$I'(t) = (1 - xKD)I(t) \qquad (6)$$

This means that I' is the result of routing I backwards (that is, calculation of inflow from outflow) through linear reservoir storage $S = -xKI$. The effect of the negative xK is achieved by taking the routing procedure from right to left; that is, in the negative direction of time (Fig. 1).

When we come to t_1 at which I' becomes zero, I would fall off logarithmically and never actually reach zero unless I' took negative values. This means that when I starts from zero and rises at a finite rate, I' must always take negative values initially.

It is clear, too, that the interval between the centers of area of $I'(t)$ and $I(t)$ is xK. We must now route I' forwards through $S = (1 - x)KQ$ to obtain Q (Fig. 1). Clearly this involve further shift of the center of area $(1 - x)K$ that the total shift is K. However I and Q not otherwise identical even when $x = 0.$ shown in Figure 1. It should be noted that negative initial values of I' result in nega initial values of Q.

If we divide out the operator in (3) we ob

$$Q = \left[-\frac{x}{1 - x} + \frac{1}{(1 - x)\{1 + (1 - x)KD\}} \right] I$$

$$Q = \frac{1}{1 + (1 - x)KD} \frac{I}{(1 - x)} - \frac{xI}{1 - x}$$

We see, therefore, that the outflow consist the sum of two parts, the first of which we call q, being the result of routing $I/(1 -$ through $S = K(1 - x)q$, and the se part being simply the inflow multiplied $-x/(1 - x)$.

There are various ways of routing thr reservoir storage. Equation (5) may alway integrated graphically, or mathematically is in a suitable form. A simple graphical solu not involving integration has been demonstr by *Nash* and *Farrell* [1955]. It frequently h pens, however, that a coefficient solution desired. Formulas for the coefficients are ca lated in the next section.

Modification of the Muskingum coefficients—

$$Q_1 = C_1 I_0 + C_2 I_1 + C_3 Q_0$$

We shall use (8) to obtain the expression the C's. In expressing Q as a function of $I_0 I_1$ Q_0 only, we must neglect second and hig derivatives of I; that is, we must assume I consist of straight-line segments. If the sec or higher derivatives are required, we must three or more values of I in (9). However, choosing time intervals which are sufficien short, the calculation using only I_0, I_1, and can be made as precise as is desired. The o difference between the present calculation the usual development of the Muskingum efficient equation is that we are not limited values of the time interval which are sm compared with K.

The solution of (8) when I is a series of strai

nents is obtained as follows. Let $m = (I_1 - I_0)/T$ be the slope of a segment.

$$q(t) = \frac{1}{1 + (1 - x)KD} I(t)$$

$$Q = q/(1 - x) - xI/(1 - x) \qquad (10)$$

$k = (1 - x)K$ and $c = \exp[-T/K(1 - x)]$ implify the notation. From (5)

$$q = 1/ke^{-t/k} \int (I_0 + mt)e^{t/k}\, dt$$

$$= 1/ke^{-t/k}[kI_0e^{t/k} + mk^2e^{t/k}(t/k - 1) + A]$$

$$= I_0 + mk(t/k - 1) + A/ke^{-t/k} \qquad (11)$$

solve for the arbitrary constant A by letting q_0 at $t = 0$ and obtain $q_0 = I_0 - mk + A/K$. bstituting in (11) we obtain

$$= I_0 + mk(t/k - 1) + (q_0 - I_0 + mk)e^{-t/k}$$

bstituting $(I_1 - I_0)/T$ for m and letting T, we obtain

$$= I_0 + k/T(T/k - 1)(I_1 - I_0) + [q_0 - I_0 + k/T(I_1 - I_0)]c$$

$$= I_0[k/T(1 - c) - c] + I_1[-k/T(1 - c) + 1] + q_0c \qquad (12)$$

ence by (10)

$$= I_0\left[\frac{k}{T}\frac{1 - c}{1 - x} - \frac{c}{1 - x}\right] + I_1\left[-\frac{k}{T}\frac{1 - c}{1 - x} + \frac{1}{1 - x} - \frac{x}{1 - x}\right] + q_0\frac{c}{1 - x}$$

t $q_0/(1 - x) = Q_0 - xI_0/(1 - x)$ which when bstituted in (12), bearing in mind that $k = (1 - x)$, gives

$$Q_1 = I_0[K/T(1 - c) - c] + I_1[-K/T(1 - c) + 1] + Q_0c \qquad (13)$$

This is the modified form of the Muskingum equation when T is not small relative to K. If T/K is taken very small the coefficients in (13) and in the Muskingum equation converge.

Conclusions—We have seen that the Muskingum method is equivalent to either routing the inflow backwards (that is, calculating I from Q) through storage $S = -xKI$ and subsequently forwards through $S = (1 - x)KQ$, or routing a multiple of the inflow $I/(1 - x)$ through $S = K(1 - x)q$ and subtracting $xI/(1 - x)$. We have also developed the values of the coefficients to be used when T/K is not small. The negative outflow, which may occur when the inflow rises steeply, has been explained as being essentially associated with the storage assumption, and not with any particular method of solution. This rather unrealistic consequence of the storage assumption suggests that some modification is desirable. As it is necessary in practice to determine x and K by experiment, it would seem more reasonable to abandon the storage assumption and consider the linear operation to consist of two parts, a pure delay and a single reservoir routing [*Hopkins*, 1956], the two parameters to be determined by experiment. The pure delay plus the storage factor K would be equal to the lag between the centers of area of inflow and outflow, and the ratio of the storage factor to the lag would form a dimensionless parameter which might be constant as a first approximation or reflect some characteristics, at present unknown, of the channel. It might be possible to determine this relation by means of a statistical correlation.

Acknowledgment—This note is published by permission of the Director, Hydraulics Research Station, Department of Scientific and Industrial Research, Howbery Park, Wallingford, Berkshire, England.

References

Clark, C. O., Storage and the unit hydrograph, *Trans. Am. Soc. Civil Engrs.*, 110, 1419–1446, 1945.

McCarthy, G. T., The unit hydrograph and flood routing, unpublished manuscript presented at a conference North Atlantic Div., Corps of Engi-

neers, War Dept., June 24, 1938 (see also *Engineering construction—flood control*, The Engineer School, Fort Belvoir, Va., pp. 147–156, 1940).

Nash, J. E. and J. P. Farrell, A graphical solution of the flood routing equation for lin storage-discharge relation, *Trans. Am. Geop Union*, **36**, 319–320, 1955.

Hopkins, C. D., Discussion on previous refere *Trans. Am. Geophys. Union*, **37**, 500–501, 195

Estimating the Total Heat Output of Natural Thermal Regions

R. F. BENSEMAN

Dominion Physical Laboratory
Department of Scientific and Industrial Research
Lower Hutt, New Zealand

Abstract—The natural flow of heat from a thermal region is a first indication of the amount of steam that might be continually drawn from bores to generate electric power. Methods are described for assessing the natural heat flow by such agencies as steaming ground, geysers, springs, fumaroles, and the underground seepage of hot water to nearby streams or lakes.

Introduction—Since 1950 New Zealand has en planning to exploit its natural thermal re- urces for power purposes. The background id objectives of the scientific work have al- ady been outlined by *Grange* [1955] but one spect has not yet been treated fully—the ini- al estimate of the total natural heat flow from thermal area.

The extent to which underground steam can e used for generating electric power depends artly on its temperature, dryness, and acid con- nt, but first it must be available in sufficient mounts. The total natural flux of heat through he surface of the ground is some indication of he available power, and indeed it may well epresent the greatest rate at which steam can e drawn continuously from the region without ignificantly reducing the underground tempera- ures in the course of a few years. A survey of he rate of escape of hot water and steam from he surface is relatively inexpensive and is herefore one of the first steps to be taken in he development of any thermal region. If de- ired, the surveys can be repeated after the bores ave been drilled and a considerable quantity of team discharged, so as to find what fraction of he bore demand is being provided at the ex- ense of the natural activity.

The various modes of heat loss that are en- countered and the methods that are used to measure them are outlined in this paper. It was decided that an over-all accuracy of 20 per cent would be acceptable. A tolerance this large al- ows the use of fairly relaxed techniques, yet it is still adequate for comparison purposes. If two areas have outputs differing by only 20 per cent, then for all practical purposes they are the same, and the decision to develop one in preference to the other would be governed by such considerations as access, drilling conditions, labor pool, housing, and so on.

Defining the area—Before an observer proceeds to any detailed measurements of the heat that is lost through various agencies, he is well advised to make a preliminary exploration of the whole region, noting the major springs and geysers, outlining the areas of hot ground, and making sure that all the thermal activity in the locality comes under review. Without this general survey much time may be wasted in making detailed measurements of features that later prove to be relatively unimportant.

Large-scale aerial photographs are an aid in such surveys; they often reveal the stunted growth that is characteristic of vegetation on hot ground. The association of thermal activity with a free water surface is also helpful. All major thermal activity in New Zealand borders a free water surface—a lake, a river, or a stream. It is thought that the visible thermal features are occasioned by hot water rising from a great depth as part of a large-scale convective circulation in the permeable rock, and it is clear that the heated water cannot rise far above the local water table, which may be evident as a river or lake. Steam generated at the underground hot water surface permeates the higher land around springs and geysers and

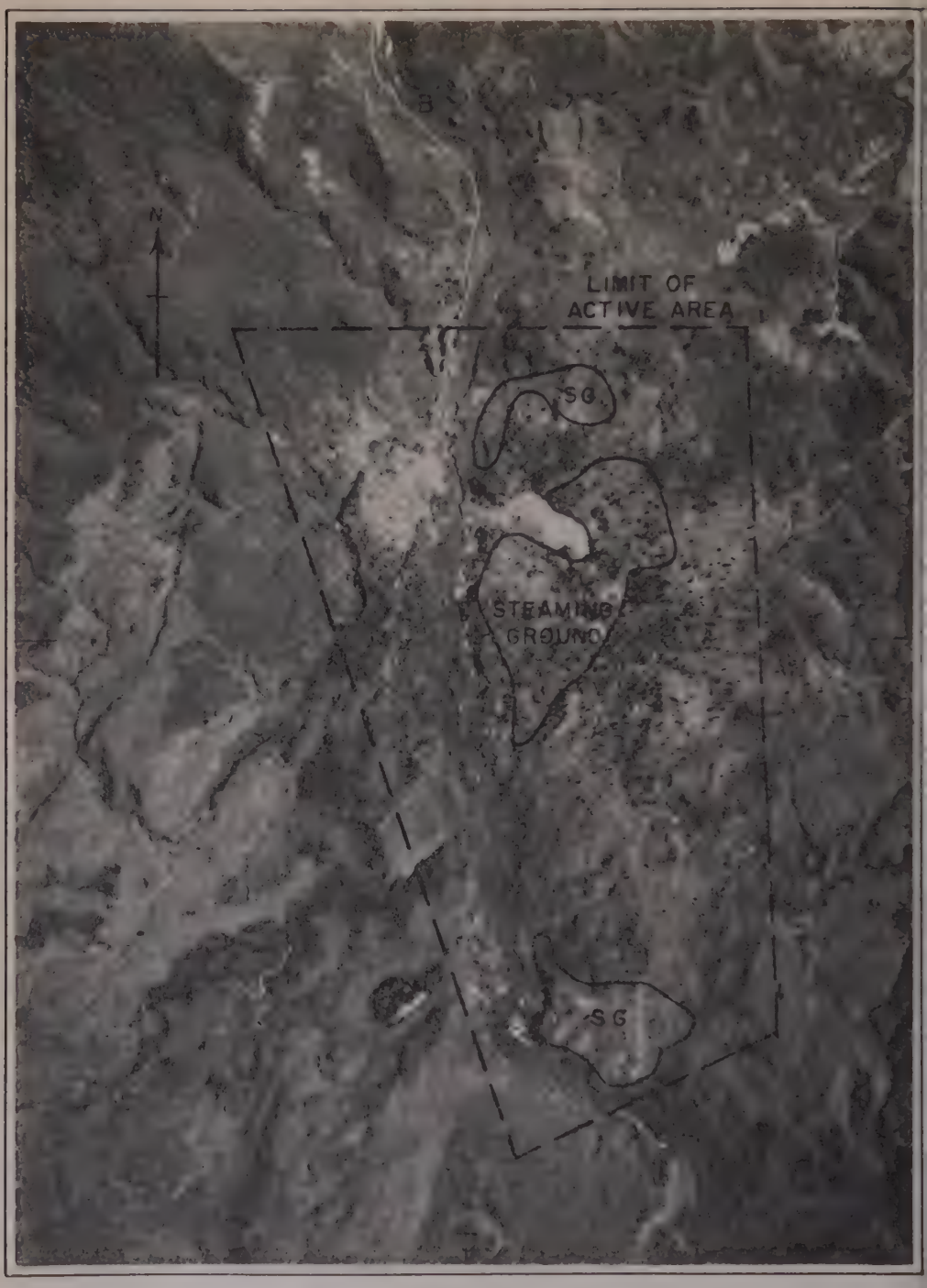

Fig. 1—Aerial Photograph of Orakei Korako Thermal Area
(Courtesy of New Zealand Lands and Survey Department)

give rise to steam fumaroles. More usually, ever, it escapes quite slowly through large cts of surface soil.

s an illustration of a typical thermal area, ure 1 shows an aerial photograph of Orakei rako, one of the regions in the North Island cribed by *Grange* [1955]. This is rugged ntry, rising some 400 feet above the Waikato er, but the geysers and springs all lie close to river. The free steam which passes up into higher ground appears at the surface within areas labeled "steaming ground." The outer ndary is a limit to the thermal region. No ns of past or present activity are found out- e it.

Avenues of natural heat loss.—The various ncies by which heat is emitted are listed be- v, approximately in order of importance.

) Steaming ground and fumaroles
) Hot springs and geysers
) Evaporation from hot water surfaces
) Seepage
) Conduction

hese will now be discussed in detail.

Steaming ground and fumaroles—The heat ss from a large fumarole can be found by easuring the temperature and velocity of the eam as it passes through a suitably sized cone aced over the vent. The largest accessible marole in New Zealand is Karapiti, which has output of 2800 Kcals/sec and a steam tem- erature of 115°C. But most fumaroles are uite small (outputs of the order of 1 Kcal/sec). hey occur in the midst of areas of steaming round, and the practice has been to take ac- ount of them by including them with the sur- ounding steaming ground and grading it ac- ordingly, as explained below.

The area of steaming ground in any single hermal region may well exceed a million square eters, and a survey depending on the use of he sampling calorimeter, or even the simpler arth temperature measurement [*Benseman,* 959a], is quite impossible. The only practical nethod has been to use the appearance of the crub growing on the steaming ground as an ndication of the intensity of the heat output.

Experimental work has shown that the con- lition of the scrub cover in steaming ground is letermined by the temperature of the earth in vhich it roots. As the earth temperature (and the heat flux) rises, the scrub becomes progressively more stunted and sparse, finally disappearing entirely in areas of very intense heat. Observers have found it relatively easy to differentiate between ten grades of steaming ground by this inspection method, and, although the approach may seem crude, independent observers seldom differ by more than one unit when assessing the same area of steaming ground. Test surveys over large areas have shown that agreement can be expected to within the allowed 20 per cent tolerance.

TABLE 1—*The relationship between the grade, earth temperature, and heat output of steaming ground*

Estimated grade	Heat output (10^{-3}cals/cm^2/sec)	Earth temperature at 35 cm
1	0.1	17
2	0.4	24
3	1.1	31
4	1.7	38
5	2.4	45
6	3.6	52
7	6.5	59
8	13	66
9	32	73
10	50	80+

The relationship between the grade of steaming ground, the earth temperature at a depth of 35 cm, and the heat flux are shown in Table 1. These figures relate to a time of year when the average earth temperature at this depth in a non-thermal area was 15°C. Measurements at other times would probably show that the lower grade steaming ground has a range of temperatures dictated by the seasonal changes in the ambient, but any corrections would have a fairly minor effect on the over-all heat flux because heat contributions by grades 1 to 4 are small in comparison with the total output from all steaming ground.

During surveys each area of steaming ground is assigned a grade of intensity and its area is estimated by inspection or from aerial photographs. The heat output is then assessed from Table 1.

Springs and geysers—In most of the thermal regions there are a few major springs and about ten times as many minor ones. At Orakei Ko-

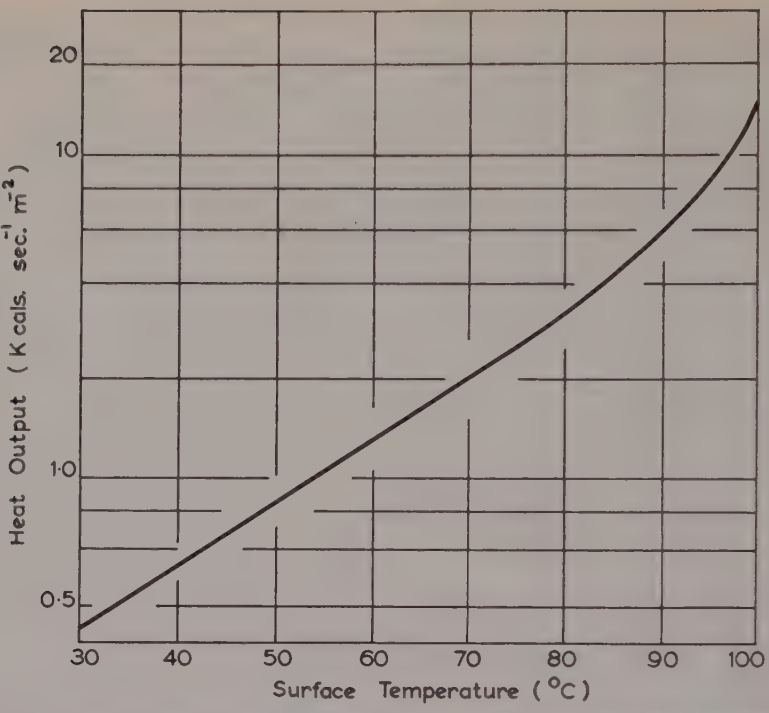

FIG. 2—The rate of loss of heat by radiation and evaporation from a hot water surface in averag weather conditions

rako, for example, the major springs produce about 80 per cent of the total visible outflow of hot water, and the same sort of relationship holds for the other large thermal areas. In view of the 20 per cent accuracy that is the aim of the survey, and in view of the errors likely to arise when discharge measurements are made on the larger springs, it is clear that the output from minor springs can be estimated by inspection or even ignored entirely.

Spring and geyser discharges are usually measured with either V-notches or weirs placed in the discharge channel. Once this has been done the temperature of the spring is measured, and the heat loss is computed relative to some realistic base temperature (normally 15°C) [*Benseman*, 1959b].

Evaporation from hot water surfaces—The heat that is lost with the steam that rises from hot water surfaces is estimated by measuring the surface area and temperature of each pool or spring and then using the curve shown in Figure 2 to arrive at a value of the heat that is lost through evaporation and radiation.

This curve is a revised version of one co structed by *Banwell* and others [1957] on t basis of small-scale laboratory tests, measu ments on larger water surfaces of the order 20 square meters, and a semiempirical form from the International Critical Tables. T curve has been derived for values of wind spe and humidity that are normally encounter in thermal areas in New Zealand; it may n apply in other areas.

Heat that is lost by excessive boiling has be ignored, for no simple and direct method measuring ebullition losses has yet been c veloped. Until such a technique is available, t preferred treatment has been to underestima this loss rather than to apply any unreliab and untested correction. The resulting error expected to be small.

Seepage—Some of the hot water that rises a thermal area may escape by undergrou paths to a nearby lake or river. When this ha pens one of the following methods may be a plicable.

(a) Determination of rise in river temper

re: If the seepage is towards a river that flows rough the thermal area, it may be possible determine the temperature rise of the river tween the points at which it enters and leaves e thermal area and from its volume of flow ake an estimate of the heat it has gained. If count is taken of heat gains from spring dis-arges (previously determined), radiation from e sun, and mechanical stirring, then anything excess of this may be attributed to seepage. is generally found that mechanical stirring d radiation contribute little heat.

(b) Determination of increase in mineral ntent: It is a feature of most New Zealand ermal areas that the mineral content of the scharge water is nearly constant. This is true hether the water is surface water taken from a ring or from 3000 ft down a bore hole. If all epage is towards a river that flows through e area, then the progressive increase in min-ral content of the river water from one end of e area to the other is a measure of the quan-ty of mineral water added. Although this gives nly the volume of water added, not its heat ontent, the information can be useful for check-ng the results obtained from the next method.

(c) Subsurface temperature survey: When ot water rises through the bed of the river or ake it sets up a characteristically curved tem-erature profile in the material of the bed; with ncreasing depth the temperature rises asymp-otically to that of the upwelling hot water, and he rise is more rapid the faster the flow. A the-oretical treatment of the temperature profile to e expected has been given by Donaldson [*Benseman*, 1956], and, although this treatment does not exactly parallel the practical condi-tions, it is easier to manipulate than the more rigorous solution that can be obtained from equations developed by *Wooding* [1957]. If either of these treatments is used and realistic boundary conditions are assumed, an estimate of the amount of heat and water seeping to the surface can be made from a survey of the ther-mal diffusivity of the material of the river or lake bed and of the excess temperature at some known depth (usually 21 cm, the length of a standard maximum thermometer).

As a comparison of the three methods, the re-sults from the Orakei Korako thermal area are given in Table 2. Temperatures and water samples were taken at points *A* and *B* shown in Figure 1, and the river bed temperatures were measured at some hundred points along the length of the river.

TABLE 2—*A comparison of seepage measurement*

Method	Water entry (liters/sec)	Heat entry (Kcals/sec)
Water temperature rise	...	21,300
Mineral increase	300	...
Theoretical estimate	240	18,200

Under the circumstances, the agreement must be regarded as good, and it suggests that where a thermal area borders a lake and the first two methods become inoperative, a temperature survey of the lake bed will allow the theoretical approach to be used with some confidence.

Conduction—The heat loss arising from conduction of heat upwards through the ground is usually only a small fraction of that caused by the convection of steam and water. In the course of extensive drilling operations in the various thermal areas it has been found that it is sufficient to assume an average surface temperature gradient of 3°C per meter for any region directly associated with thermal activity. Other measurements have shown that the pumice breccia that covers the thermal areas has a thermal conductivity of about 3×10^{-3} cgs

TABLE 3—*Estimates of the natural heat output of three thermal areas in New Zealand*

Item	Orakei Korako	Wairakei	Waiotapu
Total output (K cals/sec)	130,000	143,000	272,000
Source of heat (percentage)			
Hot springs, geysers, and evaporation from hot pools	38	39	61
Steaming ground	44	38	32
Seepage	16	13	0
Conduction	2	10	7

units, so that the heat loss by conduction can be taken to be about 1 cal/m² sec for all that area within the outer boundary of any region being considered. Large deviations from this figure will have little effect on the estimate of the total heat loss from all causes.

Results from three New Zealand thermal areas—The results of thermal surveys made of the three major thermal areas in New Zealand are summarized in Table 3. Wairakei and Orakei Korako are both alkaline areas, and it can be seen that the different avenues of heat loss are of similar relative importance in these two cases. Waiotapu, however, is dominantly an acidic region, and it can be seen that seepage and steaming ground assume less importance here than in the other two localities.

Whether a 20 per cent accuracy has been realized in these surveys will only become clear when current work has led to new estimates by independent observers. Wairakei was the region first surveyed, and there is reason to think that the heat output from its steaming ground, and consequently its total heat output, is much underestimated in Table 3.

Conclusion—The total natural heat output of thermal areas can be assessed quite readily provided a limited degree of accuracy is acceptable. All avenues of heat loss can be measured by methods that require neither elaborate equipment nor extensive sets of observations. The sequence of measurements should be adapted to suit the circumstances, but an over-all knowledge of the area comes first and helps to show where short cuts can be adopted; this is particularly true of spring discharges. Tedious measurements on small sources of heat should be avoided in view of the uncertainties in the measurement of such important items as steaming ground and seepage, and observers should keep in mind all means by which heat is lost so that there is no tendency to concentrate on one feature to the exclusion of another.

References

Banwell, C. J., E. R. Cooper, G. E. K. Thomson, K. J. McCree, Physics of the New Zealand thermal area, *New Zealand Dept. Sci. Ind. Research Bull. 123*, 27–28, 1957.

Benseman, R. F., The natural heat output of Orakei Korako, *Tech. Rept. R258*, Dominion Physical Laboratory, Lower Hutt, New Zealand, 13 pp., 1956.

Benseman, R. F., The calorimetry of steaming ground in thermal areas, *J. Geophys. Research*, 64, 123–126, 1959a.

Benseman, R. F., Subsurface discharge from thermal springs, *J. Geophys. Research*, 64, 1063–1065, 1959b.

Grange, L. I., Geothermal steam for power in New Zealand, *New Zealand Dept. Sci. Ind. Research Bull. 177*, 102 pp., 1955.

Wooding, R. A., Steady state free thermal convection of liquid in a saturated permeable medium, *J. Fluid Mech.*, 2, 273–285, 1957.

(Manuscript received December 16, 1958; revised March 26, 1959.)

Subsurface Discharge from Thermal Springs

R. F. BENSEMAN

Dominion Physical Laboratory
Department of Scientific and Industrial Research
Lower Hutt, New Zealand

Abstract—Individual hot springs in thermal regions have only a fractional discharge at the surface because a large proportion of the water leaves by underground paths. A new and more realistic concept of the activity of a spring is the 'turnover rate' (R), which allows the water throughput to be defined without reference to the surface discharge. A method for determining R is described.

Introduction—Every thermal area in New Zealand has its quota of hot pools which have temperatures ranging from a few degrees above ambient to near boiling. Superficially these pools are quite unspectacular, yet to anyone interested in questions of heat balance and heat transfer the fact that they are pools and not springs is something of a paradox. Since there is no outflow, one assumes, in the first instance, that there is no inflow. If there is no inflow, then what is the source of their heat?

One solution would be steam heating, since large quantities of heat could thus be delivered without any great accumulation of water. However, there are two factors which weigh against this hypothesis. First, there is seldom any visual sign to suggest that steam is entering the pool. But more telling still is the fact that the chemical composition of nearly all of the thermal water in any specific area is the same, irrespective of whether the water comes from a discharging spring, a geyser, a cool pool, or from 5000 feet underground. If a pool derives its heat from condensing steam there is no reason why the water in the pool should have a chloride content, for instance, that is the same as that of the water from any other form of nearby activity. The answer must lie elsewhere.

The equally attractive and obvious solution is that there *is* an inflow of hot water to the pool but the discharge is not visible from the surface; that is, there is a subsurface discharge channel. This underground discharge channel may well be outside the immediate pool basin, and heat and water requirements could be maintained by convection currents through a single port into the pool. But, whether the discharge channel is a simple leakage path from the pool proper or lies deeper in the spring system, hot water must enter the pool and eventually be rejected at a lower temperature if the pool is to maintain its temperature. The reject water is, of course, free to make its way to other springs and pools and is not necessarily lost to the local hot spring system.

Consider now the specific case of one of the springs that was selected for experimental work. Springs were chosen instead of pools because the objective of the work was to test the value of long-term discharge measurements on springs that are at present used as indicators of the stability of selected thermal areas. Although hot pools were used to introduce the idea of subsurface flows, it is not unreasonable to project the conclusions to springs and other forms of thermal activity. The spring in question had a surface area of six square meters and an average surface temperature of 80°C. There was no sign of steam entering the spring basin, so it must be assumed that the spring derived its heat from a source of hot water. The problem was to estimate how much hot water at 100°C, for instance, would be needed to maintain the temperature of this spring in the face of evaporative losses from the surface.

Previous experiments had shown that the heat lost from a free water surface at 80°C and subject to average weather conditions was about 5 Kcals/m^2/sec. Thus the spring was losing some 30 Kcals/sec by evaporative and convec-

tive cooling. If water was entering the spring system at 100°C and cooling to 80°C before leaving, it was this heat that was sustaining the spring at its average temperature of 80°C. A simple calculation shows that, to make good the 30 Kcals/sec heat loss, 1.5 liters of water would have to pass through the spring every second. But the surface discharge was measured as 0.34 liters/sec, so 1.2 liters/sec presumably flowed away underground. Other springs showed similar discrepancies between surface discharge and heat requirements. The object of the experiments was to establish independently that this division of flows was real.

Theory—If, instead of measuring the actual amount of water discharged from a spring, one defines the movement of water in terms of the 'turnover,' then a new concept of spring activity is realized. The rate of change of water (R) in a spring can be defined as the ratio of the rate at which water enters (leaves) the spring divided by the volume of the spring. The effective rates of change of water in different parts of the spring are not necessarily the same, but it should be posible to assign a value to a particular spring, just as a single temperature is used to express the temperature of the spring when, in fact, there may be some variation in the temperature throughout the spring.

Suppose that some chemical is introduced into a spring at the beginning of the experiment. If there is complete mixing between the replacement water and the water in the basin of the spring, the concentration of the alien chemical during the dilution process is given by

$$-W\frac{dC}{dt} = VC$$

Where C = Concentration of time t
V = Volume of water entering the spring in unit time
W = Volume of the spring basin.

For initial conditions, $C = C_0$ at $t = 0$, the solution is

$$C = C_0 e^{-Vt/W} = C_0 e^{-Rt}$$

Where R = Number of water changes in unit time.

Hence $\text{Log}_e C = \text{Log}_e C_0 - Rt$

By plotting the logarithm of the concentration against time, one obtains from the slope of the line which best fits the experimental points the rate of change of the water. In addition, the absolute rate of water flow through the system can be determined if the volume of the spring basin is known.

Experiments and results—Three widely spaced thermal springs were selected for field trials on the method, and various chemicals, concentrations, and sampling methods were tried.

As to choice of chemical, it was found that almost any stable soluble chemical could be used irrespective of whether it was already present in the spring waters, provided that it did not react with other minerals in the spring water or suffer selective absorption. The use of one in preference to another depended almost entirely on availability, cost, and ease of analysis. Of the several chemicals tried, NaCl, with its simple titration, was found to be the most suitable. It was found that if the concentration was raised from three to five hundred parts per million above that usually present in the spring the titration methods did not need to be overcritical. And, because absolute determinations were not needed for estimating R, it was quite in order to use unknown titrating solutions, provided the same solution was used consistently throughout each sequence of samples.

Mixing and sampling problems were much as expected. It was found that the results were repeatable to within 10 per cent if the chemical additive was introduced as a solution and the spring water was well stirred just before each sample was taken.

Typical results for the three springs mentioned earlier are given in Table 1, and the appropriate decay curves are shown in Figure 1.

It is apparent from these results that the subsurface discharge may account for between half and three-quarters of the total water throughput of these springs and that the flow rate derived by the use of chemical tracers is more realistic than that obtained by a direct measurement of the overflow. In particular, the derived rate of flow is adequate to account for the surface heat losses; the spring that is mentioned in the Introduction was found to have a flow of 1.23 liters/sec, which agrees reasonably well with the 1.5 liters/sec estimated from the balance of heat.

Conclusions—Although the results come from a small sample, it can be safely assumed that

TABLE 1—*Comparison of surface discharge and total discharge*

Spring	Turnover rate (R) (sec^{-1})	Estimated volume (liters)	Calculated total discharge (lit/sec)	Observed surface discharge (lit/sec)
1	0.103×10^{-3}	12,000	1.23	0.337
2	0.042×10^{-3}	2,400	0.10	0.034
3	0.183×10^{-3}	4,200	0.77	0.417

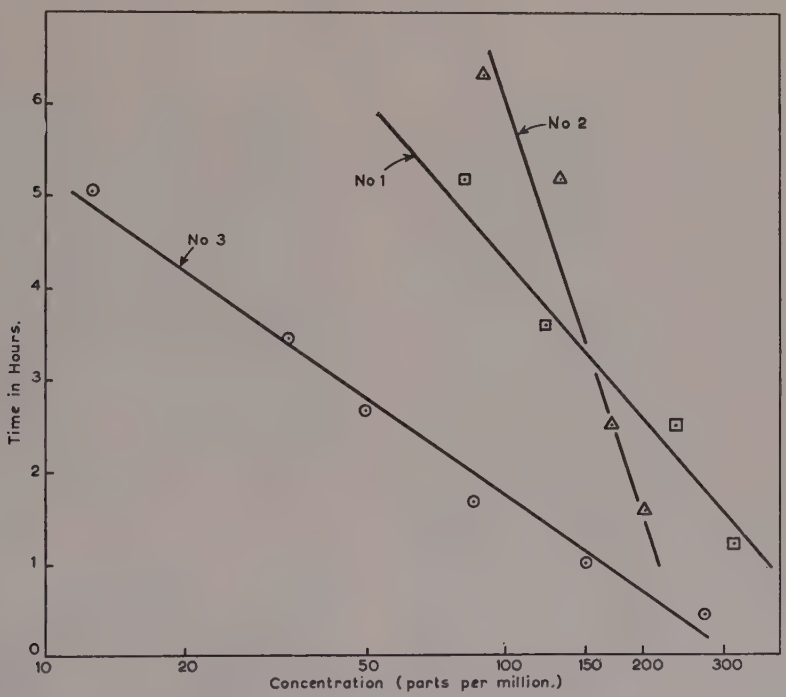

FIG. 1—Dilution history of chemical salts introduced into three hot springs

many hot springs have a significant, if unobtrusive, subsurface discharge. Consequently, any increase or decrease in the surface discharge over a period of time may not be so significant as has been thought to be the case in the past. It may mean only that there has been a redistribution of the discharge between the surface and subsurface paths. It would therefore be a worthwhile precaution to check the 'turnover rate' of springs which show significant changes in surface discharge.

Present methods of measuring the decay rate of the introduced chemical could be vastly improved. In terms of convenience and accuracy, stable-dye or electrical-conductivity methods have much to recommend them, whereas the fact that absolute determinations of the tracer concentration is unnecesary allows a wide latitude in the selection of tracer and detector.

(Manuscript received July 8, 1958; revised May 1, 1959.)

Letters to the Editor

DISCUSSION OF PAPER BY G. EARL HARBECK, JR., AND GORDON E. KOBERG, 'A METHOD OF EVALUATING THE EFFECT OF A MONOMOLECULAR FILM IN SUPPRESSING RESERVOIR EVAPORATION'

MAX A. KOHLER

U. S. Weather Bureau
Washington, D. C.

In the January issue, *Harbeck* and *Koberg* [1959] discussed a procedure recommended by *Mansfield* [1956] for field trials of hexadecanol and proposed a new approach embodying the mass transfer and energy budget techniques. The writer agrees with their statement that "The assumption that the pan or evaporimeter coefficient determined during the calibration period would be applicable after treatment is not tenable." A pan cannot reflect the changes in energy storage of an adjacent lake, and, furthermore, heat exchange through the class A pan (or sunken pans) is sufficient to cause moderate variation in the pan coefficient. The studies at Lake Mead [*Kohler* and others, 1958] indicate that the monthly class A pan coefficients would be reasonably stable were it not for these two effects.

Kohler and others [1955], in deriving lake evaporation from class A pan evaporation, in reality adjusted the pan coefficient for heat exchange (through the pan) and took into account the change in energy storage of the lake. Their equation is

$$E_L = 07.0\,[E_p + 0.00051P\alpha_p(0.37 + 0.0041u_p)(T_0 - T_a)^{0.88}] + \alpha(Q_v - Q_\vartheta) \quad (1)$$

where E_L = lake evaporation in inches per day.
E_p = class A pan evaporation in inches per day
P = atmospheric pressure in inches of mercury
α_p = portion of heat exchange through the pan dissipated by (or not available for) evaporation
u_p = wind movement at the pan (standard height) in miles per day
T_0 = mean surface water temperature in the pan in °F
T_a = mean air temperature in °F
α = portion of net advected energy ($Q_v - Q_\vartheta$) into the lake utilized for evaporation
Q_v = energy advected into the lake in equivalent inches of evaporation
Q_ϑ = change in energy storage of the lake.

The values of α and α_p are obtained from Figures 1 and 2. Since these factors depend slightly upon

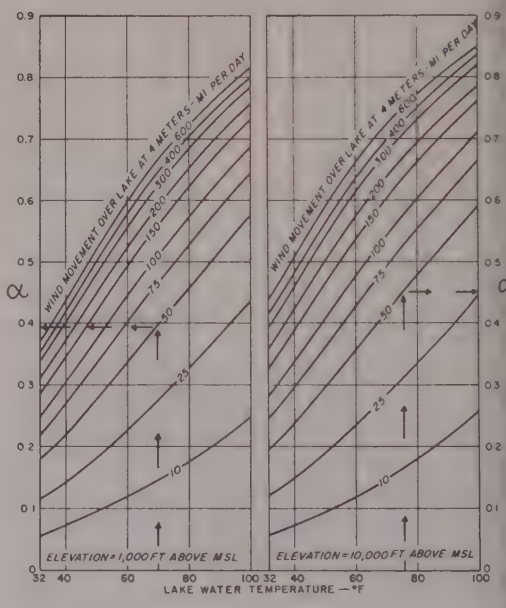

FIG. 1—Portion of advected energy (into a lake) utilized for evaporation

pressure, two relations are shown for each (1,000 and 10,000 ft, msl).

The water budget for the lake can be expressed as

$$\Delta H = I + P - S - E_L - O \qquad (2)$$

where ΔH = change in lake stage

I = inflow
P = precipitation
S = seepage out of the lake
O = outflow

and all items are expressed as inches per day over the lake surface. If we assume that all factors in equations (1) and (2) except E_L and S are known for the calibration period, simultaneous solution will provide an estimate of the seepage S. The derived value of S also reflects observational errors and errors in the procedure as a whole, but it should be much the same during the calibration and test periods if lake level and meteorological factors are reasonably similar. In this event the reduction in evaporation achieved during the test becomes the difference in E_L as computed from equations (1) and (2).

In this approach it is assumed (as did the authors) that the change in energy storage of the lake is the same, with or without the film. It will be noted from Figure 1 that 4-meter wind over the lake and water-surface temperature are needed to derive α. Except at low speeds, wind movement is not critical, and increasing the pan wind by a reasonable factor (about 2 at Lake Hefner) should be sufficiently accurate. During the test period the 'natural' water temperature must be known for α to be obtained. It will be seen, however, that an error of a few degrees in temperature has but little effect on α and would result in an appreciable error in E_L only if $(Q_s - Q_3)$ were large during the period of measurement. The natural water temperature can be assumed to be a few degrees lower than the observed value.

The natural water temperature can be estimated if representative humidity data are also available. The constant in the empirical mass transfer equation can be determined during calibration, if E_L from equation (1) is used. The saturation vapor pressure corresponding to the natural water temperature during the test can then be obtained from the mass transfer equation, again using E_L from equation (1). If this yields a natural temperature that is appreciably different from that used to compute α, a second approximation may be required.

In conclusion, it should be stated that the reliability of this approach is not known, but it does overcome the major deficiencies of the method used by *Mansfield* [1956]. Although it may not be as reliable as the method of the authors (depending upon the accuracy of the various observations), the required observational program is relatively much simpler and less expensive. All that is needed in addition to the class A evaporation station is lake-surface temperature, temperature profiles and lake levels at the beginning and end of the two periods, precipitation, and inflow and outflow volumes and temperatures. If the studies are based on periods of no inflow or outflow, and this should certainly be the case if at all possible, the observational requirements are greatly reduced. Since the additional requirements for this approach (over that of the authors) are relatively minor, it is entirely feasible to use both for comparative purposes. If the observations required for both are available, one further check can be made by replacing equation (1),

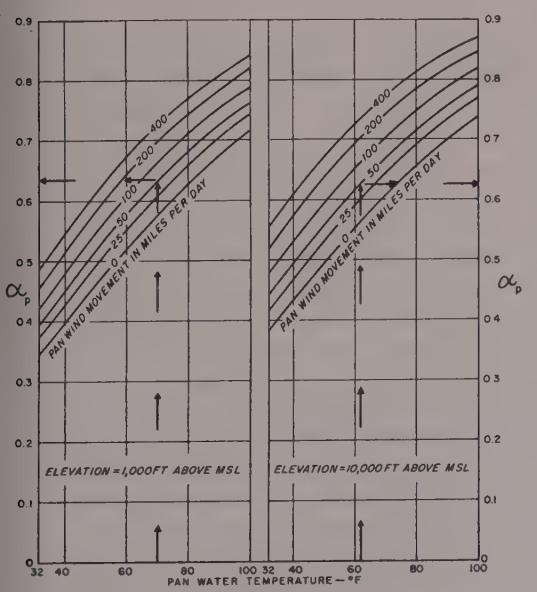

FIG. 2—Portion of advected energy (into a class A pan) utilized for evaporation

above, with a relation derived by *Kohler*, and others [1955] involving air and dewpoint temperatures, wind movement, and solar radiation.

References

Harbeck, G. E., and G. E. Koberg, A method of evaluating the effect of a monomolecular film in suppressing reservoir evaporation, *J. Geophys. Research*, 64, 89–93, 1959.

Kohler, M. A., T. J. Nordenson, and W. E. Fox, Evaporation from pans and lakes, *U. S. Weather Bur. Research Pap. 38*, 1955.

Kohler, M. A., T. J. Nordenson, and W. E. Fox, Pan and lake evaporation, *Water-loss investigations: Lake Mead studies, U. S. Geol. Surv. Prof. Pap. 298*, 38–60, 1958.

Mansfield, W. W., The use of hexadecanol for reservoir evaporation control, *Proc. 1st Intern. Conf. Reserv. Evap. Control, Southwest Research Inst.*, 33–35, 1956.

(Received April 13, 1959.)

DISCUSSION OF PAPER BY G. EARL HARBECK, JR., AND GORDON E. KOBERG, 'A METHOD OF EVALUATING THE EFFECT OF A MONOMOLECULAR FILM IN SUPPRESSING RESERVOIR EVAPORATION'

N. J. COCHRANE

Sir William Halcrow & Partners
Consulting Engineers
London, S.W.1., England

The paper is very relevant to the problem of deducing valid results from such investigations. When the difficulties of carrying out true water budgets on large bodies of water are borne in mind, the problem is seen to be most intractable.

The sequence of events quoted by the authors is not entirely complete. The first experimental work with the object of suppressing evaporation from reservoirs in Australia may be attributed to *Docking* and others [1940]. In addition, the East African Meteorological Department started work in 1954 on pans and on six reservoirs varying in area from 1 to 100 acres. *Grundy* [1957] reports a number of important results from this work:

(1) The efficiency of commercial cetyl alcohol (generally a mixture of hexadecanol and octadecanol) depends to a considerable extent on the impurities present.

(2) The effectiveness of the surface film deteriorates rapidly, and, in an experiment, half doses twice a day were significantly more suppressive than a full dose once a day.

(3) The use of cetyl alcohol in pellet or flake form was abandoned early in 1956 and a solution in kerosene and a dispersing agent was substituted.

(4) Two of the reservoirs yielded technically reliable results and indicated reductions of evaporation of 20 and just over 30 per cent.

It will be realized from the above that apart from the physical difficulties of treating a very large reservoir there are significant practical factors which modify the efficiency of the film itself.

The writer may add that he has carried out water budget analyses of Lake Nyasa for part of each year over a period of many years [*Cochrane,* 1956] and found that the natural evaporation varied considerably from year to year. He has now completed a similar investigation using lake levels of the Caspian Sea since 1837 and finds support there for the variation in the Nyasa evaporation results. The authors also quote a considerable range of values for three years from Lake Mead. It appears to follow from these results that pre-treatment evaporation from a lake should not yet be used as a control for an over-all assessment of post-treatment results from the same lake, unless both are known for many years.

The use of standard pan evaporimeters as controls does not commend itself to everyone, although their value is greater than the authors suggest. It is hoped that the authors' interesting new proposals will supplant pan controls, but there are at present several unresolved aspects which modify the presumed effectiveness of the film and it would be of interest to have the authors' comments on this.

REFERENCES

COCHRANE, N. J., The cyclic behaviour of Lakes Victoria and Nyasa, *Colonial Geol. and Mineral Resources, Gt. Brit.,* **6**, 169–175, 1956.

DOCKING, A. R., E. HEYMAN, L. F. KERLEY, AND K. N. MORTENSEN, Evaporation of water through multimolecular films, *Nature,* **146**, 265, 1940.

GRUNDY, F., The use of cetyl alcohol to reduce reservoir evaporation, *J. Inst. Water Engrs.,* **11**, no. 5, 1957.

(Received March 16, 1959.)

Authors' Reply to Preceding Discussions

G. E. Harbeck, Jr.
and
G. E. Koberg

U. S. Geological Survey
Denver, Colorado

The instrumental requirements for the alternate evaluation method suggested by Mr. Kohler are admittedly simpler than the technique we proposed, at least during periods when inflow and outflow are negligible. A water budget is required, however, and at some reservoirs it may be impossible to obtain the necessary accuracy merely because volumes of inflow and outflow may be unduly large compared with other water budget items.

Mr. Cochrane's comments on his and Mr. Grundy's work in Africa were most welcome. His findings that natural evaporation varies considerably from year to year is not confirmed by our Lake Mead results. Although the volume of evaporation did range from 699,000 to 875,-200 acre-feet during the water years 1953–1956, this variation is attributable primarily to differences in surface area. Evaporation ranged only between 85.6 and 88.9 inches during that 4-year period—a relatively small annual variation. It is not surprising that annual reservoir evaporation should be relatively constant, at least in comparison with rainfall and runoff. The annual variation in solar and atmospheric radiation, which is the energy supply for evaporation, is quite small. The annual variation in air temperature, which can be considered an indicator of the amount of incoming energy, is seldom more than a few degrees. Large year-to-year variations in evaporation might occur if there were also large variations in the sum $(Q_s - Q_o)$, but this is not likely unless there are large annual variations in inflow and outflow.

(Received May 27, 1959.)

Discussion of Paper by J. F. Lovering, 'The Nature of the Mohorovicic Discontinuity'

Hisashi Kuno

Geological Institute, University of Tokyo
Tokyo, Japan

The author's discussion [*Lovering,* 1958] is primarily based on the assumptions that the layer of gabbroic composition in the earth is much thicker than is generally accepted and that the Mohorovicic discontinuity lies within this layer and represents a level of gabbro→ eclogite transition. But he does not mention whether these assumptions are consistent with known petrological facts.

If the basaltic magmas originate through melting of the eclogite layer, as Lovering suggests, how can the world-wide occurrence of peridotite inclusions or 'olivine nodules' in basaltic rocks [*Ross* and others, 1954] be explained? From their mineralogy, especially the nature of the pyroxenes, these peridotite inclusions cannot be interpreted as being derived from early segregations of the host magmas. Again, the peridotite inclusions are found in alkali-olivine basalt and other alkali-rich mafic lavas but are absent in tholeiite [*Kuno* and others, 1957]. If the inclusions were fragments of intrusive peridotite, they would be found both in tholeiite and alkalic lavas.

In Hawaiian volcanoes, inclusions in tholeiite are gabbroic rocks (such as in Kilauea); those in alkali-olivine basalt and andesine basalt are either gabbroic rocks and peridotite (in Hualalai) or peridotite alone (in Mauna Kea); and those in nepheline basalt are either peridotite alone (at Honolulu) or peridotite and eclogite (at Salt Lake crater near Honolulu [*Winchell,* 1947]. In the last-named locality, there is complete gradation in chemistry and mineralogy between the peridotite and the eclogite (Kuno, unpublished data). Such association of inclusions strongly indicates that a gabbro layer is directly underlain by a peridotite layer and that a local eclogite lens or pocket exists at some deep level within the peridotite layer.

The tholeiite constituted the bulk of the Hawaiian primitive shield, and the alkali-olivine basalt and andesine basalt were extruded during the declining stage of the shield-building activity [*Macdonald,* 1949; *Tilley,* 1950]. *Kuno* and others [1957] suggest that the tholeiite magma was formed by partial melting of the postulated peridotite layer at comparatively shallow levels, whereas the alkali-olivine basalt magma was formed by partial melting of the same material at deeper levels. Thus the sequence of volcanic activity can be explained in relation to the model of the crust and the mantle postulated above: the successive stages of activity in each volcano were caused by different types of magmas which were generated at successively deeper levels of the mantle and captured the rocks existing at successively deeper levels of the crust and the mantle. The nepheline basalt was erupted at a stage when the shield had been deeply dissected, and it may therefore be interpreted as having been derived also from a great depth.

If a gabbro layer were directly underlain by an eclogite layer of gabbroic composition, as postulated by Lovering, inclusions of gabbro would tend to be associated with those of eclogite. Such association has not been observed in Hawaii and in Japan. In Japan gabbro inclusions are found in association with those of peridotite, and eclogite of gabbroic composition has never been observed. It might be argued that garnet and omphacite of eclogite dissociate readily upon heating by the basaltic magmas and therefore cannot be recognized as such. But this does not appear likely. So far as I have observed, garnet in eclogite inclusions has been transformed either partly or wholly to myrmekite-like intergrowth of pyroxene and spinel and is never overlooked or misidentified.

The petrological evidences appear to lead us

to the conclusion that the Mohorovicic discontinuity is a boundary between a gabbro layer and a peridotite substratum and that the gabbro→eclogite transition takes place at a certain level below the discontinuity. The peridotite above this level may belong partly to the granulite facies.

A more detailed discussion will be given in a later paper.

References

Kuno, H., K. Yamasaki, C. Iida, and K. Nagashima, Differentiation of Hawaiian magmas, *Japan. J. Geol. and Geogr.*, **28**, 179–218, 1957.

Lovering, J. F., The nature of the Mohorovicic discontinuity, *Trans. Am. Geophys. Union*, **39**, 947–955, 1958.

Macdonald, G. A., Hawaiian petrographic province, *Bull. Geol. Soc. Am.*, **60**, 1541–1596, 1949.

Ross, C. S., M. D. Foster, and A. T. Myers, Origin of dunites and of olivine-rich inclusions in basaltic rocks, *Am. Mineralogist*, **39**, 693–737, 1954.

Tilley, C. E., Some aspects of evolution of magmas, *Quart. J. Geol. Soc. London*, **106**, 37–61, 1950.

Winchell, H., Honolulu volcanic series, *Bull. Geol. Soc. Am.*, **58**, 1–48, 1947.

(Received January 29, 1959.)

AUTHOR'S REPLY TO PRECEDING DISCUSSION

J. F. LOVERING

Department of Geophysics, Australian National University
Canberra, A.C.T.

Dr. Kuno has raised some important petrological objections to a possible eclogitic composition for the earth's upper mantle. These objections are based on two points: (1) the significance of the world-wide occurrence of peridotite inclusions in basaltic rocks and (2) the significance of the non-occurrence of gabbroic with eclogitic inclusions in basaltic rocks.

(1) At the present time the petrological significance of the 'olivine nodules' in basaltic rocks is very much an open question. Previously the generally accepted view has been that the nodules are derived directly from a primary peridotite zone in the earth [*Ross* and others, 1954]. However, recent work reported by *Tilton* and others [1956] would seem to rule out a direct mantle origin for the nodules. They determined uranium, thorium, and lead concentrations in several nodules and one host basalt, together with the isotopic composition of the lead extracted from each. The details of the crystallization of the nodules and their relationships to the host basalts are still uncertain from their data. However their results show quite conclusively that the nodules must be eliminated as possible undifferentiated samples of the earth's mantle.

(2) In his discussion, Dr. Kuno has said that if a gabbro layer in the lower crust was directly underlain by an eclogite layer of gabbroic composition in the upper mantle, then inclusions of gabbro should tend to be associated with those of eclogite in basaltic magmas. In the silica-saturated tholeiitic magmas in Hawaii only gabbroic inclusions occur, whereas the silica undersaturated magmas contain gabbroic and peridotitic associations (in the alkali-olivine basalts) or eclogitic and peridotitic associations (in the nepheline basalts). Apparently gabbro and eclogite inclusions have never been found associated in either Hawaiian or Japanese basalts.

However, it will be shown in a paper currently in preparation [*Lovering*, 1959] that a number of intrusions in eastern Australia show gabbro (or pyroxene granulite), garnet granulite, eclogite, and peridotite inclusions in a matrix composed of both massive and brecciated silica-undersaturated alkali basalt. It may be significant that in most cases granulitic and eclogitic inclusions predominate over peridotitic inclusions. The point which can be made is that in these eastern Australian occurrences, at least, inclusions of both eclogitic and gabbroic types are associated in alkali basalt magmas.

Obviously the points raised by Dr. Kuno are only two of a number of petrological arguments which are relevant to both the 'peridotite' and 'eclogite' hypotheses for the upper mantle. It is important that these arguments be marshalled in one place and critically re-examined in the light of recent work. This approach to the problem is being attempted, and the writer hopes to present the work in the near future.

REFERENCES

LOVERING, J. F., Granulitic, eclogitic and peridotitic inclusions in basaltic rocks from Eastern Australia, 1959, (in preparation).

ROSS, C. S., M. D. FOSTER, AND A. T. MYERS, Origin of dunites and of olivine-rich inclusions in basaltic rocks, *Am. Mineralogist*, 39, 693–737, 1954.

TILTON, G. R., G. W. WETHERILL, L. T. ALDRICH, G. L. DAVIS, AND P. M. JEFFERY, Ages of ancient minerals, *Carnegie Inst. Washington 1955–1956 Year Book*, no. 55, 87–100, 1956.

(Received May 16, 1959.)

MEASUREMENT OF IONOSPHERIC ELECTRON DENSITIES USING AN RF PROBE TECHNIQUE

J. E. JACKSON* AND J. A. KANE*

U. S. Naval Research Laboratory
Washington 25, D. C.

An interesting variable measured during the course of the Seddon propagation experiment for the determination of ionospheric electron densities [*Seddon*, 1953; *Jackson and Seddon*, 1958] is the impedance at 7.75 Mc of the rocket-borne transmitting antenna. This antenna consists of two whips, each 14 ft long, which at 7.75 Mc form an electrically short dipole whose free-space impedance is $Z = (5.0 - j538)$ ohms. During the rocket flight the impedance is obtained by telemetering the voltages on both sides of a transformer matching network located between the antenna and the transmitter. By comparing these telemetered voltages with the impedance contour obtained by a preflight calibration of the system, both the resistive and reactive components of the antenna are obtained as a function of rocket altitude.

Above 110 km it is found that the impedance undergoes only a reactive variation from its free-space value. Because the measured impedance is primarily a negative reactance we will assume that the dipole can be treated as a capacitor. In the general case where the resistive component is not negligible one is confronted with an as yet unsolved problem, namely the behavior of a radiating dipole in a conducting medium. Assuming that in the ionosphere the measured value of capacitance C is related to the free-space capacitance C_0 by $C = KC_0$ permits the local electron density to be computed from the simplified Appleton-Hartree formula for the dielectric constant $K = 1 - 81N/f^2$, where N is the number of electrons per cubic centimeter and f is the exploring frequency in kilocycles.

This computation was performed for rocket flight NN3.08F, which was fired from Fort Churchill, Canada, at 1216 hours CST July 4, 1957. The electron densities so obtained were after multiplication by a factor of 3, plotted in Figure 1, which also shows the electron densities measured simultaneously by the propagation experiment. During the night flight of rocket NN3.11F, fired from Fort Churchill at 0017 hours CST, February 4, 1958, the impedance variation of the dipole, for the region above 110 km, was too small to be measured. This was due to the presence of a low electron density whose profile, as determined by the propagation experiment, is also included in Figure 1. In the region below 110 km the impedance measurements were essentially identical on both rockets.

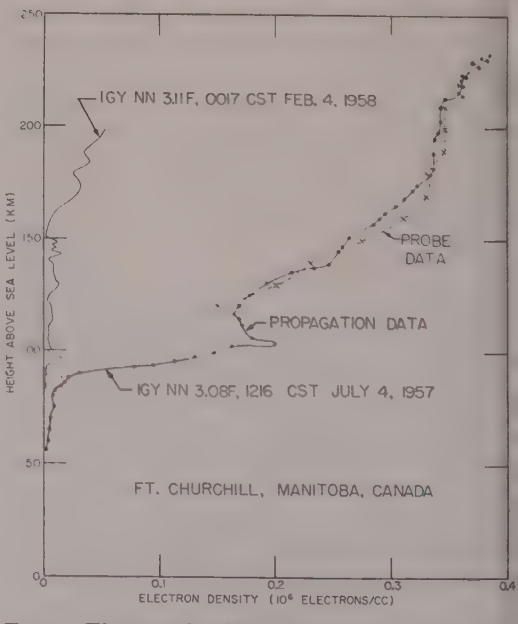

FIG. 1—Electron densities obtained by the propagation experiment and the rf probe technique

*Now with National Aeronautics and Space Administration.

flights. It is known, however, that with the power used for the propagation experiment the antenna undergoes an rf breakdown [*Jackson and Kane,* 1959] when the rocket is below 110 km, and the impedance values in this region are therefore not a measure of the ambient ionosphere.

It can be shown that the factor of 3, which is required to bring the electron densities calculated from the impedance data into agreement with the results of the propagation experiment, is due to the effect of a rocket potential of the order of 10 volts. This large rocket potential is due to the collection of electrons from the ionosphere by the antenna which for the propagation experiment requires an rf amplitude of about 150 volts. The effect of this rocket potential is to enhance the positive-ion sheath [*Jastrow and Pearse,* 1957] in which electrons are removed from that region to which the antenna capacitance is the most sensitive, namely the volume immediately surrounding the antenna. The magnitude of this effect was calculated [*Jackson and Kane,* 1959] to be sufficient to explain the above-mentioned factor of 3.

On the basis of these encouraging results a program is now under way to develop a reliable rf probe for measuring electron densities. Probably the impedance method can be substantially improved by performing the measurements with a low amplitude of rf voltage on the antenna, thereby minimizing the role of the ion sheath.

References

Seddon, J. C., Propagation measurements in the ionosphere with the aid of rockets, *J. Geophys. Research,* **58,** 323–335, 1953.

Jackson, J. E., and J. C. Seddon, Ionosphere electron density measurements with the Navy Aerobee-Hi rocket, *J. Geophys. Research,* **63,** 197–208, 1958.

Jackson, J. E., and J. A. Kane, Breakdown and detuning of transmitting antennas in the ionosphere, *NRL Rept.* 5345, in press.

Jastrow, R., and C. A. Pearse, Atmospheric drag on the satellite, *J. Geophys. Research,* **62,** 413–423, 1957.

(Received June 15, 1959.)

Report of the Committee on Cosmic-Terrestrial Relationships 1957-1959

E. H. VESTINE, Chairman
W. O. ROBERTS, Vice-Chairman

L. BERKNER
R. BRACEWELL
J. CHAMBERLAIN
C. ELVEY
J. EVANS
H. FRIEDMAN
S. FRITZ
H. KALLMANN
S. KORFF
R. McMATH
M. MORGAN
H. ODISHAW
C. PALMER
A. SHAPLEY
S. SINGER
J. SMAGORINSKY
T. SKILLMAN
A. WAYNICK
F. WHIPPLE
H. WILLETT

Introduction—The Committee has functioned during the report year by (1) holding a Symposium on Cosmic-Terrestrial Relationships at the Thirty-Ninth Annual Meeting of the American Geophysical Union (Appendix 1), (2) noting and encouraging the production of books in the general area of cosmic-terrestrial relationships (Appendix 2), and (3) preparing a short summary of progress made during the past report year in the general area of cosmic-terrestrial relationships.

Under (1) will be noted a number of papers of quite special interest, including some dealing in part with IGY activities. It is believed that another symposium of this general type, perhaps covering some additional topics, should be held soon because of new opportunities for researches based on IGY data.

(2) The Committee notes with pleasure the appearance of several new books and the several books planned or in preparation which are mentioned in Appendix 2.

(3) The Committee has noted most encouraging accomplishments in its general area of interest during the past report year. One of the most gratifying aspects has been the high degree of public awareness and interest in the various basic researches that are under way in cosmic-terrestrial relationships. The press and other media, such as television, brought many matters in our area of interest before the scientific and general public, with results of educational and other useful benefits.

The great international scientific venture of the International Geophysical Year was of material help because it brought a great number of new workers to the general area of cosmic-terrestrial relationships. It is to be hoped that a number of these new workers will continue work in geophyscis. To this end a number of the Committee members, and other interested supporters are active in various related organizations, such as the National Academy of Sciences, the American Geophysical Union, the National Science Foundation, and the IGY. They are working for a continued geophysical effort following the International Geophysical Year.

The Committee has necessarily achieved only partial coverage of the general field of cosmic-terrestrial relationships in this report. It has, however, sought to cover at least a major portion of those activities of interest to members of the American Geophysical Union.

Solar research—Sydney Chapman has considered the thermal diffusion factor for an ionized solar coronal gas at non-uniform temperature. In such a gas thermal diffusion can greatly increase the (still small) proportion of the heavy multiple ions in the hotter regions. This tendency may be of importance in the solar corona if temperature inequalities persist long enough and turbulence is not too great. In a recent paper *Chapman* [1957] has considered the thermal properties of a model coronal gas and the influence of such a gas on the outermost atmosphere of the earth. On the basis of tentative calculations on such a model, he has shown how the heat flow to the earth's atmosphere could account for the high temperatures measured in the F layer. In an extension of the subject reported in August 1957 to the ICSU Mixed Commission for the Ionosphere, he further developed the picture of the terrestrial ionosphere decreasing upwards in density until it merges with the far extension of the solar atmosphere. He stated that, though it seems improper to dogmatize as to the state of the solar gas through which the earth moves in its orbit, it is worth while to consider the possibility that it is very hot and has a density of the order of 10^3/cc near the earth. Also, in regard to the composition of the outer ionosphere, present data and theory suggest that the thermocline continues indefinitely upwards, but that the F2 layer is limited above by a nearly neutral layer of atomic hydrogen, above which lies another layer of protons and electrons. In another report to the ICSU commission, Chapman has considered the disturbances in the lower auroral ionosphere. Here he has discussed the complex particle interactions that give rise to the regions of ionization and radio-wave absorption at or below auroral heights. Further consideration has been given to the ideas previously advanced by *Chapman* and *Little* [1957] that the low-level ionizations are due to primary electrons, acting directly, or, in the lowest regions, by x-rays produced by a small minority of the primary electrons. Revised results of their calculations are discussed, and it is shown that there is no alteration of their main conclusion—that the absorption of

radio waves takes place mainly below the level of luminous aurora, and that the excess absorption by day results from photodetachment of electrons from negative ions. He concluded that in auroral regions there will be a long strip of ionized atmosphere over the band of latitude traversed by the auroral arcs, and that this strip appears to extend considerably below the level of luminosity, owing to the primary electrons. In particular, it extends much lower towards the weather and thunderstorm levels of the atmosphere than was formerly supposed.

Robert R. McMath reported that the McMath-Hulbert Observatory of the University of Michigan continued its program of basic solar research. In addition, the staff of the observatory has developed or acquired in recent years a battery of instruments that permit direct and quick comparison of solar phenomena and associated terrestrial events and is taking an active part in the IGY solar activity program. The solar telescopes and spectrographs provide observations of plages, flares, prominences, and spots. A small radio-frequency installation permits great flare-associated bursts at 200 Mc/s to be recorded. Three 'indirect' flare detectors give ionospheric data through records of variations in the 5-Mc/s WWV signal, 18-Mc/s cosmic noise, and 27-kc/s atmospherics. Variations in the earth's magnetic field are indicated on a total-force variometer and a declination-component magnetometer. Direct comparison or early evaluation of solar phenomena and their effects on the earth are proving to be of assistance in efforts to clarify certain aspects of solar-terrestrial relationships.

Geomagnetic effects of flares with major, premaximum bursts at radio frequencies $\leq$ 200 Mc/s have been investigated by *Dodson* and *Hedeman* [1958] for the interval from January 1949 to April 1956. The investigation shows a close association between such flares and subsequent sudden-commencement geomagnetic storms. Geomagnetic storms were reported by at least one observatory within less than five days after the occurrence of 92 per cent of the flares which had this type of rf emission. The average time interval between flares with 'major early bursts' and the start of subsequent geomagnetic storms was slightly less than 2½ days. Average superposed values of A_p and K_p were high on days 2, 3, and 4 after flares of importance 3 with major early bursts, but this was not the case after flares of importance 3 without this type of rf emission. According to this study, storm-producing flares occurred at all distances from the central meridian and in all importance categories. However, centrality of position and high flare importance favored greater severity in the subsequent storm.

W. O. Roberts reported that in the field of cosmic-terrestrial relationships, the High Altitude Observatory has undertaken, in collaboration with the Sun-Earth Section of the National Bureau of Standards, a detailed comparison of optical indices of solar activity with indices of geomagnetic activity. The principal conclusion is that in recent years the correspondence between any existing parameters of optical solar activity and a detailed trend of geomagnetic disturbance as represented by planetary geomagnetic A or K indices is rather weak. Another finding is that an intense flare associated, in time or position on the solar disk, with radio-noise bursts and storm activity at meter wave-lengths is the most reliable indicator of a magnetic storm. Flares which occur in sunspot groups not characterized by these radio emissions have less likelihood of producing terrestrial magnetic storms. In particular, stable, regular, round sunspots tend to be radio quiet and are not accompanied by geomagnetic disturbance.

A study of more than 100 limb flares confirms an earlier result based on a small sample [*Warwick*, 1955], that a flare is very unlikely to be accompanied by a short-wave radio fadeout (SWF) unless the flare attains a height greater than about 14,000 km above the solar photosphere. The variation with distance from the center of the solar disk of the fraction of SWF-producing flares is consistent with the interpretation of this result in terms of optical depth unity for the ionizing radiation being reached near the 14,000-km level.

Some work has been done at CRPL on a five-day index for ionospheric propagation based on E layer critical frequencies observed in routine vertical soundings. Seasonal and latitudinal effects are largely removed by extrapolating the morning and afternoon observations to a hypothetical overhead sun. Five-day means of the 'overhead' sun values from two widely separated middle latitude stations (Puerto Rico, Maui) agree within about 5 per cent during a period when the sunspot-number range was more than 200. The trend of these indices has many of the features of the course of the five-day mean sunspot number.

G. Newkirk of the High Altitude Observatory has confirmed the existence of emission lines in the spectrum of the atmosphere of the dark hemisphere of Venus, suggesting a Venusian aurora, but not with the same lines as the terrestrial aurora. Such lines were previously reported by Kosyrev (*Publ. Crimean Astrophys. Obs.*, 12, 169, 1954).

Fred L. Whipple in reporting on current work relating to cosmic-terrestrial relationships at the Smithsonian Astrophysical Observatory and the Harvard College Observatory related that statistical studies of the variation of solar-radiation intensity were made by *Sterne* and *Dieter*, [1958]. By comparing simultaneous Montezuma and Table Mountain values between 1926 and 1955 they found that the root-mean-square value of real changes in the solar constant during this interval was no greater than 0.0032 cal/cm²/min, or about 0.17 per cent of the solar constant itself.

At Lowell Observatory, H. L. Johnson and W. M. Sinton have been continuing measurements of the brightness of Uranus and Neptune in blue light. The measurements indicate no significant fluctuation in the solar constant with time.

Max Krook at Harvard has been investigating the theory of non-steady phenomena in the solar atmosphere and corona. His studies include the effects of convective instabilities and magnetic fields on the state of motion of the solar atmosphere and have shed light on the production of such events as sun spots, flares, prominences, and the production of cosmic rays.

Theoretical studies of the propagation of non-adiabatic acoustic waves in the solar atmosphere have been made by Charles Whitney, who constructed a theoretical model for solar granulation (small-scale brightness fluctuations observed on

: solar disk) which is in accord with observa-
ns.

ohn H. Waddell has been investigating, theo-
ically and observationally, the velocity fluctua-
ns in the solar photosphere and their effect on
: line-spectrum of the solar disk.

Alan S. Meltzer, from observations made at the
ramento Peak Observatory, Sunspot, New
xico, has been conducting two studies of solar
e profiles: (1) the variation of Doppler half-
lth with atomic weight and (2) the parity effect.

Donald H. Menzel continued as project director
the two Air Force contracts that support solar
earch in Cambridge and the work at the Sac-
nento Peak Observatory, Sunspot, New Mexico,
d the Radio Astronomy Station, Fort Davis,
xas. His own investigations have included the
ture of the solar corona and prominences and
o of the ionosphere and solar activity. He is
ervising a survey of all available data on cos-
c radio noise.

In collaboration with members of the staff at
ramento Peak, Richard N. Thomas analyzed
romospheric limb spectra obtained with the 16-
h coronagraph. With Jean-Claude Pecker, he
vestigated the problem of the source function
the upper photosphere and lower chromosphere.
omas completed work which demonstrated the
ference between electron and excitation tem-
ratures for the early Balmer lines and has ap-
ed it to the problem of analyzing these lines for
mospheric structure and abundance.

The structure of the sunspot zone, as shown in
e distribution of sunspots with latitude over the
lar cycle, was studied by *Bell* and *Glazer* [1957,
58].

Thomas Gold studied the evidence for cosmic-
y effects of solar origin and their relation to the
ructure of magnetic fields in the solar system
d also worked on a new theory of magnetic
orms.

John G. Wolbach is analyzing various proper-
es of solar flares, using Mount Wilson solar
aps and High Altitude Observatory flare films
ith other data to construct magnetic and visual
mposite diagrams.

F. Shirley Jones, in collaboration with Menzel,
ntinued the measurement and classification of
lar prominences, working with data from Climax
d Sacramento Peak. Analysis for the years 1949
rough 1952 has been completed.

Henry J. Smith, Astronomer-in-Charge of the
arvard program at Sacramento Peak, was prin-
pally concerned this year with the development
d testing of instrumental accessories. Using the
6-inch coronagraph, the large Littrow spectro-
raph, and E. W. Dennison's direct-intensity mi-
rophotometer, Smith recorded and analyzed spec-
a of the low chromosphere. He also extended the
alysis of spectra of bright prominences observed
ith the patrol camera spectrograph.

Elski v. P. Smith completed an analysis of Hα
pectra taken with the high-dispersion spectro-
raph of the 16-inch coronagraph, which gives in-
rmation concerning the variation of the Hα pro-
le with height in the chromosphere.

H. Friedman reported that at the U. S. Naval
esearch Laboratory solar radiation was meas-
red at a wavelength of 4.3 mm using a 10-foot
arabolic reflector with a beamwidth of 6.7 min-
utes of arc [*Coates*, 1958a]. The sun appears as a nearly uniform disk at this wavelength with a brightness temperature of about 7000°K. From these observations, together with the results of the observation of the 1954 eclipse at 8.6 mm wavelength, a new model of the solar chromosphere containing spicules was developed [*Coates*, 1958b; *Coates* and others, 1958]. At midyear a solar flare patrol was started with both optical and radio telescopes. The sun is observed in Hα, and at 4.3-mm, 3.5-cm, and 9.4-cm wavelengths.

Rocket flare patrol program—This program, an IGY project under the sponsorship of the NAS-NSF was begun in July and completed in September, 1957. New geophysical data on solar x-rays were obtained in Class 1+, 2, and 3 flares, as well as background data for the quiet sun. Flares were found to produce marked increases in short-wavelength x-ray emission. The largest flare yielded the shortest wavelength emission, about 2A. Highest fluxes observed below 7A were of the order of 10^{-2} erg/cm^2·sec. [*Friedman* and others, 1958].

Direct measurements of Lyman α (1216A) radiation in the night sky and ultraviolet fluxes (1220–1350A) from celestial sources were made from an Aerobee rocket fired at WSPG at 10:13 local time, March 29, 1957. The entire sky glowed in diffuse Lyman α emission with a slight minimum in brightness in the anti-solar direction. The integrated flux was 10^{-2} erg/cm^2·sec over the hemisphere above the rocket. An albedo of 42 per cent in Lyman α was observed below the rocket. Numerous celestial sources were detected in the 1220–1350A band, the most prominent being the Orion region, the Puppis-Vela region, and an area centered on Spica. The observed flux from the Orion region was approximately 5×10^{-3} erg/cm^2·sec steradian [*Kupperian* and others, 1958].

An analysis has been completed of the solar spectrograms obtained in a rocket flight to 115 km on February 21, 1955. Forty-five emission lines including Lyman β (1025.7A) and the Balmer line of He II (1640.5A) are identified between 1892A and 977A. The lines of highest excitation potential arise from O VI, N V, C IV and Si IV. Lyman β was about 1/60 the intensity of Lyman α (after correction for atmospheric absorption) [*Johnson* and others, 1958].

Hydromagnetics—At the Naval Research Laboratory, Smithsonian Institution, and the University of Maryland the 'induction drag' of a magnetic sphere in a conducting fluid was studied.

The properties of the current-driven hydrostatic magnetic fields in a non-rotating (a) sphere (b) infinite cylinder, and their effect on the instability of these bodies forms the subject matter of recent investigations (*Chopra* 1957a, b). It is shown that a force-free magnetic field must be a suitable combination of poloidal and toroidal components such that the magnetic energy is equally divided among them. On the other hand, a pressure-bound magnetic field may either be purely poloidal, purely toroidal, or a suitable combination of both. The equilibrium configuration of an arbitrarily deformed sphere is an oblate spheroid for a pure poloidal field and a prolate spheroid for a pure toroidal field. On the other hand, the cylinder is stable in a poloidal field, while the toroidal field

adds to its instability. The pulsations of an infinite cylinder in the presence of an external magnetic field were published earlier [*Chopra* and *Talwar* 1956; *Chopra* 1956]. The problems discussed, though highly idealized, are of interest in the understanding of the structure and stability of cosmical bodies.

Other problems in hydromagnetics that were considered are (1) the effect of a transverse magnetic field on the Poissuile flow, (2) thermodynamics of compressible hydromagnetic flow, and (3) propagation of hydromagnetic shock waves.

The effect of thermal diffusion on plane nonrelativistic hydromagnetic shock waves in a mixture of two completely ionized gases has also been considered [*Chopra,* 1958]. The problems concerning the interactions of shock waves in the presence of a magnetic field are under investigation.

Spectroscopic studies—Since spectroscopic methods are extremely valuable in the determination of temperature and chemical composition of the upper atmosphere and stellar atmospheres, a short description of work done in this field is included.

a. Linebroadening: Cross sections were measured for pressure of Li, Na, K, Ca, St, Ba, Tl, Cu, Ag, Cr, Mn, Fe, Co, and Ni lines emitted by an acetylene air flame. The evaluation of the cross sections was based on intensity-density graphs, constructed from photoelectric measurements of the total line intensities as a function of the density of the emitting atoms in the flame [*Hinnov,* 1957].

The Stark-effect broadening of hydrogen lines was investigated in a water-stabilized arc at 12,000°K and 10^{17} electrons/cm^3. The statistical theory by Holtsmark proved unsatisfactory and was modified to take into account the perturbations by the electrons [*Griem,* 1954].

b. Line intensities: For the derivation of absolute concentrations of atoms from measured intensities, knowledge of transition probabilities is essential. Because the wave-mechanical calculation of these quantities is too involved for complicated atoms, they must be determined experimentally. Such methods were worked out and applied to O^+ lines in a plasma produced in a water-stabilized arc [*Wiese,* in press].

Lunar investigations—Some simple properties of rocket orbits to and around the moon have been discussed by Singer and Wentworth. The question of the nature of the lunar atmoshpere has been re-examined in the light of recent radio astronomical observations. The conclusion is reached that the moon has only a daylight electron ionosphere rather than a krypton-xenon atmosphere, a conclusion which can be checked experimentally. Other studies of the evolution and nature of the lunar atmosphere, the lunar magnetic field, and the solar corona were undertaken by Vestine. It was concluded that the lunar atmosphere cannot exceed about 10^{-10} terrestrial atmoshperes, and that the lunar magnetic field is unlikely to exceed 200 gammas.

At NRL the distance to the moon was studied with the 50-ft reflector and a radar operating at 10.6-cm wavelength [*Yaplee,* 1958]. The distance measurements show an internal accuracy of about one-half mile. The echoing area of the moon is estimated to be about 975 square miles.

Meteors—Early calculations [*Singer,* 1952] dicated that substantial amounts of He^3 are duced in meteorites by cosmic-ray bombardm If constant average cosmic-ray intensity is sumed, the time of exposure of a meteorite a therefore, its date of creation can be calcula Several iron meteorites indicated an exposure t of 300 million years [*Singer,* 1954]. This view confirmed more recently by some H^3:He^3 m urements and especially by Öpik's calculation the 'lifetime' of an asteroid against sweep-up the planets. One view, therefore, is that a ma catastrophe, involving a collision of at least fair-sized asteroidal body took place as recen as 300 my ago. Some confusion exists concern the interpretation of the radiogenic helium meteorites; but this point could be settled perimentally [*Singer,* 1957 f]. The physical pro of meteorite creation in an interplanetary lision has been described [*Öpik* and *Singer,* 19

Extensive work has been carried out by Ö on the physical theory of meteors and their co cal relationships, including meteor cratering, properties and dynamics of interplanetary d and meteor phenomena in the atmosphere. latter subject deals with drag, mass loss, lumi ity, and more detailed physical effects on met as they traverse the ionosphere. It has been scribed simply [*Öpik,* 1958a] and is appearin the form of a monograph [*Öpik,* 1958b].

L. G. Jacchia has supervised the reduction accurate techniques of meteors photographed w the Super-Schmidt cameras under the Harv Meteor Program and has conducted research the physical nature of meteors through a st of their deceleration and fragmentation inside earth's atmosphere. He has found no clear evidence of the presence of hard-bodied met of asteroidal origin among 361 Super-Schm records analyzed. A comparison of visual photographic magnitudes showed that the 'c index' of meteors is independent of velocity bu strongly dependent on meteor brightness.

The radio meteor research program contin under the direction of Gerlad S. Hawkins. Vis meteor observations made in England betw 1930 and 1949 were analyzed by Hawkins J. P. M. Prentice, former director of the Me Section of the British Astronomical Associati Measurements of the width of meteor trails recorded on the National Geographic Socie Palomar Observatory Sky Atlas were made Hawkins, C. Payne-Gaposchkin, and F. L. Wh ple. The terrestrial data, extracted by Hawk and Richard B. Southworth from the 361 mete in the short-trail reduction program, will be va able in extending the physical theory of mete A radiometer supplied by the Air Force C bridge Research Center, through the coopera of Jules Aarons, and the observatory's 24-f radio telescope at the George R. Agassiz Stat have been used since January 1957 to measure fluctuation in intensity of the radio signals fr Cassiopeia A.

The meteor project, under the direction of F Whipple, has been continued at the observ station in Sunspot, New Mexico. The second s tion, formerly at Mayhill, was moved in A 1957 to Organ Pass, New Mexico, to lengthen baseline between the two stations. This reflect

nge in emphasis of the program. Observations present are directed toward the photography of sistent meteor trails which supply information the wind fields of the upper atmosphere and on structure of meteoroids. Photography of meteor ils continues at a reduced rate. Gunther wartz is superintendent of the New Mexico tions.

As in the past, the optical facilities of the teor project have been utilized to photograph cial rocket flights from Holloman Air Force se, Alamogordo, New Mexico. As part of a ic research program, the Air Force is 'seeding' upper atmosphere with known quantities of terials which interact with the atmospheric nponents to produce light. In the last year th ethylene gas and sodium vapor were released an attempt to determine the concentration of mic oxygen and atomic nitrogen in the atmos- ere above 100 km. Richard E. McCrosky, Allan Cook, and Richard Rodman are cooperating th the scientists of the Air Force Geophysics search Directorate in the analysis of these re- lts.

McCrosky, under the sponsorship of a Navy ntract, completed the reduction of 2500 meteors d has determined distribution statistics for eir orbital elements. This photographic study, owing the insignificant number of meteors that iginate outside the solar system and the pre- nderance of meteors closely confined to the liptic plane, confirms results obtained by radar servations.

Members of the meteor project published a ries of five papers on "Meteor Reduction ethods" [*Whipple* and *Jacchia,* 1957; *Hawkins,* 57; *McCrosky,* 1957; *Cook* and *Hughes,* 1957; *hipple* and *Wright,* 1957].

G. F. Schilling is directing basic studies towards e astrophysical utilization of the Cambridge ectron accelerator, presently under construction. s a source of continuum of ultraviolet radiation ith a power level of 6 Bev, unprecedented ex- rimental investigations of the reactions between is radiation and gases and solids will become asible. D. H. Tomboulian and D. E. Bedo from ornell University act as the principal consultants the project, and the study has reached the age of preliminary design for facilities and in- rumentation as well as the publication of funda- ental results on the average power spectrum.

John S. Rinehart is directing a newly oriented rogram of meteoritic research to resolve astro- hysical problems: specifically, a study of the rocesses that cause the ablation of meteorites uring their flight through the atmosphere; the esign and construction of an electron fluorescent -ray microanalyzer to be used especially for udying the distribution of nickel, iron, and cobalt ithin meteorites; the collection and identifica- on of airborne extraterrestrial material; the nding of an expedition to the Arizona Meteorite rater for determining the distribution of mete- ritic debris about the crater; and the determina- on of the ages of meteorites by radiochemical echniques.

The problem of photoelectric charring of dust articles in the solar system has been studied rom the theoretical point of view, and the dy- amics of the motion of dust particles has been considered [*Chopra* and *Singer,* 1958]. It is hoped that these studies will eventually be augmented by experiments with high-altitude rockets or satel- lites [*Singer,* 1956a].

Radio astronomy—At the new Radio Astronomy Station in Fort Davis, Texas, the 28-foot equa- torially mounted paraboloid antenna was com- pleted. Under the direction of Alan Maxwell, ex- perimental observations begun in August 1956 have revealed much new fine structure in the radio spectrum of noise storms and other low-in- tensity phenomena not previously recognized. A new type of solar burst was detected on the rec- ords in the form of an inverted U. Apparently it is caused by a disturbance moving outward through the solar atmosphere and then returning [*Maxwell* and *Swarup,* 1958]. All the radio ob- servations are being correlated in time with opti- cal observations of solar activity made at Sacra- mento Peak Observatory.

Equipment at Fort Davis to supplement the dynamic spectrum analyzer and 28-ft dish includes an interferometer for rapid position measurements of solar disturbances. It consists of two primary antennas, separated by 1000 meters on an east- west line, which accept simultaneous signals in the frequency range of 110–140 Mc/s. A sweep-fre- quency receiver is being planned to operate out- side the 100- to 600-Mc/s range of the existing equipment. Selected data from the Fort Davis Observatory are contributed to the IGY program.

The Naval Research Laboratory made observa- tions of the flux density of radiation from discrete radio sources at wavelengths of 1.8 cm, 3.15 cm, and 67 cm with the 50-foot reflector. The meas- ured radio radiation from the Crab Nebula [*Mayer* and others, 1957] at 3.15-cm wavelength showed a plane-polarized component in rough agreement with optical results. Contours of the radio brightness of the galaxy at 67-cm wave- length were derived for galactic longitudes from 320° to 347° and from 42° to 54°. The 1.8-cm wavelength is the shortest wavelength at which discrete radio sources have been observed.

The measurements of thermal radiation from the planets were extended to include the radiation from Jupiter at 3.15-cm wavelength [*Mayer* and others, 1958a, b]. The apparent brightness tem- peratures deduced from the 3.15-cm wavelength measurements were 600°K for Venus, 218°K for Mars, and 145°K for Jupiter.

Construction was completed on the largest radio telescope in the United States (also the largest equatorially mounted instrument in the world) at NRL's Maryland Point Observatory. Research programs with this instrument commenced in early 1958.

High altitude sounding—An aircraft-launched rocket system, the Rockair, has been developed [*Masterson* and *Ross,* 1957] and suitable instru- mentation has been designed for it. Several launch- ings were undertaken, but the method is not well suited to university research projects. It seems better suited to special meteorological studies.

A ground-launched 2-stage rocket, the Terrapin, was designed, and several test firings have been undertaken [*Singer* and *Lawrence,* 1957], as well as a very simple small one-stage rocket named the Oriole. It consists of a booster rocket on top of which sits a pencil containing instrumentation.

The diameter of the pencil has been made as small as 7/8 inch, with the result that the altitudes reached have been of the order of 100 miles.

Review papers have been written on high-altitude rocket research [*Singer,* 1956b] and on research with extreme-altitude vehicles [*Singer,* 1957e].

Cosmic-ray instrumentation was constructed for the Air Force's Farside rocket firings from Eniwetok in the autumn of 1957. Special counter and scaling circuits were designed to measure the increase in intensity with altitude to confirm previous calculations [*Singer,* 1957d] and to investigate the cause of the low-energy cutoff.

As a part of the IGY program at the State University of Iowa and the Jet Propulsion Laboratory, California Institute of Technology, an earth-encircling equatorial belt or ring of energetic radiation was discovered with the U. S. Army's Explorer satellites. Preliminary analyses indicate a mean electron energy of about 40 kev. The flux was about $10^9/cm^2 \cdot sec$, and an energy estimate is 10 $ergs/cm^2 \cdot sec$, according to Van Allen and his associates. Other results with rockoons confirmed earlier findings of a strong flux of x-rays in the ionosphere during auroral displays, referred to previously in the *IGY Bulletin.*

During the first four months of the IGY two series of IGY cosmic-ray balloon flights demonstrated that soft (x-ray) radiation is sometimes present at much lower altitudes in the atmosphere than was expected. Flights conducted by Kinsey Anderson of the State University of Iowa at Fort Churchill, Canada, during the summer of 1957 provided evidence of the close interrelations of cosmic rays, soft radiation, and geomagnetic activity. X-rays of perhaps 100 kev, observed during a magnetic storm, were attributed to bremsstrahlung from electrons incident on the atmosphere from outside. Bursts of soft radiation at balloon heights at Minneapolis were reported by J. R. Winckler and L. Peterson of the University of Minnesota as the result of another summer program of IGY balloon experiments in 1957. Measurements of this radiation were consistent with x-rays in the 50- to 70-kev range, also attributed to bremsstrahlung. In this work, however, the radiation was directly correlated with visual auroral phenomena.

At the University of Minnesota, Freier, Ney, and Waddington noted from balloon-flown photographic emulsions that the primary α-particle flux at sunspot maximum appears to be about half that at sunspot minimum. Winckler, Peterson, Arnoldy, and Hoffman noted bursts of x-rays beneath strong auroral-ray arcs. Energies of 50 to 100 kev were noted. One burst was measured at a height of only 70,000 ft. The current of electrons is at least 3×10^6 $electrons/cm^2$ sec.

An IGY Aerobee-Hi fired at Fort Churchill, Canada, carried radio-frequency mass spectrometers to measure the gas and ion composition of the upper atmosphere [*Meadows* and *Townsend,* 1958; *C. Y. Johnson* and others, 1958]. The results showed that diffusive separation was present in the atmospheric gases above 105 km. The separation appeared to being in the 90-km region. Positive ions were detected in the region from 90 to 251 km. These ions are identified as Mass 30 (NO), Mass 32 (O_2), and Mass 16 (O). During the flight a negative ion was detected at M
46 (NO_2).

During the past year data from two rock
fired at Fort Churchill, Canada, as part of
IGY Rocket Program have been analyzed [*L*
Gow and others, 1958]. Both rockets carried
experiments, one pertaining principally to lo
altitude structural parameters and the other
the high-altitude parameters. These data show
that the values of atmospheric density in the lo
regions, 30 to 45 km at 59°N, were the same
slightly less than the values obtained over
White Sands Proving Ground. At high altitud
the density at 200 km, measured during a summ
day at latitude 59°N, was 2½ times as great
that obtained on a winter day and 20 times
great as that obtained on a winter night.
measurement of the summer-day density was 6
times the corresponding White Sands value
1.4×10^{-7} $gm/meter^3$.

H. K. Kallmann, of The RAND Corporati
reported that the distribution of electron dens
with height, as observed with rockets, is reac
explained quantitatively when various atmosph
constituents are ionized by the ultraviolet
x-ray radiations. She has recently been consid
ing the possible role of x-rays in producing ra
fadeouts. She further stressed the importance
providing a summary report on the recent e
mates of electron densities based data from ro
ets and satellites.

Data taken from the flight of Aerobee 33
NRL workers at the White Sands Proving Grou
with a proton precessional magnetometer h
shown that the earth's main magnetic field
creases more rapidly than would be expected
a dipole field. Measurements of the field w
made to an altitude of 163 km with an accur
of $\pm$ 10 gammas. No discontinuities were observ
during E-region transit; hence it is assumed t
there were no ionosphere currents present at
time of firing.

Cosmic rays—S. A. Korff reported that the C
mic Ray group at New York University has
dertaken work in connection with IGY progra
sponsored in part by the NAS-NSF-IGY gra
and assisted also by the joint ONR-AEC p
gram. A neutron monitor was installed and is
operation at the University of Alaska. The mo
tor is located at Ballaines Lake, two miles no
and west of College. It commenced operati
there during 1957. The data from the meter w
sent to New York, and copies were sent to
IGY World Data Center A. Two 'Forbush ty
decreases were noted, and all tests have indica
that they were real. Several other fluctuatio
both increases and decreases, were also observ
but some of the increases were observed w
only one of the two parts of the meter was wo
ing properly and hence it is uncertain whether
liance can be placed upon the readings. The wo
is being continued and promises to yield results
much interest.

The series of neutron cosmic-ray balloon flig
was continued. In connection with these flights
great deal of work was devoted to the inst
mentation, and a fairly sophisticated system
been developed—a new hypsometer for meas
ing pressure, and a new telemetering system w
1680-Mc/s transmission and automatic track

nd recording. Much progress on the instrumentation was achieved.

Further work was also done on quantitative calculation of the rates of production of various sotopes by cosmic radiation and, in particular, by neutrons. All the neutrons that are produced eventually make new isotopes. Whereas many of he secondary and primary protons and other particles have energy enough to produce isotopes, nost of their energy is lost in production of ionization, and hence charged particles are not a major factor. The balance of the neutrons was computed. The principal unknown at present is the amount of tritium produced, which, as Libby has shown, nay be very much greater than has been supposed.

The effects of the interplanetary medium on he propagation of cosmic rays were studied [*Beiser,* 1958]. The material between the sun and he earth appears to be largely ionized, so that tangled magnetic fields of the order of a few nicrogauss, but of variable directions and magnitudes, diffuse through the region. These fields are nfluenced by charged-particle radiation from the sun, and they, in turn, affect the propagation of cosmic rays through the region. It has long been evident that fields are necessary to explain the storage phenomena evidenced by the famous flare of February 23, 1956, in which radiation reached the dark side of the earth only minutes after it reached the sunlit side.

Further, an analysis was made which showed that cosmic-ray intensity, and presumably the magnetic field of the earth, has not changed by large factors in the last 15,000 years. This analysis was in part stimulated by a report that an analysis of some old bricks showed that the earth's field was very different at the time they were baked than now, with the consequent suggestion that the basis for radiocarbon dating should be re-examined. The analysis showed that the basis for doubting radiocarbon dating is much less significant than the earlier published reports had indicated [*Beiser,* 1957].

At the University of Maryland some considerations have been noted concerning the acceleration of particles to cosmic-ray energies in the vicinity of solar flares [*Singer,* 1957c]. Effects presumed to detect cosmic-ray increases during small flares have been noted in an aircraft flying at high geomagnetic latitudes [*Corrigan* and others, 1958].

The decreases are larger in polar stations than elsewhere, and a model explaining cosmic-ray decreases during magnetic storms has been studied. This model has been developed further to explain, in particular, the absence of non-relativistic cosmic-ray particles (the so-called latitude knee or low-energy cutoff) which is prominent during years of high solar activity [*Singer,* 1957b].

As part of the IGY program cubical monitor telescopes were installed near the geomagnetic poles, at Thule, Greenland, and Wilkes Coast, Antarctica. Special high-counting-rate telescopes, designed to back up the cosmic-ray airplane flight, were installed at Climax, Colorado (11,300 ft) and Sulphur Mountain (7,500 ft), near Banff, Canada. Data are being reduced.

At Harvard E. L. Fireman continues to study stable and radioactive isotopes produced by cosmic rays in meteorites and by high-energy particles in targets. He also collaborated with J. Zähringer to measure the depth variation of tritium and argon-37 produced by high-energy protons in iron.

At NRL the intensity of the primary helium component of the cosmic radiation near the geomagnetic equator was measured with nuclear emulsions as detectors. The data were obtained in a balloon flight near the Galapagos Islands (10°N geomagnetic) at a mean pressure altitude of 15 gm/cm^2. The flux of primary helium at this latitude was found to be 22.3 ± 2.0 particles/m^2·sec·sterad. The energy spectrum of the He component has been determined by combing the NRL results with those obtained at other latitudes. The intensity of particles with total energy per nucleon exceeding W was found to be proportional to $W^{-1.5}$ [*Shapiro* and others, 1958].

At the University of Chicago, California Institute of Technology, Department of Terrestrial Magnetism, and the University of Minnesota considerable additional work on cosmic rays was presented at the Symposium noted. Meyer at Chicago measured changes in α-particle flux associated with solar events.

Magnetic variations—S. Matsushita of CRPL and High Altitude Observatory has studied relations between large magnetic-bay disturbances in the auroral zone and solar phenomena; he found that solar flares occurring one to two days earlier than the magnetic-bay disturbances, particularly those with solar-radio bursts, were occasionally associated.

Magnetic disturbance occurred most frequently and with the greatest intensity at night in the auroral zone and around *noon* in the polar zone. This shows that the behavior of the solar particles was affected by the earth's magnetic field. Those disturbances in the auroral and polar zones often occurred even on days which were very quiet in middle and lower latitudes.

In a period of several consecutive magnetically quiet days, it appeared that even outstanding solar phenomena, which usually produce magnetic disturbances and storms (for example, a solar flare of importance 3 with a major solar radio burst) were not accompanied by any disturbance, even in the auroral or polar zones. Lowered ionization in the outer atmosphere of the earth during these long periods of quiet might produce this effect; the fact that whistler atmospherics were not observed during these days is additional evidence.

Some preliminary interpretations by Matsushita of early results of a research undertaken jointly by Masahisa Sugiura (Geophysical Institute, College, Alaska), S. Matsushita (HAO-CRPL) and R. B. Norton (CRPL) indicate interesting findings for ionospheric storms. Ionospheric F2 density variations in the ratio $(N-N_{median})/N_{median}$ during strong and weak storms in low and middle latitudes were studied from the data collected during ten years (1946–1955) at 38 ionospheric stations between 60°N and 60°S, geomagnetic. Fifty-one strong and fifty-eight weak storms occurred during that period.

Storm-time variations of F2-region ionization in geomagnetic latitude ranges of 35° to 60° in both hemispheres showed a decrease (20 to 40 per cent during strong storms and 10 to 20 per cent during weak storms) after an initial short

increase of about 15 per cent for both strong and weak storms. In equatorial regions, however, storm-time variations showed the opposite phase: generally an increase (about 20 per cent for strong storms and about 15 per cent for weak) after an initial short decrease (about 10 per cent for strong storms and something less than 10 per cent for weak). The variations in the equatorial region did not show any notable seasonal changes. The variations in geomagnetic latitude range of 10° to 35°, however, had a measurable seasonal behavior; the variations in winter were of the equatorial type and those in summer were of the higher latitude type. In higher latitudes, storm-time variations in summer showed the greatest decrease.

The maximum of local time variations of F2 density during strong storms occurred at 06 to 18 h local time in geomagnetic latitude ranges of 50° to 60°N; at 18 to 06 h in 10° to 50°N, and 03 to 09 h in 10°N to 10°S.

In the auroral zone at night, slant E*s*, gradual blackout, and complete blanketing of F2 by E*s* were accompanied by magnetic-bay disturbances (and bay-shaped disturbances during storms). Differences between blackouts which occurred at night and in the daylight hours were also studied.

Further aspects of ionospheric behavior during disturbances were investigated in order to find the morphology of ionospheric storms in the auroral and polar zones. Spread echoes may be explained by many blobs due to turbulent motions and drift forces. Rapid decrease of density during storms and the 'G condition' may be explained by the following reactions:

$$O^+ + O_2 \rightarrow O_2^+ + O$$

$$O_2^+ + e \rightarrow O' + O''$$

assuming that the F2 layer may have abundant O_2 due to vertical transports from lower level by turbulence.

M. Sugiura and E. H. Vestine have collaborated in a study of the function of electric fields in the auroral regions in causing world-wide sudden commencements. Studies of the effect of electric fields that originate in the E region upon F-region height, were also undertaken for the magnetically quiet days, on a day-to-day difference.

V. P. Hessler has continued his studies of electric and magnetic fluctuations at the earth's surface. North-south earth potentials have been recorded continuously during the year at College, Alaska, with a Brown recorder at a chart speed of 6 in/hr. A fluctuation-frequency counter has been recording earth potentials for several months. An operations pen indicates every tenth cycle on the earth-potential trace. The cycle counter is sensitive to fluctuation amplitudes of 4 mv/km with a full-scale instrument range of 1000 mv/km. The records are being scaled continuously for cycles per hour and for frequency range during rapid-fluctuation disturbance.

At the University of Alaska the study of magnetic storms has been continued under the direction of M. Sugiura. The analysis is nearing completion for the great storms. Calculations are being made to determine the DS variations over the first three days of the storm so that comparisons may be made with similar results previously calculated for weak and moderate storms.

A special IGY research study was recently begun by J. C. Cain for the analysis of data from the many magnetic stations operating in Alaska during the IGY. J. A. Simpson has initiated a broad study of cosmic-ray and related data, and a group at the High Altitude Observatory, under W. G. Roberts, is engaged in theoretical studies based on IGY solar and related high-atmosphere data. These programs are part of a special program sponsored by the National Academy of Sciences.

During the past three years an increasing amount of the effort of the Physics Department, University of Maryland, has been devoted to describing a model of magnetic storms and auroras which takes account of the fact that the earth is embedded in a tenuous gas of high conductivity. The motions of charged particles in the vicinity of the earth and their behaviour as they enter the earth's atmosphere were studied [*Rhode*, 1955].

Also studied was the trapping of these charged particles in the earth's magnetic field. From these considerations it was possible to calculate the drift of the particles and to identify this drift current as the ring current flowing beyond the atmosphere, responsible for the main phase of magnetic storms. The conductivity of the gas in the earth's environment is severely cut down by the earth's magnetic field so that the shielding effects are not perfect, but the currents responsible for the sudden commencement are thought to flow mainly in the earth's upper atmosphere. This agrees with the analyses of Vestine and others and can best be understood on the basis of a shock wave model of the interaction of the solar gas with the earth's magnetic field [*Singer* 1957a].

Aurora and airglow—The problem of the acceleration of the solar protons to auroral energies has been treated recently in terms of an acceleration mechanism which exists in the immediate vicinity of the earth and acts upon the trapped particles [*Singer*, 1958]. This acceleration mechanism is produced by hydromagnetic waves traveling along the lines of force and is responsible also for the geomagnetic micropulsations. The bunching of the protons, which has to be postulated in the acceleration mechanism, fits well with the emissions of VLF radiation observed by Gallet. The result of this acceleration mechanism is a distribution of velocities of the auroral protons rather than a unique velocity, and this is in agreement with recent findings by Chamberlain.

During 1955–1956 an experiment to investigate the day airglow by means of a balloon-borne high dispersion spectrograph was begun. One test flight was carried out. The work is continuing.

During 1957 equipment was constructed to detect auroral γ-rays from the reaction N^{14} (p, γ). One test flight was carried out in an aircraft. The experiment is being redesigned for balloon flight.

In a paper for the National Institute of Sciences of India, Chapman has published the results of historical research into the great aurora which occurred on February 4, 1872.

J. Chamberlain reported that the program of observation and theoretical research on the aurora and airglow has been continued at Yerkes Observatory. A recent analysis and interpretation [*Chamberlain*, 1957] of the profiles of hydrogen lines in auroral spectra indicated that a rath-

arge dispersion in the speeds suggests that the uroral particles are accelerated in the neighborood of the earth. A review on "Theories of the Aurora" has recently been published by *Chamberlain* [1958a].

A program of the measurement and analysis of igh-dispersion plates of the auroral hydrogen lines nd of the low-dispersion spectra obtained with he IGY patrol spectrographs at Yerkes and Shingleton, Michigan, is being conducted by Chamberain and V. Pesch. It is hoped that this program vill serve as a pilot analysis for the reduction of he IGY patrol-spectrograph films.

The theoretical program on resonance scattering by atmospheric sodium is being extended. A reent collaboration by Chamberlain, Hunten (University of Saskatchewan), and Mack (University of Wisconsin) has produced paper IV on the abundance of sodium in twilight [*Chamberlain* and others, 1958]. *Brandt* and *Chamberlain* [1958] have developed the theory of the day airglow n the sodium D lines to predict the intensity and D_2/D_1 ratio as a function of sodium abundance, zenith distance of observation, and angle of incidence of sunlight. It appears that extended observation of the dayglow from balloons could result in important information on the origin of atmospheric sodium and could also give valuable information on atmospheric winds at the 85-km level.

A theoretical discussion of the origin of the oxygen red lines in the twilight and night airglow has recently been published by *Chamberlain* [1958b]. Resonance scattering by atomic oxygen in the upper atmosphere is inadequate to explain both the absolute intensity of the twilight airglow and the rate of decay after sunset. Similarly, dissociation of molecular oxygen in the Schumann-Runge region will not entirely explain the observations, although dissociation is probably a more important effect than is resonance scattering. A majority of the twilight and night airglow seems to arise from dissociative recombination of O_2^+, which is the main process by which the F layers recombine. The rate of recombination in the F layers after sunset agrees well with the observed rate of intensity decrease in the evening. Mechanisms responsible for deactivation of the red lines have been considered in a paper by *Seaton* [1958].

Continued laboratory experiments on auroral excitation problems have been devoted to the interpretation of rotational temperatures in auroral spectra. *Roesler* and others [1958] have found that nitrogen molecules excited by proton collisions at intermediate energies between 10 and 30 kev give rotational temperatures that correspond closely to the kinetic temperature. Similar results were reported by *Carleton* [1957] for very low energies (about 3 kev). However, it is less certain that high-energy protons or fast electrons that simultaneously ionize and excite the nigrogen molecule will lead to rotational temperatures that are indicative of the air temperature.

Under K. C. Clark, the division of atmospheric physics at the University of Alaska has been responsible for the auroral photography and spectroscopy programs for the IGY. All-sky cameras and spectroscopic and photometric equipment have been operated at a network of Alaskan stations. The IGY patrol spectrograph operates continuously, providing alternating 30- and 90-minute exposures resolved along the north-south magnetic meridian at an 8A resolution. The longer exposures regularly show the presence of hydrogen emission in the aurora and other regions of the sky.

A Hunten scanning spectrometer has been installed in a versatile sky-scanning mount which turns on an axis parallel to the direction of magnetic zenith and scans along auroral rays centered at the magnetic zenith. The spectrometer is being directed to problems of height-luminosity ratios of auroral lines pertaining to different excitation processes. Time-resolved spectra of emission at the magnetic zenith are obtained on a routine, all-weather basis with the Huet f/0.6 prism spectrograph. The prior occurrence of $H\alpha$ and $H\beta$ relative to auroral emissions by N_2^+ is well established on a statistical basis, but the distinction in time relative to other prominent emissions is less well established.

To distinguish between time and motion as causes of a given increase in spectral intensity, a new meridian mirror spectrograph was developed and placed in operation. This instrument uses the flat image of a curved external slot formed by a convex all-sky mirror and photographs it through a blazed transmission grating. The resolution is broadened to 24A to give optimum sensitivity to the broad $H\alpha$ line. No collimating lenses are required when the grating operates at minimum deviation. The increased speed of this spectrograph automatically gives good hydrogen detection at regular 15-minute exposures through one week. Preliminary studies of data at this increased time resolution show that hydrogen emission characteristically precedes the auroral development as the display moves south, and it characteristically disappears as the first positive emission of N_2 develops in the later stages.

The great red aurora of February 10, 1958 was recorded, often with over-exposure, by numerous all-sky cameras in Alaska. With the Huet and IGY patrol spectrographs spectra were obtained which showed unusually strong development of infrequently noted lines and intensity distributions that are characteristic of relatively high concentrations of slow electrons and protons.

W. Murcray has made some observations of the relation of atmospheric emission in the 9.6-micron band of ozone with auroral displays. Auroral emissions in the zenith were monitored during the past season with a photoelectric photometer on the wavelengths 3914, 6300, and 4861A ($H\beta$). The records on 4861A appear to show (in addition to the features noted in the spectrographic studies) that $H\beta$ is definitely present in active aurora, although it is not present at lower latitudes. Statistical studies of auroral luminosity at wavelength 3914A have been made and the results are being prepared for publication. One such result is that the diurnal variation of auroral luminosity rises to a maximum at about 0100 local time and remains constant thereafter until daylight stops observation. Further, a correlation coefficient of 0.6 was found between auroral luminosity and sporadic-E ionization as measured by $(FE_s)^2$. Preparations are being made for photometric observations of the night sky, twilight, and aurora with a rapid-scanning photometer which has a bi-refringent filter.

W. N. Abbott has been carrying out studies within the auroral program of the IGY. Data from auroral spectra are being studied for the purpose of investigating possible relations between characteristics of the auroral spectra, and excitation and collisional deactivation in relation to height and various atmospheric quantities.

Gerald Romick and C. T. Elvey have made a spectroscopic study of the variations in intensity of the hydrogen emission line Hβ during auroral activity. They made a qualitative analysis of the auroral spectrum that is incident from the magnetic zenith and estimated the intensity for Hβ (4861A) and the 4709A line of N_2^+. Their results show that the peak in intensity of the Hβ precedes that of the 4709 line by one to four hours. During this period of maximum Hβ, quiet forms of the aurora are present and the records of N–S earth potential exhibit low-amplitiude, low-frequency fluctuations. The over-all fluctuation of earth potential is highly correlated with the intensity variations of the 4709A line of N_2^+ and with the type of aurora present at the zenith.

Data from Aerobee rockets 33 [*Heppner* and *Meredith,* 1958] and 31 [*Tousey,* 1958] flown at the White Sands Proving Ground confirmed and supplemented data on the night airglow that was reported previously by NRL. It was shown that the 5577Å oxygen line originates in the region from 85 to 120 km and that maximum luminosity was at 97 to 98 km. Aerobee 33 showed a sharp lower boundary to this emitting region. The sodium D lines were found to originate between 80 and 115 km, with a possibility of faint emission extending to 140 km. Maximum luminosity was at 93–95 km. Aerobee 33 data indicated that the 6300A line of oxygen originates above 163 km and that the Meinel OH bands (9–3) and (8–2) are emitted primarily in the region from 56 to 100 km. Radiation near 2700A, presumed from Herzberg bands of O_2, was measured from Aerobee 31 and was found to have peak luminosity near 100 km.

The recording of vertical-incidence penetration frequencies and other parameters has been continued at the University of Alaska with the C–3 ionosphere sounder under contract with the National Bureau of Standards. A C–4 sweep-frequency sounder has been installed and is currently in use at oblique incidence with a fixed rhombic antenna beamed between magnetic and true north. A three-frequency HF back-equipment is also in routine operation, under an IGY contract. The latter two sets of equipment are giving information on direct scatter of radio waves from auroral ionization, and also on the oblique incidence-reflection properties of the arctic ionosphere.

Propagation of radio waves—Refraction and diffraction have been studied using the Cygnus and Cassiopeia radio sources at 223 Mc/s and 456 Mc/s. More than 12 months' data have been obtained on each of the above frequencies with phase-switch interferometers operating between two sidereally mounted radio telescopes, 28 ft in diameter. Several months' data have also been obtained at 223 Mc/s with a phase-sweep interferometer system and the same antennas. Analysis of the data has shown the following:

(1) The radio star scintillations show a rather weak diurnal variation, maximum at about midnight. The variation is very much less than at temperate latitudes.

(2) No strong elevation-angle effect occurs over the range of zenith angles from 6° to 75°. The scintillations are strongest in the zenith; they decrease with increasing zenith angle to about 60° and then increase again. This behavior is also different from that at low latitudes.

(3) Fading rates of up to about 1 cps have been observed. Limited observations have failed to reveal appreciable scintillation activity in the frequency range of 1 to 20 cps.

(4) Long-duration fades, lasting many minutes, have been observed on both the 223 Mc/s and 45 Mc/s interferometers. These fades are attributed to the occurrence of intense, localized irregularities in the ionospheric electron density—irregularities which cause the diffraction pattern on the ground to have structure smaller than the separation of the antennas (100 yards). This is a new observation, and it has recently been confirmed by observers at lower latitudes. The absence of similar reports in previous years seems to imply the presence of smaller or more intense electron clouds than in previous years.

(5) The intensity of the scintillations of the Cygnus source, averaged over a 12-month period, was significantly greater than that for the Cassiopeia source. This effect is not due to difference in zenith angle and may be associated with the smaller angular diameter of the Cygnus source. The results are consistent with the idea that the irregularities are elongated along the geomagnetic lines of force.

The scatter of radio waves from auroral ionization is being studied by a network of five 41-Mc auroral radars in Alaska. These, with three similar stations in the northern United States and one Macquarie Island, are operated as one of the USNC-IGY programs. Scaling and analysis of the data is about to begin.

The absorption of radio waves is being investigated at six Alaskan stations using 'riometers' developed at the Geophysical Institute. Seven other identical sets of equipment are being operated in the United States, Canada, Greenland and Sweden, as part of the IGY program. These stations will provide the first quantitative measurements of radio-wave absorption around and across the auroral zone. A paper describing some three years' observation of ionospheric absorption in Alaska has been published [*Little* and *Leinbach* 1958]. It gives information on the diurnal and seasonal variations in absorption activity, on the size and location of the absorbing regions, and on the relation between absorption and magnetic and auroral activity. L. Owren reported on several experiments which are being carried out in the radio physics division to determine the effect of solar fluctuations on the auroral-zone ionosphere. The radio emission from the sun at 65 Mc/s has been monitored with a total-power interferometer since February 1956. The solar radio observations are used qualitatively for local predictions of aurora activity.

Analyses of the HF transmission data secured by the Signal Corps in Alaska during 'Experiment Aurora' have been completed. Experiment Aurora extended over a 76-month period, from June 19 through October 1955, and included periods both of high and low solar activity. CW signal tran

missions at 6, 8, and 12 Mc/s short (350 km) and long (1100 km) paths parallel to and crossing the auroral zone, were recorded. The main conclusions of the analysis are:

(1) The best transmission frequency over the short paths was 4 Mc/s which showed an average monthly signal in-time of 76.5 per cent whereas the best transmission frequencies over the long paths were 8 and 12 Mc/s. The average monthly signal in–time on 8 Mc/s was 62.5 per cent. Signal in-time on these 8- and 12-Mc/s long paths showed a significant increase during the summer months. No seasonal effects were established on the other paths.

(2) The signal outages over the short paths were analyzed for a year of high and low solar activity. Almost all outages were caused by ionospheric D-layer absorption, which was mainly a daytime phenomenon peaking in the early midday hours. There was a strong seasonal variation in outage time, with large maxima occurring during the equinoctial months. The signal out-time varied with the relative sunspot numbers both seasonally and yearly. On all frequencies the out-time in 1949–1950, the high solar activity year, was about twice that in 1954, the low activity year. The short-path signal outages were also strongly correlated with the local geomagnetic activity.

(3) The propagation modes involved in auroral–zone HF transmission could not be established, in general, on the basis of such ionospheric parameters as critical frequency and virtual height near the reflection point. The probable reasons for this failure include ionospheric absorption, high incidence of sporadic ionization, and the effect of earth's magnetic field on high-latitude ionospheric soundings. Short-path 12-Mc/s transmission was found to depend primarily on sporadic ionization. Short-path 4-Mc/s daytime transmission can be explained in terms of the normal changes in the F2 and E layers with the sunspot cycle, solar control of the ionization, and D-layer absorption. Detailed seasonal variations in the relative strength of S-N and E-W propagated signals over the 4-Mc/s short paths depend on the combined effects of forward scattering by ionospheric irregularities and absorptions. Long-path 12-Mc/s daytime transmission can, in general, but not entirely, be understood in terms of F2-layer conditions and D-layer absorption. Nighttime transmission over short and long paths must be associated partly with F-layer ionization and partly with 'Night-E' and sporadic-E ionization.

(4) Auroral ionization affecting HF transmission is estimated as being present 20 per cent of the time. This figure is not expected to vary much over a sunspot cycle [*Owren* and others, 1958].

Another experiment has been reported by L. Owren and R. A. Stark concerning "HF Backscatter Soundings and Forward Pulse Transmission"; 250,000 PPI recordings secured during 1956 with a continuously operating 12-Mc/s backscatter sounder (rotating antenna system) have been studied with regard to groundscatter and long-range auroral echoes. The F-layer propagated groundscatter echoes show a daily and seasonal variation consistent with solar control of the F-layer and the characteristics of high-latitude ionospheric absorption.

The groundscatter echoes propagated by sporadic E show that nighttime-E ionization in or near the auroral zone can support HF propagation on a semi-regular basis during all seasons. During 1956 there was, on the average, sufficient ionization to propagate 12-Mc/s pulses over some one-hop ionospheric path 95 per cent of the time during the day. This figure varies from 70 per cent of the day during the midwinter months to 100 per cent during the summer season because of the seasonal variation in F-layer ionization [*Owren* and *Stark*, 1957].

Short-range auroral echoes occur mostly at night, with maximum activity near magnetic midnight, and exhibit the characteristics of aspect-sensitive backscatter. At 12 Mc/s direct backscatter from field-aligned columns of auroral ionization is received at off-perpendicular angles up to 25 degrees. The long-range auroral echoes, which are defined as those received by ionospheric modes, have two daily maxima of occurrence. The primary maximum occurs during the afternoon, the secondary maximum near magnetic midnight. The echoes have ranges between 1400 and 2400 km and azimuths within 75° of geomagnetic north. The average duration is less than 5 minutes. The long-range auroral echoes depend on F-layer propagation during the daytime and Es propagation at night. The long-range echoes have been classified in five types which include 99 per cent of all such echoes. Propagation modes have been derived for all five types and are mostly of the zig-zag or billiard-ball kind, insensitive to range. Some modes are aspect sensitive. The auroral echoes are found to originate at E-layer heights. Long-range auroral echoes occurred on the average during 19.5 per cent of the day.

Forward-pulse propagation at 12 Mc/s between College and Barrow, Alaska, was sustained by the ionosphere during 76 per cent of the one-month experiment. These pulses were mostly strong, discrete, and slowly fading. Trains of two pulses were observed 14 per cent of the time, the second pulse being always diffuse and rapidly fading. The delay time relative to the first pulse varied from 1 to 6 milliseconds. Whereas the first pulses could be shown to be propagated by a regular one-hop ionospheric mode, the delayed, diffuse pulses were found to be backscattered from auroral ionization located beyond Barrow by means of one of the five main, long-range modes.

A small program relating to the preparation of instantaneous synoptic world maps of the ionosphere is under way at CRPL. To date synoptic maps with the critical frequency of the F2 layer used as the parameter have been prepared for 1200, 1600, and 2000 UT on a magnetically quiet day (March 8, 1956) and for 1200 and 1600 UT on a disturbed day (March 22, 1956). A number of interesting points pertaining to the drift of high and low regions are suggested by this preliminary set of maps.

Two IGY Aerobee-Hi rockets at Fort Churchill were used to measure the electron distribution to as high as 240 km using the Seddon propagation experiment. NRL workers have found that these data show a very dense, low D region during the time of a polar blackout. The electron distribution in the E and F regions is quite similar to the distribution observed over the White Sands Proving Ground [*Seddon* and *Jackson*, 1958].

E. Tandberg-Hanssen [1958] has examined the

relationship at High Altitude Observatory of F1 layer virtual heights to geomagnetic disturbances and found, as expected from *Parker's* [1956] suggestions, that there appears to be about 10-km elevation of these layers at the time of geomagnetic disturbance.

J. Warwick, R. H. Lee, and H. Zirin have been giving attention to problems of ionospheric absorption and refraction. Two new instruments have been built, one a large steerable interferometer for 18- to 20-Mc/s signals of radio 'stars,' and the other a cosmic radio noise meter. Both are in use to determine solar influences on the ionosphere.

Whistlers—J. H. Pope reported that whistlers and chorus have been studied at College, Alaska, to determine the change in characteristics of these phenomena at high latitudes.

Chorus shows a diurnal variation in its occurrence and strength which differs considerably from that at low latitudes. The maximum occurs at about 1400 local time as contrasted with maxima during the morning hour for stations at lower latitudes. A consideration of the local times of maxima for various stations shows a systematic variation with geomagnetic latitude [*Pope,* 1957].

It has been found that the correlation between chorus and magnetic activity, as expressed in the daily *K* figures, undergoes a remarkable seasonal variation. The correlation is positive during solstices and negative during equinoxes. This result is contrasted with those for lower latitudes which show little or no seasonal variation in this coefficient.

Two networks of automatically operated recording stations have been installed and placed in operation as part of the IGY program. These stations are making simultaneous observations of audio-frequency atmospherics from the Arctic to the Antarctic. The results obtained, along with other correlated geophysical observations, will be studied at Dartmouth, Stanford, NRL, and elsewhere in an attempt to define more precisely the whistler mode of propagation and to explain the origin of other types of audio-frequency emissions that are commonly associated with high magnetic activity.

From a theoretical study of turbulence in the ionosphere, David Layzer has developed a new interpretation of the Richardson number and a new estimate of the rate of turbulent dissipation in the ionosphere.

Helliwell, at Stanford, has provided some results on whistlers. One network of IGY stations operates in the general vicinity of the 75°W and is under the supervision of Dartmouth College. The other IGY network includes New Zealand, Australia, Alaska, and the west coast of the United States and is supervised by Stanford University. Tape-recorded whistlers are analyzed for their dispersions which depend on the integrated electron density along the path of propagation. Density values of the order of 10^2 to 10^3 electrons/cc are found to distances of several earth radii. Information on electron density profiles and the strength of the earth's field in the outer inosphere is being sought with the aid of 'nose' whistlers.

Data on whistler-mode propagation have been obtained from a new experiment in which special pulse transmissions from NSS on 15.5 kc/s were received at Cape Horn, 10,000 km distant. Th measured time delays, from 0.3 to 0.9 sec, wer essentially the same as those from whistlers. Th confirms Storey's theory of whistler propagatio Large variations in time delay from day to da suggested marked changes in the characteristics the propogation path through the outer iono sphere. However, no clear-cut correlation wi magnetic activity could be found.

Audio atmospherics of another type, terme 'VLF emissions,' are closely associated with mag netic activity and sometimes with whistlers. The are thought to result from the entrance of sola corpuscular radiation into the outer ionosphere It has been suggested that the observed signa arise from selective traveling-wave amplificati of ambient noise in the outer ionosphere. Furth tests and study of this hypothesis are in progre The theory, if correct, might provide a new mea of measuring the properties of solar corpuscul streams [*Helliwell* and others, 1956; *Gallet* an *Helliwell,* 1957; *Helliwell* and *Gehrels,* 1958].

Meteorological relations—Carol Echols at t University of Alaska Geophysical Institute h carried out a study of solar radiation and radia heat exchange in order to determine their effe on the micrometeorology at high latitudes.

Another area of cosmic-terrestrial relationsh is in the detailed study at the High Altitude O servatory of possible influences of solar corpusc lar emission on upper atmospheric circulation the higher levels of the meteorological layers. Sp cifically, the correspondence between large a abrupt rises of geomagnetic disturbance with t magnitude of trough developments at 300 mb the fall and winter of 1956–1957 has been studie It is claimed, in the short period studied, tha there is a definite tendency towards weaken trough development and zonal wind flow at tim of lower geomagnetic activity, and the sharp d velopment of meridional atmospheric flow at 3 mb in the eight days following the occurrence of substantial geomagnetic disturbance has bee noted.

Hurd C. Willett reported that he has been ab to organize some climatic and solar data for co tinued studies in the area of solar-weather rel tionships, when funds for this work become ava able.

S. Fritz, U. S. Weather Bureau, reported abo work to determine whether the variable emissio from the sun influence the circulation or 'weathe of the troposphere and lower stratosphere. This the 'solar-weather' relations problem. The presen state of the 'art' is summarized by *Roberts* [195 and by the American Meteorological Society 1957. The A.M.S. notes that "Efforts to find co nections between solar activity and weather ha so far mainly been based on a statistical approac Some few results have been obtained that a highly suggestive. But none of these studies h yet produced any conclusive evidence that rel tionships exist. Whether any of the more encou aging results are of practical importance f weather forecasting is a question which at prese cannot be answered affirmatively." Moreover, "N physically acceptable mechanism has been pr posed yet by which variations in the solar ener output could directly or indirectly influence t lower atmosphere." Many lines of research in

both the solar and weather parameters are suggested by Roberts. But so far statistical studies are the only ones which have been carried out.

A few of the many statistical studies which have appeared in the literature are: *Wexler* [1956], *Shapiro* [1956], *Woodbridge* and others [1957]. Wexler shows relations of Northern Hemisphere pressure, temperature, and precipitation in relation to maximum and minimum of the sunspot cycle for the month of January. Computations of the temperature relation are being extended to include each month of the year.

Shapiro is extending his study of persistence in atmospheric circulation pattern to the European area.

A few of the physical quantities and possible suggested methods, with their limitations, by which the variable sun might influence the lower atmosphere have been discussed by *Fritz* [1957].

Smagorinsky reported that a number of research groups in the United States and elsewhere have been working toward the application of numerical techniques to the study of the dynamics of atmospheric evolutions. Whereas shorter-period evolutions of the order of one day are for the most part inertial, depending very little upon external sources or sinks of energy, longer-period evolutions, from 5 days to climatic time spans, become increasingly controlled by these external influences. Some effort is being made to construct models that possess the ingredients thought to be mainly responsible for these longer-period evolutions. Quite obviously, the influence of solar radiation must provide the ultimate driving force. It is not yet known how sensitive the atmospheric circulation is, particularly that of the troposphere, to variations in the solar spectrum. It is reasonable to expect that as progress is made in developing adequate models suitable for describing longer-period evolutions of the atmosphere, meaningful experiments can be performed in simulating solar variations. It would appear that only by means of such experiments can reliable quantitative estimates be made. Most of the work in this field is in a primitive state, and it may be some time before we are in a position to arrive at conclusive results regarding the nature and magnitude of solar-terrestrial influences. However, this note is offered to indicate the potential of techniques now being developed.

Appendix 1

On the recommendation of the Committee the following papers were presented by invitation at the May 1958 AGU meetings. Walter Orr Roberts served as Chairman.

(1) Sydney Chapman: The Terrestrial Implications of Thermal Conduction in the Solar Corona; invited comments: Eugene N. Parker.

(2) Joseph W. Chamberlain: The Present State of Speculation about the Origin and Acceleration of Aurora-Producing Particles; invited comments: S. F. Singer, Constance Warwick, and R. Jastrow.

(3) John A. Simpson: What We Have Learned about Planetary Magnetic Fields and the Production of Cosmic Rays from the Flare of February 23, 1956; invited comments: John R. Winckler, Scott E. Forbush, and Dana K. Bailey.

Appendix 2

The Committee notes with great satisfaction, the appearance of a number of new books in its general area of interest. Among these special note is taken of three volumes on Geophysics, I, II, and III, *Handbook of Physics,* edited by our colleague, J. Bartels, of Göttingen. It notes that several contributions by members of the AGU were included. The Committee has also noted the general excellence of the series *Advances in Geophysics,* Academic Press, edited by Helmut Landsberg. Another new book *The Planet Earth,* Pergamon Press, edited by D. R. Bates includes a modern elementary introduction to various geophysical subjects, including topics in the area of interest of this Committee.

Among a few special reports of interest may be included that of W. O. Roberts, on behalf of the Institute for Solar-Terrestrial Research, on the status of the solar-weather field. It is understood this may be revised to include new material. A volume on solar activity is also planned.

It is understood that C. T. Elvey and M. Sugiura are preparing a new book on the aurorae. Also a book on the upper atmosphere, probable title "Methods and Results of Upper Atmosphere Research," has been prepared by J. Kaplan, G. F. Schilling and H. K. Kallmann.

The Third International Symposium on Cosmical Gas Dynamics took place at the Smithsonian Astrophysical Observatory on June 24 to 29, 1957. Organized by committees from the International Astronomical Union and the International Union of Theoretical and Applied Mechanics, the symposium was sponsored by the Observatory and the U. S. Air Force. The Proceedings are to be published by the *Reviews of Modern Physics,* in cooperation with the Smithsonian Astrophysical Observatory.

The first number of a new publication, the *Smithsonian Contributions to Astrophysics,* appeared in 1957 under the editorship of F. L. Whipple. The journal appears at irregular intervals, and in it will be published important collections of data and detailed analyses which, because of their length or specialized audience, do not easily find an outlet elsewhere. Among the publications planned for the near future is a complete collection of raw data of the optical-orbital observations of Satellites 1957α and 1957β, as they were received by the Satellite Tracking Program at Cambridge, Massachusetts.

Other activities in cosmic-terrestrial relationships have been published in summary form in the *IGY Bulletin,* reprinted in *Trans. Am. Geophys. Union,* 39, 179–194, 1958, and need not be repeated here.

References

Beiser, Arthur, Variation in the geomagnetic dipole in the past 15,000 years, *J. Geophys. Research,* 62, 235–239, 1957.

Beiser, Arthur, Cosmic-ray trapping in interplanetary space, *J. Geophys. Research,* 63, 1–17, 1958.

Bell, B., and H. Glazer, Geomagnetism and the emission-line corona, *Smithsonian Contribs. Astrophys.*, **2**, 51–107, 1957.

Bell, B., and H. Glazer, Sunspots and geomagnetism, *Smithsonian Contribs. Astrophys.*, **2**, 161–179, 1958.

Brandt, J. C., and J. W. Chamberlain, Resonance scattering by atmospheric sodium—V. Theory of the day airglow, *J. Atmospheric and Terrest. Phys.*, **12**, 288, 1958.

Carleton, N. P., Excitation of nitrogen by protons of a few kev energy, *Phys. Rev.*, **107**, 110–113, 1957.

Chamberlain, J. W., On a possible velocity dispersion of auroral protons, *Astrophys. J.*, **126**, 245–252, 1957.

Chamberlain, J. W., Theories of the aurora, *Advances in Geophys.*, **4**, 109–215, 1958a.

Chamberlain, J. W., Oxygen red lines in the airglow. I. Twilight and night excitation processes, *Astrophys. J.*, **127**, 54-66, 1958b.

Chamberlain, J. W., D. M. Henten, and J. E. Mack, Resonance scattering by atmospheric sodium. IV. Abundance of sodium in twilight, *J. Atmospheric and Terrest. Phys.*, **12**, 153–165, 1958.

Chapman, Sydney, Notes on the solar corona and the terrestrial ionosphere, *Smithsonian Contribs. Astrophys.*, **2**, 1–14, 1957.

Chapman, Sydney, and C. G. Little, The non-deviation absorption of high-frequency radio waves in auroral latitudes, *J. Atmospheric and Terrest. Phys.*, **10**, 20–31, 1957.

Chopra, K. P., On the radial adiabatic pulsations of an infinite cylinder in the presence of magnetic field parallel to its axis, *Proc. Natl. Inst. Sci. India, Pt. A*, **21**, 314–320, 1956.

Chopra, K. P., Magnetic fields in a conducting fluid sphere with volume currents, *J. Geophys. Research*, **62**, 573–579, 1957a.

Chopra, K. P., Hydromagnetic instability of cosmical bodies, *Univ. Maryland Physics Dept. Tech. Rept. 90*, 1957b.

Chopra, K. P., Diffusion and planehydromagnetic shock waves, *Univ. Maryland Physics Dept. Tech. Rept. 96*, 1958.

Chopra, K. P., and S. F. Singer, Drag of a sphere moving in a conducting fluid, *Univ. Maryland Physics Dept. Tech. Rept. 97*, 1958.

Chopra, K. P., and S. P. Talwar, On the radial pulsations of an infinite cylinder with a magnetic field parallel to its axis, *Proc. Natl. Inst. Sci. India, Pt. A*, **21**, 302–313, 1956.

Coates, R. J., Measurements of solar radiation and atmospheric attenuation at 4.3 millimeters wavelength, *Proc. Inst. Radio Engrs.*, **46**, 122–126, Jan. 1958a.

Coates, R. J., A model of the chromosphere from millimeter wavelength observations, *Astrophys. J.*, **128**, 83–91, 1958b.

Coates, R. J., J. E. Gibson, and J. P. Hagen, The 1954 eclipse measurement of the 8.6-mm solar brightness distribution, *Astrophys. J.*, **128**, 406, 1958.

Cook, A. F., and R. F. Hughes, A reduction method for the motions of persistent meteor trains, *Smithsonian Contribs. Astrophys.*, **1**, 225 1957.

Corrigan, J. J., S. F. Singer, and M. J. Swetnick, Cosmic ray increases associated with small solar flares, *Bull. Am. Phys. Soc.*, **3**, 71, 1958.

Dodson, H. W., and E. R. Hedeman, Geomagnetic disturbances associated with solar flare with major premaximum bursts at radio frequencies $\geq$ 200 Mc/s, *J. Geophys. Research*, **63** 77–96, 1958.

Friedman, H., T. A. Chubb, J. E. Kupperian, Jr., R. W. Kreplin, and J. C. Lindsay, X-ray and ultraviolet emission of solar flares (IGY Project 10.3), *Ann. géophys.*, **14**, 232–235, 1958.

Fritz, S., Solar radiation and the lower atmosphere, *Proc. Natl. Acad. Sci. U. S.*, **43**, 95–10 1957.

Gallet, R. M., and R. A. Helliwell, A theory of the production of VLF noise (so-called dawn chorus) by traveling wave amplification in the exosphere of the earth, *Pap. 20, vol. II*, Symposium on the Propagation of VLF Waves, Nat Bur. Standards Boulder Labs, Boulder, Colo Jan. 23–25, 1957.

Griem, H., Starkeffektverbreiterung der Balmerlinien bei grossen Electronendichten, *Z Phys* **137**, 280–294, 1954.

Hawkins, G. S., The method of reduction short-trail meteors, *Smithsonian Contribs. Astrophys.*, **1**, 207, 1957.

Helliwell, R. A., J. H. Crary, J. H. Pope, and R. L. Smith, The 'nose' whistler—a new high latitude phenomenon, *J. Geophys. Research*, **63** 139–142, 1956.

Helliwell, R. A., and E. Gehrels, Observations of magneto-ionic duct propagation using man made signals of very low frequency, *Proc. Inst. Radio Engrs.*, 1958.

Heppner, J. P., and L. H. Meredith, Nightglow emission altitudes from rocket measurements, *J. Geophys. Research*, **63**, 51–65, 1958.

Hinnov, E., Optical cross sections from intensity density measurements, *J. Opt. Soc. Am.*, **47** 156–162, 1957.

Johnson, C. Y., J. P. Heppner, J. C. Holmes, and E. B. Meadows, Results obtained with rocket borne ion spectrometers, *Ann. géophys.*, **14**, 475 482, 1958.

Johnson, F. S., H. H. Malitson, J. D. Purcell and R. Tousey, Emission lines in the extreme ultraviolet spectrum of the sun, *Astrophys. J.* **127**, 80, 1958.

Korff, S. A., The origin and implications of the cosmic radiation, *Am. Scientist*, **45**, 281–300, 1957

Kupperian, J. E., Jr., E. T. Byram, T. A. Chubb and H. Friedman, Extreme ultraviolet radiation in the night sky, *Ann. géophys.*, **14**, 329–333 1958.

LaGow, H. E., R. Horowitz, and J. Ainsworth Rocket measurements of the arctic upper atmosphere, *Ann. géophys.*, **14**, 131, 1958.

Little, C. G., and H. Leinbach, Some measurements of high-latitude ionospheric absorption using extraterrestrial radio waves, *Proc. Inst. Radio Engrs.*, **46**, 334–348, 1958.

Masterson, J. E., and M. D. Ross, Rockair—a promising new tool for specialized high altitude research, *Jet Propulsion*, **2**, 276-278, 1957.

Maxwell, A., and G. Swarup, A new spectral characteristic in solar radio emission, *Nature* **181**, 36–38, 1958.

Mayer, C. H., T. P. McCullough, and R. M. Sloanaker, Evidence for polarized radio radiation from the Crab Nebula, *Astrophys. J.*, **126** 468–470, 1957.

Mayer, C. H., T. P. McCullough, and R. M

Sloanaker, Measurements of planetary radiation at centimeter wavelengths, *Proc. Inst. Radio Engrs.*, **46**, no. 1, 260–266, 1958a.

Mayer, C. H., T. P. McCullough, and R. M. Sloanaker, Observations of Mars and Jupiter at a wavelength of 3.15 cm, *Astrophys. J.*, **127**, 11–16, 1958b.

McCrosky, R. E., A rapid graphical method of meteor trail reduction, *Smithsonian Contribs. Astrophys.*, **1**, 215, 1957.

Meadows, E. B., and J. W. Townsend, Jr., Diffusive separation in the winter night time arctic upper atmosphere 112 to 150 km, *Ann géophys.*, **14**, 80–93, 1958.

Öpik, E. J., Problems in physics of meteors, *Am. J. Phys.*, **26**, 70–80, 1958a.

Öpik, E. J., *The physics of meteor flight in the atmosphere*, Interscience Publishers, New York, 1958b.

Öpik, E. J., and S. F. Singer, Reinterpretation of the uranium-helium ages of iron meteorites, *Trans. Am. Geophys. Union*, **38**, 566–568, 1957.

Owren, L., and R. A. Stark, Arctic radio wave propagation, *Final Rept. Task B*, Contract DA–36–039 SC–71137, 1957.

Owren, L., L. A. Ware, and G. C. Rumi, Arctic radio wave propagation, *Final Rept. Task A*, Contract DA–36–039 SC–71137, 1958.

Parker, E. N., On the geomagnetic storm effect, *J. Geophys. Research*, **61**, 625–637, 1956.

Pope, J. H., Diurnal variation in the occurrence of "dawn chorus," *Nature*, **180**, 433, 1957.

Rhodes, R. M., *A study of auroral particles*, Master's thesis, Univ. Maryland, 1955.

Roberts, W. O., Cross-Field Seminar on possible responses of terrestrial atmospheric circulation to changes in solar activity, *Bull. Am. Meteorol. Soc.*, **37**, 477–479, 1956.

Roesler, F. L., C. Y. Fan, and J. W. Chamberlain, Interpretation of rotational temperatures of auroral N_2^+ bands—I. Proton impact at intermediate energies, *J. Atmospheric and Terrest. Phys.*, **12**, 200–205, 1958.

Seaton, M. J., Oxygen red lines in the airglow—II. Collisional deactivation effects, *Astrophys. J.*, **127**, 67–74, 1958.

Seddon, J. C., and J. E. Jackson, Ionosphere electron densities and differential absorption, *Ann. géophys.*, **14**, 456–463, 1958.

Shapiro, M. M., B. Stiller, and F. W. O'Dell, Varenna Conference on Cosmic Radiation, 1957 Proceedings to be published in Suppl. II *Nuovo cimento*, 1958.

Shapiro, R., Further evidence of a solar-weather effect, *J. Meteorol.*, **13**, 335–340, 1956.

Singer, S. F., Meteorites and cosmic rays, *Nature*, **170**, 728–729, 1952.

Singer, S. F., Origin of meteorites, *Sci. American*, **191**, 36–41, 1954.

Singer, S. F., Geophysical research with artificial satellites, *Advances in Geophys.*, **3**, 301–367, 1956a.

Singer, S. F., Research in the upper atmosphere with high altitude sounding rockets, *Vistas in Astronomy*, vol. 2 (A. Beer, ed.), Pergamon Press, New York, 878–912, 1956b.

Singer, S. F., A new model of magnetic storms and aurorae, *Trans. Am. Geophys. Union*, **38**, 175–190, 1957a.

Singer, S. F., On the low energy cutoff of the cosmic radiation, *Nuovo cimento*, **6**, Suppl. II, 1957b.

Singer, S. F., A model for solar flare increases of cosmic rays, *Nuovo cimento*, **6**, Suppl. II, 1957c.

Singer, S. F., The primary cosmic radiation and its time variation, *Progress in cosmic ray and elementary particle physics*, vol. 4, (J. G. Wilson and S. Wouthuysen, ed.), Interscience Publishers, New York, 1957d.

Singer, S. F., Project Far-Side, *Missiles and Rockets*, **2**, 120–128, 1957e.

Singer, S. F., Crucial experiment concerning the origin of meteorites, *Phys. Rev.*, **105**, 765–766, 1957f.

Singer, S. F., New acceleration mechanism for auroral particles, *Bull. Am. Phys. Soc.*, **3**, 40, 1958.

Singer, S. F., and A. L. Lawrence, Terrapin—An upper atmosphere research vehicle, *Jet Propulsion*, **2**, 281–288, 1957.

Singer, S. F., and R. C. Wentworth, A method for the determination of the vertical ozone distribution from a satellite, *J. Geophys. Research*, **62**, 299–308, 1957.

Sterne, T. E., and N. Dieter, The "constancy" of the solar constant, *Smithsonian Contribs. Astrophys.*, **3**, 9–12, 1958.

Tandberg-Hanssen, E., Variations in the height of ionospheric layers during magnetic storms, *J. Geophys. Research*, **63**, 157–160, 1958.

Tousey, R., Rocket measurements of the night airglow, *Ann. géophys.*, **14**, 186–195, 1958.

Warwick, C. S., Flare height and association with SID's *Astrophys. J.*, **121**, 385–390, 1955.

Wexler, H., Variations in isolation, general circulation and climate, *Tellus*, **8**, 480–494, 1956.

Whipple, F. L., and L. G. Jacchia, Reduction methods for photographic meteor trails, *Smithsonian Contribs. Astrophys.*, **1**, 183, 1957.

Wiese, W., Experimental determination of the oscillator strengths of OII lines, *Z. Astrophys.* (in press).

Woodbridge, D. D., T. W. Pohrte, and N. Macdonald, A possible solar effect on wind patterns at high altitudes, *Tech. Rept. 4*, High Altitude Observatory, Boulder, Colo., 1957.

Yaplee, B. S., Radar echoes from the moon at a wavelength of 10 cm, *Proc. Inst. Radio Engrs.*, **46**, no. 1, 293–297, 1958.

(Received October 7, 1958.)

Abstracts of the papers presented at the Fortieth Annual Meeting, Washington, D. C., May 4-7, 1959 listed in the order of the last name of the first author

ISIDORE ADLER (U. S. Geological Survey, Washington 25, D. C.) *Application of X-Ray and Electron Probes in Mineralogical Investigations*—Recent years have seen the development of highly specialized analytical tools for the rapid and nondestructive chemical analysis of small samples. Two such devices, the x-ray probe and the electron probe, are particularly useful in the study of mineral systems. The x-ray probe operates on the principles of fluorescent x-ray analysis and is useful on samples having a lower size limit of approximately 0.3 mm diameter. The electron probe utilizes a sharply focused beam of electrons to excite the characteristic x-rays and has a lower size limit of approximately 1 to 2 microns. Both types of instruments are described and examples of the use of each are given.

H. W. ANDERSON, R. M. RICE, AND A. J. WEST (Pacific Southwest Forest and Range Experiment Station, Berkeley, Calif.) *Snow in Forest Openings and Forest Stands*—First analyses have been made of the 1958 data from 57 snow courses at the Central Sierra Snow Laboratory, near Soda Springs, California. In the year of very heavy snowfall, 1957-1958, forest effects on snow accumulation and melt were clearly evident. Snow measurements have provided some clues as to how forests may be cut to improve the timing and increase the amount of water yield. In 1958, at the time of maximum pack, the snowpack had 14 more inches of water in forest openings than in high-density forest stands. A forest with 50 per cent opening and 50 per cent forest would be expected to have 12.7 inches more water than dense forest would have. Forest openings 1 to 2 tree-heights across had more snow left on June 1, 1958, than did smaller or larger openings. Choice of the correct shape and orientation of forest openings for various slopes can increase the snow storage; L-shaped openings for east and west slopes are probably best. Selective cutting of forest stands can increase snow storage from 2 to 9 inches. June 1 snow-water storage was a maximum at forest densities less than 80 per cent. We are continuing these studies aimed at developing and testing ways that forests can be managed to improve water yield.

J. K. ANGELL (U. S. Weather Bureau, Washington, D. C.) *The Use of Transosonde Data As an Aid to Analysis and Forecasting during the Winter of 1958-1959*—During the winter of 1958-1959, transosonde positions and transosonde-derived winds were plotted routinely on the 250-mb chart by the National Weather Analysis Center (NWAC) at Suitland, Maryland. A statistical assessment is presented of the quantity and quality of transosonde data so plotted. The usefulness of transosonde data in specific instances is pointed out.

G. ARNASON (U. S. Weather Bureau, Washington, D. C.) *A Report on a New Numerical Weather Prediction Group*—Since July 1958 the U. S. Navy has maintained a small but expanding group of people engaged in numerical weather prediction. The group, called Navy Numerical Weather Problems (NANWEP) Group, is composed of both civilian and military personnel and plans to deal primarily with the solution of problems pertinent to naval operations. As these problems are intimately connected with weather prediction in general and low-level forecasting in particular, the group will devote considerable effort to the design and testing of suitable atmospheric prediction models. After a preparatory period of research and development, the activities of the group are planned to expand into routine operations.

A. ARNOLD AND M. LOWENTHAL (U. S. Army Signal Research and Development Laboratory, Elberon, N. J.) *Evaluation of Radiosonde Flights Using IBM 650 Computer*—In order to eliminate human errors as far as possible, radiosonde data and rawins are evaluated at USASRDL on the IBM 650 computer. Using the characteristic temperature-resistance response of the ML-419 temperature element, mathematical formulation of the temperatures is obtained. The humidity relationships are derived empirically. The operator selects the significant levels, records the pressure, temperature, and humidity recorder divisions, and time from the flight record, and the IBM computer carries out the computations. Elevation and azimuth angles are automatically punched on paper tape, corrections for curvature and refraction again being computed on the IBM 650.

B. R. BEAN AND L. P. RIGGS (National Bureau of Standards, Boulder, Colo.) *On the Synoptic Variation of the Radio Refractive Index*—The synoptic variation of the atmospheric radio refractive index, evaluated from standard weather observations, is examined during an outbreak of polar continental air. It is found that the reduced-to-sea-level value of the refractive index is a more sensitive synoptic parameter than the station value. The reduced value is quite sensitive to the humidity and density structure of the storm under study, while the great station elevation dependence of the station value tends to mask synoptic changes. The reduced value changes systematically with the approach and passage of the polar front wave. The present system showed a consistent increase of the reduced value in the

warm sector of the wave and a marked decrease behind the cold front.

B. R. Bean, L. P. Riggs, and J. D. Horn (National Bureau of Standards, Boulder, Colo.) *A Study of the Three-Dimensional Distribution of Radio Refractive Index*—An analysis of the three-dimensional structure of an intense outbreak of continental polar air is presented in terms of the radio refractive index of the atmosphere. Employed for the first time is a reduced index analogous to potential temperature. The reduced value more clearly shows the refractive index structure than do the classical methods used heretofore. This new unit is a measure of both atmospheric density and humidity. It shows, on a single cross section, the airmass structure and the dynamic mixing of air around the frontal interface.

Raymond Bellucci (U. S. Army Signal Research and Development Laboratory, Fort Monmouth, N. J.) *Drag Cord Anemometer*—An anemometer has been developed which provides a weighted integrated wind over a path. This development was necessitated by the requirement for a weighted, integrated wind measurement over the initial sensitive portion of a rocket trajectory. Two components of the wind force on a long length of stainless steel wire are obtained by measuring the displacement of the wire at one end while the other is held fixed. The wire is placed in a line parallel to the rocket trajectory. By this means the two components of the wind that are determined are the same two components that affect the rocket flight. The equipment has been tested by fixing it vertically at the Oakhurst Tower where wind measurements were compared with those from a set of conventional anemometers.

H. Benioff (California Institute of Technology, Pasadena, Calif.), J. C. Harrison, W. H. Munk, and L. B. Slichter (Institute of Geophysics, University of California, Los Angeles, Calif.) *A Search for the Free Oscillations*—Five-minute values were read from records taken by a gravimeter and a strain seismometer over a period of the order of a month. A power-spectral analysis reveals a white noise in the frequency range of 0.1 to 6 cycles per hour. This imposes some upper limits to the amplitude of free oscillation in the absence of earthquakes.

Charles R. Bentley and Ned A. Ostenso (Department of Geology, University of Wisconsin, Madison, Wis.) *Seismic Methods and Preliminary Results, Marie Byrd Land, Antarctica*—A preliminary report on three traverses in Marie Byrd Land is presented. Seismic investigations included reflection shots to determine ice thickness, short refraction profiles to measure near-surface velocity variations, uphole velocity measurements, and long refraction and wide-angle reflection shooting to give velocities throughout the ice cap and in the rock beneath. Gravity readings between seismic stations provided a detailed profile of ice thickness throughout the traverses. The combination of several lines of evidence strongly suggests the division of West Antarctica into two land areas that would be separated, if the ice were removed, by an area of open water running from the Ross Sea to the Bellingshausen Sea.

Alfred K. Blackadar and Abram B. Bernste (Pennsylvania State University, University Pa Pa.) *The Effect of a Horizontal Temperatu Gradient on the Surface Wind*—The deviati from geostrophic flow at the surface has been e plained in the past by several theories based different assumptions regarding the vertical var tion of the eddy-viscosity coefficient. These the ries disagree somewhat with each other and wi observations. One reason for this is that they a sume no horizontal temperature gradient. In th study the Ekman Spiral theory is modified to pe mit a linear variation with height of the geostroph wind. The surface winds predicted by this theo are compared with winds observed in the Gre Plains and at Brookhaven. The theory correct predicts the effect of a horizontal temperatu gradient but fails to predict correctly the role vertical stability. Two parameters of great imp tance in determining the surface wind are t magnitude and vertical variation of the edd viscosity coefficient, about which little is know

Paul Bock (Department of Civil Engineeri University of Delaware, Newark, Del.) *Wett Perimeter and Hydraulic Radius as Parameters Flow Equations*—The concept of hydraulic rad R has changed little (if any) since 1775. T paper attempts a new interpretation of R based a 'bumpy wetted perimeter' P_b. An expression relative roughness k is developed: $k = \epsilon B_s/4$ where ϵ = absolute roughness, B_s = 'bump sha factor, R_s = hydraulic radius (smooth). It is a demonstrated that $Q = \int^A V da$ is not mathem cally rigorous when using an expression for (such as Manning's equation) having R as parameter.

Iris Borg (Princeton University, Princeto N. J.), and John Handin and D. V. Higgs (Sh Development Co., Houston, Tex.) *Experiment Deformation of Plagioclase Single Crystals*—Jac eted cylindrical specimens of plagioclase (An single crystals have been deformed dry at 50 bars confining pressure and 400°C at a consta strain rate of one per cent per minute. Uniaxi compression experiments were carried out for tw different orientations designated A and B (cylind axes for A and B were mutually perpendicular ar each was inclined 45° to (010) in a plane quas normal to the a axis). These orientations are mo favorable for production of mechanical albite an pericline twins at this composition. Should twin be produced experimentally, these orientation would permit discrimination of the direction sens of gliding for each twin law. In both orientation there were small permanent strains of two to thre per cent followed by faulting on surfaces incline at about 36° to the direction of loading (observe macroscopically). However, the ultimate strengt of B cylinders, about 9500 bars, was nearly doub that of A cylinders.

Petrographic examination revealed that, a though both albite and pericline twinning ma have occurred to minor extents in all specimen only one of these deformation mechanisms can b clearly recognized—twin gliding according to th albite law, with $K_1 = (010)$, $N_2 = [010]$, and th direction sense positive [that is, layers parallel t (010) as viewed along $+b$ axis move toward +

axis]. There is limited evidence in one specimen for pericline twinning with $K_2 = (010)$, $N_1 = [010]$, and direction sense negative (that is, layers parallel to the rhombic section as viewed along the $+c$ axis move toward the $-b$ axis). Twinning according to other plagioclase laws was not present, and there was no evidence for translation gliding although the possibility cannot be eliminated. For both orientations the resolved shear stress coefficients for both twin planes are about equal. However, for A the direction sense is such that albite, but not pericline twinning, can occur; and for B the reverse is true. The observed strength anisotropy therefore suggests that the critical resolved shear stress for albite twinning is only about half that for pericline twinning.

F. R. Boyd and J. L. England (Geophysical Laboratory, Carnegie Institution of Washington, Washington, D. C.) *Quartz ⇄ Coesite Transition*—The quartz ⇄ coesite inversion has been determined over the temperature range of 700 to 1700°C in the pressure range of 20 to 40 kilobars. The data, corrected for friction, are best fitted by a boundary whose equation is $P = 19.5 + 0.0112\ T$ where P is in kilobars and T in degrees centigrade. The reaction has been reversed across narrow pressure intervals over the entire temperature range of the investigation. The determination was made in an internally heated tungsten carbide pressure vessel. Talc was used as the pressure medium. Calibration with the reaction Bi I ⇄ Bi II indicates a friction of 8% ± 5% at 25 kb. Additional calibration data on a transition in thallium at about 40 kb are being sought.

We have synthesized coesite in a squeezer apparatus at significantly lower load pressures than those indicated possible by the present determination of its stability field. Our data suggest the presence of pressure gradients in squeezer runs on this system, and the discrepancy may possibly be explained in this way. Present data indicate that quartz would be stable in the earth relative to coesite to depths up to about 100 kilometers.

Wallace S. Broecker and Edwin A. Olson (Lamont Geological Observatory, Columbia University, Palisades, N. Y.) *Variations in Atmospheric Radiocarbon Concentration over the Last 2000 Years*—Aside from their importance in radiocarbon dating, past variations in the C^{14} concentration of the atmosphere are of interest because they are related to certain geophysical factors. Variations may reflect fluctuations in the rate at which C^{14} has been produced by cosmic rays and thus might point to intensity fluctuations in primary cosmic radiation or in the earth's magnetic field. On the other hand, variations in the atmospheric inventory of stable carbon, such as might be produced by sudden release of large quantities of volcanic CO_2, might explain variations in the atmospheric C^{14} concentration. Finally, and perhaps most probably, the distribution of radiocarbon between atmosphere and deep oceans might vary as a result of climatically reduced changes in the rate of deep water formation, thus varying the atmospheric C^{14} concentration.

From C^{14} measurements on 12 well-dated plant samples representing the last 2000 years it is concluded that variations in the atmospheric C^{14} concentration have been restricted to a range less than 5 per cent. The samples analyzed include two that were historically dated and ten that were dated by tree-ring counting. Corrections were made for the effects of radioactive decay and isotopic fractionation. From the measurements available the small variations in radiocarbon concentration cannot now be described as cyclic. Their cause has not been established.

M. Brook and N. Kitagawa (New Mexico Institute of Mining and Technology, Socorro, N. M.) *An Interpretation of the Ratio of Cloud-to-Cloud-to-Ground Lightning Discharges*—An extension of the bipolar thunderstorm model of Holzer and Saxon leads to a model which predicts in inhomogeneous column of negative charge. The model also predicts that the total number of intracloud strokes in a storm should equal the sum of the separate return-stroke elements of all discharges to ground. The agreement between the number of cloud strokes and return-stroke elements for New Mexico is good for some storms, poor for others. Excellent agreement with the predicted equality is found for Japanese thunderstorms and for British thunderstorms of frontal origin. A thunderstorm-activity index is proposed, based upon the rate of lightning occurrence and the total duration of individual discharges.

Robert M. Brown (Brookhaven National Laboratory, Upton, Long Island, N. Y.) *An Automatic Meteorological Data Collecting System*—In common with other industrial and business organizations faced with the problem of reducing large volumes of data, the Brookhaven Meteorology Group has developed an automatic data collection system. This device is capable of accepting meteorological information in the form of either a rotation or a voltage. It then converts these inputs to digital information and records it on a paper punch. The tape punch is extremely fast, and it is possible to scan the required information every 0.6 sec. This eliminates the need for developing mean data prior to the coding.

William L. Brown (Department of Mineralogy, Pennsylvania State University, University Park, Pa.) *The Existence of Monoclinic Albite at Room Temperature*—Albite heated for long periods of time (5 to 6 months) at a temperature (1050°C) near its melting point shows changes in lattice constants, when x-rayed at room temperature, beyond those from low albite to high albite and of a different nature. There is a progressive change in the lattice constants from those of high albite through those of analbites towards the monoclinic state, until monoclinic albite—monalbite—can exist at room temperature. The rate of this change has been investigated. The lattice constants of monalbite and of the intermediate states between it and high albite are very similar to those of alkali feldspars in the analbite-sanidine series. Similar though progressively smaller changes are shown by Na-rich plagioclases up to about An_{30}.

The monalbite crystals show a rapid reversible monoclinic-triclinic displacive transformation. One crystal examined, using a low temperature Weissenberg camera, had an inversion temperature of −65 ± 5°C and its triclinicity increased rapidly

with decreasing temperature. Thus a displacive transformation can occur in $NaAlSi_3O_8$ from near its melting point to below room temperature, a range of more than 1100°C. These changes are probably due to an increase in Si/Al disorder.

James N. Brune, John E. Nafe, and Jack E. Oliver (Lamont Geological Observatory, Columbia University, Palisades, N. Y.) *A Simplified Method for the Analysis and Synthesis of Dispersed Wavetrains*—A disturbance at one point of a dispersive medium resulting from an impulse applied at another point may be represented as a superposition of traveling waves. The phase and period of the disturbance at any instant are related to the phase and period of the traveling wave component for which the phase is stationary. From the instantaneous phase of that traveling wave component the following equation may be written

$$\frac{(c - u)t}{cT} = n + d + d'$$

where c is the phase velocity, u is the group velocity, T is the period, t is the travel time, n is an integer, and d and d' are corrections for initial phase and instrumental phase shift. Since u, t, and T may be measured from a record of the disturbance, the equation may be used to compute the dispersion equation relating phase velocity and period. Although n and d are assumed, incorrect assumptions usually lead to improbable values of c. If distance and the dispersion are known, initial phases may be determined. From distance, initial phases, and phase velocities the disturbance at any point may be constructed. The practical use of the method is demonstrated by application to flexural waves in a plate, Rayleigh waves from U. S. and Russian nuclear explosions, Rayleigh waves from the Hudson Bay earthquake of January 30, 1959, and Love waves from the Fairview Peak and Fallon, Nevada, earthquakes of 1954.

Konrad J. K. Buettner (Department of Meteorology and Climatology, University of Washington, Seattle, Wash.) *How Good or Bad is Weather for Normal and Sick People?*—Every forecaster, weather analyst, or climatologist occasionally is asked the question, "How good or bad is weather for normal and sick people?" Frequently, the answer cannot be given without some knowledge of the physiological, psychological, and even clinical response of man to his varying environs. Weather and climate reports, as disseminated to the public, are given in those elements which are either easily measured or which are specifically required by various specialists, such as air pilots. For man, relative humidity is a much more important element than dew point or specific humidity. What makes weather more or less bearable to man is rarely mentioned in routine reports. A partial list of other neglected components of the atmosphere are cooling power; sweat load; effective temperature; number of heating days or cooling days; smog; concentration of ozone, acids, hydrocarbons, allergens, ions, and other possibly detrimental air components; rain frequency; duration of sunshine; sky brightness; natural indoors illumination; solar ultraviolet; and microclimate. Data on wind chill and the discomfort index are just beginning to enrich our list of climatic elements. The lack of understanding of human factors in meteorology concurs with a certain neglect of weather and climate elements by the medical profession. Matters become worse by the persistence of some archaic superstitions or unproven theses, such as the danger of 'damp' nights (Shakespeare), sunstroke, infrared radiation, the correlation of menstruation and moon phases, and the 'healthiness' of sunshine. Little proof has been given that certain places have 'health' climates. Examples of various weather types are discussed to aid the public. Among the examples treated are some of the modern conditions of clothing, housing, transportation, sanitation, and air pollution.

Konrad J. K. Buettner and Norman Thyer (University of Washington, Seattle, Wash.) *The Anti-Mountain and Anti-Valley Wind*—Previous observations by E. Ekhart and by the authors show compensation winds situated above the well-known thermal, nightly mountain wind and daily valley wind. A pibal net of single and double theodolite stations was set up in and around the Carbon River valley in Mount Rainier National Park. The lower portion of the valley has ridges of about 800 m relative height and 30° elevation, the middle portion has 45° ridges of 1000 m height and the uppermost part shows near-vertical walls above the glacier terminal. Stations which worked around the clock were erected along the valley axis on top of the ridges bordering the valley and at the upper end of the valley. Tests were also conducted on the daily period of the slope wind. Data about the three-dimensional distribution of the wind in and above the valley are shown.

Elizabeth T. Bunce and Robert A. Phinney (Woods Hole Oceanographic Institution, Woods Hole, Mass.) and Robert N. Pooley (University of Wisconsin, Madison, Wis.) *Seismic Refraction Observations in Buzzards Bay, Massachusetts*—Detailed seismic refraction measurements have been made in this shallow-water area. A towed bouyant cable carrying 12 detectors at 100-ft intervals was used. First arrivals from the basement are found on all records. Observed velocities range from 5.1 to 5.7 km/sec, and calculated depths range from 18 to 75 m below sea level. In a well-defined area of at least seven square miles, substantially lower basement velocities of 3.9 to 4.5 km/sec are found. Both observed basement velocities are suggestive of the granite-gneiss complex observed in outcrops on the western side of Buzzards Bay. Indicated sedimentary velocities, which range from 1.52 to 2.4 km/sec, are associated with second later arrivals. Complicated patterns of dispersive waves restrict the accuracy with which these later arrivals can be interpreted. This uncertainty, plus the known glacial character of the sediments, is more than sufficient to account for the poor correlation of sedimentary velocities.

H. D. Burke and A. W. Krumbach (Vicksburg Research Center, Southern Forest Experiment Sta., Vicksburg, Miss.) *Liquid Nitrogen for Sampling Wet Soils*—Metal probes containing liquid

itrogen were tested in prepared silt and sandy oam soils. The soil froze to the probe and samples ere extracted up to one foot in length. Replicate amples with moisture contents ranging from 2 to 75 per cent by weight were taken with probes and echanical sampling devices. Results indicated hat probes could be used over this range of moisure content with accuracy. Mean deviations of robe samples from mechanical samples ranged rom 0.46 to 2.42 per cent of the mean moisture ontent.

Edward M. Burt (Williams and Work, Grand Rapids, Mich.) *Evaluation of a Formula Used in Predicting Well Performance*—The formula $Q_t = (0.67\ s_a/s_{t_0})\ Q_{s_{t_0}}$ is used to establish the 'safe yield' of public supply wells. This formula attempts to 'short cut' accepted methods of estimating long-term well yields from aquifer test data obtained in exploration programs. The complexities of natural conditions and the variables in well structures defy any formula intended to provide a short cut for estimating well yields. Attention is called to the ease with which such formulae become design standards.

Joseph C. Cain (Geophysical Institute, College, Alaska) *A Preliminary Study of the IGY Magnetic Data from Alaskan Observatories*—A survey is made of the data accrued by the ten U. S. Coast and Geodetic Survey magnetic observatories operated in Alaska during the IGY. Some preliminary analyses are reported for sample magnetic disturbances, and interpretations are made on the assumption of horizontal electric currents at the 100-km level. Special attention is given to data from the newly devised differential magnetometer operated at College (64.8°N, 147.8°W geographic). Some of the problems inherent in such an instrument and a few results in terms of limited ionospheric currents are discussed.

Fred A. Camp (Department of Water and Power, The City of Los Angeles, Los Angeles, Calif.) *Hydrologic Processes of Snow and Ice at High Altitude*—Abstract published previously in *J. Geophys. Research,* 64, 685, 1959.

Michael H. Carr and Karl K. Turekian (Yale University, New Haven, Conn.) *A Preliminary Report on the Geochemistry of Cobalt*—The geochemistry of cobalt is under study utilizing the combined techniques of emission spectrography and neutron activation analysis. The latter method has proved particularly important in establishing the accuracy of the spectrographic procedure for values above 5 ‰ Co and in obtaining results on geologic materials low in cobalt. The spectrographic method has been previously described by one of us. The following procedure has been used in the neutron activation analyses. Samples and standards (a measured amount of soluble cobalt salt on aluminum foil) were irradiated together for a period of several days in the Brookhaven reactor. To the irradiated samples a cobalt carrier was added, and after sodium peroxide fusion the cobalt was isolated as potassium cobaltinitrite. Using a gamma-ray spectrometer the Co^{60} 1.17 Mev gamma activity was measured for both samples. Standards and cobalt concentrations were determined in the samples by comparison.

In this manner a series of commonly available rock standards (including G-1, W-1 and the Bureau of Standards radium standards), were analyzed for cobalt. The results are given in the following table:

Number	Rock	Co
		ppm
G 1	Granite	2.3
4979[a]	Granite	0.85
4983[a]	Granite	0.44
4982[a]	Gabbro-diorite	40.
W 1	Diabase	54.
4984[a]	Basalt	47.
4985[a]	Basalt	49.
4978[a]	Basalt	48.
4975[a]	Dunite	154
4986[a]	Kimberlite	64
99[b]	Soda-Feldspar	0.69
88[b]	Dolomite	0.37
4976[a]	Limestone	0.61
1A[b]	Argill. limestone	4.8
4980[a]	Ortho-quartzite	0.2

[a] Bureau of Standards radium standards.
[b] Other Bureau of Standards rocks.

Using the above and other activation data combined with spectrographic results, a preliminary outline of the geochemistry of cobalt is presented.

Louis P. Carstensen and Paul M. Wolff, (U. S. Navy, Suitland, Md.) *Experiments in Numerical Prediction Using Synoptic-Empirical Approximations*—A numerical forecasting procedure incorporating several empirical terms derived from synoptic experience is described. These empirical terms include effects previously used subjectively by J. J. George. The results of several hemispheric 1000-mb forecasts are presented.

Ralf C. Carter, G. T. Orlob, W. J. Kaufman, and David K. Todd (Department of Civil Engineering, University of California, Berkeley, Calif.) *Studies of Helium as a Ground-Water Tracer*—Laboratory and field experiments were conducted employing helium as a ground-water tracer. Techniques were developed for the addition and extraction of helium from water. A mass spectrometer and a pressure-volume apparatus were employed for helium measurements at concentrations in water ranging from 1.5 to 5.5 $\times$ 10^{-4} mg/liter. In the field investigation, flow was traced through a confined aquifer for a distance of 188 ft. Both laboratory and field experiments showed that helium traveled at a slightly slower velocity than did chloride. The lag was attributed to a higher diffusion capacity of helium into nonconducting portions of the medium. Advantages of helium as a ground-water tracer are its safety, low cost, relative ease of analysis, low concentrations required, and chemical inertness. Disadvantages include the

relatively large errors in analysis, difficulties of maintaining a constant recharge rate, and time required to develop equilibrium conditions in unconfined aquifers.

James E. Caskey, Jr., Fred D. White, Harold B. Harshbarger, and Forrest R. Miller (Air Weather Service, U. S. Air Force, Washington, D. C.) *Navigation Flight Planning by Electronic Computer*—A program to compute navigation information for aerial flight planning by digital computers has been developed by the Electronic Computer Branch of Air Weather Service. Given route terminals, the program rapidly computes navigation information along great-circle routes utilizing the Joint Numerical Weather Prediction Unit's 500-mb hourly barotropic forecasts. Test runs, made in a 'paper test' to determine the accuracy of computer flight plans, reveal that the forecast information is sufficiently accurate to be of value in all types of flight planning. The speed with which flight plans can be transmitted to the field would supply distant departure terminals with the same information, and Air Traffic Control could be provided with another means for more positive control. Future plans to incorporate such features as the option of change in air speed and altitude along the route will greatly enhance the applicability of this program.

J. E. Chappelear (Shell Development Company, Houston, Tex.) *A Class of Three-Dimensional Shallow-Water. Waves*—We consider the problem of the calculation of the properties of three-dimensional waves (whose surface profiles have a two-dimensional structure) using the approximations of the shallow-water theory. We find that, if we assume that the first approximation is a uniform flow, there is in the theory a critical speed nearly equal to the square root of the product of the acceleration of gravity and the depth. No steady waves can propagate slower than this velocity. Waves which have this critical velocity are essentially two-dimensional, since they differ from two-dimensional waves only by a steady current. The waves whose velocities are greater than critical may have a wide variety of behaviors, since in this case the velocity potential satisfies the homogeneous wave equation (in two-space coordinates, not the time) to the second order of approximation. Although we have not been able to construct any solution to the first approximation, other than the uniform flow, we have not been able to find a proof that the uniform flow is a unique solution.

Edwin J. Chernosky (Geophysics Research Directorate, Air Force Cambridge Research Center, Bedford, Mass.) *The Effect of Magnetic Disturbance upon Subsequent Disturbance*—The purpose of this investigation is to determine the relative activity of magnetically disturbed days to disturbed days following n days later, where n varies from 1 to 35. The data used are the daily magnetic C_4 figures for the sunspot cycle 1935 to 1944. The cycle is divided into four parts to determine changes during the cycle. C_4 values over 1.0 are here considered disturbed D and those under 0.4 quiet Q. Average values of C_4 for each day of each n-day separation are obtained and compared. The first day of each n-day pair is more active than the second for $n = 1$ to $n = 5$ and from $n = 27$ to $n = 33$ for the sunspot cycle maximum and post-maximum epochs. After $n = 5$ the second day is more active until about $n = 10$ at the sunspot maximum. At sunspot minimum the first day is more active until about $n = 13$ and after $n = 27$.

John M. Christie and C. B. Raleigh (University of California, Los Angeles, Calif.) *Deformation Lamellae in Quartz*—Fabric analysis of several quartz-tectonites reveals patterns of preferred orientation of deformation lamellae which differ from those previously described in the literature. Poles of lamellae define, in projection, a small circle girdle about an axis designated A; orientations and strengths of maxima within the girdle are not similar in all specimens. The [0001]-axes of grains containing lamellae also define a small circle girdle (of larger radius) about the same axis A. In each specimen, the great circles containing [0001] and the lamellae pole in individual grains pass through, or close to, the axis A. The lamellae demonstrably postdate the deformation which produced the preferred orientations of quartz grains in the rocks. They are not parallel to rational crystallographic planes, and are interpreted as kink-bands induced by shearing parallel to [0001] on irregular surfaces in the prism-zone. The shearing may be controlled by imperfections in the crystal structure parallel to [0001]. According to this hypothesis, A is the axis of maximum compressive stress in the deformation which produced the lamellae. This relationship may be used to obtain a dynamic interpretation of deformation lamellae in sedimentary and metamorphic rocks.

Philip F. Clapp (Extended Forecast Section, U. S. Weather Bureau, Washington, D. C.) *Preferred Levels for Application of Single-Parameter Numerical Prediction Models*—To introduce sources and sinks of vorticity in predicting the evolution of planetry waves, an attempt is made to allow for large-scale divergence fields in the equivalent-barotropic vorticity equation. This is done by an adjustment depending on average geographical variations in the level of nondivergence. Preliminary tests of this technique at 500 mb are not too promising. Results show that the non-divergent barotropic model is not likely to be successful when applied at 500 mb because of the presence of strong average divergence fields at low and high latitudes. However, similar single-parameter models may be more useful when applied to 100 mb, since here average divergence fields are much weaker.

W. E. Cobb, B. B. Phillips, and P. A. Allee (Office of Physical Research, U. S. Weather Bureau, Washington, D. C.) *Mountain-Top Measurements of Atmospheric Electricity in Northwestern United States*—Certain proposed cloud-charging mechanisms depend upon the cleanliness of the ambient air. It is therefore important to compare electrical properties occurring within the relatively clean air of the northwestern United States with those occurring within the more polluted eastern and southern areas of the country. Previous measurements of the atmospheric electric variables have been made from a mountain in western

orth Carolina. During the summer of 1958 simi-
r measurements were made from the summit of
lount Washburn (10,317 ft) in Yellowstone Park,
'yoming. These measurements included the elec-
ic field, the positive and negative electrical con-
ıctivities, the charge of individual raindrops, the
ze and charge of individual cloud droplets, and
ıe coronal discharge current from the earth's
ırface associated with high electric fields be-
ath thunderstorms. Specific results are presented
ıd interpretations made of their significance.

L. F. Conover and H. V. Senn (U. S. Weather
ureau, University of Miami, Miami, Fla.) *Use
Spiral Overlays in Tracking Hurricanes by
adar*—Overlays developed at the University of
liami under U. S. Weather Bureau contract dur-
g the study of spiral rain bands are examined
show the role they play in the hurricane's move-
ent and intensity. These have been found to be
ry useful in locating the eye when only a frag-
ent of a spiral band is visible on the radar scope.
mphasis is placed upon several features of the
iral structures which may be depended upon.
lso, configurations are illustrated which should
e avoided in applying the overlays as an observa-
onal aid. Radar reports for several hurricanes
nder radar surveillance during the 1958 season are
sed as illustrations.

A. P. Crary (Air Force Cambridge Research
enter, Bedford, Mass.) *Seismic Methods and
reliminary Results, Ross Ice Shelf and Victoria
and Plateau*—During IGY Antarctic operations,
raverse parties from Little America, Byrd, and
llsworth stations traveled over 7500 miles on
land ice, carrying out glaciological, seismic, grav-
y, and magnetic studies. During the first summer,
ıe Little America traverse worked entirely on
ıe floating Ross Ice Shelf. Reflections from the
ottom of the water were generally good, but
eflections from the ice-water interface were not
bserved with ice thicknesses of less than 500
ıeters. Most accurate information on ice thick-
ess was obtained from multiple reflections which
ıcluded at least one reflection from the ice-water
ıterface. Thickness of the ice varied from 130
ıeters near the barrier edge to over 750 meters
ı the southeastern part. Deepest water encoun-
ered was 1360 meters below sea level, but rela-
ively deep water was found at all stations near
he inland ice. In the summer of 1958–1959 the
arty traveled up the Skelton Glacier and 640
ilometers into the Victoria Land plateau, where
levations ranged from 2400 to 3000 meters. Seis-
ıic reflections were very poor, with low signal-to-
ıoise ratios despite shot holes 15 and 20 meters
leep. Material immediately under the ice, prob-
bly sandstone, had a velocity about the same as
hat of ice, 3.9 km/sec, and could not be detected
y refraction methods. With a combination of the
oor reflections from the bottom of the ice and
efractions from a 5.5- to 5.9-km/sec layer about
000 meters below the bottom of the ice, a section
nto the plateau was obtained.

John R. Crippen (U. S. Geological Survey,
Washington, D. C.) *Frequency of Deficient Dis-
harge*—One characteristic of low flow may be de-
ined as the flow below which the daily discharge of a stream can be expected to remain continuously for a given length of time. This characteristic, here termed 'deficient-period discharge,' may be either the extreme during the period of record, or that which can be expected to recur with a certain frequency in years. Relationships between deficient-period discharge and the more commonly used average discharge for the same length of period can be found and used to compute the frequency of deficient-period discharge. Frequency of deficient discharge is useful in pollution-control studies and in other studies where the length of time between periods of deficiency is important.

A. R. Croft (U. S. Forest Service, Ogden, Utah) *A Concept of Erosion Potential of Mountain Soils*—Inherent in the plant-covered soils of the steep mountains of the West are certain hydrologic functions—surface detention, infiltration, storage, and percolation—that have made possible the accumulation and development of soil. It is through these functions, over the ages, that the soil has been able to dispose of large amounts of precipitation (15 to 80 inches annually) without being washed away in the process. The longer this intimate relationship of hydrologic function to soil development exists, and the deeper the soil on steep slopes becomes, the greater is the potential for soil erosion and sedimentation. The soil's existence, then, is dependent on preservation of its hydrologic functions. Tremendous potential for destruction, once the soil's hydrology is disturbed, is shown by reports of sedimentation rates along the Wasatch mountain front in Utah. Here, recent past geologic rates of .0025 AF/SMY have increased as much as 2500 times since settlement, to about 6.25 AF/SMY. These high rates are related to changes in vegetal cover which is followed by changes in the soil's hydrologic functioning during torrential rains.

J. Cl. De Bremaecker Institut pour la Recherche Scientifique en Afrique Centrale, Bukavu, Congo Belge) *Seismicity of the West African Rift Valley*—Four seismograph stations have been operating near the West African Rift Valley since 1953. All the epicenters between 3°N and 6°S, and 24°E and 32°E have been plotted on a map. A transverse zone stretching westward from Lake Kivu for at least 450 km constitutes the most important discovery. Extinct or active volcanoes are located at the junction of this zone and the Rift. Most other epicenters are on faults bordering the Rift or on their prolongation; a few are on faults cross-cutting it. The 'extinct' volcano area north of Lake Kivu is fairly active.

The yearly release of seismic energy within a radius of 500 km around Lwiro has a mean value of 3.5×10^{20} ergs. It is probably more correct to assume a variable seismic volume and a constant elastic limit than vice versa when a whole region is investigated.

J. Cl. De Bremaecker (Institut pour la Recherche Scientifique en Afrique Centrale, Bukavu, Congo Belge) *Electronic Transducer and Tiltmeter*—Transducers may depend on the modulation of frequency or amplitudes by means of variable capacity, inductance, or resistance. A push-pull arrangement can also be used. Many of the possible

combinations have been used. The present transducer is of the mutual inductance type (variable transformer) with a mobile H-shaped primary and two fixed U-shaped secondaries. It operates at 1 kc and responds to a few millimicrons of displacement. Two such transducers will be installed on each end of an oil-and-water tube to record earth tides and long-period waves either directly or on magnetic tape.

Wallace de Laguna (Oak Ridge National Laboratory, Oak Ridge, Tenn.) *The Brookhaven Lysimeter*—A lysimeter was installed at Brookhaven National Laboratory, Long Island, N. Y., to study the distribution and amount of recharge to the water table. The soil was excavated for the installation, but it is so sandy that it could be replaced with essentially its original porosity but with an unknown increase in vertical permeability. There is virtually no direct surface runoff in this area, nearly all rain and snow infiltrating where it falls. Results showed the recharge to be about as expected, except somewhat larger than anticipated following heavy winter rains. Recharge following several hurricanes exceeded reported rainfall, probably because of incomplete catch by the rain gage in a high wind.

A. J. Dessler (Lockheed Aircraft Corp., Missiles and Space Division, Palo Alto, Calif.) *Effect of Magnetic Anomaly on Particle Radiation Trapped in the Geomagnetic Field*—Anomalies in the geomagnetic field will affect the mirror altitude of trapped particles. A negative magnetic anomaly (abnormally weak magnetic field strength) will lower the mirror altitude of the trapped particles which are reflected near the anomaly. The large negative anomaly near Capetown, South Africa, will lower the local mirror altitude by about 1000 km. Since the trapped particles drift around the earth's magnetic axis, the outward projecting 'horns' in the contours of constant radiation intensity observed by Satellite 1958ϵ may be explained on the basis of this anomaly and the equatorial drift of the trapped particles. The gap in the radiation belt as observed by Lunar Probe Pioneer III is also apparently related to this anomaly, and the intensity at the minimum relative to the adjoining maxima indicates that most of the trapped particles are reflected at comparatively low altitudes.

A. J. Dessler (Lockheed Aircraft Corp., Missiles and Space Division, Palo Alto, Calif.) and E. N. Parker (Enrico Fermi Institute for Nuclear Studies, University of Chicago, Chicago, Ill.) *Hydromagnetic Theory of Geomagnetic Storms*—A hydromagnetic theory is presented which explains the average characteristics of geomagnetic storms. Stresses can be set up in the geomagnetic field by plasma from the sun. These stresses, which are propagated to the earth as hydromagnetic waves, are shown to account for the observed average magnetic storm variations. The sudden commencement is generated by the impact of plasma from the sun on the geomagnetic field. The effect of the impact is carried to the earth's surface by hydromagnetic waves. The initial phase is due to the increased solar wind pressure. During the initial phase, instability causes small plasma clouds to become imbedded in the magnetic field. The small clouds break up and diffuse into the magnetic field to form a belt of trapped particles from the sun. It is shown that the trapped protons set up stresses, due to centrifugal force, which account for the main phase. The recovery from the main phase is attributed to the relief of the stress by the geomagnetic field by transfer of the energy of the trapped protons to neutral hydrogen by means of the ion-atom charge-exchange process, for which the measured cross section gives the correct time constant.

A. Nelson Dingle (University of Michigan, Ann Arbor, Mich.) *The Effect of Wind Direction Upon Ragweed Pollen Deposition*—Experimental studies of the dissemination of ragweed pollen from localized sources show that the locus of maximum pollen deposition does not generally follow the direction of the mean wind vector near the ground. The mechanism of pollen flotation suggests that a deviation of the locus of maximum deposition to the right of the mean wind vector may be expected because of the greater effectiveness of gust maxima, as compared with lower wind speeds, in loosening and transporting the pollen from its source.

C. H. Dix (California Institute of Technology, Pasadena, Calif.) *The Reflected Seismic Pulse*—Approximate formulas for the calculation of the displacement potentials and components are derived for reflected pulses based on Cagniard's work (Reflexion et Refraction des Ondes Seismiques Progressives, 1939). For early parts of the pulse one has to evaluate integrals, the integrands of which have two factors, one dependent only on the complex variable of integration u and the other dependent on u and on the receiver's space-time coordinates. The former part, though very complicated in appearance, is simple and smooth in the region of interest here; it can be simply expanded as a power series in u. Then the integrations can be carried out using the first terms of the expansion. For very early parts of the pulse the center of expansion is $u = 0$. For a later range one selects a suitable positive real value of u for the center for series expansion.

William L. Donn and William T. McGuinness (Lamont Geological Observatory, Columbia University, Palisades, N. Y.) *North Atlantic Ice and Ocean-Wave Results*—Ocean-wave spectra from short-period gravity waves to tide periods have been well recorded at a number of IGY island observatories. All stations show common gravity waves to 16 sec, but those recorded in deep water show a much more regular profile than when recorded in shallow water, owing to bottom and coastal effects. West Indian storm surges have been explained on the basis of distant storm swell, spring tides, and coastal conditions. Longer period waves (1 to 5 min) at shore recorders reach a maximum when waves and swell are high and are attributed to coastal surf-beat effects; these are absent at deep-water installations. Periods of 6 to 15 min associated with open coasts appear to be some coastal resonance phenomenon not yet fully investigated. Most stations show seiches of about 10 to 40 min which can mostly be explained

ıe boundary conditions. Resonant coupling can e demonstrated between long-period waves in air nd ocean. In addition to tide variations resulting rom atmospheric pressure variations and tem- erature-volume changes, some significant anom- lies have been recorded.

James Dorman (Lamont Geological Observa- ory, Columbia University, Palisades, N. Y.) *The- ry and Computation of Properties of Surface Vaves on Layered Media*—Haskell's matrix for- ıulation for surface waves on layered solid half pace has been generalized to cover all cases of urface or boundary waves in media of interbedded olid and liquid layers. The matrix theory leads to umerical methods for calculating dispersion and istribution of particle motion for layered media vhich are much simpler and faster than the de- erminant method. A program has been written or the IBM 650 to solve problems of Rayleigh nd Love waves including higher modes on a ayered half space and has been applied to models onsisting of as many as 150 layers. An energy alculation has been developed by which group elocity at a given wave period can be determined rom a single-phase velocity solution at the same eriod. This increases speed and flexibility in prac- ical work. Examples of computations on disper- ion of surface waves by typical continental and ceanic sections are shown.

William J. Evans (Federal Aviation Agency, Washington, D. C.) *Meeting the Weather Com- nunications Requirements of Jet-Age Aviation*—For many years, flight dispatchers, traffic control- lers, and meteorologists have needed more mete- orological data than could be provided over the weather-communications networks. With the ad- vent of jet flights, demands are being made for an ever-increasing amount of meteorological informa- tion. Fortunately, forward-looking planners in the old CAA recognized this problem and planned a major weather communications improvement pro- gram which will become operational within a year. Included in these plans are providing a high-speed (600 to 1000 wpm) transcontinental express circuit which will collect hourly reports from over 600 locations in less than 15 min; increasing the oper- ating speed on all networks from 75 to 100 wpm; establishing an additional 25,000 mi of new circuits, including 14 new Service A circuits to speed the flow of hourly data to major users; and providing for selective readout of reports direct from the high-speed circuit at all major forecast centers. In the years immediately ahead we are planning high-speed express circuits with error-detecting equip- ment designed to provide the necessary accuracy for direct input of synoptic data into the com- puter.

J. F. Evernden, G. H. Curtis, R. Kistler, and J. D. Obradovich (University of California, Berke- ley, Calif.) *Argon Diffusion in K-Feldspar, Biotite, Glauconite, and Illite*—Samples of K-feldspar, biotite, glauconite, and illite were heated to fusion in incremental steps, each increment being held at constant temperature from 6 to 48 hours. Argon diffusion data were obtained for five size-fractions of K-feldspar ranging from 125 to 420 microns average diameter; for two size fractions of biotite, $16.5 \times 15{,}000$ microns and 48×420 microns; and for single samples of glauconite and Fithian illite. All of the sanidine data give one accordant curve when plotted on a diffusion-coefficient versus tem- perature diagram. For 500°C, $D = 1.2 \times 10^{-13}$ cm²/sec, and for 1000°C, $D = 1.3 \times 10^{-10}$ cm²/sec. Because of uncertainty at the lower temperature, extrapolation to 0°C is unwarranted.

For biotite, depending upon the diffusion model assumed—that is, perpendicular or parallel to cleavage—$D = 10^{-10}$ cm²/sec at 1000°C (perpen- dicular), $D = 10^{-5}$ cm²/sec (parallel), and at 0°C, $D = 10^{-30}$ cm²/sec (perpendicular) and 10^{-25} cm²/sec (parallel). These and correlative data suggest that diffusion perpendicular to cleavage is dominant. Computed diffusion losses of argon from biotite of 200-micron thickness in the lower range of geologic temperatures and under the conditions of these experiments are:

Temp. (°C)	D	Time (year)	Loss (per cent)	Time (year)	Loss (per cent)
30	$0.15\text{–}1 \times 10^{-28}$	10^6	0.0002–0.0006	10^9	0.01
100	$1\text{–}5 \times 10^{-25}$	10^6	0.02–0.04	10^9	1.0
200	$0.35\text{–}1 \times 10^{-21}$	10^6	1.2–1.9	10^9	48
300	10^{-19}	10^6	19	10^9	...

In glauconite and illite, when heated under low water pressure, argon and hydroxyl water loss ap- pear to be closely correlated. The nature of the argon diffusion in glauconite is illustrated by a curve of argon-loss versus time at constant tem- perature.

Maurice Ewing (Lamont Geological Observa- tory, Columbia University, Palisades, N. Y.) *The Scotia Sea Floor*—On *Vema* cruises 14 and 15 continuous observations of topography and total magnetic field were made. Frequent atmospheric samples were obtained for tritium and CO_2 analy- sis. A continuous bathythermograph observation program supplemented by water-bottle data and large volume samples for carbon 14 analysis has been followed. Piston core samples, biological trawls, and ocean-bottom photographs have been obtained to study the ocean floor. Many seismic refraction stations were made. These observations were carried out in cooperation with the Argen-

tinians as a study of the Drake Passage, the Scotia Sea, and the South Sandwich Trench.

The geological history of this region is discussed in the light of these recent observations. Particular attention is given to the possible continuation of the Andes mountain chain and to Quaternary events. Two major magnetic anomalies strike from Tierra del Fuego into the Drake Passage. There is a large magnetic anomaly associated with the South Sandwich Trench in contrast with other trenches previously investigated. Many similarities between the Caribbean Sea and the Scotia Sea are indicated by the seismic data. Extensive areas of pebbles were photographed. The cores, however, show that this type of sedimentation does not continue to any great depth.

Henry Faul (U. S. Geological Survey, Washington 25, D. C.) *Doubts of the Paleozoic Time Scale*—K/Ar and Rb/Sr determinations on intrusive rocks of the Paleozoic era almost always give ages greater than the numerical age predicted by the currently accepted time scale. Paleozoic intrusives with narrow stratigraphic limits are rare. We have studied closely bracketed intrusives in eastern Main (early Devonian) and northeastern France (early Carboniferous). We have also measured the ages of rocks that intrude fossiliferous sediments (Lower Devonian slates in the Jackman and Mount Katahdin areas, Maine, and Permian lavas and sandstones in the Oslo region) but have no stratigraphic top limit. We report here the following preliminary values, based on measurements that are still in progress: Post-Upper Silurian, pre-Upper Devonion 390 m y (K/Ar); post-Oriskany (post-Lower Devonian) 360 m y (K/Ar); Dinantian, pre-Visean (lower Carboniferous) 340 m y (Rb/Sr) and 320 m y (K/Ar); post-Permian 260 m y (zircon, isotopic U/Pb), and 250 m y (K/Ar). The results show that one may begin to think of fairly drastic revisions in the Paleozoic time scale. However, alternate explanations could be advanced. Hasty erection of new time scales seems ill advised until the body of available data becomes so convincing that new doubts need not come up right away.

E. L. Fireman and J. DeFelice (Smithsonian Astrophysical Observatory, Cambridge, Mass.) *Argon-39 and Tritium in Meteorites*—The radioactive isotopes argon-39 (260-year half-life) and tritium (12.4-year half-life) were measured in seven iron and in two stony meteorites. Argon-39 was detected and measured in the iron meteorites Sikhote-Alin (1947), Treysa (1916), Pitts (1921), and in the stony meteorites Norton County (1948) and St. Michel (1910). The detection and measurement of argon-39 in these meteorites makes it possible to determine their argon exposure ages. On the basis of the same assumptions previously used, the ages are 4.9×10^8 years for the Sikhote-Alin meteorite, 5.7×10^8 years for the Treysa meteorite, 6.5×10^8 years for the Norton County meteorite, 1.7×10^8 years for the St. Michel meteorite, and, for the Pitts meteorite, an unusually low figure in the range of 10^7 years.

The short argon exposure ages may be interpreted in two ways: they may result from the loss of shielding material, worn off the meteorite in space by interplanetary dust and gas as suggested by Whipple; or they may represent the tim since the breakup of planets. From the lack argon-39 in the Carbo, Grant, and Washingt County meteorites whose dates of fall are u known, one can conclude that they fell more th 1500 years ago. In the case of the Cañon Diab meteorite the helium-3 content is so low that t measured absence of argon-39 and tritium does n necessarily mean that it fell long ago. The rat of tritium to argon-39 radioactivities (decays min) in the Norton County meteorite is 230 t at the time of fall. This ratio in the Sikhote-A meteorite is anomalously low, being less than to 1 at the time of fall.

Paul Frenzen (Argonne National Laborato Lemont, Ill.) *Laboratory Studies of Turbule Diffusion in Stratified Fluids*—A series of expe ments carried out in a towing tank at the Argon National Laboratory is described. Lagrangi autocorrelation functions were computed fr particle trajectories photographed in the lee of moving, rectangular grid, the velocity measu ments having been corrected for decay by method suggested by G. K. Batchelor. Autocor lation functions and their cosine transforms (L grangian spectra of turbulence) determined un conditions of stable, neutral, and unstable flu stratification are compared. Possible applicatio of the experimental model to atmospheric turb lence problems are considered.

E. M. Frisby (South Dakota State Colle Brookings, S. Dak.) *A Study of the Verti Gradient of Temperature near the Ground at Site in Southeastern South Dakota*—The pa discusses the establishment in early April 1958 a microclimatic instrument network at a site alo a west-east section of a river valley in southea ern South Dakota. It presents an hourly analy of the temperature data obtained from the si during the period May 1, 1958 to April 30, 1959.

Tetsuya Fujita (University of Chicago, Ch cago, Ill.) *Technique of Computing Hurrica Echo Velocity by the Use of Airborne Radar* Computation of echo velocity by using airbor radar pictures is rather complicated because of t motion of the plane and echoes. In this techniqu the plane's position, given in the photopanel, w eliminated first and the individual echo was ide tified by shifting the radar coordinates as much five to ten miles per minute. As an example, ech velocities around the eye wall of Hurricane Carr are shown.

Tetsuya Fujita (University of Chicago, Ch cago, Ill.) *Preliminary Report on the Developme of Animated Motion Picture in Mesometeorolog* —Mesoanalytical studies of the data from t U. S. Weather Bureau's Texas-Oklahoma netwo revealed that excellent continuity exists betwe the charts. The charts were interpolated at 7½ minute intervals, then they were photographed i several different ways. The results so far ha shown that the animation of charts is feasib and that the animated motion picture is extremel valuable both for education and research purpose

Arie Gaalswyk (Mechanical Division, Gener Mills, Minneapolis, Minn.) *Vertical Motions in*

nunderstorm Cell Indicated by a Balloon-Flight cident—An analysis is made of vertical motions dicated by the time-altitude data of a balloon ought down from the stratosphere by a thunder- orm cell. Upward air motions were sufficient to op the descent of an 800-lb load on a parachute 20,000 ft and carry it back up to 40,000 ft. From own drag characteristics of the parachute it was termined that updrafts must have exceeded 90 /sec. This maximum occurred at 30,000 ft about min after the trajectory of the balloon and the rachute load went through a transition from scending to ascending motion. A maximum ownward of 32 ft/sec occurred at 40,000 ft about min before the transition. An attempt is made relate the computed vertical motions to a verti- l cross section of the thunderstorm cell.

Paul W. Gast (University of Minnesota, Minneapolis, Minn.) *The Rubidium-Strontium Age Stone Meteorites*—The isotopic composition of rontium and the rubidium and strontium content three howardite achondrites and five chondrites ave been determined. The howardites are greatly epleted in rubidium. The Sr^{87} abundance of the owardites is constant within 0.3 per cent. The apparent ages found from the difference in the undance of Sr^{87} in the chondrites and the howrdites are discussed. Beardsley appears to be a nique chondrite. Its rubidium content is sigificantly higher than that of all other chondrites hich have been studied. Its apparent rubidiumrontium age is also greater than that of other hondrites. The isotopic composition of terrestrial trontium has also been investigated. The lowest errestrial abundance is almost identical to that ound for howardites. Thus it is suggested that the arth was formed at the time that rubidium was eparated from strontium in the achondrites.

Charles E. Giffin and J. Laurence Kulp (Lamont Geological Observatory, Columbia University, Palisades, N. Y.) *K-A Ages on the Precambrian Basement of Colorado*—The existence of orogenic events at 2600, 1300, and 100 m y in the egion of the Rocky Mountains has been fairly vell established. At least the latter two events ppear to have affected large areas of the basement n Colorado. Further reconnaissance by the K-A method has been undertaken in a search for remnants of the older basement in an attempt to delimit the areas of superimposition of the 1000 m y event on pre-existing metamorphic and igneous rocks. About 25 localities have been sampled, representing most of the larger areas of Precambrian exposure in Colorado. No evidence of the 2600-m y-old basement has been found. The youngest Precambrian event appears to have occurred at about 1000 m y, and, although centered in the Pikes Peak area, it is detectable elsewhere in the State.

Freeman Gilbert and Leon Knopoff (Institute of Geophysics, University of California, Los Angeles, Calif.) *Scattering of P Waves by the Core of the Earth*—The solution to the problem of the scattering of P waves from an impulsive point source by a fluid sphere imbedded in a homegenous, isotropic, elastic solid has been obtained. This solution is compared with the solutions to the corresponding problems of the scattering of P waves by (1) a perfectly rigid sphere, (2) a perfectly weak sphere, (3) a perfectly rigid half-plane, (4) a perfectly weak half-plane, and (5) the scattering of SH waves by a half-plane. The shape of the time response is not the same for all these cases, nor are the amplitude distributions the same. The amplitude responses are computed for incident wavelets with the dominant period of core waves; as in the impulsive cases, the amplitudes and wave forms depend critically upon the model considered. Jeffreys has applied the Airy theory of diffraction to this problem in his work on the existence of the inner core; although diffraction by the outer core cannot explain all the observations in the shadow zone, Jeffreys' method allows only a qualitative interpretation of diffraction by the core. The use of diffraction to investigate the core-mantle boundary requires a more complete theory and a careful analysis of seismic records.

Freeman Gilbert and Gordon J. F. MacDonald (Institute of Geophysics, University of California, Los Angeles, Calif.) *Free Oscillations of the Earth*—The calculations of Love, Stoneley, and Pekeris on the free oscillations of the earth have been revised and extended. Frequencies have been computed for five different earth models by a variational technique. The lowest four frequencies for each model for the first five torsional modes and the first six coupled modes have been obtained. Approximations to the periods of oscillation in the first coupled (radial) mode, obtained by the variational method, are compared with the exact solution below. The effect of the inhomogeneity of the earth is to decrease the period of the lower modes.

Item	T_1 (min)	T_2 (min)	T_3 (min)	T_4 (min)
Exact (homogeneous earth)	26.1	10.4	6.7	5.0
Variational (homogeneous earth)	26.1	10.4	6.6	4.1
Variational (Bullard model earth)	20.8	10.1	6.5	4.6

The near-surface values of the elastic parameters and of the density play a dominant role in determining the frequencies. The effect of the viscosity of the core is negligible, and the dissipation in the mantle is treated as solid friction of a constant Q type. It is suggested that careful spectral analyses of broadband seismic recordings show the presence

of the frequencies corresponding to the higher order free oscillations. The results of the spectral analyses of several Benioff strain recordings are discussed.

S. S. Goldich, A. O. Nier, J. H. Hoffman, and H. W. Krueger (University of Minnesota, Minneapolis, Minn.) *Problems of Early Precambrian Time*—Events of Early Precambrian time in Minnesota and adjacent areas are interpreted from geologic and radioactivity-dating studies. The oldest orogeny is known from geologic evidence and involved folding of Keewatin and older rocks accompanied by emplacement of the Saganaga granite. A second orogeny involved folding of the Knife Lake group and instrusion of the Vermilion granite dated at approximately 2.6 b y Gneisses mapped as part of the Giants Range batholith are dated at 2.6 b y but granite intrusions give 2.4 b y. Granites in the Rainy Lake area mapped as Algoman by Lawson are of different ages; some are dated at 2.6 b y, and others at 2.4 b y. A similar relationship is found in the Minnesota River valley where the Morton gneiss (2.6 b y) is intruded by granite 2.3 to 2.4 b y). The 2.6-b y orogeny was a major event, and intense metamorphism at this time has obscured earlier events. Efforts to date the older rocks are being continued.

S. M. Greenfield and W. W. Kellogg (Rand Corp., 1700 Main St., Santa Monica, Calif.) *Spectral Measurements from a Meteorological Satellite*—Since certain constitutents of the atmosphere have pronounced spectral absorption and emission bands, the radiation which is scattered and emitted upward from the atmosphere will depend on the distribution and temperature of these constituents. The constituents which are of primary interest in this respect are water vapor (with a band in the infrared at 6.3μ) and ozone (with bands in the ultraviolet between 0.2 and 0.3μ and in the infrared at 9.6μ). Carbon dioxide plays a somewhat lesser role. The analysis shows how atmospheric changes may be estimated by spectral measurements in the ultraviolet and infrared from a meteorological satellite.

R. F. Hadley (U. S. Geological Survey, Denver, Colo.) *The Effect of Waterspreading on Streamflow and Suspended Sediment Discharge*—A study was made on a waterspreading system in the valley of Box Creek, Converse County, Wyoming, to determine the use of water by conservation practices designed to reduce sediment yield or fluvial erosion. The waterspreading system on Box Creek consists of 27 small dams that divert the flow directly onto the flood plain, where it is used to irrigate a hay meadow of 360 ac. Two gaging stations were installed, one above the waterspreading system and one below, to measure the inflow and outflow. Analyses of flood hydrographs and sediment samples for two storms that originated above the upper gaging station, with no contribution between gages, reveal a marked decrease in peak discharge, volume of runoff, and suspended sediment load as the flow passed through the waterspreading system.

During the period June 9 to 14, 1957, the peak discharge at the upper gaging station was 1190 cfs and only 276 cfs at the lower gage. The volume of inflow measured at the upper gage was 506 ac and the volume of outflow was 350 ac ft. Similar in the period June 30 to July 4, 1957, the pe discharge was reduced from 840 to 247 cfs and t volume of runoff decreased from 485 to 355 ac between gaging stations. Data indicate that the decreases are dependent on antecedent soil-mo ture conditions. The reduction in peak discha and volume of runoff between gaging stations w accompanied by a 75 per cent reduction in to suspended sediment load. Approximately 3400 to of sediment were trapped on the flood plain these two periods.

Bradford A. Hall and F. Donald Eckelman (Department of Geology, Brown University, Pro dence 12, R. I.) *Nature and Petrologic Significan of Apparent Gravity Settling in a Dike of We erly Granodiorite, Bradford, Rhode Island*—St tistical data and weight percentages for zirc populations at successively higher elevati within a gently dipping, granodiorite dike arg against apparent evidence for gravity settling heavy minerals. Uniformity of weight percenta and reduced major axes for zircon populations the main body of the dike confirm this conclusi as do the weight percentages of other heavy m erals such as biotite, apatite, and sphene. Va tion of weight percentages, elongation frequenc volume frequencies, and reduced major axes f zircon populations in the lower contact zone attributed to magmatic sorting of zircon due laminor flow. Primary flow layers involving zirc biotite, and other heavy minerals, and the abse of abnormal amounts of heavy minerals in so gentle depressions at the base of the dike, a suggest that gravity settling has not occurred. T is consistent with evidence indicating a norm viscosity for the magma as shown by the mediu to-fine-grained character of the rock and by t absence of evidence of excessive amounts of fu tive constituents. The observations are consiste with early crystallization of zircon in felsic igneo rocks.

R. E. Hallgren and C. L. Hosler (Departme of Meteorology, Pennsylvania State Universit University Park, Pa.) *Collection Efficiency of Ice Pellet in an Ice-Crystal Cloud*—Quantitati measurements of the collection efficiency of an i pellet in a cloud of small ice crystals will be pr sented, and the influence of temperature will b described. The results will be discussed with refe ence to growth of snowflakes and to charge gener tion in thunderstorms. A brief description of th apparatus is given.

E. C. Hansen, I. Y. Borg, and J. C. Maxwe (Princeton University, Princeton, N. J.) *Dynam Significance of Quartz Lamellae*—Griggs, Turne and collaborators have demonstrated in exper mentally deformed Yule marble that the stre field can be determined from a study of twinnin induced on *e* {01$\bar{1}$2} in constituent calcite cry tals. Using oriented samples of Oriskany san stone, which is composed of randomly oriente quartz grains with well-developed lamellae an calcite cement highly twinned on *e*, stress field were obtained from the calcite and related to th quartz lamellae. Excellent correlation betwee

:rtz lamellae and calcite showed that twinning :alcite was caused by the same stress field that ormed the quartz. Triaxial stress fields were ob- ıed from samples from the limb of a fold, and corresponding quartz lamellae define two nes, each making an angle of about 35° to 40° :he maximum principal stress axis and both con- ıing the intermediate principal stress in their ersection. A biaxial stress field was determined m another sample from the crest of an anticline, l the quartz lamellae define a cone everywhere ırly 35° to 40° to the maximum principal stress s. Arrows constructed on projections in such a v that the head is at the *c* axis of a quartz grain l the shaft is a great circle defined by the *c* s and pole to a lamellae tend to point to the npression axis deduced from *c* twinning in cal- e in the same specimen. The maximum and in- mediate principal stress axes are respectively rmal and parallel to the local fold axis. This rk suggests that the orientation of lamellae in artz-bearing rocks may be useful in deducing ess fields.

Kirby J. Hanson (U. S. Weather Bureau, Wash- gton, D. C.) *Radiation Measurement on the uth Polar Snowfield: A Preliminary Report*—)servations of solar and terrestrial radiation and sociated energy exchange at the geographic uth Pole were first taken during the Interna-)nal Geophysical Year. An attempt is made to ow the problems of radiation observation when ındard instrumentation is used on a cold polar owfield. Low sun elevation during the six light onths, changing sastrugii patterns, instrument ex-)sure at temperature 150°F below calibration, ıd human limitations during the winter night all fect in varying degrees the observed fluxes of lar and terrestrial radiation. A preliminary study the radiant energy exchange is presented to ıow the absorption of solar radiation at the snow ırface and 'warm' cloud effect on surface tem- eratures during the winter night.

Mahdi S. Hantush (New Mexico Institute of Mining and Technology, Socorro, N. M.) *Analysis f Data from Pumping Wells near a River*—Meth- ds are outlined to determine the hydrologic char- cteristics of an aquifer draining or drained by a ream; specifically to determine the transmissi- ility and storage coefficients of the aquifer and he effective distance from a pumped well to the ed of the stream where the water is entering or eaving the aquifer. The procedure is based on the heory of the nonsteady flow toward a steadily ischarging well from an infinite aquifer hydrau- ically connected to a fairly straight and long tretch of a stream bed. Application of these meth- ds is illustrated by treating data from the Ingalls rea in Kansas.

Clayton H. Hardison (U. S. Geological Survey, Washington, D. C.) *Frequency of Seasonal Storage* —The average recurrence interval at which given mounts of storage will be required if a given uni- orm draft rate is to be maintained can be com- puted from the frequency of annual minimum dis- harge for various periods of consecutive days. The amounts of storage required for given draft rates at a given recurrence interval are computed from a mass curve developed from the low-flow frequency data for the same recurrence interval. Storage-required frequency curves computed in this manner are particularly applicable to the problem of designing storage to increase the flow during low-water months.

Donald R. F. Harleman and Jan M. Jordaan, Jr. (Hydrodynamics Laboratory, Department of Civil and Sanitary Engineering, Massachusetts Institute of Technology, Cambridge, Mass.) *Density Effects on Time-Dependent Turbulent Diffusion in an Idealized Estuary*—Turbulence, homogenous with distance, is generated in a 32-ft rectangular flume by the oscillation of screens supported from a spring-mounted truss which can be driven at various amplitudes and frequencies. The rate of energy dissipation in turbulence is measured and correlated with the product of screen amplitude and frequency to define a mechanical eddy viscosity. Time-dependent diffusion tests were made by initially separating the diffusant and receiving fluid by a vertical barrier at the midpoint of the flume. After the desired turbulence level was established, the barrier was removed and the time and distance variation in concentration of the diffusant fluid was observed. Analytically, the process is in the nature of one-dimensional diffusion in a semi-infinite medium with a constant concentration applied at one vertical boundary. The effect of gravitational convection, superimposed on the turbulent diffusion, caused by a small density difference between the diffusant and receiving fluid was investigated. The density difference varied from zero to 2 per cent. A comparison of the gross diffusion coefficients for runs with the same turbulence level, both with and without density differences, was obtained. The increasing importance in the diffusion process of the gravitational convection (as the general turbulence level is decreased) is demonstrated quantitatively.

J. B. Harrington and G. C. Gill (University of Michigan Research Institute, Ann Arbor, Mich.) *The Flag Sampler: A High Efficiency Sampler for Particles 10 to 100 Microns in Diameter*—The collection efficiencies of various pollen and spore samplers have been tested both in a wind tunnel and outdoors. The common sampling techniques have been found to be both inefficient and inaccurate when used under normal wind conditions. A new and inexpensive sampler is described and its efficiency compared with that of other samplers.

Harold R. Henry (U. S. Geological Survey, New York, N. Y.) *Salt Intrusion into Fresh-Water Aquifers*—In a coastal aquifer a steady flow of fresh water toward the sea can limit the encroachment of salt water into the aquifer. This action is treated, assuming steady two-dimensional flow, and assuming that the salt and fresh water are immiscible and that there is no fingering. Theoretical equations for the shape and location of the interface and for the boundary velocities are derived for several sets of boundary conditions. The uncertainty of the location of the interface is circumvented by use of a hodograph plane. In addition, a complex potential is employed and related to the hodograph by conformal mapping. Certain boundary conditions represent inversions

of gravity seepage through dams for which solutions already exist. Numerical computations are presented also for a semi-infinite aquifer having a vertical seepage face and one having a horizontal seepage face.

D. M. Hershfield and M. A. Kohler (U. S. Weather Bureau, Washington, D. C.) *An Empirical Appraisal of the Gumbel Extreme-Value Procedure*—The purpose of this study was to appraise the predictive value of the widely used Fisher-Tippett type-I distribution when fitted to rainfall data by the Gumbel method. Thousands of station-years of rainfall data have been analyzed in several ways in an attempt to evaluate the Gumbel procedure. The results provide evidence for the acceptability of the Gumbel procedure for predicting the probability of occurrence of the extreme values of rainfall.

D. M. Hershfield and W. T. Wilson (U. S. Weather Bureau, Washington, D. C.) *A Comparison of Extreme Rainfall Depths from Tropical and Nontropical Storms*—Increasing attention has been given lately to the hydrologic characteristics of rainfall produced by tropical storms. Such storms are often outstanding flood-producers. As a result they have been given a lot of attention, more or less as a class. It has been suggested that they are significantly different from other storms with respect to frequency and other hydrologic characteristics of extreme rainfall. For the region affected by storms of tropical origin, various analyses and comparisons are made with storms not regarded as having tropical origin. In the following important respects, the extreme rainfall associated with tropical storms does not stand out as being significantly different from extreme rainfall associated with other types of storms: (1) frequency distribution of annual maximum for durations of 10 minutes to 168 hours, (2) shape of area-depth curve up to 5000 square miles, (3) time distribution within largest 24- and 48-hour rainfalls, and (4) time sequence or mass curves of these rainfalls.

Martin Hertzberg (Lockheed Aircraft Corp., Missiles and Space Division, Palo Alto, Calif.) *Ion-Atom Interchange as an Important Source of Ionospheric Atomic Nitrogen*—It is shown that secondary reactions involving the positive ions O^+, O_2^+, and NO^+ and the neutral species O, N, N_2, O_2, and NO are significant in determining the composition balance of the upper atmosphere. Their importance is manifest in two ways; first, in converting atomic ions to molecular ions; second, in bringing about the dissociation of molecular nitrogen. The conclusion that atomic nitrogen is a major neutral component of the F2 region is consistent with rocket measurements of ion composition below 250 km. A tentative curve for the degree of dissociation of molecular nitrogen as a function of altitude is presented. If this conclusion is valid, the observed N^+/O^+ ion ratios above 250 km leads to the expectation that atomic oxygen is preferentially ionized by Lyman continuum radiation from the solar chromosphere.

H. H. Hess (Princeton University, Princeton, N. J.) *The AMSOC Deep Hole to the Mantle*—There probably is no project, within the scope of present capabilities, which would give more information concerning the broad picture of the earth as a planet than drilling a hole through the sediments and the so-called 'basalt' layer and finally into the upper mantle. It can be looked upon as a courageous attempt to broaden the base on which the most fundamental of earth problems rests.

A. If an authentic sample of the material below the discontinuity were obtained one could establish the following attributes for the following purposes:

(1) *Density*—The density of materials from the surface to the center of the earth has been computed by Bullen and more recently by Bullard. These computations are based on the moment of rotational inertia of the earth and are highly sensitive to the initial density assumed at the top of the mantle. If an exact figure could be given to this, the validity of the rest of the column would be greatly enhanced. The density value could also be used to great advantage in analyzing gravity anomalies over the seas.

(2) *Composition, bulk, and mineral phases*—If the composition and mineralogy of the top of the mantle were known a much more valid earth model could be constructed. High-pressure and high-temperature research could be concentrated on the type of material found rather than on some hypothetical preference. The validity of the meteorite analogy as a model for the earth's interior could be tested.

(3) *Radioactivity*—Some clue to explain the anomalously high heat flow from the floor of the ocean might be obtained.

(4) *Age*—Possibly the M discontinuity represents the primordial surface of the earth and the rock material found there formed at the beginning of the earth's history. If some means of determining its age could be found the result might be highly significant.

(5) *Isotopes of Pb, and the total Pb and U*—If primordial, the isotopic composition of the Pb corrected for the radiogenic Pb from U and Th present would significantly enhance the understanding of all Pb isotope age work.

B. What is the layer immediately above the M discontinuity with a seismic velocity near 6.5 km/sec? While it is generally said to be basalt, there is no evidence to substantiate this hypothesis other than that the velocity is appropriate. It would also be appropriate for a variety of other materials such as consolidated sediments or serpentinized peridotite. The thickness of this layer is comparatively uniform over much of the deep sea (4.5 km $\pm$ 1). It is almost inconceivable that if it consisted of basalt flows the thickness could be so uniform. That it is something in the nature of a phase transition as suggested by Sumner (1954), by Lovering (1958), and many others, seems much more likely. Perhaps it is a phase transition related to a much steeper thermal gradient in the distant past. Is it the transition from peridotite to serpentinized peridotite or from eclogite to basalt? Present evidence, serpentine dredged from fault scarps and olivine nodules of basaltic volcanoes strongly support the former hypothesis.

C. The sedimentary column from the sea floor to the material mentioned above could be sampled. Such a sample in the deep sea might give

omplete sedimentary column stretching back to he beginning of the oceans. The fossil flora and auna in this column back to the first appearance f life in the sea would be extremely interesting it could be obtained. Or perhaps one would find hat the oceans are relatively recent features on he earth's surface. In any case here is a whole ew world to explore.

D. Over-all properties of the materials through hich the hole passed could be measured to great dvantage.

(1) *Thermal*—One would like to obtain figures n the temperature gradient, conductivity, and a onsequent better understanding of heat flow.

(2) *Seismic velocity*—A seismic velocity log ould be obtained which would form a better basis or understanding seismic results at sea and per- aps for testing for seismic anistropy in different lirections around the hole.

(3) *Magnetism*—The magnetic properties of the naterials in the hole could be obtained. This vould certainly lead to a much better means of nterpreting the magnetic anomalies at sea. The lirection and sign of the remanant magnetism of he rock samples progressively down the hole could e determined, perhaps shedding some light on aleomagnetic problems.

(4) *Electrical properties*—Various types of elec- ric logging could be done, coupled with laboratory neasurements on the samples.

Above are most of the obvious objectives, but o doubt in probing into new and unexplored ter- itory the unexpected discoveries might play a arge role in the final outcome.

Some have deprecated the value of drilling this ole by postulating that the earth's crust and nantle are too heterogeneous to prove much with *ne* hole. To them I can only say that if there isn't first hole there cannot be a second. My own valuation of the data suggests, however, uni- formity rather than heterogeneity.

V. P. Hessler and E. M. Wescott (Geophysical Institute, University of Alaska, College, Alaska) *Earth-Current Rapid Fluctuations at College, Alaska*—A distinctive type of earth-current variation is regularly observed in the College records. The phenomenon consists of more or less regular fluctuations with range from a few mv/km to more than 1000 mv/km and periods ranging upward from six seconds. The fluctuations may continue from a few minutes to several hours. They have a strong diurnal variation at College with a broad maximum at 06h 00m local time (150° WMT). The fluctuations also occur at a site about 100 km southeast of College but are not observed at Barrow. Thus these rapid fluctuations display characteristics quite different from the previously classified magnetic and earth-current continuous pulsations, *pc*'s, and train pulsations, *pt*'s. Special equipment was devised to count and record the period of the fluctuations on a continuous basis. Typical rapid-fluctuation traces and charts showing their activity patterns are presented.

Bruce L. Hicks (CSL, University of Illinois, Urbana, Ill.) *The Spectrum of Small Wind Waves*—Small waves produce radar sea clutter, affect the drag coefficient of wind acting upon ocean waves, and represent the high-frequency end of the ocean-wave spectrum. More important, small wind waves are generated by and possibly dissipated by much the same processes as are the large ones at sea. Consequently the growth of small waves can serve as a naturally occurring dynamical model of the generation of large waves. In experiments, the investigator of small wind waves has an easy time compared with his counterpart at sea: average wind speed and average fetch can be defined with some precision; characterization of the wind is required only for very limited ranges of the time and distance variables; and the equipment used need not withstand the destructive effects of ocean storm waves. During 1957 and 1958 we made extensive measurements of small wind waves on a small lake near Urbana, Illinois. Experimental data consisted of about 200 measurements of rms wave amplitude h for various combinations of frequency f (center frequency of an octave-wide filter), average wind speed V, and average fetch F. We reduced the data with the help of numerous programs for Illiac, the University of Illinois' digital computer. Our principal results concern the energy spectrum of the waves for the following ranges of the variables: f, 0.8 to 12 cps; V, 0.6 to 6 m/sec; F, 10 to 700m; and h, 0.08 to 12 mm.

We define a spectrum function $\phi(f)$ such that

$$h^2 = \int_0^\infty \phi(f)\, df$$

A parameterized spectrum function of the form

$$\phi(f) = \begin{cases} b_3 V^{p_1} F^{p_2} f^{q_3} & f \leq f_0 \\ b_2 f^{-q_2} & f > f_0 \end{cases}$$

where the frequency f_0 at maximum is given by

$$f_0^{q_2+q_3} = [b_2/b_3 V^{p1} F^{p2}]$$

has been fitted by least squares to the experimental data. The appropriateness of this form of spectrum function, and in particular its dependence upon wind speed and fetch, had been indicated by our preliminary analysis of the data on small gravity waves.

The least-squares procedure included allowance for the shape of each octave-wide filter and will eventually permit estimates of the probable error of the values of the six parameters. The final analysis of CSL data will, if time permits, be compared with the recent measurements of Charles Cox on slope spectra, with the unpublished data of Burling on small wind waves, and with appropriate data on ocean waves. We believe that on the basis of such small wind-wave studies it will be possible in the future to design the difficult experiments on ocean waves so that they are more efficient and more accurate.

C. O. Hines (Radio Physics Laboratory, Defense Research Board, Ottawa, Canada) *Does the Polar Ionosphere Rotate with the Earth?*—The growing evidence that the earth is imbedded in

an ionized solar corona or interplanetary gas of appreciable density forces a re-examination of many previously-held beliefs. Among the latter may be included the belief that the upper atmosphere rotates with the earth. Viscous-drag effects now have a medium to operate against, and they are enhanced by the coupling provided by magnetic induction. Nevertheless, no systematic drag on the ionosphere's rotation has yet been reported.

An explanation of this has been provided by Dungey, but its application appears to be limited to regions away from the poles. It seems reasonable to suppose, then, that the polar atmosphere may be subject to drag effects and that these are yet to be observed. Indeed, a quantitative estimate will be presented which indicates that near the poles virtually all ionospheric levels tend to be held in a state of nonrotation. This immediately provides a completely new mechanism for the explanation of many polar and high-latitude effects, and even of some having wider distribution. A preliminary indication will be given of the type of effects concerned, and in some cases quantitative considerations will be introduced.

Walter H. Hoecker, Jr. (U. S. Weather Bureau, Washington, D. C.) *Wind-Speed Measurements in the Dallas Tornado*—Utilizing scaled movies of the Dallas tornado of April 2, 1957, measurements of the speed of debris particles, small dust clouds, and cloud fragments at various radii and heights around the tornado provides clues to the distribution of horizontal wind velocity in this tornado. Debris clouds ascending along the tornado trunk give data on the vertical wind current near the trunk. The speeds of the tracer elements are arranged in a composite of velocity distribution around the tornado, and this is compared with the theoretical *VR* vortex.

Jinghwa Hsu (Shell Development Co., Houston, Tex.) *A Theory for the Origin of Geosynclines*—The earth's crust is in approximately isostatic equilibrium; regions of thin crust are depressions. Crustal equilibrium can be disturbed by tectonic disturbances. Geosynclines, created after such disturbances when isostatic equilibrium is restored by crustal faulting, are regions of thinner crust. Further subsidence is induced by sedimentary load and by sediment compaction. Normal geosynclinal cycles start with deep marine sediments, followed by deltaic deposits, and end with shelf carbonates. Where rapid alluvial sedimentation prevents development of such cycles, regions of thin crust are overlain with thick continental deposits. The earth's mantle beneath the oceanic crust is apparently more radioactive than that under the continental crust. This supports the idea of continental accretion through partial melting of an initially radioactive mantle. Ensimatic geosynclines floored by oceanic crust are underlain by a radioactive mantle. Blanketing effects of geosyncline sediments result in weakening or melting a crust and mantle, which lead to crustal disturbance. New ensialic geosynclines are created in regions where crust is thinned through melting. Geosynclinal and orogenic cycles thus repeat themselves until the radioactivity of the mantle is concentrated in a thickened crust. The repeatedly deformed regions, now underlain by a weakly radioactive mantle, become cratons and nuclei for continental accretion.

Harry Hughes (Massachusetts Institute of Technology, Cambridge, Mass.) *The Conductivity Mechanism in the Earth's Mantle*—The electrical conductivity of corundum has been measured at pressures up to 10,000 bars and temperatures between 1350°K and 1550°K (where conduction by electrons is believed predominant) and found to decrease with pressure by about 2 per cent per 1000 bars. This is about half the rate of decrease found in peridot at relatively higher temperatures where the conductivity due to mobile metallic ions is much greater than that due to electrons. Extrapolating these results to the temperatures and pressures in the earth's mantle suggests that the conductivity observed there is not due to electrons, as is commonly thought, but is predominantly ionic.

Bengt Hultqvist and Johannes Ortner (Kiruna Geophysical Observatory, Kiruna, Sweden) and Jules Aarons (Air Force Cambridge Research Center, Bedford, Mass.) *Effects of the Solar Flare of July 7, 1958*—The very strong effects in the auroral zone of the solar flares of July 7, 1958 as observed at Kiruna Geophysical Observatory by means of magnetometers, an ionospheric sounder, a cosmic-noise absorption receiver (riometer), oblique auroral-reflection receivers, transpolar communications receivers, and cosmic-ray telescopes are reported and discussed. Several remarkable features of the terrestrial disturbances were observed: (1) Extremely strong absorption became apparent a few hours after the solar flare. In spite of a linearly increasing absorption during the first seven hours after the flare no change in height or critical frequency of the F2 layer was noted during this period. (2) The SID's reported by Pacific observatories at the time of the flare were not observed at Kiruna although Kiruna was on the sunlit side of the earth. (3) A magnetic storm and a large decrease in the counting rate of the meson component of cosmic radiation appeared simultaneously 31 hours after the flare. (4) The maximum absorption at 27.6 Mc/s recorded during this period was 23 decibels.

Marvin N. Hunter (U. S. Weather Bureau, Washington National Airport, Washington, D. C.) *The Correlation of the Zurich Sunspot Number with the Verification of Aviation Terminal Forecasts*—All regular aviation terminal forecasts made by the Weather Bureau at Washington National Airport are verified. A point system of verification is used whereby the lower the score the better the forecast; the higher the score the worse the forecast. Over the ten-year period from 1949 through 1958 more than five million hours of ceilings and visibilities have been verified and the results summarized. The average yearly verification score per terminal for each 12-hour forecast period shows some correlation with the Zurich sunspot numbers. Consideration of this correlation along with Wexler's findings as described in "Variations in Insolation, General Circulation and Climate" in *Tellus*, 1956, suggests that there is a physical basis for the variation of terminal verification scores with sunspot numbers.

P. M. Hurley, W. H. Pinson, R. F. Cormier, nd H. W. Fairbairn (Massachusetts Institute f Technology, Cambridge, Mass.) *Age Study of ower Paleozoic Glauconites*—Samples of the ineral glauconite of varying purity as deter-ined by x-ray powder diffraction were obtained rom Lower Paleozoic strata of well-established ge. K-A and Rb-Sr age measurements on these ive results in moderate agreement with each ther. In general, the glauconite ages suggested y the averages of results by the two methods are:

Geologic age	No. of localities	$*Sr^{87}/Sr^{87}$	$*Sr^{87}/Rb^{87}$ age, m y	A^{40}/K^{40} age, m y
Pennsylvanian	1			268 ± 12
Mississippian	1			250 ± 14
Lower Devonian	1	.124	320 ± 18	312 ± 14
Lower Silurian	1			370 ± 20
Lowest Ordovician	1	.333	375 ± 20	410 ± 16
Upper Cambrian	9	.334 Av.	443 ± 10	430 ± 10
Lower Cambrian	1	.163	525 ± 30	434 ± 20

* Radiogenic. $\lambda_e = 0.585 \times 10^{-10}$ yr^{-1}; $\lambda = 5.3 \times 10^{-10}$ yr^{-1} for K^{40}; $\lambda_B = 1.39 \times 10^{-11}$ yr^{-1} for Rb^{87}.

Samples from different localities along the same ed showed remarkably consistent ages. The effect n the age ratios of mild acid treatment or heat-ng to 180°C for 24 hours was negligible. A core ample taken at a depth of 6300 ft showed a 10 ercent reduction of argon age relative to surface amples on the same bed. The range of ages con-forms fairly well with the Holmes B time scale but are generally lower than certain minimum values established by well-dated igneous rock minerals elsewhere. These are: 360 ±5 m y for post-Lower Devonian intrusives in Maine, Nova Scotia, and New Brunswick; 260 ±5 m y for post-Lower Pennsylvania metamorphism in Rhode Island; and 180 ±5 for post-Lower Triassic gran-ite in Billiton, Indonesia.

E. R. Ibert and Donald W. Hood (A. and M. College of Texas, College Station, Texas) *A Simple Equilibrator for Use in Measuring Partial Pressure of Gases in Sea Water*—The construction and operating characteristics of a six-stage equi-librator built to be used in conjunction with an infrared analyser in measuring the partial pres-sure of carbon dioxide in sea water is presented. The device may be used with any measuring in-strument because it furnishes a continuous stream of equilibrated gas. A time lag of less than two minutes to steady state allows some study of fine structure of water characteristics. Operated in con-junction with a submersible pump of 200 to 600 gallons per hour capacity, the device has been used to measure partial pressures at various depths, and when operated with such a pump trailing in the water abeam of a ship under way it has been used to make a continuous study of variations in partial pressure of carbon dioxide along the ship's track. Data for both types of profiles are pre-sented.

The equilibrator itself is made up of standard laboratory aspirators mounted in such a manner that the water stream is run through the aspirators in parallel while the gas sample flows in series through the cells. The gas stream can be sampled at any stage, and it was found that each successive stage up to four shows a detectable difference in instrument reading. The temperature of operation is maintained very near that *in situ*. Because one tenth of the water actually pumped from the sam-pling site is used in the equilibration, the large transfer of water assures temperature stability. At sea no more than 0.02°C change in temperature of water was observed in operation.

Takashi Ichiye (Oceanographic Institute, Flori-da State University, Tallahassee, Fla.) *A Theory of Storm Surges on the Continental Shelf*—Long waves caused by a traveling disturbance on a con-tinental shelf of uniform depth is discussed theo-retically. In a nonrotating system the ratio of the wave speed to the speed of the disturbance is an important factor for generated waves. When the disturbance advances faster than the long waves on the shelf, there is no forerunner but resurgences with a period of proper oscillations of the shelf. In a rotating system the same condition holds for a disturbance due to a low-pressure area. However, the effect of the wind-stress curl becomes impor-tant after the passage of the main portion of the disturbance consisting of wind stresses. This effect produces resurgences even for a disturbance mov-ing more slowly than the long waves.

Takashi Ichiye (Oceanographic Institute, Flori-da State University, Tallahassee, Fla.) *Circulation and Water-Mass Distribution in the Gulf of Mexico*—Oceanographic data collected by the *Alaska* and the *Jakkula* in the Gulf of Mexico since 1951 are analyzed. The water-mass distribu-tion in the upper layer is much influenced by the surface wind drift, as seen in the location of the low-salinity water. Seasonal change of the temper-ature and salinity in the upper layer provides a basis for the classification of five water types, three coastal and two off-shore types. The average oxygen-density and phosphates-density correla-tions in the western and eastern section indicate that the eastern section is much affected by the water coming through the Yucatan Channel. On the other hand, the T-S relationships are more uniform and thus the temperature at 200 m depth

corresponds well to the current pattern derived by dynamic computation. The comparison with the hydrography of the Sea of Japan suggests that the Florida Current is more effective in mixing different water masses than is the Tsushima Current in that sea and that the vertical convection is more intensive in the Sea of Japan, which has uniform water in the subsurface layer.

C. I. Jackson (McGill University, Montreal, Canada) *Meteorological Observations in Ellesmere Island during the International Geophysical Year*—From August 1957 till August 1958 regular surface observations were taken at the Canadian IGY base at Lake Hazen, N.W.T. This is the first record from an inland site in the Canadian Arctic Archipelago and shows marked differences from the records at Alert and Eureka. Temperatures during the winter were the coldest recorded in Canada, but winds were extremely light, the mean wind speed during winter being under three miles per hour. Precipitation during the 12 months was less than two inches.

John C. Jamieson and A. W. Lawson (University of Chicago, Chicago, Ill.) *A New Device for High-Pressure X-Ray Studies*— A new x-ray diffraction unit suitable for the study of highly absorbing materials has been developed by combining the 'simple squeezer' with a clamping scheme. The pistons of the squeezer are truncated diamond cones, ⅛ inch high with basal diameters, ⅛ and ¼ inch. Pressure, applied by a small laboratory press, is clamped on the sample by a self-locking screw. The unit is then removed from the press and placed on a G. E. XRD-5 spectrometer, replacing the usual sample mount. Centering devices are provided. Assembly of the pressurized unit requires about ten minutes. Typical power patterns exhibiting the transition in HgSe will be shown. The present performance of the relatively inexpensive diamond pistons is unpredictable and the ultimate useful pressure range is as yet undetermined.

Wenceslas S. Jardetzky (Manhattan College, New York, N. Y.) *Velocity of Propagation of a Disturbance in a Heterogeneous Medium*—More precision in definition of the velocity is necessary in the case of heterogeneous media where the dilation and rotation are coupled (and no wave equations for potentials exist). To make it possible the equations of dynamics for small displacements must be considered *simultaneously* with the equations of geometric optics, the latter being interpreted as some kind of kinematical constraints. The Malus law yields the definition of the velocity of propagation. An exact relationship between the phase velocity and the factor $\beta = (\mu/\rho)^{1/2}$ is derived for the two-dimensional case. The factor β is usually defined from the equations of dynamics as the velocity of propagation. It is determined exclusively by the rigidity and density. It is shown that the phase velocity depends on the period and variations in the amplitude in addition to rigidity and density.

Francis S. Johnson (Lockheed Aircraft Corp., Missiles and Space Division, Palo Alto, Calif.) *The Distribution of Ions Above the F2 Region*—Observations made of the ion distribution in the ionosphere indicate that the ion distribution up t 550 km is controlled not by diffusion but b changes in the recombination coefficient. This ion distribution control by recombination is conclude to be in probable agreement with diffusion theory It is further concluded that the ion distributio above 550 km is controlled by diffusive equilibriu and not by recombination, although above 550 k further changes in the recombination coefficient d occur. Charge exchange reactions between oxyge ions and hydrogen atoms at an altitude near 8(km provide a source of thermal protons which fi the magnetic field and provide a medium for th propagation of radio whistlers. The neutral hydro gen distribution around the earth is deduced fro the nighttime observation of hydrogen Lyma alpha radiation; it is found that the hydroge cloud is more tenuous than has formerly been su posed. The charge exchange reaction betwee oxygen ions and hydrogen atoms is nearly reso nant, and the cross section for this reaction i probably large enough to provide the correct nu ber of protons to explain the whistler propagatio The distribution of the protons around the eart although diffusive in nature, is more affected b magnetic field than by gravity. When the magnet field is considered, the proton distribution is fou to be in excellent agreement with the whistl data. Thus, the ions responsible for whistler prop gation are terrestrial in origin, and their source o ionization is the same as that for the F region.

Frank E. Jones and Arnold Wexler (Nation Bureau of Standards, Washington, D. C.) *Barium Fluoride Humidity Element*—This pap discusses a thin-film electric hygrometer elemen developed at the National Bureau of Standard under the sponsorship of the Aerology Division o the Bureau of Aeronautics, which shows conside able promise for use in upper-air humidity sounc ing. The element consists of a thin film of bariu fluoride deposited by vacuum evaporation over metal film configuration on a glass substrate. Th electrical resistance of the element varies wit relative humidity. Of primary importance in th performance of the element is its rapid response t changes in relative humidity. For example, a —40°C the element passes through 63 per cent c a total change in indication in approximately thre seconds. The results of a study of performanc characteristics of the element are presented. Thes results indicate, in addition to the rapid respons that the element can be manufactured reproduci bly to conform to mean calibration curves; th element responds to changes in humidity over wide range of relative humidities (no upper o lower relative humidity limits were found), 'hys teresis' is small; and exposure to high humidity water spray, or water immersion had no permanen harmful effect on the functioning of the element

Yona Kahanowitz (Water Planning for Israe Tel Aviv, Israel) *Intensification of Ground-Wate Exploitation in the Coastal Plain of Israel*—A scheme is described for increasing the safe yield o Israel's coastal aquifer by reducing outflows int the sea. The fresh water–salt water interface wil be moved a definite distance inland, at a prede termined rate of advance to a new steady state This will result in the release of a one-time reserv

fresh water. The aquifer which is to yield the :-time supply, in addition to its increased regu- exploitation, consists of the coastal plain's sand i sandstone formations and is underlain by an pervious stratum dipping towards the sea. Tests ve been made on a Hele-Shaw model and quan- itive estimates of exploitation drawn up. Study s been made of the effect of rate of pumping and tance of wells from the coast on the rate of ad- ice of the interface, both in phreatic and con- ed aquifers. Out of the residual outflow neces- y to maintain the new steady state, part will be ercepted at the coast after having performed its ction.

Werner D. Kahn (Army Map Service, Wash- ton 25, D. C.) *Determination of Correction to ark II Minitrack Station Coordinates from Arti- ial Satellite Observations*—The Mark II mini- ck receives satellite signals at a frequency of 8 megacycles. Observations give the times cor- sponding to zero and 180° difference in phase of e satellite signal as it is received at two separate tennas. The predicted positions of the satellite these times are compared with the deduced sitions of the satellite for the same times. From ese comparisons, corrections to the observer's itude and longitude (but not to height above e reference ellipsoid) are obtained.

W. M. Kaula (Army Map Service, Washington , D. C.) *A Statistical and Harmonic Analysis of ravity*—Markov theory was applied to mean ee-air anomalies and mean elevations of 1° × 1° d 5° × 5° squares to obtain estimated gravity omalies to cover the entire earth. These esti- ates were adjusted to eliminate inadmissible har- onics and to agree with the nodal precession of tellite 1958β. Solutions were made for spherical rmonics up to the eighth degree of free-air grav- y anomalies and topography, the latter of which reed very closely with Prey's solution. The herical harmonic geoid height estimates have an ns amplitude of ±17 meters. The weighted mean tio of free-air gravity to topographic coefficients r degrees three through eight agrees with Airy- eiskanen compensation depth of 36 km, but in- ividual coefficient ratios vary widely from this verage.

An independent autocovariance analysis used as control on the Markov estimates obtained the llowing parameters for free-air anomalies: rms oint anomaly, ±35 mgal; rms 1° × 1° square ean, ±27.5 mgal; rms 5° × 5° square mean, ±19 gal; rms 30° × 30° square mean, ±9 mgal; ariances of harmonic degrees, sum of degrees 2 rough 6, 116 mgal^2; 7 through 12, 85 mgal^2; 13 rough 20, 108 mgal^2; 21 through 32, 78 mgal^2; ns geoid height, ±32 meters.

D. P. Keily and S. G. Millen (Department of Meteorology, Massachusetts Institute of Tech- ology, Cambridge, Mass.) *An Airborne Cloud- Drop-Size Distribution Meter*—An outboard aspi- ating electrostatic probe is described which counts nd sizes droplets in the range of 2 to 60 microns n diameter at rates up to ten thousand per second. Sample observed distributions are presented.

G. C. Kennedy, G. J. Wasserburg, and H. Heard (Institute of Geophysics, University of California, Los Angeles, Calif., and California Institute of Technology, Pasadena, Calif.) *The Upper Three-Phase Region in the System SiO_2-H_2O*—The upper three-phase region in the system SiO_2-H_2O has been explored to 10,000 bars H_2O pressure. Two triple points are encountered. One triple point is at 400 bars H_2O pressure and a temperature of 1470°C, where the phases cristobalite tridymite and liquid coexist. A second triple point occurs at 1500 bars H_2O pressure at a temperature of 1160°C, where the phases quartz tridymite and liquid coexist. The melting point of pure quartz at 3000 bars H_2O pressure is at 1100 ± 5°. Surprisingly, higher water pressures reduce the melting points but little more. At 10,000 bars H_2O pressure the melting point of quartz is at 1080°C. Some data are available on the compositions of coexisting liquids and gases along the upper three-phase boundary.

N. Kitagawa and M. Brook (New Mexico Institute of Mining and Technology, Socorro, N. M.) *Similarities and Differences between Cloud-to-Ground and Intracloud Lightning Discharges*—Electric-field changes caused by lightning discharges were investigated using both electric and electric-field-change meters displayed on wide-band oscilloscopes. The *J*-field change portion of ground discharges and the field change of the later portion of intracloud discharges are similar, many small rapid field changes (*K* changes) overlapping both *J* and cloud-field changes with almost identical time intervals. In contrast, the initial portion of the first-leader field change (*B*-field change) in a ground discharge consists of regular pulsations and bears little or no resemblance to the *J*-field change. This long-lasting and periodic initial field change is seldom observed during the course of the usual intracloud discharge. These facts indicate that the *J* process which occurs during the period between and after strokes of a multiple ground discharge is essentially identical with the usual intracloud discharge between the lower negative and upper positive charge in a thundercloud, and that the discharge between the main negative charge and the lower positive pocket of charge postulated by Schonland is definitely different in nature from the typical cloud discharges.

William H. Klein, Billy M. Lewis, Isadore Enger, and Curtis W. Crockett (U. S. Weather Bureau, Washington, D. C.) *Application of Numerical Prognostic Contour Patterns to Surface-Temperature Forecasts*—Multiple regression equations for predicting five-day mean surface temperature anomalies in the United States from anomalies of 700-mb height have recently been developed. The required heights are approximated from daily prognostic maps prepared at the 500-mb level by a barotropic model and at the 700-mb level by a baroclinic model. The temperature forecasts resulting from the numerical prognoses are verified on independent data at 39 cities in terms of the percentage of total variance explained, and the sources of error are analyzed. Additional verification is presented in terms of temperature classes at 100 stations for forecasts prepared three times a week during the past six months. Comparison is made with forecasts prepared by other methods: local temperature persistence, continuity of error,

and official forecasts of the Extended Forecast Section for this year and previous years.

Leon Knopoff and Gordon J. F. MacDonald (Institute of Geophysics, University of California, Los Angeles, Calif.) *An Equation of State for the Earth's Core*—Recent shock wave measurements (Altshuler and others, *J. Exptl. Theoret. Phys. USSR*, v. 34, 606-619, 1958) upon the compressibility of iron and eight other metals at pressures up to five megabars permits an investigation of the equation of state of the earth's core. The density of iron at $T = 0$ at 1.4 megabars (core-mantle boundary pressure) is 11.8. The density at the core boundary is estimated to be between 9.1 and 10.1, depending upon the particular earth model. The temperature correction is small. The discrepancy can only be resolved by stating that the core is not pure iron but rather that it contains significant amounts of alloying elements of lower atomic number than iron. The seismic velocity in pure iron at core pressure is also significantly different from the velocity in the core and also indicates the existence of lighter components within the core. A material of mean atomic number 23 in the core is consistent with the shock wave velocity and density measurements and with seismic observations.

F. A. Kohout (U. S. Geological Survey, Miami, Florida) *Cyclic Flow of Salt Water in the Biscayne Aquifer of Southeastern Florida*—Observations over a period of nearly 20 years confirm the fact that the salt-water front in the Biscayne aquifer along the coast of the Miami area, Florida, is dynamically stable at a position seaward of that computed according to the Ghyben-Herzberg principle, which is simply that of the U-tube. During periods of heavy recharge the fresh-water head is high enough to cause the fresh water, the salt water, and the zone of diffusion between them to move seaward. In addition to this bodily movement of the system, there is a seaward flow of diluted salt water in the zone of diffusion. When the fresh-water head is low, salt water in the lower part of the aquifer intrudes inland, but some of the diluted sea water in the zone of diffusion continues to flow seaward. Cross sections showing equipotential lines in terms of equivalent fresh-water head show that the sea water flows inland, becoming progressively diluted with fresh water, to a line along which there is no horizontal component of flow, after which it moves upward and returns to the sea. The cyclic flow acts as a deterrent to the encroachment of sea water because of return to the sea of a part of the inland flow.

Igho Hart Kornblueh (University of Pennsylvania, Philadelphia, Pa.) *Electric Space Charges and Human Health*—Years of intensive work devoted to the study of the biological effects of weather and climate have yielded a vast array of convincing results. However, some basic questions still remain unanswered. Faced with formidable technical difficulties, many investigators diverted their time and abilities to other fields of research. Lack of encouragement and support might have been another deterring factor, leaving missing links in the chain of knowledge of bioclimatology and biometeorology. Evaluation of the physiological action of single atmospheric elements encounters great obstacles. Atmospheric electricity and, particular, air ions have never attracted sufficient attention because of the relatively low ener levels involved.

About half a century ago, Sokoloff pointed the biological influence of ionized air. The initi results obtained by his followers were not co clusive. Some time later, a method permitting su pression of one and a controlled increase of other polarity far beyond the concentrations countered under natural conditions produced perimentally various somatic and mental reacti of clinical significance. The biological effects artificially ionized air were studied by many thors in this country and abroad. It appears t the ciliary rate of the trachea, the growth of cultures, certain microorganisms, and superfi wounds are directly affected while the enzym activity of the adrenal glands, respiration, bl pressure, and the action currents of the hun brain are indirectly influenced by ionization. M encouraging are the therapeutic results obtai in persons suffering from hay fever, allergic asth and burns. The desiccating, deodorizing, sedat and pain-relieving quality of negative ioniza proved of value in selected surgical procedure

Research on ionization is being directed organized on a large scale by the Pavlov Insti of Physiology of the Russian Academy of Scien in Leningrad. Over 100 hospitals, health cen and resorts are currently employing this met The techniques of artificial ionization of the as used in the United States and in the Sov Union are discussed in detail in this paper.

A. W. Krumbach (Vicksburg Research Cen Southern Forest Experiment Sta., Vicksburg, M *Effects of Microrelief on Soil-Moisture Distri tion*—The horizontal and vertical variation in moisture in relation to microrelief was stud in a loessial bottom soil near Vicksburg, Mis sippi, on a 50 × 60-ft plot. A topographic map the plot was made using 0.3-ft contour interv Total difference in elevation was 1.8 ft. One h dred and twenty observations of soil moisture bulk density in the 6- to 12-inch depth were a lyzed. Comparisons made near field maxim moisture content and near the plastic limit vealed that significant changes in soil moisture d density occurred in relation to changes in ele tion. Moisture variation was particularly p nounced at the higher moisture content. Comp sons were made for moisture content by wei and by volume.

W. C. Krumbein (Northwestern Univers Evanston, Ill.) *Trend Surface Analysis of C tour-Type Maps With Irregular Control-Po Spacing*—Trend surface analysis is a procedure separating the relatively large-scale systema changes in mapped data from essentially rand small-scale variations caused by local effects. T method can be applied to any contour-type m and has been used for analysis of gravity ma isopach maps, facies maps, and maps of igne and sedimentary rock attributes. Polynomial a lysis of maps is much facilitated by use of hi speed digital computers. An IBM 650 program this work is outlined in the paper.

When observations can be collected on a r

ngular grid, orthogonal polynomial analysis per- its convenient identification of the trend and siduals. When the observations are limited in umber or are very irregularly distributed over the ap, non-orthogonal polynomial analysis can be sed to determine at least the linear and quadratic mponents of the trend. These surfaces and the eviations on them have value in geological in- rpretation, and they suggest that, even when the mplete trend is known, maps of selected trend mponents may be useful for examining special roblems.

Wallace W. Lamoreaux (U. S. Weather Bureau, Washington, D. C.) *Salton Sea Evaporation Study*—New insight into the phenomenon of evapora- on gained from the Lake Hefner and Lake Mead vestigations prompted review of evaporation cords taken during the Salton Sea campaign of 09-1910. Two objectives were in mind for the udy: (1) to help firm up a mean annual value of ee-water evaporation for the Salton Sea area, and 2) to test further the Lake Hefner techniques of etermining evaporation. Numerous deficiencies in ie 1909-1910 data became apparent early in the udy, and some improvising became necessary. A umber of the present-day techniques were ap- lied. Results are presented and evaluated in light f some of the known shortcomings of the data.

M. Landisman, Y. Sato, and M. Ewing (La- mont Geological Observatory, Columbia Univer- ty, Palisades, N. Y.) *Surface Wave Dispersion in lastic Media Having Gradients in Their Physical roperties*—Machine calculations have been ap- lied to various cases of Love wave dispersion in lastic media having gradients in their physical roperties. Among the cases considered are several hich are directly related to the structure of the arth.

Love wave dispersion has been computed by wo different methods. In the first method, the eriod equation is solved by the explicit series ap- ropriate for the model under study. This has been one for Meissner's case, a half-space with a linear radient in shear modulus, and for Sato's case, hich is the same structure beneath two homo- eneous layers. Meissner's case has also been solved y the second method, which is a numerical solu- ion of the equation of motion, and the two ethods are in excellent agreement. This agree- ent indicates that the numerical methods may be sed to investigate Love wave dispersion in the ultigradient structures which result from travel- ime studies.

Explicit series solutions of the period equation or models with two homogenous layers over a radient half-space were used to study the struc- ure of the upper mantle under continents and ceans. These solutions have confirmed the con- lusions, reported a year ago on the basis of Love ave dispersion studies, and since confirmed in a eport by Dorman and others on Rayleigh wave ispersion:

1. Under continents a zone of low shear veloc- ties exists between depths of roughly 100 and 200 m.

2. The upper mantle beneath the oceans is dif- erent from that under the continents. Under ceans the region of low shear velocities rises to depths of about 50 km; the low velocity zone is thicker, and the velocities are lower, than under continents.

H. E. Landsberg (U. S. Weather Bureau, Washington, D. C.) *Bioclimatic Work in the Weather Bureau*—Public demands for information of a bioclimatic nature recur with high frequency in Weather Bureau service. These come both from healthy individuals and the chronically sick. The former are primarily interested in comfort conditions. The latter hope to achieve cure, or at least alleviation of symptoms, by a move from one climate to another. Some progress has been made in using ordinary climatic data for these purposes. But new indices, based on the regularly observed climatic elements, are still needed and are under development. Such anthropocentric concepts as wind chill and discomfort index have found their way into regular practice.

The whole problem of beneficial recreational climates for the young and retirement climates for the old is under investigation. There is considerable lack of reliable criteria and boundary conditions to estimate the influence of various climatic elements upon normal and abnormal physiological reactions, as well as meteorotropic ailments. In the face of this some 'common-sense' approaches have to be used until better knowledge becomes available. There is probably a need to measure other elements than those usually recorded at climatic stations and to accumulate statistics truly germane to the bioclimatic problems.

Leonard H. Larsen and Arie Poldervaart (University of Cincinnati, Cincinnati 21, Ohio, and Columbia University, New York 27, N. Y.) *Contributions to the Petrology of Bald Rock Batholith near Bidwell Bar, California*—Compton (1955) suggested that tonalites and granodiorites of the batholith mantle originated through contamination of trondhjemite magma by metabasaltic country rocks. A detailed study of 22 batholithic rocks results in a different conclusion. Values for Qu, Or, Ab, and An calculated from modes show that the rocks fall along a trend slightly below and directed toward the boundary surface between quartz and feldspars. Tonalite formation by contamination is possible but requires unlikely high proportions of metabasalt. Habit and dimensional data of zircons emphasize contrasts between trondhjemite core and granodiorite-tonalite mantle but do not support a contamination origin for the latter. When compared with Bald Mountain batholith, Oregon (Taubeneck, 1957), in which zircon characteristics are uniform throughout, different compositional trends for tonalite to granodiorite are seen. It is concluded that the Oregon batholith was injected as a uniform magma, while the California batholith was emplaced as a migma-magma in which the trondhjemite core was mostly liquid while the tonalite-granodiorite mantle consisted of mobile, viscous solid phases with interstitial melt. The liquid line of descent at Bald Mountain, Oregon, was from tonalite to granodiorite and at Bald Rock, California, from trondhjemite to leucotrondhjemite.

Fred H. Larson and Vincent McKeever (Soil Conservation Service, Upper Darby, Pa.) *Hydrol-*

ogy and the Small Dam—This paper deals with the methods used by the Soil Conservation Service in evaluating the effect of small dams on the flow characteristics of the river and the effectiveness of these changes in regard to reducing damages. Emphasis is placed on the degree of effectiveness rather than on the hydrologic methods that are being used. Examples are taken from the work of the Soil Conservation Service in the 13 northeastern states.

Douglas H. K. Lee (U. S. Quartermaster Research and Engineering Center, Natick, Mass.) *Role of Bioclimatology in the Armed Forces*—Man remains the primary mover in military operations, however esoteric the means taken to achieve results. Climate affects man directly, through its influence on disease transmission, and through its effects upon food and supplies of all kinds. Bioclimatic effects of prime military concern are those touching survival, the incidence of disease, the operational efficiency of the individual, and his morale. Residual as well as immediate effects are of considerable concern. Major research activities being conducted by the Armed Forces in the field of bioclimatology include: storage and retrieval of climatic information, principles of microclimatology, basic nature of climatic stress, psychological and social consequences of climatic conditions, provision of protection against climatic effects, control of disease vectors, and prediction of operational efficiency under given climatic conditions.

Harry E. LeGrand (P. O. Box 10602, Raleigh, N. C.) *Problems of Contrasting Ground-Water Media in Consolidated Rocks of Humid Areas*—In many humid areas underlain by consolidated rocks, a clayey residuum of weathered rock forms the uppermost ground-water medium. The water table lies in this material in many places, at least when it is at its highest seasonal stages. Where the water table is lowest, around pumped wells, it lies in the fractured bedrock. Movement of water through these contrasting media leads to complex problems not amenable to treatment by many accepted 'aquifer' concepts. In some wells penetrating consolidated rocks the drawdown and recovery of water levels are conventional, but in others they are somewhat erratic as a result of intricacies of draining, refilling, and siphoning in bedrock openings. Recharge is sluggish where air is trapped in bedrock openings below the residuum. The complexities resulting from the behavior of air-water interfaces in the two media need consideration when withdrawal of water from wells and mines in consolidated rocks is planned.

Frank Lewis (Electronic Computer Branch, Det 2, Air Weather Service, Washington, D. C.) *Short-Range Terminal Forecasting by a Non-Linear Statistical Model*—A statistical model capable of forecasting by non-linear methods has been developed and programed for the IBM 704. The regressions produced are automatically tested on independent data. Runs of the program using a single station's data for predictors and predictand show small improvements over persistence and extrapolation. The program is being adopted to accommodate predictors from several stations.

Douglas K. Lilly (U. S. Weather Bureau, Washington, D. C.) *On the Theory of Disturbances in Conditionally Unstable Atmosphere*—Cloud-sc and cyclone-scale motions in a moist, conditionall unstable atmosphere are considered. Perturbati solutions are obtained, where horizontal and ve tical distributions of moisture and stability en as parameters. Analytic and numerical results sh that small-horizontal-scale disturbances are mo unstable than those of cyclone scale and that t stability criterion of tropical-cyclone-scale distur ances is strongly dependent upon occurrence a distribution of smaller-scale convective motion Banded structure is shown to be more unstabl than solid cloud structure. Occurrence of an 'ey seems to be irrelevant to linear solutions. Surfa friction tends to promote development of cyclo scale disturbances, in the early stages.

Austin Long, Arnold Silverman, and J. La rence Kulp (Lamont Geological Observatory, C lumbia University, Palisades, N. Y.) *Precambr Mineralization of the Coeur d'Alene District, Ida* —The Coeur d'Alene district in northern Idaho the chief Pb-Zn-Ag mining area in the Cordiller region. Until recent isotopic studies were ma mineralization was assumed to have occurred late Cretaceous or early Tertiary time during subsequent to the Laramide disturbance. Fift galena samples from widely distributed mines the area and at various levels in some of the mi were analyzed for lead isotope composition a did not vary beyond the experimental error. T average value and the standard deviation are:

Average of 15 Coeur d'Alene galenas

Pb^{206}/Pb^{204}	Pb^{207}/Pb^{204}	Pb^{208}/Pb^{20}
16.44 ± 0.06	15.58 ± 0.07	$36.52 \pm 0.$

This average gives a common lead model age 1250 million years which agrees with the estimat age of pitchblende from the Sunshine Mine as c rived from U-Pb isotopic ratios. The isotopic co position of the Coeur d'Alene lead is essentia the same as that in the Sullivan Mine and relat ones in southeastern British Columbia and sugge a common source for the ore during a sin Precambrian mineralizing epoch. Precambrian le was also found in veinlets cutting Cretaceous i trusives and may indicate remobilization of s fides during the Laramide orogeny.

Gerald R. MacCarthy (University of Nor Carolina, Chapel Hill, N. C.) *Some First Motio as Recorded at Chapel Hill, N. C.*—A tabulati has been made of the character (compressional dilational) of the first motions of 101 earthqua recorded by the seismograph operated by the U versity of North Carolina at Chapel Hill, N. The azimuth of, and distance to, each epicent are included in the tabulation. No marked g graphic or temporal patterns are displayed, b the data should be of interest to anyone engag in a study of fault mechanisms.

Gordon J. F. MacDonald and Walter H. Mun (Institute of Geophysics, University of Californ Los Angeles, Calif.) *Tides and the Length of D*

Astronomic observations since 1680 give a surs singly good measure of the variation of the gth of day. Moreover they make it possible to parate the effect of tidal friction from other posle causes. Babylonian eclipses and other ancient servations lend support to the interpretation of e modern observations. Tidal dissipation ounts to 3×10^{19} ergs/sec. The astronomical servations can give no information on how this ergy is dissipated.

The work of Taylor and Jeffreys has led to the nclusion that the dissipation takes place in shalv seas, the Bering Sea in particular. It now apars that dissipation in the Bering Sea can acunt for no more than 10 per cent of the required ount. It is possible that dissipation associated th internal (baroclinic) ocean tides and with rth tides may be an important factor. Atmoseric tides are of no help, since they add to ather than subtract from) the rotational energy the earth.

S. Manabe (U. S. Weather Bureau, Washington, C.) *On the Energy Exchange between Polar ntinental Air and the Sea of Japan in Winter*—order to evaluate airmass transformations in a pical unstable situation, the sensible and latent ergy exchanges between the Sea of Japan and nosphere during winter were calculated, based on the energy budget of both sea and atmosere. For this, data obtained by the comparavely good observation network surrounding the a were utilized. As a result, during a period of pical outburst of cold air, the amount of sensible at supplied from the sea to the atmosphere was aluated to be as much as 1000 ly/day, which ems to be important even over short periods. rthermore, from a computation of the energy dget of the sea water, it might be concluded at the seasonal change of heat stored in the ean is very important for the determination of e exchange coefficient by the energy method. he budget requires that heat be transported upard more effectively than moisture. It is quite tely that the predominance of free or forced nvection determines the relative efficiencies of eat and moisture transport.

Nicholas E. Manos (Dept. of Health, Educaon, and Welfare, Washington, D. C.) *Weather in ublic Health Research*—There is a need to elete bioclimatology to a position of higher promence and prestige. Technically, there is a need r quantitation of the many known and suspected lationships between various weather elements nd certain causes of death, kinds of illness, and rms of human behavior. The multiplicity of comicating factors can be overcome if the quantitaon is based on an intensive and rigorous analysis at is conducted on a broad scale. There now xist enough health and weather data for such an nalysis. There is a need for stronger administrave support of bioclimatology. The strongest suport could come from those areas of public health search where the inclusion of weather factors is navoidable. For example, there is now a strong emand for research on the health effects of air ollution. This research has to include weather ctors. Weather factors are also associated with eart disease, strokes, arthritis, accidents, allergies, crimes, and suicides. We know that some lives have been ended prematurely by the adverse effects of weather on man. We must determine how many. If bioclimatology could offer a rigorous, well-organized body of knowledge today, it would be more actively sought after by research workers in public health. If bioclimatology can make contributions in the areas of greatest demands today, it can achieve a position of higher prominence and prestige.

Elwood Maple (Air Force Cambridge Research Center, Bedford, Massachusetts) *Sub-Audio-Frequency Geomagnetic Fluctuations, IGY Project 3.10*—Five field stations have been established at Thule, Greenland; College, Alaska; Fort Devens, Mass.; Mount Evans, Colorado; and Puerto Rico under a joint project with the Denver Research Institute (DRI), University of Denver. Each station records three components of the 1- to 50-cps fluctuations on magnetic tape for the first 15 minutes of each hour. The initial electrical reduction of the data, which will yield the relation of average signal level to time in six-octave frequency bands, is under way at DRI. Preliminary results of the program, indicating the relationship of the fluctuations to various sources such as geomagnetic disturbances and world-wide thunderstorm activity, are presented.

William Markowitz (U. S. Naval Observatory, Washington 25, D. C.) *The Dual-Rate Satellite Camera*—An experimental dual-rate satellite camera has been constructed and tested at the U. S. Naval Observatory. The camera simultaneously tracks the satellite and surrounding stars at their respective rates, thus obtaining sharp images of both. A rotating glass plate, one-half inch thick, is at the center of the field. This holds the satellite fixed during the time in which the satellite moves 0°.5. The epoch of observation is the instant when the rotating plate is parallel to a fixed plate of the same thickness, which is in the outer part of the field. The camera aperture is seven inches, and the focal length is 40 inches. The probable error of a coordinate of the satellite with respect to the stars is 5″ and the probable error in timing is 0ˢ.002 sec.

1958 δ 1 (Sputnik III rocket) was photographed on November 27, 1958, and 1958 ζ (Atlas) was photographed on January 13, 1959. At the time of photographing Atlas its altitude was 19° and its apparent magnitude was about 6; it was not then visible to the naked eye.

The camera is relatively light in weight and is suitable for field operations. The camera will be useful for observing high-altitude geodetic satellites when such objects are placed in orbit.

Donald P. Martineau (Department of Meteorology and Oceanography, New York University, New York, N. Y.) *The Gulf Stream as an Equivalent-Barotropic System*—The equivalent-barotrophy of the Gulf Stream is investigated. The cross-stream, seasonal, and down-stream variations are discussed from the results of the analysis of selected sets of hydrographic sections across the current. The surface velocities and depth of the lower boundary for an equivalent-barotropic Gulf Stream are determined to be similar to values ob-

served by GEK, LORAN-DR, and bath pitotmeter measurements; but the surface velocities are found not to represent the means of the layers comprising the current, as required for an equivalent-barotropic system. The maximum velocity and the average velocity of the easterly flowing water appear to be greatest in winter and spring and agree with other results based on mean monthly surface current data. The results show that the equivalent-barotropic Gulf Stream is deepest and densest in winter and shallowest and lightest in summer. Some reasons for this variation are suggested. The downstream variations in the dynamic and geometric properties of the equivalent-barotropic Gulf Stream are determined to be less pronounced than are the cross-stream and seasonal ones.

S. Matsushita (High Altitude Observatory, University of Colorado, Boulder, Colo.) *Geomagnetic Studies with IGY Data from Seven U. S. Stations*—This report contains studies of geomagnetism from IGY data taken at a net of seven stations in the United States. The distance between the two nearest stations is 360 to 510 km. Geomagnetic variations at these stations were usually quite similar, as would be expected. However, different variations even among adjacent stations occurred occasionally during magnetic storms. These occasions were looked for in the IGY data. Different shapes of sudden commencement of the horizontal component for the same magnetic storm occurred among these adjacent stations. From this result, behavior of the electric-current system responsible for the sudden commencement is estimated. Also differences of the vertical component of the sudden commencement at the seven stations show that there is an anomalous magnetic field in the central part of the United States. Examples of bay-shaped variation during magnetic storms, which are quite different at the closely spaced net, are also obtained and analyzed for the behavior.

S. Matsushita (High Altitude Observatory, University of Colorado, Boulder, Colo.) *On Artificial Geomagnetic and Ionospheric Storms Associated with High Altitude Explosions*—Geophysical effects of nuclear explosions at Johnston Island on August 1 and 12, 1958, were studied using IGY geomagnetic and ionospheric data collected at various stations in the Pacific area and the American continent. From this study the explosion height for August 1 is estimated at 70–80 km and for August 12 is estimated at about 40 km. Immediately following each explosion, three phenomena occurred. (1) Strong counterclockwise circular electric currents were formed in the vicinity of Johnston Island at 80–100 km height. These currents caused the immediate occurrence of artificial magnetic storms in the central Pacific. (2) High energy particles moving along the magnetic lines of force caused auroras seen from Apia, and also caused the main parts of the magnetic storms observed at Apia. (3) X-rays caused by the explosion caused the increase of the D-region absorption observed at Maui.

Irregularities of the electron density in the F-layer at Maui were caused by a pressure wave from the explosion. The degree of ionization in a wide area in the central Pacific increased by a factor of the order of ten times normal within 35 minutes after the explosion on August 1, a within about six hours on August 12. Then a stro radio absorption continued for many hours. Tstudy was supported by the National Academy Sciences as part of the International Geophysi Year Program, with assistance from the Fo Foundation.

William T. McGuinness and William Donn (Lamont Geological Observatory, Colu bia University, Palisades, N. Y.) *Long-Peri Ocean Waves at Bermuda*—St. George's Har exhibits damped ten-minute seiches when cross by atmospheric pressure jumps usually associat with squall lines. The tide gage in St. George Harbor also shows a characteristic long wave wi a period of about 40 min. This is explained as seiche oscillating between the outer reefs s rounding the Bermuda platform and shows corre tions with seasons. Oscillations of close to 8 m utes are commonly recorded off the southea coast of Bermuda. These are under investigati at present, and possible mechanisms of origin w be discussed.

J. H. Meyer, J. R. Bauer, and F. A. Wilson (L coln Laboratory, Massachusetts Institute of Te nology, Cambridge, Mass.) *Aircraft Investigati of the Mesometeorological Structure in the Lo Troposphere*—In the fields of radar and ra propagation there are a number of applications which the usual assumption of an idealized, sphe cally symmetric atmosphere does not provide su cient information to describe fully the effects the lower troposphere on radar and radio pro gation. Airborne measurements of pressure, te perature, water vapor, and radio refractive ind were made in the vicinity of Bath, Maine. T meteorological variables versus corrected heig above mean sea level are reported. Departures the variables from the condition of perfect hor ontal stratification are examined from sea level approximately 8000 ft. The horizontal variabili is represented by the comparison of individ profiles made along a path with the mean pro for that group of soundings. Several variables a presented as cross sections along the flight path illustrate the degree of inhomogeneity. The a alysis of the data provides a measure of the d parture of the lower troposphere from that of idealized, spherically symmetric atmosphere.

Dixon R. Miller (Blakeslee, Pa.) *The Depo tion of Dew and the Orographic-Turbulent Fact*—More 'air dew' was measured on the top of a h than in a frost pocket at its base. Condensati from a static vertical column above the top of t hill, above the midpoint on the slope and abo the base was computed from dew point and mi mum temperature. The ratio of the amount measured dew to the computed condensation i static vertical column is designated the orograph turbulent factor. Orographic dew is the result moisture transport over slopes and condensati through a 'contact inversion.' The contact inv sion is a thin layer or film of air adhering to ra ating surfaces. It is supersaturated at its base wh dew is forming in the absence of fog. 'Air de deposition on windward slopes and hill tops almost entirely a result of orographic-turbul

ion. At the expense of dew deposition water or is expended in radiation fog. Stirring of ersaturated air is a factor of fog initiation.

Charles B. Moore and Bernard Vonnegut rthur D. Little, Inc., Cambridge, Mass.) *Some servations of an Association between the Ar- al of Rain and the Electrical Potential Gradient Mount Withington, New Mexico*—The mech- sm of thunderstorm charging is popularly as- ned to involve the charge carried downward by ling precipitation. It is surprising that there is conclusive evidence in the literature associating nfall rates and the charge brought to the earth rain with the resulting potential gradient under cloud. Simpson reported in 1949 that the char- er of the potential gradient record seems to ar no relation to the rate of rainfall and Gunn 1953 that his . . . "data do not show a significant relation of the free charge (on a raindrop) and electric field (at the surface of the Earth)." ring the summers of 1957 and 1958 isolated mulonimbus clouds in New Mexico were studied detail. On several occasions under these 'simple' uds, major changes occurred in the potential dient recordings just before the arrival of a n 'gush' at the summit. Measurements of the arge carried by rain, point discharge current and space charge both at the summit and aloft re also obtained during several of these events. ese observations are presented with a hypothe- to explain the phenomena.

W. B. Murcray (Geophysical Institute, College, aska) *Some Properties of the Luminous Aurora Measured by a Photo-Electric Photometer*—In- nsity of the auroral radiation from the entire y as a function of time was monitored photo- ectrically at College, Alaska. Measurements ex- nded over two years. Very good correlation was und between the 3914A band of N_2^+ and the 77A line of OI. An intensity time curve of a pical auroral display is shown. A diurnal varia- on curve is obtained which is very consistent, ving the same form for weak, moderate, and rong auroras, and not showing evidence of sea- nal variation. A rapid fluctuation in the intensity radiation is reported.

V. Rama Murthy and Claire C. Patterson (Di- sion of Geological Sciences, California Institute Technology, Pasadena, Calif.) *Isotopic Com- osition of Lead in Ore and Associated Igneous Minerals in Butte, Montana*—The isotopic com- osition of lead in some coexisting sulfide minerals Butte, Montana, has been investigated. The oundance of Pb^{206} in the lead from the sulfide inerals was found to increase slightly with depth, ut this relationship could not be conclusively emonstrated because of the small number of nalyses. Pb^{206} and Pb^{208} are distinctly more oundant in the lead from the quartz monzonite ountry-rock than in the lead from the ore. The uartz (igneous rock) and ore leads are derived om two different mixtures of at least two types f leads, so that in this case the ore was not de- ved from the same source as that of the igneous ock. Lead extracted from the feldspars of the onzonite has a composition intermediate between he compositions of the quartz and ore leads, and varies with the extent of alteration of the feldspar. The composition of lead in the less altered feldspar is more like that in the quartz. This may indicate that, when the feldspar was altered, ore lead was added to the original lead of the feldspar. The composition of lead in the potash feldspar of two different pegmatites was found to be similar to that in the ore. The feldspar in both of these samples was extensively altered.

V. A. Myers and William Malkin (U. S. Weather Bureau, Washington, D. C.) *Why Is the Hurricane Surface-Wind Field Asymmetrical?*—The traditional view that the winds blow more strongly on the right side of a hurricane than on the left, because on one side the speeds of translation and rotation are additive and on the other they are subtractive, has some validity as an empirical description but is incomplete and erroneous as a dynamic explanation. A more rigorous theory is offered, based on application of the equation of motion to trajectories of the air, with friction taken into account. Surface-wind fields are computed for an idealized hurricane at different forward speeds. Various characteristics observed in the artificially constructed wind fields appear to be indicative of, and to account for, features in observed hurricane wind fields. An immediately useful application is the reconstructing of surface-wind fields in an actual hurricane.

National Hurricane Research Project, Staff (U. S. Weather Bureau, Miami, Fla.) *The Structure of Hurricane Cleo*—Data obtained by three research aircraft at altitudes of 6,000, 14,000 and 35,000 ft provide the bases for a detailed and quite complete description of the three-dimensional structure of a mature hurricane. The report will be presented in three parts.

First, time-lapse movies of the radar echoes obtained by photographing the PPI radar scope and of the visible clouds obtained by a camera in the nose of the aircraft will be presented and discussed qualitatively.

Second, a quantitative analysis of the radar echo and cloud data obtained from these films will be presented. By carefully compositing the data in a relative coordinate system centered on and moving with the storm, quantitative measurements of the areal and vertical distributions of clouds and precipitation are possible. Both horizontal and vertical cross sections will be presented to show that a surprisingly small volume of the storm is filled with strong convective clouds.

Finally, analyses of the fields of motion, pressure, temperature and humidity will be presented and their interrelationships, as well as their relationship to cloud and precipitation distribution, will be discussed.

Gerhard Neumann (New York University, New York, N. Y.) *On the Dynamical Structure of the Gulf Stream as an Equivalent-Barotropic Flow*—Some of the main features of the Gulf Stream and its horizontal-velocity profile can be accounted for by treating the stream as a non-accelerated, equivalent barotropic flow determined by pressure, Coriolis, and frictional forces. An essential part of the model is an inclined lower boundary of the stream with its depth increasing toward the Sargasso Sea.

Increasing frictional forces toward the continental side seem to account for the pressure of a counter current bordering the region of strong cyclonic horizontal shear.

Donald W. Newton (Flood Control Branch, TVA, Knoxville, Tenn.) *Storms and Floods on Small Areas*—A complete analysis of the flood potential of a watershed must include an estimate of the maximum expected-flood discharge, A simplified, easily applied procedure for areas of up to approximately 500 sq mi is outlined. The procedure is based upon a determination of the maximum expected storm. A method for making this determination is outlined which utilizes storm transportation techniques and information published by the U. S. Weather Bureau and the Corps of Engineers. A basic family of depth-area-duration curves is found by using relationships developed by the U. S. Weather Bureau and reported in *Hydrometeorological Report 33* to envelop observed storms in a meteorologically homogeneous region. These basic data are further adjusted to conform to the moisture potential of the watershed in question. Standard techniques are used to compute the precipitation excess and the flood hydrograph. Support for both the storms and floods computed by this technique in the Tennessee Valley area are found in observed events in the region.

Rolf M. Nilsestuen (Air Weather Service Climatic Center, Suitland, Md.) *Estimating Wet-Bulb Distribution*—A method has been developed for estimating the distribution of the wet-bulb temperature in a warm month for any station. It is necessary to know only the distribution of the dry-bulb temperature and the mean relative humidity at noon or the over-all mean relative humidity. The noon humidity produces a better estimate of the upper percentiles of the wet bulb, the mean humidity a better estimate of the low percentiles. In the absence of a complete temperature summary, the dry-bulb distribution may be estimated by Spreen's method, which requires only the mean temperature and the mean monthly range. The shortcut graphic method for multiple curvilinear regression described by Ezekiel was used in development. Tests on an independent sample of 35 stations indicate an accuracy for prediction purposes approaching that which might be expected from summarized data over a short period of record, yet at a small fraction of the time and cost required for making a complete frequency distribution. The study was prepared for use in air-conditioning work but may have applications in other fields where the wet-bulb distribution is required.

Paul R. Nixon and G. Paul Lawless (Western and Water Management Research Branch, U. S. Department of Agriculture, Lompoc, Calif.) *Translocation of Moisture with Time in Unsaturated Soil Profiles*—Downward translocation of moisture in soil profiles under various types of natural vegetation and in a denuded plot was observed during a prolonged rainless period. Moisture determinations were made to twenty-foot depths with a neutron scattering moisture meter. The observations were made as part of a study of groundwater recharge by deep penetration of rain water. The significant magnitude that translocated mo ture may reach is illustrated by data obtained sand under brush cover. In this case, deeply tra located moisture was equal to 159 per cent evapotranspiration during the first rainless mon Approximately 31 per cent of the moisture conte of a twenty-foot profile under a denuded plot w lost by downward migration during 240 days f lowing the last appreciable rainfall. The moistu contents of various soil layers under the plot var with time in a manner that was expressed by pow functions.

Laurence H. Nobles (Department of Geolo Northwestern University, Evanston, Ill.) *Therm Regimen of Subpolar Glaciers*—Detailed tempe ture measurements made at seven localities in t outer 30 mi of the Greenland Ice Cap at latitu 76°N reveal ice in which constant (and negativ temperatures prevail throughout the year in but the upper few meters. The upper eight to meters are subjected to the penetration of a win 'cold wave' and also to a period of summer 'wa up' which produces temperatures of 0°C for a weeks in the upper meter or so of the ice. T constant temperature measured at a depth of ei meters ranges from —13°C near the edge of ice cap to —19°C inland at an elevation of 420 and reflects the higher mean annual air tempe tures at the lower elevations nearer to the co In the ice, all transfer of heat is by conduction firn downward transfer of heat is also accomplis by penetration and refreezing of meltwater. T produces an irregular temperature curve in and a deeper 0° isotherm in firn than in ice. thermal regimen of subpolar ice is analagous that of perennially frozen ground and is the co trolling factor in producing the integrated s parallel drainage patterns, slush avalanches, a algal pits that are intrinsic to the ice surface these regions.

J. A. O'Keefe, D. Ann Eckels, and R. Kenne Squires (National Aeronautics and Space Adm istration, Washington 25, D. C.) *Zonal Harmon of the Earth's Field and the Basic Hypothesis Geodesy*—The zero-order harmonic can be termined from radar measurements of the moo distance. The harmonics of degrees 2 and 4 are terminable from the motions of the node a perigee of artificial satellites; those of degree and 5 are from the perturbations of the eccent city, inclination, node and argument of perig with periods equal to the period of revolution the line of apsides. It is pointed out that the val of these harmonics are not reconcilable with hypothesis of Heiskanen and Vening Meinesz the smoothness of the earth's field.

Vincent J. Oliver (U. S. Weather Bureau, Wa ington, D. C.) *Some Applications of Vorticity A vection Charts to Weather Forecasting*—The vor city advection at 500 mb has been determined three winter months by superimposing the ab lute vorticity printout obtained from the NN computer on the 500-mb analysis. The areas 500-mb vorticity advection are indicated by cross pattern of the two sets of isopleths. Vortic advection areas were compared with the weath patterns obtained from surface charts to determ

what extent they were related. Comparisons re also made of the relation of vorticity advec- n areas to surface cyclogenesis and anticyclo- nesis. The prognostic vorticity advection pat- ns obtained in a similar manner from the NMC -hr barotropic progs were also compared with rface weather patterns and with surface pressure tterns. These studies indicate that 500-mb vorti- y advection is a numerical tool that practicing recasters could use to great advantage.

H. Orlin (U. S. Coast and Geodetic Survey, ashington 25, D. C.) *The Three Components of e External Anomalous Gravity Field*—By means a surface coating determined from the gravity omalies at sea level and the geoid heights, the ree components of the external anomalous grav- field are computed. This technique is applied points at and above sea level, and comparisons e made with existing methods.

N. A. Ostenso, E. Thiel, G. P. Woollard, and . E. Bonini (University of Wisconsin, Madison, is.) *Gravity Measurements in Alaska*—Over the st several years a network of 513 gravity stations s been established in Alaska and the Yukon erritory. This network includes traverses over ost of the highways, the Alaska Railroad, and e Lewes-Yukon River. Less accessible areas were ached by single-engined aircraft. All values are ljusted to the Potsdam datum through reoccupa- on of pendulum stations at Fairbanks and White- rse. The free-air and Bouguer anomalies for nsities of 1.77, 2.00, 2.20, 2.40, 2.50, 2.67, 2.80, and 0 were computed on an IBM 650 digital com- ter. While this work was intended principally provide a widespread unified datum for future avity surveys, some geologic conclusions can be awn. Although the areal coverage is not sufficient r detailed interpretation, deductions regarding ustal structure can be made, and the occurrence several large anomalies implies large change in ie composition of the crystalline rock complex.

M. Ozima (Department of Geophysics, Univer- ty of Toronto, Toronto, Canada) *A New Tech- ique for Potassium-Argon Dating*—A new tech- ique for K-A dating has been investigated in hich both K and A are liberated by evaporation om the same aliquot of sample at 1350°C in a acuum. The ages so obtained are considered to ow a better precision than would be expected om separate potassium and argon analyses, as any errors tend to cancel. The reproducibility in ie determination of A^{40}/K^{40} is within ± 3 per nt. This technique is suitable for rapid routine ating.

Willard H. Parsons (Wayne State University, Detroit, Mich.), Adrian F. Richards (U. S. Navy Hydrographic Office, Washington, D. C.), and John W. Mulford (Cranbrook Institute of Sci- nce, Bloomfield Hills, Mich.) *Capelinhos Erup- ion of Fayal Volcano, Azores*—A flank eruption roke out one-half mile at sea off the west end of Fayal Island on September 27, 1957, following a eek of earth tremors. This eruption continued al- most without cessation for 13 months, the last bserved crater activity being on October 24, 1958. ll phases of the eruption have been carefully recorded in day-to-day detail by Frederico Machado of Horta, Fayal. Violent explosions for the first three weeks of the eruption built a cone one-half mile wide by 300 ft high. This island cone subsequently disappeared only to be rebuilt a week or two later. Intermittent but continuing violent ash ejections, pseudo-volcanism or phreatomagmatic explosions, characterized the eruption during its first seven months. Machado estimates a total of 0.4×10^{24} ergs was dissipated per month during this time (4.1×10^{24} for the entire 13 months' eruption). The new cone is now part of the island of Fayal, adding a peninsula of approximately a square mile and several miles of ash beaches. A broad semicircular cinder cone is three-quarters of a mile in diameter and 500 ft above sea level.

A seismic crisis occurred on May 12-13, 1958, forming east-west fractures on both the northwest and southeast flanks of Fayal, 3 to 5 miles from the eruption. A few hundred buildings were destroyed, uplift on the sea cliffs on both flanks of Fayal averaged 70 cm and new fumerolic activity broke out in the summit caldera. From May through October the eruption was essentially Strombolian in character, with lava being thrown 500 to 1000 ft above a spatter cone built inside the older cinder cone ring. Activity was intermittent; active phases lasted two to four hours, separated by shorter quiet intervals. Numerous small lava flows issued from the seaward side of the spatter cone during this six months' phase of the eruption. Machado estimated the viscosity of one flow to be 3.2×10^4 poises. Temperature readings by optical pyrometer on the lava jets from the inner cone averaged 980°C.

J. A. Peoples, Jr. (Department of Geology, University of Kansas, Lawrence, Kans.) *A Station Seismograph Calibration System*—A variable-frequency mechanical signal generator was devised in which a four-speed phonograph motor provides ample driving power. It operates on the seismometer pier without causing a noticeable increase in noise level. A simple lever system reduces the initial amplitude of 1 mm by a factor of from 50 to 1000. The period can be varied from 0.3 to 30 sec. The horizontal seismometer is supported at three points on two parallel drill rods (axes horizontal). One of the rods is rotated through a very small angular amplitude, and a small horizontal oscillation is produced. The vertical seismometer is placed on a platform scale, and the end of the weighing arm is driven by the signal generator. The three-component system (seismograph and galvanometer periods near 1.5 sec and peak magnifications 6,000 to 13,000) was satisfactorily calibrated at full sensitivity over a period range of 0.3 to 10 sec. It is believed that moderately long period systems could be satisfactorily calibrated in this way.

Willard J. Pierson, Jr. (Department of Meteorology and Oceanography, New York University, New York, N. Y.) *A Note on the Growth of the Spectrum of Wind-Generated Gravity Waves as Determined by Non-Linear Considerations*—Nonlinear wave properties lead to the conclusion according to Phillips that "where non-linear effects are important" the spectrum of wind-generated

gravity waves must have the form $S(\mu) = ag^2\omega^{-5}$. To second order, it has been shown by Tick that non-linear effects are important in producing sharp crests above a frequency corresponding to twice the frequency of the dominant peak in the wave spectrum and that the second-order contribution is due to contributions from the linear part obtained from both sum and difference frequencies. In the representation due to Tick it is possible to represent the wave spectrum as a first-order part, $S^1(\mu;v)$, and a second-order correction, $S^2(\mu;v)$.

If these results are accepted, and if several additional assumptions are made, it is shown that the first-order family of wave spectra, $S^1(\mu;v)$, for fully developed seas, cannot form a nested family of curves. The results suggest that the various theoretical forms for the first-order spectrum of a fully developed sea are each correct over a limited range of wind speeds. However, since they are nested curves, they cannot be correct over the whole range of sea states.

Paul Pomeroy (Lamont Geological Observatory, Columbia University, Palisades, N. Y.) *Background and Storm Microseisms in the Period Range 11-22 Seconds*—Microseisms with periods of 14 to 22 seconds and trace amplitudes up to 8 mm are recorded almost continuously throughout the year on the high-sensitivity vertical instruments ($T_o = 30$, $T_g = 100$ and $T_o = 15$, $T_g = 25$) currently being operated at the Palisades station of the Lamont Geological Observatory. The amplitude of this background varies by a factor of 2 to 3 between summer and winter, and it is between 0.1 and 0.01 of the maximum amplitude microseisms which fall in the period range of 6 to 8 seconds. On the standard long-period instruments ($T_o = 30$, $T_g = 100$), microseism storms with periods from 11 to 15 seconds and with trace amplitudes up to 2 mm are recorded occasionally on the north-south component. In severe storms, this background also appears on the vertical component. East-west motion has not been observed.

The microseism storm of May 28, 1958 was recorded at Palisades with periods of 10½ to 14 seconds on the north and vertical components. At Ottawa there is vertical motion indicating a Rayleigh component. At Waynesburg, St. Louis, and John Carroll the motion, entirely north-south, indicates Love waves. A detailed comparison between water-wave records at Atlantic City and seismograms at Palisades shows a strong correlation in amplitude and period which indicates that the microseisms may be caused by gravity-wave action near shore.

F. Pooler, Jr. (U. S. Weather Bureau Research Station, Robert A. Taft Sanitary Engineering Center, Cincinnati, Ohio) *A Prediction Model of Mean Urban Pollution for Use with Standard Wind Roses*—An empirical diffusion equation in which vertical diffusion is dependent on surface wind speed, and horizontal diffusion is accounted for by the observed wind direction frequencies, is described. This equation is used in conjunction with a preliminary source inventory of sulfur dioxide emissions, made as part of the current Nashville, Tennessee, air-pollution study, to estimate mean monthly sulfur dioxide concentration patterns. Comparisons are made with observ mean concentration patterns.

Frank Press (Seismological Laboratory, C fornia Institute of Technology, Pasadena, Cal *New Results on Mantle and Crustal Structur* Crustal structure in the vicinity of the Califor Nevada border is being studied by three separ methods: (1) surface wave phase velocity, gravity, and (3) explosion seismology. The two methods indicate a crustal thickness of ab 40 km. Explosion-seismology results are conco ant only if an intermediate crustal layer is p ent. Explosion data for the existence of this la are discussed and it is shown how, without su cient detail, this layer can be overlooked a erroneous conclusions can occur.

A study of G waves for purely continental pa indicates that the corresponding velocities identical or differ by no more than about 2 cent. This implies that the low-velocity zone the mantle is identical under continents and s gests that the pressure, temperature, and comp tion are also similar.

D. W. Pritchard (Chesapeake Bay Instit Johns Hopkins University, Baltimore, Md.) *Test of Mixing-Length Theories of Vertical Di sion in an Estuary and in a Pacific Atoll Lagoo* Observations of the vertical and horizontal v ations in salinity and velocity in the James R estuary have been previously employed in indirect determination of the vertical eddy of salt (Pritchard, 1954). This term is emplo here to compute a mixing length after the de tion of Prandtl. It is shown that this 'observ mixing length is qualitatively similar to a 'th retical' mixing length formulated from the ometry of the system and a stability parame related to the density stratification. Data on advection and vertical diffusion of a tracer su stance introduced into a Pacific atoll lagoon also utilized in comparing the 'observed' and 'th retical' mixing lengths. It is found that bet quantitative agreement is obtained when the infl ence of surface wind waves is included in formulation of the 'theoretical' mixing length

W. Bruce Ramsay, (U. S. Weather Bure Washington, D. C.) *The Use of Numeri Weather Forecasts for Radioactive-Fallout P dictions*—The Weather Bureau has begun wo on a numerical fallout-prediction program whi will produce a listing of the downwind areas which fallout of radioactive particles is possil from selected targets. A realistic approach to t fallout problem must include the effects of wi variability in space and time. To this end, win derived from the forecasts of the Joint Numeri Weather Prediction Unit are used to whatev extent possible. At altitudes above the JNW levels the last available observed winds are sumed to persist throughout the forecast perio The program is designed primarily for Civil D fense operations and can treat any attack patte at any time within the continental United Stat The basic philosophy of the program is one flexibility, so that future changes in JNWP pr cedures can be incorporated into the fallout pr gram with a minimum of effort. A next stage

llout forecasting, not yet begun, is a forecast of llout intensities (relative or absolute) based on e output from the present program and on cer- in assumptions concerning the radioactive clouds.

G. W. Reed, K. Kigoshi, and Anthony Turkevich (Argonne National Laboratory, and Enrico ermi Institute for Nuclear Studies, University of hicago, Chicago, Ill.) *Tl, Pb, Bi, and U Contents Meteorites*—Heavy elements have been meas- ed, by neutron activation, in several chondrites id in troilite from iron meteorites. Five of the ondrites gave elemental contents in g/g meteo- te as follows: Tl ($\sim 3 + 10^{-10}$), Pb ($0.6\text{–}4 \times 10^{-7}$), i ($1\text{–}8 \times 10^{-9}$). Four other chondrites, two carbo- aceous and two enstatite, representing extremes sofar as metal (Fe-Ni) contents are concerned ielded of the order of 100 times more Tl and Bi nd 10 times more Pb. The heavy element con- ents in troilite from two iron meteorites fall in he ranges: $10\text{–}2000 \times 10^{-10}$ g Tl/g 70×10^{-7} Pb/g, $50\text{–}200 \times 10^{-9}$ g Bi/g and $\sim 3 \times 10^{-9}$ g U/g. The amounts of Tl, Pb, and Bi in the first roup of chondrites appear to be consistent with he low percentage of troilite they contain. The osmic abundances derived from the data for the irst group of chondrites are much lower than hose reported by Suess and Urey (*Revs. Modern Phys.*, 28, 53, 1956). However, the data from the econd group fall more nearly on their curve. The results for Tl, Pb, and Bi for even the high group re still significantly lower than would appear to e needed on the basis of current theories of ucleogenesis, although the experimental evidence upports the predicted enhancement in the Pb bundances relative to Bi and Tl.

H. Riehl and J. Mihaljan (University of Chicago, Chicago, Ill.) *Analysis of the Layer of Maximum Wind*—In spite of recent technical improvements, the wind soundings currently transmitted via teletype still leave much to be desired. Methods are proposed for modifying techniques of wind calculation and reporting balloon ascents, including computation of the parameters for layer of maximum wind analysis. Methods for analyzing charts of the layer of maximum wind are discussed.

W. J. Roberts (Illinois State Water Survey Division, Urbana, Ill.) *Reducing Lake Evaporation in the Midwest*—Studies were conducted during the summers of 1957 and 1958 on two lakes in central Illinois to determine a practical method of applying monomolecular layers and to learn their effectiveness in reducing evaporation. Results showed a saving of 43 per cent in 1957 and 22 per cent in 1958 of the water normally lost by evaporation. A method was developed to determine the strength of the monolayer by measuring the latent heat gradient near the water surface.

W. O. Roberts (High Altitude Observatory, University of Colorado, Boulder, Colo.) *Recent Progress in Solar Physics*—The period of the International Geophysical Year has seen the highest peak of solar activity of modern times. The Zurich Observatory, for example, reported that 1957 had the highest yearly mean sunspot number since 1778. With the increased sunspot counts have gone increased numbers of large solar flares, strong ejective solar prominences, and considerably increased intensities of the high-ionization lines of the solar corona. All of these phenomena have been subjected to thorough observational study. Particularly intensive theoretical and observational study has been made of the physics of the solar chromosphere by Thomas, Athay, Jefferies, and others.

Rocket observations by the Naval Research Laboratory strongly suggest that instantaneous short-wave radio fadeouts accompanying solar flares result from increases of solar x-ray emission during flares, rather than from increases of Lyman alpha radiation of hydrogen, as previously suspected. The detailed physical mechanisms in solar flares, however, still are not fully understood.

The high-ionization lines of the spectrum of the solar corona, have long been known to possess extremely broad profiles. If these breadths are interpreted as being entirely due to thermal broadening, the temperatures so deduced are well above those previously derived from ionization theory and sometimes exceed 3×10^6°K in strong active regions of the solar corona. Recent theoretical work by Schwartz and Zirin suggests that the ionization temperatures previously derived were too low, and that the appropriate values agree reasonably with the line profile values derived when the profiles are interpreted as thermal.

Problems of variations of the magnetic fields of the solar surface and the solar atmosphere during flares have received recent attention, particularly from Severny in the Soviet Union. The relationship of atmospheric magnetic fields to solar radio noise emission and to the emission and acceleration of charged atomic particles from the sun have also recently assumed great importance for solar-terrestrial research, due to work of Parker, Singer, and others. The possible effects of thermal conduction in the corona, recently suggested by Chapman, also introduces new considerations for the physics of the interplanetary medium.

John C. Rose and G. P. Woollard (University of Wisconsin, Madison, Wis.) *The Accuracy of Gulf-Wisconsin Pendulum Results*—The abrupt field period changes of the Gulf-Wisconsin pendulums have resulted in period decreases as well as increases. Since 1953 the Madison base station period for the M pendulums has varied both plus and minus. It is believed that the cause of these changes is now known, and the apparatus is being modified to eliminate the cause. The objective of the modifications is to achieve a reliable field precision of 0.1 mgal.

It is important to be able to measure large gravity intervals to this accuracy in order to distinguish between geologic changes in elevation and changes in mean sea level.

Use of gravity meter intervals to locate pendulum period changes and pendulum reoccupation closures to give the amount of the period changes results in a calibration line accuracy in North America of standard deviation of 0.5 mgal, and standard error 0.1 mgal over 4600 mgals. Other pendulum results are in agreement.

J. H. Rosenbaum (Shell Development Co., Houston, Tex.) *The Long-Time Response of a*

Layered Elastic Medium to Explosive Sound—The long-time response of a layered elastic medium is considered for the particular case of a point-source explosion in a liquid layer lying above an infinitely deep liquid bottom. An asymptotic solution, valid for large values of the time variable, is obtained which expresses the response in terms of harmonic vibrations of the liquid layer. Special emphasis is placed on those vibrations which correspond to waves with small angles of incidence and which, because of radiation into the bottom, decay exponentially with time. The well-known guided-wave phenomenon, first discussed by Pekeris, is also included in the present formulation. The relatively simple nature of the problem treated here permits us to bring out clearly the method of analysis, which is applicable to more complicated problems. Numerical results are presented for some typical examples.

Alexander Sadowski (U. S. Weather Bureau, Washington, D. C.) *Use of Coastal Radars in Hurricane Forecasting*—Continuous accurate tracking of the hurricane eye and associated precipitation pattern helps in dealing with the difficult problem of forecasting hurricane movement. Coastal radars are capable of detecting both the erratic changes in direction of the eye and its general pattern of motion. Such application of coastal radars during the 1958 hurricane season is discussed. Hurricane Daisy, August 24-29, was the first storm to be tracked continuously by coastal radar. Once picked up by the Weather Bureau's radar at Cape Hatteras, Daisy was under continuous radar surveillance until it passed into the Atlantic east of Cape Cod.

Hurricane Helene, one of the most dangerous hurricanes to affect the east coast in recent years, was similarly tracked. The ADC radar of the 701st AC&W Squadron, Fort Fisher, Wilmington, N. C., was first to locate Helene when the center was some 200 nautical miles to the southeast. Next, ADC radar of 792nd AC&W Squadron, Charleston, S. C., followed Helene's movements, with the Weather Bureau's WSR-1 radar at Charleston giving reports of center fixes when Helene came within its range. Finally, Weather Bureau's SPIM radar at Cape Hatteras tracked Helene's northeastward course into the North Atlantic. Coastal radars, as well as the hurricane reconnaissance flights of the Air Force and Navy, caught the sharp turn away from land and provided the hurricane forecasters with up-to-the-minute information for their forecasts and warnings.

Personal observations of the author who operated the SPIM radar at Weather Bureau Office, Cape Hatteras, North Carolina, with another radar meteorologist, during the passage of Hurricane Daisy and Hurricane Helene are illustrated with lantern slides of radar scope photographs. Also, lantern slides are used to show hurricane paths, a real coverage by different radars, radar scope photographs of Hurricane Helene by WSR-1 radar at Charleston, S. C., and more powerful SPIM radar at Cape Hatteras, and eye locations by plastic, logarithmic spiral band curve overlays.

Alexander Sadowski (U. S. Weather Bureau, Washington, D. C.) *Use of Radar in Tornado Warnings*—Radar makes possible the continuous scanning of approximately 125,000 sq mi about[1] station. Clouds with water droplets of sufficie[nt] reflectivity to produce radar echoes can be track[ed] continuously to determine their speed and dire[c]tion for the purpose of predicting their possibl[e] future courses and the places most likely to [be] affected. Experience with the presentation of radi[o] echoes has shown that certain characteristic ec[ho] formations are associated with tornado occu[r]rences. Some such characteristic echo formation[s] are hooks on individual echoes and waves on radi[o] echo lines. The formation of a hook on a radi[o] echo was observed by the author while operatin[g] the WSR-3 radar at Wichita, Kansas, on June 1[2] 1958. The phenomena was recorded by a 35-m[m] time lapse camera on a repeater scope. The motio[n] picture film will be shown. In addition, person[al] observations will be illustrated by lantern slide[s]. The hook appeared about an hour before the to[r]nado struck El Dorado, Kansas. On the followin[g] day, another hook was observed 20 min before t[he] tornado struck Wichita, Kansas. If, as in the cas[es] presented, further experience shows that hooks [on] radar echoes appear well in advance of tornado[es] it may be possible in favorable circumstances [to] issue advance warnings on the basis of the PP[I] scope presentations before the tornado drops fr[om] the clouds.

Henry A. Salmela (Geophysics Research Dire[c]torate, Air Force Cambridge Research Cent[er] Bedford, Mass.) *Accuracy of Mean Monthly Ge[o]strophic Wind Vectors as a Function of Stati[on] Network Density*—Two experiments aimed [at] studying the accuracy of analysis of mean month[ly] contour pressure charts at three levels, with fi[ve] different densities of station network coverage [in] one experiment and four in the other, are d[e]scribed. Independent analysis of these data we[re] made by three professional meteorologists in eac[h] experiment. The results of these experiments sho[w] that, using sparse data coverage, it is possible t[o] make analyses of mean monthly upper-air chara[c]from which geostrophic winds can be obtaine[d] that are accurate enough for many purposes an[d] that these geostrophic winds can be compared wit[h] those derived over areas of optimum coverage an[d] a quantative value of the relative accuracy ca[n] be obtained.

Barry Saltzman (Department of Meteorology, Massachusetts Institute of Technology, Cam[b]ridge, Mass.) *On the Maintenance of the Large-Scale Quasi-Permanent Disturbances in the At[m]osphere*—It is proposed that the large-scale quasi-permanent flow systems are maintained against dissipative effects by the transfer of kineti[c] energy from smaller-scale disturbances which hav[e] baroclinic energy sources, the processes involved being non-linear and barotropic. An example using a limited number of double Fourier com[-]ponents, is given to illustrate the operation of suc[h] processes.

Frederick Sargent, II (University of Illinois, Urbana, Ill.) *Changes in Ideas on Climatic Origin of Disease*—The idea that disease has a climatic origin began with Hippocrates; he taught that disease was caused by meteorological change and humoral disturbance. This broad iatro-meteorologi[cal]

cal concept prevailed until the Middle Ages. At that time a new idea began to develop: The 'atmospheric constitution' was responsible for disease. This notion led to the idea that a peculiar property of the air—miasma—caused ill health and epidemic disease. When the miasmas were found to be bacteria, viruses, or parasites carried by insect vectors, the iatro-meteorological concept which emerged in the twentieth century was that weather and season conditioned man and so precipitated the onset of disease. Diseases which were thus associated with meteorological or seasonal change were called meteorotropisms. Meteorotropisms include infectious, allergic, metabolic, and cardio-vascular-renal diseases; industrial and traffic accidents; and weather-sensitivity (meteoropathy). The meteorotropism, however, has primarily a statistical basis; there is little information regarding the basic causes of the correlations. A few conditions are still classified as climatic diseases—for example, heat disease, cold injury, and mountain sickness—but included among them are syndromes, especially psychological, the climatic origin of which is dubious; namely, tropical neurasthenia ('heat neurotic reaction') and Arctic hysteria. Current miasmas are largely man-made and comprise atmospheric pollution.

W. J. Saucier (A. and M. College of Texas, College Station, Tex.) *The Structures of Jet Streams as Determined from Project Jet Stream Data*—Project Jet Stream is an observation program operated by the Geophysics Research Directorate, Air Force Cambridge Research Center, since 1953 to gather wind and other data by aircraft in the upper troposphere and tropopause regions. The specially instrumented vehicles used were a B-29 during the early phase of the program and a B-47 throughout the program. Both aircraft operated from Florida during the 1953–1954 and 1954–1955 seasons of observation. The second observational phase was the 1956–1957 season, during which the B-47 operated alone from Wright-Patterson Air Force Base. This paper summarizes the findings by the group at the A. & M. College of Texas which analyzed these data under contract with GRD. Emphasis is placed on the wind structure in those jet streams investigated by the aircraft. The mean structure of and the variabilities in the Florida jet streams are discussed in some detail. Analyses and models of the polar-front jet streams investigated by the 1956–1957 phase of Project Jet Stream are also given. Studies of turbulence distributions and of local time variations of wind in the jet stream are briefly summarized.

Richard G. Semonin (Illinois State Water Survey, Urbana, Ill.) *Artificial Precipitation Potential in Illinois as Inferred from Precipitable Water Data*—Precipitable water values for Rantoul and Peoria, Illinois, were computed by the University of Illinois' digital computor for the period April 1953 through December 1957. These data were obtained for the layer from 1000 to 400 mb. Cumulative frequency curves of precipitable water for each month were derived from the twice-daily observations. These curves were derived to aid in defining the variability of the precipitable water data. Weekly average values of precipitable water during the interval from 1953 through 1957 were determined. These were compared with weekly areal mean rainfall values obtained from several stations surrounding Rantoul and Peoria. These comparisons are interpreted with regard to cloud and precipitation modification potentialities in Illinois.

F. E. Senftle (U. S. Geological Survey, Washington 25, D. C.) and Arthur Thorpe (Howard University, Washington, D. C.) *Magnetic Susceptibility of Tektites and Some Terrestrial Glasses*—The magnetic susceptibility and intensity of magnetization of about 30 tektites from various localities have been measured. The value of susceptibility ranges from -0.2×10^{-6} to about 7.5×10^{-6} emu/gram. Tektites from a given locality have similar susceptibilities. In all cases the intensity of magnetization is zero or very small. For comparison, the same measurements have been made on about 30 obsidians. The magnetic susceptibilities cover approximately the same range, but the intensity of magnetization was found to be much higher. By heating the obsidians to 1450°C the intensity of magnetization was reduced to zero. From the above data, arguments are shown that the tektites must have been heated to greater than 1450°C and that essentially all the iron is in solution. On the other hand, the evidence shows that obsidians have not been heated to this temperature and that there is a significant amount of undissolved iron in the glass, probably as magnetite. Further, if they are extraterrestrial, they probably entered the earth's atmosphere as a glass.

A. L. Sharp (Agriculture Research Service, Lincoln, Nebr.) A. E. Gibbs (U. S. Bureau of Reclamation, Lincoln, Nebr.) W. J. Owen (Soil Conservation Service, Lincoln, Nebr.) and B. Harris (Department of Mathematics, University of Neraska, Lincoln, Nebr.) *Application of the Multiple Regression Approach in Evaluating Parameters Affecting Water Yields of River Basins*—The efficacy of the use of the multiple correlation and regression approach in evaluating parameters affecting water yields of river basins is examined. Results of several analyses of annual and monthly streamflow of Delaware River Basin in Kansas are presented to provide a background for an examination of the method. Hydrologic data, in general, and factors affecting water yield, in particular, may not fit the premises upon which the multiple regression method of analysis is based: (1) The variance of the dependent variable (streamflow) does not change with changing levels of the independent variables (precipitation for example). (2) The observed values of the dependent variable are uncorrelated random events.

Hydrologic data may not fit the further assumption that is implicit in tests of significance of multiple correlation and regression coefficients; that is, that the dependent variable (streamflow) is normally distributed about the regression line for fixed levels of the independent variables under consideration.

It is concluded that: (1) Although the multiple regression approach will result in a 'line' of best fit and 'best' estimating equation for hydrologic data, it is not safe to place too much reliance on values estimated by such equations, particularly at levels far removed from the mean, despite very

high correlation coefficients. (2) Some of the more modern statistical procedures may be better tools than the multiple regression approach for evaluating effects of watershed parameters on water yield.

JOHN SHERROD (Library of Congress, Washington, D. C.) *Documentation in Meteorology*—Results of a survey are presented which show that within the meteorological profession the interest in and knowledge of information practices in science and technology have lagged behind the progress made in this area by many other science and engineering professions. This is particularly unfortunate at this time when the relatively new science of documentation is experiencing its greatest growth and development. For correcting this situation, recommendations are made which it is hoped will awaken new interest in this neglected area and at the same time prove beneficial to the entire meteorological profession.

ANATOL J. SHNEIDEROV (1241 New Hampshire Ave., N.W., Washington, D. C.) *Microseisms Due to Magnetostriction and Electrostriction in Some Ferrous and Polarized Rock Deposits*—A theory of microseisms resulting from mechanical oscillations of magnetically and electrically polarized rock layers is proposed. The theory attempts to explain some microseismic tremors by magnetostriction and electrostriction by partially polarized ferro-magnetic and piezoelectric types of crystals which constitute the layers. Short-period electric variations coexistent with atmospheric disturbances and sea storms are usually associated with the corresponding short-period variations in the earth's magnetic field. Both such variations are considered to be capable of producing electro- and magnetostrictive pulsations of the ferro-magnetic and piezoelectric crystals. The oscillations of the crystals so induced are additive in character, so that the cumulative expansion and contraction of a rock over a distance of a few kilometers may produce microseisms of observed magnitude and frequency.

Akulov's formula used for calculation of magnetostrictive elongation l of a bed 10^6 cm long gives a maximum value $(\Delta l/l) \times 10^6 \text{ cm} \approx 1$ cm. The maximum elongation of a piezoelectric rock of a similar size is about 320 microns. Since the maximum of the microseismic oscillation effect discussed in this paper should be felt at the periphery of the body, and the minimum at its center, a geophysical (microseismic) determination of the size, form, dip, and depth of the deposit is suggested.

SAM SHULITS (U. S. Geological Survey, Department of Civil Engineering, Pennsylvania State University, University Park, Pa.) *Two Principles of Stability of River Form*—In a straight river channel the slightest irregularity produces an erratic channel. If the flow enters the straight channel at an angle, that is, through a bend, the channel is no longer sensitive to slight irregularities. This morphologic behavior is illustrated by Exner's experiments which have escaped American interest for about 35 years. Can it be postulated that, in a channel of a certain curvature, the *talweg* is more stable than in a straight channel? Wundt's broad generalization of the 'principle of least constraint' from physical mechanics seems to be applicable t river behavior. It affirms that any phenomen produced in a system by an external act is so d rected that it tends to prevent a change in th system by the external act. Vitols states that stream flowing freely in erodible soil strives t form a bed which will offer the least resistanc These thoughts are applied to river behavior.

R. S. SIGAFOOS (U. S. Geological Survey, Wash ington, D. C.) *Maximum Modern Advance of Ni qually Glacier, Washington, and Its Recession be tween 1840 and 1900*—In the last 500 years Ni qually Glacier has not advanced farther than 120 to 1400 ft downstream from the present highwa bridge, according to the estimated age of th forest beyond a conspicuous modern moraine. Th estimate is based on ages of (1) stumps cut i 1957–1958, (2) trees growing on fallen logs a sumed to be about the same age as the stump and (3) trees on mounds formed when large tre were uprooted. The last recession from the max mum advance started about 1840, as suggested b the ages of trees on the moraine plus a 1- to 1 year interval before they started to grow. Th front could not have been more than 400 to 500 downstream from the bridge in 1857 nor mo than 200 to 300 ft in 1885. The minimum interv of time since ice began to retreat is the on inference that can be drawn from the age of tre on a moraine.

LEON T. SILVER, SARAH DEUTSCH, AND C. H McKINNEY (Division of Geological Scienc California Institute of Technology, Pasaden Calif.) *Fusion Loss of Lead in the Analysis o Zircons for Isotopic Age Dating*—For the purpos of U-Th-Pb age-dating in zircon, certain cond tions must be met in the analysis of (1) lead iso topic composition, and in the determination of (2 lead concentration by isotope dilution. The tot lead of the sample generally is not homogeneous distributed in concentration, composition, or avail ability to fusion in the zircon and must be repre sentatively sampled for (1). Complete mixing o the same (total) lead with the total lead spike i necessary for determination of (2). A series o investigations of lead loss by volatilization durin the conventional borax fusion procedures indicat that both of these necessary conditions may b violated. The extent of loss seems to be a functio of both temperature and duration of fusion. Vary ing degrees and directions of discordance may b obtained from representative aliquots of a singl zircon sample depending upon the conditions o fusion and spiking. These changes may explain certain types of discordance in U-Th-Pb ages on zircons now reported in the literature. It will no explain all such discrepancies. A procedure and apparatus for minimizing or removing these sources of error by entrapment of the volatile lead is suggested.

JAMES B. SMALL (U. S. Coast and Geodetic Sur vey, Washington 25, D. C.) *Settlement Investiga tions in the Vicinity of Galveston-Houston, Texas and San Joaquin Valley, California*—The U. S Coast and Geodetic Survey has a program of re leveling a net of lines in the Galveston-Houston Texas, area at five-year intervals. Maximum set tlement of 2.8 ft occurred at Texas City (from

936–1954). In the San Joaquin Valley where settlement has reached a maximum of 20 ft at a maximum rate of 1¾ ft per year, a releveling program is undertaken at two-year intervals. Adjustments of the levelings in both regions are now completed.

J. V. Smith and W. L. Brown (Department of Mineralogy and Petrology, Pennsylvania State University, University Park, Pa.) *Single Crystal X-Ray Data on the Polymorphism of $MgSiO_3$*—Large single crystals of $MgSiO_3$ were synthesized by M. L. Keith using B_2O_3 as a flux. Specimens grown at 1200 to 1300°C were quenched to room temperature and examined by x-rays. Most consisted of twinned clino-enstatite, the twinning almost certainly indicating inversion from an orthorhombic form, presumably proto-enstatite. Strong diffuse reflections were observed in addition to those from the clino-enstatite. Very similar patterns have been obtained from meteoric pyroxenes kindly supplied by B. Mason. Some synthetic specimens gave highly complex patterns which are interpreted as coming from complex polytypes of $MgSiO_3$, forms not hitherto observed. In order to overcome the complications introduced by quenching, a furnace capable of 1300°C was built on a precession camera, and crystals were x-rayed at elevated temperatures. At the time of writing results are incomplete but it is hoped that data on the stability of the polymorphs of $MgSiO_3$ will be available by the date of the meeting.

Kenneth W. Smith and Robert G. Allen (Lockheed Nuclear Products Branch, Lockheed Aircraft Corp., Marietta, Ga.) *Forecasting the Intensity and Duration of Low-Level Temperature Inversions in a Valley*—Investigations of the intensity and duration of temperature inversions in a valley of 300-foot depth have been carried out for two years at Lockheed Nuclear Products Branch, Dawsonville, Georgia, utilizing data obtained from up-slope temperature measurements and a 320-foot instrumented tower. Three factors seem to determine inversion strength and duration; the amount of clouds below 15,000 ft, wind speed at the gradient level, and the moisture content of the lower atmosphere. A technique to forecast inversion intensity by time of day for a 24-hour period, based upon these three factors, has been developed and is currently in use operationally.

Robert Sourbeer, R. Cecil Gentry, and L. F. Conover (U. S. Weather Bureau, Miami, Fla.) *Storm in Southern Florida, January 21, 1957*—Synoptic Interpretation—A study was conducted of the storm situation of January 21, 1957, and the vorticity and horizontal divergence patterns were computed from analyzed synoptic maps at low and high elevations of the troposphere. Divergence values were also computed at many tropospheric levels for triangles where the vortices were fixed at rawinsonde stations. Computations of divergence are compared with the rainfall charts in an effort to determine the cause of the heavy rainfall which varied in amounts up to 21½ inches within a 24-hour period. Contour and streamline charts for the period are presented to show that consideration of many of the synoptic parameters ordinarily considered in analysis and forecasting would not lead one to expect such heavy rainfall. The divergence patterns move horizontally with time in such a manner that a high-level divergence area becomes superimposed over a low-level convergence area at the time of heavy rain.

Radar interpretation—The storm was under continuous surveillance between 08h 00 m and 23h 00m EST by a SP-1M 10-cm radar operated by the University of Miami at Coral Gables, Florida. Time lapse, plan position indication (PPI), and range height indication (RHI) photographs are shown for the most active portions of the storm. In these sequences, characteristics of a storm are observed in which semi-stationary cells dump large amounts of rainfall over a limited area for long periods of time. The climax of the storm is the development of two hail shafts clearly observed on both the PPI and RHI scopes.

J. B. Stall (Illinois State Water Survey, Urbana, Ill.) and L. J. Bartelli (U. S. Soil Conservation Service, Urbana, Ill.) *An Analysis of the Sediment Producing Character of Watersheds*—Lake-sedimentation data and watershed factors are correlated utilizing results on 20 lakes varying in original capacity from 3.7 to 61,309 ac ft and having watersheds from 0.09 to 258 sq mi. All watersheds are loaded within the deep loess soils of the Springfield Plain physiographic area in west central Illinois, and the results apply to this area only. Thirteen lake and watershed variables were tested by multiple correlation analysis for their significance in determining the rate at which sediment is deposited in a lake. Those variables significant at the 10 per cent level, or having significance that could probably be reproduced on the average in nine of ten new sets of data, were retained as important. Nine different equations are presented which contain from one to six independent variables, having varying accuracies for determining the dependent sediment deposition. The most accurate equation allows computation of the sediment deposition within 50 per cent confidence limits of ± 8.2 tons/ac and 95 per cent limits of 25.6 tons/ac. Included in this equation are a slope factor, age, gross erosion, capacity-inflow ratio, non-incised channel density, and a watershed shape factor. All equations are applicable to a range of sediment deposition from 3 to 102 tons/ac.

Forest Stearns (Vicksburg Research Center, Southern Forest Experiment Sta., Vicksburg, Miss.) and Charles A. Carlson (Army Mobility Research Center, Waterways Experiment Sta., Vicksburg, Miss.) *Some Correlations between Solar Radiation and Other Environmental Factors and Soil Moisture Depletion*—The relationships of solar radiation and other factors with moisture loss were examined for the purpose of broadening the usefulness of soil-moisture prediction methods. Data were obtained from an upland meadow site on loess in Mississippi. Relationships were examined by computing correlations between environmental factors and measured moisture loss. Correlations were calculated for three-day periods when soil moisture was in the upper half of its range, using drying periods only. Highest correlations of single factors with moisture loss were obtained with soil temperature and evaporation pan ($r = -0.79$ each) with a slightly lower value for solar radiation ($r = -0.76$) and progressively

lower values for air temperature, vapor pressure deficit, and humidity. Correlations with soil temperature or evaporation were not vastly improved by adding other factors in combination or with curvilinear functions. The highest correlation for a single factor was obtained between the site-derived depletion curve and measured moisture loss ($r = -0.85$). Four radiometers were also evaluated.

Duncan Stewart (Carleton College, Northfield, Minn.) *Petrography of Some Erratics from Cape Royds, Ross Island, Antarctica*—A petrographical study is made of a suite of rocks collected by the British Antarctic Expedition, 1907–1909, from Cape Royds, Ross Island, Antarctica. Of the 169 thin sections examined, 163 are of erratics. The igneous specimens constitute approximately 80 per cent of the collection, and may be described as typical East Antarctica rocks.

H. B. Stewart, Jr., G. G. Salsman, and A. J. Goodheart (U. S. Coast and Geodetic Survey, Washington, D. C.) *Surface and Subsurface Rotary Currents Measured at the Outer Edge of the Continental Shelf*—In August 1958 the Coast and Geodetic Survey anchored a Roberts radio current buoy in 42 fathoms and another in 104 fathoms at the outer edge of the Continental shelf near Georges Bank, 155 miles east of Cape Cod. Half-hourly observations of current speed and direction were made for four days from current meters suspended near the surface and near the bottom in 42 fathoms, and near the surface, mid-depth, and bottom in 104 fathoms. Nansen bottle casts were made at each station at the time of planting and recovery, and a BT was obtained at each station every six hours. Velocities up to 1.8 knots were encountered, and the currents were predominently tidal and rotary, at least to 290 ft. The meter at 590 ft, near the bottom at the break in slope, became inoperative after one day and the data were insufficient to attempt a rotary reduction. However, for the 18 simultaneous observations at 590 and 290 ft, the currents averaged 0.1 knot stronger at the bottom. Temperature-with-depth profiles plotted against time show interval waves with heights up to 100 ft and suggest periods of tidal magnitude, although the data on the latter are not conclusive. These were most pronounced in a layer of warm water at about 425 ft, where the temperature was some six degrees above that at 200 ft.

George Sutton and Jack E. Oliver (Lamont Geological Observatory, Columbia University, Palisades, N. Y.) *Seismographs of High Magnification at Long Periods*—Several types of high-magnification seismographs with peak response at periods between about 7 and 80 seconds are operated at the Palisades station of the Lamont Geological Observatory. Comparison of the seismograms from these instruments, and of the appropriate theoretical and experimental frequency-response characteristics, illustrates their value for the detection and resolution of the long-period components of both body and surface waves. New vertical-component seismographs detect surface waves from small shocks at very great distances and, apparently for the first time, record microseisms in the 10- to 30-sec period range almost continuously. Two other types of seismographs are operated throughout the world in cooperative program with other institutions during the International Geophysical Year.

Taro Takahashi (Lamont Geological Observatory, Columbia University, Palisades, N. Y.) *The Carbon Dioxide Exchange between the North and South Atlantic Oceans and the Atmosphere*—Two hundred analyses of carbon dioxide concentrations in the atmosphere and 250 measurements of the partial pressures of carbon dioxide in the ocean waters were obtained during the fourteenth cruise of the *R. V. Vema*, November 1957 to April 1958 from New York to Cape Town, Union of South Africa. Although the carbon dioxide concentrations in the atmosphere do not deviate by more than ± 6‰ (by volume in dry air) from the mean value of 317‰, the small variations within this range seem to correlate with the partial pressure of carbon dioxide in sea water. Over the North Atlantic from 30°N to the equator, the daily average of carbon dioxide in the atmosphere increased from 314‰ to 323‰. Over the South Atlantic it decreased from 323‰ to 315‰ from the equator to 55°S. The results of the measurements of the carbon dioxide partial pressures in sea water (November 1957 to January 1958) indicated that carbon dioxide was being released from the ocean into the atmosphere between 8°N and 35°S, whereas it was being absorbed into the ocean water in the areas north of 8°N and south of 35°S.

Manik Talwani, George H. Sutton, and J. Lamar Worzel (Lamont Geological Observatory, Columbia University, Palisades, N. Y.) *Crustal Sections Across the Puerto Rico Trench*—A crustal section across the Puerto Rico trench, from 450 km north to 250 km south of San Juan, was deduced from seismic refraction and gravity data. The result is a refinement of previous work made possible through more complete seismic refraction coverage and a program for high-speed electronic computation of two-dimensional gravity problems. Based on the refraction data, the crust was divided into five layers. Densities were taken from a density-velocity curve compiled by Nafe and Drake. Depths to the M discontinuity were then computed from the gravity data. Depth to M under the trench is about 20 km decreasing sharply on both sides. Northwards it reaches a minimum of about 10 km under the outer ridge, then deepens gradually to about 13 km under the southern margin of the Nares basin. South of the trench, M rises under the Puerto Rico shelf to about 17 km then deepens sharply to about 30 km beneath Puerto Rico. South of Puerto Rico the depth decreases again to about 14 km under the Venezuelan basin. Depths to M were obtained using Airy isostatic anomalies. The crustal section thus deduced differs significantly from that obtained above where density variations within the crust were considered. The shallow depth predicted for M under the outer ridge is of interest for possible future crustal drilling programs.

Manik Talwani, J. Lamar Worzel, and Maurice Ewing (Lamont Geological Observatory, Columbia University, Palisades, N. Y.) *Gravity*

Anomalies and Crustal Section Across the Tonga Trench—In 1956 gravity observations by means of the Vening Meinesz pendulum apparatus were made aboard *HMS Telemachus* in the Southwest Pacific. Several gravity profiles were obtained across the Tonga and the Kermadec trenches and for each profile large negative free-air anomalies are associated with the trenches. One of the gravity profiles across the Tonga trench was located close to the seismic profile established by Raitt and others during the Capricorn expedition of 1952–1953. The seismic structure section was projected to the line of the gravity profile. Then, by assigning densities for the respective seismic velocities of the different layers and by making a two-dimensional approximation, the free-air anomalies were computed for the section and compared with the observed values. Significant differences (~100 mgal) were found in the immediate vicinity of the trench. An attempt is made to reinterpret and modify the section in order to reconcile the gravity and seismic observations.

J. L. Thames and S. J. Ursic (Southern Forest Experiment Station, Forest Service, U. S. Department of Agriculture, Vicksburg, Miss.) *The Soil Moisture Variable in Surface Runoff Prediction*—Soil-moisture, rainfall, and surface-runoff records from a small watershed in northern Mississippi during a two-year period indicate that surface runoff is strongly correlated with storage opportunity in the top six inches of soil. A logarithmic expression was developed to describe surface runoff from individual storms as a function of amount of rainfall and antecedent storage. It was tested with data from an adjacent watershed and found to be applicable. A procedure for calculating antecedent soil-moisture storage over a watershed is presented.

E. Thiel and N. A. Ostenso (University of Wisconsin, Madison, Wis.) *Airborne Geophysical Studies in Antarctica*—The American oversnow traverse program for 1958–1959 included an airborne unit comprising an R4D and a three-man scientific team. Seven landings were made on the polar plateau along meridian 130°W between the Executive Committee Range and the Harold Byrd Mountains. Two additional landings were made to study the contact of the Ross Ice Shelf with the continental ice cap. The scientific program included seismic sounding, gravity and magnetic measurements, and glaciological studies. Velocity control for the seismic program was obtained by refraction shooting and well-logging of the 800-foot bore hole in Little America. A Varian proton precessional magnetometer was flown to obtain 2500 nautical miles of magnetic profiles in West Antarctica.

The ice along meridian 130°W is everywhere grounded and has a maximum thickness of 6000 feet, thus eliminating any possibilities of water interchange between the Ross and Weddell Seas. However, the rock surface at all stations was found to be from 600 to 3000 feet below sea level. Thus the possibility of a downwarped, ice-filled trough between the two seas is not precluded.

Lloyd G. D. Thompson (Air Force Cambridge Research Center, Bedford, Mass.) and Lucien J. B. LaCoste (LaCoste and Romberg, Austin 5, Texas) *Airborne Gravity Measurements*—Airborne tests with a LaCoste and Romberg sea gravity meter (surface type) have shown that gravity measurements in a flying aircraft are feasible. At high altitudes the aircraft was a sufficiently stable platform for the gravity meter to operate satisfactorily. Analysis of in-flight acceleration problems indicated that gravity observations could be made at high aircraft velocities with proper flight programing and navigation systems. North, south, and west traverses over an Askania tracking range gave five-minute average gravity readings which plotted into smooth profiles. An attainable accuracy of about ten milligals was indicated which meets requirements for geodetic applications where mean gravity values for one-degree squares are required.

D. Bruce Turner (U. S. Weather Bureau Research Station, Robert A. Taft Sanitary Engineering Center, Cincinnati, Ohio) *A Simple Diffusion Model for an Urban Area*—A diffusion equation, assuming a virtual point source, with $\sigma_z^2 \propto t$ and $\sigma_y^2 \propto t^2$, is used to compute relative ground-level concentrations. Patterns of relative concentrations are used with a preliminary source inventory map of sulfur dioxide sources in Nashville, Tennessee, to compute ground-level concentrations at seven locations. Wind speed, direction, and stability are considered in increments of one hour. Hourly computed concentrations are summed to yield a computed 24-hour average ground-level concentration. Gross assumptions used are: (1) no spatial variation in wind velocity; (2) influences of topography can be neglected; (3) all sources have the same effective height; (4) diffusion parameters appropriate to only two stability categories are sufficient. Evaluation of the model is made by comparison of computed with observed 24-hour average concentrations of sulfur dioxide.

A. C. Turnock and H. P. Eugster (Geophysical Laboratory, Carnegie Institution of Washington, Washington, D. C., and Department of Geology, Johns Hopkins University, Baltimore, Md.) *Subsolidus Relations of Magnetite-Hercynite and Magnetite-Hematite-Corundum Assemblages*—The subsolidus relations of magnetite-hercynite and magnetite-hematite-corundum assemblages have been determined between 500° and 900°C, at various total pressures and oxygen pressures, as a part of a larger program dealing with the phase relations of iron-rich spinels. Complete solid solution has been known to exist between magnetite (Fe_3O_4) and hercynite ($FeAl_2O_4$) above 1000°C. However, exsolution has been observed below 858 ± 8°C, and the location of the solvus is as follows (wt. %):

T	Mag. ss	Hc. ss
°C		
800	Mag75 Hc25	Mag30 Hc70
700	Mag82 Hc18	Mag18 Hc82
600	Mag88 Hc12	Mag11 Hc89
500	Mag90 Hc10	Mag 8 Hc92

The points were determined both by exsolution and solid solution reactions. The hydrothermal experiments were performed at a water pressure of 2000 bars ($P_{total} = P_{vapor}$) and the partial pressure of oxygen (P_{O_2}) of a fayalite-magnetite-quartz buffer.

Pure hercynite is not stable at a P_{O_2} significantly higher than that of a fayalite-magnetite-quartz buffer. With increasing P_{O_2} the following assemblages are found to be stable:

P_{O_2} (increasing downward)	Stable assemblage
Fayalite-magnetite-quartz buffer	Magnetite ss + hercynite ss
↓	Magnetite ss + corundum ss
Hematite-magnetite buffer	Magnetite ss + hematite ss + corundum ss

At the P_{O_2} of the hematite-magnetite buffer the compositions of the coexisting phases are as follows (wt. %, determined from cell dimensions):

T	Magnetite ss in equilibrium with hem. and cor., at 2000 bars	Hematite ss in equilibrium with mag. + cor. at 1 bar	Corundum ss in equilibrium with mag. + cor. at 1 bar
°C			
900	....	Hem92 Cor8	Cor93 Hem7
800	Mag90 Hc10	(Hem93 Cor7)	Cor94 Hem6
700	Mag94 Hc6	(Hem94 Cor6)	Cor95 Hem5
600	Mag97 Hc3	(Hem95 Cor5)	Cor96 Hem4
500	Mag98 Hc2	....	....

The effect of total pressure on the above compositions appears to be negligible. Hercynite is known to exsolve from aluminum magnetites of basic rocks. Hematite-magnetite-corundum assemblages are typical for emery deposits.

S. J. Ursic and J. L. Thames (Southern Forest Experiment Station, Forest Service, U. S. Department of Agriculture, Vicksburg, Miss.) *Effect of Cover Types and Soils on Surface Runoff*—Hydrologic and meteorologic data for individual storms were collected on three small headwater catchments on each of three cover types in northern Mississippi during 1958. Surface runoff and peak flows were greatest from abandoned fields, intermediate from depleted upland (hardwoods), and least from 20-year-old loblolly pine plantations that had been established on eroding farm land. The pine cover has been a highly effective flood-abatement measure.

The soils are silt loams of loessial origin and Coastal Plain sandy loams. Within each of the three cover types, surface runoff increased directly with the proportion of loessial soil. The presence of a shallow, slowly permeable fragipan more than doubled the amount of surface runoff and increased peak flows considerably. Detention storage above the fragipan was directly related to flow stage at the flume.

C. H. M. van Bavel (Southwest Water Conservation Laboratory, Agricultural Research Service, Phoenix, Ariz.) *Water Deficits and Irrigation Requirements in the Southern United States*—The frequency of exhaustion of available moisture supplies and the attendant water deficits have been determined for nine southern states. The results are based upon estimated daily moisture balance computed for 25 years at 264 stations. Evapotranspiration was estimated with the Penman formula. Results are given in terms of two parameters: storage capacity of the root zone and recurrence probability. Therefore, the values obtained have immediate practical value for a number of agrohydrological and agronomical applications. Among these are the estimation of irrigation requirements for river basins, farms, and individual fields, as well as estimation of drought hazard. Generalized, the results indicate typical occurrence of severe drought throughout the South during the growing season. It appears that soil storage capacity and recurrence frequency are more important in determining water deficits than is geographical location.

George Veis (Smithsonian Astrophysical Observatory, Cambridge, Mass.) *Geodetic Connections with Artificial Satellites*—The orbital method for geodetic connections with the use of satellites and the advantages of simultaneous observations of a special flashing artificial satellite are discussed.

E. H. Vestine and W. L. Sibley (Rand Corporation, Santa Monica, Calif.) *Comparison of Geomagnetic Fields in the Northern and Southern*

Hemispheres—The lines of force of the geomagnetic field at various latitudes and longitudes in the Northern Hemisphere are approximately traced to their intersection with the earth's surface in the Southern Hemisphere, using an electronic computer and the first nine Gauss coefficients. Those lines leaving the average northern auroral zone are traced to their intersection of the geomagnetic field with the earth's surface. These points of intersection are found to be very nearly at the average southern auroral zone, deduced from auroral observations and from magnetic measurements of disturbance. It is concluded, therefore, that the geomagnetic field has stability and a simple character even at distances as great as about six earth radii above the earth, measured in the equatorial plane, even during auroral displays. It is also concluded that solar streams at such times do not seriously distort the field lines connecting the auroral zones.

Bernard Vonnegut and Charles B. Moore (Arthur D. Little, Inc., Cambridge, Mass.) *Measurement of Electric Fields in the Atmosphere*—Experimental apparatus has been devised for measuring the magnitude and direction of the atmospheric electrical field from the ground and in the air from balloons and airplanes. These instruments are described and some of the preliminary results obtained with them are presented.

L. S. Walter (Pennsylvania State University, University Park, Pa.) *Determination of the PT Curves for the 'Monticellite' and 'Akermanite' Reactions of Bowen's Decarbonation Series*—The univariant stability curves of

(1) 2 calcite + diopside + forsterite $\leftrightarrows$ 3 monticellite + 2 CO_2

and

(2) calcite + diopside $\leftrightarrows$ akermanite + CO_2

have been experimentally determined as a function of P_{CO_2} and T. The curve of (1) passes through 710°C at 700 psi, through 800°C at 2500 psi, and through 900°C at 8700 psi. Akermanite breaks down to monticellite + wollastonite below approximately 725°C, but above this temperature the curve of reaction (2) passes through 750°C at 1400 psi, through 800°C at 2900 psi, and through 900°C at 7600 psi. These two curves serve as additional elements of the petrogenetic grid proposed by Bowen.

G. J. Wasserburg (California Institute of Technology, Pasadena, Calif.), G. W. Wetherill (Department of Terrestrial Magnetism, Carnegie Institution of Washington, Washington, D. C.), and L. A. Wright (California Division of Mines, Sacramento, Calif.) *Ages in the Precambrian of Death Valley, California*—Age determinations have been made on micas from the Pre-Pahrump basement in Death Valley. These are C-1, a muscovite from an underformed pegmatite crosscutting a highly foliated quartz muscovite schist, C-2. Basal Pahrump rests unconformably on the pegmatite and the schist. C-3 is a biotite from a Pre-Pahrump granite gneiss in the southern Nopah Mountains. These data show that the western continental margins have an ancient Precambrian basement. SG-Bi is a biotite from a basic pegmatite, near the Pacoima Canyon locality in the San Gabriel Mountains, of supposed Precambrian age.

Specimen	τA^{40}-K^{40}	τSr^{87}-Rb^{87}
	m y	m y
C-1	1,670	1,720
C-2	1,480	1,510
C-3	980	1,440
SG-Bi	380	380

Willis L. Webb (U. S. Army Signal Missile Support Agency, White Sands Missile Range, N. M.) *Application of Available Meteorological Missiles*—A series of test-rocket firings has been conducted during the past eighteen months to establish the operational feasibility of available rocket systems for meteorological observations. As could be expected, the most desirable systems from an instrumentation point of view are generally not the most desirable relative to the rocket-firing problem. It has been demonstrated, however, that a reasonable observation schedule can be accomplished by the judicious application of currently available rockets and sensors. The most variable of high-atmosphere meteorological parameters is the flow. Chaff was used initially for rocket wind measurements because it could be expected to provide a suitable indication of the wind in this air above balloon level. It is easy to package and deploy. Most of the available high-atmosphere wind data have been obtained through use of a chaff sensor, and it is still most applicable for point measurements and at very high altitudes.

The need for a more coherent sensor and a vehicle capable of transporting a telemetry system to provide for the measurement of other parameters has resulted in the development of a parachute system. Although one will always incur an altitude range problem, it is possible to obtain data from approximately 200,000 ft to the surface through the application of a single parachute and balloon combination. Launch and flight characteristics of the available rockets are presented for use in applying this new observational technique. Careful adherence to the design and operational restrictions indicated by these data will result in savings in the effort required for development of the various desirable measuring techniques. Experience to date indicates that one can, with available equipment, obtain profiles of several meteorological parameters from the surface to altitudes of the order of 200,000 ft at reasonable expenditure of effort.

G. W. Wetherill, G. R. Tilton, G. L. Davis, and C. A. Hopson (Carnegie Institution of Washington, Washington, D. C., and Johns Hopkins University, Baltimore, Md.) *Mineral Ages in the Baltimore-Washington Area*—The following mica ages have been found:

Specimen	Rb-Sr	K-A
	m y	m y
1. Baltimore gneiss, Towson dome, Md.	305	335
2. Baltimore gneiss, Woodstock dome, Md.	310	410
3. Baltimore gneiss, Phoenix dome, Md.	310	390
4. Hartley Augen-gneiss, Md.	315	...
5. Woodstock granite, Md.	315	295
6. Kensington gneiss, D. C.	305	370
7. Pegmatite, Baltimore, Md.	405	280

Zircons from the Baltimore gneiss have approximately concordant 1050 m y U-Pb and Th-Pb ages; feldspars from both the Baltimore gneiss and the Hartley Augen-gneiss have Rb-Sr ages of 1200 ± 200 m y. These data are interpreted as implying the existence of a basement 1050 m y old, which has been metamorphosed and intruded during the Paleozoic. The relationship of these ages to the age of the meta-sedimentary Glenarm series is discussed.

Peter K. Weyl (Exploration and Production Research Division, Shell Development Co., Houston 25, Tex.) *Pressure Solution–A Phenomenological Theory*—The phenomenon of pressure solution results from the removal of mineral matter in the region of contact between the mineral grains. We assume that this transport takes place by diffusion in a solution film between the grains. The rate of transport depends on the grain size, the effective normal stress between the grains, the diffusion constant in the film, the film thickness, and the stress coefficient of solubility. Values of these parameters required to obtain the amount of pressure solution observed in the St. Peter sandstone are reasonable. The theory predicts an increase in pressure solution with decreasing grain size. Clay films between the grains also increase the rate of pressure solution owing to the more rapid rate of diffusion in the clay layer. This explains how pre-existing clay films in the sediment may, because of the greater rate of pressure solution, develop into stylolites.

W. W. Whitaker, S. Valastro, Jr., and Milton Williams (Production Research Division, Humble Oil and Refining Co., Houston, Tex.) *The Climatic Factor in the Radiocarbon Content of Woods*—Past research has shown significant variations in radiocarbon contents of woods from different environments and in the degrees to which these radiocarbon contents reflect dilution of atmospheric carbon dioxide by carbon dioxide from fossil fuels. The present work attempts to relate these variations to climatic factors. Comparison of radiocarbon contents of individual tree rings with thickness of the rings and, in some cases, with meteorological records suggests that the radiocarbon contents of rings produced in years of heavy rainfall may be comparatively high. The year-to-year fluctuations in radiocarbon content observed in individual trees probably cannot be ascribed to rainfall alone. The apparent dependence of radiocarbon content on climate seems to be a result of a varying contribution to the tree of carbon from the pedosphere.

E. H. Timothy Whitten (Northwestern University, Evanston, Ill.) *Composition Trends in a Granite: Modal Variation and Ghost Stratigraphy in Part of the Donegal Granite, Eire*—Modal variation of quartz, color index, potash feldspar/plagioclase, and total feldspar within a 25 square mile area of the 'older granite' of Donegal was analyzed on the basis of 71 specimens. Non-orthogonal polynomial analysis was used to compute linear and quadratic trend surfaces and deviations for each variable. The IBM 650 was used for all computations.

Each variable behaved differently. Single models gave excellent trend surfaces for color index, whereas averaging data within each square mile sometimes masked important residuals. Realistic trend surfaces for quartz or total feldspar were only derived from averaged data. With averaged data the four linear trend surfaces have almost parallel strikes, and such uniform regional trends have significance in the interpretation of geologic gradients in relation to the petrogenesis of the granite.

Some deviations have been linked to observed geologic factors. Other deviations are consistent for all variables. These deviations reflect ghost stratigraphy; the latter group indicate ghost stratigraphy previously unsuspected in this area, but which is harmonious with the well-known regional picture.

William K. Widger, Jr., (Geophysics Research Directorate, Air Force Cambridge Research Center, Bedford, Mass.) *The Processing and Analysis of Satellite Weather Data*—In the near future meteorological satellites will be providing television observations of clouds over sizeable areas of the earth and radiometric measurements of the earth and its atmosphere. These radiometric measurements are expected to provide data pertinent to the atmospheric heat balance, moisture or temperature in the upper troposphere, and, using measurements made in the region of the ten micron atmospheric 'window,' a complex variety of other parameters. Present programs for the processing and analysis of these data will be discussed.

John W. Winchester (Department of Geology, Massachusetts Institute of Technology, Cambridge, Mass.) *Determination of Potassium in Biotite by Neutron Activation*—Potassium may be determined in biotite and many other common minerals by pile neutron irradiation followed by counting of the induced 12.5 hr K^{42} hard β radiation with an end-window proportional counter and selected Al absorbers. The method requires no chemical operations but involves a ten-minute irradiation of 30 to 40 mg samples and potassium acid phthalate standards, each sealed into a polyethylene packet, followed 24 to 48 hours later by counting of these packets. The procedure is rapid and precision error of an analysis may be 1 p

cent or less of the potassium value. Systematic error due to induced β activities of other elements is less than the random errors of the method. Gallium is the most seriously interfering element in biotite analysis causing 0.4% error (0.03% K) if K = 7.8% and Ga = 200‰. An analysis of standard biotite MIT No. B3203, corrected for Ga, gives 7.83 I 0.05% K.

JOHN W. WINCHESTER (Department of Geology, Massachusetts Institute of Technology, Cambridge, Mass.) *Trace-Element Analysis in Geochemistry by Neutron Activation–Discussion of Sensitivities and Errors*—The sensitivity limits for determining the elements in geological materials by pile neutron activation have been computed using recent neutron capture cross section and half-life data. These sensitivities are compared with those attainable by dc arc spectroscopy, x ray emission, and sensitive color reactions, and the sensitivities of the four analytical methods are compared with the contents of trace elements in sedimentary rocks and four igneous rock types. Analysis of one gram samples by neutron activation offers sensitivity greater than the average concentration of the elements in all major rock types (insofar as data is available) for all elements heavier than Ca. In contrast, sensitive color reactions are insufficiently sensitive for nearly all elements heavier than Mo for at least one rock type, and x-ray emission and dc arc spectroscopy are even less sensitive. High sensitivity and freedom from reagent contamination make neutron activation the most reliable analytical method for studying trace-element distribution in geological materials.

PAUL M. WOLFF, D. W. MCILHENNY, AND R. E. WALKER (U. S. Navy, Suitland, Md.) *Verification of JNWP Hurricane Forecasts from 1958*—Statistical summary of the verification of the JNWP hurricane tracks is presented together with comparative results for earlier years. The results of numerical experiments designed to assess the importance of various changes in JNWP procedure are described.

DAVID R. WONES (Geophysical Laboratory, Carnegie Institution of Washington, Washington, D. C.) *Biotites: Phase Relations of the $K_2O \cdot 6FeO \cdot Fe_2O_3 \cdot 6SiO_2 \cdot 2H_2O$ End Member*—Phase relations of a biotite of the composition $K_2O \cdot 6FeO \cdot Fe_2O_3 \cdot 6SiO_2 \cdot 2H_2O$ have been determined for total pressure (= water vapor pressure), temperature, and partial pressure of oxygen (P_{O_2}). The following six assemblages were encountered for this bulk composition (arranged in order of increasing temperature and decreasing oxygen pressure at a constant vapor pressure): (1) Fe-sanidine + hematite + vapor; (2) Fe-sanidine + magnetite + vapor; (3) biotite + vapor; (4) melt + magnetite + vapor; (5) melt + wüstite + fayalite + vapor; and (6) melt + iron + fayalite + vapor.

The locations of five univariant equilibria have been determined at 15,000 and 30,000 psi as shown in the table below.

The assemblage Fe-sanidine + magnetite + melt + biotite + vapor has been inferred from the location of the intersecting phase boundaries. Partial pressures of oxygen were controlled by using the following buffers: (1) cuprite-copper; (2) hematite-magnetite; (3) nickel oxide-nickel; (4) quartz-magnetite-fayalite; (5) magnetite-wüstite; and (6) wüstite-iron.

$(\partial P_{tot}/\partial T)_{P_{O_2}}$ of the divariant assemblage biotite + melt + magnetite + vapor shows a marked decrease with increasing P_{O_2}. This is interpreted as a decrease in the water content of the melt.

These data are an addition to the data on the phase relations of the biotite end members. Natural occurrences of this biotite should be limited to subaluminous iron-rich rocks (that is, iron formation or ferruginous quartzites) which contain either sedimentary or metasomatic potash.

JOHN A. WOOD, JR. (Smithsonian Astrophysical Observatory, Cambridge, Mass.) *Petrographic Textures in Chondrites*—Microphotographs are presented, some depicting the over-all texture of several types of chondritic meteorites, others the characteristics of some of the individual chondrules of which the chondrites are aggregated. Conclusions and inferences which may be drawn from these, regarding the origin of the meteorites, are discussed. The petrography of the chondrites appears to favor the following sequence of events. (1) Condensation of liquid droplets (and finer dust) dur-

Assemblage	P_{vapor} = 15,000 psi		P_{vapor} = 30,000 psi	
	P_{O_2} (in bars)	T (°C)	P_{O_2} (in bars)	T (°C)
Biotite + Fe-sanidine + hematite + magnetite + vapor	$\sim 10^{-19}$	470	$\sim 10^{-17}$	510
Fe-sanidine + hematite + magnetite + melt + vapor	$\sim 10^{-9}$	765	$\sim 10^{-11}$	715
Biotite + Fe-sanidine + magnetite + melt + vapor	$\sim 10^{-15}$–10^{-16}	580–735	$\sim 10^{-12}$–10^{-13}	660–715
Biotite + magnetite + wüstite + fayalite + melt + vapor	$\sim 10^{-16}$	825	$\sim 10^{-16}$	825
Mica + wüstite + iron + fayalite + melt + vapor	$\sim 10^{-20}$	765	$\sim 10^{-20}$	765

ing cooling of a hot gas cloud containing silicate and iron vapor. This condensation may have been a minor by-product of the genesis of the sun. (2) After solidification of the droplets (chondrules), accretion of this solid material into the terrestrial planets, including one or more parent meteorite planets. (3) Recrystallization and possibly even melting of the deeper chondritic material in the parent meteorite planets. The central heat responsible for this might also have produced the carbonaceous chondrites. (4) Disintegration of the parent meteorite planets into asteroids and meteorites.

The petrographic characteristics of the chondrites do not appear to support the existence of primary bodies which antedated the parent meteorite planets.

P. J. Wyllie and O. F. Tuttle (Pennsylvania State University, University Park, Pa.) *The Calcite-Portlandite Join in the System CaO-Co_2-H_2O*—An isobaric equilibrium diagram has been determined for this join at a pressure of 1000 bars in the temperature interval from 600 to 1320°C. Portlandite ($Ca(OH)_2$) melts congruently at 835 ± 5°C and calcite melts incongruently to liquid + CO_2 at 1310 ± 10°C. Because of the incongruent melting of calcite, the join is ternary at high temperatures but becomes binary below about 1150°C at this pressure. Ternary fields of calcite + liquid + vapor and liquid + vapor, and binary fields of calcite + liquid, liquid, portlandite + liquid and calcite + portlandite have been delineated. The eutectic at 685°C has the composition portlandite: calcite = 56:44, in weight per cent. With variation in pressure the eutectic remains binary from 250 bars (685°C) to at least 3000 bars (660°C). At lower pressures the join becomes ternary because all compositions melt incongruently to liquid + vapor. The addition of water vapor under pressure to compositions on the join depresses the melting temperatures, but the depression is slight (10°C at 1000 bars pressure) because only a small amount of water dissolves in the melt. The low temperature liquid in the join portlandite-calcite, consisting of 67 CaO, 19 CO_2, and 14 H_2O in weight per cent, is regarded as a simplified carbonatite magma. These results indicate that carbonatite magmas can exist at moderate temperatures over a wide range of pressures.

Edward J. Zeller (University of Kansas, Lawrence, Kans.) *Thermoluminescence as an Indicator of Past Climatic Conditions*—Samples of carbonate rocks from the Antarctic continent have shown natural thermoluminescence at much lower temperatures than rocks from temperate climates. Measurements of the rate of filling of low-temperature electron traps by artificial radiation, together with studies of rates of trap drainage at elevated temperatures, provide information concerning the thermal history of the natural samples. The amount of natural thermoluminescence present at these low temperatures is dependent upon the equilibrium between thermal drainage of the traps and the natural rate of filling. Measurements of the natural radiation rate of the carbonate samples combined with the data concerning the thermal history permit estimation of the length of time to which the rocks have been subjected to low temperatures.

Alfred J. Zmuda (Applied Physics Laboratory, Johns Hopkins University, Silver Spring, Md.) *Preliminary Results on Some Hydromagnetic Effects Related to the Geomagnetic Field*—In the model of the terrestrial dynamo discussed by E. C. Bullard, the dominant motion in the earth's core is one with a radial variation of angular velocity. Fluid motion of this type contributes prominently to the hydromagnetic interactions which maintain that part of the geomagnetic field associated with a dipole aligned along the earth's rotational axis. This dynamo motion will also influence other parts of the geomagnetic field, especially that portion related to a dipole lying in the equatorial plane. The hydromagnetic problem connected with the nonuniform rotation and the equatorial dipole is discussed and some preliminary results are presented.

Alfred J. Zmuda (Applied Physics Laboratory, Johns Hopkins University, Silver Spring, Md.) *Some Characteristics of the Upper-Air Magnetic Field and Ionospheric Currents*—Published rocket data on the scalar magnetic intensity were compared with values computed through the extrapolation of the vector surface field. Agreement between the two sets of data is good. For the cases where the rockets penetrated the ionospheric currents, it was determined that the current densities lies in general between 10^{-5} and 10^{-6} amp/meter^2 depending on the time of the rocket flight. The computed currents are treated in relation to the equatorial electrojet and the currents that produce the normal magnetic daily variation.

AMERICAN GEOPHYSICAL UNION

1515 Massachusetts Avenue, N.W., Washington 5, D. C.

Established by the National Research Council in 1919 for the development of the science of geophysics through scientific publication and the advancement of professional ideals.

APPLICATION FOR MEMBERSHIP

Please refer to qualifications on reverse side and designate below type of membership desired:

Member ($10) ☐ Associate ($10) ☐ Student ($3) ☐

Application forms for Corporation Membership are available upon request.

1. _____
Surname *First Name* *Middle Name*

2. _____
Preferred mailing address for publications

_____
Permanent address

3. _____ 4. _____
Place *Month* *Day* *Year of Birth* *Country of citizenship/naturalization*

5. _____
Nature of work and title and/or military rank; name and address of organization with which you are associated.

6. Check section or sections with which affiliation is desired.

☐ Geodesy
☐ Seismology
☐ Meteorology
☐ Geomagnetism and Aeronomy
☐ Oceanography
☐ Volcanology, Geochemistry, and Petrology
☐ Hydrology
☐ Tectonophysics

7. **EXPERIENCE (List below)**

Dates: From To Name and address of organization Title, duties, nature of work

8. **EDUCATION (List below)**

Dates: From To School Address Major Subject Degree, if any

*9. References: Please list below names and addresses of two or three references; include members of the AGU or others who know you well.

*10. Titles of technical contributions or publications, particularly those in the geophysical sciences, and where published.

*11. Brief statement of any special interests or qualifications in the geophysical sciences.

Date_____ _____
Written Signature

* Applicants for student membership may omit Questions 9, 10, and 11, but must fill in Question 12. Please return form with check or money order payable to American Geophysical Union, 1515 Massachusetts Ave., N.W., Washington 5, D. C.

(over)

12. (STUDENT MEMBERS ONLY) The person whose signature appears on the reverse side is known to me and is a student majoring in _____ (subject) at _____ (Name of college or university) expected to graduate in _____ (year) with the degree of _____

☐ He is a full-time student, or ☐ a teaching or research assistant enrolled in more than half of a full-time academic program.

_____
(Signature of faculty sponsor)

☐ Check here if faculty sponsor is a member of AGU and willing to act as a regular sponsor for associate membership as well.

_____
(Typed or printed name of sponsor)

_____
(Title)

QUALIFICATIONS FOR MEMBERSHIP IN THE AMERICAN GEOPHYSICAL UNION

The membership of the AGU shall consist of Members, Associate Members, Student Members, and Corporation Members.

Those eligible as candidates for election to the grade of MEMBER shall be:

Member (a) Persons who have made an active contribution to geophysical research through observation, publication, teaching, or administration. Definite evidence should be presented to the Membership Committee. "Publication" may include books, articles, unpublished manuscripts, inventions, or development of geophysical instruments.

(b) Persons who have made active practical application of geophysical research. It should be shown that the nominee's work has not been purely routine, but that it has tended to create new knowledge of, or to broaden or strengthen the application of, geophysical research. In general, the minimum qualifications for membership will be not less than three years of professional experience in some phase of geophysics.

Those eligible as candidates for election to the grade of ASSOCIATE MEMBER shall be:

Associate Member Persons who have an active interest in physical processes of the Earth or technical assistance in the application of geophysics. In general, the minimum qualification for associate membership will be acceptable training or experience in some field of geophysics or allied science.

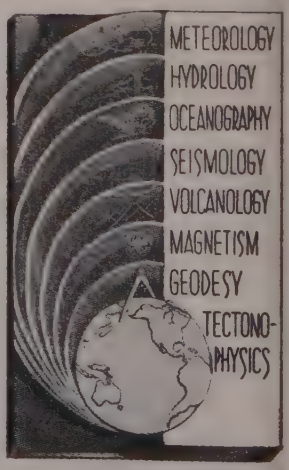

Corporation Member Corporations and other interested organizations shall be eligible as candidates for election to CORPORATION MEMBERSHIP. They shall have the privilege of designating a representative who has the rights and privileges of Members (use special form).

Student Member Those eligible as candidates for election to the grade of STUDENT MEMBER shall be persons who are graduate or undergraduate students in residence at least half-time and who are specializing in the geophysical sciences. Teaching or research assistants enrolled in more than half of a full-time academic program may also be eligible for Student Membership. Student Members shall have all the privileges of Members except that they shall not vote or hold office.

American Geophysical Union

PROPOSAL FOR CORPORATION MEMBERSHIP

To the Executive Committee, American Geophysical Union
1515 Massachusetts Ave., N.W., Washington 5, D. C.

Gentlemen:

As an indication of our interest in the aims and activities of the American Geophysical Union, and to assist in maintaining and extending its program of publication and other work in the development of the geophysical sciences, the undersigned applies for Corporation Membership in the AGU and, until further notice, agrees to pay annual dues, currently at the rate of $100 per unit of corporation membership, in accordance with the information set forth on the back of this sheet.

Company or Organization _____

By _____ Title _____
(Signature)

Address _____

City _____ State _____

General fields of activity _____

_____

_____

_____

The following person is designated as our representative in this membership _____
_____ Title _____

Number of units of membership desired (this will be taken as one unless otherwise indicated) _____

Place _____

Date _____

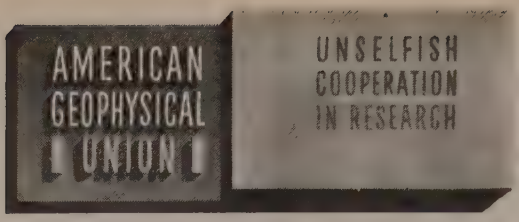

INFORMATION CONCERNING CORPORATION MEMBERSHIP

The American Geophysical Union is a non-profit scientific organization established by the National Research Council. It is the American National Committee of the International Union of Geodesy and Geophysics, and its Executive Committee is the Committee on Geophysics of the National Research Council.

Extracts from the Statutes:

Article 3. Membership—The membership of the American Geophysical Union shall be as follows:

(e) *Corporation Members*—Corporations and other organizations interested in geophysics elected by the Executive Committee of the Union. The designated representative of each such organization shall enjoy the privileges of a Member.

Extracts from the By-Laws:

(2) . . . Members of class (e) shall pay dues of $100 for each calendar year; . . .

(21) One copy of each issue of (a) the *Transactions*, (b) *Journal of Geophysical Research*, (c) any published *List of Members and Officers*, and (d) any other publication which may be approved for *free distribution* to the membership by the Executive Committee of the Union, shall be sent to each . . . Corporation Member. . . . Each . . . organization in good standing may purchase any available publication of the Union at a discount from printed price list to non-members. The General Secretary is authorized to establish discounts for sales of publications.

Action of the Executive Committee, November 29, 1946:

(1) A list of corporation members shall be published on one or more pages immediately after the final page of text in each issue of the *Transactions*.

(2) A list of corporation members shall be included in the Membership Directory as a distinct unit.

AMERICAN GEOPHYSICAL UNION

1515 Massachusetts Ave., N.W.
Washington 5, D. C.

Contents

(*Continued from back cover*)

(Journal of Geophysical Research, Vol. 64, No. 8, August 1959

Contents

(*Continued inside back cover*)